

# *Symmetry Implications for Wilson Line Correlators in QCD at High Energies*

Judith Magdalena Alcock-Zeilinger

Supervisor: A/Prof. Heribert Weigert



Thesis Presented for the Degree of  
DOCTOR OF PHILOSOPHY  
in the Department of Physics  
UNIVERSITY OF CAPE TOWN

Submitted for Examination: July 2017

Revised: November 2017



# Abstract

In modern collider experiments such as the LHC or DESY, reaction channels from quantum chromodynamics (QCD) dominate particle production. In the high energy limit, the number of gluons produced is so large, that these gluons dominate the initial conditions of heavy ion collisions and influence subsequent transitions of the produced hot dense matter into a quark gluon plasma (QGP). These initial gluon dominated configurations are called the color glass condensate (CGC). The energy dependence of observables in this situation is described by a renormalization group equation, the Jalilian-Marian–Iancu–McLerran–Weigert–Leonidov–Kovner (JIMWLK) equation.

The theoretical foundation of the CGC treatment are factorization theorems that allow one to separate hard and soft contributions. In particular, the interaction between a hard projectile with the CGC occurs via the exchange of soft gluons. Such an interaction is said to be eikonal and is described by path-ordered exponentials in the gauge group  $SU(N)$  called Wilson lines. By virtue of these Wilson lines being group elements, they impart additional structure on the interaction: Since confinement requires the individual partons in the projectile and target to assemble into color neutral configurations before and after the interaction, the group structure requires these color neutral configurations to be in a singlet representation of  $SU(N)$  over the appropriate Fock space.

Surprisingly little is known about the representation theory of  $SU(N)$  over a mixed space  $V^{\otimes m} \otimes (V^*)^{\otimes n}$ . While the standard methods are well suited for classification purposes, even computer implementations become inefficient in practice beyond the most elementary examples. In this thesis, we explore the representation theory of  $SU(N)$  with a focus on applications in the QCD context. In doing so, we develop computational tools for the birdtrack formalism, which allow a new, computationally efficient construction of Hermitian Young projection and transition operators based on the measure of lexical disorder of Young tableaux. These operators allow for a computationally efficient algorithm to construct the singlet projection operators (and thus singlet states) of  $SU(N)$  over the Fock space encoding quarks, antiquarks and gluons,  $V^{\otimes m} \otimes (V^*)^{\otimes n}$ . These singlet projectors are immediately applicable to QCD as they facilitate the construction of Wilson line correlators.

Many additional results with regards to the representation theory of  $SU(N)$  over  $V^{\otimes m} \otimes (V^*)^{\otimes n}$  were found along the way. Most notable is a counting argument giving the number of irreducible representations of  $SU(N)$  over any mixed space  $V^{\otimes m} \otimes (V^*)^{\otimes n}$ . These additional results are also given in this thesis.

# Plagiarism Declaration

I know the meaning of plagiarism and declare that all of the work in this thesis, save for that which is properly acknowledged, is my own.

---

Judith Magdalena Alcock-Zeilinger  
Student number: ZLNJUD001

Date: 26<sup>th</sup> of July 2017

## Inclusion of Publications in my Thesis

I confirm that I have been granted permission by the University of Cape Town's Doctoral Degrees Board to include the following publications in my PhD thesis, and where co-authorships are involved, my co-authors have agreed that I may include the publications:

1. J. Alcock-Zeilinger and H. Weigert, "Simplification Rules for Birdtrack Operators", *J. Math. Phys.* **58** no. 5, (2017) 051701 (*c.f.* Ref. [1], included as chapter 2).
2. J. Alcock-Zeilinger and H. Weigert, "Compact Hermitian Young Projection Operators", *J. Math. Phys.* **58** no. 5, (2017) 051702 (*c.f.* Ref. [2], included as chapter 3).
3. J. Alcock-Zeilinger and H. Weigert, "Transition Operators", *J. Math. Phys.* **58** no. 5, (2017) 051703 (*c.f.* Ref. [3], included as chapter 4).

On pages iv–vi, I state the contribution each author has made to these publications.

---

Judith Magdalena Alcock-Zeilinger  
Student number: ZLNJUD001

Date: 26<sup>th</sup> of July 2017

---

## Contribution to Refs. [1–3] by each author

The publications in question were co-authored between myself and my supervisor A/Prof. Heribert Weigert. While I derived all the main results in each of these papers, A/Prof. Weigert had the initial idea to look into the topics discussed in Refs. [1–3]. Furthermore, A/Prof. Weigert provided guidance throughout the entire process. All diagrams/graphics in papers [1–3] were created by me.

I will now give a detailed account of the contributions each person has made to each paper:

### Paper [1] (chapter 2): “Simplification Rules for Birdtrack Operators”

This paper is almost exclusively my own work. I derived (and proved) all original results given in this paper by myself, A/Prof. Weigert provided guidance for the overall presentation of the results.

### Paper [2] (chapter 3): “Compact Hermitian Young Projection Operators”

The initial idea to look into a Hermitian version of Young projection operators came from A/Prof. Weigert. Sections 3.1–3.2 and the beginning of section 3.3 (before section 3.3.1), which form an introduction to this paper, are a collaboration between A/Prof. Weigert and myself.

Section 3.3.1 describes the Hermitian conjugation for linear maps in the birdtrack formalism. This section is mainly due to A/Prof. Weigert, and I provided the diagrams.

Section 3.3.2 gives a motivation for why the standard (non-Hermitian) Young projection operators are not sufficient for our purposes. While the general idea behind this section emerged from discussions between A/Prof. Weigert and myself, the examples and calculations presented in this section were done by me.

Section 3.3.3 first summarizes the construction method for Hermitian Young projection operators by Keppeler and Sjö Dahl (KS) [4]. We then give the first simplified version of the KS Hermitian Young projection (in Corollary 3.1). The original work presented in this section is wholly mine, A/Prof. Weigert gave advice for presentation of the known results.

Section 3.3.4 (including Lemma 3.1) gives a proof that the Hermitian Young projection operators constructed according to Corollary 3.1 fulfill a nested hierarchy: The subspace onto which a particular operator projects is included in the subspace corresponding to its ancestor operator. This section has been a collaboration between A/Prof. Weigert and myself, each person contributed approximately half the work.

**Section 3.4 gives the main results of this paper:** In section 3.4.1, we first give a compact construction formula for Hermitian Young projection operators corresponding to lexically ordered tableaux (Theorem 3.4). This result gives a basis for a compact construction principle for *all* Hermitian Young projection operators, which uses the measure of lexical disorder (MOLD) of the corresponding Young tableau (Theorem 3.5), see section 3.4.2. Section 3.4.3 discusses the advantages of the MOLD operators over the previously existing KS operators. Section 3.4 is my own work, A/Prof. Weigert gave advice with regards to the pedagogical presentation of the material. The proofs of Theorems 3.4 and 3.5 (which are given in appendix 3.C) are also exclusively my own work, with the exception of the very last step of the proof of Theorem 3.5, for which I received the help of A/Prof. Weigert.

Section 3.5 is the conclusion of this paper, on which A/Prof. Weigert and myself collaborated. In particular, A/Prof. Weigert provided the outlook on applications of the results of this paper in the QCD context. The

---

summary of results, as well as the discussion on the computational efficiency of our MOLD operators are from me.

Appendices 3.A (a review of Littlewood’s contribution to Young’s projection operators) and 3.B (a proof that the (non-Hermitian) Young projection operators do not commute with their ancestor operators) are a collaboration between A/Prof. Weigert and myself. A/Prof. Weigert had the initial idea to look into these topics and gave guidance with respect to the presentation. The calculations in these appendices were done by me.

As already mentioned, appendix 3.C (which gives the proofs of the main results (Theorems 3.4 and 3.5) of this paper) is my own work.

## Paper [3] (chapter 4): “Transition Operators”

The idea, that transition operators between equivalent irreducible representations of  $SU(N)$  must exist, stems from A/Prof. Weigert. This idea prompted us to look into the topic in the first place.

Sections 4.1–4.2 and the beginning of section 4.3 (up until section 4.3.1) form the introduction of this paper, giving the relevant background material. These sections are a collaboration between A/Prof. Weigert and myself.

Section 4.3.1 gives the transition operators between the (non-Hermitian) Young projection operators. A/Prof. Weigert and myself collaborated on this section, where each of us contributed approximately half the work.

Section 4.3.2 proves that the totality of projection and transition operators span the algebra of invariants of  $SU(N)$  over  $V^{\otimes m}$ : For the Young projection operators, this proof holds up to  $m \leq 4$ , but for the MOLD projectors and their unitary transition operators (to be constructed in section 4.5), this proof holds for all  $m$ . Section 4.3.2 is completely my work. Section 4.3.3 gives an example of the Young projection and transition operators over  $V^{\otimes 3}$ , which was also done by me.

Section 4.4 (up until and including section 4.4.1) gives a review of the properties of the Hermitian Young projection operators which were previously discussed in chapter 3 (Ref. [2]). This review is a collaboration between A/Prof. Weigert and myself.

In section 4.4.2, the proof given in section 4.3.2 (stating that the projection and transition operators span the algebra of invariants of  $SU(N)$ ) is translated into the language of Clebsch-Gordan operators. Section 4.4.3 discusses the multiplication table of the algebra of invariants of  $SU(N)$  in terms of a basis of projection and transition operators. Both, sections 4.4.2 and 4.4.3, are mainly due to A/Prof. Weigert.

**Section 4.5 gives the main results of this paper:** We first review the construction principle of the MOLD operators (see chapter 3, Ref. [2]) in section 4.5.1. Section 4.5.2 gives a general construction principle for the transition operators between Hermitian Young projection operators (Theorem 4.4) with a proof. It is then motivated that the operators obtained from Theorem 4.4, albeit obeying all the desired properties, are not as compact as they could be. Theorem 4.5 gives an alternative, *graphical* construction method (based on cutting and gluing the projection operators), which immediately yields the more *compact* version of the transition operators. Section 4.5 is my own work, A/Prof. Weigert provided guidance with regards to the presentation of the material in this section. The proof of Theorem 4.5 is given in appendix 4.D, which is also my own work.

Section 4.6 gives all projection and transition operators of  $SU(N)$  over  $V^{\otimes 3}$  and over  $V^{\otimes 4}$ . This section is due to me.

---

Section 4.7 is the conclusion of this paper, on which A/Prof. Weigert and myself collaborated, each of us contributing approximately half the work. In addition, I made Figures 4.2 and 4.3, which show all projection and transition operators (with the corresponding dimension) up to the 4<sup>th</sup> generation for Young operators and MOLD operators respectively.

A/Prof. Weigert and I collaborated on appendix 4.A (a discussion on dimensionally null operators), where the initial idea came from A/Prof. Weigert.

Appendix 4.B gives an example illustrating the action of the tableau permutation  $\rho_{\Theta\Phi}$ . The idea behind this section, as well as all the calculations come from me, but A/Prof. Weigert provided crucial insight which manifests in the presentation of the material.

In appendix 4.C, we provide an example illustrating the consequence of the non-Hermiticity of Young projection operators. The material presented in this appendix is from me.

As already mentioned, appendix 4.D (which includes the proof of Theorem 4.5) is my work.



# Acknowledgements

I would like to thank all my funding agencies for the financial support throughout this project: I was supported (in sequence) by the postgraduate funding office of the University of Cape Town (2014), the National Research Foundation (2015) and the Science Faculty PhD Fellowship of the University of Cape Town (2016-2017).

Furthermore, I would like to thank my supervisor A/Prof. Heribert Weigert for his guidance and the many, many, MANY hours of discussions — I really profited tremendously from them. Our conversations, often over coffee or beer (most of which had been sponsored by A/Prof. Weigert), not only granted me a deeper understanding of the topics we discussed, but also influenced my strategy in tackling new problems with an open mind and a can-do attitude. Lastly, I am deeply indebted to A/Prof. Weigert for carefully reading through numerous drafts of this thesis, thus allowing me to make it the best it can possibly be.

A big hug and thanks goes out to my husband Ryan, for supporting me through the ups and downs of this project. You were my stronghold through all difficulties and never stopped believing in me. I am also very grateful to my parents Alois and Christa, for their constant, loving moral support and their cheerful enthusiasm throughout the entire process. To all three of you: Danke, dass ihr immer für mich da wart, ich hätte es nicht ohne euch geschafft. Ein “Prosit” zu diesem abenteuerlichen Lebensabschnitt, der nun endlich sein Ende gefunden hat. A special thanks also to my mother for creating the beautiful letter “S” on page 1.

I would further like to thank many postgraduate students of the UCT Physics Department that spent countless hours chatting to me, thus enormously improving my understanding of physics and maths (and, in some cases, life as a whole). In no particular order, thanks to Charlotte Hillebrand-Viljoen, Isobel Kolbe, Andrianiaina Rasoanaivo, Robert Moerman, Daniel Adamiak, Luke Lippstreu and Jonathan Rayner.

I am also very grateful to Steven Kukard for proof-reading this thesis, spotting all kinds of grammar and punctuation errors that I would have overlooked.

Last but not least, I would like to thank God for giving me this opportunity. In the words of Collossians 3:23 “Whatever you do, work at it with your whole heart, as working for the LORD, not for human masters” — this is what kept me going through the more trying times in the course of this PhD project.

Reflecting on this list, I truly have a lot to be thankful for.



# Contents

<i>Title Page</i>	<i>1</i>
<i>Abstract</i>	<i>i</i>
<i>Plagiarism Declaration</i>	<i>ii</i>
<i>Inclusion of Publications in my Thesis</i>	<i>iii</i>
<i>Acknowledgements</i>	<i>vii</i>
<i>Table of Contents</i>	<i>ix</i>
<i>List of Figures</i>	<i>xi</i>
<i>Prologue</i>	<i>1</i>
<b>1 High Energy Physics and Wilson Line Correlators</b>	<b>3</b>
<b>1.1 QCD interactions at high energies — in a nutshell</b>	<b>3</b>
1.1.1 Scattering at high energies	3
1.1.2 Interactions in different kinematic limits	6
1.1.2.1 Proton mass dominates: energies below $\Lambda_{\text{QCD}}$	7
1.1.2.2 Photon energy dominates: the Bjorken limit	8
1.1.2.3 Momentum transfer dominates: the Regge-Gribov limit	9
<b>1.2 Wilson lines at high energies</b>	<b>10</b>
1.2.1 Gauge theories	11
1.2.1.1 A brief overview of gauge theories	11
1.2.1.2 Non-abelian gauge theories	12
1.2.2 Geometric interpretation of a Wilson line: parallel transport	13
1.2.3 Physics interpretation of a Wilson line	14

1.2.3.1	Feynman rules of Wilson lines .....	14
1.2.3.2	Eikonal approximation .....	15
1.2.3.3	Summary .....	18
1.2.4	Wilson lines as elements of $SU(N)$ .....	18
<b>1.3</b>	<b>The color glass condensate .....</b>	<b>21</b>
1.3.1	McLerran–Venugopalan model .....	21
1.3.2	Evolution with high energy .....	25
<b>1.4</b>	<b>The JIMWLK equation .....</b>	<b>26</b>
1.4.1	What does JIMWLK do? — a summary .....	27
1.4.2	A derivation of the JIMWLK equation at leading order .....	29
1.4.2.1	Diagrammatic notation for Wilson lines .....	30
1.4.2.2	Generating functionals and $k$ -point Wilson line correlators .....	32
1.4.2.3	Diagrammatic notation for singlet states and the target average .....	34
1.4.2.4	Cross section without fluctuations in the color field .....	36
1.4.2.5	Fluctuations in the color field .....	39
1.4.2.6	Functional differentiation of a Wilson line .....	41
1.4.2.7	Wilson line correlators from differentiation with respect to the source .....	43
1.4.2.8	Diagrammatic notation for fluctuations in the color field .....	44
1.4.2.9	Cross section with fluctuations in the color field .....	48
1.4.2.10	Cancellations and the largest time Theorem .....	49
1.4.2.11	Finite difference equation leading to JIMWLK .....	54
<b>1.5</b>	<b>Parametrization of JIMWLK .....</b>	<b>55</b>
1.5.1	Validity of the parametrization .....	56
1.5.2	Form of the parametrization .....	57
1.5.3	Faithfully parametrizing the JIMWLK Hamiltonian .....	59
1.5.4	Beyond the Gaussian truncation .....	60
1.5.5	Symmetries of the correlators and the parametrization of JIMWLK .....	61
<b>1.6</b>	<b>Symmetry implications for Wilson line correlators .....</b>	<b>63</b>
1.6.1	Wilson line correlators and JIMWLK evolution .....	64
<b>Research Statement</b> .....	<b>65</b>	
1.6.2	Coincidence limits of Wilson line correlators .....	65
1.6.3	Pulling singlets apart: further limits in Wilson line correlators .....	70
<b>1.7</b>	<b>Thesis Outline .....</b>	<b>72</b>

---

Appendix to chapter 1 .....	75
1.A Functional differentiation of a Wilson line: differentiating with respect to a parameter .....	75
<b>I Singlets and Wilson Line Correlators</b> .....	<b>79</b>
<b>2 Simplification Rules for Birdtrack Operators</b> .....	<b>81</b>
2.1 Introduction .....	81
2.2 Notation, conventions and known results .....	83
2.2.1 Tableaux .....	83
2.2.2 Birdtracks .....	84
2.3 Cancellation rules .....	89
2.3.1 Cancellation of wedged Young projectors .....	89
2.3.2 Cancellation of factors between bracketing sets .....	92
2.4 Propagation rules .....	98
2.4.1 Proof of Theorem 2.2 (propagation rules) .....	103
2.4.1.1 Unpacking the theorem conditions .....	104
2.4.1.2 Strategy of the proof .....	105
2.4.1.3 Propagating transpositions .....	105
2.4.1.4 Propagating antisymmetrizers .....	110
2.4.2 Proof of Theorem 2.3 (generalized propagation rules) .....	111
2.5 Chapter conclusion .....	112
<b>3 Compact Hermitian Young Projection Operators</b> .....	<b>115</b>
3.1 Introduction & outline .....	115
3.1.1 Historical overview .....	115
3.1.2 Where non-Hermitian projection operators fail to deliver .....	119
3.1.3 Shorter is better .....	121
3.2 Tableaux, projectors, birdtracks, and conventions .....	121
3.2.1 Birdtracks & projection operators .....	121
3.2.2 Notation & conventions .....	124
3.2.2.1 Structural relationships between Young tableaux of different sizes .....	124
3.2.2.2 Embeddings and images of linear operators .....	126
3.2.3 Cancellation rules .....	127

<b>3.3 Hermitian Young projection operators</b> .....	<b>129</b>
3.3.1 Hermitian conjugation of linear maps in birdtrack notation .....	129
3.3.2 Why equation (3.15) and its generalization cannot hold for Young projection operators.	132
3.3.3 Hermitian Young projection operators: KS and beyond .....	134
3.3.3.1 KS construction principle .....	134
3.3.3.2 Beyond the KS construction .....	136
3.3.4 Spanning subspaces with Hermitian operators .....	137
<b>3.4 An algorithm to construct compact expressions of Hermitian Young projection operators</b> .....	<b>140</b>
3.4.1 Lexically ordered Young tableaux .....	140
3.4.2 Young tableaux with partial lexical order .....	142
3.4.2.1 A Short Analysis of the MOLD Theorem 3.5.....	144
3.4.3 The advantage of using MOLD .....	145
<b>3.5 Chapter conclusion &amp; outlook</b> .....	<b>146</b>
<b>Appendix to chapter 3</b> .....	<b>149</b>
<b>3.A Littlewood-Young projection operators</b> .....	<b>149</b>
<b>3.B Young projectors that do not commute with their ancestors</b> .....	<b>153</b>
<b>3.C Proofs of the construction principles for Hermitian Young projection operators</b> ...	<b>154</b>
3.C.1 Proof of Theorem 3.4 “lexical Hermitian Young projectors” .....	154
3.C.1.1 Propagation rules .....	154
3.C.1.2 Proof of Theorem 3.4: .....	156
3.C.2 Proof of Theorem 3.5 “partially lexical Hermitian Young projectors” (or MOLD Theorem)	161
<b>4 Transition Operators</b> .....	<b>167</b>
<b>4.1 Introduction</b> .....	<b>167</b>
<b>4.2 Background: birdtracks, Young tableaux, notations and conventions</b> .....	<b>170</b>
4.2.1 Birdtracks, scalar products, and Hermiticity .....	170
4.2.2 The hierarchical nature of Young tableaux .....	173
4.2.3 From Young tableaux to Young operators.....	174
4.2.4 Cancellation rules .....	178
<b>4.3 Young projection and transition operators over <math>V^{\otimes m}</math> for small <math>m</math>: an inspiration for a multiplet adapted basis for <math>\text{API}(\text{SU}(N), V^{\otimes m})</math></b> .....	<b>179</b>
4.3.1 Transition operators for Young projectors over $V^{\otimes m}$ for $m \leq 4$ .....	180
4.3.2 A multiplet adapted basis for $\text{API}(\text{SU}(N), V^{\otimes m})$ .....	181

---

4.3.3	An example: the full algebra over $V^{\otimes 3}$ in a Young projector basis .....	182
<b>4.4</b>	<b>Orthogonal projector bases .....</b>	<b>184</b>
4.4.1	Hermitian projection operators.....	184
4.4.2	A full orthogonal basis for $\text{API}(\text{SU}(N), V^{\otimes m})$ via Clebsch-Gordan operators .....	185
4.4.3	The multiplication table of the algebra of invariants .....	188
<b>4.5</b>	<b>Unitary transition operators for Hermitian Young projectors .....</b>	<b>190</b>
4.5.1	Construction methods of Hermitian Young projection operators.....	191
4.5.2	Unitary transition operators for Hermitian Young projectors .....	193
<b>4.6</b>	<b>Examples .....</b>	<b>198</b>
4.6.1	$\text{API}(\text{SU}(N), V^{\otimes 3})$ — the full algebra of 3 quarks .....	198
4.6.2	$\text{API}(\text{SU}(N), V^{\otimes 4})$ — the full algebra of 4 quarks .....	199
<b>4.7</b>	<b>Chapter conclusion &amp; outlook.....</b>	<b>204</b>
	<b>Appendix to chapter 4 .....</b>	<b>205</b>
<b>4.A</b>	<b>Dimensional zeros.....</b>	<b>205</b>
<b>4.B</b>	<b>Illustrating the action of <math>\rho_{\Theta\Phi}</math> on Hermitian Young projection operators: an example</b>	<b>206</b>
<b>4.C</b>	<b>Consequences of non-Hermiticity: an example.....</b>	<b>208</b>
<b>4.D</b>	<b>Proof of Theorem 4.5 “compact transition operators” .....</b>	<b>209</b>
4.D.1	The significance of the cutting-and-gluing procedure.....	209
4.D.2	Proof of Theorem 4.5 .....	210
<b>5</b>	<b>Singlets: A Construction Algorithm for the Singlets of <math>\text{SU}(N)</math>, and What They Tell Us About Wilson Line Correlators .....</b>	<b>215</b>
<b>5.1</b>	<b>The necessity of a new construction algorithm for singlet projectors of <math>\text{SU}(N)</math> .....</b>	<b>215</b>
5.1.1	Theory of invariants & birdtracks.....	216
5.1.2	The irreducible representations of $\text{SU}(N)$ over $V^{\otimes m}$ : Young tableaux .....	217
5.1.3	The irreducible representations of $\text{SU}(N)$ over $V^{\otimes m} \otimes (V^*)^{\otimes n}$ with standard methods: Littlewood-Richardson tableaux .....	218
5.1.4	Projection operators from Littlewood-Richardson tableaux using the Leibniz formula for determinants.....	223
5.1.4.1	Leibniz rule for determinants .....	223
5.1.4.2	The irreducible representations of $\text{SU}(N)$ over $V \otimes V^*$ from Littlewood-Richardson tableaux .....	225
5.1.4.3	A comment on the dimension of projection operators obtained from LR-tableaux.....	229
<b>5.2</b>	<b>Singlet projection operators .....</b>	<b>229</b>

5.2.1	Singlet projectors over $V^{\otimes k} \otimes (V^*)^{\otimes k}$ : Kronecker $\delta$ 's .....	230
5.2.1.1	A short review of Clebsch-Gordan operators .....	230
5.2.1.2	Projection and transition operators as a basis for the algebra of invariants ....	231
5.2.1.3	Singlet projectors and transition operators over $V^{\otimes k} \otimes (V^*)^{\otimes k}$ from Clebsch-Gordan operators .....	234
5.2.1.4	Constructing singlet projectors over $V^{\otimes k} \otimes (V^*)^{\otimes k}$ from the projector basis $\mathfrak{S}_k$	239
5.2.1.5	Transition operators and an example of the complete singlet algebra over $V^{\otimes k} \otimes (V^*)^{\otimes k}$ .....	242
5.2.1.6	Singlet projectors of $SU(N)$ over $V^{\otimes k}$ in a different basis .....	243
5.2.1.7	Using the primitive invariants $S_k$ or the standard Young projector basis to construct singlet projectors .....	245
5.2.2	Singlet projectors over $V^{\otimes m} \otimes (V^*)^{\otimes n}$ : $\varepsilon$ -tensors .....	246
5.2.2.1	Baryon singlet projector $A_{123}$ .....	246
5.2.2.2	Singlets over $V^{\otimes m} \otimes (V^*)^{\otimes n}$ from singlets over $V^{\otimes k} \otimes (V^*)^{\otimes k}$ .....	248
<b>5.3</b>	<b>Wilson line correlators .....</b>	<b>250</b>
5.3.1	Coincidence limits: a tale of two bases .....	251
5.3.1.1	Symmetrizers and antisymmetrizers .....	252
5.3.1.2	(Anti-) fundamental and adjoint lines .....	254
5.3.2	Wilson line correlators of $3q + 3\bar{q}$ and their coincidence limits .....	255
5.3.2.1	Hermitian Young projector basis .....	255
5.3.2.2	Fierz basis .....	257
5.3.3	Singlets containing Levi-Civita tensors .....	259
<b>Appendix to chapter 5 .....</b>		<b>261</b>
<b>5.A</b>	<b>Simplifying the <math>1q + 1\bar{q}</math> Littlewood-Richardson operators (5.43) .....</b>	<b>261</b>
<b>5.B</b>	<b>Calculations in the birdtrack formalism .....</b>	<b>265</b>
5.B.1	Scalar product & orthogonality .....	265
5.B.2	Orthogonal singlet projection operators .....	266
5.B.3	Dimension of the representations corresponding to singlet projection operators .....	267
5.B.4	Transition operators between singlet projectors .....	267
<b>5.C</b>	<b>Untwisting <math>\varepsilon</math>-tensors without inducing a factor of <math>i^{\pm\phi}</math> .....</b>	<b>270</b>



---

<b>II</b>	<b>Incidental Results Regarding Multiplets of <math>SU(N)</math></b>	<b>271</b>
<b>6</b>	<b>On Mixed Multiplets of <math>SU(N)</math>: Counting and General Results</b>	<b>273</b>
6.1	Introduction .....	273
6.2	The projector basis of the algebra of invariants.....	275
6.2.1	Transition operators from intertwining operators.....	275
6.2.2	The projector basis is orthogonal .....	277
6.3	A counting argument of the number of irreducible representations of $SU(N)$ .....	278
6.4	An explicit formula for the number of irreducible representations of $SU(N)$ over $V^{\otimes m} \otimes (V^*)^{\otimes n}$ .....	282
6.5	Birdtracks and the recursion formula for the number of irreducible representations of $SU(N)$ over $V^{\otimes m} \otimes (V^*)^{\otimes n}$ .....	285
6.6	A graphical bijection between the Young tableaux in $\mathcal{Y}_{m+1}$ and the Littlewood-Richardson tableaux in $\mathcal{Y}_{m,1}$ .....	287
<b>7</b>	<b>The Irreducible Representations of <math>SU(N)</math> over the 4-Particle Fock Spaces: An Example</b>	<b>291</b>
7.1	The projector basis over the 4-particle Fock spaces .....	292
7.2	The $4q$ -algebra.....	294
7.2.1	The projection operators of the $4q$ -algebra.....	294
7.2.2	The full $4q$ -algebra: transition operators .....	295
7.2.3	The $4\bar{q}$ -algebra.....	296
7.3	The $3q + 1\bar{q}$ -algebra .....	296
7.3.1	The projection operators of the $3q + 1\bar{q}$ -algebra .....	296
7.3.2	The full $3q + 1\bar{q}$ -algebra: transition operators .....	299
7.3.3	The $1q + 3\bar{q}$ -algebra .....	301
7.4	The $2q + 2\bar{q}$ -algebra .....	302
7.4.1	The projection operators of the $2q + 2\bar{q}$ -algebra in an (anti-)symmetrizer basis .....	302
7.4.2	The full $2q + 2\bar{q}$ -algebra: transition operators .....	305
7.4.3	An alternative basis for the $2q + 2\bar{q}$ -algebra.....	307
7.5	Spin: the special case $N = 2$ .....	309
7.5.1	$SU(2)$ over 4-particle Fock spaces .....	309
7.5.2	$SU(2)$ over $V^{\otimes 4}$ (dimensional zeros) .....	310
7.5.2.1	The operators of $SU(2)$ : the standard method vs. simplifying projectors .....	311
7.5.3	$SU(2)$ over $V^{\otimes 3} \otimes V^*$ .....	312

7.5.4	SU(2) over $V^{\otimes 2} \otimes (V^*)^{\otimes 2}$ .....	317
7.5.5	SU(2) over $V^{\otimes 2} \otimes (V^*)^{\otimes 2}$ — an alternative basis .....	320
<b>8</b>	<b>On Traces of Primitive Invariants</b> .....	<b>321</b>
8.1	Introduction and overview .....	321
8.2	Traces of primitive invariants in $S_k$ .....	322
8.2.1	Traces of birdtracks .....	322
8.2.2	A graph-theoretic approach to transpositions and permutations .....	323
8.2.3	Traces of permutations and minimum number of transpositions .....	331
8.2.4	Transpositions of inverses and Hermitian conjugates .....	334
8.3	Traces of primitive invariants and products thereof .....	335
8.3.1	Antifundamental factors in the product space .....	335
8.3.2	Traces of primitive invariants in $S_{m,n}$ .....	337
8.3.3	Traces of products of primitive invariants .....	340
<b>III</b>	<b>Conclusion</b> .....	<b>345</b>
<b>9</b>	<b>Towards a Full Mathematical Theory: Outlook</b> .....	<b>347</b>
9.1	A formula for the normalization constants? .....	347
9.2	Coincidence limits of Wilson lines beyond what is already established .....	348
9.3	Irreducible representations of SU( $N$ ) over $V^{\otimes m} \otimes (V^*)^{\otimes n}$ .....	349
9.3.1	Systematic knowledge of dimensionally null operators of SU( $N$ ) over the 4-particle Fock spaces .....	349
9.3.2	Comparing the projector bases $\mathfrak{S}_3$ and $\mathfrak{S}_{2,1}$ .....	352
9.3.2.1	Systematic knowledge of dimensionally null operators of SU( $N$ ) over the 3-particle Fock spaces .....	355
<b>10</b>	<b>Summary and Outlook</b> .....	<b>357</b>
10.1	Thesis summary .....	357
10.2	Outlook .....	360
10.2.1	Wilson line correlators in high energy QCD .....	361
10.2.1.1	Transverse-momentum-dependent parton distributions (TMDs) .....	361
10.2.1.2	Energy loss .....	363
10.2.1.3	Non-global jet observables and the Banfi-Marchesini-Smye equation .....	364
10.2.2	Parametrization of Wilson line correlators .....	364

10.2.2.1 Beyond the Gaussian truncation: results at third order .....	365
10.2.2.2 Generalized structure constants .....	366
10.2.3 Changing bases for singlet projection operators .....	367
10.2.4 Multiplets and physics .....	368
<b>10.3 Concluding remarks .....</b>	<b>368</b>
 <b>Bibliography .....</b>	 <b>369</b>



# List of Figures

1.1	Schematic drawing of spacetime for interactions with a high rapidity separation in lightcone coordinates .....	4
1.2	Deep inelastic scattering (DIS) Feynman diagram with relevant kinematic variables .....	6
1.3	Phase space diagram of rapidity $Y = \ln \frac{1}{x_{\text{Bj}}}$ versus transverse resolution $\ln Q^2$ .....	8
1.4	Feynman diagrams for the sub-process $q \rightarrow gqg$ .....	17
1.5	Schematic diagram depicting the idea behind the JIMWLK renormalization group equation ...	26
1.6	Explanation of diagrams depicting the amplitude of a singlet over $V^{\otimes m} \otimes (V^*)^{\otimes n}$ scattering off a target at fixed resolution and small $x_{\text{Bj}}$ .....	36
1.7	Explanation of diagrams depicting the amplitude of a $q\bar{q}$ -singlet scattering off a target at fixed resolution and small $x_{\text{Bj}}$ .....	39
1.8	Diagrammatic notation for the sum over vertex insertions $t^a$ .....	48
1.9	Cancellations for the $\langle \text{in}   \text{in} \rangle$ -states in the cross section .....	51
1.10	Cancellations for the $\langle \text{out}   \text{out} \rangle$ -states in the cross section .....	52
1.11	Cancellations for the $\langle \text{in}   \text{out} \rangle$ -states in the cross section .....	52
1.12	Path of a Wilson line partitioned into infinitely many pieces .....	76
2.1	General structure of an operator $O$ satisfying all conditions of the propagation rule Theorem 2.2	106
2.2	Shortening and exposing the Hermiticity of a KS operator .....	112
3.1	Ancestry tree of the Hermitian Young projection operators up to $V^{\otimes 4}$ .....	141
3.2	Size comparison of a particular KS operator to its MOLD equivalent .....	146
3.3	Similarities and differences between a column-ordered Young tableau and its parent tableau ...	159
4.1	Branching tree for the Young tableaux up to $V^{\otimes 4}$ .....	173
4.2	Ancestry tree of the Young projection operators up to $V^{\otimes 4}$ together with their transition operators .....	202
4.3	Ancestry tree of the Hermitian Young projection operators up to $V^{\otimes 4}$ together with their unitary transition operators .....	203

5.1	Branching tree for the Littlewood-Richardson tableaux over $V^{\otimes 2} \otimes (V^*)^{\otimes 2}$ .....	222
5.2	Structure of a general singlet projection operator over $V^{\otimes m} \otimes (V^*)^{\otimes n}$ .....	249
5.3	Relating a general singlet projection operator over $V^{\otimes m} \otimes (V^*)^{\otimes n}$ to a particular singlet over $V^{\otimes \alpha} \otimes (V^*)^{\otimes \alpha}$ .....	249
6.1	Exemplifying the recursion formula for the number of irreducible representations of $SU(N)$ over a 5-particle product space .....	286
7.1	The Young tableaux with 4 boxes and the corresponding Young diagrams .....	294
7.2	Branching tree for the Littlewood-Richardson tableaux over $V^{\otimes 3} \otimes V^*$ .....	300

# Prologue



Symmetries govern the laws of nature. Understanding such symmetries leads to a deeper understanding of nature. This was already intuitively clear to early researchers: In the 6<sup>th</sup> century BC, the Greek philosopher Anaximander conceived a model of the solar system in which each of the planets and the sun itself moved in perfect circles — the epitome of symmetry — around the earth [5].

As this model could not account for certain observed phenomena (such as the retrograde motion or the varying brightness of certain planets in the night sky), Ptolemy in ca. 140 AD refined this model by adding epicycles, which are smaller (perfect) circles along the circular orbit along which the planets and the sun supposedly travel around the earth [6]. The major flaw with this model of course was that it was *geocentric*, i.e. the earth was placed in the centre of the solar system. In 1543, Copernicus [7] revised this model and placed the sun at the centre of the solar system — a *heliocentric* model —, with the earth and all other planets orbiting it in perfect circles. Today we know that the planet’s orbits are not perfectly circular but in fact slightly elliptic [6]. Copernicus’ model, despite being obsessively insistent upon symmetry, was nonetheless surprisingly accurate.

However, the important role of symmetry in physics is not just wishful thinking imposed by the human mind, but was quantified by Emmy Noether in 1918 [8, 9] when she formulated a theorem (now referred to as *Noether’s Theorem*) that states that every continuous symmetry obeyed by a physics theory gives rise to a conservation law. This theorem was made possible by the formulation of *group theory*, which is a branch of abstract algebra that goes back to the 19<sup>th</sup> century, *c.f.*, for example, [10]. The term “group” (coined by Camille Jordan [10]) refers to an algebraic construct that gives precise mathematical meaning to what is in physics referred to as symmetry.

Thus began a journey of the development of group theory and physics, the two ever crossing paths, influencing each other. There are far too many instances in which physics research has had a breakthrough due to symmetry considerations to be all listed here. However, the following milestone is worth mentioning:

In the early 1960’s, Murray Gell-Mann [11] and Georg Zweig [12, 13] proposed a theory of “wee particles” (a term coined by Feynman [14], now known as quarks), which make up many of the then known particles, such as protons and neutrons. Purely from symmetry considerations governing the laws of these new fundamental particles, Gell-Mann and Yuval Ne’emam [15] independently predicted the existence of a new particle  $\Omega^-$ , which had not yet been discovered. Shortly after its theoretical prediction, the existence of the  $\Omega^-$  was experimentally confirmed in 1964 [16, 17].

Today, the important role of symmetries in physics has found axiomatic acceptance. And while the idea to study the underlying symmetry of a theory in order to advance the theory itself is by no means new, there are still a lot of questions pertaining to such symmetries that have yet to be answered. In this thesis we will focus on the symmetry aspects in the context of high energy quantum chromodynamics (QCD). In particular, we find that the objects that most naturally describe interactions in a particular kinematic limit of interest here are Wilson lines, which themselves are elements of the special unitary group  $SU(N)$ . Therefore, keeping in mind that we ultimately strive to apply our results in a QCD context, this thesis focuses on the study of the symmetry-group  $SU(N)$ .



# Chapter 1

## High Energy Physics and Wilson Line Correlators

*This chapter sets the background for this thesis. The most important aspects of high energy quantum chromodynamics (QCD) in the small- $x_{Bj}$  limit are discussed. We begin with an overview of QCD interactions at high energies, working towards the kinematic limit in which Bjorken- $x$  ( $x_{Bj}$ ) is small. In this limit, one may perform the eikonal approximation, giving rise to Wilson lines. Thereafter, we briefly describe the color glass condensate, which is a highly dense gluonic matter that appears in the small- $x_{Bj}$  limit of QCD. The McLerran–Venugopalan model attempts to describe the gluon distribution function in the CGC, but it was found that the peculiar dynamics within the CGC require a renormalization group (RG) formulation of the gluon distribution instead. The relevant RG equation is the Jalilian-Marian–Iancu–McLerran–Weigert–Leonidov–Kovner (JIMWLK) equation. We give a derivation of this equation at leading order, making use of modern diagrammatic notation. For practical purposes, a parametrization of the JIMWLK equation is required. This parametrization, however, presupposes knowledge about a subclass of projection operators of the special unitary group, which are not as well understood as the literature might lead us to believe. This motivates the research presented in the remainder of this thesis.*

### 1.1 QCD interactions at high energies — in a nutshell

#### 1.1.1 Scattering at high energies

In a typical scattering experiment, one spatial direction is singled out, namely the direction along which the collision takes place (i.e. the beam axis); we will take the beam direction to be the  $x^3$ -axis. It is convenient in such a setting to work in light cone coordinates,

$$x^\pm := \frac{1}{\sqrt{2}}(x^0 \pm x^3) \quad \text{and} \quad \mathbf{x} := (x^1, x^2)^t, \quad (1.1)$$

where  $x^\pm$  lie on the light cone (one of these can be interpreted as “time”), and the vector  $\mathbf{x}$  lies in the plane transverse to the beam axis (*c.f.* Figure 1.1). The two objects involved in the collision are referred to as the *projectile* and the *target*. If the energies involved in such a collision are very large, their worldlines approach

the  $x^-$ - and  $x^+$ -axes respectively. Thus, the target and the projectile experience a large rapidity separation, as is illustrated in Figure 1.1.

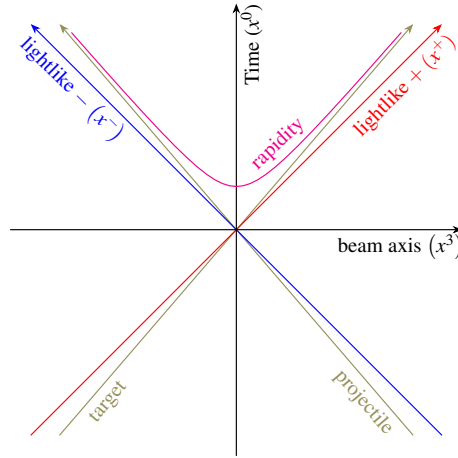


Figure 1.1: The rapidity separation between the projectile and the target is measured as the hyperbolic angle between the respective worldlines in the centre-of-mass frame. As the participants of the collision approach the light cone, their rapidity separation increases. The  $x^3$ -direction is normal to the transverse plane mapped by  $\mathbf{x}$ . [18]

As an example, consider the projectile to be a dilute object (for example an electron) travelling in the direction  $x^-$ . The target is taken to be a more dense object, which, here, is drawn as a superposition of *color*<sup>1</sup> charged partons<sup>2</sup> travelling along the  $x^+$ -direction:



Consider now the rest frame of the projectile. As the rapidity separation between target and projectile increases, the target becomes more and more Lorentz contracted until it has nearly  $\delta$  function support in the  $x^-$ -direction. On the other hand, time dilation almost purges the  $x^+$ -dependence of the color field, making it essentially constant in  $x^+$ . Naively speaking, the target  $b$  is an infinitely flat disc with very large diameter in which the individual color charges are frozen in place, approaching the projectile face-on. These considerations inspire the following component-wise definition of  $b$ :

$$b^i = b^- = 0, \quad b^+ = \beta(\mathbf{x})\delta(x^-), \quad (1.3)$$

where  $\beta(\mathbf{x})$  is a distribution of the color charges in the target in the transverse plane [18]. Thus, a more

<sup>1</sup>The spelling of this charge of partons (color) follows that used by Fritzsche and Gell-Mann [19].

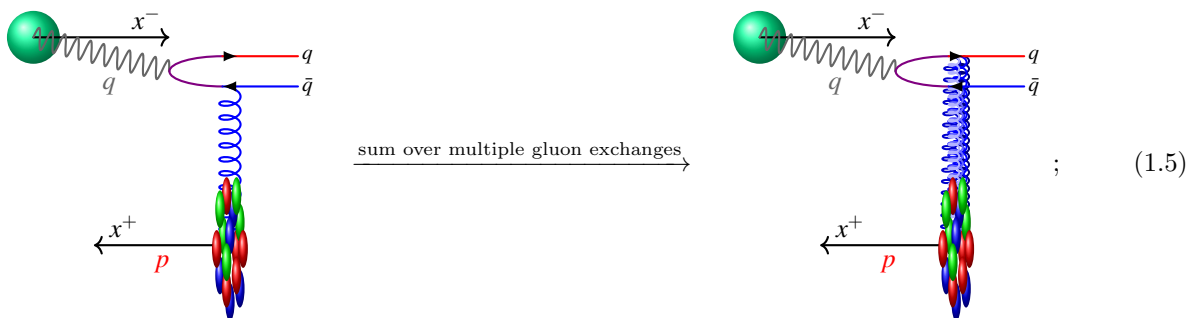
<sup>2</sup>An example of such a target could be a large nucleus, but it can be argued that in certain kinematic limits even a hadron can be viewed as a dense gluonic target [20].

accurate picture of this scattering experiment is



The exact form of the distribution function  $\beta(\mathbf{x})$  depends on the kinematics of the particular collision. In the small- $x_{Bj}$  regime at fixed resolution (this is also referred to as the Regge-Gribov limit, see, for example, [21]), the projectile will perceive the target as a superposition of color charges of fixed size. Due to the high energy in the collision, the target will be saturated with gluons, causing it to be modelled as a coherent color field in the color glass condensate framework [21–23]; this is discussed in more detail in section 1.3.

Due to the  $\delta$ -function-like support of the target in the projectile’s rest frame, the interaction will be instantaneous and eikonal of nature. In other words, the interaction occurs solely via a rotation in color space and is mathematically described by Wilson lines. Such an interaction typically takes place by the projectile emitting a photon, which splits into a globally color neutral configuration — a *global color singlet* — of color carrying objects, for example a  $q\bar{q}$ -dipole. This singlet interacts with the target via the exchange of gluons, where diagrams in which  $n$  gluon exchanges take place are of the order  $(\alpha_s \ln \frac{1}{x_{Bj}})^n$  [21]. In the Regge-Gribov limit, where we take  $x_{Bj}$  to be small, contributions with a large number of gluon exchanges cannot be neglected, and a resummation of diagrams has to be carried out,



this resummation of diagrams gives rise to Wilson lines (*c.f.* section 1.2.3).

The Wilson lines describing the eikonal interaction are elements of the gauge group  $SU(N)$  of QCD (*c.f.* section 1.2.4), where  $N$  is taken to be  $N_c$  (the number of colors), and thus impart additional (group) structure on the interaction that would otherwise not be present. It is this added structure that warrants the study of the gauge group  $SU(N)$ . In particular, the structures entering a cross section have to be globally singlet with respect to the gauge group  $SU(N)$  to adhere to color confinement. The main part of this thesis is dedicated to the study of  $SU(N)$  with a focus on projection operators corresponding to the irreducible representations of  $SU(N)$  over a product space  $V^{\otimes m} \otimes (V^*)^{\otimes n}$ . One of our main results is an algorithm giving a construction principle for *all* projection operators corresponding to the *singlet representations* of  $SU(N)$  over  $V^{\otimes m} \otimes (V^*)^{\otimes n}$ .

### 1.1.2 Interactions in different kinematic limits

In this section, we use deep inelastic scattering (DIS) as a case study to discuss the kinematics we are ultimately interested in. Our review summarizes the arguments given in [18, 21].

In a DIS experiment, a dilute projectile (for example, an electron) probes a dense target at very high energies. The “deep inelasticity” property refers to the fact that (to overwhelming probability) the target is shattered after the collision. This nomenclature parallels that of classical mechanics where inelastic collisions allow for energy loss that may manifest in one of the participants breaking after the collision.

Suppose the interaction between the projectile and the target occurs via the exchange of a photon in the  $t$ -channel. The relevant kinematic variables are summarized in Figure 1.2 and eqns. (1.6).

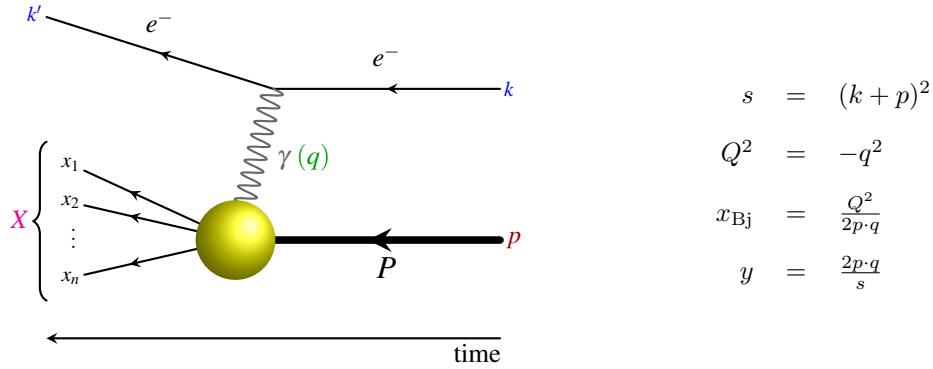


Figure 1.2: In this DIS event (time is read from right to left), an incoming electron  $e^-$  with momentum  $k$  emits a photon  $\gamma$  (projectile, probe) with momentum  $q$ ; after this emission, the electron has momentum  $k'$ . The photon  $\gamma$  then interacts with an incoming proton  $P$  (target), which carries a momentum  $p$ ; this interaction is indicated by the yellow blob. The nature of this interaction depends on the particular kinematic regime. The target is then shattered into particles with individual momenta  $x_i$ , which have a total momentum  $X$ . We choose to draw the time axis in this way for the different parts of the Feynman diagram to be in 1-to-1 correspondence with the terms in the associated equation. The quantities listed on the right hand side are the Lorentz invariants of this interaction. [18, 21]

The relevant kinematic variables are [21] the total energy of the interaction

$$s := (p + k)^2, \quad \text{where } p \text{ and } k \text{ are the 4-momenta of the target and projectile respectively,} \quad (1.6a)$$

the virtuality of the photon

$$Q^2 := -q^2 > 0, \quad \text{where } q \text{ is the spacelike momentum of the photon,} \quad (1.6b)$$

the momentum fraction Bjorken- $x$  ( $x_{\text{Bj}}$ )

$$x_{\text{Bj}} := \frac{Q^2}{2p \cdot q}, \quad (1.6c)$$

and the inelasticity of the collision

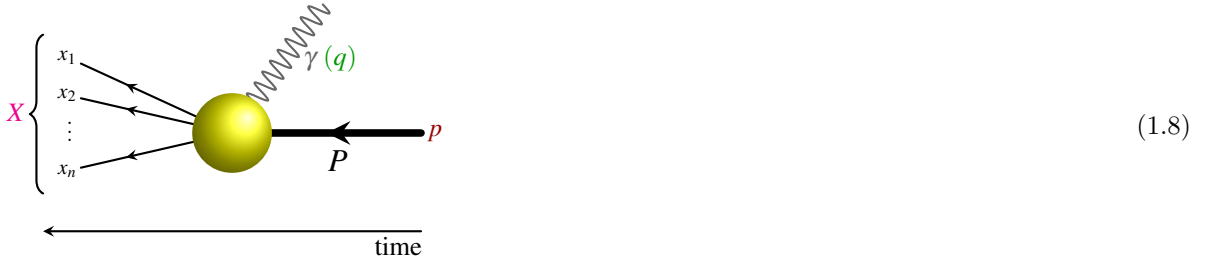
$$y := \frac{2p \cdot q}{s} . \quad (1.6d)$$

Since energy-momentum is conserved at each vertex, we find that the outgoing momentum of the electron  $k'$  and the total momentum  $X$  of the shattered fragments of the former proton can be expressed in terms of the measurable quantities  $k$ ,  $q$  and  $p$ ,

$$k' = k - q \quad (1.7a)$$

$$X = k + p - k' = p + q . \quad (1.7b)$$

From now on, we will focus on the sub-diagram



of Figure 1.2. An analysis of the momentum  $X$  in various limits determines the nature of the interaction (indicated by the yellow blob in (1.8)) between the photon and the target. Let us expand  $X^2$  as

$$X^2 = (p + q)^2 = p^2 + 2p \cdot q + q^2 . \quad (1.9)$$

Since the proton must be on-shell, its 4-momentum squared will give the mass of the proton,  $p^2 = m_p^2$ . Factoring the quantity  $2p \cdot q$  out of each term in (1.9) and using the definition of  $x_{\text{Bj}}$  as given in Figure 1.2, we can rewrite  $X^2$  as

$$X^2 = 2p \cdot q \left( \frac{m_p^2}{2p \cdot q} + 1 - x_{\text{Bj}} \right) . \quad (1.10)$$

Different limiting cases determine which term in (1.10) gives the dominant contribution to  $X^2$ . The various scenarios populate different regions in the phase space depicted in Figure 1.3. We discuss the different kinematic limits in sections 1.1.2.1 to 1.1.2.3. For this thesis, the Regge-Gribov limit discussed in section 1.1.2.3 will be of most interest, which is why this section goes into more detail than the previous sections, 1.1.2.1 and 1.1.2.2.

### 1.1.2.1 Proton mass dominates: energies below $\Lambda_{\text{QCD}}$

If the bulk of the contribution to  $X^2$  comes from the term  $\frac{m_p^2}{2p \cdot q}$ , then we must have that

$$x_{\text{Bj}} = \frac{Q^2}{2p \cdot q} \ll \frac{m_p^2}{2p \cdot q} \quad \implies \quad Q^2 \ll m_p^2 . \quad (1.11)$$

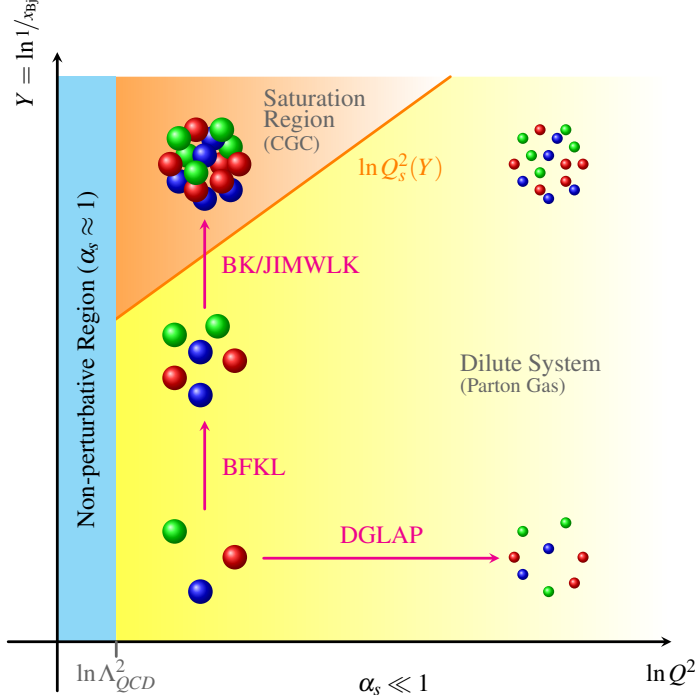


Figure 1.3: A schematic depiction of the phase space as a function of the transverse resolution  $Q^2$  and the rapidity  $Y = \ln \frac{1}{x_{\text{Bj}}}$ . As the total energy increases (via increasing either  $Q^2$  or  $Y$ ), more and more particles are produced. Since the number of particles grows linearly with  $Y$  but only logarithmically with  $Q^2$ , the system remains dilute for large enough values of  $Q^2$  (even for large  $Y$ ), but becomes a saturated medium — the color glass condensate (CGC) — for large  $Y$  at fixed  $Q^2$ . In this graphic, we marked the boundary between the parton gas and the CGC (the curve  $\ln Q_s^2(Y)$ , where  $Q_s$  is the *saturation scale*) by a straight line for the sake of simplicity, but actually it should be a parabola with ever increasing slope. In particular, there will be a value of  $Q^2$  beyond which the CGC cannot be produced, irrespective of the value of  $Y$ . [18, 21]

Since the proton mass  $m_p$  is approximately  $938 \text{ MeV}/c^2$  [24], eq. (1.11) implies that  $Q^2$  must be of the order  $10^1 \text{ MeV}$  to be negligible compared to  $m_p$ . However, this corresponds to the region  $Q^2 < \Lambda_{\text{QCD}}^2$  since  $\Lambda_{\text{QCD}}$  is of order of  $200 \text{ MeV}$  ([25] quotes  $\Lambda_{\text{QCD}} \approx 200 \text{ MeV}$ , while [26] evaluates  $\Lambda_{\text{QCD}} \approx 250 \text{ MeV}$  in the  $\overline{\text{MS}}$ -scheme). In this region the coupling constant  $\alpha_s$  becomes large ( $\mathcal{O}(\alpha_s) \approx 1$ ), which moves us outside the region of applicability of perturbation theory [27].

### 1.1.2.2 Photon energy dominates: the Bjorken limit

In the Bjorken limit, we consider a high energy event in which we assume that  $Q^2$  is the most dominant contribution to  $X^2$ , in other words

$$Q^2, s \rightarrow \infty, \quad \text{while } x_{\text{Bj}} \text{ remains fixed.} \quad (1.12)$$

Since the photon momentum  $q$  is spacelike ( $q^2 < 0$ ), the quantity  $Q^2 := -q^2 > 0$  sets the transverse resolution of the target [18].<sup>3</sup> Hence, the limit (1.12) describes a situation in which the probe perceives the target as a

<sup>3</sup>Intuitively, this can be understood as follows: If the photon probing the target has low momentum, it is likely to be scattered off the target. Thus, to the photon, the nucleus appears to be made of “large” constituents. On the other hand, if the photon momentum is large, it will pierce through the target as if there was no spacial obstacle at all. In this case, the target appears

dilute collection of color charges; even as the total energy of the collision is increased and thus more and more partons (gluons) are produced, the system remains dilute due to the concurrent increase in resolution. Thus, the photon is able to resolve the individual components of the target and hence experiences a hard interaction with an individual parton. It should be noted that the interaction between the constituents within the target (during the time of the interaction with the probe) is suppressed due to time-dilation [21]. Schematically, therefore, the yellow blob of eq. (1.8) (resp. Figure 1.2) becomes



where, here, the interaction occurs between the photon and the parton  $q_1$ ; the remaining partons act as spectators in the interaction.

### 1.1.2.3 Momentum transfer dominates: the Regge-Gribov limit

Lastly, we consider the case where  $p \cdot q$  is the dominant contribution to  $X^2$  in (1.10). For this to be the case, we in particular require that Bjorken- $x$  is small,  $x_{Bj} \ll 1$ . This is achieved in a limit in which

$$x_{Bj} \rightarrow 0, s \rightarrow \infty, \quad \text{while } Q^2 \text{ remains fixed}, \quad (1.14)$$

which is referred to as the Regge-Gribov limit [21]. In this limit  $X^2 \approx 2p \cdot q$  since  $p \cdot q \gg Q^2, m_p^2$ , which allows us to write

$$x_{Bj} \approx \frac{Q^2}{X^2}. \quad (1.15)$$

Thus, for small Bjorken- $x$ , we may interpret  $x_{Bj}$  as the fractional momentum transfer from the probe to the target in the collision.

As  $x_{Bj}$  decreases (and  $s$  increases), the target becomes more and more populated with color charges. However, since the transverse resolution  $Q^2$  remains fixed, and since we know that the total size of the target remains essentially unchanged even if the energy increases,<sup>4</sup> these color charges appear to overlap in the view of the probe. Once this happens, recombination effects start occurring, until eventually the recombination of charges balances the production of new gluons, causing the medium to saturate; this saturation phenomenon was confirmed by HERA data [29, 30]. Thus, the Regge-Gribov limit moves us into the top left corner of the phase space diagram in Figure 1.3 — the region of the color glass condensate (CGC) [18, 21].

In this region of phase space, the probe encounters not a dilute system of partons, but a dense color field. The probe therefore does not interact with individual color charges within the nucleons, but rather couples to

---

to the photon as a dilute system of “small” constituents through which a path could easily be found. Readers should be careful to not take this picture too literally: whilst the *apparent* size of the partons in the target nucleus does indeed change, these partons are actually point-like particles irrespective of the value of  $Q^2$ .

<sup>4</sup>This follows from the fact that the total (inelastic) cross section of, for example, a  $pp$ -collision hardly changes as the energy is increased [28, Figure 3].

the entire color field [18, 21] — we move from individual degrees of freedom to collective degrees of freedom. In addition, due to the high Lorentz contraction of the target, the only effect that the probe can experience from the interaction is a rotation in color space. That is to say that the interaction is *eikonal* and thus described via Wilson lines (section 1.2). Since the photon itself is color neutral, it first has to split into a color neutral combination of color carrying partons (a *color singlet*) before the interaction can take place [27]. For example, if the photon splits into a  $q\bar{q}$ -pair, the yellow blob in diagram (1.8) (resp. Figure 1.2) looks like



We remind the reader that even though the interaction here is indicated by the exchange of one gluon between the  $q\bar{q}$ -dipole and the target (mainly in order not to clutter the graphic), the eikonal interaction is actually a sum of contributions where multiple soft gluons are exchanged (*c.f.* eq. (1.5)).

A remark with regards to the dependence of picture (1.16) on the reference frame is in order: So far, we have assumed that the target has a  $\delta$  function support, thus localizing the interaction. While this is indeed the case in the rest frame of the projectile, or in the infinite momentum frame, the target certainly extends along  $x^-$  in the target's rest frame. However, as is pointed out in [18], the ratio between the thickness of the target,<sup>5</sup> and the distance between the photon splitting into a color singlet and the interaction, is of the order  $\frac{1}{x_{Bj}}$  (which is huge in the limit  $x_{Bj} \rightarrow 0$ ) irrespective of the reference frame. Furthermore, due to the high longitudinal momentum of the probe, it does not experience a deflection in the transverse direction as a result of the interaction. What becomes clear in the target rest frame, however, is that the probe interacts with a multitude of scattering centres, which causes several gluons to be exchanged in the interaction [18] (*c.f.* eq. (1.5)).

## 1.2 Wilson lines at high energies

Up to this point, we have casually claimed that interactions whose sole effect is a rotation in color space are described by Wilson lines. We now wish to make this more precise. We first give a brief summary of the origin of Wilson lines in non-abelian gauge theories.

Thereafter, we wish to give an interpretation of the concept of Wilson lines. We first approach the topic from a geometric standpoint and briefly summarize the derivation of Wilson lines from the parallel transport equation (section 1.2.2).

We then shift our focus to a physics interpretation, which will give validity to our original claim that Wilson lines describe the interaction between a projectile and a target in the Regge-Gribov limit. We first give an

<sup>5</sup>If we consider the target to be a nucleus, then its  $x^-$ -support goes as  $A^{1/3}$ , where  $A$  is its nuclear number [18].



outline of the derivation of the the Feynman rules of Wilson lines in section 1.2.3.1. This will allow one to view a Wilson line as a quark emitting/absorbing a multitude of gluons, where the gluons are summed over. We then present the “reverse argument” where we start from a Feynman diagram describing a quark emitting a number of gluons. Through the *eikonal approximation* (which essentially says that the emitted gluons are soft), a resummation of diagrams with a varying number of gluon exchanges once again yields a Wilson line, as shown in section 1.2.3.2.

Lastly, we describe several properties of Wilson lines in section 1.2.4. This will allow us to conclude that Wilson lines are elements of the special unitary group  $SU(N)$ . Even though we keep this section brief, the conclusion is key for the main body of this thesis, which analyzes Wilson line correlators from a group theoretic viewpoint.

## 1.2.1 Gauge theories

### 1.2.1.1 A brief overview of gauge theories

Nature obeys a multitude of symmetries, be it rotational, translational or a symmetry of a more abstract kind. These symmetries are mathematically expressed as groups, that is, in order for a field theory to faithfully capture a particular natural phenomenon, it has to be constrained by the group describing the associated symmetry. Such theories are called *gauge theories* and the corresponding groups are referred to as *gauge groups* [31–34].

Consider the Dirac-Lagrangian for a particular fermion field  $\psi$  living in the Fock space  $V$  [25]

$$\mathcal{L}_{\text{Dirac}} = -i\bar{\psi}(x)\not{\partial}\psi(x) + m\bar{\psi}(x)\psi(x) , \quad (1.17)$$

where we used Feynman slash notation,

$$\not{\partial} := \gamma^\mu \partial_\mu \quad (1.18)$$

and  $\gamma^\mu$  are the Dirac matrices [35]. Suppose that the theory described by  $\mathcal{L}_{\text{Dirac}}$  obeys a symmetry encapsulated by a group  $G$ , that is  $\mathcal{L}_{\text{Dirac}}$  stays invariant under the transformation

$$\psi(x) \longrightarrow \mathbf{g}\psi(x) \quad \text{and} \quad \bar{\psi}(x) \longrightarrow \bar{\psi}(x)\mathbf{g}^{-1} \quad (1.19)$$

for every group element  $\mathbf{g} \in G$ . The central idea of gauge symmetry is to make the symmetry *local*, thus promoting the group parameters to functions of spacetime,  $\mathbf{g} \rightarrow \mathbf{g}(x)$ . Hence, for  $G$  to be the gauge group of a certain theory described by  $\mathcal{L}_{\text{Dirac}}$  (for field theories corresponding to a physical observable  $G$  is a semi-simple Lie group [36]), a transformation with the group element  $\mathbf{g}(x) \in G$ ,

$$\psi(x) \longrightarrow \mathbf{g}(x)\psi(x) \quad \text{and} \quad \bar{\psi}(x) \longrightarrow \bar{\psi}(x)[\mathbf{g}(x)]^{-1} , \quad (1.20)$$

has to leave the Lagrangian (1.17) *unchanged*. This statement is certainly always true for the second term of  $\mathcal{L}_{\text{Dirac}}$ ,

$$m\bar{\psi}(x)\psi(x) \longrightarrow m\bar{\psi}(x)\underbrace{[\mathbf{g}(x)]^{-1}\mathbf{g}(x)}_{=1}\psi(x) = m\bar{\psi}(x)\psi(x) , \quad (1.21a)$$

but with the first term we run into trouble since

$$i\bar{\psi}(x)\not{\partial}\psi(x) \longrightarrow i\bar{\psi}(x)[\mathbf{g}(x)]^{-1}\not{\partial}(\mathbf{g}(x)\psi(x)) \neq i\bar{\psi}(x)\not{\partial}\psi(x) ; \quad (1.21b)$$

the physical symmetry of the theory is no longer captured by the Lagrangian  $\mathcal{L}_{\text{Dirac}}$ . To resolve this problem we must replace the partial derivative  $\partial_\mu$  with a covariant derivative  $D_\mu$  [31–34],

$$D_\mu := \partial_\mu - igA_\mu(x) , \quad A_\mu(x) := A_\mu^a(x)t^a \text{ is called the } \textit{gauge field} , \quad (1.22)$$

the  $t^a$  are the generators of the gauge group, and  $g$  is the coupling constant. If we act this derivative on a vector  $\psi(x)$  undergoing the gauge transformation (1.20),

$$D_\mu\psi(x) \xrightarrow{\text{gauge transformation (1.20)}} D_\mu(\mathbf{g}(x)\psi(x)) , \quad (1.23)$$

we find (after simple algebraic manipulations) that  $D_\mu\psi(x)$  transforms as

$$D_\mu\psi(x) \longrightarrow D_\mu(\mathbf{g}(x)\psi(x)) = \mathbf{g}(x)D_\mu\psi(x) . \quad (1.24)$$

This transformation law of the covariant derivative indeed renders the term  $-i\bar{\psi}(x)\not{D}\psi(x)$  invariant under a gauge transformation,

$$-i\bar{\psi}(x)\not{D}\psi(x) \xrightarrow{\text{gauge transformation (1.20)}} -i\bar{\psi}(x)\underbrace{[\mathbf{g}(x)]^{-1}\mathbf{g}(x)}_{=\mathbb{1}}\not{D}\psi(x) = -i\bar{\psi}(x)\not{D}\psi(x) . \quad (1.25)$$

In order to be fully prepared for the exposition of section 1.2.2, we will tie all the quantities discussed in the present section into the language of differential geometry [37] (for a comprehensive introduction to differential geometry, see [38] and other textbooks): The Minkowski space  $\mathbb{M}^4$  describing 4-dimensional spacetime (one time direction  $x^0$  and three spatial directions  $x^1, x^2, x^3$ ) acts as a base manifold for the vector bundle  $V\mathbb{M}^4$ , which itself is a manifold. Since for each  $x \in \mathbb{M}^4$  the vector  $\psi(x)$  lies in the vector space  $V_x\mathbb{M}^4$ , which is a fibre in the bundle  $V\mathbb{M}^4$ , the fermion field  $\psi$  is a section through this bundle. The gauge field  $A_\mu(x)$  takes value in the Lie algebra of the gauge group and allows us to define the connection  $D_\mu$  on the vector bundle  $V\mathbb{M}^4$ .

### 1.2.1.2 Non-abelian gauge theories

In order to incorporate the interaction of the gauge field  $A_\mu(x)$  into the Lagrangian, one adds a term  $\frac{1}{4}F^{\mu\nu}F_{\mu\nu}$  [31–34],

$$\mathcal{L}_{\text{gauge}} = -i\bar{\psi}(x)\not{D}\psi(x) + m\bar{\psi}(x)\psi(x) + \frac{1}{2}\text{tr}(F^{\mu\nu}F_{\mu\nu}) , \quad (1.26)$$

where  $F^{\mu\nu}$  is referred to as the *field strength tensor*. The exact form of this tensor will depend on the particular field theory. Most quantum field theories (for example, quantum chromodynamics (QCD) or quantum electrodynamics (QED)) fall into the class of Yang-Mills theories [39], which describe  $F^{\mu\nu}$  as

$$F^{\mu\nu} = \partial^\mu A^\nu - \partial^\nu A^\mu + [A^\mu, A^\nu] . \quad (1.27)$$


If the gauge group (and hence the Lie algebra) is abelian, the last term in (1.27) vanishes, reducing  $F^{\mu\nu}$  to

$$F^{\mu\nu} = \partial^\mu A^\nu - \partial^\nu A^\mu . \quad (1.28)$$

An example of an abelian gauge theory is QED, which has gauge group  $U(1)$ . On the other hand, for a non-abelian gauge group, all terms in (1.27) are nonzero, and the Lagrangian will include a term proportional to  $A^2$ . This term gives rise to vertices where the gauge field couples to itself. In other words, non-abelian gauge theories allow for vertices of the type



$$\text{or} \quad (1.29)$$

where  represents a gauge boson, while abelian gauge theories do not (see, e.g., [27] for a textbook exposition). The gauge group of QCD is  $SU(3)$ , making it a non-abelian gauge theory. Thus, the gauge bosons of QCD (the gluons) can self-interact through vertices such as (1.29).

This potential of gauge bosons to self-interact in a non-abelian gauge theory brings forth various challenges: In the context of JIMWLK, we wish to determine the energy dependence of an observable interacting eikonally with a gluon field  $A$ . Since gluons require very little energy to be produced, by virtue of their vanishing mass, space is filled with gluons — we call this the background field  $b$  (this is the same  $b$  as given in eq. (1.3) to describe the target of the interaction). In a general calculation, one has to take an average over various configurations of the background field  $b$  since the exact configuration of color charges cannot be known. If there is no additional energy added to the system, then  $A = b$ . If, however, we increase the energy deposited in the interaction (equivalently we increase the rapidity  $Y = \ln \frac{1}{x_{Bj}}$ ), one necessarily generates fluctuations  $\alpha$  to the background field in the form of creating additional gluons,

$$A = b \quad \xrightarrow{\text{increase energy}} \quad A = b + \alpha . \quad (1.30)$$

The nonlinearity in such an interaction comes from the fact that the additional gluons  $\alpha$  can themselves interact with the background field.

## 1.2.2 Geometric interpretation of a Wilson line: parallel transport

Consider once again the mass term in the Lagrangian (1.26),

$$m\bar{\psi}(x)\psi(x) . \quad (1.31)$$

For each  $x \in \mathbb{M}^4$ , the object  $\bar{\psi}(x)$  is an element of the dual vector space  $V_x^*\mathbb{M}^4$  acting on  $\psi(x) \in V_x\mathbb{M}^4$ , where  $V_x\mathbb{M}^4$  is a particular fibre in the bundle  $V\mathbb{M}^4$  at the point  $x$ . Suppose there exists a path  $\gamma$  between two points  $y$  and  $x$  ( $x, y \in \mathbb{M}^4$ ), which lies entirely on the manifold  $\mathbb{M}^4$ . One could conceivably move the vector  $\psi(y) \in V_y\mathbb{M}^4$  along this path by means of some transportation device  $U_{[\gamma, x, y]}$  to obtain the vector  $\psi(x)$ ,

$$\psi(x) = U_{[\gamma, x, y]}\psi(y) . \quad (1.32)$$

However, for  $U_{[\gamma,x,y]}\psi(y)$  to yield the vector  $\psi(x)$  and not some other element of the tangent space  $V_x\mathbb{M}^4$ ,  $U_{[x,y]}$  has to satisfy the parallel transport equation [36, 37, 40]

$$\frac{d}{d\tau}U_{[\gamma,x,y]} = -ig \left( \frac{d\gamma^\mu}{d\tau} A_\mu(\gamma) \right) U_{[\gamma,x,y]}, \quad (1.33)$$

where  $\tau$  parametrizes the path  $\gamma$ . One may solve eq. (1.33) for  $U_{[\gamma,x,y]}$  to obtain the following path-ordered exponential:

$$U_{[\gamma,x,y]} = \text{Pexp} \left\{ -ig \int_y^x d\gamma^\mu A_\mu(\gamma) \right\}; \quad (1.34)$$

the object  $U_{[\gamma,x,y]}$  defined in eq. (1.34) is referred to as a *Wilson line*. Thus, a Wilson line describes an operator that transforms (transports) a particular field component  $\psi(x)$  (equivalently,  $U_{[\gamma,x,y]}^\dagger$  transports the dual  $\bar{\psi}(x)$ ) along the manifold  $\mathbb{M}$  into  $\psi(y)$  (resp.  $\bar{\psi}(y)$ ).

### 1.2.3 Physics interpretation of a Wilson line

#### 1.2.3.1 Feynman rules of Wilson lines

Let us now establish a physical picture for Wilson lines by discussing their Feynman rules. These may be derived by pursuing the steps laid out below, which are summarized from [37].

For simplicity, we consider  $\gamma$  to be a straight line path parametrized by  $\tau$ ,  $\gamma^\mu = \eta^\mu \tau$ , where  $\eta^\mu$  gives the direction of the straight line, and  $\tau \in (-\infty, \infty)$ ,

$$U_{[\gamma,x,y]} \longrightarrow U_{[\eta,\infty,-\infty]} = \text{Pexp} \left\{ (-ig) \int_{-\infty}^{\infty} d\tau \eta \cdot A(\gamma(\tau)) \right\}. \quad (1.35)$$

As will become clear in section 1.4.2.6 in the derivation of the JIMWLK equation, a Wilson line following a straight path is sufficient for the purposes of this thesis.

- Taylor expand the path-ordered exponential and thus write it as a sum. The  $m^{\text{th}}$  term of this sum will consist of an ordered product of integrals,

$$(-ig)^m \int_{-\infty}^{\infty} d\tau_m \dots \int_{-\infty}^{\tau_3} d\tau_2 \int_{-\infty}^{\tau_2} d\tau_1 \left( \eta \cdot A(\gamma(\tau_m)) \right) \dots \left( \eta \cdot A(\gamma(\tau_2)) \right) \left( \eta \cdot A(\gamma(\tau_1)) \right). \quad (1.36)$$

- Fourier transform the gauge field in each term:

$$A_\mu(\eta^\mu \tau) \longrightarrow \int \frac{d^4 k}{(4\pi)^2} e^{-i\tau(\eta \cdot k)} A_\mu(k). \quad (1.37)$$

- Exchange the order of integration  $\int dk \leftrightarrow \int d\tau$  in each term of the sum. For the  $m^{\text{th}}$  term, this means

$$\begin{aligned} (-ig\eta)^m \int \frac{d^4 k_1 d^4 k_2 \dots d^4 k_m}{(4\pi)^{2m}} A(k_m) A(k_{m-1}) \dots A(k_1) \times \\ \times \int_{-\infty}^{\infty} d\tau_m \dots \int_{-\infty}^{\tau_3} d\tau_2 \int_{-\infty}^{\tau_2} d\tau_1 e^{-i\eta \cdot \sum_{j=1}^m \tau_j k_j}; \end{aligned} \quad (1.38)$$

we have suppressed the Lorentz indices on the gauge fields  $A$  and on the directional vector  $\eta$ , but we understand that each  $\eta$  is contracted with exactly one  $A$ .

- The integrals over the variables  $\tau_i$  are essentially Fourier transforms of Heaviside step functions, for example,

$$\int_{-\infty}^{\tau_2} d\tau_1 e^{-i\tau_1 \eta \cdot k_1} = \int_{-\infty}^{\infty} d\tau_1 \theta(\tau_2 - \tau_1) e^{-i\tau_1 \eta \cdot k_1} = \frac{i}{-\eta \cdot k_1 + i\epsilon} e^{-i\tau_2 \eta \cdot k_1}, \quad (1.39a)$$

where  $\epsilon$  is a small parameter. For the  $m^{\text{th}}$  term (1.38) in the series expansion of the Wilson line, we thus have

$$\int_{-\infty}^{\infty} d\tau_m \dots \int_{-\infty}^{\tau_3} d\tau_2 \int_{-\infty}^{\tau_2} d\tau_1 e^{-i\eta \cdot \sum_{j=1}^m \tau_j k_j} = \prod_{f=1}^m \left( \frac{i}{-\eta \cdot \sum_{j=1}^f k_j + i\epsilon} e^{-i\tau_m \eta \cdot k_f} \right). \quad (1.39b)$$

After these steps are performed, the Wilson line (1.35) takes the form

$$U_{[\eta, \infty, -\infty]} = \sum_{m=1}^{\infty} (-ig\eta)^m \int \frac{d^4 k_1 \dots d^4 k_m}{(4\pi)^{2m}} A(k_m) \dots A(k_1) \prod_{f=1}^m \left( \frac{i}{-\eta \cdot \sum_{j=1}^f k_j + i\epsilon} e^{-i\tau_m \eta \cdot k_f} \right). \quad (1.40)$$

The sum of momenta  $(-\sum_{j=1}^f k_j)$  in the denominator physically arises from multiple gluon emissions: by conservation of energy-momentum at a vertex, a quark with momentum  $p$  radiating a gluon with momentum  $k_1$  has momentum  $p - k_1$  after the emission. If it radiates a further gluon with momentum  $k_2$ , the quark's momentum will be reduced to  $p - (k_1 + k_2)$ , and so forth.

Recall that we used the short-hand notation  $A = A^a t^a$  (*c.f.* eq. (1.22)). Making the generators  $t^a$  explicit and identifying the Wilson line propagator and the gluon vertex as

$$\text{Wilson line propagator:} \quad \frac{i}{-\eta \cdot k_j + i\epsilon} \quad (1.41a)$$

$$\text{Gluon vertex:} \quad -ig\eta^\mu t^a, \quad (1.41b)$$

the Wilson line  $U_{[\eta, \infty, -\infty]}$  may be thought of as a sum of all Feynman diagrams where a particle moving along the straight line path  $\gamma^\mu = \eta^\mu \tau$  radiates/absorbs multiple gluons along the way.

### 1.2.3.2 Eikonal approximation

Let us now tackle the subject from the opposite direction and see how a particular (sum of) Feynman diagram(s) gives rise to Wilson lines. The exposition of this section closely follows [37].

Consider a quark radiating a gluon. It will be shown that if we sum over multiple gluon exchanges and the radiated gluons are soft, then the Dirac propagator and the gluon vertex of the corresponding Feynman diagrams turn into the Wilson line propagator and gluon vertex of eqns. (1.41).

Suppose a quark with momentum  $p$  emits a gluon with momentum  $k$ ,



where time flows from right to left, and the grey blob  $F$  incorporates all possible diagrams containing the depicted vertex. Suppose that the gluon that is emitted by the quark is *soft* (this is also referred to as the *eikonal limit*),

$$k \ll p, \quad (1.43)$$

such that the straight line trajectory of the quark is not (significantly) altered by the emission of the gluon.

Using standard Feynman rules [25, 31, 37], the diagram (1.42) becomes

$$F \frac{i(\not{p}-\not{k})-m}{(p-k)^2-m^2+i\epsilon} \underbrace{(-igt^a\gamma^\mu)}_{\text{gluon vertex (Dirac)}} u(p) \quad (1.44)$$

↑ remainder    ↑ Dirac propagator    ↑ quark

where  $F$  depends of the particularities of the blob  $F$  in the diagram,  $m$  is the total mass of the quark and the gluon,  $\epsilon$  is a small parameter, and  $u(p)$  encodes all information about the quark. We once again used Feynman slash notation (*c.f.* eq. (1.18)). We emphasize that, for the purpose of this thesis, the emitted gluon in the diagram (1.42) attaches to the background field, such that an additional factor  $A^{\mu a}$  appears in eq. (1.44). For now, we will suppress  $A^{\mu a}$ , but we will make this factor explicit at the end of our calculation.

In the eikonal limit (1.43), the momentum of the radiated gluon is negligible in comparison to the quark momentum, implying that  $\not{p}-\not{k} \approx \not{p}$ . Furthermore, since the gluon is massless, the total mass  $m$  of the quark and the gluon reduces to the quark mass  $m = m_q$ . Therefore, when expanding the term  $(p-k)^2 - m^2$ , we obtain

$$(p-k)^2 - m^2 = \underbrace{p^2}_{=m_q^2} - 2p \cdot k + \underbrace{k^2}_{\ll p^2} - \underbrace{m^2}_{=m_q^2} \approx -2p \cdot k. \quad (1.45)$$

Since we are in the high energy regime of QCD, the contribution from the quark momentum dominates over that of its rest mass,  $p \gg m_q = m$ . Taking all these approximations into account, the Feynman diagram (1.44) reduces to

$$F \frac{i p_\nu \gamma^\nu}{-2p \cdot k + i\epsilon} (-igt^a \gamma^\mu) u(p), \quad (1.46)$$

where we have resolved  $\not{p}$  into  $p_\nu \gamma^\nu$  according to eq. (1.18). Let us rearrange terms in eq. (1.46): Firstly, notice that  $(-igt^a)$  commutes with both  $\gamma^\mu$  and  $u(p)$ , such that we can write

$$F \frac{i p_\nu \gamma^\nu \gamma^\mu}{-2p \cdot k + i\epsilon} u(p) (-igt^a). \quad (1.47)$$

Secondly, by the Dirac equation [41], we have that

$$0 = \not{p}u(p) = p_\nu \gamma^\nu u(p). \quad (1.48)$$

Thus, we may add a term  $\gamma^\mu p_\nu \gamma^\nu u(p)$  to the numerator of eq. (1.47),

$$F \frac{i p_\nu (\gamma^\nu \gamma^\mu + \gamma^\mu \gamma^\nu)}{-2p \cdot q + i\epsilon} u(p) (-igt^a), \quad (1.49)$$

where we used the fact that  $\gamma^\mu$  and  $p_\nu$  commute (notice the *different* indices on  $p$  and  $\gamma$  implying that no contraction between the two quantities occurs). The term in the round brackets in the numerator of eq. (1.49) is merely the anti-commutator of two  $\gamma$ -matrices, which is given by [25]

$$\{\gamma^\mu \gamma^\nu\} = 2g^{\mu\nu}, \quad g^{\mu\nu} \text{ is the metric.} \quad (1.50)$$

Expressing  $p_\nu$  as  $|p|\eta_\nu$ , where  $\eta_\nu$  is a normalized direction vector, eq. (1.49) becomes

$$F \frac{i2|p|\eta_\nu g^{\mu\nu}}{-2|p|\eta \cdot k + 2|p|\frac{i\epsilon}{2|p|}} (-igt^a) u(p). \quad (1.51)$$

It remains to define  $i\epsilon' := \frac{i\epsilon}{2|p|} < i\epsilon$  and cancel a common factor  $2|p|$  in the fraction to obtain (*c.f.* eqns. (1.41))

$$F \frac{i}{-\eta \cdot k + i\epsilon'} (-ig\eta^\mu t^a) u(p). \quad (1.52)$$

↑ remainder      ↑ Wilson propagator      } gluon vertex (Wilson)      ↑ quark

Eq. (1.52) describes a Wilson line propagator along the path of the quark emitting a gluon on the way.

Instead of emitting one gluon (such that one gluon is in the out state), the quark also may emit a multitude of soft gluons. However, here the calculation becomes more involved, as one has to consider several Feynman diagrams. For example, Figure 1.4 depicts some diagrams that produce two gluons in the out state.

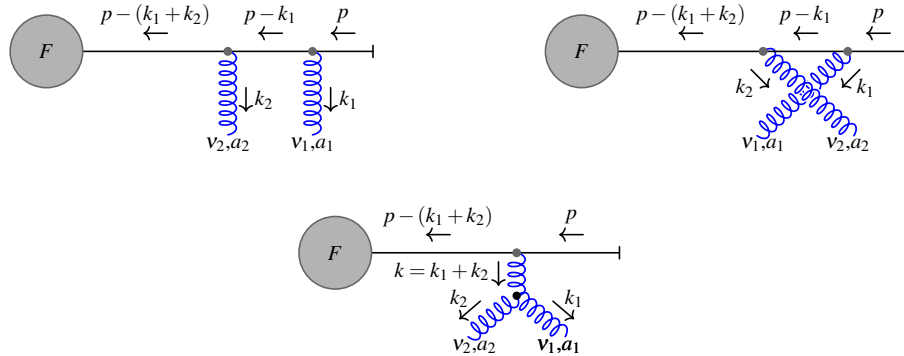


Figure 1.4: This graphic contains several diagrams in which a quark radiates two gluons (top row) or one gluon (bottom row), such that there are two gluons in the out state. All these diagrams need to be taken into account when considering the sub-process interaction  $q \rightarrow gqg$ .

Amazingly, when all diagrams of a given order are added up, one obtains an *ordered* product — this was proven to all orders in [42]. Thus, resumming the contributions of all Feynman diagrams where a quark radiates a soft gluon to all orders yields a Wilson line,

$$F \left( \sum_{m=0}^{\infty} \frac{i\eta^{\nu_m} A^{\nu_m a_m}(k_m)}{\eta \cdot \sum_{i=1}^m k_i + i\epsilon} \cdots \frac{i\eta^{\nu_2} A^{\nu_2 a_2}(k_2)}{\eta \cdot \sum_{i=1}^2 k_i + i\epsilon} \frac{i\eta^{\nu_1} A^{\nu_1 a_1}(k_1)}{\eta \cdot k_1 + i\epsilon} (-ig)^m t^{a_m} \dots t^{a_2} t^{a_1} \right) u(p) = F U_{[\eta, \infty, -\infty]} u(p), \quad (1.53)$$

where we have made the external/background gluons  $A$  explicit again, as discussed previously.

### 1.2.3.3 Summary

In the previous sections, 1.2.3.1 and 1.2.3.2, we showed that a Wilson line describes a parton radiating/absorbing several low-energy (soft) gluons, where a sum over the number of gluons is implied. Since the path of the particle will not be altered significantly when radiating a soft gluon, one may approximate this path by a straight line. This physical picture justifies the following schematic of a Wilson line,

$$U_{[\eta, \infty, -\infty]} = \sum_{\text{gluons}} \text{---} \begin{array}{c} \color{blue}{\text{~~~~~}} \\ \color{blue}{\text{~~~~~}} \\ \color{blue}{\text{~~~~~}} \\ \dots \\ \color{blue}{\text{~~~~~}} \\ \color{blue}{\text{~~~~~}} \end{array} \text{---}, \quad (1.54)$$

where the red dots at the end of the gluon coils indicate that the gluon attaches to the background field. In other words, in the eikonal approximation, Wilson lines allow us to re-sum all Feynman diagrams describing a quark emitting any number of soft (external/background) gluons to all orders.

### 1.2.4 Wilson lines as elements of $SU(N)$

In this section, we will establish various properties of Wilson lines, which will allow us to conclude that Wilson lines are indeed elements of the special unitary group  $SU(N)$ .

1. *Identity*: The Wilson line can become the identity matrix in two ways: either the path  $\gamma$  along which the Wilson line is taken has zero length,

$$U_{[\gamma, x, x]} = \text{Pexp} \left\{ -ig \int_x^x d\gamma^\mu A_\mu^a(\gamma) t^a \right\} = \text{Pexp} \{0\} = \mathbb{1}, \quad (1.55a)$$

or the gauge field  $A_\mu$  vanishes along the path of the Wilson line,

$$U_{[\gamma, x, y]} = \text{Pexp} \left\{ -ig \int_y^x d\gamma^\mu 0 \right\} = \text{Pexp} \{0\} = \mathbb{1}. \quad (1.55b)$$

2. *Unitarity* [37, 43]: The inverse of a Wilson line is obtained by “reversing the effects” of the differential equation (1.33). In other words, one needs to employ anti-path-ordering, and flip the sign of the integral to “traverse the path in the opposite direction” [44],

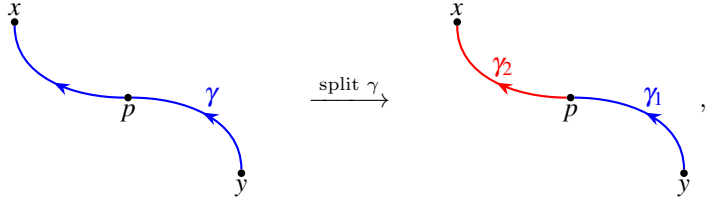
$$(U_{[\gamma, x, y]})^{-1} = \left( \text{Pexp} \left\{ -ig \int_y^x d\gamma^\mu A_\mu(\gamma) \right\} \right)^{-1} = \bar{\text{Pexp}} \left\{ +ig \int_y^x d\gamma^\mu A_\mu(\gamma) \right\}. \quad (1.56a)$$



In doing so, one reverses the order in the product and exchanges  $-i \rightarrow +i$ , which is exactly the same procedure one employs when forming the Hermitian conjugate. Hence we conclude that Wilson lines are unitary,  $U_{[\gamma,x,y]}^{-1} = U_{[\gamma,x,y]}^\dagger$ , implying that

$$U_{[\gamma,x,y]}^\dagger U_{[\gamma,x,y]} = U_{[\gamma,x,y]} U_{[\gamma,x,y]}^\dagger = \mathbb{1} . \quad (1.56b)$$

3. *Closure under multiplication:* Consider a Wilson line along a path  $\gamma$  from  $y$  to  $x$  containing a point  $p$ . We may split  $\gamma$  into two segments,  $\gamma_1$  and  $\gamma_2$ , where  $\gamma_1$  runs from  $y$  to  $p$  along  $\gamma$ , and  $\gamma_2$  follows  $\gamma$  from  $p$  to  $x$ ,



$$, \quad (1.57)$$

such that

$$\begin{aligned} U_{[\gamma,x,y]} &= \text{Pexp} \left\{ -ig \int_y^x d\gamma^\mu A_\mu^a(\gamma) t^a \right\} \\ &= \text{Pexp} \left\{ \left( -ig \int_y^p d\gamma_1^\mu A_\mu^a(\gamma_1) t^a \right) + \left( -ig \int_p^x d\gamma_2^\mu A_\mu^a(\gamma_2) t^a \right) \right\} . \end{aligned} \quad (1.58)$$

The path-ordering will ensure that all integrals over points on the curve  $\gamma_1$  come to stand to the right of all integrals over points in  $\gamma_2$  such that the Wilson line  $U_{[\gamma,x,y]}$  can be expressed as a product of two Wilson lines along the paths  $\gamma_1$  and  $\gamma_2$  respectively,

$$U_{[\gamma,x,y]} = U_{[\gamma_2,x,p]} U_{[\gamma_1,p,y]} , \quad \gamma_1 \cup \gamma_2 = \gamma . \quad (1.59)$$

This result however was to be expected [44]: We started our discussion on Wilson lines by defining the object  $U_{[\gamma,x,y]}$ , the device that parallel transports the vector  $\psi(y)$  to the point  $x$ , such that  $U_{[\gamma,x,y]} \psi(y) = \psi(x)$  (c.f. eq. (1.32)). Thus, for the paths  $\gamma$ ,  $\gamma_1$  and  $\gamma_2$ , as defined in (1.57), we must have

$$\psi(x) = U_{[\gamma_2,x,p]} \psi(p) = U_{[\gamma_2,x,p]} (U_{[\gamma_1,p,y]} \psi(y)) = U_{[\gamma_2,x,p]} U_{[\gamma_1,p,y]} \psi(y) , \quad (1.60)$$

and also

$$\psi(x) = U_{[\gamma,x,y]} \psi(y) , \quad (1.61)$$

which again implies that

$$U_{[\gamma_2,x,p]} U_{[\gamma_1,p,y]} = U_{[\gamma,x,y]} . \quad (1.62)$$

More generally, the path of a Wilson line may be broken up consecutively into smaller segments, allowing

us to write a particular Wilson line as a product of shorter Wilson lines,

$$U_{[\gamma,x,y]} = U_{[\gamma_n,x,p_n]} U_{[\gamma_{n-1},p_n,p_{n-1}]} \cdots U_{[\gamma_1,p_2,p_1]} U_{[\gamma_0,p_1,y]} , \quad \gamma_0 \cup \gamma_1 \cup \cdots \cup \gamma_{n-1} \cup \gamma_n = \gamma . \quad (1.63)$$

4. *Determinant:* We present a proof given in [44] to show that the determinant of  $SU(N)$  is 1: One can write the determinant of  $U_{[\gamma,x,y]}$  as

$$\det(U_{[\gamma,x,y]}) = e^{\text{tr}(\ln U_{[\gamma,x,y]})} . \quad (1.64)$$

Taking the derivative with respect to  $x$  yields Jacobi's formula for the derivative of determinants [45]

$$\frac{\partial}{\partial x} \det(U_{[\gamma,x,y]}) = e^{\text{tr}(\ln U_{[\gamma,x,y]})} \text{tr} \left( \frac{\partial}{\partial x} \ln U_{[\gamma,x,y]} \right) = \det(U_{[\gamma,x,y]}) \text{tr} \left( U_{[\gamma,x,y]}^{-1} \frac{\partial}{\partial x} U_{[\gamma,x,y]} \right) . \quad (1.65)$$

From the explicit form (1.34) of  $U_{[\gamma,x,y]}$ , the derivative  $\frac{\partial}{\partial x} U_{[\gamma,x,y]}$  is calculated to be

$$\frac{\partial}{\partial x} U_{[\gamma,x,y]} = (-ig) U_{[\gamma,x,y]} A_\mu^a(\gamma) t^a , \quad (1.66)$$

such that eq. (1.65) reduces to

$$\frac{\partial}{\partial x} \det(U_{[\gamma,x,y]}) = (-ig) \det(U_{[\gamma,x,y]}) \text{tr} (A_\mu^a(\gamma) t^a) . \quad (1.67)$$

Adding in all previously suppressed matrix indices,  $t^a = [t^a]_{ij}$ ,  $\text{tr} (A_\mu^a(\gamma) t^a)$  is understood to be

$$\text{tr} (A_\mu^a(\gamma) t^a) \longrightarrow \text{tr} (A_\mu^a(\gamma) [t^a]_{ij}) = A_\mu^a(\gamma) \text{tr} ([t^a]_{ij}) . \quad (1.68)$$

Since the generators  $[t^a]_{ij}$  of  $SU(N)$  are traceless, it follows that

$$\frac{\partial}{\partial x} \det(U_{[\gamma,x,y]}) = 0 ; \quad (1.69)$$

the determinant of  $U_{[\gamma,x,y]}$  is *constant* with respect to  $x$ . Using the initial condition  $U_{[\gamma,y,y]} = \mathbb{1}$  (see eq. (1.55a)), we must have

$$\det(U_{[\gamma,x,y]}) = \det(U_{[\gamma,y,y]}) = \det(\mathbb{1}) = 1 , \quad (1.70)$$

as required.

In summary, the properties discussed in this section verify that Wilson lines are elements of the special unitary group  $SU(N)$ . Intuitively, this was to be expected since, by its very definition

$$U_{[\gamma,x,y]} = \text{Pexp} \left\{ -ig \int_y^x d\gamma^\mu A_\mu^a(\gamma) t^a \right\}_\gamma , \quad (1.71)$$

a Wilson line is a (path-ordered) exponential of the group generators  $t^a$ .

## 1.3 The color glass condensate

The color glass condensate (CGC) [21, 46, 47] is a state of matter that is densely populated by gluons. The high gluon density gives rise to screening effects within the medium. Thus, the correlation length between particles becomes short, which in turn limits interactions between individual partons in the CGC to short distances — short enough for the coupling to be weak. In such a situation, one may model the conglomerate of partons (quarks and gluons) as a classical field of color charges.

The CGC owes its name to its properties:

- *color*: as already mentioned, the CGC describes a state of matter comprised of a multitude of particles (quarks and gluons) that carry color charge.
- *glass*: Due to the time-dilation of the highly boosted system, the individual color charges seem frozen in the transverse plane in time, making the CGC behave like a solid on short time scales. In particular, during the time of the interaction one only observes a snapshot of a fixed parton configuration.
- *condensate*: Due to the limited resolution of the color charges in the CGC by the probe, recombination effects of gluons become more and more prominent as the gluon population increases. Eventually, gluon production and recombination will balance out, causing the system to reach saturation — a feature it shares with condensates.

Besides being the name given to a particular state of matter, the CGC is an effective field theory which allows one to describe a system that is highly populated by gluons. Due to the weak coupling arising from the high population density, such a system is not accessible to standard perturbation theory.

### 1.3.1 McLerran–Venugopalan model

Attempts to find the gluon distribution functions for very small values of  $x_{Bj}$  have been made since the 1970's. All of these attempts use techniques that are strictly only applicable in the low density situation: One usually models the interaction probing the gluon field by an exchange of multiple reggeized gluons in a vacuum. Using these methods, one may derive the BFKL-equation [48, 49], which captures the evolution of the gluon distribution function (at low density) with  $x_{Bj}$  (*c.f.* Figure 1.3).

A paradigm shift in the approach to calculating these gluon distribution functions came about in the 1990's when McLerran and Venugopalan (MV) [22, 23] proposed a model in which the gluon background field is *not* viewed as a dilute system,<sup>6</sup> but rather as a dense collection of gluons with finite apparent sizes. One essentially moves from a vacuum background, as in [48], to a background field consisting of a very large number of gluons. These gluons are produced by color sources representing the valence partons. Since then, the so-called MV-model has been generalized in a multitude of directions and one may find it applied to descriptions of varying sophistication, for example in [20, 50].

Physically speaking, a collection of highly energetic valence quarks radiate a (large) number of typically soft gluons. These gluons constitute a background field  $b$ <sup>7</sup> whose distribution one wishes to calculate. Since

<sup>6</sup>Unlike the Bjorken limit in which the partons constitute a *dilute* system (see section 1.1.2.2).

<sup>7</sup>We use the same letter as for the target of a high energy collision, *c.f.* eq. (1.3), since we will eventually model the target as a CGC-medium.

these radiated gluons are soft, the momentum of the valence partons is hardly altered, allowing us to model the valence partons as no-recoil sources confined to the lightcone (i.e. moving in the  $x^+$ -direction, see Figure 1.1). Due to the non-abelian nature of QCD (*c.f.* section 1.2.1.2) the gluons making up  $b$  may radiate further gluons, generating cascading gluon chains. These fluctuations  $\alpha$  of  $b$  may be calculated using weak coupling methods [22, 23].

This picture motivates a cut-off  $\Lambda_0^+$  for the  $x^+$ -momentum of the color charges (using the notation of [21]), separating them into the background field  $b$  and fluctuations  $\alpha$ . According to an argument of [22], one may model  $b$  as a classical field and treat  $\alpha$  as quantum corrections to  $b$ . Thus, the cut-off  $\Lambda_0^+$  essentially separates particle and field degrees of freedom [20]. We repeat the argument of [22] here:

In order to justify the high density of gluons prerequisite for this description in a physical situation, [22] considers a high energy collision in the infinite momentum frame. In this reference frame, Lorentz contraction in the  $x^-$ -direction confines the valence partons to the lightcone. Adopting a path integral formalism, the valence partons are modelled by sources  $J$ , which have a  $\delta$ -function-like support due to the boost factor  $e^{-Y}$  ( $Y$  is the rapidity),

$$J^{\mu a} = \delta^{\mu+} \delta(x^-) \delta^2(\mathbf{x}) \rho^a(x) , \quad (1.72)$$

where  $\rho^a(x)$  gives the color charge density of the source  $J^{\mu a}$ , and  $\delta(x^-) \delta^2(\mathbf{x})$  tells us that such a source is a point-particle whose worldline is localized in  $x^-$  and in  $\mathbf{x}$ .<sup>8</sup>

It is argued in [22] that the regions of space occupied by the target may be broken up into a grid such that each piece of size  $da^2$  contains a large number of valence partons (the grid size sets the resolution at which this approximation holds). Due to the large number of partons in a particular transverse region  $da^2$ , the sources  $J$  may be treated as *classical*: The ground state of the field configuration about which perturbation theory is performed is the ground state obtained from the Yang-Mills equation [39]

$$[D_\mu, F^{\mu\nu}] = J^\nu , \quad \text{where } J^\nu := J^{\nu a} t^a , \quad (1.73)$$

and  $t^a$  are the generators of the gauge group  $SU(N)$ . In other words, eq. (1.73) defines the saddle point (about which we perturb) of the path integral.

Recall that we are working in the infinite momentum frame in which the gluon field is enhanced in the  $x^+$ -direction by a factor  $e^Y$  and suppressed in the  $x^-$ -direction by a factor  $e^{-Y}$  due to a Lorentz boost in  $x^3$  (i.e. the field experiences spatial contraction and time dilation in  $x^\pm$  respectively). Hence, internal interactions between the sources during the time of interaction with the projectile are extremely unlikely. Therefore, one may model the valence partons as a collection of *static* charges in the transverse plane. Concluding that the  $J$ 's are a statistically large sample of static, classical sources, [22] argues that they must distribute themselves in the transverse plane with a Gaussian weight.

Furthermore, since the valence quarks comprising the target must combine into a color neutral configuration due to confinement, the average color charge of the sources must be zero. This is encapsulated by the fact that the 1-point correlator  $\langle \rho^a \rangle$  vanishes [22]. Hence, the average color of the background field  $b$  must be zero. The only net color charge that can be generated, therefore, stems from the fluctuations. This tells us that the Gaussian describing the transverse distribution of the source charges for the gluon field must peak

---

<sup>8</sup>In [22] the function  $\rho^a$  is denoted by  $\mathcal{Q}^a$ , but in the later paper [23, eq. (14)]  $\mathcal{Q}^a(x^+, \mathbf{x})$  is identified as  $\rho^a(\mathbf{x})$ .

at zero net color. In summary, [22] proposes the model

$$\mathcal{M}_{\text{MV}}[\rho] = \exp \left\{ - \int d^2 \mathbf{x} \frac{1}{2\mu^2} \text{tr} (\rho^2(\mathbf{x})) \right\}, \quad (1.74)$$

where  $\mu^2$  is proportional to the average charge density per unit transverse area. The follow-on paper [23] of [22] addresses some of the issues that arise from a low transverse resolution  $Q^2$ . In this case, rather than modelling the sources  $J$  as point particles in the transverse plane, the  $J$ 's are taken to be uniformly distributed in  $\mathbf{x}$ ,

$$J^{\mu a}(x^-, \mathbf{x}) = \delta^{\mu+} \delta(x^-) \rho^a(\mathbf{x}). \quad (1.75)$$

The weight  $\mathcal{M}_{\text{MV}}[\rho]$  in the generating functional (1.77) is however still Gaussian,

$$\mathcal{M}_{\text{MV}}[\rho] = \exp \left\{ - \int d^2 \mathbf{x} \frac{1}{2\mu^2} \text{tr} (\rho^2(\mathbf{x})) \right\}. \quad (1.76)$$

The gluon distribution function (within the target) is then calculated by finding the two point correlator of the field  $A = b + \alpha$  from the path integral formalism with the generating functional

$$\mathfrak{Z} = \int [d\rho][dA][d\psi^\dagger d\psi] e^{iS + ig \int d^4 x \text{tr}(A^+(x)\rho(x))\delta(x^-)} \mathcal{M}_{\text{MV}}[\rho], \quad (1.77)$$

where  $S$  is the gluon action in the presence of the sources  $J$  [22]. We'd like to draw attention to the integral  $\int [d\rho]$ , which describes an averaging procedure over the source configurations  $\rho$ .

One may now set out to find a solution for the gauge field  $A^\mu$  in order to eventually obtain the gluon distribution  $\langle A^\nu A^\mu \rangle$ : Recall that  $J^{+a}(x^-, \mathbf{x})$  is a classical source satisfying the Yang-Mills equation (1.73). The fact that the target is highly boosted along the  $x^+$ -direction (which allowed us to arrive at the particular form (1.75) of the source  $J^{\mu a}$ ) introduces a hierarchy of the various components of the tensor  $F^{\mu\nu}$  [20, 51]: The plus-components  $F^{i+}$  and  $F^{+i}$  are enhanced by a factor  $e^{+\eta}$  (where  $\eta$  is the boost factor), the spacial components  $F^{ij}$  are unaffected by the boost, and the minus-components  $F^{i-}$  and  $F^{-i}$  are suppressed by a factor  $e^{-\eta}$ , such that

$$F^{i+}, F^{+i} \gg e^\eta F^{ij}, F^{+-}, F^{-+} \gg e^{-\eta} F^{i-}, F^{-i}. \quad (1.78)$$

Therefore, the most dominant component of the Yang-Mills eq. (1.73) is

$$[D_i, F^{i+}] = J^+ = \delta(x^-) \rho(\mathbf{x}), \quad \text{where } \rho(\mathbf{x}) := \rho^a(\mathbf{x}) t^a. \quad (1.79)$$

Since the gauge field  $A^\mu$  satisfies the analogous hierarchy of the field strength tensor,

$$A^+ \gg e^\eta A^i \gg e^{-\eta} A^-, \quad (1.80)$$

it is tempting to check whether eq. (1.79) has a solution in which only the  $A^+$ -component does not vanish,

$$[D_i, F^{i+}] = \left[ \partial_i + \underbrace{ig A_i}_{=0}, \partial^i A^+ - \underbrace{\partial^+ A^i - ig[A^i, A^+] }_{=0} \right]$$

$$= \partial_i \partial^i A^+ = \delta(x^-) \rho(\mathbf{x}) . \quad (1.81)$$

This equation can indeed be solved for  $A^+$ . As is often done, one may want to choose the lightcone gauge in which the plus-component of the gauge field  $A$  vanishes,<sup>9</sup> even though the hierarchy (1.80) suggests this to be an “unnatural” gauge. This can be accomplished by means of a gauge transformation  $U$ ,

$$\tilde{A}^+ := U \left( A^+ - \frac{1}{ig} \partial^+ \right) U^{-1} \stackrel{!}{=} 0 . \quad (1.82)$$

Then one finds that  $\tilde{A}^i$  is of the form [20, 51]

$$\tilde{A}^i(x) = \theta(x^-) \mathbf{a}^i(\mathbf{x}) , \quad (1.83)$$

where  $\mathbf{a}^i(\mathbf{x})$  depends on the gauge transformation  $U$  in a complicated way. With this form of  $\tilde{A}^i$ , it can eventually be shown [22] that the gluon distribution in the small- $x_{Bj}$  system is of the Weizacker-Williams form. This is physically justified [20]: Since the color sources are confined to a thin sheet on the lightcone, the free equations of motion must govern the kinematics of the field everywhere except on the sheet. Furthermore, the charge density on the sheet must be given by the discontinuity across the sheet.

Substituting the solution (1.83) of  $\tilde{A}^i$  into the Yang-Mills equation (1.73), the commutator term

$$\left[ \tilde{A}_i, \partial^\mu \tilde{A}^i \right] \quad (1.84)$$

has the interesting singular structure  $\delta(x^-) \theta(x^-)$  [20]. In order to properly understand this structure, one must consider the distribution of valence partons (modelled by the sources  $J$ ) to extend in the longitudinal direction.<sup>10</sup> To do so, [20] introduce the rapidity  $Y$ ,

$$Y := Y_0 + \ln \left( \frac{x_0^-}{x^-} \right) , \quad (1.85)$$

where  $Y_0$  is the rapidity of the target and  $x_0^-$  is the Lorentz contracted size of the target,

$$x_0^- \sim \frac{R}{\gamma} , \quad \gamma \text{ is the Lorentz factor} , \quad (1.86)$$

and  $R$  is the uncontracted target size. Furthermore, [20] realized that gluons (emitted from the valence partons) that have longitudinal momenta larger than  $\Lambda_0^+$  themselves contribute to the sources. Thus, the charge per unit spacetime  $\mu$  must be considered as rapidity dependent,  $\mu \rightarrow \mu(Y)$ . Similarly, the source strength  $\rho$  becomes rapidity dependent,  $\rho(\mathbf{x}) \rightarrow \rho(Y, \mathbf{x})$ , such that one must consider the functional distribution

$$\mathcal{M}_{\text{MV}}[\rho] = \exp \left\{ - \int_0^\infty dY \int d^2 \mathbf{x} \frac{\text{tr}(\rho^2(Y, \mathbf{x}))}{2\mu^2(Y, Q^2)} \right\} \quad (1.87)$$

rather than (1.76); as explained in [18], this weight is gauge invariant. We once again stress that (1.87) is a

<sup>9</sup>This was done in the original paper [23] already at the level of the Young-Mills equation, such that the latter reduces to

$$-\partial_i \partial^+ A^i + ig [A_i, \partial^+ A^i] = \delta(x^-) \rho(\mathbf{x}) .$$

However, the discussion is much simpler if we start with a gauge in which  $A^+ \neq 0$ .

<sup>10</sup>In other words, the gluon distribution has  $\delta$  function support  $\delta(x^-)$  in the infinite momentum frame, but not, e.g., in the rest frame of the target.

model, which is to say that it has not been derived from QCD.<sup>11</sup>

Ref. [20] suggests that renormalization group (RG) techniques should be used to systematically integrate out the fluctuations (gluons) contributing to the color sources (adjusting the momentum cut-off  $\Lambda_0^+$  with the rapidity  $Y$ ) in order to include them in the background field. In other words, one seeks to perform the integral over the gauge field  $\int[dA]$  for all rapidities higher than some cut-off rapidity  $Y_*$ , such that the result of this integration can be completely encoded into the functional weight  $\mathcal{M}_{MV}$  as

$$\begin{aligned} \mathfrak{Z} &= \int_0^{Y_*} [dA] \int [d\rho] \cdots \mathcal{M}_{MV}[\rho] + \underbrace{\int_{Y_*}^{\infty} [dA] \int [d\rho] \cdots \mathcal{M}_{MV}[\rho]}_{\text{perform integration over } A} \\ &\stackrel{\text{RG step}}{=} \int_0^{Y_*} [dA] \int [d\rho] \cdots \tilde{\mathcal{M}}_{MV}[\rho, Y_*] =: \tilde{\mathfrak{Z}}, \end{aligned} \quad (1.88)$$

such that

$$\frac{d}{dY_*} \tilde{\mathfrak{Z}} = 0; \quad (1.89)$$

the dots  $\cdots$  in eq. (1.88) stand for

$$\int [d\psi^\dagger d\psi] e^{iS + ig \int d^4x \text{tr}(A^+(x)\rho(x))\delta(x^-)} \quad (1.90)$$

(*c.f.* eq. (1.77)). While the functional form (1.87) makes physical sense, it is a model (an Ansatz) that was not derived from QCD. Therefore, it is not clear whether it is a good starting point for a renormalization group argument such as (1.88). In fact, it will turn out that the relevant RG equation does not have the MV-model as its starting point, *c.f.* section 1.4.

In the following section, 1.3.2, we give an intuitive sketch of the main idea behind an RG approach. In section 1.4.1 we make this approach more concrete in the context of the *JIMWLK*<sup>12</sup> framework: JIMWLK is an RG equation determining the rapidity dependence of the gluon distribution functions at small  $x_{Bj}$ . We will give a derivation of the JIMWLK equation in section 1.4.2.

### 1.3.2 Evolution with high energy

One important feature of the color glass condensate is the separation between hard and soft gluons, i.e. the separation of gluons into the background field  $b$  and fluctuations  $\alpha$ . As the energy  $s$  (equivalently, the rapidity separation  $Y$  between the projectile and the target) is increased, fluctuations in the background field (target) become more and more prominent. Thus, the separation of gluons into  $b$  and  $\alpha$ , and consequently the averaging procedure introduced by the MV-model, has to be adjusted with  $Y$ . This is schematically depicted in Figure 1.5.

<sup>11</sup>The JIMWLK equation, however, is derived from QCD principles, which will become clear in section 1.4.

<sup>12</sup>The name is an acronym of the authors who first derived it (see section 1.3.2).

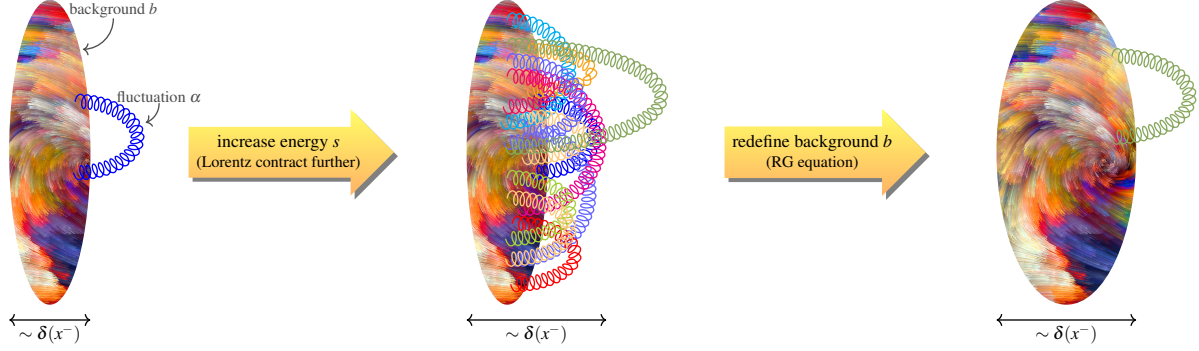


Figure 1.5: As the energy  $s$  deposited in the collision area increases, fluctuations  $\alpha$  in the background color field  $b$  become more and more relevant. In the Bjorken limit ( $Q^2$  increases,  $Y$  fixed),  $b$  is modelled as a dilute system of partons, while the Regge-Gribov limit ( $Y$  increases,  $Q^2$  fixed) requires  $b$  to be viewed as a dense, coherent color field. The relevant renormalization group equation for each limit prescribes how the cut-off dividing the color charges into background field and fluctuations is to be adjusted with increasing  $s$ . (The image used for the background field  $b$  is taken from [52].)

This is done by means of a renormalization group (RG) equation.<sup>13</sup> In the Bjorken limit, the relevant RG equations are the DGLAP (Dokshitzer–Gribov–Lipatov–Altarelli–Parisi, pronounced “dee-glap”) equations [53–55]. On the other hand, in the Regge-Gribov limit, the JIMWLK (Jalilian-Marian–Iancu–McLerran–Weigert–Leonidov–Kovner, pronounced “gym-walk”) equation [20, 56–59] or the equivalent Balitsky hierarchies [60] achieve the desired result. In the large- $N_c$  limit, the JIMWLK equation reduces to the BK (Balitsky–Kovchegov) [60–62] equation. On the other hand, if one considers the case where the system is dilute, the JIMWLK equation reduces to the BFKL (Balitsky–Fadin–Kuraev–Lipatov) equation [48, 49] (see e.g. [46]). The regions of phase space where the various equations are applicable are indicated in Figure 1.3.

In this thesis, we are mainly interested in the Regge-Gribov limit. In the following section 1.4, we give an overview of the JIMWLK equation, including a derivation at leading order in section 1.4.2. Thereafter, we discuss symmetries of the JIMWLK equation and  $SU(N)$  gauge theories as a whole (section 1.6), preparing us for the main matter of this thesis.

## 1.4 The JIMWLK equation

In its essence, the JIMWLK framework tracks the rapidity evolution of an observable when interacting eikonally with a target. In particular, it is a renormalization group equation that *adjusts* the averaging procedure over the color field with which the probe interacts as the rapidity increases: As in the MV-model, one separates the color degrees of freedom of the target into those belonging to the background field  $b$  (a Lorentz contracted, time-dilated color field), and those of the fluctuations  $\alpha$ . However, as pointed out in [20], the cut-off scale separating the degrees of freedom has to be adjusted with the energy of the collision. Thus, renormalization group arguments are needed to faithfully accomplish this separation of degrees of freedom.

Depending on the viewpoint one takes, these field fluctuations generated in the interaction are modelled as

<sup>13</sup>For a textbook introduction to the renormalization group see, for example, [25, chpt. 12], [33, chpt. 18], [31, chpt. 12.1], or [32, chpt. 2.5].



either part of the target or the projectile [18]: One either considers these fluctuations as gluons produced by the field  $b$ , which then interact with the probe, or one may view  $\alpha$  as gluons radiated by the probe to interact with  $b$  — we adopt the second viewpoint to derive the JIMWLK equation in section 1.4.2.

Before going through the derivation of JIMWLK at leading order, we wish to briefly discuss the structure of the equation in section 1.4.1.

### 1.4.1 What does JIMWLK do? — a summary

As already mentioned, the ultimate goal of JIMWLK is to find the gluon distribution function of observables in the Regge-Gribov limit; such an observable is located in the top-left corner of the phase space diagram Figure 1.3 (the saturation region). It soon became clear that such a distribution function cannot be derived directly from QCD, but what can be calculated is the evolution of the gluon distribution with increasing energy [20]. In particular, since we are interested in the Regge-Gribov limit, an increase in energy is achieved via an increase in rapidity  $Y$  (equivalently, a decrease in  $x_{\text{Bj}}$ , since  $Y = \ln \frac{1}{x_{\text{Bj}}}$ ) while keeping the transverse resolution  $Q^2$  fixed (*c.f.* eq. (1.14)).

The JIMWLK evolution for the gluon distribution function is derived somewhat indirectly (the outline of the derivation described here follows the treatment of [18], and will be used in the following section 1.4.2): At small  $x_{\text{Bj}}$ , an interaction between a projectile and a target is (to a good approximation) eikonal. Thus, the projectile is best described by a Wilson line correlator  $\mathcal{A}$ .<sup>14</sup>  $\mathcal{A}$  must undergo an averaging procedure over all background fields  $b$  (representing the target) with which the eikonal interaction occurs,

$$\langle \mathcal{A} \rangle_b, \quad (1.91)$$

since there is no way of knowing, a priori, the exact field configuration of  $b$ . The averaging procedure is determined through QCD and is given by

$$\langle \cdots \rangle_b = \int D[b] \cdots Z[b] \quad (1.92)$$

observable (curved arrow from  $\langle \cdots \rangle_b$  to  $\cdots$ )  
background field (arrow from  $b$  to  $D[b]$ )  
Haar measure (arrow from  $D[b]$  to  $\int$ )  
distribution function (arrow from  $Z[b]$  to  $\cdots$ )

where  $Z[b]$  is intimately linked with the gluon distribution function  $Z[\rho]$ , as  $b$  and  $\rho$  are related via a differential equation: In the absence of fluctuations  $\alpha$ , the gauge field  $A$  is entirely comprised of the background field  $b$ ,  $A = b$ . From eq. (1.81) it then follows that  $\partial_i \partial^i b^+ = \rho \delta(x^-)$  [18]. Since, furthermore, the only variables in the correlator  $\mathcal{A}$  that depend on  $b$  are the Wilson lines  $U$  via<sup>15</sup>

$$U_{[\mathbf{x}, +\infty, -\infty]} = \text{Pexp} \left\{ -ig \int_{-\infty}^{+\infty} dx^- \underbrace{A_x^{+a} t_x^a}_{=b_x^{+a}} \right\} \Rightarrow b_x^+ = b_x^{+a} t_x^a = \frac{i}{g} U_{[\mathbf{x}, +\infty, x^-]}^{-1} \left( \frac{\partial}{\partial x^-} U_{[\mathbf{x}, +\infty, -\infty]} \right) U_{[\mathbf{x}, x^-, -\infty]}^{-1}, \quad (1.93)$$

<sup>14</sup>For more complicated projectiles,  $\mathcal{A}$  becomes a matrix of Wilson line correlators, see section 1.6 and section 5.3 in chapter 5.

<sup>15</sup>Often, it is written that  $b^+ = \frac{i}{g} U^{-1} (\partial_x^- U)$  or  $b^+ = \frac{i}{g} (\partial_x^- U) U^{-1}$ . These are special cases of eq. (1.93), in which either  $x^- < 0$  such that  $U_{[\mathbf{x}, x^-, -\infty]} = \mathbb{1}$ , or  $x^- > 0$  such that  $U_{[\mathbf{x}, \infty, x^-]} = \mathbb{1}$ , *c.f.* eqns. (1.159).

one may perform a change of variables [18]

$$\{D[b], Z[b]\} \longrightarrow \{D[U], Z[U]\} . \quad (1.94)$$

In this change of variables, the Haar measure [63]  $D[b]$  (which is just a flat, Euclidean measure) becomes<sup>16</sup>

$$D[b] \longrightarrow D[U] = \delta(UU^\dagger - \mathbb{1}) \delta(\det(U) - 1) dU , \quad (1.95)$$

where  $dU$  is the flat measure over  $U$ , [18].

As the rapidity  $Y$  is increased, more and more gluon fluctuations feature in the interaction. In particular, after a sufficiently large interval (of  $Y$ ), the interaction between  $\mathcal{A}$  and the gluon fluctuations  $\alpha$  can no longer be ignored — one must give  $\alpha$  the same treatment as the background field  $b$ , causing the average to become

$$\langle \mathcal{A} \rangle_b \longrightarrow \langle \mathcal{A} \rangle_{\alpha, b} . \quad (1.96)$$

At this point, it is wiser to incorporate the fluctuation  $\alpha$  into the background field  $b$  rather than performing two averaging procedures. This requires us to adjust  $\langle \cdots \rangle_b$  on the fly as we increase  $Y$ . In doing so, we make the average  $\langle \cdots \rangle_b$  rapidity-dependent,

$$\langle \cdots \rangle_b \longrightarrow \langle \cdots \rangle_b(Y) . \quad (1.97)$$

To see how this adjustment is done correctly, one considers the average  $\langle \cdots \rangle_b$  at a particular rapidity  $Y_0$ . We then increase the rapidity to  $Y$  ( $Y > Y_0$ ), at which point the fluctuations  $\alpha$  become non-negligible. Comparing the two averages of  $\mathcal{A}$  yields a finite difference equation,

$$\langle \mathcal{A} \rangle_b(Y_0) - \langle \mathcal{A} \rangle_{\alpha, b}(Y) = \mathcal{K} , \quad (1.98)$$

where  $\mathcal{K}$  is a quantity to be determined. One can continue increasing the rapidity even further to obtain more finite difference equations — this is the essence of a renormalization group argument. However, since the procedure will not alter as the rapidity becomes larger,<sup>17</sup> one step (for example from  $Y_0$  to  $Y$ ) is sufficient. Taking the limit as  $Y - Y_0 \rightarrow 0$  allows one to reformulate equation (1.98) as<sup>18</sup>

$$\frac{d}{dY} \langle \mathcal{A} \rangle_b(Y) = - \langle H_{\text{JIMWLK}} \mathcal{A} \rangle_b(Y) , \quad (1.99)$$

where  $H_{\text{JIMWLK}}$  is called the JIMWLK Hamiltonian. All steps of the derivation outlined up to this point will be discussed in more detail in section 1.4.2.

To obtain an evolution equation for the gluon distribution function  $Z[U]$  from (1.99), a little bit more work needs to be done. The details of the calculations involved in this reformulation will not be discussed in this

---

<sup>16</sup>That this measure is left- and right-invariant under the multiplication with a group element  $U \in \text{SU}(N)$  (see the definition of a Haar measure [63–65]) can be verified via direct calculation.

<sup>17</sup>This is due to the fact that Wilson lines will be mapped into Wilson lines by the conservation of color at each vertex of a Feynman diagram.

<sup>18</sup>This will be explained in detail in section 1.4.2.

thesis but can be found in [18, 66]: Due to the form of the averaging procedure,

$$\langle \cdots \rangle_b(Y) = \int D[U] \cdots Z[U]$$

↖ observable ↗  
↑ rapidity  
↑ Haar measure  
↑ distribution function

(1.100)

one may rewrite the JIMWLK equation (1.99) for an observable  $\mathcal{A}$  as

$$\begin{aligned}
 \frac{d}{dY} \int D[U] Z[U] \mathcal{A} &= \int D[U] Z[U] H_{\text{JIMWLK}} \mathcal{A} \\
 \frac{d}{dY} \langle Z[U] | \mathcal{A} \rangle &= \langle Z[U] | H_{\text{JIMWLK}} | \mathcal{A} \rangle ,
 \end{aligned}$$
(1.101)

where we suggestively defined a scalar product  $\langle \cdot | \cdot \rangle$  through  $\int D[U]$  (this is not to be confused with the averaging procedure  $\langle \cdots \rangle(Y)$ , which involves the functional distribution  $Z[U]$ ). Treating  $U$  and  $U^\dagger$  as independent variables,<sup>19</sup> it can be shown that  $H_{\text{JIMWLK}}$  is Hermitian [18],

$$\langle Z[U] | H_{\text{JIMWLK}} | \mathcal{A} \rangle = \langle Z[U] | H_{\text{JIMWLK}}^\dagger | \mathcal{A} \rangle ,$$
(1.102)

allowing us to view  $H_{\text{JIMWLK}}$  to be acting on the distribution  $Z[U]$  rather than on  $\mathcal{A}$ . Then,  $\mathcal{A}$  acts as a test function in the evolution equation, allowing us to conclude that

$$\frac{d}{dY} Z[U] = -H_{\text{JIMWLK}} Z[U] .$$
(1.103)

Thus, the JIMWLK equation gives the rapidity-evolution of a gluon distribution function  $Z[U]$ . If it could be solved,<sup>20</sup> it would in fact give the gluon distribution function itself.

The JIMWLK Hamiltonian is currently known up to next-to-leading order (NLO) [68], but research to fully understand the NNLO contributions is ongoing. In the following section, we give a derivation of  $H_{\text{JIMWLK}}$  up to leading order using the strategy described in this section.

## 1.4.2 A derivation of the JIMWLK equation at leading order

In this section, we give a brief derivation of the JIMWLK equation at leading order (LO) for observables consisting of quarks, antiquarks and, at most, 1 gluon in the final state. While there is a multitude of sources giving a derivation of JIMWLK at LO (*c.f.* [18, 21, 69, 70], just to name a few) the derivation presented here combines the treatments given in [18, 71]: we begin in the spirit of [18], but then switch over to the diagrammatic notation of [71], as we feel that this notation makes the latter part of the derivation more accessible.

<sup>19</sup>This does not break the group constraints (such as  $UU^\dagger = \mathbb{1}$ ), since these constraints are additionally imposed by the Haar measure  $D[U]$  (see eq (1.95)).

<sup>20</sup>The JIMWLK equation cannot be solved analytically, but a numerical solution via a Langevin description exists for the leading order [18, 67]. For an analytic treatment, one usually parametrizes the evolution equation — this will be discussed in section 1.5.



conjugate amplitude of (1.105) is given by

$$\text{wavy line with two red arrows pointing right} \rightarrow ([U_{\mathbf{x}}]_{ik} \delta_{kl} [U_{\mathbf{y}}^\dagger]_{lj})^\dagger = [U_{\mathbf{y}}]_{jl} \delta_{lk} [U_{\mathbf{x}}^\dagger]_{ki} . \quad (1.109)$$

Since

$$[U_{\mathbf{x}}^\dagger]_{ik} = ([U_{\mathbf{x}}^\dagger]_{ki})^\dagger \neq [U_{\mathbf{x}}^\dagger]_{ki} \quad \text{and} \quad [U_{\mathbf{y}}]_{lj} = ([U_{\mathbf{y}}]_{jl})^\dagger \neq [U_{\mathbf{y}}]_{jl} , \quad (1.110)$$

the graphical notation (1.104) is not able to express the conjugate amplitude (1.109) due to the different placement of the indices on the Wilson lines. We therefore introduce more notation to accommodate this:

$$[U_{\mathbf{x}}^\dagger]_{ij} \rightarrow i \overleftarrow{\text{wavy line with red arrow}} j \quad \text{and} \quad [U_{\mathbf{y}}]_{ji} \rightarrow i \overrightarrow{\text{wavy line with red arrow}} j . \quad (1.111)$$

Using this notation, together with convention (1.107) for the Kronecker  $\delta$ , we can write the product (1.109) as

$$[U_{\mathbf{y}}]_{jl} \delta_{lk} [U_{\mathbf{x}}^\dagger]_{ki} = \text{wavy line with red arrows } \xrightarrow{\text{suppressing indices}} \text{wavy line with red arrows} , \quad (1.112)$$

where we understand that the bar acts on the entire tensor product of Wilson lines. (This notation will be revisited in chapter 5, section 5.1.4.1.) Thus, the conjugate amplitude is also mirrored by the birdtrack,

$$\left( \text{wavy line with red arrows} \right)^\dagger = \text{wavy line with red arrows} \xrightarrow{\text{birdtracks}} \text{wavy line with red arrows} . \quad (1.113)$$

In the present chapter, we want to make the target with which the eikonal interaction occurs explicit. We will denote the target by a grey box  $\blacksquare$ . Thus, a particular tensor product of Wilson lines  $U^{(\dagger)}$  together with the target is depicted as

$$U_{\mathbf{x}_1} \otimes \cdots \otimes U_{\mathbf{x}_m} \otimes U_{\mathbf{y}_1}^\dagger \otimes \cdots \otimes U_{\mathbf{y}_n}^\dagger \otimes \text{target} \rightarrow \begin{array}{c} \overleftarrow{\text{wavy line with red arrow}} U_{\mathbf{x}_1} \\ \vdots \\ \overleftarrow{\text{wavy line with red arrow}} U_{\mathbf{x}_m} \\ \overrightarrow{\text{wavy line with red arrow}} U_{\mathbf{y}_1}^\dagger \\ \vdots \\ \overrightarrow{\text{wavy line with red arrow}} U_{\mathbf{y}_n}^\dagger \\ \blacksquare \text{target} \end{array} . \quad (1.114)$$

The product (1.114) acts on the component of the quark–antiquark Fock space  $\mathcal{F}$ ,

$$\mathcal{F} := 0 \oplus \bigoplus_{\substack{i=1 \\ j=1}}^{\infty} \left\{ (V^{\otimes i}) \oplus ((V^*)^{\otimes j}) \oplus (V^{\otimes i} \otimes (V^*)^{\otimes j}) \right\} ; \quad (1.115)$$

consisting of  $m$  fundamental and  $n$  antifundamental, namely  $V^{\otimes m} \otimes (V^*)^{\otimes n} \otimes \text{target}$ .

Lastly, a Wilson line in the adjoint representation  $\tilde{U}_z^{ab}$  (corresponding to a gluon) will be denoted as<sup>21</sup>

$$\tilde{U}_z^{ab} \rightarrow a \overleftarrow{\text{wavy line with red arrow}} b \quad \text{and} \quad (\tilde{U}_z^{ab})^\dagger \rightarrow b \overrightarrow{\text{wavy line with red arrow}} a = b \overleftarrow{\text{wavy line with red arrow}} a = b \overrightarrow{\text{wavy line with red arrow}} a , \quad (1.116)$$

<sup>21</sup>In later sections we will change this notation slightly to better suit our purposes, but for now we strive for consistency between [71] and the material presented here.

where the last two equalities hold, since  $\tilde{U}_z^{ab}$  is real,

$$\left(\tilde{U}_z^{ab}\right)^* := \left(2\text{tr}\left(t^a U_z t^b U_z^\dagger\right)\right)^* = 2\left(\text{tr}\left(t^a U_z t^b U_z^\dagger\right)\right)^\dagger = 2\text{tr}\left(U_z t^b U_z^\dagger t^a\right) = \tilde{U}_z^{ab} . \quad (1.117)$$

This relation also clearly exhibits that an adjoint Wilson line can be decomposed into a fundamental and an antifundamental Wilson line, and is therefore contained in a Fock space component of the form (1.114).

It should be noted that, since  $U^{(\dagger)}$  is a group element of  $\text{SU}(N)$ , it may take the value of the identity  $\mathbb{1}$  even at the time of interaction between the particle worldline and the target. Physically, this corresponds to the situation where no interaction between the affected parton and the target took place. We would like to explicitly distinguish situations where all Wilson lines in (1.114) are gauge equivalent to unity (no interaction) with situations in which at least one Wilson line in the correlator is non-trivial (interaction) — ultimately, we are interested in the  $T$ -matrix element, not the  $S$ -matrix element, which necessitates this distinction. Diagrammatically, we will tell these cases apart by [71]

- laying a blue rectangle behind the tower of  $U^{(\dagger)}$ 's if we want to indicate an interaction
- drawing a dashed line behind the  $U^{(\dagger)}$ 's to indicate that each  $U^{(\dagger)}$  is gauge equivalent to  $\mathbb{1}$  and thus no interaction took place,

$\underbrace{\begin{array}{c} \text{---} \text{---} \text{---} \\ \vdots \\ \text{---} \text{---} \text{---} \\ \vdots \\ \text{---} \text{---} \text{---} \end{array}}_{\text{general tensor product of Wilson lines}} \longrightarrow \underbrace{\begin{array}{c} \text{---} \text{---} \text{---} \\ \vdots \\ \text{---} \text{---} \text{---} \\ \vdots \\ \text{---} \text{---} \text{---} \end{array}}_{\text{not all Wilson lines = 1 interaction}} \quad \text{or} \quad \underbrace{\begin{array}{c} \text{---} \text{---} \text{---} \\ \vdots \\ \text{---} \text{---} \text{---} \\ \vdots \\ \text{---} \text{---} \text{---} \end{array}}_{\text{all Wilson lines = 1 no interaction}} \quad (1.118)$

#### 1.4.2.2 Generating functionals and $k$ -point Wilson line correlators

Creating  $n$ -point correlators via functional differentiation of the generating functional corresponding to the theory at hand is a textbook topic (see for example [25, sec. 9.2]). In this method, one defines an object  $\bar{\mathcal{Z}}[J]$  called the *generating functional* as a functional integral over an exponential of the appropriate Lagrangian density  $\mathcal{L}$  including a source term. For example, if we are interested in a theory of a scalar field  $\phi(x)$ , then the appropriate generating functional is

$$\bar{\mathcal{Z}}[J] := \int \mathcal{D}[\phi] \exp\left\{ \int d^4x \left( \mathcal{L}[\phi] + J(x)\phi(x) \right) \right\} , \quad (1.119)$$

where  $J(x)$  is called the *source* and the integration  $\int \mathcal{D}[\phi]$  may be interpreted as an averaging procedure over the field configurations  $\phi$ . It is readily seen that  $n$  functional derivatives with respect to the source  $J$  at points  $x_1 \dots x_n$  gives rise to an  $n$ -point correlator of the field,

$$\frac{\delta}{\delta J(x_n)} \cdots \frac{\delta}{\delta J(x_2)} \frac{\delta}{\delta J(x_1)} \bar{\mathcal{Z}}[J] \Big|_{J=0} = \langle \phi(x_n) \dots \phi(x_2) \phi(x_1) \rangle . \quad (1.120)$$

It will be mathematically convenient to adopt this language of generating functionals here. In particular, we will consider the generating functional  $\bar{\mathcal{Z}}[J^\dagger, J, \tilde{J}]$ , which depends on three sources  $J^\dagger$ ,  $J$  and  $\tilde{J}$ ,

$$\bar{\mathcal{Z}}[J^\dagger, J, \tilde{J}] := \left\langle e^{\mathcal{S}_{\text{ext}}^{q\bar{q}g}[b, J^\dagger, J, \tilde{J}]} \right\rangle_{b, \alpha} , \quad (1.121a)$$

where  $\langle \dots \rangle_{b,\alpha}$  denotes an averaging procedure over the background field  $b$  and the fluctuation  $\alpha$ , and the action  $\mathcal{S}_{\text{ext}}^{q\bar{q}g}$  describes the coupling of quarks, antiquarks and gluons to the external sources  $J^\dagger$ ,  $J$  and  $\tilde{J}$  respectively,<sup>22</sup>

$$\mathcal{S}_{\text{ext}}^{q\bar{q}g}[b, J^\dagger, J, \tilde{J}] := \int d^2\mathbf{x} \left\{ \text{tr} \left( (J_{\mathbf{x}}^\dagger)^t U_{\mathbf{x}}[A_{\mathbf{x}}^+] \right) + \text{tr} \left( (J_{\mathbf{x}})^t U_{\mathbf{x}}^\dagger[A_{\mathbf{x}}^+] \right) + \text{tr} \left( (\tilde{J}_{\mathbf{x}}^\mu)^t \alpha_{\mathbf{x}}^\mu \right) \right\}. \quad (1.121b)$$

The generating functional  $\bar{\mathcal{Z}}[J^\dagger, J, \tilde{J}]$  is *not* to be confused with  $Z[U]$  describing the distribution of the gluons in the background field (*c.f.* eq. (1.100)), but the two are related: in particular,  $\bar{\mathcal{Z}}[J^\dagger, J, \tilde{J}]$  is the functional Fourier transform of  $Z[U]$  up to group theory constraints.

It should be noted that [18] omits the term proportional to the fluctuation  $\alpha$ , as it is anticipated that all correlators obtained from this term will eventually cancel due to the largest time Theorem [73, 74]. In this thesis, however, we prefer to keep the term  $\text{tr} \left( (\tilde{J}_{\mathbf{x}})^t \alpha_{\mathbf{x}}^+ \right)$  in  $\mathcal{S}_{\text{ext}}^{q\bar{q}g}$  and explicitly show that all contributions originating from it cancel, following the arguments made in [71].

In eq. (1.121b) we used the abbreviated notation

$$A_{\mathbf{x}}^+ := A_{\mathbf{x}}^+ t^a, \quad \alpha_{\mathbf{x}}^\mu := \alpha_{\mathbf{x}}^{\mu a} t_x^a, \quad \text{where } t_x^a \text{ is a group generator,} \quad (1.122a)$$

and

$$\text{tr} \left( (J_{\mathbf{x}}^\dagger)^t U_{\mathbf{x}}[A_{\mathbf{x}}^+] \right) = \left[ (J_{\mathbf{x}}^\dagger)_{ij} \right]^t \left( U_{\mathbf{x}}[A_{\mathbf{x}}^+] \right)_{ji} = (J_{\mathbf{x}}^\dagger)_{ij} \left( U_{\mathbf{x}}[A_{\mathbf{x}}^+] \right)_{ij}. \quad (1.122b)$$

The mathematical benefit of the generating functional as defined in eqns. (1.121) is that it allows us to easily extract arbitrary  $n$ -point Wilson line correlators by means of functional differentiation with respect to the sources  $J_{\mathbf{x}}^{(\dagger)}$  and  $\tilde{J}_{\mathbf{z}}$ : Introducing the shorthand notation  $\{J\} \equiv 0$  to mean  $J \stackrel{\dagger}{=} J^\dagger \stackrel{\dagger}{=} \tilde{J} \stackrel{\dagger}{=} 0$ , we, for example, have that

$$\frac{\delta}{\delta J_{\mathbf{x}}} \bar{\mathcal{Z}}[J^\dagger, J, \tilde{J}] \Big|_{\{J\} \equiv 0} = \left\langle \frac{\delta}{\delta J_{\mathbf{x}}} e^{\mathcal{S}_{\text{ext}}^{q\bar{q}g}[b, J^\dagger, J, \tilde{J}]} \right\rangle_{\alpha, b} \Big|_{\{J\} \equiv 0} = \left\langle U_{\mathbf{x}}^\dagger e^{\mathcal{S}_{\text{ext}}^{q\bar{q}g}[b, J^\dagger, J, \tilde{J}]} \right\rangle_{\alpha, b} \Big|_{\{J\} \equiv 0} = \langle U_{\mathbf{x}}^\dagger \rangle_b. \quad (1.123)$$

In the last step all  $\alpha$ -dependence was removed by setting  $\tilde{J} = 0$  such that  $\langle \dots \rangle_{\alpha, b} \rightarrow \langle \dots \rangle_b$ . For a  $k$ -point Wilson line correlator, one merely has to take  $k$  derivatives, for example

$$\frac{\delta}{\delta J_{\mathbf{x}_1}^\dagger} \dots \frac{\delta}{\delta J_{\mathbf{x}_m}^\dagger} \frac{\delta}{\delta J_{\mathbf{y}_1}} \dots \frac{\delta}{\delta J_{\mathbf{y}_n}} \bar{\mathcal{Z}}[J^\dagger, J, \tilde{J}] \Big|_{\{J\} \equiv 0} = \langle U_{\mathbf{x}_1} \otimes \dots \otimes U_{\mathbf{x}_m} \otimes U_{\mathbf{y}_1}^\dagger \otimes \dots \otimes U_{\mathbf{y}_n}^\dagger \rangle_b. \quad (1.124)$$

Similarly, one may perform a differentiation with respect to the source  $\tilde{J}$  to obtain a gluon in the final state,

$$\frac{\delta}{\delta \tilde{J}_{\mathbf{z}}} \bar{\mathcal{Z}}[J^\dagger, J, \tilde{J}] \Big|_{\{J\} \equiv 0} = \langle \alpha_{\mathbf{z}}^\mu \rangle_{\alpha, b}. \quad (1.125)$$

The observant reader will have noticed that this 1-point correlator vanishes identically [18]. While this

<sup>22</sup>Note that the sources here are matrices. The transpose of  $(J^{(\dagger)})^t$  in  $\mathcal{S}_{\text{ext}}^{q\bar{q}g}$  is needed such that differentiation with respect to  $J^{(\dagger)}$  yields the Wilson lines  $U^{(\dagger)}$  and not their transpose  $(U^{(\dagger)})^t$ ,

$$\frac{\partial}{\partial J_{\mathbf{x}}^\dagger} \text{tr} \left( (J_{\mathbf{y}}^\dagger)^t U_{\mathbf{y}} \right) = U_{\mathbf{x}}, \quad \text{but} \quad \frac{\partial}{\partial J_{\mathbf{x}}^\dagger} \text{tr} \left( J_{\mathbf{y}}^\dagger U_{\mathbf{y}} \right) = (U_{\mathbf{x}})^t.$$

certainly will come in handy at a later stage in our derivation of JIMWLK, we choose to keep the term  $\langle \alpha_{\mathbf{z}}^+ \rangle_{\alpha,b}$  around for the time being for reasons that will become apparent in sections 1.4.2.5 and 1.4.2.7.

It will be convenient to introduce the shorthand notation

$$\frac{\delta^{m,n}}{\delta \mathbf{J}_{\mathbf{x},\mathbf{y}}} := \frac{\delta}{\delta J_{\mathbf{x}_1}^\dagger} \cdots \frac{\delta}{\delta J_{\mathbf{x}_m}^\dagger} \frac{\delta}{\delta J_{\mathbf{y}_1}} \cdots \frac{\delta}{\delta J_{\mathbf{y}_n}} \quad (1.126a)$$

$$\mathbf{U}_{\mathbf{x},\mathbf{y}}^{m,n} := U_{\mathbf{x}_1} \otimes \cdots \otimes U_{\mathbf{x}_m} \otimes U_{\mathbf{y}_1}^\dagger \otimes \cdots \otimes U_{\mathbf{y}_n}^\dagger \quad (1.126b)$$

such that eq. (1.124) becomes

$$\frac{\delta^{m,n}}{\delta \mathbf{J}_{\mathbf{x},\mathbf{y}}} \bar{\mathcal{Z}}[J^\dagger, J, \tilde{J}] \Big|_{\{J\} \equiv 0} = \langle \mathbf{U}_{\mathbf{x},\mathbf{y}}^{m,n} \rangle_b . \quad (1.127)$$

As we stated in the beginning of this section, we derive the JIMWLK equation at LO with at most one gluon in the final states. Thus, we are interested in generating Wilson lines from  $Z$  by differentiating at most once with respect to  $\tilde{J}$ . The most general such form is

$$\left( \frac{\delta^{m,n}}{\delta \mathbf{J}_{\mathbf{x},\mathbf{y}}} + \frac{\delta^{m,n}}{\delta \mathbf{J}_{\mathbf{x},\mathbf{y}}} \frac{\delta}{\delta \tilde{J}_{\mathbf{z}}} \right) \bar{\mathcal{Z}}[J^\dagger, J, \tilde{J}] \Big|_{\{J\} \equiv 0} = \langle \mathbf{U}_{\mathbf{x},\mathbf{y}}^{m,n} \rangle_b + \langle \mathbf{U}_{\mathbf{x},\mathbf{y}}^{m,n} \otimes \langle \alpha_{\mathbf{z}}^\mu \rangle_\alpha \rangle_b , \quad (1.128)$$

where again the second term in the sum (1.128) vanishes by virtue of the 1-point correlator being zero, but we will keep both terms of (1.128) for the time being.

### 1.4.2.3 Diagrammatic notation for singlet states and the target average

For the Wilson line correlators discussed in the previous section to describe a physical quantity, the index legs corresponding to individual Wilson lines have to combine into color neutral configurations before as well as after the interaction — this is a consequence of confinement. This was discussed in section 1.1.2.3, where the color neutral photon was said to split into a globally color neutral configuration of color charged objects.

Mathematically, it is the representation of  $\text{SU}(N)$ , in which the states  $|i\rangle, |j\rangle \in V^{\otimes m} \otimes (V^*)^{\otimes n}$  are given, that provides information about the  $m q + n \bar{q}$ -configuration interacting with the target (i.e. the configuration that is acted upon by the product of Wilson lines  $\mathbf{U}_{\mathbf{x},\mathbf{y}}^{m,n}$ ). For example, if the state  $|i\rangle$  is in the adjoint representation, it is interpreted as a gluon.  $|i\rangle$  is said to be color neutral if in the limit where all coordinate dependence of the Wilson lines coincide, a *coincidence limit*, it satisfies

$$\mathbf{U}_{\mathbf{x},\mathbf{y}}^{m,n} |i\rangle \xrightarrow{\mathbf{x}_1=\dots=\mathbf{x}_m=\mathbf{y}_1=\dots=\mathbf{y}_n} \mathbf{U}^{m,n} |i\rangle = |i\rangle \quad (1.129a)$$

$$\langle i | (\mathbf{U}_{\mathbf{x},\mathbf{y}}^{m,n})^\dagger \xrightarrow{\mathbf{x}_1=\dots=\mathbf{x}_m=\mathbf{y}_1=\dots=\mathbf{y}_n} \langle i | (\mathbf{U}^{m,n})^\dagger = \langle i | , \quad (1.129b)$$

and similarly for  $|j\rangle$ . Such states are also referred to as *global color singlet states* of  $\text{SU}(N)$ .

Consider the Wilson line correlator  $\langle \mathbf{U}_{\mathbf{x},\mathbf{y}}^{m,n} \rangle_b$  and insert a full set of states on either side of  $\mathbf{U}_{\mathbf{x},\mathbf{y}}^{m,n}$  as

$$\langle \mathbf{U}_{\mathbf{x},\mathbf{y}}^{m,n} \rangle_b = \left\langle \left( \sum_j |j\rangle \langle j| \right) \mathbf{U}_{\mathbf{x},\mathbf{y}}^{m,n} \left( \sum_i |i\rangle \langle i| \right) \right\rangle_b = \sum_{j,i} |j\rangle \langle j | \mathbf{U}_{\mathbf{x},\mathbf{y}}^{m,n} |i\rangle \rangle_b \langle i| ; \quad (1.130)$$



we were able to take  $|j\rangle$  and  $\langle i|$  out of the average, as these states do *not* depend on the background field  $b$ . Due to confinement, all non-singlet states are irrelevant in a *physical* correlator, thus causing (1.130) to reduce to

$$\sum_{j,i} |j\rangle \langle \langle j | \mathbf{U}_{\mathbf{x},\mathbf{y}}^{m,n} | i \rangle \rangle_b \langle i| \longrightarrow \sum_{j,i \text{ singlets}} |j\rangle \langle \langle j | \mathbf{U}_{\mathbf{x},\mathbf{y}}^{m,n} | i \rangle \rangle_b \langle i| \quad (1.131)$$

when requiring it to correspond to a physically meaningful object. Thus, the relevant object to consider when working with Wilson line correlators is  $\langle \langle j | \mathbf{U}_{\mathbf{x},\mathbf{y}}^{m,n} | i \rangle \rangle_b$ , where  $|i\rangle, |j\rangle$  are globally color singlet. Finding an algorithm to construct such states for an arbitrary combination of fundamental and antifundamental lines will be one of the main tasks fulfilled in this thesis, *c.f.* chapter 5.

Diagrammatically, we denote a color neutral state  $|i\rangle$  as



$$\text{color-neutral state}; \quad (1.132)$$

this notation is inspired by Clebsch-Gordan operators, which have no index line exiting on the right if the representation corresponding to such an index line would be 1-dimensional (i.e. a *singlet* representation) [72], *c.f.* later chapter 5. The arrows on the index legs in (1.132) indicate whether the particle is in the fundamental or the antifundamental representation,

$$\text{fundamental rep.: } \longleftarrow \quad \text{antifundamental rep.: } \longrightarrow. \quad (1.133)$$

The arrows may be suppressed if the representation of the affected leg is clear: Since the Wilson lines acting on these legs will always point in the same direction as the representational arrows (1.133), we will often neglect the representation arrow and only retain the Wilson line arrow. For the remainder of this section, we assume that the singlet states  $|i\rangle$  are orthonormal. That an orthonormal basis of singlet states can always be found is made clear in chapter 5, where we also provide a construction algorithm.

Lastly, following [71], we represent the average over the color configuration in the target  $\langle \dots \rangle_{b,\alpha}$  (*c.f.* our discussion in section 1.3.1) as

$$\langle \dots \rangle_{b,\alpha} \longrightarrow \text{---} \text{---} \text{---}; \quad (1.134)$$

the goal of the JIMWLK equation is to make this target  $Y$ -dependent to adjust for the increasingly important gluon fluctuations at higher energies.

The graphic notation introduced so far is summarized in Figure 1.6.

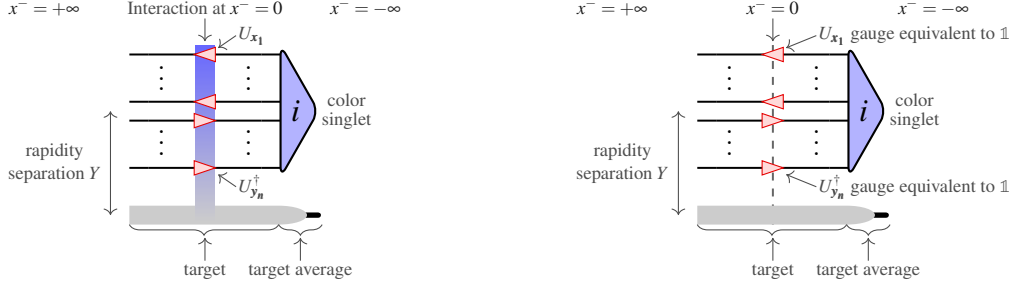


Figure 1.6: These figures summarize the diagrammatic notation that is used in this section. The left graphic depicts a singlet  $|i\rangle$  consisting of  $m$  quarks and  $n$  antiquarks interacting eikonally (all gluon interactions sum into Wilson lines  $U^{(\dagger)}$ ) with the target. The interaction is marked by the blue slab at the interaction time  $x^- = 0$ . In the right graphic, all Wilson lines are gauge equivalent to unity, which is to say that these Wilson lines are independent of the transverse coordinates  $\mathbf{x}, \mathbf{y}$ . Since  $|i\rangle$  is a singlet state satisfying eqns. (1.129),  $|i\rangle$  is unaffected by such a configuration of Wilson lines, implying that no interaction has taken place. This is denoted by the dashed line (rather than a blue slab) at the “interaction time”  $x^- = 0$ . Note that a large rapidity separation between projectile and target is required for the interaction to assemble into Wilson lines (*c.f.* eq. (1.5) and section 1.2). [71]

#### 1.4.2.4 Cross section without fluctuations in the color field

We are now in a position to calculate the cross section describing the eikonal interaction between a  $k$ -point correlator and a target. At this point, we consider the  $k$ -point correlator to consist of fundamental and antifundamental Wilson lines only, setting fluctuations in the color field (i.e. adjoint lines in the correlator) to zero; this will give us a basis with which we may compare the cross section of a Wilson line correlator with a 1-gluon fluctuation.

Using the language of generating functionals introduced in section 1.4.2.2, we set  $\tilde{J}$  to zero to eliminate the fluctuations in the background field,

$$\left\langle \left( \frac{\delta^{m,n}}{\delta \mathbf{J}_{\mathbf{x}, \mathbf{y}}} + \frac{\delta^{m,n}}{\delta \mathbf{J}_{\mathbf{x}, \mathbf{y}}} \frac{\delta}{\delta \tilde{J}_{\mathbf{z}}} \right) e^{\mathcal{S}_{\text{ext}}^{q\bar{q}g}[b, J^\dagger, J, \tilde{J}]} \right\rangle_{b, \alpha} \Big|_{\{J\} \equiv 0} \xrightarrow{\tilde{J}=0} \left\langle \frac{\delta^{m,n}}{\delta \mathbf{J}_{\mathbf{x}, \mathbf{y}}} e^{\mathcal{S}_{\text{ext}}^{q\bar{q}g}[b, J^\dagger, J]} \right\rangle_b \Big|_{\{J\} \equiv 0}, \quad (1.135)$$

where we used notation (1.126a) for the collective source derivative  $\frac{\delta^{m,n}}{\delta \mathbf{J}_{\mathbf{x}, \mathbf{y}}}$ . Incidentally, this result is exactly what we would have obtained even if we had kept  $\tilde{J}$ , by virtue of the 1-point correlator  $\langle \alpha_{\mathbf{z}}^\mu \rangle_\alpha$  being zero [18],

$$\left( \frac{\delta^{m,n}}{\delta \mathbf{J}_{\mathbf{x}, \mathbf{y}}} + \frac{\delta^{m,n}}{\delta \mathbf{J}_{\mathbf{x}, \mathbf{y}}} \frac{\delta}{\delta \tilde{J}_{\mathbf{z}}} \right) \bar{\mathcal{Z}}[J^\dagger, J, \tilde{J}] \Big|_{\{J\} \equiv 0} = \langle \mathbf{U}_{\mathbf{x}, \mathbf{y}}^{m,n} \rangle_b + \left\langle \mathbf{U}_{\mathbf{x}, \mathbf{y}}^{m,n} \otimes \underbrace{\langle \alpha_{\mathbf{z}}^\mu \rangle_\alpha}_{=0} \right\rangle_b = \langle \mathbf{U}_{\mathbf{x}, \mathbf{y}}^{m,n} \rangle_b. \quad (1.136)$$

To calculate the total cross section diagrammatically, we adopt the convention of [18, 71] and refer to the case where all Wilson lines are gauge equivalent to unity as the *in*-state, and the situation where not all Wilson

lines are gauge equivalent to  $\mathbb{1}$  as the *out*-state,

$$|\text{in}\rangle = \text{[diagram]} \quad \text{and} \quad |\text{out}\rangle = \text{[diagram]}. \quad (1.137)$$

The  $T$ -matrix contribution  $|\text{out}\rangle - |\text{in}\rangle$ ,

$$|\text{out}\rangle - |\text{in}\rangle = \text{[diagram]} - \text{[diagram]}, \quad (1.138)$$

then determines the total cross section

$$\sigma_{\text{tot}} = \left| |\text{out}\rangle - |\text{in}\rangle \right|^2 = \langle \text{out} | \text{out} \rangle - \langle \text{out} | \text{in} \rangle - \langle \text{in} | \text{out} \rangle + \langle \text{in} | \text{in} \rangle \quad (1.139)$$

due to the optical Theorem [25]. The states  $\langle \text{in} | := |\text{in}\rangle^\dagger$  and  $\langle \text{out} | := |\text{out}\rangle^\dagger$  are graphically obtained by flipping the diagram about its vertical axis and reversing the arrows [72] (this will be made precise in section 3.3.1 of chapter 3), and then adding a bar over the tensor product of Wilson lines according to eq. (1.111),

$$\left( \text{[diagram]} \right)^\dagger = \text{[diagram]} \quad \text{and} \quad \left( \text{[diagram]} \right)^\dagger = \text{[diagram]}, \quad (1.140)$$

such that the cross section becomes

$$\left\langle \left\langle j \right| \frac{\delta^{m,n}}{\delta \mathbf{J}_{\mathbf{x}, \mathbf{y}}} e^{\mathcal{S}_{\text{ext}}^{qqg}[b, J^\dagger, J, \bar{J}]} \right| \left| i \right\rangle \right\rangle_{b, \alpha} \Big|_{\{J\} \equiv 0} = \left( \text{[diagram]} - \text{[diagram]} \right) \left( \text{[diagram]} - \text{[diagram]} \right). \quad (1.141)$$

Note that we projected onto the singlet states  $|i\rangle, \langle j|$  to remind the reader that a physical observable corresponds to a *singlet* Wilson line correlator, but the general calculation does not require this projection (*c.f.* [18]). Furthermore, by keeping  $|i\rangle$  and  $|j\rangle$  distinct, we allow for the fact that the Wilson lines after the interaction may re-combine into different singlet states than before the interaction. This is possible if the algebra of singlets is large enough to admit more than one singlet state (*c.f.* Theorems 5.2 and 5.4 in chapter 5). However, all cross-terms in which all Wilson lines are gauge equivalent to  $\mathbb{1}$  will vanish unless  $|i\rangle = |j\rangle$ , since the singlet states  $|i\rangle$  are assumed to be orthonormal.

Let us now look at each term in (1.141) in more detail: When multiplying out the brackets, we connect the

Wilson lines of the various states. “Time”  $x^-$  thus runs as (*c.f.* Figure 1.6)

$$(1.142)$$

In connecting the Wilson lines graphically, we actually perform an integration over the transverse momenta. This produces a  $\delta$  function in the transverse variables which, in turn, identifies the transverse coordinates of the Wilson lines on either side of the the cut  $x^- = +\infty$  [71]. Thus, each product of Wilson lines  $U_{\mathbf{y}}^\dagger U_{\mathbf{x}}$  appearing in the  $\langle \text{out} | \text{out} \rangle$ -term<sup>23</sup> becomes  $U_{\mathbf{x}}^\dagger U_{\mathbf{x}} = \mathbb{1}$  such that

$$(1.143)$$

where the last step follows from the orthonormality of the singlet states  $|i\rangle$ . The cross section (1.141) therefore reduces to

$$(1.144)$$

To confirm this, consider the familiar example of a photon splitting into a  $q\bar{q}$ -dipole, which then interacts eikonally with a dense gluonic target. Diagrammatically, the cross section of such an interaction is given by [71] (*c.f.* Figure 1.7)

$$(1.145)$$

where we chose to explicitly represent the photon as  $\text{Wavy}$ . Due to the transverse momentum integration

<sup>23</sup>Notice that the Wilson lines appearing in the  $|\text{in}\rangle$ -state do not carry a coordinate dependence by virtue of their being gauge equivalent to unity (see Figure 1.6). Thus, no simplification from the integration over the transverse momenta takes place in the  $\langle \text{in} | \text{in} \rangle$ ,  $\langle \text{in} | \text{out} \rangle$  and  $\langle \text{out} | \text{in} \rangle$  terms.

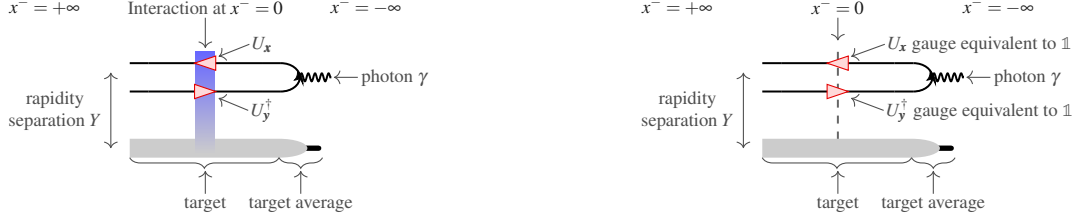


Figure 1.7: These diagrams depict an eikonal interaction between a projectile and a target with a rapidity separation  $Y$ . In our case, the projectile is a photon which splits into a  $q\bar{q}$ -pair. This dipole interacts eikonally with a target at  $x^- = 0$ . The Wilson lines emanating from the interaction are marked by the pink arrowheads. The blue slab in the left diagram indicates that not all Wilson lines are gauge equivalent to unity, and hence an interaction has taken place. In the right diagram, the dashed line at  $x^- = 0$  indicates that all Wilson lines are gauge equivalent to  $\mathbb{1}$ , and thus no interaction with the target has taken place. In both diagrams, the target undergoes an averaging procedure over the gluon field. [71]

that is implicit to the graphical procedure of connecting index lines, one obtains

$$\begin{aligned}
 \left| \begin{array}{c} \text{Diagram 1} \\ \text{Diagram 2} \end{array} \right|^2 &= \begin{array}{c} \text{Diagram 3} \\ \text{Diagram 4} \\ \text{Diagram 5} \\ \text{Diagram 6} \end{array} \\
 &= 2 \cdot \begin{array}{c} \text{Diagram 7} \\ \text{Diagram 8} \end{array} - \left\{ \begin{array}{c} \text{Diagram 9} \\ \text{Diagram 10} \end{array} \right\} . \quad (1.146)
 \end{aligned}$$

$\text{tr}(U_y^\dagger U_y U_x^\dagger U_x) = \text{tr}(\mathbb{1})$     
  $\text{tr}(U_y U_x^\dagger) = (\text{tr}(U_y^\dagger U_x))^\dagger$     
  $\text{tr}(U_y^\dagger U_x)$     
  $\text{tr}(\mathbb{1})$

Let us denote the size of the dipole as  $\mathbf{r} := \mathbf{x} - \mathbf{y}$ , and the dipole *amplitude* by

$$\mathcal{N}_{\mathbf{x}\mathbf{y}} := \frac{\langle \text{tr}(\mathbb{1} - U_{\mathbf{y}}^\dagger U_{\mathbf{x}}) \rangle_b}{N} , \quad (1.147)$$

where  $N$  is taken to be  $N_c$  (the number of colors). Then, the total cross section is [71]

$$\sigma_{\text{total}} = 2 \int d^2\mathbf{r} \int_0^1 d\chi |\Psi(\chi, r^2, Q^2)|^2 \int d^2\mathbf{w} \mathcal{N}_{\mathbf{x}\mathbf{y}} , \quad (1.148)$$

where  $\mathbf{w} = \frac{1}{2}(\mathbf{x} + \mathbf{y})$ , and  $|\Psi(\chi, r^2, Q^2)|^2$  describes the probability of finding a  $q\bar{q}$ -dipole with size  $\mathbf{r}$  and longitudinal momentum fraction  $\chi$  at a fixed resolution  $Q^2$  within the photon.

#### 1.4.2.5 Fluctuations in the color field

As the energy (equivalently the rapidity  $Y$ ) increases, fluctuations in the background field become non-negligible. That is, we have to replace the background field  $b$  by a field  $A$  that includes corrections (fluctuations)  $\alpha$ ,

$$b \longrightarrow A = b + \alpha , \quad (1.149)$$

as was already discussed in eq. (1.30). At leading order, we consider the correction to be a single gluon. There are three ways in which such a gluon can enter the Wilson line correlator: It can connect two parton-lines (the two partons interact by means of a gluon), it can start and end on the same parton-line (self-energy),

or it may start on a parton-line and enter into the final state.<sup>24</sup> These considerations determine which terms we keep and which we neglect at leading order when expanding the generating functional

$$\left\langle e^{\mathcal{S}_{\text{ext}}^{q\bar{q}g}[b+\alpha, J^\dagger, J, \tilde{J}]} \right\rangle_{b,\alpha} \quad (1.150)$$

about the background field  $b$ .

We begin by splitting the exponential into a product of terms containing the fluctuation  $\alpha$  indirectly via  $U^{(\dagger)}$ , and terms with direct dependence on  $\alpha$ ,

$$\left\langle e^{\mathcal{S}_{\text{ext}}^{q\bar{q}g}[b+\alpha, J^\dagger, J, \tilde{J}]} \right\rangle_{b,\alpha} = \left\langle e^{\int d^2\mathbf{x} \{ \text{tr}((J_{\mathbf{x}}^\dagger)^t U_{\mathbf{x}}[A_{\mathbf{x}}^\dagger]) + \text{tr}((J_{\mathbf{x}})^t U_{\mathbf{x}}^\dagger[A_{\mathbf{x}}^\dagger]) \}} \cdot e^{\int d^2\mathbf{x} \{ \text{tr}((\tilde{J}_{\mathbf{x}}^\mu)^t \alpha_{\mathbf{x}}^\mu) \}} \right\rangle_{b,\alpha}. \quad (1.151)$$

We then perform a Taylor expansion of  $A$  about  $b$  on each exponential separately, recalling that the Taylor expansion of a product is the product of Taylor expansions,

$$\begin{aligned} \left\langle e^{\mathcal{S}_{\text{ext}}^{q\bar{q}g}[b+\alpha, J^\dagger, J, \tilde{J}]} \right\rangle_{b,\alpha} &= \left\langle \left( 1 + \int_u \alpha_u^{+a} \frac{\delta}{\delta b_u^{+a}} + \frac{1}{2} \int_{uv} \alpha_u^{+a} \frac{\delta}{\delta b_u^{+a}} \alpha_v^{+b} \frac{\delta}{\delta b_v^{+b}} + \mathcal{O}(A^3) \right) \times \right. \\ &\quad \left. \times \left( 1 + \int_w \alpha_w^{+c} \frac{\delta}{\delta \alpha_w^{+c}} + \mathcal{O}(\alpha^2) \right) e^{\mathcal{S}_{\text{ext}}^{q\bar{q}g}[b, J^\dagger, J, \tilde{J}]} \right\rangle_{b,\alpha}, \end{aligned} \quad (1.152a)$$

where we used the shorthand notation

$$\int_u := \int d^4u \quad \text{and} \quad \int_{uv} := \int d^4u \int d^4v. \quad (1.152b)$$

Note that we truncated the second expansion already at order  $\mathcal{O}(\alpha^2)$ . This was done because we would like to consider correlators with at most 1 gluon in the final state, while terms with two derivatives  $\frac{\delta}{\delta \alpha_u^{+a}} \frac{\delta}{\delta \alpha_v^{+b}}$  would give rise to two gluons in the final state.

Recall that the average over the fields is linear (it is merely an integral over field configurations as given in eq. (1.100)), so we may distribute  $\langle \cdots \rangle_{b,\alpha}$  over the sum. Additionally, we multiply out the brackets in (1.152a) and rearrange terms,

$$\begin{aligned} \left\langle e^{\mathcal{S}_{\text{ext}}^{q\bar{q}g}[b+\alpha, J^\dagger, J, \tilde{J}]} \right\rangle_{b,\alpha} &= \left\langle e^{\mathcal{S}_{\text{ext}}^{q\bar{q}g}[b, J^\dagger, J, \tilde{J}]} \right\rangle_b \\ &\quad + \int_u \left\langle \langle \alpha_u^{+a} \rangle_\alpha [b] \left( \frac{\delta}{\delta b_u^{+a}} + \frac{\delta}{\delta \alpha_u^{+a}} \right) e^{\mathcal{S}_{\text{ext}}^{q\bar{q}g}[b, J^\dagger, J, \tilde{J}]} \right\rangle_b \\ &\quad + \frac{1}{2} \int_{uv} \left\langle \langle \alpha_u^{+a} \alpha_v^{+b} \rangle_\alpha [b] \left( \frac{\delta}{\delta b_u^{+a}} \frac{\delta}{\delta b_v^{+b}} + \frac{\delta}{\delta b_u^{+a}} \frac{\delta}{\delta \alpha_v^{+b}} \right) e^{\mathcal{S}_{\text{ext}}^{q\bar{q}g}[b, J^\dagger, J, \tilde{J}]} \right\rangle_b \\ &\quad + \mathcal{O}(A^3). \end{aligned} \quad (1.153)$$

The first term in this expansion simply gives the cross section with no gluon fluctuations (eq. (1.144)) once differentiation with respect to the sources  $J^{(\dagger)}$  and  $\tilde{J}$  has been performed. The term proportional to the 1-point correlator  $\langle \alpha_u^{+a} \rangle_\alpha$  is

$$\int_u \left\langle \langle \alpha_u^{+a} \rangle_\alpha [b] \left( \frac{\delta}{\delta b_u^{+a}} \mathcal{S}_{\text{ext}}^{q\bar{q}g}[b, J^\dagger, J, \tilde{J}] + \frac{\delta}{\delta \alpha_u^{+a}} \mathcal{S}_{\text{ext}}^{q\bar{q}g}[b, J^\dagger, J, \tilde{J}] \right) e^{\mathcal{S}_{\text{ext}}^{q\bar{q}g}[b, J^\dagger, J, \tilde{J}]} \right\rangle_b. \quad (1.154a)$$

<sup>24</sup>We will see that all terms arising from the last of the three contributions cancel amongst themselves due to the largest time Theorem [71] (see section 1.4.2.10).

It should be noted that, even though the 1-point correlator itself is zero, differentiation of (1.154a) remedies this dilemma by bringing down an additional factor of  $\alpha$ , turning the 1-point correlator into a 2-point correlator, as will be explained in section 1.4.2.7.

Expanding the brackets in the term proportional to the 2-point correlator  $\langle \alpha_u^{+a} \alpha_v^{+b} \rangle_\alpha$  in (1.153) gives

$$\begin{aligned} & \frac{1}{2} \int_{uv} \left\langle \left\langle \alpha_u^{+a} \alpha_v^{+b} \right\rangle_\alpha [b] \times \right. \\ & \quad \times \left\{ \left( \frac{\delta}{\delta b_u^{+a}} \mathcal{S}_{\text{ext}}^{q\bar{q}g}[b, J^\dagger, J, \tilde{J}] \right) \left( \frac{\delta}{\delta b_v^{+b}} \mathcal{S}_{\text{ext}}^{q\bar{q}g}[b, J^\dagger, J, \tilde{J}] \right) + \left( \frac{\delta}{\delta b_u^{+a}} \frac{\delta}{\delta b_v^{+b}} \mathcal{S}_{\text{ext}}^{q\bar{q}g}[b, J^\dagger, J, \tilde{J}] \right) \right. \\ & \quad + 2 \left( \frac{\delta}{\delta b_u^{+a}} \mathcal{S}_{\text{ext}}^{q\bar{q}g}[b, J^\dagger, J, \tilde{J}] \right) \left( \frac{\delta}{\delta \alpha_v^{+b}} \mathcal{S}_{\text{ext}}^{q\bar{q}g}[b, J^\dagger, J, \tilde{J}] \right) + 2 \left( \frac{\delta}{\delta b_u^{+a}} \frac{\delta}{\delta \alpha_v^{+b}} \mathcal{S}_{\text{ext}}^{q\bar{q}g}[b, J^\dagger, J, \tilde{J}] \right) \left. \right\} \times \\ & \quad \times e^{\mathcal{S}_{\text{ext}}^{q\bar{q}g}[b, J^\dagger, J, \tilde{J}]} \Bigg\rangle_b . \end{aligned} \quad (1.154b)$$

We notice that the last term in (1.154b),

$$\frac{\delta}{\delta b_u^{+a}} \frac{\delta}{\delta \alpha_v^{+b}} \mathcal{S}_{\text{ext}}^{q\bar{q}g}[b, J^\dagger, J, \tilde{J}] , \quad (1.155)$$

vanishes identically since  $\frac{\delta}{\delta \alpha_v^{+b}} \mathcal{S}_{\text{ext}}^{q\bar{q}g}[b, J^\dagger, J, \tilde{J}]$  is independent of the background field  $b$ . We may thus drop this term in eq. (1.154b).

To facilitate a discussion of the remaining terms of eqns. (1.154), we need to calculate the derivative of  $\mathcal{S}_{\text{ext}}^{q\bar{q}g}[b, J^\dagger, J, \tilde{J}]$  with respect to the fluctuation  $\alpha$ ,

$$\begin{aligned} \frac{\delta}{\delta \alpha_v^{+b}} \mathcal{S}_{\text{ext}}^{q\bar{q}g}[b, J^\dagger, J, \tilde{J}] &= \frac{\delta}{\delta \alpha_v^{+b}} \int d^2 \mathbf{x} \left\{ \text{tr} \left( (J_{\mathbf{x}}^\dagger)^t U_{\mathbf{x}}[A_{\mathbf{x}}^+] \right) + \text{tr} \left( (J_{\mathbf{x}})^t U_{\mathbf{x}}^\dagger[A_{\mathbf{x}}^+] \right) + \text{tr} \left( (\tilde{J}_{\mathbf{x}}^\mu)^t \alpha_{\mathbf{x}}^\mu \right) \right\} \\ &= \int d^2 \mathbf{x} \left\{ \text{tr} \left( (\tilde{J}_{\mathbf{x}}^\mu)^t \frac{\delta}{\delta \alpha_v^{+b}} \alpha_{\mathbf{x}}^{\mu a} t_x^a \right) \right\} \\ &= \int d^2 \mathbf{x} \left\{ \text{tr} \left( (\tilde{J}_{\mathbf{x}}^\mu)^t \delta^{+\mu} \delta_{v-x-} \delta_{0v+} \delta_{\mathbf{x}v}^2 \delta^{ab} t_x^a \right) \right\} \\ &= \delta_{v-x-} \delta_{0v+} \text{tr} \left( (\tilde{J}_v^+)^t t_v^b \right) , \end{aligned} \quad (1.156a)$$

as well as the derivative with respect to the background field  $b$ ,

$$\begin{aligned} \frac{\delta}{\delta b_v^{+b}} \mathcal{S}_{\text{ext}}^{q\bar{q}g}[b, J^\dagger, J, \tilde{J}] &= \frac{\delta}{\delta b_v^{+b}} \int d^2 \mathbf{x} \left\{ \text{tr} \left( (J_{\mathbf{x}}^\dagger)^t U_{\mathbf{x}}[A_{\mathbf{x}}^+] \right) + \text{tr} \left( (J_{\mathbf{x}})^t U_{\mathbf{x}}^\dagger[A_{\mathbf{x}}^+] \right) + \text{tr} \left( (\tilde{J}_{\mathbf{x}}^\mu)^t \alpha_{\mathbf{x}}^\mu \right) \right\} \\ &= \int d^2 \mathbf{x} \left\{ \text{tr} \left( (J_{\mathbf{x}}^\dagger)^t \frac{\delta}{\delta b_v^{+b}} U_{\mathbf{x}}[A_{\mathbf{x}}^+] \right) + \text{tr} \left( (J_{\mathbf{x}})^t \frac{\delta}{\delta b_v^{+b}} U_{\mathbf{x}}^\dagger[A_{\mathbf{x}}^+] \right) \right\} . \end{aligned} \quad (1.156b)$$

Eq. (1.156b) introduces functional derivatives of the Wilson lines, which will be discussed in the following section.

#### 1.4.2.6 Functional differentiation of a Wilson line

The Lorentz contraction of the target localizes the interaction between projectile and target to  $x^- = 0$ . Thus, as explained in section 1.4.2.1, the only point at which  $U_{\mathbf{x}}$  is non-trivial is when the particle worldline pierces the  $x^- = 0$  plane at the transverse coordinate  $\mathbf{x}$ . Therefore, instead of taking  $U_{\mathbf{x}}$  to run along the

curved path that is the particle worldline, we may consider it a straight line from  $-\infty$  to  $+\infty$  parallel to the  $x^-$ -direction, piercing the  $x^- = 0$  plane at the particular transverse coordinate  $\mathbf{x}$ . We modify our notation to make this path explicit:

$$U_{\mathbf{x}} = U_{[\mathbf{x}, +\infty, -\infty]} . \quad (1.157)$$

In appendix 1.A, we show that the functional derivative of  $U_{[\mathbf{x}, +\infty, -\infty]}$  with respect to the background field  $b_v^{+b}$  is given by (c.f. eq. (1.270))

$$\frac{\delta}{\delta b_v^{+b}} U_{[\mathbf{x}, +\infty, -\infty]} = (-ig) \delta_{\mathbf{x}\mathbf{v}}^2 \delta_{v+0} U_{[\mathbf{x}, +\infty, v^-]} t_v^b U_{[\mathbf{x}, v^-, -\infty]} . \quad (1.158)$$

Since the Wilson lines at hand are all trivial except at  $x^- = 0$ , a Wilson line over a finite path piercing the  $x^- = 0$  plane may be extended to infinity, while any Wilson line over a path not piercing the  $x^- = 0$  plane is gauge equivalent to unity. We therefore have:

$$\text{if } v^- > 0: \quad U_{[\mathbf{x}, +\infty, v^-]} = \mathbb{1} \quad \text{and} \quad U_{[\mathbf{x}, v^-, -\infty]} = U_{[\mathbf{x}, +\infty, -\infty]} = U_{\mathbf{x}} \quad (1.159a)$$

$$\text{if } v^- < 0: \quad U_{[\mathbf{x}, +\infty, v^-]} = U_{[\mathbf{x}, +\infty, -\infty]} = U_{\mathbf{x}} \quad \text{and} \quad U_{[\mathbf{x}, v^-, -\infty]} = \mathbb{1} . \quad (1.159b)$$

Using eqns. (1.159), we can write the derivative  $\frac{\delta}{\delta b_v^{+b}} U_{[\mathbf{x}, +\infty, -\infty]}$  given in (1.158) as

$$\frac{\delta}{\delta b_v^{+b}} U_{\mathbf{x}} = (-ig) \delta_{\mathbf{x}\mathbf{v}}^2 \delta_{v+0} (\theta(v^-) t_v^b U_{\mathbf{x}} + \theta(-v^-) U_{\mathbf{x}} t_v^b) . \quad (1.160a)$$

Similarly, the derivative of the antifundamental Wilson line is

$$\frac{\delta}{\delta b_v^{+b}} U_{\mathbf{x}}^\dagger = (+ig) \delta_{\mathbf{x}\mathbf{v}}^2 \delta_{v+0} (\theta(v^-) U_{\mathbf{x}}^\dagger t_v^b + \theta(-v^-) t_v^b U_{\mathbf{x}}^\dagger) . \quad (1.160b)$$

Substituting this back into eq. (1.156b) yields

$$\begin{aligned} \frac{\delta}{\delta b_v^{+b}} \mathcal{S}_{\text{ext}}^{q\bar{q}g}[b, J^\dagger, J, \tilde{J}] &= (-ig) \delta_{v+0} \left\{ \theta(v^-) [\text{tr}((J_v^\dagger)^t t_v^b U_v) - \text{tr}((J_v)^t U_v^\dagger t_v^b)] \right. \\ &\quad \left. + \theta(-v^-) [\text{tr}((J_v^\dagger)^t U_v t_v^b) - \text{tr}((J_v)^t t_v^b U_v^\dagger)] \right\} , \end{aligned} \quad (1.161)$$

where we were able to perform the integration over  $\mathbf{x}$  due to the presence of  $\delta_{\mathbf{x}\mathbf{v}}^2$ . Squaring this term gives the contribution

$$\begin{aligned} &\left( \frac{\delta}{\delta b_u^{+a}} \mathcal{S}_{\text{ext}}^{q\bar{q}g}[b, J^\dagger, J, \tilde{J}] \right) \cdot \left( \frac{\delta}{\delta b_v^{+b}} \mathcal{S}_{\text{ext}}^{q\bar{q}g}[b, J^\dagger, J, \tilde{J}] \right) = (-ig)^2 \delta_{u+0} \delta_{v+0} \\ &\times \left\{ \theta(u^-) [\text{tr}((J_u^\dagger)^t t_u^a U_u) - \text{tr}((J_u)^t U_u^\dagger t_u^a)] + \theta(-u^-) [\text{tr}((J_u^\dagger)^t U_u t_u^a) - \text{tr}((J_u)^t t_u^a U_u^\dagger)] \right\} \\ &\times \left\{ \theta(v^-) [\text{tr}((J_v^\dagger)^t t_v^b U_v) - \text{tr}((J_v)^t U_v^\dagger t_v^b)] + \theta(-v^-) [\text{tr}((J_v^\dagger)^t U_v t_v^b) - \text{tr}((J_v)^t t_v^b U_v^\dagger)] \right\} . \end{aligned} \quad (1.162)$$

The calculation of the second derivative  $\frac{\delta}{\delta b_u^{+a}} \frac{\delta}{\delta b_v^{+b}} \mathcal{S}_{\text{ext}}^{q\bar{q}g}[b, J^\dagger, J, \tilde{J}]$  involves steps similar to those performed to arrive at eq. (1.161). We obtain

$$\frac{\delta}{\delta b_u^{+a}} \frac{\delta}{\delta b_v^{+b}} \mathcal{S}_{\text{ext}}^{q\bar{q}g}[b, J^\dagger, J, \tilde{J}] = (-ig)^2 \delta_{\mathbf{u}\mathbf{v}}^2 \delta_{u+0} \delta_{v+0} \left\{ \right.$$



$$\begin{aligned}
 & \theta(u^-)\theta(v^-) \operatorname{tr} \left( \theta(u^- - v^-) \left( (J_{\mathbf{u}}^\dagger)^t t_u^a t_v^b U_{\mathbf{u}} + (J_{\mathbf{u}})^t U_{\mathbf{u}}^\dagger t_v^b t_u^a \right) \right. \\
 & \quad \left. + \theta(v^- - u^-) \left( (J_{\mathbf{u}}^\dagger)^t t_v^b t_u^a U_{\mathbf{u}} + (J_{\mathbf{u}})^t U_{\mathbf{u}}^\dagger t_u^a t_v^b \right) \right) \\
 & + \theta(u^-)\theta(-v^-) \operatorname{tr} \left( (J_{\mathbf{u}}^\dagger)^t t_u^a U_{\mathbf{u}} t_v^b + (J_{\mathbf{u}})^t t_v^b U_{\mathbf{u}}^\dagger t_u^a \right) \\
 & + \theta(-u^-)\theta(v^-) \operatorname{tr} \left( (J_{\mathbf{u}}^\dagger)^t t_v^b U_{\mathbf{u}} t_u^a + (J_{\mathbf{u}})^t t_u^a U_{\mathbf{u}}^\dagger t_v^b \right) \\
 & \theta(-u^-)\theta(-v^-) \operatorname{tr} \left( \theta(u^- - v^-) \left( (J_{\mathbf{u}}^\dagger)^t U_{\mathbf{u}} t_u^a t_v^b + (J_{\mathbf{u}})^t t_v^b t_u^a U_{\mathbf{u}}^\dagger \right) \right. \\
 & \quad \left. + \theta(v^- - u^-) \left( (J_{\mathbf{u}}^\dagger)^t U_{\mathbf{u}} t_v^b t_u^a + (J_{\mathbf{u}})^t t_u^a t_v^b U_{\mathbf{u}}^\dagger \right) \right) \Bigg\}, \tag{1.163}
 \end{aligned}$$

where the functions  $\theta(u^- - v^-)$  and  $\theta(v^- - u^-)$  keep track of the order of the vertex insertions  $t_u^a$  and  $t_v^b$ , depending on which of the two coordinates  $u^-$  or  $v^-$  corresponds to the earlier/later “time”.

#### 1.4.2.7 Wilson line correlators from differentiation with respect to the source

In order to calculate the cross section from the series expansion (1.153), we must take the derivative

$$\left( \frac{\delta^{m,n}}{\delta \mathbf{J}_{\mathbf{x},\mathbf{y}}} + \frac{\delta^{m,n}}{\delta \mathbf{J}_{\mathbf{x},\mathbf{y}}} \frac{\delta}{\delta \tilde{J}_{\mathbf{z}}} \right) \Bigg|_{\{J\} \equiv 0} \tag{1.164}$$

of each term, as discussed in eq. (1.128). The following observations, however, invoke simplification when taking this derivative:

- Each term in (1.153) containing an  $\alpha$ -derivative  $\frac{\delta}{\delta \alpha_v^{+b}} \mathcal{S}_{\text{ext}}^{q\bar{q}g}$  is directly proportional to the source  $\tilde{J}$ , *c.f.* eq. (1.156a). This is still true after we perform the differentiation  $\frac{\delta^{m,n}}{\delta \mathbf{J}_{\mathbf{x},\mathbf{y}}}$ . Thus, setting all sources to zero ( $\{J\} \equiv 0$ ) will cause these terms to vanish,

$$\frac{\delta^{m,n}}{\delta \mathbf{J}_{\mathbf{x},\mathbf{y}}} \left( \frac{\delta}{\delta \alpha_v^{+b}} \mathcal{S}_{\text{ext}}^{q\bar{q}g}[b, J^\dagger, J, \tilde{J}] \right) \Bigg|_{\{J\} \equiv 0} = 0. \tag{1.165a}$$

Additionally, the term

$$\langle \alpha_u^{+a} \alpha_v^{+b} \rangle_\alpha \frac{\delta^{m,n}}{\delta \mathbf{J}_{\mathbf{x},\mathbf{y}}} \frac{\delta}{\delta \tilde{J}_{\mathbf{z}}} \left( \frac{\delta}{\delta b_u^{+a}} \mathcal{S}_{\text{ext}}^{q\bar{q}g}[b, J^\dagger, J, \tilde{J}] \right) \left( \frac{\delta}{\delta \alpha_v^{+b}} \mathcal{S}_{\text{ext}}^{q\bar{q}g}[b, J^\dagger, J, \tilde{J}] \right) \Bigg|_{\{J\} \equiv 0} \tag{1.165b}$$

will be proportional to the 3-point correlator  $\langle \alpha_u^{+a} \alpha_v^{+b} \alpha_z^{+c} \rangle_\alpha$  since the derivative with respect to  $\tilde{J}$  induces an additional term  $\alpha_z^{+c}$  (*c.f.* eq. (1.125)). As the 3-point correlator of  $\alpha$  is a next-to-leading-order (NLO) contribution, (1.165b) does not contribute to the total cross section at LO.

- For each term not containing an  $\alpha$ -derivative of  $\mathcal{S}_{\text{ext}}^{q\bar{q}g}$ , differentiation with respect to  $\tilde{J}$  will give rise to a  $p$ -point correlator of  $\alpha$  where  $p = 1$  or  $p = 3$ , as we have observed in eq. (1.128). Since the 1-point correlator of  $\alpha$  vanishes, and the 3-point correlator is a NLO contribution, the terms

$$\frac{\delta^{m,n}}{\delta \mathbf{J}_{\mathbf{x},\mathbf{y}}} \frac{\delta}{\delta \tilde{J}_{\mathbf{z}}} \left( \frac{\delta}{\delta b_v^{+b}} \mathcal{S}_{\text{ext}}^{q\bar{q}g}[b, J^\dagger, J, \tilde{J}] \right) \Bigg|_{\{J\} \equiv 0} \tag{1.165c}$$

do not contribute to the total cross section at leading order. That being said,

$$\langle \alpha_u^{+a} \rangle_\alpha \frac{\delta^{m,n}}{\delta \mathbf{J}_{\mathbf{x},\mathbf{y}}} \left( \frac{\delta}{\delta b_u^{+a}} \mathcal{S}_{\text{ext}}^{q\bar{q}g} [b, J^\dagger, J, \tilde{J}] \right) \Big|_{\{J\} \equiv 0} \propto \langle \alpha_u^{+a} \rangle_\alpha . \quad (1.165d)$$

Since the 1-point correlator  $\langle \alpha_u^{+a} \rangle_\alpha$  vanishes, the contribution of (1.165d) to the total cross section will be zero.

- Lastly, the product rule yields terms where the source-derivatives act on the exponential only, for example,

$$\left( \frac{\delta}{\delta \{\alpha, b\}_v^{+b}} \mathcal{S}_{\text{ext}}^{q\bar{q}g} [b, J^\dagger, J, \tilde{J}] \right) \cdot \left\{ \left( \frac{\delta^{m,n}}{\delta \mathbf{J}_{\mathbf{x},\mathbf{y}}} + \frac{\delta^{m,n}}{\delta \mathbf{J}_{\mathbf{x},\mathbf{y}}} \frac{\delta}{\delta \tilde{J}_{\mathbf{z}}} \right) e^{\mathcal{S}_{\text{ext}}^{q\bar{q}g} [b+\alpha, J^\dagger, J, \tilde{J}]} \right\} \Big|_{\{J\} \equiv 0} . \quad (1.165e)$$

Since the prefactor  $\frac{\delta}{\delta \{\alpha, b\}_v^{+b}} \mathcal{S}_{\text{ext}}^{q\bar{q}g}$  is proportional to the sources  $J, J^\dagger, \tilde{J}$  (*c.f.* eqns. (1.156)), setting the sources to zero according to  $\{J\} \equiv 0$  will cause terms such as (1.165e) to vanish.

With these considerations, the surviving terms of (1.153), when acted upon by the source-derivatives to obtain the cross section

$$\left\langle \left( \frac{\delta^{m,n}}{\delta \mathbf{J}_{\mathbf{x},\mathbf{y}}} + \frac{\delta^{m,n}}{\delta \mathbf{J}_{\mathbf{x},\mathbf{y}}} \frac{\delta}{\delta \tilde{J}_{\mathbf{z}}} \right) e^{\mathcal{S}_{\text{ext}}^{q\bar{q}g} [b+\alpha, J^\dagger, J, \tilde{J}]} \right\rangle_{b,\alpha} \Big|_{\{J\} \equiv 0} , \quad (1.166)$$

are

$$\left\langle \left( \frac{\delta^{m,n}}{\delta \mathbf{J}_{\mathbf{x},\mathbf{y}}} + \frac{\delta^{m,n}}{\delta \mathbf{J}_{\mathbf{x},\mathbf{y}}} \frac{\delta}{\delta \tilde{J}_{\mathbf{z}}} \right) e^{\mathcal{S}_{\text{ext}}^{q\bar{q}g} [b+\alpha, J^\dagger, J, \tilde{J}]} \right\rangle_{b,\alpha} \Big|_{\{J\} \equiv 0} = \left\langle \left( \frac{\delta^{m,n}}{\delta \mathbf{J}_{\mathbf{x},\mathbf{y}}} + \frac{\delta^{m,n}}{\delta \mathbf{J}_{\mathbf{x},\mathbf{y}}} \frac{\delta}{\delta \tilde{J}_{\mathbf{z}}} \right) e^{\mathcal{S}_{\text{ext}}^{q\bar{q}g} [b, J^\dagger, J, \tilde{J}]} \right\rangle_b \Big|_{\{J\} \equiv 0} \quad (1.167a)$$

$$+ \int_u \left\langle \langle \alpha_u^{+a} \rangle_\alpha [b] \left\{ \frac{\delta^{m,n}}{\delta \mathbf{J}_{\mathbf{x},\mathbf{y}}} \frac{\delta}{\delta \tilde{J}_{\mathbf{z}}} \left( \frac{\delta}{\delta \alpha_u^{+a}} \mathcal{S}_{\text{ext}}^{q\bar{q}g} [b, J^\dagger, J, \tilde{J}] \right) \right\} e^{\mathcal{S}_{\text{ext}}^{q\bar{q}g} [b, J^\dagger, J, \tilde{J}]} \right\rangle_b \Big|_{\{J\} \equiv 0} \quad (1.167b)$$

$$+ \frac{1}{2} \int_{uv} \left\langle \langle \alpha_u^{+a} \alpha_v^{+b} \rangle_\alpha [b] \left\{ \frac{\delta^{m,n}}{\delta \mathbf{J}_{\mathbf{x},\mathbf{y}}} \left( \frac{\delta}{\delta b_u^{+a}} \mathcal{S}_{\text{ext}}^{q\bar{q}g} [b, J^\dagger, J, \tilde{J}] \right) \left( \frac{\delta}{\delta b_v^{+b}} \mathcal{S}_{\text{ext}}^{q\bar{q}g} [b, J^\dagger, J, \tilde{J}] \right) \right\} \right\rangle_b \Big|_{\{J\} \equiv 0} \quad (1.167c)$$

$$+ \frac{\delta^{m,n}}{\delta \mathbf{J}_{\mathbf{x},\mathbf{y}}} \left( \frac{\delta}{\delta b_u^{+a}} \frac{\delta}{\delta b_v^{+b}} \mathcal{S}_{\text{ext}}^{q\bar{q}g} [b, J^\dagger, J, \tilde{J}] \right) \left\{ e^{\mathcal{S}_{\text{ext}}^{q\bar{q}g} [b, J^\dagger, J, \tilde{J}]} \right\} \Big|_{\{J\} \equiv 0} ; \quad (1.167d)$$

notice that the terms (1.167b) would be missing from the cross section if we had eliminated all terms including the 1-point correlator  $\langle \alpha_u^{+a} \rangle_\alpha$  already in eqns. (1.125) resp. (1.136).

#### 1.4.2.8 Diagrammatic notation for fluctuations in the color field

Eq. (1.167) has become quite unwieldy, so we abandon the traditional notation used so far in favour of the diagrammatic notation of [71]. We will interpret each term of (1.167) separately, establishing a connection to Feynman diagrams (analogously to what was done in [18]), in order to motivate a suitable diagrammatic notation.

The first term (1.167a) merely gives the cross section without any gluon fluctuations (*c.f.* eq. (1.136)). Thus, we may recycle the diagrams used in section 1.4.2.4.

The second term (1.167b) containing an  $\alpha$ -derivative of  $\mathcal{S}_{\text{ext}}^{q\bar{q}g}$ ,

$$\frac{\delta^{m,n}}{\delta \mathbf{J}_{\mathbf{x},\mathbf{y}}} \frac{\delta}{\delta \tilde{J}_{\mathbf{z}}} \int_u \left\langle \langle \alpha_u^{+a} \rangle_\alpha \left( \frac{\delta}{\delta \alpha_v^{+b}} \mathcal{S}_{\text{ext}}^{q\bar{q}g} [b, J^\dagger, J, \tilde{J}] \right) \right\rangle_b, \quad (1.168)$$

will give rise to a sum of Wilson line correlators of the form

$$\sum_{\text{positions of } t^a} \langle \alpha_u^{+a} \alpha_z^{+b} \rangle_\alpha U_{\mathbf{x}_1} \otimes \cdots \otimes t^a U_{\mathbf{x}_j} \otimes \cdots \otimes U_{\mathbf{x}_m} \otimes U_{\mathbf{y}_1}^\dagger \otimes \cdots \otimes U_{\mathbf{y}_n}^\dagger \otimes t^b, \quad (1.169)$$

where we sum over all positions at which the generator  $t^a$  can attach to a Wilson line  $U^{(\dagger)}$ . (We neglected prefactors and many indices on purpose in eq. (1.169), in order to direct the eye of the reader to the most important features of this equation, namely the positions of  $t^a$  and  $t^b$ . Furthermore, we recall that the  $\tilde{J}$ -derivative turned the 1-point correlator  $\langle \alpha_u^{+a} \rangle_\alpha$  into a 2-point correlator.) The terms in (1.169) correspond to Feynman diagrams consisting of  $(m+n)$  Wilson lines  $U^{(\dagger)}$  and a gluon propagator  $\langle \alpha_u^{+a} \alpha_z^{+b} \rangle_\alpha$ . One end of the gluon propagator is connected to a Wilson line via a vertex insertion  $t^a$  (in our case, this is  $t^a U_{\mathbf{x}_j}$ ), the other end enters the final state due to the term  $t^b$  in this tensor product. All other Wilson lines not connected to the additional gluon interact solely with the background field  $b$ . Whether the gluon interacts with the background field as well depends on whether it is produced (radiated from the Wilson line) before or after  $x^- = 0$ ; this is reflected in the position of  $t^a$  relative to the Wilson line, and in the Heaviside step function of the longitudinal coordinate (*c.f.* eq. (1.161)). The appropriate Feynman diagrams for (1.168) (where we suppress all Wilson lines not affected by the gluon fluctuation  $\langle \alpha_u^{+a} \alpha_z^{+b} \rangle_\alpha$ ) are

$$(1.170a)$$

and similarly for the  $\bar{q}$ -contributions,

$$(1.170b)$$

where time runs from bottom to top to mirror the depiction of spacetime in Figure 1.1 (the diagrams (1.170) are inspired by [18]). We will see that contributions from the diagrams (1.170) largely cancel due to the largest time Theorem [71], *c.f.* section 1.4.2.10.

Our calculation of the derivative of  $\mathcal{S}_{\text{ext}}^{q\bar{q}g}$  in eq. (1.162) shows that

$$\frac{\delta^{m,n}}{\delta \mathbf{J}_{\mathbf{x},\mathbf{y}}} \int_{u,v} \left\langle \langle \alpha_u^{+a} \alpha_v^{+b} \rangle_\alpha \left( \frac{\delta}{\delta b_u^{+a}} \mathcal{S}_{\text{ext}}^{q\bar{q}g} [b, J^\dagger, J, \tilde{J}] \right) \left( \frac{\delta}{\delta b_v^{+b}} \mathcal{S}_{\text{ext}}^{q\bar{q}g} [b, J^\dagger, J, \tilde{J}] \right) e^{\mathcal{S}_{\text{ext}}^{q\bar{q}g} [b, J^\dagger, J, \tilde{J}]} \right\rangle_b \Big|_{\{J\} \equiv 0} \quad (1.171)$$

gives a sum of the form (again suppressing additional prefactors)

$$\sum_{\text{positions of } t^a, t^b} \langle \alpha_u^{+a} \alpha_v^{+b} \rangle_\alpha U_{\mathbf{x}_1} \otimes \cdots \otimes t^a U_{\mathbf{x}_i} \otimes \cdots \otimes U_{\mathbf{x}_m} \otimes U_{\mathbf{y}_1}^\dagger \otimes \cdots \otimes U_{\mathbf{y}_j}^\dagger t^b \otimes \cdots \otimes U_{\mathbf{y}_n}^\dagger, \quad (1.172)$$

where we sum over all possible positions at which the generators  $t^a, t^b$  can attach to two *distinct* Wilson lines. Each term in eq. (1.172) corresponds to Feynman diagrams in which two Wilson lines of the correlator are connected with a gluon propagator  $\langle \alpha_u^{+a} \alpha_v^{+b} \rangle_\alpha$  by means of the vertex insertions  $t^a$  and  $t^b$  (in the case (1.172), these are the Wilson lines  $U_{\mathbf{x}_i}$  and  $U_{\mathbf{y}_j}^\dagger$ ). The Heaviside step functions of the longitudinal coordinates (*c.f.* eq. (1.162)) determine whether the gluon attaches to the (anti-) quark Wilson lines in a way that allows an interaction between  $\alpha$  and  $b$ , or not. All remaining Wilson lines in the correlator (that are not connected to the gluon) interact with the target only. Suppressing such Wilson lines for the purpose of brevity, we obtain the following diagrams [18]:

$$= U_{\mathbf{x}} t^a \otimes t^b U_{\mathbf{y}}^\dagger + U_{\mathbf{x}} t^a \otimes U_{\mathbf{y}}^\dagger t^b + t^a U_{\mathbf{x}} \otimes t^b U_{\mathbf{y}}^\dagger + t^a U_{\mathbf{x}} \otimes U_{\mathbf{y}}^\dagger t^b, \quad (1.173)$$

and similarly if the gluon propagator connects  $qq$ ,  $\bar{q}q$  or  $\bar{q}\bar{q}$ -pairs.

Lastly, from eq. (1.163) we see that the correlator

$$\frac{\delta^{m,n}}{\delta \mathbf{J}_{\mathbf{x},\mathbf{y}}} \int_{u,v} \left\langle \langle \alpha_u^{+a} \alpha_v^{+b} \rangle_\alpha \left( \frac{\delta}{\delta b_u^{+a}} \frac{\delta}{\delta b_v^{+b}} \mathcal{S}_{\text{ext}}^{q\bar{q}g} [b, J^\dagger, J, \tilde{J}] \right) e^{\mathcal{S}_{\text{ext}}^{q\bar{q}g} [b, J^\dagger, J, \tilde{J}]} \right\rangle_b \Big|_{\{J\} \equiv 0} \quad (1.174)$$

will give a sum of terms of the form (suppressing additional prefactors)

$$\sum_{\text{positions of } t^a, t^b} \langle \alpha_u^{+a} \alpha_v^{+b} \rangle_\alpha U_{\mathbf{x}_1} \otimes \cdots \otimes t^a U_{\mathbf{x}_j} t^b \otimes \cdots \otimes U_{\mathbf{x}_m} \otimes U_{\mathbf{y}_1}^\dagger \otimes \cdots \otimes U_{\mathbf{y}_n}^\dagger, \quad (1.175)$$

where we sum over all possible positions at which the generators  $t^a, t^b$  can attach to the *same* Wilson line  $U^{(\dagger)}$ . Eq. (1.175) describes Feynman diagrams in which an individual (anti-) quark line (in our case  $U_{\mathbf{x}_j}$ ) is dressed by a gluon (the gluon propagator  $\langle \alpha_u^{+a} \alpha_v^{+b} \rangle_\alpha$  attaches to the Wilson line via vertex insertions,  $t^a U_{\mathbf{x}_j} t^b$ ), all other Wilson lines in the correlator are unaffected by this gluon and interact with the target background field  $b$  only. Furthermore, whether the gluon represented by  $\langle \alpha_u^{+a} \alpha_v^{+b} \rangle_\alpha$  itself interacts with the background field depends on the Heaviside step functions of the longitudinal coordinates (in (1.163)), and on the positions at which the gluon attaches to the Wilson line  $U^{(\dagger)}$ . Thus, the term (1.174) gives rise to

diagrams such as [18]

$$\begin{aligned}
 & \text{Diagram with gluon loop} = \text{Diagram 1} + \text{Diagram 2} + \text{Diagram 3}, \\
 & \text{Labels: } t^a t^b U_x, \quad t^a U_x t^b, \quad U_x t^a t^b.
 \end{aligned}
 \tag{1.176a}$$

where we suppress Wilson lines unaffected by the fluctuation  $\alpha$ . Similar diagrams arise when a  $\bar{q}$ -line is dressed with the gluon, except that the order of the gluon insertions is reversed,

$$\begin{aligned}
 & \text{Diagram with gluon loop} = \text{Diagram 1} + \text{Diagram 2} + \text{Diagram 3}, \\
 & \text{Labels: } t^b t^a U_y^\dagger, \quad t^b U_y^\dagger t^a, \quad U_y^\dagger t^b t^a.
 \end{aligned}
 \tag{1.176b}$$

The Feynman diagrams corresponding to the various contributions of the cross section (1.167) inspires a diagrammatic notation: Following [71], we introduce a graphical notation for the sum of vertex insertions  $t^a$ ,

$$\text{Diagram} := \text{Diagram 1} + \dots + \text{Diagram 2} - \dots - \text{Diagram 3};
 \tag{1.177a}$$

notice that the gluon couples with a prefactor  $(-ig)$  to a Wilson line  $U$  in the fundamental representation, but with a prefactor  $(+ig)$  to a Wilson line  $U^\dagger$  in the antifundamental representation (*c.f.* eqns. (1.160)), causing the different signs in eq. (1.177a). In this notation, the diagrams in eqns. (1.170), (1.173) and (1.176) are re-grouped, for example

$$\text{Diagram} \rightarrow \text{Diagram 1} + qq, \bar{q}q, \bar{q}\bar{q}\text{-contributions} + \text{Diagram 2} + \bar{q}\text{-contribution}.
 \tag{1.177b}$$

This diagrammatic notation is summarized in Figure 1.8.

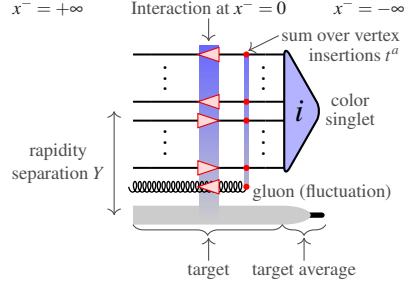


Figure 1.8: This figure compliments the graphical notation introduced in Figure 1.6. Here, we introduce a notation for the sum over vertex insertions  $t^a$  (c.f. eq. (1.177a)) that describes the coupling of the projectile to the fluctuation  $\alpha$  of the background field.

### 1.4.2.9 Cross section with fluctuations in the color field

As we have already done for the cross section without gluon fluctuations in section 1.4.2.4, we would now like to use the graphical notation (1.177) to define the  $|\text{in}\rangle$ - and  $|\text{out}\rangle$ -states analogous to eqns. (1.137). The analysis of the previous section fully justifies these to be given by the following sum of diagrams,

$$|\text{in}\rangle = \begin{array}{c} \text{diagram 1} \\ \text{diagram 2} \\ \text{diagram 3} \\ \text{diagram 4} \\ \text{diagram 5} \\ \text{diagram 6} \end{array} \quad (1.178a)$$

$$|\text{out}\rangle = \begin{array}{c} \text{diagram 1} \\ \text{diagram 2} \\ \text{diagram 3} \\ \text{diagram 4} \\ \text{diagram 5} \\ \text{diagram 6} \end{array} \quad (1.178b)$$

The  $T$ -matrix element  $|\text{out}\rangle - |\text{in}\rangle$  gives rise to the following expression for the cross section,

$$\begin{array}{c} \text{diagram } j \\ \left( \begin{array}{c} \text{diagram 1} \\ \text{diagram 2} \\ \text{diagram 3} \\ \text{diagram 4} \\ \text{diagram 5} \\ \text{diagram 6} \end{array} \right) - \left( \begin{array}{c} \text{diagram 1} \\ \text{diagram 2} \\ \text{diagram 3} \\ \text{diagram 4} \\ \text{diagram 5} \\ \text{diagram 6} \end{array} \right) \end{array} \Bigg|^2 \begin{array}{c} \text{diagram } i \\ \text{diagram } i \end{array} \quad (1.179)$$

Multiplying out the terms in (1.179) involves connecting the index lines of two diagrams in the product at  $x^- = +\infty$ . We remind the reader that this graphical procedure corresponds to performing an integral over the transverse momenta, as explained in section 1.4.2.4 (c.f. eq. (1.143)); we will discuss the consequences of this integration in section 1.4.2.10. In total, we obtain  $12^2 = 144$  terms, which can be grouped into the following categories:

1. 4 terms without gluon fluctuations,

(1.180a)

these terms merely describe the cross section without gluon fluctuations given in eq. (1.144).

2. 64 terms where we have a gluon entering the final state from either  $\langle \text{in, out} |$  or  $|\text{in, out} \rangle$  but not both, for example,

(1.180b)

these contributions vanish identically since the  $m\bar{q} + n\bar{q}$  Fock space component has no overlap with the  $m\bar{q} + n\bar{q} + g$  Fock space component.

3. 16 terms where the gluon enters the final state in both  $\langle \text{in, out} |$  and  $|\text{in, out} \rangle$  to obtain 1-loop diagrams, for example,

(1.180c)

4. 24 1-loop diagrams where the gluon does not enter the final state, such as

(1.180d)

5. 36 terms with two loops, for example

(1.180e)

since these are next-to-leading order terms, we ignore these at LO calculation.

Thus, at leading order, we obtain  $4 + 16 + 24$  terms of the type (1.180a), (1.180c) and (1.180d) respectively. Figures 1.9, 1.10 and 1.11 organize these terms according to  $\langle \text{in}|\text{in} \rangle$ ,  $\langle \text{out}|\text{out} \rangle$  and  $\langle \text{in}|\text{out} \rangle$  (equivalently  $\langle \text{out}|\text{in} \rangle$ ) contributions. (Figures 1.9 to 1.11 were inspired by [71, Figure 3].)

#### 1.4.2.10 Cancellations and the largest time Theorem

It turns out that the terms arising from eqns. (1.180c) and (1.180d) largely cancel amongst themselves. This happens through a combination of two phenomena: transverse coordinate identification of adjacent Wilson

lines (*c.f.* eq. (1.143)) and largest time cancellations [71].

We have already encountered the first of the two phenomena in our discussion on the cross section without gluon fluctuations in section 1.4.2.4. There, we found that connecting Wilson lines graphically through the multiplication of the diagrams corresponds to an integration over the transverse momenta, which consequently identifies the transverse coordinates of neighbouring Wilson lines. This, together with the unitarity of Wilson lines, leads to simplifications of the terms originating from the  $\langle \text{out} | \text{out} \rangle$ -overlap (*c.f.* eq. (1.143)),

$$U_x U_y^\dagger \xrightarrow[x=y]{\text{identify transverse coordinates}} U_x U_x^\dagger = \mathbb{1}. \quad (1.181)$$

For example



$$(1.182)$$

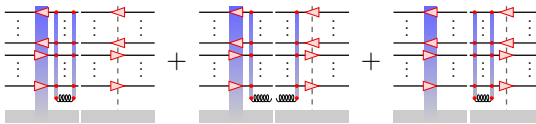
In this section, we leave a gap between the amplitude and the complex conjugate amplitude in the graphical representation of the product in order to highlight the largest time  $x^- = +\infty$  (*c.f.* eq. (1.142)) — nonetheless, all lines are understood to be connected such that an integration over the transverse momenta takes place.

The second ingredient needed to effect the cancellation of many terms in the cross section (1.179) is the largest time Theorem [73, 74]: Two diagrams, which differ only by a vertex insertion (in that one diagram has a particular vertex inserted to the left of the largest time and the other has the same vertex inserted to the right of the largest time), sum up to zero. In particular, this implies



$$(1.183a)$$

and



$$(1.183b)$$

similar cancellations hold for all other products of diagrams that differ only by a sum of generator insertions on either side of the largest time  $x^- = +\infty$ .

These identities (integration over transverse momenta and eqns. (1.183)) give rise to cancellations between a large number of diagrams. This is summarized in Figures 1.9 to 1.11 [71], where we depict all diagrams summing to zero in the same row (outlined by a solid box). In fact, only the three diagrams in the last row (no outline) of Figure 1.11 remain.

Alternatively, the diagrams in Figures 1.9 and 1.11 may be re-grouped column-wise (shaded boxes with dashed outlines), merely to see that the diagrams within the new groups still cancel among themselves [71].



This is due to the identity

$$\begin{array}{c} \text{Diagram 1} \end{array} + \begin{array}{c} \text{Diagram 2} \end{array} + \begin{array}{c} \text{Diagram 3} \end{array} = 0, \quad (1.184a)$$

describing the fact that there cannot be any JIMWLK evolution (i.e. radiation and re-absorption of a gluon) if there is no interaction with the target, and

$$\begin{array}{c} \text{Diagram 4} \end{array} + \begin{array}{c} \text{Diagram 5} \end{array} = 0 \quad \text{and} \quad \begin{array}{c} \text{Diagram 6} \end{array} + \begin{array}{c} \text{Diagram 7} \end{array} = 0, \quad (1.184b)$$

which tells us that no gluon can be emitted into the final state without an interaction taking place. Both identities (1.184) are given in [71] and can be verified through explicit calculation.

In this viewpoint, one is again left with only three diagrams which do not cancel; these are depicted in the last column (shaded box with no outline) in Figure 1.11.

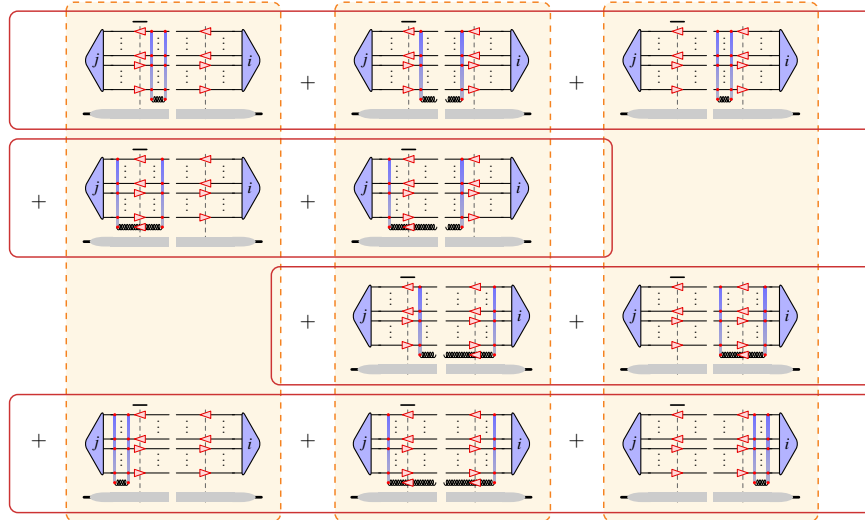


Figure 1.9:  $\langle \text{in} | \text{in} \rangle$ -states: The largest time Theorem (eqns. (1.183)) causes the cancellation of terms in the same row (boxes with solid outlines), where the largest time  $x^- = +\infty$  occurs in the centre of the diagrams (c.f. eq. (1.142)). On the other hand, identities (1.184) effect the cancellation of all terms in the same column (shaded boxes with dashed outline).

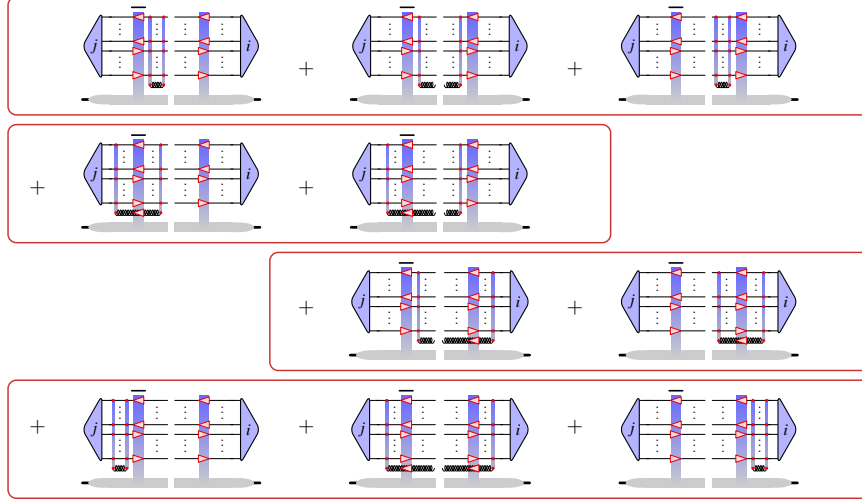


Figure 1.10:  $\langle \text{out} | \text{out} \rangle$ -states: Each row of diagrams in this figure cancels due to final state cancellations. For the first three rows this cancellation is trivially seen when considering the largest time  $x^- = +\infty$  in the centre of each diagram (*c.f.* eq. (1.142)). The diagrams in the last row first require a simplification that stems from the integral over the transverse momenta (*c.f.* eq. (1.182)) before the largest time Theorem is applicable.

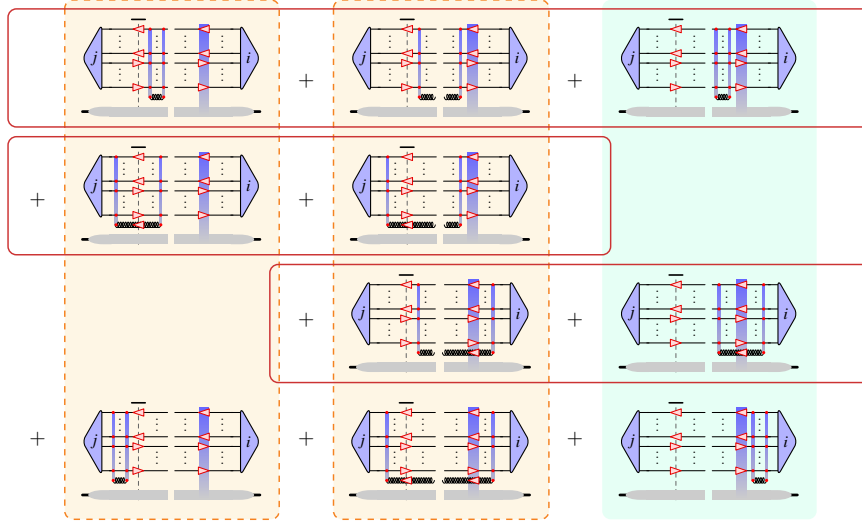


Figure 1.11:  $\langle \text{in} | \text{out} \rangle$ -states (the  $\langle \text{out} | \text{in} \rangle$ -states are obtained from the diagrams in this figure via Hermitian conjugation): The cancellation of terms can be viewed in two ways — column-wise or row-wise. The largest time Theorem (eqns. (1.183)) causes cancellations amongst the diagrams within the first three rows (boxes with solid outlines) respectively; we remain with the terms appearing in the bottom row (no outline). Alternatively, identities (1.184) give rise to column-wise (shaded boxes with dashed outline) cancellations: the terms in the first column cancel due to identity (1.184a), and the terms in the second column cancel pair-wise according to (1.184b). Thus we are left with the terms in the last column (shaded box, no outline). In both cases, the remaining diagrams give the JIMWLK evolution at leading order, but with different interpretations. (Notice that there is an overall minus sign for the sum in this figure.)

In summary, all terms in Figures 1.9 and 1.10 cancel among themselves, and only three terms in Figure 1.11 survive. These three terms are either

$$\begin{array}{c}
 \text{---} \left[ \text{Diagram 1} \right] - \left[ \text{Diagram 2} \right] - \left[ \text{Diagram 3} \right] \\
 \text{---} \left[ \text{Diagram 1} \right] - \left[ \text{Diagram 2} \right] - \left[ \text{Diagram 3} \right]
 \end{array} \quad (1.185a)$$

or

$$\begin{array}{c}
 \text{---} \left[ \text{Diagram 1} \right] - \left[ \text{Diagram 2} \right] - \left[ \text{Diagram 3} \right], \\
 \text{---} \left[ \text{Diagram 1} \right] - \left[ \text{Diagram 2} \right] - \left[ \text{Diagram 3} \right]
 \end{array} \quad (1.185b)$$

depending on whether one considers the terms to cancel across rows or across columns in the figure. Notice however that the sums (1.185a) and (1.185b) are equal, as the final result cannot depend on which cancellation method we choose. Even more strikingly, it can be shown [71] that the diagrams in eqns. (1.185) are equal term by term,

$$\begin{array}{ccc}
 \left[ \text{Diagram 1} \right] & \left[ \text{Diagram 2} \right] & \left[ \text{Diagram 3} \right] \\
 \parallel & \parallel & \parallel \\
 \left[ \text{Diagram 1} \right] & \left[ \text{Diagram 2} \right] & \left[ \text{Diagram 3} \right]
 \end{array} \quad (1.186)$$

although, they receive different physical interpretations [71]: eq. (1.185a) contains only terms in which particular (anti-) fundamental lines are dressed with gluon corrections, while eq. (1.185b) includes a term in which the gluon enters the final state — we conclude that JIMWLK evolution cannot differentiate between these two physically distinct situations.

Since eqns. (1.185) are completely equivalent, we are free to choose representation (1.185a) for the sum of non-vanishing terms in the cross section. We may suppress the tower of Wilson lines that is gauge-equivalent to  $\mathbb{1}$  (using identity (1.129b) for the singlet state  $\langle j|$ ) and simply write

$$\begin{array}{c}
 \text{---} \left[ \text{Diagram 1} \right] - \left[ \text{Diagram 2} \right] - \left[ \text{Diagram 3} \right] \\
 \text{---} \left[ \text{Diagram 1} \right] - \left[ \text{Diagram 2} \right] - \left[ \text{Diagram 3} \right]
 \end{array} \quad (1.187)$$

The same analysis given for the diagrams in Figure 1.11 also applies to the cross-terms arising from the  $\langle \text{out}|\text{in} \rangle$ -overlap, as the latter can be obtained from the former by simply mirroring diagrams about the vertical axis. Thus,  $\langle \text{out}|\text{in} \rangle$  will produce another copy of the sum (1.187).

## 1.4.2.11 Finite difference equation leading to JIMWLK

Due to the cancellations described in section 1.4.2.10, the cross section (1.179) simplifies dramatically, leaving only six (out of 144) non-vanishing terms in the cross section,<sup>25</sup>

$$\begin{aligned}
 & \left\langle \langle j | \left| \left( \frac{\delta^{m,n}}{\delta \mathbf{J}_{\mathbf{x},\mathbf{y}}} + \frac{\delta^{m,n}}{\delta \mathbf{J}_{\mathbf{x},\mathbf{y}}} \frac{\delta}{\delta \tilde{J}_{\mathbf{z}}} \right) e^{\mathcal{S}_{\text{ext}}^{q\bar{q}g}[b+\alpha, J^\dagger, J, \tilde{J}]} \right|^2 | i \rangle \right\rangle_{b,\alpha} \Big|_{\{J\} \equiv 0} = \\
 & \underbrace{2 \cdot \left( \text{Diagram 1} \right) - \left( \text{Diagram 2} \right)^\dagger - \left( \text{Diagram 3} \right)}_{= \delta_{ij} \text{tr}(\mathbf{1})} - 2 \cdot \left( \text{Diagram 4} + \text{Diagram 5} + \text{Diagram 6} \right), \\
 & = \left\langle \langle j | \left| \left( \frac{\delta^{m,n}}{\delta \mathbf{J}_{\mathbf{x},\mathbf{y}}} + \frac{\delta^{m,n}}{\delta \mathbf{J}_{\mathbf{x},\mathbf{y}}} \frac{\delta}{\delta \tilde{J}_{\mathbf{z}}} \right) \exp \left\{ \mathcal{S}_{\text{ext}}^{q\bar{q}g}[b, J^\dagger, J, \tilde{J}] \right\} \right|^2 | i \rangle \right\rangle_{b,\alpha} \Big|_{\{J\} \equiv 0}
 \end{aligned} \tag{1.188}$$

where we suppressed the tensor product of Wilson lines in which all Wilson lines are gauge-equivalent to  $\mathbf{1}$  due to identities (1.129). Furthermore, we were able to identify the first three diagrams as the cross section without gluon fluctuations (*c.f.* eq. (1.144) in section 1.4.2.4).

Notice that each term in the second bracket on the RHS of eq. (1.188) includes an integral over the field fluctuation  $\alpha$  in the form of the two-point correlator  $\langle \alpha_u^+ \alpha_v^{+b} \rangle_\alpha$ . We know from section 1.3.1 that the longitudinal momentum of the fluctuation has a cut-off  $\Lambda_0^+$ . As we increase the rapidity from  $Y_0$  to  $Y$  (according to the RG argument explained in section 1.4.1), the momentum cut-off is adjusted to  $\Lambda^+$ . Hence, performing the  $\alpha$ -integral over a finite momentum interval  $\Lambda^+ - \Lambda_0^+$  induces a factor  $\ln \frac{1}{x_{\text{Bj}}} - \ln \frac{1}{x_{\text{Bj}0}} = \ln \frac{x_{\text{Bj}0}}{x_{\text{Bj}}}$ , where  $x_{\text{Bj}0}$  is the momentum fraction of the previous iteration in the RG argument; the details of this calculation are given in in [57]. Let us perform the integration (thus making the factor  $\ln \frac{x_{\text{Bj}0}}{x_{\text{Bj}}}$  explicit) and rearrange terms of eq. (1.188) to obtain the following finite difference equation,

$$\begin{aligned}
 & \left\langle \langle j | \left| \left( \frac{\delta^{m,n}}{\delta \mathbf{J}_{\mathbf{x},\mathbf{y}}} + \frac{\delta^{m,n}}{\delta \mathbf{J}_{\mathbf{x},\mathbf{y}}} \frac{\delta}{\delta \tilde{J}_{\mathbf{z}}} \right) \left( e^{\mathcal{S}_{\text{ext}}^{q\bar{q}g}[b+\alpha, J^\dagger, J, \tilde{J}]} - e^{\mathcal{S}_{\text{ext}}^{q\bar{q}g}[b, J^\dagger, J, \tilde{J}]} \right) \right|^2 | i \rangle \right\rangle_{b,\alpha} \Big|_{\{J\} \equiv 0} \\
 & = \left( \text{Diagram 1} \right) \left( \ln \left( \frac{x_{\text{Bj}0}}{x_{\text{Bj}}} \right) \underbrace{\left( \text{Diagram 4} + \text{Diagram 5} + \text{Diagram 6} \right)}_{=:-H_{\text{JIMWLK}} \mathbf{U}_{\mathbf{x},\mathbf{y}}^{m,n}} \right) \left( \text{Diagram 2} \right), \tag{1.189}
 \end{aligned}$$

where we suppressed the factor 2 on the right-hand side (one may always absorb this constant into another constant appearing on the right). The difference on the left-hand side of this equation represents the comparison of two stages in the renormalization group argument as explained in section 1.4.1, eq. (1.98). Let us take a limit such that the energy difference between the previous and current iterations of the RG argument goes to zero. In this limit, the fluctuation  $\alpha \rightarrow 0$  such that  $b + \alpha \rightarrow b$  and  $\mathcal{S}_{\text{ext}}^{q\bar{q}g}[b, J^\dagger, J, \tilde{J}] \rightarrow \mathcal{S}_{\text{ext}}^{q\bar{q}g}[b, J^\dagger, J]$ .

<sup>25</sup>We again projected onto the singlet states  $|i\rangle, \langle j|$  to remind the reader that we are ultimately interested in cross sections involving physical observables, which are represented by singlet correlators. The calculations however would still hold without projecting onto singlet states.

Simultaneously, this limit induces  $x_{Bj} \rightarrow x_{Bj0}$ . Bringing the term  $\ln\left(\frac{x_{Bj0}}{x_{Bj}}\right)$  to the left hand of the equation then yields

$$\frac{d}{d \ln(1/x_{Bj})} \left\langle \frac{\delta^{m,n}}{\delta \mathbf{J}_{\mathbf{x}, \mathbf{y}}} e^{\mathcal{S}_{\text{ext}}^{q\bar{q}g}[b, J^\dagger, J]} \right\rangle (Y) \Big|_{\{J\} \equiv 0} = \underbrace{\left( \text{Diagram 1} + \text{Diagram 2} + \text{Diagram 3} \right)}_{-H_{\text{JIMWLK}} \mathbf{U}_{\mathbf{x}, \mathbf{y}}^{m,n}}, \quad (1.190)$$

where we have suppressed the integration variable  $b$  in the average,  $\langle \dots \rangle_b \rightarrow \langle \dots \rangle$ . Recalling that the rapidity  $Y$  and Bjorken- $x$  are related via  $Y = \ln\left(\frac{1}{x_{Bj}}\right)$ , we finally obtain the JIMWLK equation (1.99) at leading order,

$$\frac{d}{dY} \left( \underbrace{\left( \text{Diagram 1} - \text{Diagram 2} \right)}_{\langle \mathcal{A} \rangle (Y)} \right) = \underbrace{\left( \text{Diagram 3} + \text{Diagram 4} + \text{Diagram 5} \right)}_{-\langle H_{\text{JIMWLK}} \mathcal{A} \rangle (Y)}, \quad (1.191)$$

where we have identified the Wilson lines projected onto singlet states  $\langle j | \mathbf{U}_{\mathbf{x}, \mathbf{y}}^{m,n} | i \rangle$  as our observable  $\mathcal{A}_{ji}$  (*c.f.* eq. (1.192)).

## 1.5 Parametrization of JIMWLK

It turns out that no exact analytical solution to the JIMWLK equation can be found, although at leading order it can be solved numerically via a Langevin description [18, 67]. Thus, in order to perform analytic calculations in practice, one approximates the averaging procedure  $\langle \dots \rangle (Y)$  using a parametrization. In our context, the most common approximation (after a large- $N_c$  approximation, which violates gauge invariance) is the *Gaussian truncation* [18, 71, 75]; the name can be attributed to the fact that, if the approximation is truncated at leading order, the average  $\langle \dots \rangle (Y)$  has a Gaussian weight. Let us go through the steps at arriving at the Gaussian truncation and its generalizations (i.e. truncations at higher order).

Consider a matrix of Wilson line correlators  $\langle \mathcal{A} \rangle (Y)$  describing the eikonal interaction of a projectile (for  $\langle \mathcal{A} \rangle (Y)$  to be a physical observable it needs to be a Wilson line correlator projected onto a color singlet state in  $V^{\otimes m} \otimes (V^*)^{\otimes n}$ ) and a target. Clearly,  $\langle \mathcal{A} \rangle (Y)$  is a  $k \times k$  matrix with matrix elements

$$\mathcal{A}_{ji} = \left( \text{Diagram} \right), \quad (1.192)$$

where  $k$  is the number of singlet representations of  $\text{SU}(N)$  over  $V^{\otimes m} \otimes (V^*)^{\otimes n}$  (*c.f.* the later chapter 5). While we explicitly depict  $\mathcal{A}_{ji}$  with Wilson lines that are not all gauge equivalent to unity (*c.f.* eq. (1.118)), we will later consider various coincidence limits of the Wilson lines within  $\mathcal{A}_{ji}$  (see section 1.6.2). The evolution of

$\langle \mathcal{A} \rangle (Y)$  with rapidity is governed by the JIMWLK equation

$$\frac{d}{dY} \langle \mathcal{A} \rangle (Y) = - \langle H_{\text{JIMWLK}} \mathcal{A} \rangle (Y) . \quad (1.193a)$$

Since eq. (1.193a) cannot be solved analytically in general, we aim to parametrize the evolution described by the JIMWLK Hamiltonian. The calculation at leading order in eq. (1.191) shows that the singlet states  $|i\rangle, |j\rangle$  are not affected by the JIMWLK evolution, but remain intact as  $Y$  changes. In particular, evolving a Wilson line correlator (which is projected onto the singlet states  $|i\rangle, |j\rangle$ ) will return a (sum of) Wilson line correlator(s) projected onto singlet states living in the *same* algebra as  $|i\rangle, |j\rangle$ . Hence,  $\frac{d}{dY} \langle \mathcal{A} \rangle (Y)$  is expected to be of the form

$$\frac{d}{dY} \langle \mathcal{A} \rangle (Y) = - \mathcal{M}(Y) \langle \mathcal{A} \rangle (Y) , \quad (1.193b)$$

where also  $\mathcal{M}(Y)$  is understood to be a  $k \times k$  matrix. In particular,  $\mathcal{M}(Y)$  must inherit the block-structure of  $\mathcal{A}$ , in the sense that all matrix elements that vanish in  $\mathcal{A}$  must also vanish in  $\mathcal{M}(Y)$ . This behaviour of JIMWLK evolution can intuitively be understood by noticing that the explicit form of  $H_{\text{JIMWLK}}$  at LO in eq. (1.191) determines the evolution of Wilson line correlators to occur through the exchange of exactly two gluons — one “carries color away”, the other “brings color back” such that the overall color exchange is zero [51].

There are two major benefits of eq. (1.193b) over the full JIMWLK equation: The first is that it can easily be integrated to yield an expression for  $\langle \mathcal{A} \rangle (Y)$ ,

$$\langle \mathcal{A} \rangle (Y) = \text{P}_Y \exp \left\{ - \int_{Y_0}^Y d\tilde{Y} \mathcal{M}(\tilde{Y}) \right\} \langle \mathcal{A} \rangle (Y_0) . \quad (1.194)$$

Secondly, since  $\mathcal{M}(Y)$  is linear (as it is a  $k \times k$  matrix), we can hope to parametrize the operator  $\text{P}_Y \exp \left\{ - \int_{Y_0}^Y d\tilde{Y} \mathcal{M}(\tilde{Y}) \right\}$  — unlike the JIMWLK Hamiltonian, which lives in a curved manifold.

However, there are two issues that need to be addressed:

1. So far, we have given an intuitive reason for the existence of a parametrization of the form (1.193b) for the JIMWLK Hamiltonian. It still remains to be verified that our expectation did not betray us. This will be accomplished in section 1.5.1, where we also give the criteria stating when the parametrization (1.193b) will be valid.
2. Secondly, for (1.193b) to be a matrix equation, the operator  $\text{P}_Y \exp \left\{ - \int_{Y_0}^Y dY' \mathcal{M}(Y') \right\}$  must have a specific form. This will be discussed in section 1.5.2.

### 1.5.1 Validity of the parametrization

In short, the parametrization (1.193b) is valid as long as the Wilson line correlator  $\langle \mathcal{A} \rangle (Y)$  is invertible [51]. If the inverse  $(\langle \mathcal{A} \rangle (Y))^{-1}$  exists, then the left-hand side of the JIMWLK equation (1.193a) may be multiplied

by the unit element  $(\langle \mathcal{A} \rangle (Y))^{-1} \langle \mathcal{A} \rangle (Y)$ ,

$$\frac{d}{dY} \mathcal{A}(Y) = \underbrace{\left( \frac{d}{dY} \langle \mathcal{A} \rangle (Y) \right) (\langle \mathcal{A} \rangle (Y))^{-1} \langle \mathcal{A} \rangle (Y)}_{=:-\mathcal{M}(Y)} = -\mathcal{M}(Y) \langle \mathcal{A} \rangle (Y), \quad (1.195)$$

yielding a definition of  $\mathcal{M}(Y)$ .

Thus, the question to be answered is: When does  $\langle \mathcal{A} \rangle (Y)$  have an inverse? Clearly, the matrix  $\langle \mathcal{A} \rangle (Y)$  is invertible if all its eigenvalues are nonzero. Suppose that  $\mathcal{A}$  has a zero eigenvalue. This implies (by eq. (1.195)) that the corresponding eigenvalue of  $\mathcal{M}(Y)$  must be infinite. Since  $\mathcal{M}(Y)$  parametrizes  $H_{\text{JIMWLK}}$ , an infinite eigenvalue of  $\mathcal{M}(Y)$  indicates an IR or UV divergence of  $H_{\text{JIMWLK}}$ . However, it can be shown that the JIMWLK Hamiltonian remains finite for color singlets [76].<sup>26</sup> Therefore, all eigenvalues of  $\mathcal{A}$  must be nonzero, yielding  $\langle \mathcal{A} \rangle (Y)$  to be invertible.

Intuitively, this was to be expected: If all Wilson lines in  $\langle \mathcal{A} \rangle (Y)$  are set to unity, the matrix  $\langle \mathcal{A} \rangle (Y)$  itself becomes the unit matrix. Since this matrix is a physical observable, it should smoothly divert from the unit matrix as we vary the Wilson lines away from  $\mathbb{1}$ . Hence, it is plausible to assume that  $\mathcal{A}(Y)$  is invertible, at least in some neighbourhood of the unit matrix.

## 1.5.2 Form of the parametrization

The modern form of the parametrization of the JIMWLK equation (see the later eq. (1.201)) found its inspiration in the MV-model (*c.f.* eq. (1.87)). In the present section, we give a brief overview of how this comes about.

Consider an observable described by a Wilson line correlator  $\mathcal{A}$ . Its rapidity-dependent expectation value is given via the averaging procedure prescribed by the MV-functional distribution (1.87). Ignoring fluctuations  $\alpha$  such that the gauge field  $A$  becomes roughly equal to the background field,  $A = b + \alpha \approx b$ , one may relate the sources  $\rho$  to the background field  $b$  using eq. (1.81),

$$\partial_i \partial^i b_{\mathbf{x}}^{+a} = \rho^a(\mathbf{x}) \delta(x^-) \implies \partial_i \partial^i \tilde{b}_{\mathbf{x}}^{+a} = \rho^a(\mathbf{x}), \quad \text{where } \tilde{b}_{\mathbf{x}}^{+a} \delta(x^-) := b_{\mathbf{x}}^{+a}. \quad (1.196)$$

This allows one to write the MV-functional distribution (1.87) in terms of the background field as [20]

$$\begin{aligned} \langle \mathcal{A} \rangle (Y) &= \int [d\rho] \left( P_Y \exp \left\{ - \int_{Y_0}^Y d\tilde{Y} \int d^2 \mathbf{x} \frac{\rho^a(\tilde{Y}, \mathbf{x}) \rho^a(\tilde{Y}, \mathbf{x})}{\mu^2(\tilde{Y}, Q^2)} \right\} \mathcal{A} \right) \\ &= \int [d\rho] \left( P_Y \exp \left\{ - \int_{Y_0}^Y d\tilde{Y} \int d^2 \mathbf{x} \frac{(\partial_i \partial^i \tilde{b}_{\mathbf{x}}^{+a}(\tilde{Y})) (\partial_j \partial^j \tilde{b}_{\mathbf{x}}^{+a}(\tilde{Y}))}{\mu^2(\tilde{Y}, Q^2)} \right\} \mathcal{A} \right) \end{aligned} \quad (1.197)$$

(where we have made the range of  $\tilde{Y}$  *explicit* in the limits of the integral). The expectation value (1.197) may now be calculated for several Wilson line correlators  $\mathcal{A}$ . The details on how this can be accomplished

<sup>26</sup>The JIMWLK kernel can be split into an IR safe part (the BK-kernel), and a part that potentially causes IR divergences. However, this second part can be shown to vanish when the Wilson line correlator is projected onto singlet states on both sides, i.e.  $\mathbf{U} = \sum_{i,j} |j\rangle \langle j| \mathbf{U} |i\rangle \langle i|$  where both  $|i\rangle, |j\rangle$  are singlets, causing such a correlator to be IR safe. On the other hand, if  $|i\rangle, |j\rangle$  are *not* global color singlets, then the contribution from the IR-divergent part of the JIMWLK kernel is suppressed by a factor  $e^{-\infty}$  at leading order [76].

in general are laid out in [20]. However, already the example where  $\mathcal{A}$  is taken to be the  $q\bar{q}$ -dipole singlet  $\mathcal{A} = \text{tr}(U_{\mathbf{x}}U_{\mathbf{y}}^\dagger)$  given in [18] exposes several general features of the averaging procedure (1.197). We thus recapitulate it here: As argued in detail in [77], one may change variables to express the Wilson line  $U$  as a rapidity-ordered exponential rather than a path-ordered exponential, such that [18],<sup>27</sup>

$$U_{\mathbf{x}} = \text{Pexp} \left\{ -ig \int_{-\infty}^{\infty} dx^- b_{\mathbf{x}}^{+a} t_{\mathbf{x}}^a \right\} = \text{P}_Y \text{exp} \left\{ -i \int_{Y_0}^Y d\tilde{Y} \beta_{\tilde{Y}, \mathbf{x}} \right\}, \quad (1.198)$$

where the function  $\beta_{\tilde{Y}, \mathbf{x}}$  can be determined through the change of variables. Owing to the fact that eq. (1.197) is local in  $Y$  (the Gaussian weight in (1.197) depends only on one value of rapidity), the MV-average (1.197) of a correlator of Wilson lines (1.198) inserts a 2-point correlator (connecting two Wilson lines) at the largest rapidity  $Y$ . To paraphrase [18], the expectation value of the dipole operator to lowest order can be graphically represented as

$$-d_f C_f \int_{Y_0}^Y d\tilde{Y} \left( \text{diagram} \right) := -d_f C_f \int_{Y_0}^Y d\tilde{Y} \left\{ \left( \text{diagram} \right) + \left( \text{diagram} + \text{diagram} \right) \right\} \left( \text{diagram} \right) \quad (1.199)$$

(mirroring notation (1.177) for the sum over vertex insertions), where the hatched blob denotes the 2-point correlator that is inserted by the MV-average, and the target is suppressed. To higher orders, due to locality in rapidity, the 2-point correlator still attaches at the latest value of rapidity (i.e. at the very left, in a graphical sense) [18, 20]

$$\int_{Y_0}^Y d\tilde{Y}_n \int_{Y_0}^{\tilde{Y}_n} d\tilde{Y}_{n-1} \dots \int_{Y_0}^{\tilde{Y}_1} d\tilde{Y}_0 \left\{ \left( \text{diagram} \right) \dots \left( \text{diagram} \right) \right\} \left( \text{diagram} \right). \quad (1.200)$$

The same effect can also be achieved through a simpler functional: Consider the following Ansatz for the averaging procedure  $\langle \mathcal{A} \rangle(Y)$  (for an arbitrary observable  $\mathcal{A}$ ),

$$\langle \mathcal{A} \rangle(Y) = \left\langle \text{P}_Y \text{exp} \left\{ - \int_{Y_0}^Y d\tilde{Y} \int d^2\mathbf{x} d^2\mathbf{y} G_{\tilde{Y}, \mathbf{x}\mathbf{y}}^{(\delta)} \delta^{ab} \bar{\nabla}_{\mathbf{x}}^a i \bar{\nabla}_{\mathbf{y}}^b \right\} \mathcal{A} \right\rangle(Y_0), \quad (1.201)$$

where  $G_{\tilde{Y}, \mathbf{x}\mathbf{y}}^{(\delta)}$  is a 2-point function yet to be determined and  $\bar{\nabla}_{\mathbf{x}}^a$  is defined in terms of the functional derivative  $\frac{\delta}{\delta U_{\mathbf{x}}}$  [18, 78]

$$i \bar{\nabla}_{\mathbf{x}}^a := t^a U_{\mathbf{x}} \frac{\delta}{\delta U_{\mathbf{x}}}, \quad (1.202a)$$

such that

$$i \bar{\nabla}_{\mathbf{x}}^a U_{\mathbf{y}} = t^a U_{\mathbf{x}} \delta_{\mathbf{x}\mathbf{y}}^{(2)} \quad \text{and} \quad i \bar{\nabla}_{\mathbf{x}}^a U_{\mathbf{y}}^\dagger = -U_{\mathbf{x}}^\dagger t^a \delta_{\mathbf{x}\mathbf{y}}^{(2)}. \quad (1.202b)$$

In the modern literature [30, 71, 79, 80], the Ansatz (1.201) is also referred to as the *Gaussian truncation*. By its very definition, the Ansatz (1.201) mirrors the action of the MV-averaging procedure and inserts a

<sup>27</sup>We have again neglected the fluctuations  $\alpha$  such that  $A = b + \alpha \approx b$ .



2-point propagator  $G^{(\delta)}$  to the left of the Wilson lines in a general correlator  $\langle \mathcal{A} \rangle (Y_0)$ ,

$$\left[ \frac{d}{d\tilde{Y}} \left\langle \text{P}_Y \exp \left\{ - \int_{Y_0}^Y d\tilde{Y} \int d^2\mathbf{x} d^2\mathbf{y} G_{\tilde{Y},\mathbf{x}\mathbf{y}}^{(\delta)} \delta^{ab} i\bar{\nabla}_{\mathbf{x}}^a i\bar{\nabla}_{\mathbf{y}}^b \right\} \mathcal{A} \right\rangle (Y_0) \right]_{ji} = \text{Diagram}, \quad (1.203)$$

where we have suppressed the superscript  $(\delta)$  in the graphical representation. However, not only is the parametrization (1.201) much easier to calculate than the average from the MV-model (since the latter requires one to compute complicated integrals that the former does not), but eq. (1.201) does not require the Wilson lines to be rapidity ordered as the parametrization itself is ordered in  $Y$ . This makes the Gaussian truncation (1.201) preferable over the MV-model (1.197).

It is easy to show that the Gaussian truncation satisfies the desired matrix equation (1.193b), one only needs to insert a full set of singlet states  $\sum_k |k\rangle\langle k|$ ,

$$\text{Diagram} = \sum_k \underbrace{\text{Diagram}_1}_{[\mathcal{M}(Y)]_{jk}} \underbrace{\text{Diagram}_2}_{[\langle \mathcal{A} \rangle (Y)]_{ki}} = [\mathcal{M}(Y)]_{jk} [\langle \mathcal{A} \rangle (Y)]_{ki}, \quad (1.204)$$

where a sum over repeated indices is applied in the last step. Therefore, the operator (1.201) does indeed give rise to a matrix  $\mathcal{M}(Y)$  acting on the matrix of correlators  $\langle \mathcal{A} \rangle (Y)$ . (If the algebra is so small that it allows only one singlet state, for example API  $(\text{SU}(N), V \otimes V^*)$ , then  $\mathcal{M}(Y)$  will be a scalar and  $\langle \mathcal{A} \rangle (Y)$  is a single correlator.)

### 1.5.3 Faithfully parametrizing the JIMWLK Hamiltonian

Inspired by the symmetry of the JIMWLK Hamiltonian eq. (1.191),<sup>28</sup>

$$-H_{\text{JIMWLK}} \mathbf{U}_{\mathbf{x},\mathbf{y}}^{m,n} := \text{Diagram}_1 + \text{Diagram}_2 + \text{Diagram}_3 \quad (1.205)$$

(for the notation  $\mathbf{U}_{\mathbf{x},\mathbf{y}}^{m,n}$ , *c.f.* eq. (1.126b)), we employ a parametrization that mimics the symmetry of  $H_{\text{JIMWLK}}$ , such as (up to first order) [51]

$$\left\langle \text{P}_Y \exp \left\{ - \int_{Y_0}^Y d\tilde{Y} \int d^2\mathbf{x} d^2\mathbf{y} \left( G_{\tilde{Y},\mathbf{x}\mathbf{y}}^{(\delta)} \delta^{ab} i\bar{\nabla}_{\mathbf{x}}^a i\bar{\nabla}_{\mathbf{y}}^b + L_{\tilde{Y},\mathbf{x}\mathbf{y}}^{(\delta)} \delta^{ab} i\bar{\nabla}_{\mathbf{x}}^a i\nabla_{\mathbf{y}}^b + K_{\tilde{Y},\mathbf{x}\mathbf{y}}^{(\delta)} \delta^{ab} i\nabla_{\mathbf{x}}^a i\nabla_{\mathbf{y}}^b \right) \right\} \mathcal{A} \right\rangle (Y_0), \quad (1.206)$$

where  $\nabla_{\mathbf{x}}^a$  acts to the right of the Wilson lines [18, 78],

$$i\nabla_{\mathbf{x}}^a U_{\mathbf{y}} := -U_{\mathbf{x}} t^a \delta_{\mathbf{x}\mathbf{y}}^{(2)} \quad \text{and} \quad i\nabla_{\mathbf{x}}^a U_{\mathbf{y}}^\dagger := t^a U_{\mathbf{x}}^\dagger \delta_{\mathbf{x}\mathbf{y}}^{(2)}, \quad (1.207)$$

<sup>28</sup>In [71] it is made clear that  $H_{\text{JIMWLK}}$  does not depend on the  $U^{(\dagger)}$ 's on which it acts, which is why eq. (1.205) appears without the tensor product  $\mathbf{U}_{\mathbf{x},\mathbf{y}}^{m,n}$  there.

such that

$$\left[ \frac{d}{dY} (\text{eq. (1.206)}) \right]_{ji} \longrightarrow \left( \text{Diagram 1} + \text{Diagram 2} + \text{Diagram 3} \right) \quad (1.208)$$

We note that the propagator  $L_{\tilde{Y}, \mathbf{x}\mathbf{y}}^{(\delta)}$  does not interact with the target in the middle term in (1.208). This immediately disqualifies a parametrization including the middle term in (1.208), as such a term breaks the symmetry of the Hamiltonian it ultimately tries to describe:  $H_{\text{JIMWLK}}$  is invariant under the following transformation of the Wilson lines  $\mathbf{U}_{\mathbf{x}, \mathbf{y}}^{m, n}$  (c.f. eq. (1.126b)):

$$\mathbf{U}_{\mathbf{x}, \mathbf{y}}^{m, n} \longrightarrow \mathbf{U}_L \mathbf{U}_{\mathbf{x}, \mathbf{y}}^{m, n} \mathbf{U}_R^\dagger, \quad (1.209)$$

where

$$\mathbf{U}_L := \underbrace{U_{\mathbf{z}_L} \otimes \dots \otimes U_{\mathbf{z}_L}}_{m \text{ times}} \otimes \underbrace{U_{\mathbf{z}_L}^\dagger \otimes \dots \otimes U_{\mathbf{z}_L}^\dagger}_{n \text{ times}} \quad (1.210a)$$

$$\mathbf{U}_R := \underbrace{U_{\mathbf{z}_R} \otimes \dots \otimes U_{\mathbf{z}_R}}_{m \text{ times}} \otimes \underbrace{U_{\mathbf{z}_R}^\dagger \otimes \dots \otimes U_{\mathbf{z}_R}^\dagger}_{n \text{ times}}, \quad (1.210b)$$

for two arbitrary transverse coordinates  $\mathbf{z}_L$  and  $\mathbf{z}_R$ . This is trivially true for the left and right term in (1.205). For the middle term in the JIMWLK Hamiltonian, the invariance with respect to the transformation (1.209) holds, since the interaction of the gluon with the target counteracts the vertex insertion  $t^a$  from standing in the way of the cancellation of  $\mathbf{U}_L$  and  $\mathbf{U}_R$ . However, since the middle term in the parametrization (1.206) does not interact with the target, it is invariant under the transformation if and only if  $\mathbf{z}_L = \mathbf{z}_R$ , and hence does not capture the more general invariance of  $H_{\text{JIMWLK}}$ . Therefore, the parametrization (1.206) can only include the first and last terms,

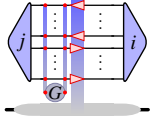
$$\left[ \frac{d}{dY} \left\langle \text{P}_Y \exp \left\{ - \int_{Y_0}^Y d\tilde{Y} \int d^2\mathbf{x} d^2\mathbf{y} \left( G_{\tilde{Y}, \mathbf{x}\mathbf{y}}^{(\delta)} \delta^{ab} i \bar{\nabla}_x^a i \bar{\nabla}_y^b + K_{\tilde{Y}, \mathbf{x}\mathbf{y}}^{(\delta)} \delta^{ab} i \nabla_x^a i \nabla_y^b \right) \right\} \mathcal{A} \right\rangle (Y_0) \right]_{ji} = \left( \text{Diagram 1} + \text{Diagram 2} \right) \quad (1.211)$$

However, this means that the parametrization (1.211) cannot describe the middle term of the JIMWLK Hamiltonian (1.205) — we can only hope that this term emerges from a generalization of (1.211) to higher orders (i.e. higher  $n$ -point functions).

#### 1.5.4 Beyond the Gaussian truncation

One may attempt to find a better parametrization of the JIMWLK Hamiltonian by including higher order terms. In the spirit of eq. (1.201) (or, equivalently, eq. (1.211)), we generalize the left action involving

$G_{Y,\mathbf{x}_1\mathbf{x}_2}^{(\delta)}$  to (*c.f.* [80], where we absorbed numerical factors into the parameters  $G$ )



$$\left\langle \left\langle \int_{\mathbf{x}_1\mathbf{x}_2} G_{Y,\mathbf{x}_1\mathbf{x}_2}^{(\delta)} \delta^{a_1 a_2} i \bar{\nabla}_{\mathbf{x}_1}^{a_1} i \bar{\nabla}_{\mathbf{x}_2}^{a_2} \right. \right. \quad (1.212a)$$

$$\left. + \int_{\mathbf{x}_1\mathbf{x}_2\mathbf{x}_3} \left( G_{Y,\mathbf{x}_1\mathbf{x}_2\mathbf{x}_3}^{(d)} d^{a_1 a_2 a_3} + G_{Y,\mathbf{x}_1\mathbf{x}_2\mathbf{x}_3}^{(f)} f^{a_1 a_2 a_3} \right) i \bar{\nabla}_{\mathbf{x}_1}^{a_1} i \bar{\nabla}_{\mathbf{x}_2}^{a_2} i \bar{\nabla}_{\mathbf{x}_3}^{a_3} \right. \quad (1.212b)$$

$$\left. + \int_{\mathbf{x}_1\mathbf{x}_2\mathbf{x}_3\mathbf{x}_4} \left( \sum_j G_{Y,\mathbf{x}_1\mathbf{x}_2\mathbf{x}_3\mathbf{x}_4}^{(j)} C_j^{a_1 a_2 a_3 a_4} \right) i \bar{\nabla}_{\mathbf{x}_1}^{a_1} i \bar{\nabla}_{\mathbf{x}_2}^{a_2} i \bar{\nabla}_{\mathbf{x}_3}^{a_3} i \bar{\nabla}_{\mathbf{x}_4}^{a_4} \right. \quad (1.212c)$$

$$\left. + \dots \right\} \mathcal{A} \rangle (Y_0) \Big]_{ji},$$

where

$$\int_{\mathbf{x}_1\mathbf{x}_2\mathbf{x}_3\mathbf{x}_4\dots} := \int \int \int \int d\mathbf{x}_1 d\mathbf{x}_2 d\mathbf{x}_3 d\mathbf{x}_4 \dots, \quad (1.213)$$

and similarly for the right action involving  $K_{Y,\mathbf{x}_1\mathbf{x}_2}^{(\delta)}$  (*c.f.* eq. (1.211)). In eq. (1.212),  $f^{a_1 a_2 a_3}$  and  $d^{a_1 a_2 a_3}$  are structure tensors of  $SU(N)$ , and the  $C_j^{a_1 a_2 a_3 a_4}$  are color factors of rank 4.

Only retaining the operators acting from the left (i.e. setting all functions  $K_{Y,\mathbf{x}_1\dots\mathbf{x}_n}^{(j)}$  to zero), this approximation was used up to third order to investigate the odderon contribution to observables [80]. On the other hand, determining the symmetries of the color factors  $C_j^{a_1\dots a_n}$  beyond the third order is not a trivial task, and current research is being conducted to answer this question (*c.f.*, for example, [81, 82]). We comment on this topic again in section 10.2.2.2 at the end of this thesis.

We emphasize that truncating the series given in (1.212) at the  $n^{\text{th}}$  order leaves gauge invariance intact. The underlying cause for this is that the truncation happens at the level of the Lie algebra (i.e. in the exponent) rather than on the manifold itself. Thus, even when (1.212) is truncated, the resulting object still lies in the group manifold.

### 1.5.5 Symmetries of the correlators and the parametrization of JIMWLK

Let us parallel transport the initial condition  $\langle \mathcal{A} \rangle (Y_0)$  (*c.f.* (1.211)) from  $Y_0$  to  $Y$  using some transformations  $U_{[Y,Y_0]}^L$  and  $U_{[Y,Y_0]}^R$  acting on the left and right of  $\langle \mathcal{A} \rangle (Y_0)$  respectively,

$$\langle \mathcal{A} \rangle (Y) \rightarrow U_{[Y,Y_0]}^L \langle \mathcal{A} \rangle (Y_0) U_{[Y,Y_0]}^R. \quad (1.214)$$

The  $Y$ -derivative of  $\langle \mathcal{A} \rangle (Y)$  is then given by

$$\begin{aligned} \frac{d}{dY} \left( \overbrace{U_{[Y,Y_0]}^L \langle \mathcal{A} \rangle (Y_0) U_{[Y,Y_0]}^R}^{\langle \mathcal{A} \rangle (Y)} \right) &= \left( \frac{d}{dY} U_{[Y,Y_0]}^L \right) \langle \mathcal{A} \rangle (Y_0) U_{[Y,Y_0]}^R + U_{[Y,Y_0]}^L \langle \mathcal{A} \rangle (Y_0) \left( \frac{d}{dY} U_{[Y,Y_0]}^R \right) \\ &= \left( \frac{d}{dY} U_{[Y,Y_0]}^L \right) \left( U_{[Y,Y_0]}^L \right)^{-1} \overbrace{U_{[Y,Y_0]}^L \langle \mathcal{A} \rangle (Y_0) U_{[Y,Y_0]}^R}^{\langle \mathcal{A} \rangle (Y)} \end{aligned}$$

$$+ \underbrace{U_{[Y,Y_0]}^L \langle \mathcal{A} \rangle (Y_0) U_{[Y,Y_0]}^R}_{\langle \mathcal{A} \rangle (Y)} \left( U_{[Y,Y_0]}^R \right)^{-1} \left( \frac{d}{dY} U_{[Y,Y_0]}^R \right)^{-1}, \quad (1.215)$$

where we have inserted the unit elements  $\left( U_{[Y,Y_0]}^L \right)^{-1} U_{[Y,Y_0]}^L = \mathbb{1}$  and  $U_{[Y,Y_0]}^R \left( U_{[Y,Y_0]}^R \right)^{-1} = \mathbb{1}$  in the second step. Defining the operators  $\mathcal{E}^L(Y)$  and  $\mathcal{E}^R(Y)$  as

$$\mathcal{E}^L(Y) := - \left( \frac{d}{dY} U_{[Y,Y_0]}^L \right) \left( U_{[Y,Y_0]}^L \right)^{-1} \quad \text{and} \quad \mathcal{E}^R(Y) := - \left( U_{[Y,Y_0]}^R \right)^{-1} \left( \frac{d}{dY} U_{[Y,Y_0]}^R \right), \quad (1.216)$$

the  $Y$ -evolution of  $\langle \mathcal{A} \rangle (Y)$  can be written as

$$\frac{d}{dY} \langle \mathcal{A} \rangle (Y) = - \left( \mathcal{E}^L(Y) \langle \mathcal{A} \rangle (Y) + \langle \mathcal{A} \rangle (Y) \mathcal{E}^R(Y) \right), \quad (1.217)$$

where  $\mathcal{E}^L(Y)$  and  $\mathcal{E}^R(Y)$  are once again  $k \times k$  matrices acting on  $\langle \mathcal{A} \rangle (Y)$  from the left, respectively, right. If a particular element of  $\langle \mathcal{A} \rangle (Y)$  is zero, then the corresponding elements in  $\mathcal{E}^L(Y)$  and  $\mathcal{E}^R(Y)$  must vanish as well, as was already the case for  $\mathcal{M}(Y)$  in (1.193b).

The parametrization (1.217) can easily be reformulated to yield a matrix equation of the form (1.193b) [51]: Multiplying the right-hand side of eq. (1.217) with  $\langle \mathcal{A} \rangle^{-1}(Y) \langle \mathcal{A} \rangle (Y) = \mathbb{1}$ ,

$$\frac{d}{dY} \langle \mathcal{A} \rangle (Y) = - \left( \mathcal{E}^L(Y) \langle \mathcal{A} \rangle (Y) + \langle \mathcal{A} \rangle (Y) \mathcal{E}^R(Y) \right) \langle \mathcal{A} \rangle^{-1}(Y) \langle \mathcal{A} \rangle (Y), \quad (1.218)$$

and defining

$$\mathcal{M}(Y) := \mathcal{E}^L(Y) + \langle \mathcal{A} \rangle (Y) \mathcal{E}^R(Y) \langle \mathcal{A} \rangle^{-1}(Y) \quad (1.219)$$

once again yields the parametrization (1.193b), which acts on the left of  $\langle \mathcal{A} \rangle (Y)$  only. Thus, we have confirmed that eq. (1.193b) is fully general. However, recent research [83] indicates that, even though a truncation of the one sided parametrization (1.193b) leaves the result gauge invariant, it does not necessarily reflect the symmetries of the matrix of correlators  $\langle \mathcal{A} \rangle (Y)$ : If, for example, we decompose  $\langle \mathcal{A} \rangle (Y)$  into its symmetric and antisymmetric parts,

$$\langle \mathcal{A} \rangle (Y) = \frac{\langle \mathcal{A} \rangle (Y) + \langle \mathcal{A} \rangle^t(Y)}{2} + \frac{\langle \mathcal{A} \rangle (Y) - \langle \mathcal{A} \rangle^t(Y)}{2}, \quad (1.220)$$

Then the JIMWLK evolution of each portion must reflect its symmetry. In other words,

$$\frac{d}{dY} \left( \frac{\langle \mathcal{A} \rangle (Y) + \langle \mathcal{A} \rangle^t(Y)}{2} \right) \quad \text{is symmetric} \quad (1.221a)$$

$$\frac{d}{dY} \left( \frac{\langle \mathcal{A} \rangle (Y) - \langle \mathcal{A} \rangle^t(Y)}{2} \right) \quad \text{is antisymmetric.} \quad (1.221b)$$

On the other hand, the parametrization (1.219) on a symmetric matrix  $\frac{1}{2}(\langle \mathcal{A} \rangle (Y) + \langle \mathcal{A} \rangle^t(Y))$  does not necessarily yield a symmetric matrix when it is truncated at a particular order — *all* orders are required [83].

Recent research [83] suggests that the easiest way to maintain the symmetry properties (1.221) of  $\langle \mathcal{A} \rangle (Y)$  is to retain a two-sided approach *à la* eq. (1.217), with certain conditions imposed on the relationship between

the  $n$ -point functions in  $\mathcal{E}^L(Y)$  and  $\mathcal{E}^R(Y)$ . This ensures that the symmetries of the matrix of correlators  $\langle \mathcal{A} \rangle(Y)$  is not destroyed by the parametrization of the evolution equation. In this thesis, we focus on the symmetries of the correlators in  $\langle \mathcal{A} \rangle(Y)$ :

## 1.6 Symmetry implications for Wilson line correlators

Up to this point, we have given a summary of QCD interactions at high energies in the Regge-Gribov limit, and of how observables in such a limit (i.e. Wilson line correlators) depend on the energy deposited into the collision area (*c.f.* the JIMWLK equation in section 1.4). Let us recapitulate the key points discussed so far.

Confinement is a phenomenon of QCD that is, to this day, theoretically not well understood in the sense that it is unclear which feature of QCD forces color charged objects to be confined into color neutral states. However, one of the consequences of confinement is clear: all objects that carry net color charge (i.e. quarks and gluons) are necessarily bound together in globally color neutral states such as baryons or mesons. It is thus of paramount importance to understand color neutral states, so-called *singlet-states*, in order to perform QCD calculations for cross sections on physically meaningful objects.

In the weak coupling region of QCD (where  $\alpha_s \ll 1$ ), a Feynman diagram containing fewer gluon vertices is kinematically favoured over a Feynman diagram containing many gluon vertices, as each vertex introduces a factor  $\propto \alpha_s$  in the corresponding Feynman integral. However, as we move to the high energy (equivalently high rapidity  $Y$ ) region of QCD, the vertex factor receives a logarithmic enhancement such that it becomes  $\propto \alpha_s \ln Y$ , which is of order 1. Consequently, higher order Feynman diagrams can no longer be neglected; a resummation of Feynman diagrams to all orders (in the number of gluons being exchanged) is necessary. As shown in section 1.2.3, this resummation yields the interaction to be described by Wilson lines. Since the Wilson lines themselves are elements of the gauge group  $SU(N)$  of QCD (*c.f.* section 1.2.4), they impart additional structure on the correlators describing the projectile. (This structure would not have been present at lower energies where the resummation of Feynman diagrams, which produces Wilson lines, does not take place!) In particular, this implies that the color singlets mentioned in this section are in fact singlet with respect to the gauge group  $SU(N)$ .

In conclusion, Wilson line correlators need to be understood well in order to proceed with (most) research in the small- $x_{Bj}$  limit of QCD. For the remainder of this section, the particulars of how Wilson line correlators will be studied in this thesis will be explained:

Section 1.6.1 focuses on the color singlets onto which the Wilson line correlators are projected. The fact that Wilson lines are elements of  $SU(N)$  has group theoretic implications on color singlets; these implications will be examined. We will find that surprisingly little is known about the singlet states of  $SU(N)$ , leading to the formulation of the main goal to be achieved in this thesis.

In section 1.6.2, the group theoretic implications of the Wilson line correlators on the parametrization of JIMWLK are explained. This analysis presupposes knowledge about the singlet states of  $SU(N)$ , therefore substantiating the need for the research that is presented in this thesis.

### 1.6.1 Wilson line correlators and JIMWLK evolution

As already stated, the color neutral states into which color charged objects combine are in fact the singlet states of  $SU(N)$ , by virtue of the Wilson lines being elements of the special unitary group. Each Wilson line correlator considered in this thesis (such as those we encountered thus far) is of the form

$$\langle j | \mathbf{U} | i \rangle, \quad (1.222)$$

where  $\mathbf{U} := U_{\mathbf{x}} \otimes U_{\mathbf{x}'}^\dagger \otimes U_{\mathbf{y}} \otimes U_{\mathbf{y}'}^\dagger$ , and  $\mathbf{x}, \mathbf{x}', \mathbf{y}, \mathbf{y}'$  are transverse coordinates. (We chose to alter the notation  $\mathbf{U}_{\mathbf{x}, \mathbf{y}}^{m, n}$  (c.f. eq. (1.126b)) to  $\mathbf{U}$  for the remainder of this thesis in order not to clutter the equations. However, the coordinate dependence on the factors in  $\mathbf{U}$  will always be made clear.) The states  $|i\rangle, |j\rangle =: \langle j |^\dagger$  are *global* singlet states of  $SU(N)$ , which is to say that  $|i\rangle$  and  $|j\rangle$  satisfy

$$\mathbf{U} |i, j\rangle = |i, j\rangle \quad \text{and} \quad \langle i, j | \mathbf{U}^\dagger = \langle i, j | \quad \text{if} \quad \mathbf{x} = \mathbf{x}' = \mathbf{y} = \mathbf{y}'. \quad (1.223)$$

Furthermore, Wilson lines *carry singlets into singlets*. This is a consequence of the conservation of color at each vertex<sup>29</sup> in the underlying sum of Feynman diagrams. This was also observed in the cross sections (1.144) (without fluctuations) and (1.179) (with fluctuations), where the singlet state  $|i\rangle$  once again becomes a singlet state  $|j\rangle$  after the interaction.

In the case of a  $q\bar{q}$ -dipole, there exists only one possible singlet.<sup>30</sup> Therefore, the  $q\bar{q}$ -pair must attain the same singlet state after the eikonal interaction as it had before, as can be observed in eq. (1.146). For two  $q\bar{q}$ -dipoles the situation becomes more interesting, since there are two possible singlets that can be formed [71],

$$\frac{1}{d_f} \begin{array}{c} \curvearrowright \\ \curvearrowleft \end{array} \quad \text{and} \quad \frac{1}{\sqrt{d_A}} \begin{array}{c} \curvearrowright \\ \curvearrowright \\ \curvearrowleft \\ \curvearrowleft \end{array}, \quad d_f := N, \quad d_A := N^2 - 1. \quad (1.224)$$

In practical calculations (for example, when considering the energy evolution by means of the JIMWLK equation), all of these states have to be considered simultaneously, since one singlet state may be mapped into another through the eikonal interaction. In other words, instead of a single correlator, one takes into account the following matrix of correlators [71],

$$\langle \mathcal{A} \rangle (Y) := \begin{pmatrix} \frac{1}{d_f^2} \begin{array}{c} \text{Diagram 1} \\ \text{Diagram 2} \end{array} & \frac{1}{d_f \sqrt{d_A}} \begin{array}{c} \text{Diagram 3} \\ \text{Diagram 4} \end{array} \\ \frac{1}{d_f \sqrt{d_A}} \begin{array}{c} \text{Diagram 5} \\ \text{Diagram 6} \end{array} & \frac{1}{d_A} \begin{array}{c} \text{Diagram 7} \\ \text{Diagram 8} \end{array} \end{pmatrix}. \quad (1.225)$$

Therefore, in order to properly encapsulate the  $Y$ -evolution of a particular Wilson line correlator over  $V^{\otimes m} \otimes (V^*)^{\otimes n}$ , *all* Wilson line correlators over this Fock space have to be known, as they will contribute towards the evolution. Consequently, knowledge of all singlet states of  $SU(N)$  over  $V^{\otimes m} \otimes (V^*)^{\otimes n}$  is required for such a calculation.

After carefully researching this topic, we found that the textbook method of constructing Hermitian projection

<sup>29</sup>For a textbook exposition, see [27].

<sup>30</sup>In chapter 5, a counting argument for singlets over  $V^{\otimes m} \otimes (V^*)^{\otimes m}$  is given (see Theorem 5.2), thus proving this claim.

operators onto the irreducible (singlet) representations of  $SU(N)$  over a mixed space  $V^{\otimes m} \otimes (V^*)^{\otimes n}$  is theoretical at best: There exists a clear algorithm to achieve this goal, but the computational effort involved is so large that it soon become impractical (we explain this algorithm and where it fails us in detail in chapter 5). Therefore, the goal of this thesis is simple:

**Research Statement:** We provide a general, practically useful construction algorithm for all singlet projection operators of  $SU(N)$  over any mixed product space  $V^{\otimes m} \otimes (V^*)^{\otimes n}$ .

The details on how we plan to achieve this, as well as an overview of other important results of this thesis, are given in section 1.7, where the outline of this thesis is presented. First, however, let us comment on how singlet states help to constrain the parameters  $G_{\mathbf{x}_1 \dots \mathbf{x}_n}^{(j)}$  and  $K_{\mathbf{x}_1 \dots \mathbf{x}_n}^{(j)}$  used in the parametrization of the JIMWLK equation (*c.f.* eq. (1.212)). This will immediately provide the first application of the singlet states to be constructed in this thesis.

### 1.6.2 Coincidence limits of Wilson line correlators

In a general Wilson line correlator, the tensor product  $\mathbf{U}$  consists of  $m$  fundamental and  $n$  antifundamental Wilson lines, which are all at *distinct* transverse coordinates (*c.f.* eq. (1.222)),

$$\mathbf{U} := U_{\mathbf{x}_1} \otimes \dots \otimes U_{\mathbf{x}_m} \otimes U_{\mathbf{y}_1}^\dagger \otimes \dots \otimes U_{\mathbf{y}_n}^\dagger \in \underbrace{SU(N) \times \dots \times SU(N)}_{(m+n) \text{ factors}}. \quad (1.226)$$

Such a tensor product gives a representation of the product group  $SU(N) \times \dots \times SU(N)$  ( $m+n$  factors) on  $V^{\otimes m} \otimes (V^*)^{\otimes n}$ . Since the states  $|i\rangle, |j\rangle$  are *globally* singlet with respect to  $SU(N)$ , the Wilson line correlator simplifies in the limit where all transverse coordinates are set equal, i.e. the limit

$$\mathbf{U} \xrightarrow[=y_1=\dots=y_n]{x_1=\dots=x_m} U_{\mathbf{x}_1} \otimes \dots \otimes U_{\mathbf{x}_1} \otimes U_{\mathbf{x}_1}^\dagger \otimes \dots \otimes U_{\mathbf{x}_1}^\dagger \in \underbrace{SU(N) \times \dots \times SU(N)}_{(m+n) \text{ factors}} \quad (1.227)$$

yields  $\mathbf{U}|i, j\rangle = |i, j\rangle$  and  $\langle i, j|\mathbf{U}^\dagger = \langle i, j|$ . In this case, the tensor product  $\mathbf{U}$  realizes a representation of the group  $SU(N)$  on the product space  $V^{\otimes m} \otimes (V^*)^{\otimes n}$ , since there exists a map  $U_{\mathbf{x}_1} \mapsto \mathbf{U}$  (where  $U_{\mathbf{x}_1} \in SU(N)$ ). The limit (1.227) will from now on be referred to as a *total coincidence limit*, since the transverse coordinates of the associated Wilson lines coincide.

But, what happens if only *some* of the coordinates are set equal? It should be noted that such a *partial coincidence limit* reduces the factors in the product group for which  $\mathbf{U}$  realizes a representation on  $V^{\otimes m} \otimes (V^*)^{\otimes n}$ , for example,

$$\begin{aligned} \mathbf{U} \xrightarrow{x_1=x_2} U_{\mathbf{x}_1} \otimes U_{\mathbf{x}_1} \otimes U_{\mathbf{x}_3} \otimes \dots \otimes U_{\mathbf{x}_m} \otimes U_{\mathbf{y}_1}^\dagger \otimes \dots \otimes U_{\mathbf{y}_n}^\dagger &\in \underbrace{SU(N) \times \dots \times SU(N)}_{(m+n) \text{ factors}} \\ \text{realizes a representation of } \underbrace{SU(N) \times \dots \times SU(N)}_{(m+n)-1 \text{ factors}} &\text{ on } V^{\otimes m} \otimes (V^*)^{\otimes n}, \end{aligned} \quad (1.228)$$

since the first two factors in the product  $\mathbf{U}$  realize a representation of  $SU(N)$  on  $V^{\otimes 2}$ . Therefore, as more and more partial coincidence limits are taken, one expects more and more simplification to take place in the

associated Wilson line correlators. We will discuss the effects of partial coincidence limits on Wilson line correlators by means of an example.

Consider once again two  $q\bar{q}$ -dipoles (*c.f.* (1.225)), but let us condense the graphical notation used thus far. Firstly, we note that the rapidity dependent average  $\langle \dots \rangle (Y)$  was graphically denoted by  $\blacktriangleleft \dots \blacktriangleright$  (*c.f.* eq. (1.134)). In what follows, we will suppress the interaction with the target, thus making the notation  $\langle \dots \rangle (Y)$  for the average preferable,

$$\blacktriangleleft \left( \begin{array}{cc} \frac{1}{d_f^2} & \frac{1}{d_f \sqrt{d_A}} \\ \frac{1}{d_f \sqrt{d_A}} & \frac{1}{d_A} \end{array} \right) \blacktriangleright \rightarrow \left\langle \left( \begin{array}{cc} \frac{1}{d_f^2} & \frac{1}{d_f \sqrt{d_A}} \\ \frac{1}{d_f \sqrt{d_A}} & \frac{1}{d_A} \end{array} \right) \right\rangle (Y). \quad (1.229)$$

Furthermore, we will suppress the target itself; only the Wilson lines  $\blacktriangleleft$  in the diagram will remind us of the interaction taking place,<sup>31</sup>

$$\langle \mathcal{A} \rangle (Y) = \left\langle \left( \begin{array}{cc} \frac{1}{d_f^2} & \frac{1}{d_f \sqrt{d_A}} \\ \frac{1}{d_f \sqrt{d_A}} & \frac{1}{d_A} \end{array} \right) \right\rangle (Y). \quad (1.230)$$

Different bases of the singlet states will be beneficial for different coincidence limits. For example, the basis given in eq. (1.230) is particularly suited for studying the coincidence limits between either the top pair of Wilson lines,

$$U_{\mathbf{x}} \otimes U_{\mathbf{x}'}^\dagger \otimes U_{\mathbf{y}} \otimes U_{\mathbf{y}'}^\dagger \xrightarrow{\mathbf{x} \rightarrow \mathbf{x}'} U_{\mathbf{x}} \otimes U_{\mathbf{x}}^\dagger \otimes U_{\mathbf{y}} \otimes U_{\mathbf{y}'}^\dagger, \quad (1.231)$$

or the bottom pair ( $\mathbf{y} \rightarrow \mathbf{y}'$ ), as either of these limits will cause the off-diagonal elements of the matrix (1.230) to vanish [71],

$$\left\langle \left( \begin{array}{cc} \frac{1}{d_f^2} & \frac{1}{d_f \sqrt{d_A}} \\ \frac{1}{d_f \sqrt{d_A}} & \frac{1}{d_A} \end{array} \right) \right\rangle (Y) \xrightarrow[\text{or } \mathbf{y} \rightarrow \mathbf{y}']{\mathbf{x} \rightarrow \mathbf{x}'} \left\langle \left( \begin{array}{cc} \frac{1}{d_f} & 0 \\ 0 & \frac{1}{d_A} \end{array} \right) \right\rangle (Y). \quad (1.232)$$

The simplification exhibited in (1.232) boils down to the fact that the group generators  $[t^a]_{ik}$  are traceless (*c.f.* section 5.3.1.2 in chapter 5 for a more in-depth explanation). In order to use this property of the generators to our advantage for a coincidence limit between the central two Wilson lines ( $\mathbf{x}' \rightarrow \mathbf{y}$ ), or the top-most and bottom-most Wilson line ( $\mathbf{x} \rightarrow \mathbf{y}'$ ), a reordering (permutation) of index lines in the matrix (1.230) is

<sup>31</sup>We have highlighted the correlators on the diagonal for visual clarity.



necessary:

$$\langle \mathcal{A} \rangle (Y) = \left\langle \left( \begin{array}{cc} \frac{1}{d_f^2} \text{diag} & \frac{1}{d_f \sqrt{d_A}} \text{diag} \\ \frac{1}{d_f \sqrt{d_A}} \text{diag} & \frac{1}{d_A} \text{diag} \end{array} \right) (Y) \right\rangle = \left\langle \left( \begin{array}{cc} \frac{1}{d_f^2} \text{diag} & \frac{1}{d_f \sqrt{d_A}} \text{diag} \\ \frac{1}{d_f \sqrt{d_A}} \text{diag} & \frac{1}{d_A} \text{diag} \end{array} \right) (Y) \right\rangle, \quad (1.233)$$

where we merely disentangled the index lines in the second step for clarity. Under such a reordering, the off-diagonal elements of the matrix (1.233) once again vanish in the coincidence limits  $\mathbf{x} \rightarrow \mathbf{y}'$  and  $\mathbf{y} \rightarrow \mathbf{x}'$  [71].

Instead of viewing the matrix (1.233) as a permutation of index lines in the matrix (1.230), it may be viewed as a change of basis. The corresponding change of basis matrix is

$$\begin{pmatrix} \frac{1}{d_f} \text{diag} \\ \frac{1}{\sqrt{d_A}} \text{diag} \end{pmatrix} = \begin{pmatrix} \frac{1}{N} & 1 \\ \frac{N+1}{N} & -\frac{1}{N} \end{pmatrix} \begin{pmatrix} \frac{1}{d_f} \text{diag} \\ \frac{1}{\sqrt{d_A}} \text{diag} \end{pmatrix}. \quad (1.234)$$

Besides coincidence limits between a fundamental and an antifundamental Wilson line, one may also consider coincidence limits of two Wilson lines in the same representation. To achieve the maximum possible simplification of the matrix of correlators when such a limit is imposed, one should consider the singlet states  $|i\rangle, |j\rangle$  in a basis of (anti-)symmetrizers [71, app. C]: In birdtrack notation, (anti-)symmetrizers are written as [72]

$$\begin{array}{|} \hline \text{---} \\ \hline \end{array} = \frac{1}{2} \left( \begin{array}{|} \hline \text{---} \\ \hline \end{array} + \begin{array}{|} \hline \text{---} \\ \hline \end{array} \right) \quad \text{and} \quad \begin{array}{|} \hline \text{---} \\ \hline \end{array} = \frac{1}{2} \left( \begin{array}{|} \hline \text{---} \\ \hline \end{array} - \begin{array}{|} \hline \text{---} \\ \hline \end{array} \right), \quad (1.235)$$

which give rise to the following normalized basis states:

$$\sqrt{\frac{2}{N(N+1)}} \begin{array}{|} \hline \text{---} \\ \hline \end{array} = \sqrt{\frac{2}{N(N+1)}} \cdot \frac{1}{2} \left( \begin{array}{|} \hline \text{---} \\ \hline \end{array} + \begin{array}{|} \hline \text{---} \\ \hline \end{array} \right) \quad (1.236a)$$

$$\sqrt{\frac{2}{N(N-1)}} \begin{array}{|} \hline \text{---} \\ \hline \end{array} = \sqrt{\frac{2}{N(N-1)}} \cdot \frac{1}{2} \left( \begin{array}{|} \hline \text{---} \\ \hline \end{array} - \begin{array}{|} \hline \text{---} \\ \hline \end{array} \right). \quad (1.236b)$$

Using the basis (1.236), the matrix of correlators  $\langle \mathcal{A} \rangle (Y)$  becomes

$$\langle \mathcal{A} \rangle (Y) = \left\langle \left( \begin{array}{cc} \frac{2}{N(N+1)} \text{diag} & \frac{2}{N\sqrt{N^2-1}} \text{diag} \\ \frac{2}{N\sqrt{N^2-1}} \text{diag} & \frac{2}{N(N-1)} \text{diag} \end{array} \right) (Y) \right\rangle, \quad (1.237)$$

where we have reordered the product of Wilson lines  $\mathbf{U}$  to

$$\mathbf{U} = U_{\mathbf{x}} \otimes U_{\mathbf{x}'}^\dagger \otimes U_{\mathbf{y}} \otimes U_{\mathbf{y}'}^\dagger \xrightarrow{\text{re-order}} U_{\mathbf{x}} \otimes U_{\mathbf{y}} \otimes U_{\mathbf{x}'}^\dagger \otimes U_{\mathbf{y}'}^\dagger =: \tilde{\mathbf{U}}. \quad (1.238)$$

As already claimed, the coincidence limit of the top two Wilson lines ( $\mathbf{x} \rightarrow \mathbf{y}$ ) or the bottom two Wilson lines ( $\mathbf{x}' \rightarrow \mathbf{y}'$ ) yields great simplifications in the (anti-) symmetrizer basis, as it causes the off-diagonal elements of (1.237) to vanish,

$$\left\langle \begin{pmatrix} \frac{2}{N(N+1)} \text{diag} & \frac{2}{N\sqrt{N^2-1}} \text{diag} \\ \frac{2}{N\sqrt{N^2-1}} \text{diag} & \frac{2}{N(N-1)} \text{diag} \end{pmatrix} (Y) \xrightarrow[\text{or } \mathbf{x}' \rightarrow \mathbf{y}']{\mathbf{x} \rightarrow \mathbf{y}} \begin{pmatrix} \frac{2}{N(N+1)} \text{diag} & 0 \\ 0 & \frac{2}{N(N-1)} \text{diag} \end{pmatrix} (Y). \quad (1.239)$$

The reason for this simplification is that such a limit essentially connects the symmetrizer and antisymmetrizer in more than one index line (*c.f.* the later section 5.3.1.1).

Since eq. (1.237) gives the 4-point correlator in yet another basis, we may establish a change of basis between (1.237) and the matrix (1.230). Let us explicitly construct this change of basis: Since the two bases have a different ordering of the Wilson lines (*c.f.* eq. (1.238)), we first need to reorder the Wilson lines in the matrix (1.230) so that a change of basis can be constructed. For example, the element  $a_{12}$  of the matrix (1.230) should be rewritten as

$$a_{12} := \underbrace{\text{diag}}_{\langle j|} \underbrace{\text{diag}}_{\mathbf{U}} \underbrace{\text{diag}}_{|i\rangle} \xrightarrow{\text{re-order}} \underbrace{\text{diag}}_{\langle j|} \underbrace{\text{diag}}_{\mathbf{U}} \underbrace{\text{diag}}_{|i\rangle} = \underbrace{\text{diag}}_{\langle \tilde{\psi}^S|} \underbrace{\text{diag}}_{\tilde{\mathbf{U}}} \underbrace{\text{diag}}_{|\tilde{\phi}^S\rangle} \quad (1.240)$$

Thus, the basis states to be considered for the change of basis are

$$\frac{1}{d_f} \text{diag} \quad \text{and} \quad \frac{1}{\sqrt{d_A}} \text{diag}. \quad (1.241)$$

To write the first of these two states in the basis (1.236), it suffices to disentangle the index lines,

$$\frac{1}{d_f} \text{diag} \xrightarrow{\text{disentangle}} \frac{1}{d_f} \text{diag} = \frac{1}{d_f} \left( \text{diag} - \text{diag} \right). \quad (1.242)$$

To write the second basis state of eq. (1.241) in the basis of (anti-) symmetrizers, one has to apply the Fierz identity [72]

$$\text{diag} = \text{diag} + \frac{1}{N} \text{diag} \quad (1.243)$$

to the state and once again disentangle the index lines,

$$\frac{1}{\sqrt{d_A}} \text{Fierz} \left( \text{diagram} \right) = \frac{1}{\sqrt{d_A}} \left( \text{diagram} - \frac{1}{N} \text{diagram} \right) = \frac{1}{\sqrt{d_A}} \left( \text{diagram} - \frac{1}{N} \text{diagram} \right) \stackrel{\text{disentangle}}{=} \frac{1}{\sqrt{d_A}} \left( \text{diagram} - \frac{1}{N} \text{diagram} \right). \quad (1.244)$$

It remains to apply the definition of symmetrizers and antisymmetrizers (1.235) in order to write eq. (1.244) in terms of the (anti-)symmetrizer basis,

$$\frac{1}{\sqrt{d_A}} \text{Fierz} \left( \text{diagram} \right) = \frac{1}{\sqrt{d_A}} \left( \text{diagram} - \frac{1}{N} \text{diagram} \right) = \frac{1}{\sqrt{d_A}} \left( 1 - \frac{1}{N} \right) \text{diagram} + \frac{1}{\sqrt{d_A}} \left( 1 + \frac{1}{N} \right) \text{diagram}. \quad (1.245)$$

Thus, the basis change between (1.230) and (1.237) is

$$\begin{pmatrix} \frac{1}{d_f} \text{diagram} \\ \frac{1}{\sqrt{d_A}} \text{diagram} \end{pmatrix} = \begin{pmatrix} \sqrt{\frac{N(N+1)}{2}} \frac{1}{d_f} & -\sqrt{\frac{N(N-1)}{2}} \frac{1}{d_f} \\ \sqrt{\frac{N(N+1)}{2}} \frac{1}{\sqrt{d_A}} \left( 1 - \frac{1}{N} \right) & \sqrt{\frac{N(N-1)}{2}} \frac{1}{\sqrt{d_A}} \left( 1 + \frac{1}{N} \right) \end{pmatrix} \begin{pmatrix} \sqrt{\frac{2}{N(N+1)}} \text{diagram} \\ \sqrt{\frac{2}{N(N-1)}} \text{diagram} \end{pmatrix}. \quad (1.246)$$

As we have seen so far, a suitable choice of basis yields simplification in the matrix of correlators  $\langle \mathcal{A} \rangle (Y)$  under a particular coincidence limit. In other words, the constraint equations imposed by a certain coincidence limit become simple in an appropriate basis. For example, eq. (1.232) implies the following constraint equations,

$$a_{12} := \text{diagram} \stackrel{\substack{\mathbf{x} \rightarrow \mathbf{x}' \\ \text{or } \mathbf{y} \rightarrow \mathbf{y}'}}{\rightarrow} 0 \quad (1.247a)$$

$$a_{21} := \text{diagram} \stackrel{\substack{\mathbf{x} \rightarrow \mathbf{x}' \\ \text{or } \mathbf{y} \rightarrow \mathbf{y}'}}{\rightarrow} 0. \quad (1.247b)$$

For bases less suited to a particular coincidence limit, the according constraint equations become more involved, in that not a particular Wilson line correlator vanishes, but rather a linear combination of various correlators in the matrix becomes zero. As an example, the constraint equations of the matrix elements of (1.237) under the coincidence limit  $\mathbf{x} = \mathbf{x}'$  are

$$\left( 1 - \frac{1}{N} \right) \left( \text{diagram} - \text{diagram} \right) + \left( 1 + \frac{1}{N} \right) \left( \text{diagram} - \text{diagram} \right) \stackrel{\substack{\mathbf{x} \rightarrow \mathbf{x}' \\ \text{or } \mathbf{y} \rightarrow \mathbf{y}'}}{\rightarrow} 0, \quad (1.248)$$

and its Hermitian conjugate. This immediately follows when applying the basis change (1.246) to eqns. (1.247).

Such constraint equations impose additional structures on the  $n$ -point functions appearing in the parametrization of the JIMWLK Hamiltonian (*c.f.* eq. (1.212)): In particular if a specific matrix-element  $\mathcal{A}_{ij}$  vanishes, then  $[\mathcal{E}^L(Y)]_{ij}$  and  $[\mathcal{E}^R(Y)]_{ij}$  (*c.f.* eq. (1.217)) must vanish as well, as stated in section 1.5.5. As was demonstrated in the present section, particular coincidence limits cause certain Wilson line correlators (or linear combinations thereof) to vanish in  $\mathcal{A}$ . This structure must be inherited by  $\mathcal{E}^L(Y)$  and  $\mathcal{E}^R(Y)$ .

### 1.6.3 Pulling singlets apart: further limits in Wilson line correlators

Besides the structures that the singlet Wilson line correlators impose on the parametrization of the JIMWLK Hamiltonian, the study of singlet Wilson line correlators allows us to make physical statements about the corresponding observables:

Let us return to the  $2q + 2\bar{q}$ -correlators presented in eq. (1.230), where  $\mathbf{x}, \mathbf{x}'$  are the transverse coordinates of the top  $q\bar{q}$ -pair, and  $\mathbf{y}, \mathbf{y}'$  label the transverse positions of the bottom  $q\bar{q}$ -dipole,

The diagram shows two equivalent representations of a Wilson line correlator. On the left, two vertical lines (one blue, one red) are connected at the top and bottom by two horizontal lines (one blue, one red). On the right, four horizontal lines are shown, with the top two labeled  $U_x$  and  $U_{x'}^\dagger$ , and the bottom two labeled  $U_y$  and  $U_{y'}^\dagger$ .

$$(1.249)$$

It was shown [71] that the parametrized evolution

$$\frac{d}{dY} \langle \mathcal{A} \rangle (Y) = -\mathcal{M}(Y) \langle \mathcal{A} \rangle (Y) , \quad (1.250)$$

(*c.f.* eq. (1.193b), only the left parametrization is used) of these correlators in the Gaußian truncation can be written as

$$\mathcal{M}(Y) = \begin{pmatrix} m_{11}(Y) & m_{12}(Y) \\ m_{21}(Y) & m_{22}(Y) \end{pmatrix} , \quad (1.251a)$$

where the matrix elements are given by

$$m_{11}(Y) = C_f (\mathcal{G}'_{Y,xx'} + \mathcal{G}'_{Y,yy'}) \quad (1.251b)$$

$$m_{12}(Y) = \frac{\sqrt{d_A}}{2C_A} (\mathcal{G}'_{Y,xy} + \mathcal{G}'_{Y,x'y'} - \mathcal{G}'_{Y,x'y} - \mathcal{G}'_{Y,xy'}) = m_{21}^\dagger(Y) \quad (1.251c)$$

$$m_{22}(Y) = \left( C_f - \frac{C_A}{2} \right) (\mathcal{G}'_{Y,xx'} + \mathcal{G}'_{Y,yy'}) + \frac{C_d + C_A}{4} (\mathcal{G}'_{Y,xy} + \mathcal{G}'_{Y,x'y'}) - \frac{C_d - C_A}{4} (\mathcal{G}'_{Y,xy'} + \mathcal{G}'_{Y,x'y}) . \quad (1.251d)$$

Here, the constants  $C_{f,A}$  are the Casimirs of the fundamental and adjoint representations,  $C_d \delta^{ae} := d^{abc} d^{bce} = \frac{N^2-4}{N} \delta^{ae}$ , and  $\mathcal{G}'_{Y,xy}$  is related to the parameters  $G$  in the parametrization (1.203) as

$$\mathcal{G}'_{Y,xy} := G_{Y,xy} - \frac{1}{2} (G_{Y,xx} + G_{Y,yy}) . \quad (1.252)$$


Clearly,  $\mathcal{G}'_{Y,xy}$  is symmetric under the exchange of  $\mathbf{x}$  and  $\mathbf{y}$ , and vanishes if  $\mathbf{x} = \mathbf{y}$ .

Suppose one tries to pull the top  $q\bar{q}$ -dipole far apart from the bottom  $q\bar{q}$ -dipole in each of the correlators in (1.230),

$$|\mathbf{x} - \mathbf{x}'| , |\mathbf{y} - \mathbf{y}'| \ll \left| \frac{\mathbf{x} + \mathbf{x}'}{2} - \frac{\mathbf{y} + \mathbf{y}'}{2} \right| . \quad (1.253)$$

For the correlator in the top left corner

$$\frac{1}{d_f^2} \text{Diagram} \quad (1.254)$$

such a procedure will move the two “sub-singlets”  away from each other, yielding a product of two independent  $q\bar{q}$ -singlets.

For the remaining three  $2q + 2\bar{q}$ -correlators,

$$\frac{1}{d_f \sqrt{d_A}} \text{Diagram}, \quad \frac{1}{d_f \sqrt{d_A}} \text{Diagram}, \quad \frac{1}{d_A} \text{Diagram}, \quad (1.255)$$

increasing the spatial distance between the  $q\bar{q}$ -pairs amounts to isolating two gluons from each other. In a full QCD description, confinement renders these operators zero. Interestingly, this aspect of confinement is reproduced in eqns. (1.251):

- Consider the first two operators in eq. (1.255). Making the distance between the top and bottom  $q\bar{q}$ -pair large can be likened to making the size of the top dipole and the bottom dipole small individually. We already saw that the operators  $\frac{1}{d_f \sqrt{d_A}} \text{Diagram}$  and  $\frac{1}{d_f \sqrt{d_A}} \text{Diagram}$  vanish in both limits  $|\mathbf{x} - \mathbf{x}'| \rightarrow 0$  and  $|\mathbf{y} - \mathbf{y}'| \rightarrow 0$  (*c.f.* eqns. (1.247)). Hence, their evolution is expected to be zero also in the limit (1.253). Indeed, this is mirrored by  $m_{12}(Y)$ ,  $m_{21}(Y)$  obtained by [71] (*c.f.* eqns. (1.251)): In the limit (1.253), the 2-point functions  $\mathcal{G}'$  in  $m_{12}(Y)$ ,  $m_{21}(Y)$  depend on two coordinates that are separated by a very large distance. In this case the functions  $\mathcal{G}'$  become large [71],

$$\mathcal{G}'_{Y,xy} \xrightarrow{|\mathbf{x}-\mathbf{y}|\rightarrow\infty} \infty, \quad (1.256)$$

causing the evolution of the two operators  $\frac{1}{d_f \sqrt{d_A}} \text{Diagram}$  and  $\frac{1}{d_f \sqrt{d_A}} \text{Diagram}$  to go as  $\sim e^{-\infty}$  — their JIMWLK evolution is exponentially suppressed in this limit.

- On the other hand, the last operator in eq. (1.255) does not vanish in either limit  $|\mathbf{x} - \mathbf{x}'| \rightarrow 0$  or  $|\mathbf{y} - \mathbf{y}'| \rightarrow 0$  (*c.f.* eq. (1.232)), but rather reduces to a  $2g$ -singlet (if both these limits are implemented simultaneously). However, making the distance between the two gluons large (i.e. in the limit (1.253)) would produce two isolated gluons — this is forbidden by confinement. The parametrization (1.251) again obeys this aspect of confinement: In the limit (1.253) the two functions  $\mathcal{G}'_{Y,xx'}$  and  $\mathcal{G}'_{Y,yy'}$  in  $m_{22}(Y)$  are negligible compared to the remaining 2-point functions  $\mathcal{G}'$ , which, in turn, become large in this limit (*c.f.* eq. (1.256)). Therefore, the JIMWLK evolution of the operator  $\frac{1}{d_A} \text{Diagram}$  is exponentially suppressed in the limit (1.253).

From the analysis presented in this section, it is of utmost importance, firstly, to know the singlet states with which we construct the Wilson line correlators, and, secondly, to study the coincidence limits of the correlators. The following section gives a road map for how we obtain the singlet states for the Wilson line correlators in this thesis.

## 1.7 Thesis Outline

As stated in the research statement on page 65, an effective study of Wilson line correlators (and its (partial) coincidence limits) over  $V^{\otimes m} \otimes (V^*)^{\otimes n}$  presupposes knowledge of the singlet states of  $SU(N)$  over  $V^{\otimes m} \otimes (V^*)^{\otimes n}$ . However, these singlet states are much less known than a glance at the literature may lead us to believe: In practical examples, one usually considers  $n$ -point Wilson line correlators for small  $n$ , for which the appropriate singlet states can easily be guessed (see for example [71]). There exists an algorithm for constructing the projection operators onto the irreducible representations of  $SU(N)$  over  $V^{\otimes m} \otimes (V^*)^{\otimes n}$  (which includes the singlet representations), but this algorithm is useful only for classification purposes, as it is extremely computationally expensive (this will be exemplified in chapter 5, section 5.1.3). We therefore provide an alternative construction algorithm for the singlet projection operators (and thus the singlet states) in part I of this thesis.

In the present chapter, the birdtrack formalism was already identified as a useful tool for our purposes. In chapter 2, we give (and prove) several easily implementable simplification rules for birdtrack operators comprised of symmetrizers and antisymmetrizers. These rules fall into two classes: *cancellation* rules, which can be used to shorten the birdtrack expression of a particular operator, and *propagation* rules, which allow one to commute certain sets of symmetrizers and antisymmetrizers.<sup>32</sup> The second set of rules is particularly useful for making the Hermiticity of an operator visually apparent.

In chapter 3, these simplification rules will be put to use when we shift our focus to the irreducible representations of  $SU(N)$  over the space  $V^{\otimes m}$ . We first review the classical methods of constructing the projection operators onto the desired representations due to Young [84] and improved by Littlewood [85]. However, the projectors constructed in this way lack Hermiticity, which is a crucial problem for our purposes. We then present a more modern approach by Keppeler and Sjö Dahl (KS) [4], which produces Hermitian Young projection operators. However, the KS operators, beyond the most elementary examples, require a large computational effort to construct. The main result of chapter 3 is an alternative construction principle for compact (and thus easily obtainable) Hermitian Young projection operators, based on the measure of lexical disorder (MOLD) of a Young tableau (Theorem 3.5). The *MOLD operators* are completely equivalent to the KS operators and thus inherit all the desired properties of their KS equivalent. The MOLD construction algorithm relies heavily on the simplification rules of chapter 2.

In chapter 4, we will augment the MOLD operators with what we call *transition operators* to constitute a basis for the algebra of primitive invariants of  $SU(N)$  over  $V^{\otimes m}$ , see section 4.3.2. These transition operators facilitate a change of basis between projection operators corresponding to equivalent irreducible representations of  $SU(N)$  over  $V^{\otimes m}$ . The highlight of chapter 4 is an easy-to-implement graphical construction method for transition operators directly from the MOLD operators (Theorem 4.5).

Chapter 5 is the heart of this thesis, as we will see all of the work done in chapters 2 to 4 bear fruit when constructing the singlet projection operators of  $SU(N)$  over a mixed product space  $V^{\otimes m} \otimes (V^*)^{\otimes n}$ . We first remind the reader about the textbook method used to construct the projection operators corresponding to the irreducible representations of  $SU(N)$  over  $V^{\otimes m} \otimes (V^*)^{\otimes n}$  (of which the singlet projectors form a subset) in section 5.1. In doing so, we find that this method is beyond laborious, to the point where it becomes essentially unusable in any practical calculation.

<sup>32</sup>In general, symmetrizers and antisymmetrizers do not commute, see eq. (2.16)

In section 5.2 we will present a **general algorithm to construct the singlet projectors in an easy, computationally efficient way**. We begin by discussing that the singlets over  $V^{\otimes k} \otimes (V^*)^{\otimes k}$  (note that there are an equal number of factors  $V$  and  $V^*$  in this product space) can be found by simply bending the basis elements of the algebra of invariants of  $SU(N)$  over  $V^{\otimes k}$  in section 5.2.1. Since the MOLD projection and transition operators span this algebra, they are prime candidates for the construction of singlets (*c.f.* Theorem 5.2).

It is then argued that all the singlet projectors constructed in this way project onto equivalent representations, and we give a general construction principle for the transition operators between singlets (Theorem 5.3). As an example, we construct and examine the singlet projectors and transition operators of  $SU(N)$  over  $V^{\otimes 3} \otimes (V^*)^{\otimes 3}$  in various bases, most of which were obtained by bending elements of bases of the algebra of invariants of  $SU(N)$  over  $V^{\otimes 3}$ .

Section 5.2.2 moves on to the more general product space  $V^{\otimes m} \otimes (V^*)^{\otimes n}$ . We explain that these projectors are singlets only for certain values of  $N$  and that, for this choice of  $N$ , they are completely equivalent to the singlets of  $SU(N)$  over  $V^{\otimes \alpha} \otimes (V^*)^{\otimes \alpha}$  for a particular integer  $\alpha$  (*c.f.* Theorem 5.4).

In light of the fact that we wish to use singlets to study Wilson line correlators, and thus infer properties about the parametrization of the JIMWLK equation (*c.f.* section 1.6.2), we examine the Wilson line correlators over the  $3q + 3\bar{q}$ -algebra in section 5.3.2. In analogy to the discussion of the  $2q + 2\bar{q}$  correlators in section 1.6.2, we will study various coincidence limits between Wilson lines. In the  $3q + 3\bar{q}$  example, we will find a nested hierarchy of smaller correlators as limiting cases of larger ones.

In the course of this PhD project, many “incidental” results pertaining to the representation theory of  $SU(N)$  over  $V^{\otimes m} \otimes (V^*)^{\otimes n}$  were obtained. These results are given in part **II** of this thesis. Most notably, a counting argument for the number of irreducible representations of  $SU(N)$  over  $V^{\otimes m} \otimes (V^*)^{\otimes n}$  was found, by establishing a relation between the Hermitian projection operators and the Hermitian primitive invariants of  $SU(N)$  over  $V^{\otimes m} \otimes (V^*)^{\otimes n}$  (Theorem 6.2). This theorem gives rise to numerous other results, which will be given in chapter 6. In chapter 7, these results are exemplified: We examine the projection and transition operators (in a particular basis) of  $SU(N)$  over all Fock spaces  $V^{\otimes m} \otimes (V^*)^{\otimes n}$  such that  $m+n = 4$ . At the end of the chapter, the special case  $N = 2$  (relating to the theory of spin) is discussed. Chapter 8 lists a multitude of theorems pertaining to the traces of primitive invariants of  $SU(N)$  over  $V^{\otimes(m+n)}$  and  $V^{\otimes m} \otimes (V^*)^{\otimes n}$ .

We end this thesis with a discussion on possible future research projects. Chapter 9 focuses on the mathematical aspects of this thesis. We list several possible research directions, following on from the results of this thesis, in the pursuit of a full mathematical theory. Chapter 10 discusses possible future research in a multitude of fields in high energy QCD. Such fields include transverse-momentum-dependent parton distributions (TMDs), energy loss, and the parametrization of the JIMWLK equation itself.





# Appendix to chapter 1

## 1.A Functional differentiation of a Wilson line: differentiating with respect to a parameter

In this appendix, we provide a proof for formula (1.158) given in section 1.4.2.6. While such a proof can be found in textbooks [86, eq. (5.15)], the proof given here originated from personal communication with A/Prof. Weigert [51].

Consider the Wilson line

$$U_{[\gamma, B, A]}[A_{\gamma(t)}^\nu] = \text{Pexp} \left\{ -ig \int_A^B d\gamma(t) A_{\gamma(t)}^{\nu a} t_{\gamma(t)}^a \right\}, \quad (1.257)$$

where

$$A_{\gamma(t)}^{\nu a} := b_{\gamma(t)}^{\nu a} + \alpha_{\gamma(t)}^{\nu a}, \quad (1.258)$$

and the path  $\gamma(t)$ ,  $t \in [t_0, t_1]$ , is depicted in Figure 1.12. Instead of taking the functional derivative  $\frac{\delta}{\delta b_{\gamma(t^*)}^{\mu b}}$  of  $U_{[\gamma, B, A]}$ , we construct a 1-parameter family and differentiate with respect to the parameter: Consider the 1-parameter family  $b_{\gamma(t)}^{\nu a}(s)$  defined as

$$b_{\gamma(t)}^{\nu a}(s) := b_{\gamma(t)}^{\nu a} + s \delta^{\nu\mu} \delta^{ab} \delta^{(4)}(\gamma(t) - \gamma(t^*)), \quad \text{such that} \quad A_{\gamma(t)}^{\nu a}(s) := b_{\gamma(t)}^{\nu a}(s) + \alpha_{\gamma(t)}^{\nu a}, \quad (1.259)$$

where  $t^* \in [t_0, t_1]$ . If the parameter  $s$  is set to 0, then  $b_{\gamma(t)}^{\nu a}(s)$  reduces to the original background field  $b_{\gamma(t)}^{\nu a}$ . A derivative with respect to  $s$  at  $s = 0$ ,  $\frac{d}{ds} \Big|_{s=0}$ , acts on the gauge field  $A_{\gamma(t)}^{\nu a}$  in exactly the same way as the functional derivative  $\frac{\delta}{\delta b_{\gamma(t^*)}^{\mu b}}$ ,

$$\frac{d}{ds} \Big|_{s=0} A_{\gamma(t)}^{\nu a}(s) = 0 + \delta^{\nu\mu} \delta^{ab} \delta^{(4)}(\gamma(t) - \gamma(t^*)) + 0 \quad (1.260a)$$

$$\frac{\delta}{\delta b_{\gamma(t^*)}^{\mu b}} A_{\gamma(t)}^{\nu a} = \delta^{\nu\mu} \delta^{ab} \delta^{(4)}(\gamma(t) - \gamma(t^*)) + 0. \quad (1.260b)$$

Since the Wilson line  $U_{[\gamma, B, A]}$  depends on the background field  $b$  only through the gauge field  $A$ , replacing

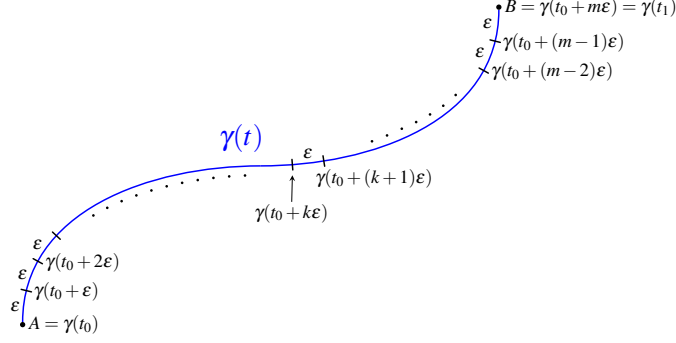


Figure 1.12: We partition the path  $\gamma$  of a Wilson line  $U_{[\gamma, B, A]}$  into  $m$  pieces of length  $\varepsilon := \frac{\text{length}(\gamma)}{m}$ , and then take the limit  $m \rightarrow \infty$ . The path  $\gamma$  depends on the parameter  $t$ ,  $t \in [t_0, t_1]$ , such that  $\gamma(t_0) = A$  and  $\gamma(t_1) = B$ .

$A_{\gamma(t)}^{\nu a}$  by  $A_{\gamma(t)}^{\nu a}(s)$ ,

$$U_{[\gamma, B, A]}[s, A_{\gamma(t)}^{\nu}] = \text{Pexp} \left\{ -ig \int_A^B d\gamma(t) A_{\gamma(t)}^{\nu a}(s) t_{\gamma(t)}^a \right\}, \quad (1.261)$$

and differentiating with respect to the parameter  $s$  will yield the desired result  $\frac{\delta}{\delta b_{\gamma(t^*)}^{\mu b}} U_{[\gamma, B, A]}[A_{\gamma(t)}^{\nu}]$ .

Before taking the  $s$ -derivative of the Wilson line (1.261), let us partition its path into infinitely many pieces of length  $\varepsilon$  (c.f. Figure 1.12) such that

$$U_{[\mathbf{x}, B, A]}[s, A_{\gamma(t)}^{\nu}(s)] = \lim_{m \rightarrow \infty} \prod_{k=0}^{m-1} U_{[\mathbf{x}, \gamma(t_0 + (k+1)\varepsilon), \gamma(t_0 + k\varepsilon)]}[s, A_{\gamma(t)}^{\nu}(s)], \quad (1.262)$$

in accordance with property (1.63) of Wilson lines.

In the limit  $m \rightarrow \infty$ , each Wilson line of length  $\varepsilon = \frac{\text{length}(\gamma)}{m} \rightarrow 0$  becomes<sup>33</sup>

$$U_{[\mathbf{x}, \gamma(t_0 + (k+1)\varepsilon), \gamma(t_0 + k\varepsilon)]}[s, A_{\gamma(t)}^{\nu}(s)] \xrightarrow{\varepsilon \rightarrow 0} \exp \left( -ig\varepsilon \frac{d\gamma}{dt} A_{\gamma(t)}^{\nu a}(s) t_{\gamma(t)}^a \Big|_{t=t_0 + k\varepsilon} \right), \quad (1.263)$$

where, due to the infinitesimal length of the path, we no longer have path-ordering in the exponential. By the product rule, the  $s$ -derivative of the Wilson line (1.262) becomes

$$\begin{aligned} & \frac{d}{ds} \Big|_{s=0} U_{[\gamma, B, A]}[s, A_{\gamma(t)}^{\nu}(s)] \\ &= \frac{d}{ds} \Big|_{s=0} \lim_{m \rightarrow \infty} \prod_{k=0}^{m-1} \exp \left( -ig\varepsilon \frac{d\gamma}{dt} A_{\gamma(t)}^{\nu a}(s) t_{\gamma(t)}^a \Big|_{t=t_0 + k\varepsilon} \right) \\ &= \lim_{m \rightarrow \infty} \sum_{k=0}^{m-1} \left\{ U_{[\gamma, B, \gamma(t_0 + k\varepsilon)]}[s, A_{\gamma(t)}^{\nu}(s)] \times \right. \\ & \quad \left. \times \exp \left\{ -ig\varepsilon \frac{d\gamma}{dt} A_{\gamma(t)}^{\nu a}(s) t_{\gamma(t)}^a \Big|_{t=t_0 + k\varepsilon} \right\} (-ig) \varepsilon \frac{d\gamma}{dt} \left( \frac{d}{ds} A_{\gamma(t)}^{\nu a}(s) t_{\gamma(t)}^a \Big|_{t=t_0 + k\varepsilon} \right) \times \right. \end{aligned}$$

<sup>33</sup>Notice that this would be an approximation if we merely required  $\varepsilon$  to be small, but since  $\varepsilon$  will be taken to 0, eq. (1.263) is exact.

$$\times U_{[\gamma, \gamma(t_0+k\varepsilon), A]}[s, A_{\gamma(t)}^\nu(s)] \Big|_{s=0} . \quad (1.264)$$

We recognize the infinite sum as a Riemann sum with the measure

$$\lim_{m \rightarrow \infty} \varepsilon \frac{d\gamma}{dt} \Big|_{t=t_0+k\varepsilon} \longrightarrow d\gamma(t_0+k\varepsilon) . \quad (1.265)$$

Further invoking the derivative at  $s = 0$  finally yields

$$\begin{aligned} \frac{\delta}{\delta b_{\gamma(t^*)}^{\mu b}} U_{[\gamma, B, A]}[A_{\gamma(t)}^\nu] &\stackrel{\text{eq. (1.260)}}{=} \frac{d}{ds} \Big|_{s=0} U_{[\gamma, B, A]}[s, A_{\gamma(t)}^\nu(s)] = \\ &= (-ig) \int_A^B [d\gamma(t_0+k\varepsilon)] \left\{ U_{[\gamma, B, \gamma(t_0+k\varepsilon)]}[A_{\gamma(t)}^\nu] \times \right. \\ &\quad \left. \times \left( \delta^{\nu\mu} \delta^{ab} \delta^{(4)}(\gamma(t_0+k\varepsilon) - \gamma(t^*)) t_{\gamma(t_0+k\varepsilon)}^a \right) U_{[\gamma, \gamma(t_0+k\varepsilon), A]}[A_{\gamma(t)}^\nu] \right\} . \end{aligned} \quad (1.266)$$

Let us now connect the result (1.266) to the context of section 1.4.2.6, in which eq. (1.266) will ultimately be applied: In section 1.4.2.6, we consider a Wilson line whose path extends to infinity, such that  $B, A \rightarrow \pm\infty$  respectively. Furthermore,  $\gamma(t)$  will be a straight line path parallel to the  $x^-$ -direction,

$$\gamma(t_0+k\varepsilon) \longrightarrow x^- , \quad (1.267)$$

and constant in  $x^+$ , which allows us to set  $x^+ = 0$ . Such a path is uniquely defined by the transverse coordinate  $\mathbf{x}$  at which it pierces the  $x^- = 0$  plane, such that we can write

$$U_{[\gamma, B, A]} \longrightarrow U_{[\mathbf{x}, \infty, -\infty]} . \quad (1.268)$$

In section 1.4.2.6, we are looking to take the functional derivative of the Wilson line (1.268) with respect to the background field  $b_v^{+b}$  (*c.f.* eq. (1.156b)), which translates into

$$\gamma(t^*) \longrightarrow v^- \quad \text{such that} \quad \delta^{\nu\mu} \delta^{ab} \delta^{(4)}(\gamma(t_0+k\varepsilon) - \gamma(t^*)) \longrightarrow \delta^{\nu+} \delta^{ab} \delta^{(4)}(x-v) . \quad (1.269)$$

Lastly, changing the integration variable to  $x^-$  in accordance with eq. (1.267), the integral (1.266) collapses due to the presence of  $\delta^{(4)}(x-v)$ , leaving us with

$$\begin{aligned} \frac{\delta}{\delta b_v^{+b}} U_{[\mathbf{x}, \infty, -\infty]} &\stackrel{\text{eq. (1.266)}}{=} (-ig) \int_{-\infty}^{\infty} dx^- U_{[\mathbf{x}, \infty, x^-]} \delta^{\nu+} \delta^{ab} \delta^{(4)}(x-v) t_x^a U_{[\mathbf{x}, x^-, -\infty]} \\ &= (-ig) \delta^{\nu+} \delta_{0v^+} \delta_{\mathbf{x}v}^{(2)} U_{[\mathbf{x}, \infty, v^-]} t_v^b U_{[\mathbf{x}, v^-, -\infty]} , \end{aligned} \quad (1.270)$$

as was claimed in eq. (1.158).



*Part I*

*Singlets and Wilson Line Correlators*



## Chapter 2

# Simplification Rules for Birdtrack Operators

This chapter has been published under the same name in the Journal of Mathematical Physics [1]. In some instances, the present paper (chapter) refers to additional results not given in the paper. Where such work is included in this thesis, a remark in square brackets and italics has been added to refer the reader to the appropriate chapter of this thesis.

**Abstract:** *This paper derives a set of easy-to-use tools designed to simplify calculations with birdtrack operators comprised of symmetrizers and antisymmetrizers. In particular, we present cancellation rules allowing one to shorten the birdtrack expressions of operators, and propagation rules identifying the circumstances under which it is possible to propagate symmetrizers past antisymmetrizers and vice versa. We exhibit the power of these simplification rules by means of a short example in which we apply the tools derived in this paper on a typical operator that can be encountered in the representation theory of  $SU(N)$  over the product space  $V^{\otimes m}$ . These rules form the basis for the construction of compact Hermitian Young projection operators and their transition operators addressed in companion papers [2, 3] [chapters 3 and 4].*

### 2.1 Introduction

In the 1970's, Penrose [87, 88] developed a graphical method of dealing with objects typically encountered in the representation theory of semi-simple compact Lie groups, as is used in quantum field theory (QFT). This new formalism was subsequently applied in a collaboration with MacCallum [89]. It is clear from Penrose's work that these graphical tools found their inspiration in Feynman diagrams and thus allow visually intuitive calculations of quantities in the QCD context, since  $SU(N)$  is the gauge group of QCD.

Penrose's graphical formalism obtained a more modern treatment by Cvitanović [72] in early part of the 21<sup>st</sup> century. It is Cvitanović who dubbed the diagrams *birdtracks*.

Birdtracks are gaining in their popularity as a computational tool for a modern treatment of group theory, in particular the representation theory of semi-simple Lie groups, and their applications to QFT. There, however, do not exist any *practical* tools that allow the easy manipulation of birdtracks in the literature. The authors suspect that this is the reason why birdtracks are not yet as widely used as they *ought* to be.

This paper aims to narrow this gap by providing several easy-to-use rules that greatly simplify dealing with birdtrack operators.

We will lay our focus on operators that are derived from Young projection operators [84], and the simplification rules presented in this paper are thus best suited for such operators. The reason for this is the authors' interest in the applications of these tools in a QCD context where factorization invariably involves color singlet projections of Wilson line correlators (see e.g. [71, 78, 90, 91] for a varied set of fields with possible applications). Since  $SU(N)$  is the gauge group of QCD, Young projection operators come into play through the theory of invariants, which relates the irreducible representations of  $SU(N)$  over  $V^{\otimes n}$  to the Young tableaux of size  $n$  (see [92, 93] and other standard textbooks). However, the lack of Hermiticity of Young projection operators disqualifies them from the application to QCD calculations [94] [chapter 5].

Keppeler and Sjö Dahl made a first step towards overcoming this problem in [4], where they present a recursive algorithm to construct Hermitian versions of Young projection operators in the birdtrack formalism. However, the KS operators soon become unwieldy and thus impractical to work with in automated calculations owing to computing time and memory resources necessary in their construction and application.

Using the simplification rules presented in this paper, the KS operators can be simplified drastically — an example of this is given in Figure 2.2.

This direct application, however, is not where these simplification rules exhaust their usefulness. Further applications are presented in a list of companion papers:

1. In [2] [chapter 3] we present an alternative construction algorithm for Hermitian Young projection operators, which directly leads to significantly more compact and explicitly Hermitian expressions of the operators.
2. The simplification rules are a crucial prerequisite for an algorithm that allows us to construct transition operators between (Hermitian) Young projection operators corresponding to equivalent irreducible representations of  $SU(N)$  [3] [chapter 4], which further furnish the construction of an orthogonal basis for the algebra of invariants on  $V^{\otimes m}$ .
3. This orthogonal basis can then be used to form a basis for the singlet states necessary to determine all color neutral Wilson line correlators [94] [chapter 5], which find direct applications in many branches of QCD. First applications (in a context that can be covered with direct calculations) can be found in [71, 80].

In this paper, we present two classes of simplification rules — they form the foundation for all three companion papers:

1. rules that determine whether certain symmetrizers or antisymmetrizers can be cancelled from an operator (section 2.3), and
2. rules describing when it is possible to propagate sets of (anti-)symmetrizers through certain parts of the operator (section 2.4).

Each result in these sections is accompanied by an example. In section 2.5 (Figure 2.2), we exhibit the applicability of these rules.

Before we set out to describe the simplification rules, we need to lay the groundwork by summarizing the conventions used in this paper in section 2.2.



## 2.2 Notation, conventions and known results

There exists a multitude of (sometimes contradicting) nomenclature and conventions in the literature with regards to Young tableaux, birdtracks, and related objects. This section serves to clarify the conventions used in this paper, as well as to collect a list of previously known results that are needed for this paper.

### 2.2.1 Tableaux

Consider an arrangement of  $m$  boxes filled with unique integers between 1 and  $k$  (for  $k \geq m$ ), for example,

$$\begin{array}{|c|c|c|} \hline 1 & 10 & 3 \\ \hline & 6 & 5 & 4 \\ \hline & & 7 & \\ \hline & 9 & 2 & 8 \\ \hline \end{array} . \tag{2.1}$$

In this paper, we will refer to such a construct as a *semi-standard irregular tableau*. In particular, the term “semi-standard” will refer to the requirement that each number appears *at most once* within a tableau. A special case of such a tableau is a *Young tableau*, in which we require  $k \stackrel{\text{def}}{=} m$ , and the boxes to be top-aligned and left-aligned, as well as the numbers in the boxes to increase within each row from left to right and within each column from top to bottom (see [93, 95, 96] and many other standard textbooks<sup>1</sup>). For example,

$$\begin{array}{|c|c|c|c|} \hline 1 & 3 & 5 & 6 \\ \hline 2 & 4 & 7 & \\ \hline 8 & & & \\ \hline \end{array} \tag{2.2}$$

is a Young tableau of size 8. In this paper, we shall denote a Young tableau by an upper case Greek letter, usually  $\Theta$  or  $\Phi$ , and a semi-standard irregular tableau by  $\tilde{\Theta}$  or  $\tilde{\Phi}$ . Furthermore, we will denote the set of all Young tableaux of size  $n$  by  $\mathcal{Y}_n$ .<sup>2</sup> For example,

$$\mathcal{Y}_3 := \left\{ \begin{array}{|c|c|c|} \hline 1 & 2 & 3 \\ \hline \end{array}, \begin{array}{|c|c|} \hline 1 & 2 \\ \hline 3 \\ \hline \end{array}, \begin{array}{|c|c|} \hline 1 & 3 \\ \hline 2 \\ \hline \end{array}, \begin{array}{|c|} \hline 1 \\ \hline 2 \\ \hline 3 \\ \hline \end{array} \right\} . \tag{2.3}$$

For a particular Young tableau  $\Theta \in \mathcal{Y}_n$ , we refer to  $\Theta_{(m)} \in \mathcal{Y}_{n-m}$  (for  $m < n$ ) as the *ancestor tableau* of  $\Theta$   $m$  generations back if  $\Theta_{(m)}$  is obtained from  $\Theta$  by removing the boxes  $\boxed{n}$ ,  $\boxed{n-1}$   $\dots$   $\boxed{n-m}$  from  $\Theta$ . For example, if

$$\Theta := \begin{array}{|c|c|c|c|} \hline 1 & 2 & 4 & 5 \\ \hline 3 & 6 & 8 & \\ \hline 7 & 9 & & \\ \hline \end{array} \quad \text{and} \quad \Phi := \begin{array}{|c|c|c|c|} \hline 1 & 2 & 4 & 5 \\ \hline 3 & & & \\ \hline \end{array} , \tag{2.4}$$

then  $\Phi$  is the ancestor tableau of  $\Theta$  four generations back, and we write  $\Phi = \Theta_{(4)}$ .

In this paper, we will need another kind of tableau, namely the *amputated tableau*, which we define as follows:

<sup>1</sup>In some references, the presently described tableau may also be referred to as a *standard* Young tableau (c.f., for example, [93, 95, 96]).

<sup>2</sup>The size of the set  $\mathcal{Y}_n$  is finite for *any* integer  $n$ , as is shown in [97].

**Definition 2.1 – Amputated Tableaux:**

Let  $\tilde{\Theta}$  be a tableau.<sup>3</sup> Furthermore, let  $\mathcal{R}$  be a particular row in  $\tilde{\Theta}$  and  $\mathcal{C}$  be a particular column in  $\tilde{\Theta}$ . Then, we form the column-amputated tableau of  $\tilde{\Theta}$  according to the row  $\mathcal{R}$ ,  $\check{\mathcal{C}}_c[\mathcal{R}]$ , by removing all columns of  $\tilde{\Theta}$  which do not overlap with the row  $\mathcal{R}$ . Similarly, we form the row-amputated tableau of  $\tilde{\Theta}$  according to the column  $\mathcal{C}$ ,  $\check{\mathcal{C}}_r[\mathcal{C}]$ , by removing all rows of  $\tilde{\Theta}$  which do not overlap with the column  $\mathcal{C}$ .

It should be noted that if  $\tilde{\Theta}$  is semi-standard, then  $\check{\mathcal{C}}_c[\mathcal{R}]$  and  $\check{\mathcal{C}}_r[\mathcal{C}]$  will also be semi-standard. As an example, consider the semi-standard irregular tableau

$$\tilde{\Theta} = \begin{array}{|c|c|c|c|} \hline 1 & 2 & 3 & 4 \\ \hline & & 6 & 5 \\ \hline & & & 7 & 8 \\ \hline \end{array}, \tag{2.5}$$

where we have shaded the row  $\mathcal{R} := (1, 2, 3, 4)$  and hatched the column  $\mathcal{C} := (3, 6)^t$ . Then, the column- and row-amputated tableaux according to  $\mathcal{R}$  and  $\mathcal{C}$  respectively are given by

$$\check{\mathcal{C}}_c[\mathcal{R}] = \begin{array}{|c|c|c|c|} \hline 1 & 2 & 3 & 4 \\ \hline & & 6 & 5 \\ \hline & & & 7 \\ \hline \end{array},$$

where the column  $(8)^t$  was removed since it does not have an overlap with the row  $\mathcal{R} = (1, 2, 3, 4)$ ,  $(1, 2, 3, 4) \cap (8)^t = \emptyset$ ,<sup>4</sup> and

$$\check{\mathcal{C}}_r[\mathcal{C}] = \begin{array}{|c|c|c|c|} \hline 1 & 2 & 3 & 4 \\ \hline & & 6 & 5 \\ \hline \end{array},$$

where the row  $(7, 8)$  was removed from  $\tilde{\Theta}$ , as it does not have an overlap with the column  $\mathcal{C} = (3, 6)^t$ ,  $(3, 6)^t \cap (7, 8) = \emptyset$ .

### 2.2.2 Birdtracks

As is clear by the title of this paper, we aim to provide simplification rules for birdtrack operators. In particular, this paper focuses on operators comprised of symmetrizers and antisymmetrizers. In this section, we give a *short* overview of the birdtrack notation [72] and its correspondence to Young projection operators [93]. For a more extensive introduction to birdtracks, readers are referred to [72], which also serves as the main resource for this section.

For each semi-standard tableau  $\tilde{\Theta}$  (be it irregular or Young), one may construct the corresponding sets of symmetrizers  $\mathbf{S}_{\tilde{\Theta}}$  and antisymmetrizers  $\mathbf{A}_{\tilde{\Theta}}$ <sup>5</sup> — this is in fact a generalization to the standard construction principle of symmetrizers and antisymmetrizers corresponding to Young tableaux [72, 84, 93]. Each row  $\mathcal{R}$  of the tableau will correspond to a symmetrizer over the numbers appearing in  $\mathcal{R}$ , and each column  $\mathcal{C}$  corresponds to an antisymmetrizer over the numbers in  $\mathcal{C}$ . For example, the symmetrizer over elements 1

<sup>3</sup>We do not require  $\tilde{\Theta}$  to be a Young tableau for this definition, a more general kind of tableau (e.g. a semi-standard irregular tableau) will suffice.

<sup>4</sup>Where we transferred the familiar set notation to rows of tableaux.

<sup>5</sup>If the tableau  $\tilde{\Theta}$  consists of  $m$  boxes filled with unique integers between 1 and  $k$  for  $k > m$ , we will draw an empty index line for each integer  $\leq k$  not appearing in the tableau  $\tilde{\Theta}$  in birdtrack notation.

and 2,  $\mathbf{S}_{12}$ , corresponds to the tableau

$$\boxed{1 \mid 2} . \quad (2.6)$$

This symmetrizer  $\mathbf{S}_{12}$  is given by  $\frac{1}{2}(\text{id} + (12))$ , where  $\text{id}$  is the identity and  $(12)$  denotes the transposition swapping elements 1 and 2. For example,  $\mathbf{S}_{12}$  acts on a tensor  $T^{ab}$  as

$$\mathbf{S}_{12}T^{ab} = \frac{1}{2}(T^{ab} + T^{ba}). \quad (2.7)$$

Graphically, we denote the symmetrizer  $\mathbf{S}_{12} = \frac{1}{2}(\text{id} + (12))$  as

$$\mathbf{S}_{12} = \frac{1}{2} \left( \begin{array}{c} \longleftrightarrow \\ \longleftrightarrow \end{array} + \begin{array}{c} \curvearrowright \\ \curvearrowleft \end{array} \right). \quad (2.8)$$

This operator is read from right to left,<sup>6</sup> as it is viewed to act as a linear map from the space  $V \otimes V$  into itself. In this paper, the elements of  $S_n$  (the permutation group of  $n$  objects) and linear combinations thereof will always be interpreted as elements of  $\text{Lin}(V^{\otimes n})$  (the space of linear maps over  $V^{\otimes n}$ ). Following [72], we will refer to the permutations of  $S_n$  as the *primitive invariants* (of  $\text{SU}(N)$  over  $V^{\otimes n}$ ), and thus denote the real subalgebra of  $\text{Lin}(V^{\otimes n})$  that is spanned by these primitive invariants by  $\text{API}(\text{SU}(N), V^{\otimes n}) \subset \text{Lin}(V^{\otimes n})$ .

Following [72], we denote a symmetrizer over an index set  $\mathcal{N}$ ,  $\mathbf{S}_{\mathcal{N}}$ , by an empty (white) box over the index lines in  $\mathcal{N}$ . Thus, the symmetrizer  $\mathbf{S}_{12}$  is denoted by  $\overleftrightarrow{\square}$ . Similarly, an antisymmetrizer over an index-set  $\mathcal{M}$ ,  $\mathbf{A}_{\mathcal{M}}$ , is denoted by a filled (black) box over the appropriate index lines. For example,

$$\mathbf{A}_{12} = \overleftarrow{\blacksquare} \quad \text{corresponds to the tableau} \quad \boxed{\begin{array}{c} 1 \\ 2 \end{array}}, \quad (2.9)$$

since antisymmetrizers correspond to columns of tableaux. It should be noted that (sets of) (anti-)symmetrizers are Hermitian with respect to the canonical scalar product on  $V^{\otimes m}$  (inherited from  $V$ ), that is,

$$\mathbf{S}_{\bar{\Theta}}^\dagger = \mathbf{S}_{\bar{\Theta}} \quad \text{and} \quad \mathbf{A}_{\bar{\Theta}}^\dagger = \mathbf{A}_{\bar{\Theta}}. \quad (2.10)$$

This is easiest seen in the birdtrack formalism, where Hermitian conjugation (with respect to the canonical scalar product) of an operator  $A$  corresponds to flipping  $A$  about its vertical axis and reversing the arrows (followed, in general by complex conjugation, which plays no role in the real algebra  $\text{API}(\text{SU}(N), V^{\otimes m})$  of interest to us here) [72].

For each tableau  $\bar{\Theta}$ , one can then define an operator  $\bar{Y}_{\bar{\Theta}}$  as the product of  $\mathbf{S}_{\bar{\Theta}}$  and  $\mathbf{A}_{\bar{\Theta}}$

$$\bar{Y}_{\bar{\Theta}} := \mathbf{S}_{\bar{\Theta}} \mathbf{A}_{\bar{\Theta}}; \quad (2.11)$$

this is in fact the generalization of Young operators [72, 84, 93] (*c.f.* eq. (2.13)) to semi-standard tableaux.

---

<sup>6</sup>This is no longer strictly true for birdtracks representing primitive invariants of  $\text{SU}(N)$  over a mixed product  $V^{\otimes m} \otimes (V^*)^{\otimes n}$ , where  $V^*$  is the dual vector space of  $V$ . A more informative discussion on this is out of the scope of this paper; readers are referred to [72] [or the later chapters 5 to 8].

As an example, the operator corresponding to the tableau (2.5) is given by

$$\tilde{\Theta} = \begin{array}{|c|c|c|c|} \hline 1 & 2 & 3 & 4 \\ \hline & & 6 & 5 \\ \hline & & & 7 & 8 \\ \hline \end{array} \longrightarrow \bar{Y}_{\tilde{\Theta}} = \begin{array}{c} \leftarrow \text{---} \text{---} \text{---} \text{---} \rightarrow \\ \leftarrow \text{---} \text{---} \text{---} \rightarrow \\ \leftarrow \text{---} \text{---} \text{---} \rightarrow \\ \leftarrow \text{---} \text{---} \text{---} \rightarrow \\ \leftarrow \text{---} \text{---} \text{---} \rightarrow \\ \leftarrow \text{---} \text{---} \text{---} \rightarrow \\ \leftarrow \text{---} \text{---} \text{---} \rightarrow \\ \leftarrow \text{---} \text{---} \text{---} \rightarrow \end{array} . \quad (2.12)$$

As already alluded to in the previous paragraph, Young projection operators are merely a special kind of the operators discussed so far, namely that where  $\tilde{\Theta} = \Theta$  is a Young tableau. One aspect that makes Young projection operators special is that there exists a unique constant  $\alpha_{\Theta} \neq 0$  such that<sup>7</sup>

$$Y_{\Theta} := \alpha_{\Theta} \cdot \underbrace{\mathbf{S}_{\Theta} \mathbf{A}_{\Theta}}_{=\bar{Y}_{\Theta}} \quad (2.13)$$

is idempotent; the object  $Y_{\Theta}$  is referred to as the *Young projection operator* corresponding to  $\Theta$ . For an operator  $\bar{Y}_{\tilde{\Theta}}$  corresponding to a semi-standard irregular tableau  $\tilde{\Theta}$ , it is not necessarily true that a nonzero constant  $c$  can be found that would yield  $Y_{\tilde{\Theta}} := c \cdot \bar{Y}_{\tilde{\Theta}}$  idempotent.<sup>8</sup> Therefore, we adapt the following notation:  $\bar{Y}_{\tilde{\Theta}}$  shall denote the operator corresponding to a (semi-standard irregular or Young) tableau  $\tilde{\Theta}$  according to (2.11), while the symbol  $Y_{\Theta}$  will refer to the *unique* Young projection operator corresponding to  $\Theta$  that is furnished with the appropriate constant  $\alpha_{\Theta}$  yielding  $Y_{\Theta}$  to be idempotent, *c.f.* eq. (2.13).

Let us now summarize the most important properties of Young projection operators [84, 93]:

1. *Idempotency*: The Young projection operator  $Y_{\Theta}$  corresponding to a Young tableau  $\Theta$  in  $\mathcal{Y}_n$  satisfies

$$Y_{\Theta} \cdot Y_{\Theta} = Y_{\Theta} \quad \text{for all } n. \quad (2.14a)$$

2. *Orthogonality*: If  $\Theta$  and  $\Phi$  are two Young tableaux in  $\mathcal{Y}_n$ , then the corresponding Young projection operators  $Y_{\Theta}$  and  $Y_{\Phi}$  are mutually orthogonal as projectors,

$$Y_{\Theta} \cdot Y_{\Phi} = \delta_{\Theta\Phi} Y_{\Theta} \quad \text{for } n = 1, 2, 3, 4, \quad (2.14b)$$

and more generally (for all  $n$ ) if  $\Theta$  and  $\Phi$  have different shapes.

3. *Completeness*: The Young projection operators corresponding to all Young tableaux in  $\mathcal{Y}_n$  sum up do the identity operator on  $V^{\otimes n}$ ,

$$\sum_{\Theta \in \mathcal{Y}_n} P_{\Theta} = \mathbf{1}_n \quad \text{for } n = 1, 2, 3, 4, \quad (2.14c)$$

but not beyond.

Generalizations of the Young projection operators that remove the restrictions on  $n$  on the latter two of these three properties allow one to fully classify the irreducible representations of  $\text{SU}(N)$  over  $V^{\otimes n}$  via Young tableaux in  $\mathcal{Y}_n$  [72, 85, 92, 98]. All these generalization build on the generally valid idempotency property of Young projectors, which will also be the only property we will rely on in this paper.

<sup>7</sup> $\alpha_{\Theta}$  is a combinatorial constant involving the Hook length of the tableau  $\Theta$  [72, 95, 96].

<sup>8</sup>This is easiest seen by means of an example: It can be verified via direct calculation that the operator corresponding to

$\begin{array}{|c|c|c|} \hline 1 & 2 & 3 \\ \hline & 6 & 5 \\ \hline & & 4 \\ \hline \end{array}$  is not proportional to a projection operator.

The Hermitian conjugate of a Young projection operator (2.13) is given by

$$Y_{\Theta}^{\dagger} = (\alpha_{\Theta} \cdot \mathbf{S}_{\Theta} \mathbf{A}_{\Theta})^{\dagger} = \alpha_{\Theta}^{\dagger} \cdot \mathbf{A}_{\Theta}^{\dagger} \mathbf{S}_{\Theta}^{\dagger} = \alpha_{\Theta} \cdot \mathbf{A}_{\Theta} \mathbf{S}_{\Theta} , \quad (2.15)$$

using the fact that  $\alpha_{\Theta}$  is a *real* constant (see [72, 95, 96] and other standard textbooks). In general, sets of symmetrizers and antisymmetrizers corresponding to a Young tableau do not commute,

$$[\mathbf{S}_{\Theta}, \mathbf{A}_{\Theta}] \neq 0 , \quad (2.16)$$

implying that Young projection operators are not Hermitian; the lack of Hermiticity of Young projection operators and the implications thereof are discussed in [2] [chapter 3].

As a last example, we construct the birdtrack Young projection operator corresponding to the following Young tableau:

$$\Theta = \begin{array}{|c|c|c|} \hline 1 & 3 & 4 \\ \hline 2 & 5 & \\ \hline \end{array} . \quad (2.17)$$

Since  $Y_{\Theta}$  must be comprised of symmetrizers corresponding to the rows of  $\Theta$  and antisymmetrizers corresponding to the columns of  $\Theta$ , we find that

$$Y_{\Theta} = \underbrace{2}_{\alpha_{\Theta}} \cdot \mathbf{S}_{134} \mathbf{S}_{25} \mathbf{A}_{12} \mathbf{A}_{35} , \quad (2.18)$$

where  $\alpha_{\Theta} = 2$  ensures the idempotency of  $Y_{\Theta}$ . In birdtrack notation, this Young projection operator becomes

$$Y_{\Theta} = \underbrace{2}_{\alpha_{\Theta}} \cdot \underbrace{\text{[birdtrack diagram]}}_{Y_{\Theta}} , \quad (2.19)$$


where we have used the bar-notation introduced previously (*c.f.* eqns. (2.11) and (2.13)). The benefit of the bar-notation is that it allows one to ignore additional scalar factors: Let  $O$  be a birdtrack operator comprised of symmetrizers and antisymmetrizers. Then, we define  $\bar{O}$  to be the equivalence class of operators that are proportional to the graphical part of  $O$  only, such that

$$\omega \cdot \bar{O} = \bar{O} , \quad \text{but in general} \quad \omega \cdot O \neq O \quad (2.20)$$

for any nonzero scalar  $\omega$ .

In expression (2.19) for  $Y_{\Theta}$  we were able to draw the two symmetrizers underneath each other since they are *disjoint*, and similarly for the two antisymmetrizers. In fact, the symmetrizers (resp. antisymmetrizers) corresponding to a semi-standard tableau will *always* be disjoint, since each number can occur at most once by the definition of semi-standard tableaux.

Any operator  $O \in \text{Lin}(V^{\otimes n})$  can be embedded into  $\text{Lin}(V^{\otimes m})$  for  $m > n$  in several ways, simply by letting the embedding act as the identity on  $(m - n)$  of the factors; how to select these factors is a matter of what one plans to achieve. The most useful convention for our purposes is to let  $O$  act on the first  $n$  factors and operate with the identity on the remaining last  $(m - n)$  factors. We will call this the *canonical embedding*.

On the level of birdtracks, this amounts to letting the index lines of  $O$  coincide with the top  $n$  index lines of  $\text{Lin}(V^{\otimes m})$ , and the bottom  $(m - n)$  lines of the embedded operator constitute the identity birdtrack of size  $(m - n)$ . For example, the operator  $\bar{Y}_{\begin{smallmatrix} 1 & 2 \\ 3 \end{smallmatrix}}$  is canonically embedded into  $\text{Lin}(V^{\otimes 5})$  as

$$(2.21)$$

Furthermore, we will use the same symbol  $O$  for the operator as well for its embedded counterpart. Thus,  $\bar{Y}_{\begin{smallmatrix} 1 & 2 \\ 3 \end{smallmatrix}}$  shall denote both the operator on the left, as well as on the right-hand side of the embedding (2.21).

Lastly, if a *Hermitian* projection operator  $A$  projects onto a subspace completely contained in the image of a Hermitian projection operator  $B$ , then we denote this as  $A \subset B$ , transferring the familiar notation of sets to the associated projection operators. In particular,  $A \subset B$  if and only if

$$A \cdot B = B \cdot A = A, \tag{2.22}$$

for the following reason: If the subspaces obtained by consecutively applying the operators  $A$  and  $B$  in any order is the same as that obtained by merely applying  $A$ , then the subspaces onto which  $A$  and  $B$  project not only need to overlap (as otherwise  $A \cdot B = B \cdot A = 0$ ), but the subspace corresponding to  $A$  must be completely contained in the subspace of  $B$  - otherwise the last equality of (2.22) would not hold.

Hermiticity is crucial for these statements: since we have seen that sets of symmetrizers and antisymmetrizers individually are Hermitian, (2.22) holds for such sets: a symmetrizer  $\mathcal{S}_{\mathcal{N}}$  can be absorbed into a symmetrizer  $\mathcal{S}_{\mathcal{N}'}$ , as long as the index set  $\mathcal{N}$  is a subset of  $\mathcal{N}'$ , and the same statement holds for antisymmetrizer [72]. For example,

$$(2.23)$$

Thus, by the above notation,  $\mathcal{S}_{\mathcal{N}'} \subset \mathcal{S}_{\mathcal{N}}$ , if  $\mathcal{N} \subset \mathcal{N}'$ . Or, as in our example,

$$(2.24)$$

In this sense, eq. (2.24) is a simplification rule in its own right, as it allows us to “cancel” (anti-)symmetrizers that can be absorbed into longer (anti-)symmetrizers. In particular, (2.24) implies that the image of any (anti-) symmetrizer is contained in the image of its ancestor (anti-) symmetrizers!<sup>9</sup> This nested inclusion of ancestor operators breaks down for the standard Young projection operators whenever they are not Hermitian [2] [chapter 3], as for example

$$(2.25)$$

<sup>9</sup>Where we transfer the nomenclature of ancestor-tableaux to the corresponding (anti-)symmetrizers.

but

$$\underbrace{\begin{array}{c} \leftarrow \text{---} \blacksquare \text{---} \leftarrow \\ \leftarrow \text{---} \blacksquare \text{---} \leftarrow \\ \leftarrow \text{---} \blacksquare \text{---} \leftarrow \end{array}}_{Y_{\begin{array}{|c|} \hline 1 \\ \hline 2 \\ \hline \end{array}}} \cdot \frac{4}{3} \cdot \underbrace{\begin{array}{c} \leftarrow \text{---} \square \text{---} \leftarrow \\ \leftarrow \text{---} \square \text{---} \leftarrow \\ \leftarrow \text{---} \square \text{---} \leftarrow \end{array}}_{Y_{\begin{array}{|c|} \hline 1 \ 3 \\ \hline 2 \\ \hline \end{array}}} = \frac{4}{3} \cdot \begin{array}{c} \leftarrow \text{---} \blacksquare \text{---} \leftarrow \\ \leftarrow \text{---} \blacksquare \text{---} \leftarrow \\ \leftarrow \text{---} \blacksquare \text{---} \leftarrow \end{array} \neq \frac{4}{3} \cdot \begin{array}{c} \leftarrow \text{---} \square \text{---} \leftarrow \\ \leftarrow \text{---} \square \text{---} \leftarrow \\ \leftarrow \text{---} \square \text{---} \leftarrow \end{array}, \quad (2.26)$$

which can be verified by direct calculation. On the other hand, the image of a Hermitian Young projection operator is contained in the images of its ancestor Hermitian projectors [2] [chapter 3].

The direction of the arrow on the index lines of the birdtrack encode whether the line acts on the vector space  $V$  (arrow pointing from right to left) or its dual  $V^*$  (arrow pointing from left to right) [72]. In this paper, we will only consider birdtracks acting on a space  $V^{\otimes m}$  (never on the dual) and thus only encounter birdtracks with arrows pointing from right to left. To reduce clutter, we will therefore suppress the arrows and (for example) simply write

$$\begin{array}{c} \diagdown \quad \diagup \\ \diagup \quad \diagdown \end{array} \quad \text{when we mean} \quad \begin{array}{c} \leftarrow \quad \leftarrow \\ \leftarrow \quad \leftarrow \\ \leftarrow \quad \leftarrow \end{array}. \quad (2.27)$$

We are now in a position to discuss the main result of this paper: We describe two classes of simplification rules for birdtrack operators  $O$  comprised of symmetrizers and antisymmetrizers, namely:

1. *Cancellation rules*: These describe a set of rules to *cancel* certain symmetrizers and antisymmetrizers within an operator  $O$ . The usefulness of these rules is that they can make a long expression significantly shorter, and thus more practical and less computationally expensive to work with. These rules are described in section 2.3.
2. *Propagation rules*: These describe the circumstances under which it is possible to commute a particular symmetrizer through a (set of) antisymmetrizer(s), and vice versa. These rules can be used to create a situation in which the cancellation rules (see part 1) can be used, or to make certain features of a particular operator  $O$  (for example its Hermiticity) explicit. These rules can be found in section 2.4.

These simplification rules come into their own when they are applied to birdtrack operators in group-theoretic calculations. For example, we extensively used these rules in our papers on a compact construction of Hermitian Young projection operators [2] [chapter 3] and transition operators [3] [chapter 4]. A further example is given in section 2.5 (Figure 2.2).

## 2.3 Cancellation rules

### 2.3.1 Cancellation of wedged Young projectors

We begin by presenting two main cancellation rules, Theorem 2.1 and Corollary 2.2. The benefit of these rules is that they can be used to shorten the birdtrack expressions of certain operators (sometimes inducing a constant factor), and thus make the resulting expression more useful for practical calculations.

**■ Theorem 2.1 – cancellation of wedged Young projectors:**

Consider an operator  $O$  consisting of an alternating product of altogether four symmetrizers and anti-symmetrizers, with the middle pair being proportional to a Young projection operator,

$$O = \mathbf{A}_{\Phi_1} \mathbf{S}_{\Theta} \mathbf{A}_{\Theta} \mathbf{S}_{\Phi_2} = \mathbf{A}_{\Phi_1} \bar{Y}_{\Theta} \mathbf{S}_{\Phi_2}, \quad (2.28)$$

such that  $\mathbf{S}_{\Theta} \supset \mathbf{S}_{\Phi_2}$  and  $\mathbf{A}_{\Theta} \supset \mathbf{A}_{\Phi_1}$ , i.e.  $\mathbf{S}_{\Theta} \mathbf{S}_{\Phi_2} = \mathbf{S}_{\Phi_2} = \mathbf{S}_{\Phi_2} \mathbf{S}_{\Theta}$  and  $\mathbf{A}_{\Theta} \mathbf{A}_{\Phi_1} = \mathbf{A}_{\Phi_1} = \mathbf{A}_{\Phi_1} \mathbf{A}_{\Theta}$  (c.f. eq. (2.22)). Then, we can drop  $\bar{Y}_{\Theta}$  while acquiring a scalar factor  $1/\alpha_{\Theta}$ :

$$\mathbf{A}_{\Phi_1} \bar{Y}_{\Theta} \mathbf{S}_{\Phi_2} = \frac{1}{\alpha_{\Theta}} \mathbf{A}_{\Phi_1} \mathbf{S}_{\Phi_2}. \quad (2.29)$$

Corresponding cancellations apply if all symmetrizers are exchanged for antisymmetrizers and vice versa.

Using  $Y_{\Theta}$  instead of  $\bar{Y}_{\Theta}$  removes the constant. The form presented here is that usually encountered in practical calculations.

Before looking at a general proof for this statement, we will develop the strategy for it through an example. To this end, take  $O$  to be

$$O = \underbrace{\text{[diagram]}}_{\mathbf{A}_{\Phi_1}} \underbrace{\text{[diagram]}}_{\mathbf{S}_{\Theta}} \underbrace{\text{[diagram]}}_{\mathbf{A}_{\Theta}} \underbrace{\text{[diagram]}}_{\mathbf{S}_{\Phi_2}}. \quad (2.30)$$

The central sets of symmetrizers and antisymmetrizers correspond to the Young tableau

$$\Theta = \begin{array}{|c|c|} \hline 1 & 2 \\ \hline 3 & \\ \hline \end{array} \quad (2.31)$$

embedded into  $\text{Lin}(V^{\otimes 5})$ . The inclusion criterion can be verified in multiple ways:

- Thinking in terms of *image* inclusions, we note that  $\mathbf{S}_{\Theta} \supset \mathbf{S}_{\Phi_2}$  (since  $\mathbf{S}_{\Theta} = \{\mathbf{S}_{12}\} \supset \{\mathbf{S}_{125}\} = \mathbf{S}_{\Phi_2}$ ) and  $\mathbf{A}_{\Theta} \supset \mathbf{A}_{\Phi_1}$  (since  $\mathbf{A}_{\Theta} = \{\mathbf{A}_{13}\} \supset \{\mathbf{A}_{13}, \mathbf{A}_{24}\} = \mathbf{A}_{\Phi_1}$ ).

- Equivalently, in terms of birdtracks, we see that

$$\underbrace{\text{[diagram]}}_{\mathbf{S}_{\Theta}} \underbrace{\text{[diagram]}}_{\mathbf{S}_{\Phi_2}} = \underbrace{\text{[diagram]}}_{\mathbf{S}_{\Phi_2}} = \underbrace{\text{[diagram]}}_{\mathbf{S}_{\Phi_2}} \underbrace{\text{[diagram]}}_{\mathbf{S}_{\Theta}} \quad \text{and} \quad \underbrace{\text{[diagram]}}_{\mathbf{A}_{\Phi_1}} \underbrace{\text{[diagram]}}_{\mathbf{A}_{\Theta}} = \underbrace{\text{[diagram]}}_{\mathbf{A}_{\Phi_1}} = \underbrace{\text{[diagram]}}_{\mathbf{A}_{\Theta}} \underbrace{\text{[diagram]}}_{\mathbf{A}_{\Phi_1}}. \quad (2.32)$$

Let us explore how the cancellation of eq. (2.29) comes about in example (2.30): First, note that due to eq. (2.32) we may rewrite  $O$  as

$$O = \underbrace{\text{[diagram]}}_{\mathbf{A}_{\Phi_1}} \underbrace{\text{[diagram]}}_{\mathbf{S}_{\Theta}} \underbrace{\text{[diagram]}}_{\mathbf{A}_{\Theta}} \underbrace{\text{[diagram]}}_{\mathbf{S}_{\Phi_2}} \stackrel{\text{eq. (2.32)}}{=} \underbrace{\text{[diagram]}}_{\mathbf{A}_{\Phi_1} \mathbf{A}_{\Theta}} \underbrace{\text{[diagram]}}_{\mathbf{S}_{\Theta} \mathbf{S}_{\Phi_2}} = \underbrace{\text{[diagram]}}_{Y_{\Theta}^{\dagger}} \underbrace{\text{[diagram]}}_{Y_{\Theta}^{\dagger}}. \quad (2.33)$$



Idempotency of  $Y_\Theta$  implies  $\bar{Y}_\Theta^\dagger \bar{Y}_\Theta^\dagger = 1/\alpha_\Theta \bar{Y}_\Theta^\dagger$ , so that

$$O = \frac{1}{\alpha_\Theta} \cdot \begin{array}{c} \text{A}_{\Phi_1} \text{A}_\Theta \rightarrow \text{A}_{\Phi_1} \\ \text{S}_\Theta \text{S}_{\Phi_2} \rightarrow \text{S}_{\Phi_2} \end{array} \begin{array}{c} \text{---} \\ \text{---} \\ \text{---} \\ \text{---} \end{array} \xrightarrow{\text{eq. (2.32)}} \frac{1}{\alpha_\Theta} \cdot \begin{array}{c} \text{---} \\ \text{---} \\ \text{---} \\ \text{---} \end{array} \begin{array}{c} \text{A}_{\Phi_1} \text{S}_{\Phi_2} \end{array} \quad (2.34)$$

This example exhibits a clear three step pattern that immediately furnishes the general proof:

1. Factor  $\mathbf{S}_\Theta$  from  $\mathbf{S}_{\Phi_2}$  and  $\mathbf{A}_\Theta$  from  $\mathbf{A}_{\Phi_1}$  to generate  $\bar{Y}_\Theta^\dagger \bar{Y}_\Theta^\dagger$  (this is possible since  $\mathbf{S}_\Theta \supset \mathbf{S}_{\Phi_2}$  and  $\mathbf{A}_\Theta \supset \mathbf{A}_{\Phi_1}$  as required by the Theorem),

$$O = \text{A}_{\Phi_1} \underbrace{\text{A}_\Theta \text{S}_\Theta}_{\bar{Y}_\Theta^\dagger} \underbrace{\text{A}_\Theta \text{S}_\Theta}_{\bar{Y}_\Theta^\dagger} \text{S}_{\Phi_2} \quad (2.35)$$

2. use idempotency of  $Y_\Theta$  so simplify  $\bar{Y}_\Theta^\dagger \bar{Y}_\Theta^\dagger = 1/\alpha_\Theta \bar{Y}_\Theta^\dagger$ ,

$$O = \frac{1}{\alpha_\Theta} \cdot \text{A}_{\Phi_1} \underbrace{\text{A}_\Theta \text{S}_\Theta}_{\bar{Y}_\Theta^\dagger} \text{S}_{\Phi_2} \quad (2.36)$$

3. reabsorb  $\mathbf{S}_\Theta$  into  $\mathbf{S}_{\Phi_2}$  and  $\mathbf{A}_\Theta$  into  $\mathbf{A}_{\Phi_1}$ ,

$$O = \frac{1}{\alpha_\Theta} \cdot \text{A}_{\Phi_1} \underbrace{\text{A}_\Theta \text{S}_\Theta}_{\bar{Y}_\Theta^\dagger} \text{S}_{\Phi_2} = \frac{1}{\alpha_\Theta} \cdot \text{A}_{\Phi_1} \text{S}_{\Phi_2} \quad (2.37)$$

□

In some applications, one finds the ingredients of Theorem 2.1 embedded into chains of Young projectors [2, 4] [*c.f. chapter 3*], we thus explicitly formulate the following Corollary:

■ **Corollary 2.1 – cancellation of wedged ancestor operators:**

Consider two Young tableaux  $\Theta$  and  $\Phi$  such that they have a common ancestor tableau  $\Gamma$ . Let  $Y_\Theta$ ,  $Y_\Phi$  and  $Y_\Gamma$  be their respective Young projection operators, all embedded in an algebra that encompasses all three. Then

$$Y_\Theta Y_\Gamma Y_\Phi = Y_\Theta Y_\Phi \quad (2.38)$$

This Corollary immediately follows from Theorem 2.1, since the product  $Y_\Theta Y_\Gamma Y_\Phi$  will be of the form

$$Y_\Theta Y_\Gamma Y_\Phi = \alpha_\Theta \alpha_\Gamma \alpha_\Phi \cdot \underbrace{\text{S}_\Theta \text{A}_\Theta \text{S}_\Gamma \text{A}_\Gamma \text{S}_\Phi \text{A}_\Phi}_O \quad (2.39)$$

where the marked factor constitutes  $O$  as defined in equation (2.28) in Theorem 2.1.

### 2.3.2 Cancellation of factors between bracketing sets

In this section, we present another cancellation theorem that allows us to significantly shorten certain operators. The results presented here follow immediately from a result attributed to von Neumann in [99] (in Lemma 2.1, we paraphrase a more modern version of von Neumann's lemma given in [93, Lemma IV.5]). Before we state von Neumann's lemma, we need to define *horizontal* and *vertical* permutations of a Young tableau [93]:

■ **Definition 2.2 – horizontal and vertical permutations:**

Let  $\tilde{\Theta}$  be a semi-standard (Young or irregular) tableau such that  $n$  is the largest integer appearing in  $\tilde{\Theta}$ . Then,  $\mathbf{h}_{\tilde{\Theta}}$  shall denote the subset of all permutations in  $S_n$  that only operate within the rows of  $\tilde{\Theta}$ , i.e. that do not swap numbers across rows. We call this the set of horizontal permutations of  $\tilde{\Theta}$ . Similarly, we define the set of vertical permutations of  $\tilde{\Theta}$ ,  $\mathbf{v}_{\tilde{\Theta}}$ , to be the subset of permutations in  $S_n$  that only operate within the columns of  $\tilde{\Theta}$ , i.e. those that do not swap numbers across columns.

By definition of semi-standard tableaux (which requires each integer to appear at most once within the tableau  $\tilde{\Theta}$ ), it is clear that

$$\mathbf{h}_{\tilde{\Theta}} \cap \mathbf{v}_{\tilde{\Theta}} = \{\text{id}\}, \quad (2.40)$$

where  $\text{id}$  is the identity permutation in  $S_n$ .

For example, if

$$\Theta = \begin{array}{|c|c|} \hline 1 & 3 \\ \hline 2 & 5 \\ \hline 4 & \\ \hline \end{array}, \quad (2.41)$$

then

$$\mathbf{h}_{\Theta} = \{\text{id}, (13), (25), (13)(25)\} \quad (2.42)$$

and

$$\mathbf{v}_{\Theta} = \{\text{id}, (12), (14), (24), (124), (142), (35), (12)(35), (14)(35), (24)(35), (124)(35), (142)(35)\}. \quad (2.43)$$

With these definitions, we restate a lemma attributed to von Neumann in [99] (we use the more modern notation of this lemma given in [93, Lemma IV.5]):

■ **Lemma 2.1 – von Neumann's Lemma:**

Let  $\Theta \in \mathcal{Y}_n$  be a Young tableau and let  $\rho$  be a (linear combination of) permutation(s) in  $S_n$ . If  $\rho$  satisfies

$$h_{\Theta} \rho v_{\Theta} = \text{sign}(v_{\Theta}) \rho \quad (2.44)$$

for all  $h_{\Theta} \in \mathbf{h}_{\Theta}$  and for all  $v_{\Theta} \in \mathbf{v}_{\Theta}$ , then  $\rho$  is proportional to the Young projection operator corresponding to  $\Theta$ ,

$$\rho = \lambda \cdot Y_{\Theta}. \quad (2.45)$$

Furthermore, if we write  $\rho$  as a sum of permutations,

$$\rho = \sum_{\sigma \in S_n} a_\sigma \sigma, \quad (2.46)$$

where the  $a_\sigma$  are constants, then the constant  $\lambda$  in eq. (2.45) is proportional to the coefficient of the identity in the series expansion of  $\rho$ ,

$$\lambda = \frac{\mathcal{H}_\Theta}{b_O} a_{\text{id}}, \quad (2.47)$$

where  $\mathcal{H}_\Theta$  denotes the hook length of  $\Theta$  [95, 96] and  $b_O$  is the product of (length of (anti-)symmetrizer)! for all symmetrizers and antisymmetrizers in  $O$  [72].

The last statement is not included in the original version shown in [93], but follows from the proof presented there.

It should be noted that in [93], symmetrizers and antisymmetrizers are not normalized: for example, we define  $\mathbf{S}_{12} := \frac{1}{2}(\text{id} + (12))$  while [93] defines  $\mathbf{S}_{12} := \text{id} + (12)$ . Thus, the constant  $b_O$  arises in our statement of the Lemma 2.1, but is not present in [93]. Furthermore, [93]'s statement of this Lemma compares the algebra element  $\rho$  with the *irreducible symmetrizer*  $e_\Theta$ , which differs from  $Y_\Theta$  by the constant  $\mathcal{H}_\Theta$ , (keeping in mind the different normalizations of symmetrizers and antisymmetrizers used in this paper and in [93]). This leads to the constant  $\mathcal{H}_\Theta$  in our rendition of the Lemma.

Lemma 2.1 immediately gives rise to the following special case:

**■ Corollary 2.2 – Cancellation of parts of the operator:**

Let  $\Theta \in \mathcal{Y}_n$  be a Young tableau and  $M$  be an element of the algebra of primitive invariants  $\text{API}(\text{SU}(N), V^{\otimes n})$ . Then, there exists a (possibly vanishing) constant  $\lambda$  such that

$$O := \mathbf{S}_\Theta M \mathbf{A}_\Theta = \lambda \cdot Y_\Theta. \quad (2.48)$$

If furthermore the operator  $O$  is nonzero, then  $\lambda \neq 0$ .

*Proof of Corollary 2.2:* From the definition of horizontal and vertical permutations (Definition 2.2) it is clear that

$$h_\Theta \mathbf{S}_\Theta = \mathbf{S}_\Theta \quad \text{for all } h_\Theta \in \mathbf{h}_\Theta \quad (2.49a)$$

$$\mathbf{A}_\Theta v_\Theta = \text{sign}(v_\Theta) \mathbf{A}_\Theta \quad \text{for all } v_\Theta \in \mathbf{v}_\Theta, \quad (2.49b)$$

where  $\text{sign}(\rho)$  denotes the signature of the permutation  $\rho$ .<sup>10</sup> Since  $O := \mathbf{S}_\Theta M \mathbf{A}_\Theta$  (eq. (2.48)), it immediately follows that, for all  $h_\Theta \in \mathbf{h}_\Theta$  and all  $v_\Theta \in \mathbf{v}_\Theta$

$$\begin{aligned} h_\Theta O &= \underbrace{h_\Theta \mathbf{S}_\Theta}_{\mathbf{S}_\Theta} M \mathbf{A}_\Theta & Ov_\Theta &= \mathbf{S}_\Theta M \underbrace{\mathbf{A}_\Theta v_\Theta}_{\text{sign}(v_\Theta) \mathbf{A}_\Theta} \\ &= \mathbf{S}_\Theta M \mathbf{A}_\Theta & &= \text{sign}(v_\Theta) \mathbf{S}_\Theta M \mathbf{A}_\Theta \\ &= O & &= \text{sign}(v_\Theta) O. \end{aligned}$$

<sup>10</sup> $\text{sign}(\rho)$  is  $\pm 1$  depending on whether  $\rho$  decomposes into an even or odd number of transpositions. Tung in [93] means the same when he writes  $(-1)^{\text{sign}(\rho)}$ .

More compactly, these conditions become

$$h_\Theta O v_\Theta = \text{sign}(v_\Theta) O \quad \text{for all } h_\Theta \in \mathbf{h}_\Theta \text{ and } v_\Theta \in \mathbf{v}_\Theta. \quad (2.50)$$

However, according to Lemma 2.1 [93, Lemma IV.5], relation (2.50) holds *if and only if*  $O$  is proportional to the Young projection operator  $Y_\Theta$ ; that is, there exists a constant  $\lambda$  such that

$$O = \lambda \cdot Y_\Theta. \quad (2.51)$$

From this, it follows immediately that  $\lambda \neq 0$  if and only if  $O \neq 0$ , thus establishing our claim.  $\square$

One of the main cases of interest is a situation where the structure of  $O$  (and thus  $M$ ) is such that we know from the outset that it is nonzero. A necessary but not sufficient condition is that none of the antisymmetrizers contained in  $O$  may exceed the length  $N$  — if this occurs, we refer to it as a *dimensional zero*. We will re-visit this scenario at the end of this section.

Two necessary and sufficient conditions ensuring  $O \neq 0$  are presented below, conditions 2.1 and 2.2 (condition 2.3 is a combination of conditions 2.1 and 2.2). We do not claim that the conditions given in this section represent an exhaustive list of cases yielding  $O \neq 0$ , but rather that these cases occur most commonly in practical examples [2, 3] [chapters 3 and 4].

**■ Condition 2.1 – inclusion of (anti-)symmetrizers:**

Let  $O$  be of the form (2.48),  $O = \mathbf{S}_\Theta M \mathbf{A}_\Theta$ , and  $M$  be given by

$$M = \mathbf{A}_{\Phi_1} \mathbf{S}_{\Phi_2} \mathbf{A}_{\Phi_3} \mathbf{S}_{\Phi_4} \cdots \mathbf{A}_{\Phi_{k-1}} \mathbf{S}_{\Phi_k}, \quad (2.52)$$

such that  $\mathbf{A}_{\Phi_i} \supset \mathbf{A}_\Theta$  for every  $i \in \{1, 3, \dots, k-1\}$  and  $\mathbf{S}_{\Phi_j} \supset \mathbf{S}_\Theta$  for every  $j \in \{2, 4, \dots, k\}$ . Then  $O$  is a nonzero element of  $\text{API}(\text{SU}(N), V^{\otimes n}) \subset \text{Lin}(V^{\otimes n})$ .

*Proof:* The operator  $O = \mathbf{S}_\Theta M \mathbf{A}_\Theta$  with  $M$  given in (2.52) is defined to be a product of alternating symmetrizers and antisymmetrizers. In particular, the outermost sets of symmetrizers and antisymmetrizers,  $\mathbf{S}_\Theta$  and  $\mathbf{A}_\Theta$  respectively, correspond to a Young tableau  $\Theta$ . By the definition of Young tableaux, this implies that each symmetrizer in  $\mathbf{S}_\Theta$  has *at most* one common leg with each antisymmetrizer in  $\mathbf{A}_\Theta$  (this is the underlying reason why  $\bar{Y}_\Theta = \mathbf{S}_\Theta \mathbf{A}_\Theta \neq 0$ ). Furthermore, since  $\mathbf{S}_{\Phi_j} \supset \mathbf{S}_\Theta$  for every  $j \in \{2, 4, \dots, k\}$  and  $\mathbf{A}_{\Phi_i} \supset \mathbf{A}_\Theta$  for every  $i \in \{1, 3, \dots, k-1\}$ , the same applies for every other (not necessarily neighbouring) pair  $\mathbf{S}_{\Xi_i}$  and  $\mathbf{A}_{\Xi_j}$  occurring in  $O$ . This guarantees that the operator  $O$  as defined in (2.52) is nonzero.  $\square$

As an example of condition 2.1 consider the operator

$$O = \underbrace{\text{---}}_{\mathbf{S}_\Theta} \underbrace{\text{---}}_{\mathbf{A}_{\Phi_1}} \underbrace{\text{---}}_{\mathbf{S}_{\Phi_2}} \underbrace{\text{---}}_{\mathbf{A}_\Theta}. \quad (2.53)$$

In  $O$ , the sets  $\mathbf{S}_\Theta$  and  $\mathbf{A}_\Theta$  correspond to the Young tableau

$$\Theta := \begin{array}{|c|c|c|} \hline 1 & 2 & 5 \\ \hline 3 & 4 & \\ \hline \end{array}. \quad (2.54)$$

The inclusion conditions are  $\mathbf{A}_{\Phi_1} = \{\mathbf{A}_{13}\} \supset \{\mathbf{A}_{13}, \mathbf{A}_{24}\} = \mathbf{A}_{\Theta}$  and  $\mathbf{S}_{\Phi_2} = \{\mathbf{S}_{12}, \mathbf{S}_{34}\} \supset \{\mathbf{S}_{125}, \mathbf{S}_{34}\} = \mathbf{S}_{\Theta}$ .<sup>11</sup> Then, according to Corollary 2.2, we may cancel the wedged sets  $\mathbf{A}_{\Phi_1}$  and  $\mathbf{S}_{\Phi_2}$  at the cost of a nonzero constant  $\kappa$ ,

$$Q = \kappa \cdot \underbrace{\text{[Diagram]}}_{\mathbf{S}_{\Theta}} \underbrace{\text{[Diagram]}}_{\mathbf{A}_{\Theta}} = \kappa \cdot \bar{Y}_{\Theta}. \quad (2.55)$$

The simplification is notable and nontrivial. It is useful in all situations where the end result is simple enough and we have an external criterion to constrain the product of any of the unknown proportionality factors  $\kappa$  acquired in the possible repeated application of Corollary 2.2.

A second way of constructing nonzero operators is by relating symmetrizers and antisymmetrizers of different Young tableaux with a permutation. To this end, we require the following definition.

**Definition 2.3 – tableau permutation:**

Consider two Young tableaux  $\Theta, \Phi \in \mathcal{Y}_n$  with the same shape. Then,  $\Phi$  can be obtained from  $\Theta$  by permuting the numbers of  $\Theta$ ; clearly, the permutation needed to obtain  $\Phi$  from  $\Theta$  is unique. Denote this permutation by  $\rho_{\Theta\Phi}$ ,

$$\Theta = \rho_{\Theta\Phi}(\Phi) \quad \iff \quad \Phi = \rho_{\Theta\Phi}^{-1}(\Theta) = \rho_{\Phi\Theta}(\Theta). \quad (2.56)$$

To construct  $\rho_{\Theta\Phi}$  explicitly, write the Young tableau  $\Theta$  and  $\Phi$  next to each other such that  $\Theta$  is to the left of  $\Phi$  and then connect the boxes in the corresponding position of the two diagrams, such as

$$\Theta \rightarrow \text{[Diagram]} \leftarrow \Phi. \quad (2.57)$$

Write two columns of numbers from 1 to  $n$  next to each other in ascending order; the left column represents the entries of  $\Theta$  and the right column represents the entries of  $\Phi$ . Connect the entries in the left and the right column in correspondence to (2.57). The resulting tangle of lines is the birdtrack corresponding to  $\rho_{\Theta\Phi}$  and thus determines the permutation.

As an example, the permutation  $\rho_{\Theta\Phi}$  between the tableaux

$$\Theta = \begin{array}{|c|c|} \hline 1 & 2 \\ \hline 3 & \\ \hline \end{array} \quad \text{and} \quad \Phi = \begin{array}{|c|c|} \hline 1 & 3 \\ \hline 2 & \\ \hline \end{array} \quad (2.58)$$

is given by

$$\Theta \rightarrow \begin{array}{|c|c|} \hline 1 & 2 \\ \hline 3 & \\ \hline \end{array} \leftarrow \Phi \quad \implies \quad \rho_{\Theta\Phi} = \overline{\text{[Diagram]}}. \quad (2.59)$$

<sup>11</sup>In this particular case, one can even notice that the set  $\mathbf{A}_{\Phi_2}$  corresponds to the ancestor tableau  $\Theta_{(2)}$  and the set  $\mathbf{S}_{\Phi_3}$  corresponds to the ancestor tableau  $\Theta_{(1)}$  of  $\Theta$ . Hence,  $Q$  can be written as  $Q = \mathbf{S}_{\Theta} \mathbf{A}_{\Theta_{(2)}} \mathbf{S}_{\Theta_{(1)}} \mathbf{A}_{\Theta}$ .

Let  $\Theta$  and  $\Phi$  be two Young tableaux of the same shape and construct the permutation  $\rho_{\Theta\Phi}$ . Furthermore, consider a general operator  $K_\Theta$  comprised of sets of (anti-) symmetrizers which can be absorbed into  $\mathbf{S}_\Theta$  and  $\mathbf{A}_\Theta$  respectively, and let  $H_\Phi$  be an operator comprised of sets of (anti-)symmetrizers which can be absorbed into  $\mathbf{S}_\Phi$  and  $\mathbf{A}_\Phi$  respectively. Except for isolated examples, the product  $K_\Theta \cdot H_\Phi$  vanishes.<sup>12</sup> However, it turns out that

$$H_\Phi \cdot \underbrace{\rho_{\Theta\Phi}^{-1}}_{\rho_{\Phi\Theta}} K_\Theta \rho_{\Theta\Phi} \neq 0 \quad \text{for all } \Theta, \Phi \in \mathcal{Y}_n \text{ for all } n. \quad (2.60)$$

To better understand this, we accompany the general argument with an example: Consider the Young tableaux

$$\Theta = \begin{array}{|c|c|c|} \hline 1 & 3 & 5 \\ \hline 2 & 4 & \\ \hline 6 & & \\ \hline \end{array} \quad \text{and} \quad \Phi = \begin{array}{|c|c|c|} \hline 1 & 2 & 6 \\ \hline 3 & 5 & \\ \hline 4 & & \\ \hline \end{array}. \quad (2.61)$$

The permutation  $\rho_{\Theta\Phi}$  as defined in Definition 2.3 is given by

$$\rho_{\Theta\Phi} = \begin{array}{c} \text{---} \\ \diagdown \quad \diagup \\ \diagup \quad \diagdown \\ \text{---} \end{array}. \quad (2.62)$$

For a general Young tableau  $\Psi \in \mathcal{Y}_n$ , we denote the irregular tableau that is obtained from  $\Psi$  by deleting the boxes with entries  $a_1$  up to  $a_m$  ( $m \leq n$ ) by  $\Psi \setminus \{a_1, \dots, a_m\}$ . Even though  $\Psi \setminus \{a_1, \dots, a_m\}$  is not a Young tableau in general, it remains semi-standard. Thus, the (anti-)symmetrizers in the sets  $\mathbf{S}_{\Psi \setminus \{a_1, \dots, a_m\}}$  and  $\mathbf{A}_{\Psi \setminus \{a_1, \dots, a_m\}}$  are disjoint and the sets themselves individually remain Hermitian projection operators. These sets can further be absorbed into  $\mathbf{S}_\Psi$  and  $\mathbf{A}_\Psi$  respectively since  $\mathbf{S}_{\Psi \setminus \{a_1, \dots, a_m\}}$  is merely the set of symmetrizers  $\mathbf{S}_\Psi$  with the legs  $a_1$  up to  $a_m$  deleted, and similarly for  $\mathbf{A}_{\Psi \setminus \{a_1, \dots, a_m\}}$ . Thus, they satisfy the absorption relations

$$\mathbf{S}_{\Psi \setminus \{a_1, \dots, a_m\}} \mathbf{S}_\Psi = \mathbf{S}_\Psi = \mathbf{S}_\Psi \mathbf{S}_{\Psi \setminus \{a_1, \dots, a_m\}} \quad \text{and} \quad \mathbf{A}_{\Psi \setminus \{a_1, \dots, a_m\}} \mathbf{A}_\Psi = \mathbf{A}_\Psi = \mathbf{A}_\Psi \mathbf{A}_{\Psi \setminus \{a_1, \dots, a_m\}}, \quad (2.63)$$

this is easiest seen via the birdtracks corresponding to the semi-standard irregular tableau  $\Psi \setminus \{a_1, \dots, a_m\}$ .

A quick look at our example elucidates how equation (2.63) comes about in general: In (2.61), we may remove boxes from  $\Theta$  at will — consider for example

$$\begin{array}{ccc} \begin{array}{|c|c|c|} \hline 1 & 3 & 5 \\ \hline 2 & 4 & \\ \hline 6 & & \\ \hline \end{array} & \begin{array}{|c|c|c|} \hline 1 & 3 & 5 \\ \hline 2 & 4 & \\ \hline 6 & & \\ \hline \end{array} & \begin{array}{|c|c|c|} \hline 1 & 3 & 5 \\ \hline 2 & 4 & \\ \hline 6 & & \\ \hline \end{array} \\ \downarrow & \downarrow & \downarrow \\ \begin{array}{|c|c|c|} \hline 1 & & 5 \\ \hline 2 & 4 & \\ \hline & & \\ \hline \end{array} & \begin{array}{|c|c|c|} \hline 1 & 3 & \\ \hline 2 & & \\ \hline & & \\ \hline \end{array} & \begin{array}{|c|c|c|} \hline 1 & 3 & 5 \\ \hline & 4 & \\ \hline 6 & & \\ \hline \end{array} \\ \Theta \setminus \{3, 6\} & \Theta \setminus \{4, 5, 6\} & \Theta \setminus \{2\} \end{array}. \quad (2.64)$$

<sup>12</sup>This is true since the product of (most!) Young projection operators corresponding to different Young tableaux of the same shape in  $\mathcal{Y}_n$  vanishes [85, 93].

It is clear from this list that only some of the resulting tableaux will be Young tableaux, most will not. Using tableaux such as (2.64), we construct an operator  $K_\Theta$  consisting of (anti-)symmetrizers which can be absorbed into  $\mathbf{S}_\Theta$  and  $\mathbf{A}_\Theta$ , for example,

$$\begin{aligned}
 K_\Theta &:= \mathbf{S}_{\Theta \setminus \{3,6\}} \mathbf{A}_{\Theta \setminus \{2\}} \mathbf{S}_\Theta \mathbf{A}_\Theta \mathbf{S}_{\Theta \setminus \{2\}} \mathbf{A}_{\Theta \setminus \{3,6\}} \mathbf{S}_{\Theta \setminus \{4,5,6\}} \\
 &= \text{[birdtrack diagram]} .
 \end{aligned} \tag{2.65}$$

Conjugating the operator  $K_\Theta$  by the permutation  $\rho_{\Theta\Phi}$  yields

$$\text{[birdtrack diagram]} ; \tag{2.66}$$

Each of the sets of (anti-)symmetrizers in (2.66) corresponds to one of the tableaux

$$\begin{array}{ccc}
 \begin{array}{c} \Phi \\ \begin{array}{|c|c|c|} \hline 1 & 2 & 6 \\ \hline 3 & 5 & \\ \hline 4 & & \\ \hline \end{array} \\ \downarrow \\ \begin{array}{|c|c|c|} \hline 1 & & 6 \\ \hline 3 & 5 & \\ \hline & & \\ \hline \end{array} \\ \Phi \setminus \{2,4\} \end{array} &
 \begin{array}{c} \Phi \\ \begin{array}{|c|c|c|} \hline 1 & 2 & 6 \\ \hline 3 & 5 & \\ \hline 4 & & \\ \hline \end{array} \\ \downarrow \\ \begin{array}{|c|c|} \hline 1 & 2 \\ \hline 3 & \\ \hline \end{array} \\ \Phi \setminus \{4,5,6\} \end{array} &
 \begin{array}{c} \Phi \\ \begin{array}{|c|c|c|} \hline 1 & 2 & 6 \\ \hline 3 & 5 & \\ \hline 4 & & \\ \hline \end{array} \\ \downarrow \\ \begin{array}{|c|c|c|} \hline 1 & 2 & 6 \\ \hline & 5 & \\ \hline 4 & & \\ \hline \end{array} \\ \Phi \setminus \{3\} \end{array} .
 \end{array} \tag{2.67}$$

The tableaux in (2.67) are obtained by superimposing the tableaux in (2.64) on  $\Phi$  in a cookie cutter fashion. By construction, all the  $\mathbf{S}_{\Phi \setminus \{b_1, \dots, b_m\}}$  (resp.  $\mathbf{A}_{\Phi \setminus \{b_1, \dots, b_m\}}$ ) can be absorbed into  $\mathbf{S}_\Phi$  (resp.  $\mathbf{A}_\Phi$ ), as claimed in eq. (2.63).

The pattern is completely general and in no way restricted to the particular example used to demonstrate it. Let us summarize:

■ **Condition 2.2 – relating (anti-)symmetrizers across tableaux:**

Let  $O$  be of the form  $O = \mathbf{S}_\Theta M \mathbf{A}_\Theta$ , eq. (2.48). Let  $\Theta, \Phi \in \mathcal{Y}_n$  be two Young tableaux with the same shape and construct the permutation  $\rho_{\Theta\Phi}$  between the two tableaux according to Definition 2.3. Furthermore, let  $\mathcal{D}_\Theta$  be a product of symmetrizers and antisymmetrizers, each of which can be absorbed into  $\mathbf{S}_\Theta$  and  $\mathbf{A}_\Theta$  respectively. If  $M$  is of the form

$$M = \rho_{\Theta\Phi} \mathcal{D}_\Phi \rho_{\Phi\Theta} , \tag{2.68}$$

then the operator  $O$  is nonzero.

It immediately follows that a combination of conditions 2.1 and 2.2 also renders the operator  $O$  nonzero:

■ **Condition 2.3 – combining conditions 2.1 and 2.2:**

Let  $O$  be an operator of the form  $O = \mathbf{S}_\Theta M \mathbf{A}_\Theta$  and let  $M$  be given by

$$M = M^{(1)} M^{(2)} \dots M^{(l)}, \quad (2.69)$$

such that for each  $M^{(i)}$  either condition 2.1 or 2.2 holds; this implies that each (anti-)symmetrizer in  $M$  can be absorbed into  $\mathbf{S}_\Theta$  or  $\mathbf{A}_\Theta$  respectively. Then  $O$  is nonzero.

**Dimensional zeros:** Let us conclude this section with a short discussion on how the operator  $O$  becomes dimensionally zero. Since in either of the three conditions presented in this section all sets of antisymmetrizers in  $M$  can be absorbed into  $\mathbf{A}_\Theta$ ,

$$\mathbf{A}_j \mathbf{A}_\Theta = \mathbf{A}_\Theta = \mathbf{A}_\Theta \mathbf{A}_j, \quad (2.70)$$

for every  $\mathbf{A}_j$  in  $M$ , it follows immediately that the antisymmetrizer in  $O$  that contains the most legs (i.e. the “longest” antisymmetrizer in  $O$ ) must be part of the set  $\mathbf{A}_\Theta$ , as otherwise eq. (2.70) could not hold. Thus,  $O$  is not dimensionally zero if  $\mathbf{A}_\Theta$  is not dimensionally zero. Furthermore, since  $Y_\Theta \propto \mathbf{S}_\Theta \mathbf{A}_\Theta$ , it suffices to require that  $N$  is large enough for the Young projection operator  $Y_\Theta$  to be nonzero to ensure that the operator  $O$  in any of the conditions 2.1–2.3 is not dimensionally zero. Thus, in cancelling parts of the operator  $O$  (to give it the structural form of  $Y_\Theta$ ), one does not remove any indication of it being dimensionally zero: dimensional zeros of  $O$  occur exactly when  $Y_\Theta$  is zero.

The cancellation rules given in this section are of enormous practical use, as they allow us to shorten birdtrack operators, often significantly so. In particular, we use Corollary 2.2 in the construction of compact Hermitian Young projection operators [2] [chapter 3] and the construction of transition operators [3] [chapter 4].

## 2.4 Propagation rules

In this section, we present propagation rules that allow us to propagate certain symmetrizers through sets of antisymmetrizers, and vice versa. These rules are particularly useful to make the Hermiticity of certain birdtrack operators visually explicit. We demonstrate their effectiveness in [2] [chapter 3] and with a specific example in our conclusions [section 2.5] (see Figure 2.2).

The structure of our proof of these propagation rules has been strongly inspired by an example presented in the appendix of Keppeler and Sjödal’s (KS) paper on Hermitian Young projection operators [4]. In this example, KS clearly realized that symmetrizers sometimes can be propagated through sets of antisymmetrizers, and vice versa, by “swapping” appropriate sets of antisymmetrizers around. However, the general conditions under which this is possible were not identified by KS, and a proof is also not present in [4].

■ **Theorem 2.2 – propagation of (anti-)symmetrizers:**

Let  $\Theta$  be a Young tableau and  $O$  be a birdtrack operator of the form

$$O = \mathbf{S}_\Theta \mathbf{A}_\Theta \mathbf{S}_{\Theta \setminus \mathcal{R}}, \quad (2.71)$$

in which the symmetrizer set  $\mathbf{S}_{\Theta \setminus \mathcal{R}}$  arises from  $\mathbf{S}_\Theta$  by removing precisely one symmetrizer  $\mathbf{S}_{\mathcal{R}}$ . By definition,



$\mathbf{S}_{\mathcal{R}}$  corresponds to a row  $\mathcal{R}$  in  $\Theta$  such that

$$\mathbf{S}_{\Theta} = \mathbf{S}_{\Theta \setminus \mathcal{R}} \mathbf{S}_{\mathcal{R}} = \mathbf{S}_{\mathcal{R}} \mathbf{S}_{\Theta \setminus \mathcal{R}} . \quad (2.72)$$

If the column-amputated tableau of  $\Theta$  according to the row  $\mathcal{R}$ ,  $\mathcal{O}_c[\mathcal{R}]$ , is **rectangular**, then the symmetrizer  $\mathbf{S}_{\mathcal{R}}$  may be propagated through the set  $\mathbf{A}_{\Theta}$  from the left to the right, yielding

$$O = \mathbf{S}_{\Theta} \mathbf{A}_{\Theta} \mathbf{S}_{\Theta \setminus \mathcal{R}} = \mathbf{S}_{\Theta \setminus \mathcal{R}} \mathbf{A}_{\Theta} \mathbf{S}_{\Theta} , \quad (2.73)$$

which implies that  $O$  is Hermitian.<sup>13</sup> We may think of this procedure as moving the missing symmetrizer  $\mathbf{S}_{\mathcal{R}}$  through the intervening antisymmetrizer set  $\mathbf{A}_{\Theta}$ . Eq. (2.72) immediately allows us to augment this statement to

$$\mathbf{S}_{\Theta} \mathbf{A}_{\Theta} \mathbf{S}_{\Theta \setminus \mathcal{R}} = \mathbf{S}_{\Theta \setminus \mathcal{R}} \mathbf{A}_{\Theta} \mathbf{S}_{\Theta} = \mathbf{S}_{\Theta} \mathbf{A}_{\Theta} \mathbf{S}_{\Theta} . \quad (2.74)$$

If the roles of symmetrizers and antisymmetrizers are exchanged, we need to verify that the row-amputated tableau  $\mathcal{O}_r[\mathcal{C}]$  with respect to a column  $\mathcal{C}$  is rectangular to guarantee that

$$\mathbf{A}_{\Theta} \mathbf{S}_{\Theta} \mathbf{A}_{\Theta \setminus \mathcal{C}} = \mathbf{A}_{\Theta \setminus \mathcal{C}} \mathbf{S}_{\Theta} \mathbf{A}_{\Theta} = \mathbf{A}_{\Theta} \mathbf{S}_{\Theta} \mathbf{A}_{\Theta} . \quad (2.75)$$

This amounts to moving the missing antisymmetrizer  $\mathbf{A}_{\mathcal{C}}$  through the intervening symmetrizer set  $\mathbf{S}_{\Theta}$ .

To clarify the statement of the Propagation Theorem 2.2, consider for example the operator  $O$

$$O := \begin{array}{c} \text{---} \\ \text{---} \\ \text{---} \\ \text{---} \\ \text{---} \\ \text{---} \end{array} \begin{array}{c} \text{---} \\ \text{---} \\ \text{---} \\ \text{---} \\ \text{---} \\ \text{---} \end{array} , \quad (2.76)$$

$\underbrace{\hspace{1.5cm}}_{\mathbf{S}_{\Theta}} \quad \underbrace{\hspace{1.5cm}}_{\mathbf{A}_{\Theta}} \quad \underbrace{\hspace{1.5cm}}_{\mathbf{S}_{\Theta \setminus \mathcal{R}}}$

where the Young tableau  $\Theta$  is

$$\Theta = \begin{array}{|c|c|c|} \hline 1 & 2 & 3 \\ \hline 4 & 5 & \\ \hline 6 & 7 & \\ \hline \end{array} . \quad (2.77)$$

The operator (2.76) meets the conditions laid out in Theorem 2.2: The sets  $\mathbf{S}_{\Theta}$  and  $\mathbf{S}_{\Theta \setminus \mathcal{R}}$  differ only by one symmetrizer, namely  $\mathbf{S}_{\mathcal{R}} = \mathbf{S}_{67}$ , which corresponds to the row (6, 7) of the tableau  $\Theta$ . Indeed, we find that the amputated tableau  $\mathcal{O}_c[(6, 7)]$  is rectangular,

$$\mathcal{O}_c[(6, 7)] = \begin{array}{|c|c|} \hline 1 & 2 \\ \hline 4 & 5 \\ \hline 6 & 7 \\ \hline \end{array} , \quad (2.78)$$

where we have highlighted the row corresponding to the symmetrizer  $\mathbf{S}_{67}$  in blue. We therefore may commute

<sup>13</sup>Recall the Hermiticity of (sets of) (anti-)symmetrizers (eq. (2.10)).

the symmetrizer  $\mathbf{S}_{67}$  from the left of  $O$  to the right in accordance with the Propagation Theorem 2.2,

$$O := \begin{array}{c} \text{---} \\ \text{---} \\ \text{---} \\ \text{---} \end{array} \begin{array}{c} \text{---} \\ \text{---} \\ \text{---} \\ \text{---} \end{array} = \begin{array}{c} \text{---} \\ \text{---} \\ \text{---} \\ \text{---} \end{array} \begin{array}{c} \text{---} \\ \text{---} \\ \text{---} \\ \text{---} \end{array}. \quad (2.79)$$

Furthermore, if we factor the symmetrizer  $\mathbf{S}_{67}$  out of the set  $\mathbf{S}_\Theta$  (i.e. if we write  $\mathbf{S}_\Theta = \mathbf{S}_{67}\mathbf{S}_\Theta$ ) before commuting it through, we obtain

$$O := \begin{array}{c} \text{---} \\ \text{---} \\ \text{---} \\ \text{---} \end{array} \begin{array}{c} \text{---} \\ \text{---} \\ \text{---} \\ \text{---} \end{array} = \begin{array}{c} \text{---} \\ \text{---} \\ \text{---} \\ \text{---} \end{array} \begin{array}{c} \text{---} \\ \text{---} \\ \text{---} \\ \text{---} \end{array} \xrightarrow{\text{Thm. 2.2}} \begin{array}{c} \text{---} \\ \text{---} \\ \text{---} \\ \text{---} \end{array} \begin{array}{c} \text{---} \\ \text{---} \\ \text{---} \\ \text{---} \end{array} = \begin{array}{c} \text{---} \\ \text{---} \\ \text{---} \\ \text{---} \end{array} \begin{array}{c} \text{---} \\ \text{---} \\ \text{---} \\ \text{---} \end{array}. \quad (2.80)$$

We thus kept  $\mathbf{S}_{67}$  on both sides of the operator, making the Hermiticity of  $O$  manifest.

Having understood the statement of the Propagation Theorem 2.2, we will foreshadow the strategy of the proof (which is given in section 2.4.1). Consider the operator

$$P := \begin{array}{c} \text{---} \\ \text{---} \\ \text{---} \\ \text{---} \end{array} \begin{array}{c} \text{---} \\ \text{---} \\ \text{---} \\ \text{---} \end{array}, \quad (2.81)$$

which satisfies all conditions posed in the Propagation Theorem 2.2. It thus immediately follows from the theorem that

$$\begin{array}{c} \text{---} \\ \text{---} \\ \text{---} \\ \text{---} \end{array} \begin{array}{c} \text{---} \\ \text{---} \\ \text{---} \\ \text{---} \end{array} = \begin{array}{c} \text{---} \\ \text{---} \\ \text{---} \\ \text{---} \end{array} \begin{array}{c} \text{---} \\ \text{---} \\ \text{---} \\ \text{---} \end{array} = \begin{array}{c} \text{---} \\ \text{---} \\ \text{---} \\ \text{---} \end{array} \begin{array}{c} \text{---} \\ \text{---} \\ \text{---} \\ \text{---} \end{array}. \quad (2.82)$$

We would, however, like to show how this comes about explicitly, thus alluding to the strategy used in the proof of Theorem 2.2. In particular, we will use a trick originally used by Keppeler and Sjödaahl in the appendix of [4].

We begin by factoring a transposition out of each symmetrizer on the left; this will not alter the operator  $P$  in any way since

$$\begin{array}{c} \text{---} \\ \text{---} \end{array} = \begin{array}{c} \text{---} \\ \text{---} \end{array} = \begin{array}{c} \text{---} \\ \text{---} \end{array}. \quad (2.83)$$

We thus have that

$$P = \begin{array}{c} \text{---} \\ \text{---} \\ \text{---} \\ \text{---} \end{array} \begin{array}{c} \text{---} \\ \text{---} \\ \text{---} \\ \text{---} \end{array} = \begin{array}{c} \text{---} \\ \text{---} \\ \text{---} \\ \text{---} \end{array} \begin{array}{c} \text{---} \\ \text{---} \\ \text{---} \\ \text{---} \end{array}, \quad (2.84)$$

where we have marked the top and bottom antisymmetrizer in  $P$  as ① and ② respectively. It is important to notice that these two antisymmetrizers would be indistinguishable if it weren't for the labelling. We may thus exchange them (paying close attention to which line enters and exits which antisymmetrizer), without

changing the operator  $P$ ,

$$(2.85)$$

We have thus effectively commuted the transpositions marked in red through the set of antisymmetrizers from the left to the right. We may now absorb the transposition on top into the right symmetrizer,

$$(2.86)$$

We therefore showed that

$$(2.87)$$

It now remains to add up the two different expressions of  $P$  found in (2.87), and multiply this sum by a factor  $1/2$ ,

$$(2.88)$$

However, since

$$(2.89)$$

equation (2.88) simply becomes

$$(2.90)$$

Performing the above process “in reverse” then yields

$$(2.91)$$

as desired. That this strategy can be applied to the operator (2.76) can be seen via factoring out a symmetrizer

of length 2 from each symmetrizer,

$$O = \text{[diagram]} = \text{[diagram with factors]} =: \tilde{O}. \quad (2.92)$$

The part marked  $\tilde{O}$  in (2.92) can now be dealt with exactly as in the previous example, allowing one to commute the symmetrizer  $S_{67}$  from the left to the right. It remains to reabsorb the extra symmetrizers to obtain the desired result (2.80),

$$O = \text{[diagram]} = \text{[diagram with absorption]} = \text{[diagram]}. \quad (2.93)$$

In particular, the ability to factor out an operator  $\tilde{O}$  within  $O$  is encoded in the requirement that the amputated tableau  $\check{\Theta}_c[\mathcal{R}]$  be rectangular, as is discussed in section 2.4.1.3.

More generally, if  $\Theta = \tilde{\Theta}$  is a semi-standard irregular tableau, then the following set of conditions on the amputated tableau will determine whether certain symmetrizers can be propagated through antisymmetrizers and vice versa:

■ **Theorem 2.3 – generalized propagation rules:**

A form of the Propagation Theorem 2.2 holds also if  $\Theta = \tilde{\Theta}$  is a semi-standard irregular tableau:

$$S_{\tilde{\Theta}} A_{\tilde{\Theta}} S_{\tilde{\Theta} \setminus \mathcal{R}} = S_{\tilde{\Theta} \setminus \mathcal{R}} A_{\tilde{\Theta}} S_{\tilde{\Theta}} = S_{\tilde{\Theta}} A_{\tilde{\Theta}} S_{\tilde{\Theta}} \quad (2.94)$$

if all rows in  $\check{\Theta}_c[\mathcal{R}]$  have equal lengths, and

$$A_{\tilde{\Theta}} S_{\tilde{\Theta}} A_{\tilde{\Theta} \setminus \mathcal{C}} = A_{\tilde{\Theta} \setminus \mathcal{C}} S_{\tilde{\Theta}} A_{\tilde{\Theta}} = A_{\tilde{\Theta}} S_{\tilde{\Theta}} A_{\tilde{\Theta}} \quad (2.95)$$

if all columns in  $\check{\Theta}_r[\mathcal{C}]$  have equal lengths.

Requiring the amputated tableaux to have rows (resp. columns) of equal lengths rather than them being rectangular allows for the fact that  $\check{\Theta}$  (for  $\tilde{\Theta}$  being a semi-standard irregular tableau) may contain disjoint pieces — this cannot happen for Young tableaux.<sup>14</sup>

The proof of Theorem 2.2 only has to be altered in minor ways to become a proof of the generalized Propagation Theorem 2.3. These alterations are given in section 2.4.2.

As an example of Theorem 2.3, consider the semi-standard irregular tableau

$$\tilde{\Theta} = \begin{array}{|c|c|c|c|} \hline & 1 & 2 & 3 & 4 \\ \hline 7 & 5 & 6 & & \\ \hline 8 & 9 & & & \\ \hline \end{array} \quad \text{with corresponding operator } \bar{Y}_{\tilde{\Theta}} = \text{[diagram]} \quad (2.96)$$

<sup>14</sup>It should be noted that missing boxes within a row/column reduce its length, for example the first row of the tableau 

1	2	3
4	5	

 has length 3 but the second row only has length 2, thus corresponding to symmetrizers of length 3 and 2 respectively.

(cf. eq. (2.12)).  $\tilde{\Theta}$  is neither a Young tableau nor does it uniquely specify  $\tilde{Y}_{\tilde{\Theta}}$  as we could, for example, swap  $\boxed{3}$  and  $\boxed{4}$  around and still obtain an appropriate tableau for  $\tilde{Y}_{\tilde{\Theta}}$ . Let us now consider the operator

$$O = \underbrace{\underbrace{\text{S}_{\tilde{\Theta}} \quad \text{A}_{\tilde{\Theta}} \quad \text{S}_{\tilde{\Theta} \setminus \mathcal{R}}}_{\tilde{Y}_{\tilde{\Theta}}}} , \quad (2.97)$$

where we would like to commute the symmetrizer  $\mathcal{S}_{\mathcal{R}} = \mathcal{S}_{89}$  from the left set  $\mathcal{S}_{\tilde{\Theta}}$  to the right set  $\mathcal{S}_{\tilde{\Theta} \setminus \mathcal{R}}$ . This symmetrizer corresponds to the row (8, 9) in  $\tilde{\Theta}$ ,

$$\tilde{\Theta} = \begin{array}{|c|c|c|c|} \hline & 1 & 2 & 3 & 4 \\ \hline 7 & 5 & 6 & & \\ \hline & 8 & 9 & & \\ \hline \end{array} . \quad (2.98)$$

All rows in the column-amputated tableau of  $\tilde{\Theta}$  according to the row (8, 9) have equal lengths,

$$\check{\Theta}_c[(8, 9)] = \begin{array}{|c|c|} \hline 1 & 2 \\ \hline 5 & 6 \\ \hline 8 & 9 \\ \hline \end{array} . \quad (2.99)$$

Thus, by Theorem 2.3 we may propagate the symmetrizer  $\mathcal{S}_{89}$  from the left to the right, yielding

$$O = \text{S}_{\tilde{\Theta}} \text{A}_{\tilde{\Theta}} \text{S}_{\tilde{\Theta} \setminus \mathcal{R}} = \text{S}_{\tilde{\Theta}} \text{A}_{\tilde{\Theta}} \text{S}_{\tilde{\Theta}} = \text{S}_{\tilde{\Theta} \setminus \mathcal{R}} \text{A}_{\tilde{\Theta}} \text{S}_{\tilde{\Theta}} . \quad (2.100)$$

The reason why the propagation rule also works in this general case is because an operator  $\tilde{O}$  can be identified within  $O$  in a similar way as was done in (2.92) (see section 2.4.2).

### 2.4.1 Proof of Theorem 2.2 (propagation rules)

In this section, we provide a proof for eq. (2.74) of the Propagation Theorem 2.2,

$$O = \mathcal{S}_{\Theta} \mathbf{A}_{\Theta} \mathcal{S}_{\Theta \setminus \mathcal{R}} = \mathcal{S}_{\Theta} \mathbf{A}_{\Theta} \mathcal{S}_{\Theta} = \mathcal{S}_{\Theta \setminus \mathcal{R}} \mathbf{A}_{\Theta} \mathcal{S}_{\Theta} . \quad (2.101)$$

The proof of eq. (2.75) (i.e. where the operator  $O$  is of the form  $O := \mathbf{A}_{\Theta} \mathcal{S}_{\Theta} \mathbf{A}_{\Theta \setminus \mathcal{C}}$ ) only changes in minor ways; these differences are discussed in section 2.4.1.4.

The steps of the proof given in the present section can become rather abstract; we therefore chose to accompany them with several schematic drawings for clarification.

The strategy of this proof will be as follows: We start by understanding what the conditions posed in Theorem 2.2 (in particular the requirement that the amputated tableau be rectangular) imply for the operator  $O$ . Then, we use a trick originally given in [4] to propagate the constituent permutations of the symmetrizer  $\mathcal{S}_{\mathcal{R}}$  through the set  $\mathbf{A}_{\Theta}$  to the right of  $O$ . We recall that each symmetrizer is by definition the sum of its

constituent permutations,

$$\mathbf{S}_{\mathcal{R}} = \frac{1}{\text{length}(\mathbf{S}_{\mathcal{R}})!} \sum_{\rho} \rho, \quad (2.102)$$

where  $\rho$  are the constituent permutations of  $\mathbf{S}_{\mathcal{R}}$ , for example

$$\underbrace{\begin{array}{|c|} \hline \hline \hline \hline \hline \\ \hline \end{array}}_{\mathbf{s}_{123}} = \frac{1}{3!} \left( \underbrace{\begin{array}{|c|} \hline \hline \hline \hline \\ \hline \end{array}}_{\text{id}} + \underbrace{\begin{array}{|c|} \hline \times \\ \hline \end{array}}_{(12)} + \underbrace{\begin{array}{|c|} \hline \times \\ \hline \end{array}}_{(13)} + \underbrace{\begin{array}{|c|} \hline \times \\ \hline \end{array}}_{(23)} + \underbrace{\begin{array}{|c|} \hline \times \\ \hline \end{array}}_{(123)} + \underbrace{\begin{array}{|c|} \hline \times \\ \hline \end{array}}_{(132)} \right). \quad (2.103)$$

The operators resulting from this propagation-process will then be summed up in the appropriate manner<sup>15</sup> to recombine to the symmetrizer  $\mathbf{S}_{\mathcal{R}}$  on the right hand side of  $O$ , yielding the desired result. Let us thus begin:

Let  $O := \mathbf{S}_{\Theta} \mathbf{A}_{\Theta} \mathbf{S}_{\Theta \setminus \mathcal{R}}$  be an operator as stated in the Propagation Theorem 2.2, and let the sets  $\mathbf{S}_{\Theta}$  and  $\mathbf{S}_{\Theta \setminus \mathcal{R}}$  only differ by one symmetrizer,  $\mathbf{S}_{\mathcal{R}}$ , with  $\mathbf{S}_{\mathcal{R}}$  corresponding to the row  $\mathcal{R}$  in the Young tableau  $\Theta$ . We will represent  $O$  schematically as

$$O = \begin{array}{|c|c|c|} \hline \mathbf{S}_{\Theta \setminus \mathcal{R}} & \mathbf{A}_{\Theta} & \mathbf{S}_{\Theta \setminus \mathcal{R}} \\ \hline \mathbf{S}_{\mathcal{R}} & & \\ \hline \end{array}, \quad (2.104)$$

where we used the fact that  $\mathbf{S}_{\Theta} = \mathbf{S}_{\Theta \setminus \mathcal{R}} \mathbf{S}_{\mathcal{R}}$  (c.f. eq. (2.72)).

#### 2.4.1.1 Unpacking the theorem conditions:

For the amputated tableau  $\mathcal{O}_c[\mathcal{R}]$  to be rectangular, we clearly require all columns that overlap with the row  $\mathcal{R}$  to have the same length. However, this is equivalent to saying that every row other than row  $\mathcal{R}$  in  $\Theta$  has to have length greater than or equal to  $\text{length}(\mathcal{R})$ : Suppose  $\mathcal{R}'$  is a row in  $\Theta$  with  $\text{length}(\mathcal{R}') < \text{length}(\mathcal{R})$ . Hence, by definition of Young tableaux, the row  $\mathcal{R}'$  is situated below the row  $\mathcal{R}$ . Furthermore, by the left-alignedness of Young tableaux, this means that all the columns that overlap with  $\mathcal{R}'$  also overlap with  $\mathcal{R}$ ; let us denote this set of columns overlapping with the row  $\mathcal{R}'$  by  $C_{\mathcal{R}'}$ . In addition, there will be at least one column that overlaps with  $\mathcal{R}$  but does not overlap with  $\mathcal{R}'$ , since  $\text{length}(\mathcal{R}) > \text{length}(\mathcal{R}')$ ; let us denote this column by  $\mathcal{C}$ . Schematically, this situation can be depicted as

$$\begin{array}{|c|c|c|c|c|} \hline \text{ } & \text{ } & \text{ } & \text{ } & \text{ } \\ \hline \text{ } & \text{ } & \text{ } & \text{ } & \text{ } \\ \hline \text{ } & \text{ } & \text{ } & \text{ } & \text{ } \\ \hline \text{ } & \text{ } & \text{ } & \text{ } & \text{ } \\ \hline \end{array} \quad (2.105)$$

It then follows by the top-alignedness of Young tableaux that  $\mathcal{C}$  is strictly shorter than the columns in the set  $C_{\mathcal{R}'}$ , as is indicated in (2.105). This poses a contradiction, as we need all columns that overlap with  $\mathcal{R}$  to be of the same length for the tableau  $\mathcal{O}_c[\mathcal{R}]$  to be rectangular. Hence, there cannot be a row in  $\Theta$  whose length is strictly less than the length of  $\mathcal{R}$ .

<sup>15</sup>Similar to what was done in the example (2.88).

Let  $C_{\mathcal{R}}$  denote the set of columns overlapping with the row  $\mathcal{R}$ . Since  $\mathcal{R}$  is established to be (one of) the shortest row(s) in  $\Theta$ , the top-alignedness and left-alignedness conditions of Young tableaux imply that every other row in  $\Theta$  also overlaps with every column in  $C_{\mathcal{R}}$ .

In the language of symmetrizers, the discussion given above can be formulated as:

1.  $\mathbf{S}_{\mathcal{R}}$  (corresponding to the row  $\mathcal{R}$  of  $\Theta$ ) is (one of) the shortest symmetrizer(s) in the set  $\mathbf{S}_{\Theta}$ .
2. Each leg of  $\mathbf{S}_{\mathcal{R}}$  enters an antisymmetrizer in  $\mathbf{A}_{\Theta}$  of equal length; let us denote this subset of antisymmetrizer by  $\mathbf{A}'_{\mathcal{S}_{\mathcal{R}}}$  (this set of antisymmetrizers correspond to the set of columns  $C_{\mathcal{R}}$ ).
3. Each symmetrizer in  $\mathbf{S}_{\Theta}$  has one common leg with each antisymmetrizer in  $\mathbf{A}'_{\mathcal{S}_{\mathcal{R}}}$  (since each row in  $\Theta$  overlaps with each column in  $C_{\mathcal{R}}$ ).
4. Since, by the assumption of the Propagation Theorem,  $\mathbf{S}_{\Theta \setminus \mathcal{R}}$  and  $\mathbf{S}_{\Theta}$  only differ by the symmetrizer  $\mathbf{S}_{\mathcal{R}}$ , each symmetrizer in the set  $\mathbf{S}_{\Theta \setminus \mathcal{R}}$  has a common leg with each antisymmetrizer in the set  $\mathbf{A}'_{\mathcal{S}_{\mathcal{R}}}$ .

#### 2.4.1.2 Strategy of the proof:

In this proof, we will use the fact that the symmetrizer  $\mathbf{S}_{\mathcal{R}}$  by definition is the sum of all permutations of the legs over which  $\mathbf{S}_{\mathcal{R}}$  is drawn. If  $\mathbf{S}_{\mathcal{R}}$  has length  $k$ , then this sum will consist of  $k!$  terms, and there will be a constant prefactor  $1/k!$ ; this was exemplified in (2.103). In particular, if  $\lambda$  is a particular permutation in the expansion of  $\mathbf{S}_{\mathcal{R}}$ , then we will show that  $O = O^{\lambda}$ , where  $O^{\lambda}$  is defined to be the operator  $O$  with the permutation  $\lambda$  added on the right side in the place where  $\mathbf{S}_{\mathcal{R}}$  would be; schematically drawn, we will show that

$$O = \begin{array}{|c|c|c|} \hline \mathbf{S}_{\Theta \setminus \mathcal{R}} & \mathbf{A}_{\Theta} & \mathbf{S}_{\Theta \setminus \mathcal{R}} \\ \hline \vdots & \vdots & \vdots \\ \hline \mathbf{S}_{\mathcal{R}} & & \\ \hline \end{array} \stackrel{?}{=} \begin{array}{|c|c|c|} \hline \mathbf{S}_{\Theta \setminus \mathcal{R}} & \mathbf{A}_{\Theta} & \mathbf{S}_{\Theta \setminus \mathcal{R}} \\ \hline \vdots & \vdots & \vdots \\ \hline \mathbf{S}_{\mathcal{R}} & & \lambda \\ \hline \end{array} =: O^{\lambda} . \quad (2.106)$$

Since the constituent permutations of a symmetrizer over a subset of factors in  $V^{\otimes n}$  form a sub-group of  $S_n$  [93], it immediately follows that every constituent permutation of  $\mathbf{S}_{\mathcal{R}}$  can be written as a product of constituent transpositions of  $\mathbf{S}_{\mathcal{R}}$ .<sup>16</sup> It thus suffices to show that (2.106) holds for  $\lambda$  being a constituent transposition of  $\mathbf{S}_{\mathcal{R}}$  (i.e. that we may propagate a transposition from the left symmetrizer  $\mathbf{S}_{\mathcal{R}}$  to the right), as then any other permutation can be produced by the successive propagation of transpositions.

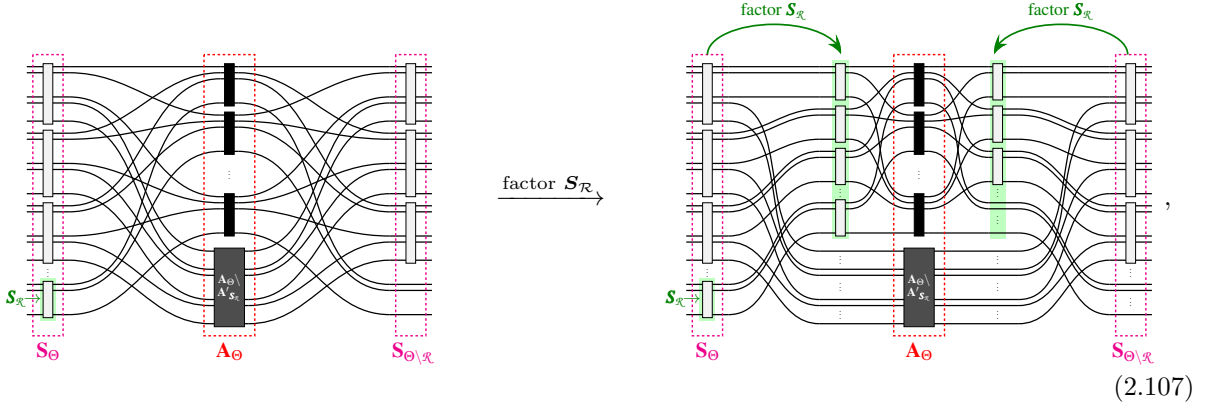
#### 2.4.1.3 Propagating transpositions:

The technique used to permute transpositions through the set of antisymmetrizers, as described in the previous paragraph, was inspired by an example presented in the appendix of [4].

Suppose the set  $\mathbf{A}'_{\mathcal{S}_{\mathcal{R}}}$  (introduced in condition 2 of the previous discussion) contains  $n$  antisymmetrizers. Then, by observations 1 to 4, the length of  $\mathbf{S}_{\mathcal{R}}$  will be exactly  $n$ , and each other symmetrizer in  $\mathbf{S}_{\Theta}$  (and thus also each symmetrizer in  $\mathbf{S}_{\Theta \setminus \mathcal{R}}$ ) will have length at least  $n$ . We may then factor “the symmetrizer  $\mathbf{S}_{\mathcal{R}}$ ”

<sup>16</sup>A proof that any permutation in  $S_n$  can be written as the product of transpositions can be found in [100] and other standard textbooks.

(i.e. a symmetrizer of length  $n$ ) out of each symmetrizer in the sets  $\mathbf{S}_\Theta$  and  $\mathbf{S}_{\Theta \setminus \mathcal{R}}$ ,



where we lumped together the antisymmetrizers  $\mathbf{A}'_{S_{\mathcal{R}}}$  and the rest ( $\mathbf{A}_\Theta \setminus \mathbf{A}'_{S_{\mathcal{R}}}$ ). We will denote the left set of  $\mathbf{S}_{\mathcal{R}}$ 's (which were factored out of  $\mathbf{S}_\Theta$ ) by  $\{\mathbf{S}_{\mathcal{R}}\}_l$ , and the right set of  $\mathbf{S}_{\mathcal{R}}$ 's (which were factored out of  $\mathbf{S}_{\Theta \setminus \mathcal{R}}$ ) by  $\{\mathbf{S}_{\mathcal{R}}\}_r$ , see Figure 2.1. From now onwards, we will focus the part  $\tilde{O}$  within the operator  $O$ , which is highlighted blue in Figure 2.1.

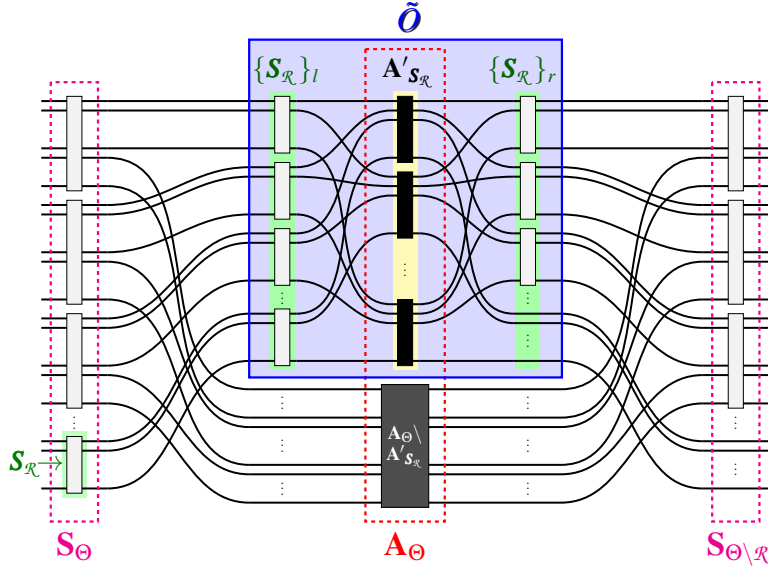


Figure 2.1: This diagram schematically depicts the operator  $O$  (c.f. eq. (2.104)) with a symmetrizer  $\mathbf{S}_{\mathcal{R}}$  factored out of each symmetrizer in  $\mathbf{S}_\Theta$  and in  $\mathbf{S}_{\Theta \setminus \mathcal{R}}$ . The left set of  $\mathbf{S}_{\mathcal{R}}$ 's will be denoted by  $\{\mathbf{S}_{\mathcal{R}}\}_l$ , and the right set of  $\mathbf{S}_{\mathcal{R}}$ 's by  $\{\mathbf{S}_{\mathcal{R}}\}_r$ . In this proof, we will focus on the part of the operator that is highlighted in blue. This part will be denoted by  $\tilde{O}$ .

**The significance of the operator  $\tilde{O}$  in Figure 2.1:** The left part of  $\tilde{O}$ , namely  $\{\mathbf{S}_{\mathcal{R}}\}_l \cdot \mathbf{A}'_{S_{\mathcal{R}}}$ , by itself corresponds to a rectangular tableau, as each symmetrizer has the same length and each antisymmetrizer has the same length. This will be important, since we will need  $\tilde{O}$  to stay unchanged under a swap of any pair of antisymmetrizers in  $\mathbf{A}'_{S_{\mathcal{R}}}$  in order to commute the constituent permutations of  $\mathbf{S}_{\mathcal{R}}$  through the intervening set  $\mathbf{A}'_{S_{\mathcal{R}}}$  (in analogy to what was done in example (2.85) — this will become evident below). Note that  $\tilde{O}$  would not stay unchanged under such a swap if the antisymmetrizers in  $\mathbf{A}'_{S_{\mathcal{R}}}$  had different lengths and would



thus be distinguishable. In particular, the operator  $\tilde{O}$  corresponds to the amputated tableau  $\mathcal{O}_c[\mathcal{R}]$ , which is indeed rectangular by requirement of the Propagation Theorem 2.2. This requirement, therefore, translates into the ability of finding an operator  $\tilde{O}$  within the operator  $O$ , thus allowing the necessary propagation of permutations.

Suppose that  $\mathbf{S}_\Theta$  contains exactly  $m$  symmetrizers (hence  $\mathbf{S}_{\Theta \setminus \mathcal{R}}$  contains  $(m-1)$  symmetrizers). Then also  $\{\mathcal{S}_{\mathcal{R}}\}_l$  contains  $m$  symmetrizers and  $\{\mathcal{S}_{\mathcal{R}}\}_r$  contains  $(m-1)$  symmetrizers.

Furthermore, since each symmetrizer in  $\{\mathcal{S}_{\mathcal{R}}\}_l$  has a common leg with each of the  $n$  antisymmetrizer in  $\mathbf{A}'_{\mathcal{S}_{\mathcal{R}}}$ , we may choose the  $k^{th}$  leg exiting each symmetrizer in  $\{\mathcal{S}_{\mathcal{R}}\}_l$  to enter the  $k^{th}$  antisymmetrizer in  $\mathbf{A}'_{\mathcal{S}_{\mathcal{R}}}$ .<sup>17</sup>

We may schematically draw this, as

$$(2.108)$$

In (2.108), we have labelled the index lines for clarity; from Figure 2.1 it however should be noted that the  $i^{th}$  index in the above graphic is not necessarily the  $i^{th}$  index line in the operator  $O$ . The part of the operator  $O$  highlighted in blue in Figure 2.1, operator  $\tilde{O}$ , can then be represented as

$$(2.109)$$

where the last symmetrizer in the set  $\{\mathcal{S}_{\mathcal{R}}\}_l$  is the symmetrizer  $\mathcal{S}_{\mathcal{R}}$  that we eventually wish to commute through to the right. In (2.109), we labeled the first and the second antisymmetrizer of the set  $\mathbf{A}'_{\mathcal{S}_{\mathcal{R}}}$  by ① and ② respectively for future reference.

As previously stated, we strive to commute constituent transpositions  $(ij)$  of the symmetrizer  $\mathcal{S}_{\mathcal{R}} \in \{\mathcal{S}_{\mathcal{R}}\}_l$  through the set of antisymmetrizers  $\mathbf{A}'_{\mathcal{S}_{\mathcal{R}}}$  to the right set  $\{\mathcal{S}_{\mathcal{R}}\}_r$ . We achieve this goal in the following way: We first factor the transposition  $(ij)$  out of *each* symmetrizer in  $\{\mathcal{S}_{\mathcal{R}}\}_l$ . By doing so, the  $i^{th}$  leg of each symmetrizer now enters the  $j^{th}$  antisymmetrizer and vice versa (all the other legs remain unchanged). We may now “remedy” this change by swapping the  $i^{th}$  and  $j^{th}$  antisymmetrizer, similar to what we did

<sup>17</sup>We may always choose to order index legs this way, since, within a symmetrizer, we may re-order index lines at will without changing the symmetrizer.

in example (2.85). For instance, if  $i = 1$  and  $j = 2$ , we factor the transposition (12) out of each of the symmetrizers of  $\{\mathcal{S}_{\mathcal{R}}\}_l$ ,

$$\tilde{O} = \begin{array}{c} \begin{array}{c} 1 \\ 2 \\ \vdots \\ n \\ n+1 \\ n+2 \\ \vdots \\ 2n \\ \vdots \\ (m-1)n+1 \\ (m-1)n+2 \\ \vdots \\ m \cdot n \end{array} \end{array}, \quad (2.110)$$

The diagram shows a tensor network with multiple horizontal legs. On the left, there are vertical bars representing symmetrizers, with labels 1, 2, ..., n, n+1, n+2, ..., 2n, ..., (m-1)n+1, (m-1)n+2, ..., m · n. A vertical red bar is positioned to the left of the first set of symmetrizers. A vertical black bar is positioned between the first and second sets of symmetrizers. Two antisymmetrizers are marked with red circles containing '1' and '2'.

and then swap the first and second antisymmetrizer, which are marked as ① and ② respectively. The key observation to make is that the antisymmetrizers ① and ② would be indistinguishable if it weren't for the labeling. Thus, the set  $\mathbf{A}'_{\mathcal{S}_{\mathcal{R}}}$  remains unchanged even when the swap between antisymmetrizers  $i$  (①) and  $j$  (②) is carried out. This trick of swapping identical antisymmetrizers was initially used by KS in an example in the appendix of [4].

After we swapped the two antisymmetrizers, the  $i^{\text{th}}$  leg of each symmetrizer in  $\{\mathcal{S}_{\mathcal{R}}\}_l$  once again enters the  $i^{\text{th}}$  antisymmetrizer, and same is true for the  $j^{\text{th}}$  leg. However, now the legs exiting the  $i^{\text{th}}$  antisymmetrizer in  $\mathbf{A}'_{\mathcal{S}_{\mathcal{R}}}$  enter the symmetrizers in  $\{\mathcal{S}_{\mathcal{R}}\}_r$  in the  $j^{\text{th}}$  position, and the legs exiting the  $j^{\text{th}}$  antisymmetrizer enter the symmetrizers in  $\{\mathcal{S}_{\mathcal{R}}\}_r$  in the  $i^{\text{th}}$  position. Thus, we have effectively commuted the transpositions  $(ij)$  past the set  $\mathbf{A}'_{\mathcal{S}_{\mathcal{R}}}$ ,

$$\tilde{O} = \begin{array}{c} \begin{array}{c} 1 \\ 2 \\ \vdots \\ n \\ n+1 \\ n+2 \\ \vdots \\ 2n \\ \vdots \\ (m-1)n+1 \\ (m-1)n+2 \\ \vdots \\ m \cdot n \end{array} \end{array}. \quad (2.111)$$

The diagram is similar to (2.110) but with the antisymmetrizers ① and ② swapped. The vertical red bar is now on the right, and the vertical black bar is in the middle. The labels on the left are the same as in (2.110).

All but one of the propagated transpositions  $(ij)$  can then be absorbed into the symmetrizers of the set  $\{\mathcal{S}_{\mathcal{R}}\}_r$ . One transposition, however, will remain, as there is no symmetrizer<sup>18</sup> in the set  $\{\mathcal{S}_{\mathcal{R}}\}_r$  to absorb

<sup>18</sup>I.e. the missing symmetrizer  $\mathcal{S}_{\mathcal{R}}$  on the right-hand side of the operator  $O$ .

this transposition,

$$\tilde{O} = \text{Diagram} \quad (2.112)$$

We then re-absorb the sets  $\{\mathcal{S}_{\mathcal{R}}\}_l$  and  $\{\mathcal{S}_{\mathcal{R}}\}_r$  into  $\mathbf{S}_{\Theta}$  and  $\mathbf{S}_{\Theta \setminus \mathcal{R}}$  respectively. This clearly leaves the transposition  $(ij)$  un-absorbed. Thus, we have shown that

$$O = \text{Diagram} = O^{\lambda} \quad (2.113)$$

for  $\lambda = (ij)$  being a transposition. We can repeat the above procedure with any constituent transposition of  $\mathcal{S}_{\mathcal{R}}$ .

If  $\lambda$  is a constituent permutation (not necessarily a transposition) of  $\mathcal{S}_{\mathcal{R}}$ , we can also propagate  $\lambda$  to the right-hand side, since any such permutation  $\lambda$  can be written as a product of constituent transpositions: Propagating the permutation  $\lambda$  then corresponds to successively propagating its constituent transpositions through to the right, yielding

$$\tilde{O} = \text{Diagram} \quad (2.114)$$

for any constituent permutation  $\lambda$  of  $\mathcal{S}_{\mathcal{R}}$ .

In order to obtain the missing symmetrizer on the right, it remains to add up all the terms  $O^{\lambda}$  — since  $\mathcal{S}_{\mathcal{R}}$  is assumed to have length  $n$ , there will be exactly  $n!$  such terms. By relation (2.113), we know that each of these terms is equal to  $O$ , yielding the following sum,

$$\frac{1}{n!} \sum_1^{n!} \left( \text{Diagram} \right) = \frac{1}{n!} \sum_{\lambda \in S_n} \left( \text{Diagram} \right) \quad (2.115)$$

The left-hand side of the above equation merely becomes  $\frac{n!}{n!}O = O$ . The right-hand side yields the desired

symmetrizer,<sup>19</sup> such that

$$O = \mathbf{S}_\Theta \mathbf{A}_\Theta \mathbf{S}_\Theta = \begin{array}{c} \boxed{\mathbf{S}_{\Theta \setminus \mathcal{R}}} \vdots \boxed{\mathbf{A}_\Theta} \vdots \boxed{\mathbf{S}_{\Theta \setminus \mathcal{R}}} \\ \boxed{\mathbf{S}_\mathcal{R}} \vdots \vdots \boxed{\mathbf{S}_\mathcal{R}} \end{array}, \quad (2.116)$$

where we used the fact that  $\mathbf{S}_\Theta = \mathbf{S}_{\Theta \setminus \mathcal{R}} \mathbf{S}_\mathcal{R} = \mathbf{S}_\mathcal{R} \mathbf{S}_{\Theta \setminus \mathcal{R}}$  by assumption of Theorem 2.2 (c.f. eq. (2.72)). In particular, using the fact that  $O$  as given in (2.116) is clearly Hermitian,  $O^\dagger = O$ ,<sup>20</sup> we find that

$$O = \begin{array}{c} \boxed{\mathbf{S}_{\Theta \setminus \mathcal{R}}} \vdots \boxed{\mathbf{A}_\Theta} \vdots \boxed{\mathbf{S}_{\Theta \setminus \mathcal{R}}} \\ \boxed{\mathbf{S}_\mathcal{R}} \vdots \vdots \end{array} = \begin{array}{c} \boxed{\mathbf{S}_{\Theta \setminus \mathcal{R}}} \vdots \boxed{\mathbf{A}_\Theta} \vdots \boxed{\mathbf{S}_{\Theta \setminus \mathcal{R}}} \\ \boxed{\mathbf{S}_\mathcal{R}} \vdots \vdots \boxed{\mathbf{S}_\mathcal{R}} \end{array} = \begin{array}{c} \boxed{\mathbf{S}_{\Theta \setminus \mathcal{R}}} \vdots \boxed{\mathbf{A}_\Theta} \vdots \boxed{\mathbf{S}_{\Theta \setminus \mathcal{R}}} \\ \vdots \vdots \boxed{\mathbf{S}_\mathcal{R}} \end{array} = O^\dagger, \quad (2.117)$$

as required.

#### 2.4.1.4 Propagating antisymmetrizers:

The proof of the Propagation Theorem 2.2 for an operator  $Q$  of the form  $Q := \mathbf{A}_\Theta \mathbf{S}_\Theta \mathbf{A}_{\Theta \setminus \mathcal{C}}$  is very similar to the proof given for the operator  $O$ . However, there are some differences on which we wish to comment here: If we want to propagate an antisymmetrizer  $\mathbf{A}_\mathcal{C}$  corresponding to a column  $\mathcal{C}$  in  $\Theta$  from  $\mathbf{A}_\Theta$  to  $\mathbf{A}_{\Theta \setminus \mathcal{C}}$ , we first check that the amputated tableau  $\mathcal{A}_r[\mathcal{C}]$  is rectangular. If so, we are able to isolate an operator  $\tilde{Q}$  within  $Q$  in analogy to how we isolated  $\tilde{O}$  within  $O$  (see Figure 2.1), where

$$\tilde{Q} := \{\mathbf{A}_\mathcal{C}\}_l \mathbf{S}'_{\mathbf{A}_\mathcal{C}} \{\mathbf{A}_\mathcal{C}\}_r. \quad (2.118)$$

When we propagate a transposition  $(ij)$  from the left to the right of  $\tilde{Q}$ , we need to tread with care as this will induce a factor of  $(-1)$ . This factor, however, will be vital in the recombination process that recreates the antisymmetrizer  $\mathbf{A}_\mathcal{C}$  by summing constituent permutations: Suppose the set  $\{\mathbf{A}_\mathcal{C}\}_l$  contains  $m$  antisymmetrizers, then the set  $\{\mathbf{A}_\mathcal{C}\}_r$  contains  $(m-1)$  antisymmetrizers. If we now factor a transposition  $(ij)$  out of each antisymmetrizer in  $\{\mathbf{A}_\mathcal{C}\}_l$  on the left of  $\tilde{Q}$ , we obtain a factor of  $(-1)^m$ . Swapping the  $i^{\text{th}}$  and  $j^{\text{th}}$  symmetrizers will not induce an extra minus-sign, but absorbing the transpositions into the antisymmetrizers in the set  $\{\mathbf{A}_\mathcal{C}\}_r$  will produce an extra factor of  $(-1)^{m-1}$ . Thus, for each transposition we commute through, we obtain a factor of  $(-1)^{2m-1} = -1$ , which is the signature of a transposition. In particular, each permutation  $\lambda$  (consisting of a product of transpositions) will induce a prefactor of  $\text{sign}(\lambda)$  when commuted through, yielding

$$\tilde{Q} = \text{sign}(\lambda) \tilde{Q}^\lambda. \quad (2.119)$$

However, since an antisymmetrizer is by definition the sum of its constituent permutations *weighted by their signatures*, for example,

$$\mathbf{1} = \frac{1}{3!} \left( \overline{\overline{\overline{\quad}}} - \overline{\overline{\times}} - \overline{\times} - \overline{\overline{\times}} + \overline{\times} + \overline{\times} \right), \quad (2.120)$$

<sup>19</sup>This was already exhibited in example (2.88).

<sup>20</sup>By the Hermiticity of (sets of) (anti-)symmetrizer, see eq. (2.10).

equation (2.119) is exactly what we need in order to be able to reconstruct the antisymmetrizer  $\mathbf{A}_C$  on the right of the operator  $\tilde{Q}$  by summing up the terms  $\text{sign}(\lambda)\tilde{Q}^\lambda$ . Re-absorbing  $\{\mathbf{A}_C\}_l$  into  $\mathbf{A}_\Theta$  and  $\{\mathbf{A}_C\}_r$  into  $\mathbf{A}_{\Theta \setminus C}$  yields the desired eq. (2.75).  $\square$

### 2.4.2 Proof of Theorem 2.3 (generalized propagation rules)

Let  $\tilde{\Theta}$  be a semi-standard irregular tableau, and let  $O$  be an operator of the form

$$O = \mathbf{S}_{\tilde{\Theta}} \mathbf{A}_{\tilde{\Theta}} \mathbf{S}_{\tilde{\Theta} \setminus \mathcal{R}}, \quad (2.121)$$

where  $\mathcal{R}$  denotes a particular row in  $\tilde{\Theta}$ . Having gone through the proof of Theorem 2.2, it is clear that the symmetrizer  $\mathbf{S}_{\mathcal{R}}$  can be propagated through the set  $\mathbf{A}_{\tilde{\Theta}}$  if the following conditions are met:

1. Each leg in  $\mathbf{S}_{\mathcal{R}}$  needs to enter an antisymmetrizer of the same length to perform the swapping procedure described in section 2.4.1.3. Call the set of antisymmetrizers sharing legs with  $\mathbf{S}_{\mathcal{R}}$   $\mathbf{A}'_{\mathcal{S}_{\mathcal{R}}}$ . If  $\mathbf{S}_{\mathcal{R}}$  has length  $n$ , then  $\mathbf{A}'_{\mathcal{S}_{\mathcal{R}}}$  contains exactly  $n$  antisymmetrizers.
2. The remaining symmetrizers in  $O$  may have
  - 0 legs in common with the antisymmetrizers in  $\mathbf{A}'_{\mathcal{S}_{\mathcal{R}}}$ , i.e. they are not affected by swapping the antisymmetrizers in  $\mathbf{A}'_{\mathcal{S}_{\mathcal{R}}}$  and thus do not contribute to  $\tilde{O}$  (c.f. section 2.4.1.3), or
  - $n$  legs in common with the antisymmetrizers in  $\mathbf{A}'_{\mathcal{S}_{\mathcal{R}}}$  (one with each antisymmetrizer) in order to be able to absorb any permutation arising from swapping the antisymmetrizers in  $\mathbf{A}'_{\mathcal{S}_{\mathcal{R}}}$ .

The requirement that  $\check{\mathcal{O}}_c[\mathcal{R}]$  only contains rows of equal length ensures that the above conditions are met:

Differently to Young tableaux, if  $\tilde{\Theta}$  is a semi-standard irregular tableau, then removing columns in order to form  $\check{\mathcal{O}}_c[\mathcal{R}]$  may remove whole rows in the process, for example

$$\tilde{\Theta} = \begin{array}{|c|c|c|c|} \hline & & 5 & 1 \\ \hline 7 & 2 & 3 & 6 \\ \hline 4 & 8 & & \\ \hline \end{array} \longrightarrow \check{\mathcal{O}}_c[(4, 8)] \begin{array}{|c|c|} \hline 7 & 2 \\ \hline 4 & 8 \\ \hline \end{array}, \quad (2.122)$$

where the row (5, 1) was removed. However, the symmetrizers corresponding to such rows have no common legs with the antisymmetrizers in  $\mathbf{A}'_{\mathcal{S}_{\mathcal{R}}}$ , as is evident from the example ( $\mathbf{S}_{51}$  shares no legs with  $\mathbf{A}_{74}$  and  $\mathbf{A}_{28}$ ). This is also due to the fact that  $\tilde{\Theta}$  is semi-standard, thus not allowing any of its entries to occur more than once.

Hence, the only symmetrizers that share index legs with the antisymmetrizers in  $\mathbf{A}'_{\mathcal{S}_{\mathcal{R}}}$  are those corresponding to the rows of  $\tilde{\Theta}$  which have not been fully deleted (although maybe in part) in  $\check{\mathcal{O}}_c[\mathcal{R}]$ . Let us denote the set of these symmetrizers by  $\mathbf{S}'_{\mathcal{S}_{\mathcal{R}}}$ . The requirement that each row in  $\check{\mathcal{O}}_c[\mathcal{R}]$  has the same length ensures that each symmetrizer in  $\mathbf{S}'_{\mathcal{S}_{\mathcal{R}}}$  shares exactly one leg with each antisymmetrizer in  $\mathbf{A}'_{\mathcal{S}_{\mathcal{R}}}$  and thus has length  $\geq n$  (this was already argued in section 2.4.1.1).

Thus, all conditions required to perform the propagating procedure already explained in sections 2.4.1.2 and 2.4.1.3 are met, allowing us to propagate  $\mathbf{S}_{\mathcal{R}}$  through  $\mathbf{A}'_{\mathcal{S}_{\mathcal{R}}}$  at will,

$$O = \mathbf{S}_{\tilde{\Theta}} \mathbf{A}_{\tilde{\Theta}} \mathbf{S}_{\tilde{\Theta} \setminus \mathcal{R}} = \mathbf{S}_{\tilde{\Theta}} \mathbf{A}_{\tilde{\Theta}} \mathbf{S}_{\tilde{\Theta}} = \mathbf{S}_{\tilde{\Theta} \setminus \mathcal{R}} \mathbf{A}_{\tilde{\Theta}} \mathbf{S}_{\tilde{\Theta}}. \quad (2.123)$$

The proof for symmetrizers and antisymmetrizers exchanged follows similar steps and is thus left as an exercise to the reader.  $\square$

## 2.5 Chapter conclusion

We have established two classes of rules that allow us to simplify and manipulate birdtrack operators. The first such class are the *cancellation rules* (Theorem 2.1 and Corollary 2.2) allowing us to shorten the birdtrack expression of an operator. The simplification reached in this process is often very significant, as is exemplified in Figure 2.2. Shorter expressions of operators are desirable, as they are more practical to work with in that they allow for faster automated computation. Furthermore, short expressions offer a visual assessment of their action, making them more intuitive.

The second class of rules are *propagation rules* (Theorems 2.2 and 2.3). Their use lies in the ability to make Hermitian birdtrack operators explicitly symmetric, thus exposing their innate Hermiticity. Since birdtracks are a graphical tool designed to make working with them more intuitive, it is desirable to visually expose the inherent properties of the birdtrack operators.

To illustrate how powerful these simplification rules are, we show their effect on the Hermitian KS projector [4] associated with the Young tableau

$$\Phi := \begin{array}{|c|c|c|c|} \hline 1 & 2 & 4 & 7 \\ \hline 3 & 6 & & \\ \hline 5 & 8 & & \\ \hline 9 & & & \\ \hline \end{array} . \tag{2.124}$$

The recursive KS algorithm leads to a Hermitian Young projection operator  $P_\Phi$ , with  $\bar{P}_\Phi$  being of impressive length: It contains 127 sets of symmetrizers and antisymmetrizers, and its Hermiticity is not visually apparent (see Figure 2.2). The cancellation rules achieve a tremendous simplification: the result contains only 13 sets. Furthermore, multiple applications of the propagation rules can be used to translate this into an explicitly symmetric form.

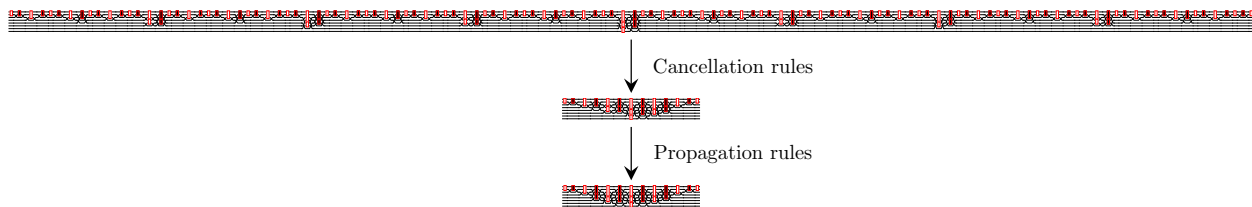


Figure 2.2: For a size comparison, this figure shows the birdtrack arising from the iterative KS construction in the top line, the much shortened version arising from the cancellation rules in the second line, and the explicitly symmetric version achieved via the propagation rules in the third line.

In fact, the shorter, explicitly symmetric result can be constructed directly, without first constructing the KS operator and then applying the cancellation rules; we provide the tools to do so in a separate paper [2]

[chapter 3]. The algorithm allowing us to do this is based on the measure of lexical disorder (MOLD) of a Young tableau [2] [chapter 3]. When used to construct the Hermitian Young projection operators in *Mathematica*, the reduction in computational cost is impressive: On a modern laptop, the final result shown in Figure 2.2 is obtained approximately 18600 times faster than the KS equivalent even before simplification rules are implemented to shorten the latter. Thus, the MOLD construction offers a significant improvement over the KS construction. The proof of the MOLD algorithm relies heavily on the manipulation rules laid out in this paper.

Augmenting the Hermitian Young projection operators with transition operators yields an alternative basis of the algebra of invariants of  $SU(N)$  over  $V^{\otimes m}$  [3] [chapter 4]. The construction algorithm of the transition operators again is built upon the simplification rules presented in this paper. With a basis for  $\text{API}(SU(N), V^{\otimes m})$  consisting of projection and transition operators, one can construct a *mutually orthogonal, complete* basis for the singlet states of  $SU(N)$  over  $V^{\otimes m} \otimes (V^*)^{\otimes m}$  (and more generally over  $V^{\otimes m} \otimes (V^*)^{\otimes n}$ ) [94] [chapter 5]. These singlets are directly applicable to QCD, as they are needed to form Wilson line correlators used in the framework of Jalilian-Marian-Iancu-McLerran-Weigert Leonidov-Kovner (JIMWLK) [20, 56–59] evolution (see e.g. [71]), as well as a modern treatment of jet-evolution equations (see e.g. [78]), the infrared structure of QCD in the form of gluon exchange webs (see e.g. [90]), generalized parton distributions (GPDs) and transverse-momentum-dependent parton distributions (TMDs) (see e.g. [91]). The references here only serve to mark a specific reference point we find intriguing and are by no means exhaustive: In fact, almost every branch of QCD in which the factorization theorems (see, e.g. [101]) apply makes use of Wilson line correlators, and any attempt at completeness would be futile.

Besides their physics applications (which is the most appealing quality to the authors of this paper), birdtracks are also immensely useful in the study of the representation theory of semi-simple Lie groups, as is exhibited in [2, 4, 72, 102]. With the recent interest in Hermitian Young projection operators, birdtracks promise interesting further development in this branch of mathematics. It is hoped that the simplification rules given here encourage the use of birdtracks as a viable tool for calculation.





## Chapter 3

# Compact Hermitian Young Projection Operators

This chapter has been published under the same name in the Journal of Mathematical Physics [2]. In some instances, the present paper (chapter) refers to additional results not given in the paper. Where such work is included in this thesis, a remark in square brackets and italics has been added to refer the reader to the appropriate chapter of this thesis.

**Abstract:** *In this paper, we describe a compact and practical algorithm to construct Hermitian Young projection operators for irreducible representations of the special unitary group  $SU(N)$ , and discuss why ordinary non-Hermitian Young projection operators are unsuitable for physics applications. The proof of this construction algorithm uses the iterative method described by Keppeler and Sjö Dahl in [4]. We further show that Hermitian Young projection operators share desirable properties with Young tableaux, namely a nested hierarchy when “adding a particle”. We close by exhibiting the enormous advantage of the Hermitian Young projection operators constructed in this paper over those given by Keppeler and Sjö Dahl.*

### 3.1 Introduction & outline

#### 3.1.1 Historical overview

More than a hundred years ago, the representation theory of compact, semi-simple Lie groups, in particular also of  $SU(N)$ , was a hot topic of research. Most known to physicists is the work done by Clebsch and Gordan, where the product representations of  $SU(N)$  can be classified using the Clebsch-Gordan coefficients [25, 92, 93]. This is the textbook method for  $N = 2$  to find the irreducible representations of spin of an  $m$ -particle configuration by giving an explicit change of basis. While this method is perfectly adequate also for  $N \neq 2$ , it requires one to choose the parameter  $N$  at the start of the calculation. Thus, this approach is of little use to us, as we mainly strive to apply representation theory in a context of QCD, where it is often essential for  $N$  (representing  $N_c$ , the number of colors in this case) to be a parameter to be varied at the end of the calculation to get a better understanding of underlying structures [71, 75, 80].

Shortly after the research by Clebsch and Gordan was conducted, Elié Cartan introduced another method of finding the irreducible representations of Lie groups via finding certain subalgebras of the associated

Lie algebras [103] since known as Cartan subalgebras. This method is based on finding the highest weights corresponding to the irreducible representations, and then constructing all basis states within it. This process was used by Gell-Mann in 1961 [15, 104] when he introduced the *eight-fold way* (here  $N$  represents  $N_f$  the number of flavors) to order hadrons into flavor multiplets such as the baryon octet and decuplet featuring prominently in any introductory text on particle physics and as a motivation to study representation theory in many a mathematical introduction to the topic [27, 65, 92]. Usually, one also fixes the parameter  $N$  from the outset when using this method. While it is possible keep  $N$  as a parameter<sup>1</sup> Cartan's method is of restricted use in practical applications as it requires us to construct all  $N^m$  associated basis elements to fully characterize the irreducible representations required to span  $V^{\otimes m}$ : For an unspecified  $N$ , this becomes a daunting task.

In 1928, approximately three decades after Cartan's work, Alfred Young conceived a combinatorial method of classifying the idempotents on the algebra of permutations [84]. This method was subsequently used in the 1930's to establish a connection between these idempotents and the irreducible representations of compact, semi-simple Lie groups, now known as the *Schur-Weyl duality*, [98]. This duality is based on the *theory of invariants*, [72, 98], which exploits the invariants (in particular the *primitive invariants*) of a Lie group  $G$  and constructs projection operators corresponding to the irreducible representations of  $G$ . Since the present paper will rely on the theory of invariants, a short overview is in order: We will deal with a product representations of  $SU(N)$  constructed from its fundamental representation on a given vector space  $V$  with  $\dim(V) = N$ , whose action will simply be denoted by  $v \mapsto Uv$  for all  $U \in SU(N)$  and  $v \in V$ . Choosing a basis  $\{e_{(i)} | i = 1, \dots, \dim(V)\}$  such that  $v = v^i e_{(i)}$ , this becomes  $v^i \mapsto U^i_j v^j$ . This immediately induces a product representation of  $SU(N)$  on  $V^{\otimes m}$  if one uses this basis of  $V$  to induce a basis on  $V^{\otimes m}$  so that a general element  $\mathbf{v} \in V^{\otimes m}$  takes the form  $\mathbf{v} = v^{i_1 \dots i_m} e_{(i_1)} \otimes \dots \otimes e_{(i_m)}$ :

$$\mathbf{U} \circ \mathbf{v} = \mathbf{U} \circ v^{i_1 \dots i_m} e_{(i_1)} \otimes \dots \otimes e_{(i_m)} := \underbrace{U^{i_1}_{j_1} \dots U^{i_m}_{j_m}}_{=: \mathbf{U}} v^{j_1 \dots j_m} e_{(i_1)} \otimes \dots \otimes e_{(i_m)}. \quad (3.1)$$

Since all the factors in  $V^{\otimes m}$  are identical, the notion of permuting the factors is a natural one and leads to a linear map on  $V^{\otimes m}$  according to

$$\rho \circ \mathbf{v} = \rho \circ v^{i_1 \dots i_m} e_{(i_1)} \otimes \dots \otimes e_{(i_m)} := v^{i_{\rho(1)} \dots i_{\rho(m)}} e_{(i_1)} \otimes \dots \otimes e_{(i_m)} \quad (3.2)$$

where  $\rho$  is an element of  $S_m$ , the group of permutations of  $m$  objects.<sup>2</sup> From the definitions (3.1) and (3.2), one immediately infers that the product representation commutes with all permutations on any  $\mathbf{v} \in V^{\otimes m}$ :

$$\mathbf{U} \circ \rho \circ \mathbf{v} = \rho \circ \mathbf{U} \circ \mathbf{v}. \quad (3.3)$$

In other words, any such permutation  $\rho$  is an *invariant* of  $SU(N)$  (or in fact any Lie group  $G$  acting on  $V$ ):

$$\mathbf{U} \circ \rho \circ \mathbf{U}^{-1} = \rho. \quad (3.4)$$

It can further be shown that these permutations in fact span the space of all linear invariants of  $SU(N)$  over  $V^{\otimes m}$  [72]. The permutations are thus referred to as the *primitive invariants* of  $SU(N)$  over  $V^{\otimes m}$ . The full

<sup>1</sup>This is an elusive piece of knowledge: Fulton [95, chapter 8.2, Lemma 4], for example, provides the basis for finding highest weight vectors directly from tableaux without fixing  $N$ .

<sup>2</sup>Permuting the basis vectors instead involves  $\rho^{-1}$ :  $v^{\rho(i_1) \dots \rho(i_m)} e_{(i_1)} \otimes \dots \otimes e_{(i_m)} = v^{i_1 \dots i_m} e_{(i_{\rho^{-1}(1)})} \otimes \dots \otimes e_{(i_{\rho^{-1}(m)})}$ .

space of linear invariants is then given by<sup>3</sup>

$$\text{API}(\text{SU}(N), V^{\otimes m}) := \left\{ \sum_{\sigma \in S_m} \alpha_\sigma \sigma \mid \alpha_\sigma \in \mathbb{R}, \sigma \in S_m \right\} \subset \text{Lin}(V^{\otimes m}) . \quad (3.5)$$

Note we are exclusively focusing on  $\text{API}(\text{SU}(N), V^{\otimes m})$  and make no efforts to directly discuss the invariants on  $V^{\otimes m} \otimes (V^*)^{\otimes n}$ . For  $\text{SU}(N)$  these are implicitly included due to the presence of  $\epsilon^{i_1 \dots i_N}$  as a second invariant besides  $\delta^i_j$  — the construction of explicit algorithms tailored to expose this structure are beyond the scope of this paper. For a more comprehensive introduction to invariant theory, readers are referred to [72, 93, 98, 105].

If we denote by  $\mathcal{Y}_m$  the complete set of irreducible representations of  $\text{SU}(N)$  on  $V^{\otimes m}$ , (according to Young this is in fact the set of Young tableaux with  $m$ -boxes), then a meaningful set of projection operators  $\{L_\Theta \in \text{API}(\text{SU}(N), V^{\otimes m}) \mid \Theta \in \mathcal{Y}_m\}$  (where the  $L_\Theta$  are not identically zero) onto the invariant subspaces must satisfy the following three properties

1. The operators must be idempotent, that is they satisfy

$$L_\Theta \cdot L_\Theta = L_\Theta . \quad (3.6a)$$

2. The operators are mutually *transversal* [4] in the sense that their images only intersect at 0,

$$L_\Theta \cdot L_\Phi = 0 \quad \text{if } \Theta \neq \Phi . \quad (3.6b)$$

3. The complete set of projection operators for  $\text{SU}(N)$  over  $V^{\otimes m}$  sum up to the identity element of  $V^{\otimes m}$ ,

$$\sum_{\Theta \in \mathcal{Y}_m} L_\Theta = \text{id}_{V^{\otimes m}} . \quad (3.6c)$$

Projection operators in  $\text{API}(\text{SU}(N), V^{\otimes m})$ , derived from Young tableaux that satisfy all three conditions without restrictions, together with equation (3.3) then classify all irreducible representations of  $\text{SU}(N)$ , [4, 72, 85, 92, 93].

Young projectors  $Y_\Theta$  are suitable for this purpose only for  $m = 1, 2, 3, 4$ : They fail to satisfy conditions (3.6b) and (3.6c) from  $m = 5$  onwards so that additional work is needed to ensure that the theory addresses *all* irreducible representations contained in  $V^{\otimes m}$ . In [85, section 5.4], Littlewood describes how to “correct” Young projectors  $Y_\Theta$  for  $m \geq 5$  to restore conditions (3.6b) and (3.6c). We call the resulting operators Littlewood-Young (LY) projectors and denote them  $L_\Theta$  to distinguish them from the original Young projectors  $Y_\Theta$ . A short account of their construction using our notation is given in appendix 3.A for completeness.

For classification purposes, one does *not* require the operators  $L_\Theta$  to be Hermitian, and from  $m = 3$  a growing fraction of the LY projectors lack that often useful feature.

On the positive side, the LY projection operators are compact and can be constructed keeping  $N$  as a parameter, both desirable properties for the practitioner.

With Young’s (and Littlewood’s) contributions, the representation theory of compact, semi-simple Lie groups was considered a fully understood and complete theory from approximately 1950 onward, even though many

---

<sup>3</sup>One may equally well define the algebra of primitive invariants over the field of complex numbers  $\mathbb{C}$ , but the real numbers  $\mathbb{R}$  are sufficient for our purposes here.

misconceptions, especially about the full extent of the theory remained, in particular among casual practitioners.

In the 1970's, Penrose devised a graphical method of dealing with primitive invariants of Lie groups including Young projection operators [87, 88], which was subsequently applied in a collaboration with MacCallum [89]. This graphical method, now dubbed the *birdtrack formalism*, was modernized and further developed by Cvitanović [72] in recent years. The immense benefit of the birdtrack formalism is that it makes the actions of the operators visually accessible and thus more intuitive. For illustration, we give as an example the permutations of  $S_3$  written both in their cycle notation (see [93] for a textbook introduction) as well as birdtracks:

$$\begin{array}{cccccc}
 \begin{array}{c} \leftarrow \\ \leftarrow \\ \leftarrow \\ \underbrace{\hspace{1.5cm}} \\ \text{id} \end{array}, &
 \begin{array}{c} \leftarrow \quad \leftarrow \\ \searrow \quad \swarrow \\ \swarrow \quad \searrow \\ \leftarrow \quad \leftarrow \\ \underbrace{\hspace{1.5cm}} \\ (12) \end{array}, &
 \begin{array}{c} \leftarrow \quad \leftarrow \\ \searrow \quad \swarrow \\ \swarrow \quad \searrow \\ \leftarrow \quad \leftarrow \\ \underbrace{\hspace{1.5cm}} \\ (13) \end{array}, &
 \begin{array}{c} \leftarrow \quad \leftarrow \\ \searrow \quad \swarrow \\ \swarrow \quad \searrow \\ \leftarrow \quad \leftarrow \\ \underbrace{\hspace{1.5cm}} \\ (23) \end{array}, &
 \begin{array}{c} \leftarrow \quad \leftarrow \\ \searrow \quad \swarrow \\ \swarrow \quad \searrow \\ \leftarrow \quad \leftarrow \\ \underbrace{\hspace{1.5cm}} \\ (123) \end{array}, &
 \begin{array}{c} \leftarrow \quad \leftarrow \\ \searrow \quad \swarrow \\ \swarrow \quad \searrow \\ \leftarrow \quad \leftarrow \\ \underbrace{\hspace{1.5cm}} \\ (132) \end{array}.
 \end{array} \tag{3.7}$$

The action of each of the above permutations on a tensor product  $v_1 \otimes v_2 \otimes v_3$  is clear, for example

$$(123)(v_1 \otimes v_2 \otimes v_3) = v_3 \otimes v_1 \otimes v_2. \tag{3.8}$$

In the birdtrack formalism, this equation is written as

$$\begin{array}{c} \leftarrow \\ \leftarrow \\ \leftarrow \\ \underbrace{\hspace{1.5cm}} \\ v_1 \\ v_2 \\ v_3 \end{array} = \begin{array}{c} v_3 \\ v_1 \\ v_2 \end{array}, \tag{3.9}$$

where each term in the product  $v_1 \otimes v_2 \otimes v_3$  (written as a tower  $\begin{smallmatrix} v_1 \\ v_2 \\ v_3 \end{smallmatrix}$ ) can be thought of as being moved along the lines of  $\begin{array}{c} \leftarrow \\ \leftarrow \\ \leftarrow \\ \underbrace{\hspace{1.5cm}} \end{array}$ . Birdtracks are thus naturally read from right to left, as is also indicated by the arrows on the legs.<sup>4</sup>

The representation theory of  $SU(N)$  found a short-lived revival in 2014, when Keppeler and Sjö Dahl presented a construction algorithm for Hermitian projection operators (based on the idempotents already found by Young) [4]. This paper arose out of a need for *Hermitian* operators in a physics context. In their paper, the birdtrack formalism was used to devise a recursive construction algorithm for Hermitian projection operators. This algorithm does produce Hermitian operators satisfying the requirements (3.6) (idempotency, transversality, and decomposition of unity) for a classification tool and allows to keep  $N$  as a parameter, just as the Littlewood-Young operators devised much earlier.

We will argue below that Hermiticity provides more than just cosmetic advantages: We show that Hermitian Young projection operators mimic the tableau hierarchy of Young tableaux. We directly trace this back to Hermiticity — the Littlewood-Young projection operators like any non-Hermitian corrected version of Young projectors must fail in this regard.

To the practitioner, this comes at a high price: the expressions created by Keppeler and Sjö Dahl's algorithm soon become extremely long and thus computationally expensive and impractical. In this paper, we give a considerably more efficient and thus more *practical* construction algorithm for Hermitian Young projection operators yielding compact expressions.

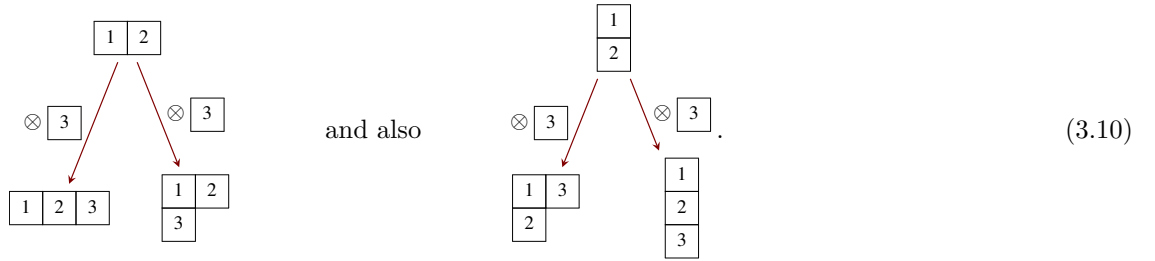
<sup>4</sup>The direction of the arrows thus encodes whether the leg is acting on  $V$  or its dual  $V^*$ , *c.f.* section 3.3.1.

The remainder of this present section 3.1 gives a detailed outline of this paper and lists all goals that will be achieved along the way.

### 3.1.2 Where non-Hermitian projection operators fail to deliver

Among practitioners, many misconceptions still exist with regards to Young projection operators and their corrected forms. The probably most generic one stems from the presentation of Young tableaux and their corresponding projection operators in the literature: It is usually explained in parallel that

1. Young tableaux follow a progressive hierarchy, in the sense that tableaux consisting of  $n$  boxes can be obtained from Young tableaux of  $(n - 1)$  boxes merely by adding the box  $\boxed{n}$  in the appropriate place. For example, the tableaux  $\begin{array}{|c|c|} \hline 1 & 2 \\ \hline 3 & \\ \hline \end{array}$  and  $\begin{array}{|c|c|c|} \hline 1 & 2 & 3 \\ \hline \end{array}$  can both be obtained from the tableau  $\begin{array}{|c|c|} \hline 1 & 2 \\ \hline \end{array}$ ,



Since this is a key concept, we will need some notation and nomenclature to refer to it. In general, for a *particular* Young tableau  $\Theta$  with  $(n - 1)$  boxes, we will denote the set of all Young tableaux that can be obtained from  $\Theta$  by adding the box  $\boxed{n}$  by

$$\{\Theta \otimes \boxed{n}\}; \quad (3.11)$$

this set will also be referred to as the *child-set* of  $\Theta$ .

2. This is complemented by the fact that the *corrected Young projection operators* (e.g. the *LY-operators*) span the full space, that is

$$\sum_{\Theta \in \mathcal{Y}_n} L_{\Theta} = \text{id}_n \quad (3.12)$$

where  $\mathcal{Y}_n$  is understood to be the set of *all* Young tableaux consisting of  $n$  boxes (for a fixed  $n$ ), and  $\text{id}_n$  is the identity operator on the space  $V^{\otimes n}$ . (As mentioned earlier, this also holds for the standard Young projection operators for  $m \leq 4$ .) Equation (3.12) is also known as the *completeness relation* of Littlewood-Young projection operators. In particular for  $n = 2, 3$  (where the  $L_{\Theta}$  reduce to  $Y_{\Theta}$ , c.f. appendix 3.A),

$$Y_{\begin{array}{|c|c|} \hline 1 & 2 \\ \hline \end{array}} + Y_{\begin{array}{|c|} \hline 1 \\ \hline 2 \\ \hline \end{array}} = \text{id}_2 \quad (3.13)$$

and

$$Y_{\begin{array}{|c|c|c|} \hline 1 & 2 & 3 \\ \hline \end{array}} + Y_{\begin{array}{|c|c|} \hline 1 & 2 \\ \hline 3 & \\ \hline \end{array}} + Y_{\begin{array}{|c|c|} \hline 1 & 3 \\ \hline 2 & \\ \hline \end{array}} + Y_{\begin{array}{|c|} \hline 1 \\ \hline 2 \\ \hline 3 \\ \hline \end{array}} = \text{id}_3. \quad (3.14)$$

The completeness relations offer decompositions of unity in both cases.

The hierarchy relation (3.10) of Young tableaux, and the completeness relation (3.12) of LY projection operators, then might lead the unwary reader to (incorrectly) infer that the tableau hierarchy (3.10) automatically implies that this decomposition of unity is in fact *nested*, i.e. that the child tableaux correspond to projection operators that furnish decompositions of their parent projectors so that the identities

$$Y_{\begin{smallmatrix} \boxed{123} \\ \boxed{3} \end{smallmatrix}} + Y_{\begin{smallmatrix} \boxed{12} \\ \boxed{3} \end{smallmatrix}} \stackrel{?}{=} Y_{\begin{smallmatrix} \boxed{12} \\ \end{smallmatrix}} \quad \text{and} \quad Y_{\begin{smallmatrix} \boxed{13} \\ \boxed{2} \end{smallmatrix}} + Y_{\begin{smallmatrix} \boxed{1} \\ \boxed{2} \\ \boxed{3} \end{smallmatrix}} \stackrel{?}{=} Y_{\begin{smallmatrix} \boxed{1} \\ \boxed{2} \end{smallmatrix}} \quad (3.15)$$

would hold. Both of these “equations” can easily be shown to be false by direct calculation. The authors have not found any literature that clearly states that relation (3.10) holds for Young tableaux only, and does not have a counterpart in terms of Littlewood-Young projection operators.

In physics applications, (3.12) is often not sufficient, and we require a counterpart of the structure in (3.10) for a suitable set of projection operators, thus repairing the failure of “equation” (3.15). The desired analogue exists, it is given by the Hermitian Young projection operators introduced by Keppeler and Sjödaahl (KS) [4].<sup>5</sup> In the present paper, we will explicitly demonstrate that the tableau hierarchy (3.10) can be transferred to the KS operators in the desired manner: Using  $P_\Theta$  to denote the Hermitian Young projection operator corresponding to the tableau  $\Theta$ , it turns out that the decompositions in our example are indeed nested, so that

$$P_{\begin{smallmatrix} \boxed{123} \\ \boxed{3} \end{smallmatrix}} + P_{\begin{smallmatrix} \boxed{12} \\ \boxed{3} \end{smallmatrix}} = P_{\begin{smallmatrix} \boxed{12} \\ \end{smallmatrix}} \quad \text{and} \quad P_{\begin{smallmatrix} \boxed{13} \\ \boxed{2} \end{smallmatrix}} + P_{\begin{smallmatrix} \boxed{1} \\ \boxed{2} \\ \boxed{3} \end{smallmatrix}} = P_{\begin{smallmatrix} \boxed{1} \\ \boxed{2} \end{smallmatrix}} \quad (3.16)$$

hold, and that this generalizes to all Hermitian projectors corresponding to Young tableaux. Thus, the first goal of this paper will be to show that this pattern holds in general:

■ **Goal 1:**

*We are interested in a nested decomposition of projection operators in analogy to the the hierarchy relation of Young tableaux (exemplified in eq. (3.10)) to operators, thus generalizing eq. (3.16) to*

$$\sum_{\Phi \in \{\Theta \otimes \boxed{n}\}} P_\Phi = P_\Theta \quad \text{where } \Phi \in \mathcal{Y}_n \text{ and } \Theta \in \mathcal{Y}_{n-1}. \quad (3.17)$$

1. *We will look at two particular examples which illustrate that the summation property (3.17) does not hold for Young projection operators, section 3.3.2. In particular, we will find that assuming (3.17) holds for Young projectors over  $V^{\otimes n}$  and all their ancestors (up to some value of  $n$ ) forces one to falsely conclude that these projectors are Hermitian. This serves as a motivation that the summation property should hold for Hermitian Young projection operators.*
2. *In section 3.3.4, we will find our intuition restored when we prove that eq. (3.17) indeed holds for all Hermitian Young projectors. This will be accomplished by using a shortened version of the KS operators; a construction principle for these shortened operators is given in section 3.3.3.2.*

---

<sup>5</sup>While the nested hierarchy (3.17) (and its generalization (3.18)) is obeyed by the KS operators, it was not explicitly discussed in [4]. For up to 4 index lines, [72] constructed Hermitian Young projection operators and also discussed their nested hierarchy property, without proceeding to a general construction algorithm. In the present paper we wish to contrast the standard Young projection operators with the Hermitian Young projection operators, and so we choose to explicitly show the nested hierarchy of the Hermitian projectors here.

3. This then automatically extends over any number of generations of tableaux (c.f. eq. (3.112)),

$$\sum_{\Phi \in \{\Theta \otimes \boxed{m} \otimes \cdots \otimes \boxed{n}\}} P_{\Phi} = P_{\Theta} \quad \text{for } \Phi \in \mathcal{Y}_n \text{ and } \Theta \in \mathcal{Y}_{m-1}, m < n, \quad (3.18)$$

section 3.3.4.

### 3.1.3 Shorter is better

Having motivated the necessity of Hermitian Young projection operators, we will now shift our focus to their application. In particular, the authors of this paper are foremost interested in applications in a QCD context such as is laid out in [94] [chapter 5]. With this objective in mind, the Hermitian Young projection operators conceived by KS [4] become impractical as the number of factors in  $V^{\otimes m}$  grows: the expressions become too long and thus computationally expensive; a quality, that is explained in section 3.4.3.

An array of practical tools [1] [chapter 2] particularly suited for the *birdtrack formalism* [72], in which the Hermitian Young projection operators by KS were constructed, allows to devise a new construction principle for Hermitian Young projection operators, which we could not resist to dub *MOLD construction*. As elements in the algebra of invariants, the MOLD operators are identical to the KS operators, however their expressions in terms of symmetrizers and antisymmetrizers, as well as the number of steps used in the construction, is shorter, often dramatically so. We gain access to all the desired properties of the KS operators at a much lower computational cost: their *idempotency*, their *mutual transversality*, their *completeness relation*,<sup>6</sup> and also the hierarchy relation (3.17). A clear comparison between the MOLD and the KS constructions and the resulting expressions for the Hermitian Young projection operators can be found in section 3.4.3. This constitutes the second goal of this paper:

#### ■ Goal 2:

*We will provide a construction principle for Hermitian Young projection operators that produces compact, and thus practically useful expressions for these operators, section 3.4. An explicit comparison of projection operators obtained from the MOLD and the KS algorithms is given in 3.4.3.*

## 3.2 Tableaux, projectors, birdtracks, and conventions

Before we set out to achieve Goals 1 and 2, we will provide a short sketch of birdtracks and the way in which they relate to Young tableaux in section 3.2.1, mainly to prepare for section 3.2.2 where we establish the notation used in this paper. For a more comprehensive introduction to the birdtrack formalism refer to [72].

### 3.2.1 Birdtracks & projection operators

Our aim in this section is to establish a link between Young tableaux [93] and birdtracks [72, 87–89], as it is our ultimate goal is to use these tools in a QCD context, where  $SU(N)$  with  $N = N_c = 3$  is the gauge group of the theory [94] [chapter 5], in a manner that allows us to keep  $N$  as a parameter in order to have direct access to additional structure, not least the large  $N_c$  limit.

<sup>6</sup>All of these properties of the KS operators are described in Theorem 3.3 and in [4].

As mentioned earlier, one way to generate the projection operators corresponding to the irreducible representations of  $SU(N)$  without being forced to choose a numerical value for  $N$  at the outset is via the method of Young projection operators, which can be constructed from Young tableaux, see for example [92, 93, 95, 96] and other standard textbooks.

We therefore begin with a short memory-refresher on Young tableaux, our main source for this will be [93]. A *Young tableau* is defined to be an arrangement of  $m$  boxes which are left-aligned and top-aligned, and each box is filled with a unique integer between 1 and  $m$  such that the numbers increase from left to right in each row and from top to bottom in each column.<sup>7</sup> For example, among the two conglomerations of boxes

$$\Theta = \begin{array}{|c|c|c|} \hline 1 & 3 & 6 \\ \hline 2 & 5 & 7 \\ \hline 4 & & \\ \hline \end{array} \quad \text{and} \quad \tilde{\Theta} = \begin{array}{|c|c|c|c|} \hline 3 & 4 & 1 & \\ \hline 2 & 6 & 7 & 5 \\ \hline \end{array}, \quad (3.19)$$

$\Theta$  is a Young tableau but  $\tilde{\Theta}$  is not since  $\tilde{\Theta}$  is neither top aligned nor are the numbers increasing within each column and row. The study of Young tableaux is the topic of several books, e.g. [95], and is thus too vast a topic to fully explore here.

Throughout this paper,  $\mathcal{Y}_n$  will denote the set of all Young tableaux consisting of  $n$  boxes. For example,

$$\mathcal{Y}_3 := \left\{ \begin{array}{|c|c|c|} \hline 1 & 2 & 3 \\ \hline \end{array}, \begin{array}{|c|c|} \hline 1 & 2 \\ \hline 3 & \\ \hline \end{array}, \begin{array}{|c|c|} \hline 1 & 3 \\ \hline 2 & \\ \hline \end{array}, \begin{array}{|c|} \hline 1 \\ \hline 2 \\ \hline 3 \\ \hline \end{array} \right\} = \left\{ \begin{array}{|c|c|} \hline 1 & 2 \\ \hline \end{array} \otimes \begin{array}{|c|} \hline 3 \\ \hline \end{array} \right\} \cup \left\{ \begin{array}{|c|} \hline 1 \\ \hline 2 \\ \hline \end{array} \otimes \begin{array}{|c|} \hline 3 \\ \hline \end{array} \right\}. \quad (3.20)$$

We will denote a particular Young tableau by an upper case Greek letter, usually  $\Theta$  or  $\Phi$ .

To establish the connection with birdtrack notation, let us consider a symmetrizer over elements 1 and 2,  $\mathcal{S}_{12}$ , corresponding to a Young tableau

$$\begin{array}{|c|c|} \hline 1 & 2 \\ \hline \end{array}, \quad (3.21)$$

as symmetrizers always correspond to rows of Young tableaux [93]. We know that this symmetrizer  $\mathcal{S}_{12}$  is given by  $\frac{1}{2}(\text{id} + (12))$ , where  $\text{id}$  is the identity and  $(12)$  denotes the transposition that swaps elements 1 and 2. Graphically, we would denote this linear combination as [72]

$$\mathcal{S}_{12} = \frac{1}{2} \left( \begin{array}{c} \leftarrow \quad \leftarrow \\ \leftarrow \quad \leftarrow \end{array} + \begin{array}{c} \leftarrow \quad \leftarrow \\ \leftarrow \quad \leftarrow \end{array} \right). \quad (3.22)$$

This operator is read from right to left,<sup>8</sup> as it is viewed to act as a linear map from the space  $V \otimes V$  into itself. In this paper, permutations and linear combinations thereof will always be interpreted as elements of  $\text{Lin}(V^{\otimes n})$ , where  $\text{Lin}(V^{\otimes n})$  denotes the space of linear maps over  $V^{\otimes n}$ . In particular, we will denote the sub-space of  $\text{Lin}(V^{\otimes n})$  that is spanned by the primitive invariants of  $SU(N)$  by  $\text{API}(SU(N), V^{\otimes n})$ .

Following [72], we denote a symmetrizer over an index-set  $\mathcal{N}$ ,  $\mathcal{S}_{\mathcal{N}}$ , by an empty (white) box over the index lines in  $\mathcal{N}$ . Thus, the symmetrizer  $\mathcal{S}_{12}$  is denoted by  $\begin{array}{c} \leftarrow \quad \leftarrow \\ \leftarrow \quad \leftarrow \end{array} \begin{array}{|c|c|} \hline \\ \hline \end{array}$ . Similarly, an antisymmetrizer over an index-set

<sup>7</sup>In some references, the presently described tableau may also be referred to as a *standard* Young tableau [95, 96].

<sup>8</sup>This is no longer strictly true for birdtracks representing primitive invariants of  $SU(N)$  over  $V^{\otimes m} \otimes (V^*)^{\otimes n}$ , which includes dual vector spaces. A more informative discussion on this is out of the scope of this paper; readers are referred to [72] [chapters 5 to 8 of this thesis].



$\mathcal{M}$ ,  $\mathbf{A}_{\mathcal{M}}$ , is denoted by a filled (black) box over the appropriate index lines. For example,

$$\mathbf{A}_{12} = \begin{array}{c} \leftarrow \blacksquare \rightarrow \\ \leftarrow \blacksquare \rightarrow \end{array} \text{ corresponds to the Young tableau } \begin{array}{|c|} \hline 1 \\ \hline 2 \\ \hline \end{array}, \quad (3.23)$$

since antisymmetrizers correspond to columns of Young tableaux [93]. For any Young tableau  $\Theta$ , one can form an idempotent, the so-called Young projection operator corresponding to  $\Theta$  [72, 84, 93, 95, 96]: Let  $\mathbf{S}_{\mathcal{R}_i}$  denote the symmetrizer corresponding to the  $i^{\text{th}}$  row of the tableau  $\Theta$ , and let  $\mathbf{S}_{\Theta}$  denote the set (or product, it does not matter since the symmetrizers  $\mathbf{S}_{\mathcal{R}_i}$  are disjoint by the definition of a Young tableau) of all symmetrizers  $\mathbf{S}_{\mathcal{R}_i}$ ,

$$\mathbf{S}_{\Theta} = \mathbf{S}_{\mathcal{R}_1} \cdots \mathbf{S}_{\mathcal{R}_k}. \quad (3.24)$$

Similarly, let

$$\mathbf{A}_{\Theta} = \mathbf{A}_{\mathcal{C}_1} \cdots \mathbf{A}_{\mathcal{C}_l} \quad (3.25)$$

where  $\mathbf{A}_{\mathcal{C}_j}$  corresponds to the  $j^{\text{th}}$  column of  $\Theta$ . Then, the object

$$Y_{\Theta} := \alpha_{\Theta} \cdot \mathbf{S}_{\Theta} \mathbf{A}_{\Theta} \quad (3.26)$$

is an idempotent, where  $\alpha_{\Theta}$  is a combinatorial factor involving the hook length of the tableau  $\Theta$  [95, 96].  $Y_{\Theta}$  is called the *Young projection operator* corresponding to  $\Theta$ . Besides being idempotent<sup>9</sup>

$$Y_{\Theta} \cdot Y_{\Theta} = Y_{\Theta}, \quad (3.27a)$$

Young projection operators on  $V^{\otimes n}$  are also mutually transversal if  $n < 5$ : If  $\Theta$  and  $\Phi$  are two Young tableaux consisting of the same number of boxes, then

$$Y_{\Theta} \cdot Y_{\Phi} = \delta_{\Theta\Phi} Y_{\Theta} \quad \text{for } n = 1, 2, 3, 4, \quad (3.27b)$$

and for general  $n$  provided the shapes of the associated tableaux are different.

Furthermore, again for  $m < 5$ , Young projection operators satisfy a completeness relation, that is, the Young projection operators corresponding to the tableaux in  $\mathcal{Y}_n$  sum up to the identity operator on the space  $V^{\otimes n}$ ,

$$\sum_{\Theta \in \mathcal{Y}_n} Y_{\Theta} = \mathbb{1}_n \quad n = 1, 2, 3, 4. \quad (3.27c)$$

Both properties (3.27b) and (3.27c) can be restored for  $m \geq 5$  by suitable subtractions without compromising (3.27a) in the process (see [85, sec. 5.4] or in [106, sec. II.3.6]), *c.f.* eqns. (3.6) and appendix 3.A. These three properties allow the (corrected) Young projection operators associated to the Young tableaux in  $\mathcal{Y}_n$  to fully classify the irreducible representations of  $\text{SU}(N)$  over  $V^{\otimes n}$  [72, 93, 98, 105]. The Hermitian replacements for these operators given in [4, 82, 102] share all three properties without restrictions on  $n$  and are formulated in terms of  $Y_{\Theta}$  entirely, relying on the unrestricted nature of (3.27a). This remains to be the

<sup>9</sup>This property is surprisingly hard to prove without the simplification rules paraphrased in section 3.2.3 [1] [chapter 2].

case for the improved algorithms presented here.

It should be noted that, since all symmetrizers in  $\mathbf{S}_\Theta$  (resp. antisymmetrizers in  $\mathbf{A}_\Theta$ ) are disjoint, each index line enters *at most* one symmetrizer (resp. antisymmetrizer) in birdtrack notation. Thus, one may draw all symmetrizers (resp. antisymmetrizers) underneath each other.

As an example, we construct the birdtrack Young projection operator corresponding to the following Young tableau,

$$\Theta = \begin{array}{|c|c|c|} \hline 1 & 3 & 4 \\ \hline 2 & 5 & \\ \hline \end{array}. \quad (3.28)$$

$Y_\Theta$  is given by

$$Y_\Theta = 2 \cdot \mathbf{S}_{134} \mathbf{S}_{25} \mathbf{A}_{12} \mathbf{A}_{35}, \quad (3.29)$$

where the constant 2 is the combinatorial factor that ensures the idempotency of  $Y_\Theta$ . In birdtrack notation, the Young projection operator  $Y_\Theta$  becomes

$$Y_\Theta = 2 \cdot \begin{array}{c} \text{[Diagram: Birdtrack representation of } Y_\Theta \text{ with 5 lines and 4 operators]} \end{array}, \quad (3.30)$$

where we were able to draw the two symmetrizers in  $\mathbf{S}_\Theta$  and the antisymmetrizers in  $\mathbf{A}_\Theta$  underneath each other, as claimed.

### 3.2.2 Notation & conventions

In the literature, there is a great multitude of (sometimes conflicting) conventions and notations regarding birdtracks, Young symmetrizers and other quantities used in this paper. We will devote this section to laying down the conventions that will be used here.

#### 3.2.2.1 Structural relationships between Young tableaux of different sizes

Throughout this paper,  $Y_\Theta$  shall denote the normalized Young projection operator corresponding to a Young tableau  $\Theta$ , and  $P_\Theta$  will refer to the normalized Hermitian Young projection operator corresponding to  $\Theta$ . Furthermore, for any operator  $O$  consisting of symmetrizers and antisymmetrizers, the symbol  $\bar{O}$  will refer to the equivalence class of operators that are proportional to the product of symmetrizers and antisymmetrizers of  $O$  without any *additional* scalar factors. For example,

$$Y_\Theta := \underbrace{\frac{4}{3}}_{=:\alpha_\Theta} \underbrace{\text{[Diagram: Birdtrack part of } Y_\Theta \text{]}}_{=:\bar{Y}_\Theta}. \quad (3.31)$$

Thus, for a birdtrack operator  $O$ , comprised solely of symmetrizers and antisymmetrizers,  $\bar{O}$  denotes the *graphical* part alone,

$$O := \omega \bar{O}, \quad (3.32)$$

where  $\omega$  is some scalar. The benefit of this notation is that the barred operator stays unchanged under multiplication with a nonzero scalar  $\lambda$ ,

$$\lambda \cdot \bar{O} = \bar{O} \quad \text{but in general} \quad \lambda \cdot O \neq O. \quad (3.33)$$

It should be noted that  $\bar{Y}_\Theta$  and  $\bar{P}_\Theta$  are only quasi-idempotent, while  $Y_\Theta$  and  $P_\Theta$  are idempotent. We will denote the normalization constants of  $Y_\Theta$  and  $P_\Theta$  by  $\alpha_\Theta$  and  $\beta_\Theta$  respectively, such that

$$Y_\Theta := \alpha_\Theta \bar{Y}_\Theta \quad \text{and} \quad P_\Theta := \beta_\Theta \bar{P}_\Theta; \quad (3.34)$$

where  $\alpha_\Theta$  can be obtained from the hook length formula [72, 95, 96] and the normalization constant  $\beta_\Theta$  is given together with the appropriate construction principle for  $P_\Theta$  (we encounter three different versions, one each for the original KS construction in Theorem 3.3, the simplified KS construction in Corollary 3.1, and the MOLD version in Theorem 3.5).

It is a well-known fact that Young tableaux in  $\mathcal{Y}_n$  can be built from Young tableaux in  $\mathcal{Y}_{n-1}$  by adding the box  $\boxed{n}$  at an appropriate place as to not destroy the properties of Young tableaux; such places are referred to as *outer corners* [96]. In this way, the Young tableau  $\Theta = \begin{array}{|c|c|c|} \hline 1 & 2 & 3 \\ \hline 4 & & \\ \hline \end{array}$  generates the subset  $\{\Theta \otimes \boxed{5}\}$  of  $\mathcal{Y}_5$ ,

$$\begin{array}{c} \Theta = \begin{array}{|c|c|c|} \hline 1 & 2 & 3 \\ \hline 4 & & \\ \hline \end{array} \in \mathcal{Y}_4 \\ \swarrow \quad \downarrow \quad \searrow \\ \begin{array}{|c|c|c|} \hline 1 & 2 & 3 \\ \hline 4 & & \\ \hline 5 & & \\ \hline \end{array} \quad \begin{array}{|c|c|c|} \hline 1 & 2 & 3 \\ \hline 4 & 5 & \\ \hline \end{array} \quad \begin{array}{|c|c|c|c|} \hline 1 & 2 & 3 & 5 \\ \hline 4 & & & \\ \hline \end{array} \in \{\Theta \otimes \boxed{5}\} \subset \mathcal{Y}_5 \end{array} \quad (3.35)$$

This operation is not a map from  $\mathcal{Y}_n$  to  $\mathcal{Y}_{n+1}$  in the mathematical sense as it does not yield a unique result; instead, we obtain a map from  $\mathcal{Y}_n$  to the power set (the set of all subsets) of  $\mathcal{Y}_{n+1}$ ,  $\mathcal{P}(\mathcal{Y}_{n+1})$ . The reverse operation, taking away the box with the highest entry, *is* a map from  $\mathcal{Y}_{n+1}$  to  $\mathcal{Y}_n$ : Let us denote this map by  $\pi$ .  $\pi$  can then repeatedly be applied to the resulting tableau,

$$\begin{array}{|c|c|c|} \hline 1 & 3 & 6 \\ \hline 2 & 5 & \\ \hline 4 & & \\ \hline \end{array} \xrightarrow{\pi} \begin{array}{|c|c|} \hline 1 & 3 \\ \hline 2 & 5 \\ \hline 4 & \\ \hline \end{array} \xrightarrow{\pi} \begin{array}{|c|c|} \hline 1 & 3 \\ \hline 2 & \\ \hline 4 & \\ \hline \end{array} \xrightarrow{\pi} \begin{array}{|c|c|} \hline 1 & 3 \\ \hline 2 & \\ \hline \end{array}. \quad (3.36)$$

### ■ Definition 3.1 – parent map and ancestor tableaux:

Let  $\Theta \in \mathcal{Y}_n$  be a Young tableau. We define its parent tableau  $\Theta_{(1)} \in \mathcal{Y}_{n-1}$  to be the tableau obtained from  $\Theta$  by removing the box  $\boxed{n}$  of  $\Theta$ .<sup>10</sup> Furthermore, we will define a parent map  $\pi$  from  $\mathcal{Y}_n$  to  $\mathcal{Y}_{n-1}$ , for a particular  $n$ ,

$$\pi : \mathcal{Y}_n \rightarrow \mathcal{Y}_{n-1}, \quad (3.37a)$$

<sup>10</sup>We note that the tableau  $\Theta_{(1)}$  is always a Young tableau if  $\Theta$  was a Young tableau, since removing the box with the highest entry cannot possibly destroy the properties of  $\Theta$  (and thus  $\Theta_{(1)}$ ) that make it a Young tableau.

which acts on  $\Theta$  by removing the box  $\boxed{n}$  from  $\Theta$ ,

$$\pi : \Theta \mapsto \Theta_{(1)}. \quad (3.37b)$$

In general, we define the successive action of the parent map  $\pi$  by

$$\mathcal{Y}_n \xrightarrow{\pi} \mathcal{Y}_{n-1} \xrightarrow{\pi} \mathcal{Y}_{n-2} \xrightarrow{\pi} \dots \xrightarrow{\pi} \mathcal{Y}_{n-m}, \quad (3.38a)$$

and denote it by  $\pi^m$ ,

$$\pi^m : \mathcal{Y}_n \rightarrow \mathcal{Y}_{n-m}, \quad \pi^m := \mathcal{Y}_n \xrightarrow{\pi} \mathcal{Y}_{n-1} \xrightarrow{\pi} \mathcal{Y}_{n-2} \xrightarrow{\pi} \dots \xrightarrow{\pi} \mathcal{Y}_{n-m}. \quad (3.38b)$$

We will further denote the unique tableau obtained from  $\Theta$  by applying the map  $\pi$   $m$  times,  $\pi^m(\Theta)$ , by  $\Theta_{(m)}$ , and refer to it as the ancestor tableau of  $\Theta$   $m$  generations back,

$$\pi^m : \Theta \mapsto \Theta_{(m)}. \quad (3.38c)$$

### 3.2.2.2 Embeddings and images of linear operators

Any operator  $O \in \text{Lin}(V^{\otimes n})$  can be embedded into  $\text{Lin}(V^{\otimes m})$  for  $m > n$  in several ways, simply by letting the embedding act as the identity on  $(m - n)$  of the factors; how to select these factors is a matter of what one plans to achieve. The most useful convention for our purposes is to let  $O$  act on the first  $n$  factors and operate with the identity on the last  $(m - n)$  factors. We will call this the *canonical embedding*. On the level of birdtracks, this amounts to letting the index lines of  $O$  coincide with the top  $n$  index lines of  $\text{Lin}(V^{\otimes m})$ , and the bottom  $(m - n)$  lines of the embedded operator constitute the identity birdtrack of size  $(m - n)$ . For example, the operator  $\bar{Y}_{\begin{smallmatrix} \boxed{1} \boxed{2} \\ \boxed{3} \end{smallmatrix}}$  is canonically embedded into  $\text{Lin}(V^{\otimes 5})$  as



$$(3.39)$$

Furthermore, we will use the same symbol  $O$  for the operator as well as for its embedded counterpart. Thus,  $\bar{Y}_{\begin{smallmatrix} \boxed{1} \boxed{2} \\ \boxed{3} \end{smallmatrix}}$  shall denote both the operator on the left as well as on the right hand side of the embedding (3.39).

Lastly, if a *Hermitian* projection operator  $A$  projects onto a subspace completely contained in the image of a Hermitian projection operator  $B$ , then we denote this as  $A \subset B$ , transferring the familiar notation of sets to the associated projection operators. In particular,  $A \subset B$  if and only if

$$A \cdot B = B \cdot A = A \quad (3.40)$$

for the following reason: If the subspaces obtained by the consecutive application of the operators  $A$  and  $B$  in any order is the same as that obtained by merely applying  $A$ , then not only need the subspaces onto which  $A$  and  $B$  project overlap (as otherwise  $A \cdot B = B \cdot A = 0$ ), but the subspace corresponding to  $A$  must be completely contained in the subspace of  $B$  — otherwise the last equality of (3.40) would not hold. Hermiticity is crucial for these statements — they thus do not apply to most Young projection operators on  $V^{\otimes m}$  if  $m \geq 3$ . A familiar example for this situation is the relation between symmetrizers of different length:

a symmetrizer  $\mathbf{S}_{\mathcal{N}}$  can be absorbed into a symmetrizer  $\mathbf{S}_{\mathcal{N}'}$ , as long as the index set  $\mathcal{N}$  is a subset of  $\mathcal{N}'$ , and the same statement holds for antisymmetrizer, [72]. For example,

$$\begin{array}{c} \leftarrow \leftarrow \leftarrow \\ \leftarrow \leftarrow \leftarrow \\ \leftarrow \leftarrow \leftarrow \\ \leftarrow \leftarrow \leftarrow \\ \leftarrow \leftarrow \leftarrow \\ \leftarrow \leftarrow \leftarrow \end{array} \begin{array}{c} \leftarrow \leftarrow \leftarrow \\ \leftarrow \leftarrow \leftarrow \\ \leftarrow \leftarrow \leftarrow \\ \leftarrow \leftarrow \leftarrow \\ \leftarrow \leftarrow \leftarrow \\ \leftarrow \leftarrow \leftarrow \end{array} = \begin{array}{c} \leftarrow \leftarrow \leftarrow \\ \leftarrow \leftarrow \leftarrow \\ \leftarrow \leftarrow \leftarrow \\ \leftarrow \leftarrow \leftarrow \\ \leftarrow \leftarrow \leftarrow \\ \leftarrow \leftarrow \leftarrow \end{array} = \begin{array}{c} \leftarrow \leftarrow \leftarrow \\ \leftarrow \leftarrow \leftarrow \\ \leftarrow \leftarrow \leftarrow \\ \leftarrow \leftarrow \leftarrow \\ \leftarrow \leftarrow \leftarrow \\ \leftarrow \leftarrow \leftarrow \end{array} . \quad (3.41)$$

Thus, by the above notation,  $\mathbf{S}_{\mathcal{N}'} \subset \mathbf{S}_{\mathcal{N}}$ , if  $\mathcal{N} \subset \mathcal{N}'$ . Or, as in our example,

$$\begin{array}{c} \leftarrow \leftarrow \leftarrow \\ \leftarrow \leftarrow \leftarrow \\ \leftarrow \leftarrow \leftarrow \\ \leftarrow \leftarrow \leftarrow \\ \leftarrow \leftarrow \leftarrow \\ \leftarrow \leftarrow \leftarrow \end{array} \subset \begin{array}{c} \leftarrow \leftarrow \leftarrow \\ \leftarrow \leftarrow \leftarrow \\ \leftarrow \leftarrow \leftarrow \\ \leftarrow \leftarrow \leftarrow \\ \leftarrow \leftarrow \leftarrow \\ \leftarrow \leftarrow \leftarrow \end{array} . \quad (3.42)$$

In particular, it follows immediately from the definition of the ancestor tableau (Definition 3.1, eq. (3.38c)) that

$$\mathbf{S}_{\Theta_{(k)}} \mathbf{S}_{\Theta} = \mathbf{S}_{\Theta} = \mathbf{S}_{\Theta} \mathbf{S}_{\Theta_{(k)}} \quad \text{and} \quad \mathbf{A}_{\Theta_{(k)}} \mathbf{A}_{\Theta} = \mathbf{A}_{\Theta} = \mathbf{A}_{\Theta} \mathbf{A}_{\Theta_{(k)}} \quad (3.43)$$

for every ancestor tableau  $\Theta_{(k)}$  of  $\Theta$ .

### 3.2.3 Cancellation rules

We suspect that one of the reasons why the birdtrack formalism has not yet gained as much popularity as it ought is because there exist virtually no practical rules which allow easy manipulation of birdtrack operators in the literature. In [1] [chapter 2], we establish various rules designed to easily manipulate birdtrack operators comprised of symmetrizers and anti-symmetrizers. Since all operators considered in this paper are of this form, the simplification rules of [1] [chapter 2] are immediately applicable: None of the proofs of the construction algorithms in this paper would have been possible without these rules. Thus, we choose to summarize the most important results of [1] [chapter 2] here. For the proofs of these rules, readers are referred to [1] [chapter 2].

The simplification rules of [1] [chapter 2] fall into two classes:

1. *Cancellation rules* (Theorems 3.1 and 3.2, section 3.2.3): these rules are to cancel large chunks of birdtrack operators, thus making them shorter (often significantly so) and more practical to use. The cancellation rules are used in several places in this paper, in particular in the proof of the shortened KS operators (Corollary 3.1) and the proof of the construction of MOLD operators (Theorem 3.5). Since the cancellation rules are used multiple times throughout this paper, we recapitulate these rules in this present section.
2. *Propagation rules* (Theorem 3.6, section 3.C.1.1): these rules allow one to commute (sets of) symmetrizers through (sets of) antisymmetrizers and vice versa. The propagation rules come in handy when trying to expose the implicit Hermiticity of a birdtrack operator. In this paper, we use these rules in the proof of Theorem 3.4, which is why we defer the re-statement of the propagation rules to appendix 3.C.1 where also the proof of Theorem 3.4 can be found.

#### ■ Theorem 3.1 – cancellation of wedged ancestor-operators:

Consider two Young tableaux  $\Theta$  and  $\Phi$  such that they have a common ancestor tableau  $\Gamma$ . Let  $Y_{\Theta}$ ,  $Y_{\Phi}$  and  $Y_{\Gamma}$  be their respective Young projection operators, all embedded in an algebra that is able to contain all three.

Then

$$Y_{\Theta} Y_{\Gamma} Y_{\Phi} = Y_{\Theta} Y_{\Phi}. \quad (3.44)$$

For example, consider the Young tableaux

$$\Theta = \begin{array}{|c|c|c|} \hline 1 & 2 & 5 \\ \hline 3 & 4 & \\ \hline \end{array} \quad \text{and} \quad \Phi = \begin{array}{|c|c|c|} \hline 1 & 2 & 4 \\ \hline 3 & & \\ \hline \end{array}, \quad (3.45)$$

which have the common ancestor

$$\Gamma = \begin{array}{|c|c|} \hline 1 & 2 \\ \hline 3 & \\ \hline \end{array}. \quad (3.46)$$

Then, the product  $Y_{\Theta} Y_{\Gamma} Y_{\Phi}$  is given by

$$Y_{\Theta} Y_{\Gamma} Y_{\Phi} = 4 \cdot \underbrace{\text{diagram}}_{Y_{\Theta}} \underbrace{\text{diagram}}_{Y_{\Gamma}} \underbrace{\text{diagram}}_{Y_{\Phi}}, \quad (3.47)$$

where  $\alpha_{\Theta} \alpha_{\Gamma} \alpha_{\Phi} = 4$ . According to Theorem 3.1, we are allowed to cancel the operator  $Y_{\Gamma}$  hence reducing the above product to

$$Y_{\Theta} Y_{\Gamma} Y_{\Phi} = 4 \cdot \underbrace{\text{diagram}}_{Y_{\Theta}} \underbrace{\text{diagram}}_{Y_{\Phi}} = 3 \cdot \underbrace{\text{diagram}}_{Y_{\Theta}} \underbrace{\text{diagram}}_{Y_{\Phi}}, \quad (3.48)$$

where  $\alpha_{\Theta} \alpha_{\Phi} = 3$ .

A more general cancellation-Theorem is:

**■ Theorem 3.2 – cancellation of parts of the operator:**

Let  $\Theta \in \mathcal{Y}_n$  be a Young tableau and  $M$  be an element of  $\text{API}(\text{SU}(N), V^{\otimes n})$ . Then, there exists a (possibly vanishing) constant  $\lambda$  such that

$$O := \mathbf{S}_{\Theta} M \mathbf{A}_{\Theta} = \lambda \cdot Y_{\Theta}. \quad (3.49)$$

If furthermore the operator  $O$  is nonzero, then  $\lambda \neq 0$ . One instance in which  $O$  is guaranteed to be nonzero is if  $M$  is of the form

$$M = \mathbf{A}_{\Phi_1} \mathbf{S}_{\Phi_2} \mathbf{A}_{\Phi_3} \mathbf{S}_{\Phi_4} \cdots \mathbf{A}_{\Phi_{k-1}} \mathbf{S}_{\Phi_k}, \quad (3.50)$$

where  $\mathbf{A}_{\Phi_i} \supset \mathbf{A}_{\Theta}$  for every  $i \in \{1, 3, \dots, k-1\}$  and  $\mathbf{S}_{\Phi_j} \supset \mathbf{S}_{\Theta}$  and for every  $j \in \{2, 4, \dots, k\}$ .

As an example, consider the operator

$$O := \text{diagram} = \{\mathbf{S}_{125}, \mathbf{S}_{34}\} \cdot \{\mathbf{A}_{13}\} \cdot \{\mathbf{S}_{12}, \mathbf{S}_{34}\} \cdot \{\mathbf{A}_{13}, \mathbf{A}_{24}\}. \quad (3.51)$$

This operator meets all conditions of the above Theorem 3.2: The sets  $\{\mathbf{S}_{125}, \mathbf{S}_{34}\}$  and  $\{\mathbf{A}_{13}, \mathbf{A}_{24}\}$  together

constitute the birdtrack of a Young projection operator  $\tilde{Y}_\Theta$  corresponding to the tableau

$$\Theta := \begin{array}{|c|c|c|} \hline 1 & 2 & 5 \\ \hline 3 & 4 & \\ \hline \end{array}. \quad (3.52)$$

The set  $\{\mathbf{A}_{13}\}$  corresponds to the ancestor tableau  $\Theta_{(2)}$ , and the set  $\{\mathbf{S}_{12}, \mathbf{S}_{34}\}$  corresponds to the ancestor tableau  $\Theta_{(1)}$  and can thus be absorbed into  $\mathbf{A}_\Theta$  and  $\mathbf{S}_\Theta$  respectively, *c.f.* eq. (3.43). Hence  $O$  can be written as

$$O = \mathbf{S}_\Theta \mathbf{A}_{\Theta_{(2)}} \mathbf{S}_{\Theta_{(1)}} \mathbf{A}_\Theta. \quad (3.53)$$

Then, according to the above Cancellation Theorem 3.2, we may cancel the wedged ancestor sets  $\mathbf{A}_{\Theta_{(2)}}$  and  $\mathbf{S}_{\Theta_{(1)}}$  at the cost of a nonzero constant  $\tilde{\lambda}$ . In particular, we find that

$$O = \tilde{\lambda} \cdot \underbrace{\text{birdtrack diagram}}_{\tilde{Y}_\Theta}, \quad (3.54)$$

which is proportional to  $\tilde{Y}_\Theta$ .

### 3.3 Hermitian Young projection operators

Throughout this paper, we will be working with linear maps over linear spaces, in particular with maps in  $\text{API}(\text{SU}(N), V^{\otimes m}) \subset \text{Lin}(V^{\otimes m})$ . All the familiar tools from linear algebra (as can be found in [107] and other standard textbooks) apply but will likely *look* unfamiliar when employed in the language of birdtracks. We thus devote this section to translate the most important tools for this paper into the birdtrack formalism.

#### 3.3.1 Hermitian conjugation of linear maps in birdtrack notation

We begin by recalling the definition of Hermitian conjugation for linear maps. Let  $U$  and  $W$  be linear spaces, and let  $\langle \cdot, \cdot \rangle_U : U \times U \rightarrow \mathbb{F}$ , where  $\mathbb{F}$  is a field usually taken to be  $\mathbb{C}$  or  $\mathbb{R}$ , denote the scalar product defined on  $U$ , and similarly for  $W$ . Furthermore, let  $P : U \rightarrow W$  be an operator. The scalar products then furnish a definition of the Hermitian conjugate of  $P$  (denoted by  $P^\dagger : W \rightarrow U$ ) in the standard way:

$$\langle w, Pu \rangle_W \stackrel{!}{=} \langle P^\dagger w, u \rangle_U \quad (3.55)$$

for any  $u \in U$  and  $w \in W$  [107]. In our case,  $u$  and  $w$  will be elements of  $V^{\otimes m}$ , both  $u$  and  $w$  appear as tensors with  $m$  upper indices,<sup>11</sup>

$$u^{j_1 \dots j_m} \quad \text{and} \quad w^{i_1 \dots i_m}, \quad (3.56)$$

<sup>11</sup>At this point we recall that the basis vectors  $\mathbf{e}$  of  $V^{\otimes m}$  are denoted with lower indices; therefore  $u$  and  $w$  act on the  $\mathbf{e}$ 's as linear maps.

and  $P : V^{\otimes m} \rightarrow V^{\otimes m}$ . Eq. (3.55) is equivalent to requiring the following diagram to commute,

$$\begin{array}{ccc}
 V^{\otimes m} \otimes V^{\otimes m} & \xrightarrow{\mathbb{1}_m \otimes P} & V^{\otimes m} \otimes V^{\otimes m} \\
 P^\dagger \otimes \mathbb{1}_m \downarrow & & \downarrow \langle \cdot, \cdot \rangle \\
 V^{\otimes m} \otimes V^{\otimes m} & \xrightarrow{\langle \cdot, \cdot \rangle} & \mathbb{C}
 \end{array} . \quad (3.57)$$

The scalar product between these maps is then defined in the usual way,  $\langle u, w \rangle = u^\dagger w \in \mathbb{C}$ . The map  $u^\dagger$  is an element of the dual space  $(V^*)^{\otimes m}$  and thus needs to be equipped with *lower* indices<sup>12</sup> (note that the index convention used here differs from that in [72]),

$$u^\dagger = (u^{j_1 \dots j_m})^* =: u_{j_1 \dots j_m}. \quad (3.58)$$

Complex conjugation  $*$  is necessary, since the vector space  $V$  may be complex. Hence, we have that

$$\langle u, w \rangle = u^\dagger w = u_{i_1 \dots i_m} w^{i_1 \dots i_m} \in \mathbb{C}. \quad (3.59)$$

In the above, all indices of  $u^\dagger$  and  $w$  were contracted so that the outcome of the scalar product lies in a field, in our case  $\mathbb{C}$ . Graphically, let us represent a tensor with  $j$  lower indices and  $i$  upper indices by a box which has  $j$  legs entering on the right and  $i$  legs exiting on the left,

$$T^{a_1 a_2 \dots a_i}_{b_1 b_2 \dots b_j} \rightarrow \begin{array}{c} \begin{array}{c} \leftarrow a_1 \\ \leftarrow a_2 \\ \vdots \\ \leftarrow a_{i-1} \\ \leftarrow a_i \end{array} \left[ \begin{array}{c} T \\ \vdots \end{array} \right] \begin{array}{c} \rightarrow b_1 \\ \rightarrow b_2 \\ \vdots \\ \rightarrow b_{j-1} \\ \rightarrow b_j \end{array} \end{array} . \quad (3.60)$$

Therefore, the tensors  $u_{i_1 \dots i_m}$  and  $w^{i_1 \dots i_m}$  will have  $m$  legs exiting on the right and left respectively,

$$u_{i_1 \dots i_m} \rightarrow \begin{array}{c} \leftarrow i_1 \\ \leftarrow i_2 \\ \vdots \\ \leftarrow i_{m-1} \\ \leftarrow i_m \end{array} \left[ \begin{array}{c} u \\ \vdots \end{array} \right] \quad \text{and} \quad w^{i_1 \dots i_m} \rightarrow \begin{array}{c} \rightarrow i_1 \\ \rightarrow i_2 \\ \vdots \\ \rightarrow i_{m-1} \\ \rightarrow i_m \end{array} \left[ \begin{array}{c} w \\ \vdots \end{array} \right] ; \quad (3.61)$$

from now on, we will suppress the index labels of the birdtracks corresponding to the tensors in question. The scalar product  $\langle u, w \rangle$  is diagrammatically represented as

$$\langle u, w \rangle = \begin{array}{c} \leftarrow \leftarrow \leftarrow \leftarrow \\ \left[ \begin{array}{c} u \\ \vdots \\ w \end{array} \right] \\ \rightarrow \rightarrow \rightarrow \rightarrow \end{array} , \quad (3.62)$$

where the contraction of indices is indicated via the connection of corresponding index lines in the birdtrack. In (3.62), we see that the birdtrack corresponding to  $\langle u, w \rangle$  does not have any index lines exiting on either the right or the left, indicating that it is indeed a scalar. We will now consider a scalar product  $\langle u, Pw \rangle$ , where  $P : \text{Lin}(V^{\otimes m}) \rightarrow \text{Lin}(V^{\otimes m})$  is an operator, to find its Hermitian dual  $P^\dagger$ .  $P$  must have  $m$  lower and  $m$  upper indices,

$$P^{i_1 \dots i_m}_{j_1 \dots j_m} \rightarrow \begin{array}{c} \leftarrow i_1 \\ \leftarrow i_2 \\ \vdots \\ \leftarrow i_{m-1} \\ \leftarrow i_m \end{array} \left[ \begin{array}{c} P \\ \vdots \end{array} \right] \begin{array}{c} \rightarrow j_1 \\ \rightarrow j_2 \\ \vdots \\ \rightarrow j_{m-1} \\ \rightarrow j_m \end{array} , \quad (3.63)$$

<sup>12</sup>Since basis vectors  $\omega$  of  $(V^*)^{\otimes m}$  have upper indices.



where the  $j$ -indices act on an element of  $\text{Lin}(V^{\otimes m})$  via index contraction. The scalar product  $\langle u, Pw \rangle$  will then be given by

$$\langle u, Pw \rangle = (u^{i_1 \dots i_m})^* P^{i_1 \dots i_m}_{j_1 \dots j_m} w^{j_1 \dots j_m} \rightarrow \begin{array}{c} \leftarrow i_1 \\ \leftarrow i_2 \\ \vdots \\ \leftarrow i_{m-1} \\ \leftarrow i_m \end{array} \left[ \begin{array}{c} \leftarrow j_1 \\ \leftarrow j_2 \\ \vdots \\ \leftarrow j_{m-1} \\ \leftarrow j_m \end{array} \right] P \begin{array}{c} \leftarrow j_1 \\ \leftarrow j_2 \\ \vdots \\ \leftarrow j_{m-1} \\ \leftarrow j_m \end{array} \rightarrow w \end{array} = \begin{array}{c} \leftarrow i_1 \\ \leftarrow i_2 \\ \vdots \\ \leftarrow i_{m-1} \\ \leftarrow i_m \end{array} \left[ \begin{array}{c} \leftarrow j_1 \\ \leftarrow j_2 \\ \vdots \\ \leftarrow j_{m-1} \\ \leftarrow j_m \end{array} \right] P \begin{array}{c} \leftarrow j_1 \\ \leftarrow j_2 \\ \vdots \\ \leftarrow j_{m-1} \\ \leftarrow j_m \end{array} \rightarrow w \end{array} . \quad (3.64)$$

The adjoint  $P^\dagger$  of  $P$  is defined to be the object such that relation (3.55) holds. Thus,  $P^\dagger$  acts on the dual space,  $P^\dagger : \text{Lin}((V^*)^{\otimes m}) \rightarrow \text{Lin}((V^*)^{\otimes m})$ , which again means that it has  $m$  upper and  $m$  lower indices, but now the  $j$ -indices act on the element of  $\text{Lin}((V^*)^{\otimes m})$ ,

$$P^\dagger = (P^{i_1 \dots i_m}_{j_1 \dots j_m})^* = P_{i_1 \dots i_m}^{j_1 \dots j_m} . \quad (3.65)$$

It should be noted that once again, the raising and lowering of indices induces a complex conjugation of the tensor components, as we have already seen for  $u$  in (3.58).<sup>13</sup> The same caveat applies to the associated birdtrack diagrams in which we have to mirror the operator about its vertical axis and reverse the direction of the arrows:

$$\left( \begin{array}{c} \leftarrow i_1 \\ \leftarrow i_2 \\ \vdots \\ \leftarrow i_{m-1} \\ \leftarrow i_m \end{array} \left[ \begin{array}{c} \leftarrow j_1 \\ \leftarrow j_2 \\ \vdots \\ \leftarrow j_{m-1} \\ \leftarrow j_m \end{array} \right] P \begin{array}{c} \leftarrow j_1 \\ \leftarrow j_2 \\ \vdots \\ \leftarrow j_{m-1} \\ \leftarrow j_m \end{array} \right)^\dagger = \begin{array}{c} \leftarrow j_1 \\ \leftarrow j_2 \\ \vdots \\ \leftarrow j_{m-1} \\ \leftarrow j_m \end{array} \left[ \begin{array}{c} \leftarrow i_1 \\ \leftarrow i_2 \\ \vdots \\ \leftarrow i_{m-1} \\ \leftarrow i_m \end{array} \right] P \begin{array}{c} \leftarrow i_1 \\ \leftarrow i_2 \\ \vdots \\ \leftarrow i_{m-1} \\ \leftarrow i_m \end{array} . \quad (3.66)$$

This results in all contracted index lines lining up correctly. For example,

$$\begin{aligned} Y_{\begin{array}{|c|} \hline \boxed{12} \\ \hline \boxed{3} \end{array}} &= \frac{4}{3} \cdot \begin{array}{c} \leftarrow \leftarrow \leftarrow \\ \leftarrow \leftarrow \leftarrow \\ \leftarrow \leftarrow \leftarrow \\ \leftarrow \leftarrow \leftarrow \end{array} \Rightarrow Y_{\begin{array}{|c|} \hline \boxed{12} \\ \hline \boxed{3} \end{array}}^\dagger = \frac{4}{3} \cdot \begin{array}{c} \leftarrow \leftarrow \leftarrow \\ \leftarrow \leftarrow \leftarrow \\ \leftarrow \leftarrow \leftarrow \\ \leftarrow \leftarrow \leftarrow \end{array} \\ &= \frac{1}{3} \left( \begin{array}{c} \leftarrow \leftarrow \leftarrow \\ \leftarrow \leftarrow \leftarrow \\ \leftarrow \leftarrow \leftarrow \\ \leftarrow \leftarrow \leftarrow \end{array} + \begin{array}{c} \leftarrow \leftarrow \leftarrow \\ \leftarrow \leftarrow \leftarrow \\ \leftarrow \leftarrow \leftarrow \\ \leftarrow \leftarrow \leftarrow \end{array} - \begin{array}{c} \leftarrow \leftarrow \leftarrow \\ \leftarrow \leftarrow \leftarrow \\ \leftarrow \leftarrow \leftarrow \\ \leftarrow \leftarrow \leftarrow \end{array} - \begin{array}{c} \leftarrow \leftarrow \leftarrow \\ \leftarrow \leftarrow \leftarrow \\ \leftarrow \leftarrow \leftarrow \\ \leftarrow \leftarrow \leftarrow \end{array} \right) = \frac{1}{3} \left( \begin{array}{c} \leftarrow \leftarrow \leftarrow \\ \leftarrow \leftarrow \leftarrow \\ \leftarrow \leftarrow \leftarrow \\ \leftarrow \leftarrow \leftarrow \end{array} + \begin{array}{c} \leftarrow \leftarrow \leftarrow \\ \leftarrow \leftarrow \leftarrow \\ \leftarrow \leftarrow \leftarrow \\ \leftarrow \leftarrow \leftarrow \end{array} - \begin{array}{c} \leftarrow \leftarrow \leftarrow \\ \leftarrow \leftarrow \leftarrow \\ \leftarrow \leftarrow \leftarrow \\ \leftarrow \leftarrow \leftarrow \end{array} - \begin{array}{c} \leftarrow \leftarrow \leftarrow \\ \leftarrow \leftarrow \leftarrow \\ \leftarrow \leftarrow \leftarrow \\ \leftarrow \leftarrow \leftarrow \end{array} \right) . \end{aligned} \quad (3.67)$$

Therefore,

$$\langle P^\dagger u, w \rangle = (u^{j_1 \dots j_m})^* (P^{i_1 \dots i_m}_{j_1 \dots j_m})^* w^{i_1 \dots i_m} \rightarrow \begin{array}{c} \leftarrow j_1 \\ \leftarrow j_2 \\ \vdots \\ \leftarrow j_{m-1} \\ \leftarrow j_m \end{array} \left[ \begin{array}{c} \leftarrow i_1 \\ \leftarrow i_2 \\ \vdots \\ \leftarrow i_{m-1} \\ \leftarrow i_m \end{array} \right] P \begin{array}{c} \leftarrow i_1 \\ \leftarrow i_2 \\ \vdots \\ \leftarrow i_{m-1} \\ \leftarrow i_m \end{array} \rightarrow w \end{array} = \begin{array}{c} \leftarrow j_1 \\ \leftarrow j_2 \\ \vdots \\ \leftarrow j_{m-1} \\ \leftarrow j_m \end{array} \left[ \begin{array}{c} \leftarrow i_1 \\ \leftarrow i_2 \\ \vdots \\ \leftarrow i_{m-1} \\ \leftarrow i_m \end{array} \right] P \begin{array}{c} \leftarrow i_1 \\ \leftarrow i_2 \\ \vdots \\ \leftarrow i_{m-1} \\ \leftarrow i_m \end{array} \rightarrow w \end{array} ; \quad (3.68)$$

in direct correspondence with equation (3.64). For birdtrack operators, the Hermitian conjugate can thus be graphically formed by reflecting the birdtrack about its vertical axis and reversing the arrows, for example

$$\begin{array}{c} \leftarrow \leftarrow \leftarrow \\ \leftarrow \leftarrow \leftarrow \\ \leftarrow \leftarrow \leftarrow \end{array} \xrightarrow{\text{reflect}} \begin{array}{c} \leftarrow \leftarrow \leftarrow \\ \leftarrow \leftarrow \leftarrow \\ \leftarrow \leftarrow \leftarrow \end{array} \xrightarrow{\text{rev. arr.}} \begin{array}{c} \leftarrow \leftarrow \leftarrow \\ \leftarrow \leftarrow \leftarrow \\ \leftarrow \leftarrow \leftarrow \end{array} \quad \text{i.e.} \quad \left( \begin{array}{c} \leftarrow \leftarrow \leftarrow \\ \leftarrow \leftarrow \leftarrow \\ \leftarrow \leftarrow \leftarrow \end{array} \right)^\dagger = \begin{array}{c} \leftarrow \leftarrow \leftarrow \\ \leftarrow \leftarrow \leftarrow \\ \leftarrow \leftarrow \leftarrow \end{array} . \quad (3.69)$$

The mirroring of birdtracks under Hermitian conjugation immediately implies the unitarity of the primitive invariants (and thus that we are dealing with a unitary representation of  $S_m$  on  $V^{\otimes m}$ ): the inverse permutation of any primitive invariant  $\rho \in S_m$  is obtained by traversing the lines of the birdtrack corresponding to  $\rho$  in

<sup>13</sup>The projection operators considered in this paper are real and thus remain unaffected by complex conjugation. This is no longer true for group elements or representations.

the opposite direction [72], for example

$$\begin{array}{c} \leftarrow \\ \leftarrow \\ \leftarrow \\ \leftarrow \end{array} \cdot \begin{array}{c} \leftarrow \\ \leftarrow \\ \leftarrow \\ \leftarrow \end{array} = \begin{array}{c} \leftarrow \\ \leftarrow \\ \leftarrow \\ \leftarrow \end{array} \implies \begin{array}{c} \leftarrow \\ \leftarrow \\ \leftarrow \\ \leftarrow \end{array} = \left( \begin{array}{c} \leftarrow \\ \leftarrow \\ \leftarrow \\ \leftarrow \end{array} \right)^{-1}. \quad (3.70)$$

However, since “traversing the lines in the opposite direction” clearly corresponds to flipping the birdtrack about its vertical axis and reversing the direction of the arrows, we have that

$$\rho^{-1} = \rho^\dagger \quad \forall \rho \in S_m ; \quad (3.71)$$

the primitive invariants are unitary.

These obvious Hermiticity properties of the primitive invariants make it easy to judge Hermiticity of an operator once it is expanded in this basis set. This is no longer the case in other representations: While any mirror symmetric birdtrack represents a Hermitian operator, the converse is not true in all representations. Despite a lack of apparent mirror symmetry, the product birdtrack

$$\begin{array}{c} \leftarrow \\ \leftarrow \\ \leftarrow \\ \leftarrow \end{array} \begin{array}{c} \leftarrow \\ \leftarrow \\ \leftarrow \\ \leftarrow \end{array} \quad (3.72)$$

is Hermitian, as can be shown by either using the simplification rules of Theorem 3.6 (app. 3.C.1.1) which allow us to recast (3.72) in an explicitly mirror symmetric form, or by expanding it fully in terms of primitive invariants.

In this paper, we will always consider birdtrack operators with lines directed from right to left (as is indicated by the arrows on the legs). To reduce clutter, we will from now on suppress the arrows and (for example) simply write

$$\text{X} \quad \text{when we mean} \quad \begin{array}{c} \leftarrow \\ \leftarrow \\ \leftarrow \\ \leftarrow \end{array}. \quad (3.73)$$

### 3.3.2 Why equation (3.15) and its generalization cannot hold for Young projection operators

In this section, we will have a look at the summation property

$$\sum_{\Phi \in \{\Theta \otimes \square\}} Y_\Phi \stackrel{?}{=} Y_\Theta \quad \text{for } \Theta \in \mathcal{Y}_{n-1}, \quad (3.74)$$

and how it fails to apply to Young projection operators. We will examine two particular examples: We will assume that the summation property (3.74) holds for the standard (not necessarily Hermitian) Young projection operators over  $V^{\otimes 3}$  and  $V^{\otimes 4}$ , which will force us to conclude that the corresponding Young projectors are Hermitian in both cases — clearly a false statement. This motivates us to check whether the summation property (3.74) does hold for *Hermitian* Young projection operators, thus completing part 1 of Goal 1.

Let us begin with our first example: In section 3.1.2 equation (3.15), we claimed that

$$Y_{\begin{smallmatrix} \boxed{123} \\ \boxed{3} \end{smallmatrix}} + Y_{\begin{smallmatrix} \boxed{12} \\ \boxed{3} \end{smallmatrix}} \neq Y_{\begin{smallmatrix} \boxed{12} \end{smallmatrix}}, \quad (3.75)$$

where  $Y_{\Theta}$  is the Young projection operator corresponding to the tableau  $\Theta$ . We have now acquired the necessary tools to show why the two sides fail to match. Assuming equality in (3.75) and adopting birdtrack notation, this relation takes the form

$$\begin{array}{|c|} \hline \hline \hline \hline \\ \hline \end{array} + \frac{4}{3} \cdot \begin{array}{|c|} \hline \hline \hline \hline \\ \hline \end{array} \stackrel{?}{=} \begin{array}{|c|} \hline \hline \hline \\ \hline \end{array} \quad (3.76)$$

and would imply that

$$\frac{4}{3} \cdot \begin{array}{|c|} \hline \hline \hline \hline \\ \hline \end{array} \stackrel{?}{=} \begin{array}{|c|} \hline \hline \hline \\ \hline \end{array} - \begin{array}{|c|} \hline \hline \hline \\ \hline \end{array}. \quad (3.77)$$

From section 3.3.1, the right hand side of (3.77) is Hermitian, leading us to conclude that the left hand side is Hermitian as well. This is clearly not true (as is evident from the expansions in (3.67), specifically the last terms shown),

$$Y_{\begin{smallmatrix} \boxed{12} \\ \boxed{3} \end{smallmatrix}} \neq Y_{\begin{smallmatrix} \boxed{12} \\ \boxed{3} \end{smallmatrix}}^\dagger. \quad (3.78)$$

Thus we have arrived at a contradiction. In a similar way, it can be falsely concluded that  $Y_{\begin{smallmatrix} \boxed{13} \\ \boxed{2} \end{smallmatrix}}$  is Hermitian.

Let us now illustrate a slightly more advanced example involving an additional step which was not present in the example for  $n = 3$ . We will explicitly discuss the case  $n = 4$ . Let us assume that equation (3.74) holds for  $n = 3$ ,

$$Y_{\begin{smallmatrix} \boxed{123} \\ \boxed{3} \end{smallmatrix}} + Y_{\begin{smallmatrix} \boxed{12} \\ \boxed{3} \end{smallmatrix}} \stackrel{?}{=} Y_{\begin{smallmatrix} \boxed{12} \end{smallmatrix}} \quad \text{and} \quad Y_{\begin{smallmatrix} \boxed{1} \\ \boxed{2} \\ \boxed{3} \end{smallmatrix}} + Y_{\begin{smallmatrix} \boxed{13} \\ \boxed{2} \end{smallmatrix}} \stackrel{?}{=} Y_{\begin{smallmatrix} \boxed{1} \\ \boxed{2} \end{smallmatrix}} \quad (3.79)$$

and also for  $n = 4$ ,

$$Y_{\begin{smallmatrix} \boxed{123} \\ \boxed{3} \end{smallmatrix}} \stackrel{?}{=} Y_{\begin{smallmatrix} \boxed{1234} \\ \boxed{4} \end{smallmatrix}} + Y_{\begin{smallmatrix} \boxed{123} \\ \boxed{4} \end{smallmatrix}} \quad (3.80a)$$

$$Y_{\begin{smallmatrix} \boxed{12} \\ \boxed{3} \end{smallmatrix}} \stackrel{?}{=} Y_{\begin{smallmatrix} \boxed{124} \\ \boxed{3} \end{smallmatrix}} + Y_{\begin{smallmatrix} \boxed{12} \\ \boxed{34} \end{smallmatrix}} + Y_{\begin{smallmatrix} \boxed{12} \\ \boxed{3} \\ \boxed{4} \end{smallmatrix}} \quad (3.80b)$$

$$Y_{\begin{smallmatrix} \boxed{13} \\ \boxed{2} \end{smallmatrix}} \stackrel{?}{=} Y_{\begin{smallmatrix} \boxed{134} \\ \boxed{2} \end{smallmatrix}} + Y_{\begin{smallmatrix} \boxed{13} \\ \boxed{24} \end{smallmatrix}} + Y_{\begin{smallmatrix} \boxed{13} \\ \boxed{2} \\ \boxed{4} \end{smallmatrix}} \quad (3.80c)$$

$$Y_{\begin{smallmatrix} \boxed{1} \\ \boxed{2} \\ \boxed{3} \end{smallmatrix}} \stackrel{?}{=} Y_{\begin{smallmatrix} \boxed{14} \\ \boxed{3} \end{smallmatrix}} + Y_{\begin{smallmatrix} \boxed{1} \\ \boxed{2} \\ \boxed{3} \\ \boxed{4} \end{smallmatrix}}. \quad (3.80d)$$

Equations (3.80a) and (3.80d), if indeed valid, tell us that the operators  $Y_{\begin{smallmatrix} \boxed{123} \\ \boxed{4} \end{smallmatrix}}$  and  $Y_{\begin{smallmatrix} \boxed{14} \\ \boxed{2} \\ \boxed{3} \end{smallmatrix}}$  are Hermitian.<sup>14</sup> To show that the remaining operators are Hermitian, we notice that a similarity transformation with an element

<sup>14</sup>This can be concluded in the same way that we previously found that  $Y_{\begin{smallmatrix} \boxed{12} \\ \boxed{3} \end{smallmatrix}}$  is Hermitian.

$\rho$  of  $S_4$  of the form

$$Y_i \mapsto \rho^\dagger Y_i \rho \tag{3.81}$$

does not change the Hermiticity of the operator  $Y_i$ . Thus, for example the operator  $(34) \cdot Y_{\begin{smallmatrix} \boxed{1} & \boxed{2} & \boxed{3} \\ \boxed{4} \end{smallmatrix}} \cdot (34)$ , where  $(34) \in S_4$  is a transposition, is still ‘‘Hermitian’’. It is now easy to check (via direct calculation) that<sup>15</sup>

$$(34) \cdot Y_{\begin{smallmatrix} \boxed{1} & \boxed{2} & \boxed{3} \\ \boxed{4} \end{smallmatrix}} \cdot (34) = Y_{\begin{smallmatrix} \boxed{1} & \boxed{2} & \boxed{4} \\ \boxed{3} \end{smallmatrix}} \quad \text{and} \quad (234) \cdot Y_{\begin{smallmatrix} \boxed{1} & \boxed{2} & \boxed{3} \\ \boxed{4} \end{smallmatrix}} \cdot (243) = Y_{\begin{smallmatrix} \boxed{1} & \boxed{3} & \boxed{4} \\ \boxed{2} \end{smallmatrix}}, \tag{3.82}$$

where  $(243)^\dagger = (234)$ , and similarly

$$(34) \cdot Y_{\begin{smallmatrix} \boxed{1} & \boxed{4} \\ \boxed{2} \\ \boxed{3} \end{smallmatrix}} \cdot (34) = Y_{\begin{smallmatrix} \boxed{1} & \boxed{3} \\ \boxed{2} \\ \boxed{4} \end{smallmatrix}} \quad \text{and} \quad (234) \cdot Y_{\begin{smallmatrix} \boxed{1} & \boxed{4} \\ \boxed{2} \\ \boxed{3} \end{smallmatrix}} \cdot (243) = Y_{\begin{smallmatrix} \boxed{1} & \boxed{2} \\ \boxed{3} \\ \boxed{4} \end{smallmatrix}}. \tag{3.83}$$

We therefore conclude that also the Young projection operators  $Y_{\begin{smallmatrix} \boxed{1} & \boxed{2} & \boxed{4} \\ \boxed{3} \end{smallmatrix}}$ ,  $Y_{\begin{smallmatrix} \boxed{1} & \boxed{3} & \boxed{4} \\ \boxed{2} \end{smallmatrix}}$ ,  $Y_{\begin{smallmatrix} \boxed{1} & \boxed{3} \\ \boxed{2} \\ \boxed{4} \end{smallmatrix}}$  and  $Y_{\begin{smallmatrix} \boxed{1} & \boxed{2} \\ \boxed{3} \\ \boxed{4} \end{smallmatrix}}$  are Hermitian.

The remaining two operators  $Y_{\begin{smallmatrix} \boxed{1} & \boxed{2} \\ \boxed{3} & \boxed{4} \end{smallmatrix}}$  and  $Y_{\begin{smallmatrix} \boxed{1} & \boxed{3} \\ \boxed{2} & \boxed{4} \end{smallmatrix}}$  can thus be written as linear combinations of Hermitian operators, using equations (3.80b) and (3.80c),

$$Y_{\begin{smallmatrix} \boxed{1} & \boxed{2} \\ \boxed{3} & \boxed{4} \end{smallmatrix}} = Y_{\begin{smallmatrix} \boxed{1} & \boxed{2} \\ \boxed{3} \end{smallmatrix}} - \left( Y_{\begin{smallmatrix} \boxed{1} & \boxed{2} & \boxed{4} \\ \boxed{3} \end{smallmatrix}} + Y_{\begin{smallmatrix} \boxed{1} & \boxed{2} \\ \boxed{3} \\ \boxed{4} \end{smallmatrix}} \right) \tag{3.84a}$$

$$Y_{\begin{smallmatrix} \boxed{1} & \boxed{3} \\ \boxed{2} & \boxed{4} \end{smallmatrix}} = Y_{\begin{smallmatrix} \boxed{1} & \boxed{3} \\ \boxed{2} \end{smallmatrix}} - \left( Y_{\begin{smallmatrix} \boxed{1} & \boxed{3} & \boxed{4} \\ \boxed{2} \end{smallmatrix}} + Y_{\begin{smallmatrix} \boxed{1} & \boxed{3} \\ \boxed{2} \\ \boxed{4} \end{smallmatrix}} \right), \tag{3.84b}$$

leading us to conclude that they are Hermitian as well. Thus, we have found that *all* Young projection operators corresponding to Young tableaux in  $\mathcal{Y}_4$  are Hermitian — a contradiction. It should be noted that, since the Littlewood-Young projection operators over  $V^{\otimes m}$  reduce to the Young projectors for  $m \leq 4$ , we conclude that also the LY-operators cannot satisfy the summation property (3.74) (at least for  $m \leq 4$ ).

In fact, one may continue this game for one more level (to the Young projectors over  $V^{\otimes 5}$ ) before the tricks given in the above examples seize to suffice and one has to come up with new tools.

Nonetheless, the key message to take away from this section is that the reason why the Young operators do not obey the summation property (3.74) is their lack of Hermiticity. This provides a strong hint that (3.74) might hold for a Hermitian version of the Young projection operators (as was already claimed in section 3.1.2). In section 3.3.4, we show explicitly that this is true, completing part 2 of Goal 1.

In order to be able to do so, we first need to describe how to obtain Hermitian Young projection operators. This will be the subject of section 3.3.3.

---

<sup>15</sup>In fact, [93] defines the Young projection operator of a tableau  $\Theta$  that can be obtained from  $\Phi$  by reordering the entries of  $\Phi$  according to a permutation  $\rho$  as  $Y_\Theta := \rho^\dagger Y_\Phi \rho$ .

### 3.3.3 Hermitian Young projection operators: KS and beyond

#### 3.3.3.1 KS construction principle

A construction principle for Hermitian Young projection operators has recently been found by Keppeler and Sjö Dahl [4]. We will now paraphrase their construction method (see Theorem 3.3), as it forms a basis for proving that the summation property eq. (3.74) (resp. eq. (3.17)) and its generalizations indeed hold for Hermitian Young projectors, section 3.3.4. We will further use Theorem 3.3 as a starting point for a new construction principle, which yields much more compact expressions for Hermitian Young projection operators, section 3.4. We will give Keppeler and Sjö Dahl's algorithm without proof; a formal proof can be found in [4].

**■ Theorem 3.3 – KS Hermitian Young projectors [4]:**

Let  $\Theta \in \mathcal{Y}_n$  be a Young tableau. If  $n \leq 2$ , then the Hermitian Young projection operator  $P_\Theta$  corresponding to the tableau  $\Theta$  is given by

$$P_\Theta := Y_\Theta. \quad (3.85)$$

This provides a termination criterion for an iterative process that obtains  $P_\Theta$  from  $P_{\Theta_{(1)}}$  via

$$P_\Theta := P_{\Theta_{(1)}} Y_\Theta P_{\Theta_{(1)}}, \quad (3.86)$$

once  $n > 2$ . In (3.86)  $P_{\Theta_{(1)}}$  is understood to be canonically embedded in the algebra  $\text{API}(\text{SU}(N), V^{\otimes n})$ . Thus,  $P_\Theta$  is recursively obtained from the full chain of its Hermitian ancestor operators  $P_{\Theta_{(m)}}$ .

The above operators generalize properties (3.27) of Young projection operators to all  $n$ :

$$\text{Idempotency:} \quad P_\Theta \cdot P_\Theta = P_\Theta \quad (3.87a)$$

$$\text{Transversality:} \quad P_\Theta \cdot P_\Phi = \delta_{\Theta\Phi} P_\Theta \quad (3.87b)$$

$$\text{Completeness:} \quad \sum_{\Theta \in \mathcal{Y}_n} P_\Theta = \mathbb{1}_n \quad (3.87c)$$

As an example, consider the Young tableau

$$\Theta = \begin{array}{|c|c|c|} \hline 1 & 2 & 4 \\ \hline 3 & 5 & \\ \hline \end{array}, \quad (3.88)$$

with ancestor tableaux<sup>16</sup>

$$\Theta_{(1)} = \begin{array}{|c|c|c|} \hline 1 & 2 & 4 \\ \hline 3 & & \\ \hline \end{array}, \quad \Theta_{(2)} = \begin{array}{|c|c|} \hline 1 & 2 \\ \hline 3 & \\ \hline \end{array} \quad \text{and} \quad \Theta_{(3)} = \begin{array}{|c|c|} \hline 1 & 2 \\ \hline \end{array}. \quad (3.89)$$

When constructing the Hermitian Young projection operator  $P_\Theta$  according to the KS Theorem 3.3, we first have to find  $P_{\Theta_{(3)}}$ ,  $P_{\Theta_{(2)}}$  and  $P_{\Theta_{(1)}}$ . According to the Theorem,  $P_{\Theta_{(3)}} = Y_{\Theta_{(3)}}$ , since  $\Theta_{(3)} \in \mathcal{Y}_2$ . Then,

<sup>16</sup>We do not have to consider the ancestor  $\Theta_{(4)}$ , since  $\Theta_{(3)} \in \mathcal{Y}_2$  and thus terminates the recursion (3.86).

following the iterative procedure of the KS Theorem,  $P_{\Theta(2)}$  and  $P_{\Theta(1)}$  are given by

$$P_{\Theta(2)} = P_{\Theta(3)} Y_{\Theta(2)} P_{\Theta(3)} = Y_{\Theta(3)} Y_{\Theta(2)} Y_{\Theta(3)} \quad (3.90)$$

$$P_{\Theta(1)} = P_{\Theta(2)} Y_{\Theta(1)} P_{\Theta(2)} = \underbrace{Y_{\Theta(3)} Y_{\Theta(2)} Y_{\Theta(3)}}_{=P_{\Theta(2)}} Y_{\Theta(1)} \underbrace{Y_{\Theta(3)} Y_{\Theta(2)} Y_{\Theta(3)}}_{=P_{\Theta(2)}}. \quad (3.91)$$

Then, the desired operator  $P_{\Theta}$  is

$$P_{\Theta} = P_{\Theta(1)} Y_{\Theta} P_{\Theta(1)} = \underbrace{Y_{\Theta(3)} Y_{\Theta(2)} Y_{\Theta(3)} Y_{\Theta(1)} Y_{\Theta(3)} Y_{\Theta(2)} Y_{\Theta(3)}}_{=P_{\Theta(1)}} Y_{\Theta} \underbrace{Y_{\Theta(3)} Y_{\Theta(2)} Y_{\Theta(3)} Y_{\Theta(1)} Y_{\Theta(3)} Y_{\Theta(2)} Y_{\Theta(3)}}_{=P_{\Theta(1)}}. \quad (3.92)$$

As a birdtrack,  $P_{\Theta}$  can be written as

$$P_{\Theta} = \frac{128}{9} \cdot \underbrace{\left[ \text{birdtrack diagram} \right]}_{\bar{P}_{\Theta(1)}}, \quad (3.93)$$

where

$$\frac{128}{9} = (\alpha_{\Theta(3)})^8 (\alpha_{\Theta(2)})^4 (\alpha_{\Theta(1)})^2 \alpha_{\Theta} \quad (3.94)$$

is the appropriate normalization constant arising from the KS algorithm.

Let us emphasize that KS have proven that this or any other operator constructed with their algorithm is Hermitian. The operator (3.93) is however not symmetric under a flip about its vertical axis, and thus Hermiticity is not visually obvious. An additional advantage of the construction algorithm described in the later section 3.4 is that it will necessarily yield mirror-symmetric operators, making their Hermiticity immediately visible.

### 3.3.3.2 Beyond the KS construction

The results regarding Hermitian Young projection operators presented up until now are all taken from [4]. We will now move beyond the established results and show that

1. the KS operators can be simplified to yield more compact expressions (*c.f.* Corollary 3.1)<sup>17</sup>
2. the KS operators obey the summation property (3.74) (resp. (3.17))

$$\sum_{\Phi \in \{\Theta \otimes \square\}} P_{\Phi} = P_{\Theta}; \quad (3.95)$$

this will be shown in section 3.3.4.

In [1] [chapter 2], we found several simplification rules for birdtrack operators, some of which are summarized

<sup>17</sup>While the simplification in Corollary 3.1 is already significant, the alternative construction given in section 3.4 will be even more efficient.

in section 3.2.3. In particular, Theorem 3.1 can be used to shorten the above operator (3.93) to

$$P_{\Theta} = Y_{\Theta_{(3)}} Y_{\Theta_{(2)}} Y_{\Theta_{(1)}} Y_{\Theta} Y_{\Theta_{(1)}} Y_{\Theta_{(2)}} Y_{\Theta_{(3)}} \quad (3.96)$$

$$= 8 \cdot \underbrace{\left[ \text{Diagram with 7 boxes and crossings} \right]}_{\bar{Y}_{\Theta_{(3)}} \bar{Y}_{\Theta_{(2)}} \bar{Y}_{\Theta_{(1)}} \bar{Y}_{\Theta} \bar{Y}_{\Theta_{(1)}} \bar{Y}_{\Theta_{(2)}} \bar{Y}_{\Theta_{(3)}}}, \quad (3.97)$$

where  $(\alpha_{\Theta_{(3)}} \alpha_{\Theta_{(2)}} \alpha_{\Theta_{(1)}})^2 \alpha_{\Theta} = 8$ . The above expression for  $P_{\Theta}$  is clearly considerably shorter than the expression given in (3.93). In fact, Theorem 3.1 allows us to systematically shorten the KS projection operators, exposing a new, much simpler general form:

■ **Corollary 3.1 – staircase form of Hermitian Young projectors:**

Let  $\Theta \in \mathcal{Y}_n$  be a Young tableau. Then, the corresponding Hermitian Young projection operator  $P_{\Theta}$  is given by

$$P_{\Theta} = Y_{\Theta_{(n-2)}} Y_{\Theta_{(n-3)}} Y_{\Theta_{(n-4)}} \cdots Y_{\Theta_{(2)}} Y_{\Theta_{(1)}} Y_{\Theta} Y_{\Theta_{(1)}} Y_{\Theta_{(2)}} \cdots Y_{\Theta_{(n-4)}} Y_{\Theta_{(n-3)}} Y_{\Theta_{(n-2)}}. \quad (3.98)$$

This result simply follows from a repeated application of Theorem 3.1, where we notice that  $\Theta_{(n-2)} \in \mathcal{Y}_2$  necessarily.

Even though this simplification is already quite substantial, it is by no means the simplest form achievable. We will present a new construction principle in section 3.4, creating even more compact and thus easier usable Hermitian Young projection operators. The proof of this construction will however make use of the KS Theorem 3.3, see appendix 3.C.

### 3.3.4 Spanning subspaces with Hermitian operators

We are finally in a position to show that

$$\sum_{\Phi \in \{\Theta \otimes \bar{n}\}} P_{\Phi} = P_{\Theta} \quad (3.99)$$

holds for every  $\Theta \in \mathcal{Y}_{n-1}$  if the  $P_{\Xi}$  are the Hermitian operators introduced previously. In section 3.1.2, we gave the particular example

$$P_{\begin{smallmatrix} \boxed{1} & \boxed{2} & \boxed{3} \\ \boxed{3} \end{smallmatrix}} + P_{\begin{smallmatrix} \boxed{1} & \boxed{2} \\ \boxed{3} \end{smallmatrix}} = P_{\begin{smallmatrix} \boxed{1} & \boxed{2} \end{smallmatrix}} \quad (3.100)$$

which holds for the *Hermitian* Young operators  $P_{\Xi}$  but fails to hold for their Young operator counterparts.

To prove (3.99) in general, we first need to show that a projection operator  $P_{\Theta}$  projects onto a subspace of the image of an operator  $P_{\Theta_{(m)}}$ , where  $\Theta_{(m)}$  is an ancestor tableau of  $\Theta$ . In particular, this will mean that the image of an operator  $P_{\Theta}$  is a subset of the image of its parent operator  $P_{\Theta_{(1)}}$ .

■ **Lemma 3.1 – Subspaces corresponding to Hermitian Young projection operators are nested:**

Let  $\Theta \in \mathcal{Y}_n$  be a Young tableau and let  $\Theta_{(m)}$  be its ancestor tableau, with  $m < n$ . Furthermore, let  $P_{\Theta}$  and  $P_{\Theta_{(m)}}$  be the Hermitian Young projection operators corresponding to these tableaux. Then, the image of  $P_{\Theta}$

lies entirely in the image of  $P_{\Theta(m)}$ ,

$$P_{\Theta}P_{\Theta(m)} = P_{\Theta} = P_{\Theta(m)}P_{\Theta} . \quad (3.101)$$

An immediate consequence of this Lemma is that a Hermitian Young projection operator  $P_{\Theta}$  commutes with its ancestor operator  $P_{\Theta(m)}$ . In appendix 3.B, we first exemplify that Young projectors do not necessarily obey the analogous image inclusion properties  $Y_{\Theta}Y_{\Theta(m)} = Y_{\Theta}$  and/or  $Y_{\Theta(m)}Y_{\Theta} = Y_{\Theta}$ . We prove that, where the image inclusion fails to hold, the associated commutator  $[Y_{\Theta(m)}, Y_{\Theta}]$  does not vanish.

Image inclusion will play an integral part in the proof of eq. (3.99) and thus highlights where the proof would break down for the (not necessarily Hermitian) Young projectors.

Before we give the proof of Lemma 3.1, We wish to draw attention to how this proof makes use of some of the simplification rules given in section 3.2.3, as this will be mirrored in the proofs of the main Theorems given in appendix 3.C.

*Proof of Lemma 3.1:* To prove the inclusion of the subspaces, it suffices to show that the product of the operators satisfies eq. (3.101) (c.f. eq. (3.40)). What this relation implies is that if we first act the product  $P_{\Theta(m)}P_{\Theta}$  (or equivalently  $P_{\Theta}P_{\Theta(m)}$ ) on an object  $x$ , we obtain the same outcome as if we only act  $P_{\Theta}$  on  $x$ . Hence,  $P_{\Theta}$  must correspond to a smaller subspace than  $P_{\Theta(m)}$ , and this subspace must completely be contained in the subspace corresponding to  $P_{\Theta(m)}$ . From the shortened KS construction (Corollary 3.1), the Hermitian Young projection operators  $P_{\Theta}$  and  $P_{\Theta(m)}$  are given by

$$P_{\Theta} = Y_{\Theta(n-2)}Y_{\Theta(n-3)} \cdots Y_{\Theta(m+1)} \underbrace{Y_{\Theta(m)}} \cdots Y_{\Theta(1)} \underbrace{Y_{\Theta}} Y_{\Theta(1)} \cdots \underbrace{Y_{\Theta(m)}} Y_{\Theta(m+1)} \cdots Y_{\Theta(n-3)} Y_{\Theta(n-2)} \quad (3.102)$$

$$P_{\Theta(m)} = Y_{\Theta(n-2)}Y_{\Theta(n-3)} \cdots Y_{\Theta(m+1)} \underbrace{Y_{\Theta(m)}} Y_{\Theta(m+1)} \cdots Y_{\Theta(n-2)} Y_{\Theta(n-2)} . \quad (3.103)$$

When forming the product  $P_{\Theta}P_{\Theta(m)}$ , we see a lot of cancellation of wedged ancestor operators due to Theorem 3.1,

$$\begin{aligned} P_{\Theta} \cdot P_{\Theta(m)} &= Y_{\Theta(n-2)} \cdots \underbrace{Y_{\Theta(m)}} \cdots Y_{\Theta(1)} \underbrace{Y_{\Theta}} Y_{\Theta(1)} \cdots \underbrace{Y_{\Theta(m)} \cdots Y_{\Theta(n-2)} \cdot Y_{\Theta(n-2)} \cdots Y_{\Theta(m)}}_{= Y_{\Theta(m)}} \cdots Y_{\Theta(n-2)} \\ &= Y_{\Theta(n-2)} \cdots \underbrace{Y_{\Theta(m)}} \cdots Y_{\Theta(1)} \underbrace{Y_{\Theta}} Y_{\Theta(1)} \cdots \underbrace{Y_{\Theta(m)}} \cdots Y_{\Theta(n-2)} . \end{aligned} \quad (3.104)$$

The above can easily be identified to be the operator  $P_{\Theta}$ , yielding the first equality  $P_{\Theta}P_{\Theta(m)} = P_{\Theta}$ . The second equality can similarly be shown, leading to the desired result.  $\square$

Let us now prove the summation property (3.99) for Hermitian Young projection operators: Recall the completeness relation of Hermitian Young projection operators, eq. (3.87c),

$$\sum_{\Theta \in \mathcal{Y}_{n-1}} P_{\Theta} = \text{id}_{n-1} , \quad (3.105)$$

where  $\text{id}_k$  is the identity operator on the space  $V^{\otimes k}$ . Equation (3.105) can be canonically embedded into the space  $V^{\otimes n}$  as was discussed in section 3.2.2.2. In order to make the embedding of the operator  $P_{\Theta}$  explicit, we



will — for this section *only* — make the identity operator on the last factor explicitly visible in the birdtrack spirit and denote the embedded operator by the symbol  $\underline{P}_\Theta$ .<sup>18</sup> The embedded equation (3.105) thus is

$$\sum_{\Theta \in \mathcal{Y}_{n-1}} \underline{P}_\Theta = \text{id}_n . \quad (3.106)$$

Even though (3.106) is a decomposition of unity, a finer decomposition of  $\text{id}_n$  (also using only transversal objects) is obtained with Hermitian Young projection operators corresponding to Young tableaux in  $\mathcal{Y}_n$ ,

$$\sum_{\Phi \in \mathcal{Y}_n} P_\Phi = \text{id}_n . \quad (3.107)$$

Since clearly  $\mathcal{Y}_n$  is the union of all the sets  $\{\Theta \otimes \boxed{n}\}$ , for all  $\Theta \in \mathcal{Y}_{n-1}$ , the sum (3.107) can be split into

$$\sum_{\Phi \in \mathcal{Y}_n} P_\Phi = \sum_{\Theta \in \mathcal{Y}_{n-1}} \left( \sum_{\Psi \in \{\Theta \otimes \boxed{n}\}} P_\Psi \right) = \text{id}_n . \quad (3.108)$$

Since both (3.106) and (3.108) are a decomposition of  $\text{id}_n$ , they must be equal to each other, yielding

$$\sum_{\Theta \in \mathcal{Y}_{n-1}} \underline{P}_\Theta = \sum_{\Theta \in \mathcal{Y}_{n-1}} \left( \sum_{\Psi \in \{\Theta \otimes \boxed{n}\}} P_\Psi \right) . \quad (3.109)$$

Let us now multiply the above equation with a particular operator  $\underline{P}_{\Theta'}$  on  $V^{\otimes n}$ , where  $\Theta'$  is a particular tableau in  $\mathcal{Y}_{n-1}$ . Due to the transversality property (eq. (3.87b), Theorem 3.3) and the inclusion property (eq. (3.101), Lemma 3.1) of Hermitian Young projectors,<sup>19</sup> it follows that

$$\sum_{\Theta \in \mathcal{Y}_{n-1}} \delta_{\Theta\Theta'} \underline{P}_\Theta = \sum_{\Theta \in \mathcal{Y}_{n-1}} \left( \delta_{\Theta\Theta'} \sum_{\Psi \in \{\Theta \otimes \boxed{n}\}} P_\Psi \right) \quad (3.110)$$

$$\underline{P}_{\Theta'} = \sum_{\Psi \in \{\Theta' \otimes \boxed{n}\}} P_\Psi , \quad (3.111)$$

yielding the desired equation (3.99). This concludes part 2 of Goal 1.

Since the Hermitian operators sum up to their Hermitian parent operators (eq. (3.111)), and these in turn sum to their Hermitian parent operators, the summation property necessarily holds over multiple generations. This statement also follows straight from Lemma 3.1, which states that the image of a Hermitian Young projection operator  $P_\Theta$  is contained in the image of its Hermitian ancestor operator  $P_{\Theta(m)}$ , where  $m$  can be *any* positive integer. Therefore, if  $\mathcal{Y}_{\Theta,n} := \{\Theta \otimes \boxed{m} \otimes \cdots \otimes \boxed{n}\}$  is the subset of  $\mathcal{Y}_n$  containing all tableaux that have  $\Theta \in \mathcal{Y}_{m-1}$  as their ancestor, then

$$\sum_{\Phi \in \mathcal{Y}_{\Theta,n}} P_\Phi = P_\Theta , \quad (3.112)$$

<sup>18</sup>In birdtrack notation, the canonically embedded operator  $\underline{P}_\Theta$  will be  $P_\Theta$  with an extra index line on the bottom, making the notation  $\underline{P}_\Theta$  intuitive.

<sup>19</sup>This is where the proof would break down for the standard Young projection operators even for  $n \leq 4$ , as they explicitly do not satisfy the image inclusion property (3.101), *c.f.* appendix 3.B.

confirming eq. (3.18). For example, if  $\Theta = \begin{array}{|c|c|c|} \hline 1 & 2 & 3 \\ \hline \end{array}$ , then  $P_\Theta$  can be written as a sum of the following Hermitian Young projection operators corresponding to tableaux in  $\mathcal{Y}_5$ ,

$$\underbrace{P_{\begin{array}{|c|c|c|c|c|} \hline 1 & 2 & 3 & 4 & 5 \\ \hline \end{array}} + P_{\begin{array}{|c|c|c|c|} \hline 1 & 2 & 3 & 4 \\ \hline 5 \\ \hline \end{array}} + P_{\begin{array}{|c|c|c|c|} \hline 1 & 2 & 3 & 5 \\ \hline 4 \\ \hline \end{array}} + P_{\begin{array}{|c|c|c|} \hline 1 & 2 & 3 \\ \hline 4 & 5 \\ \hline \end{array}} + P_{\begin{array}{|c|c|c|} \hline 1 & 2 & 3 \\ \hline 4 & 5 \\ \hline 4 & 5 \\ \hline \end{array}} = \underbrace{P_{\begin{array}{|c|c|c|} \hline 1 & 2 & 3 \\ \hline \end{array}}}_{P_\Theta}. \quad (3.113)$$

This concludes the last part (part 3) of the first Goal of this paper.

Figure 4.3 (inspired by [72, Fig. 9.1]) shows all Hermitian Young projectors corresponding to Young tableaux in  $\mathcal{Y}_n$  up to and including  $n = 4$ . The arrows indicate which operators sum to which ancestor operators. (We will augment Figure 4.3 with *transition operators* in [3, Fig. 3] [*chapter 4, Figure 4.3*]).

### 3.4 An algorithm to construct compact expressions of Hermitian Young projection operators

We will now come to Goal 2 of this paper and provide a construction principle that allows us to directly arrive at *compact expressions* for Hermitian Young projection operators (see Theorem 3.5 below). This construction yields much shorter expressions than the previously encountered KS algorithm (Theorem 3.3), or even the shortened version of Theorem 3.1, as is exemplified in Figure 3.2.

#### 3.4.1 Lexically ordered Young tableaux

It turns out that the ordering of the numbers within the Young tableau plays a vital role in our algorithm. Thus, we will first establish what we mean by the lexical order of a Young tableau. To do so, we will introduce column- and row-words:<sup>20</sup>

**■ Definition 3.2 – column- and row-words & lexical ordering:**

Let  $\Theta \in \mathcal{Y}_n$  be a Young tableau. We define the column-word of  $\Theta$ ,  $\mathfrak{C}_\Theta$ , to be the column vector whose entries are the entries of  $\Theta$  as read column-wise from left to right. Similarly, the row-word of  $\Theta$ ,  $\mathfrak{R}_\Theta$ , is defined to be the row vector whose entries are those of  $\Theta$  read row-wise from top to bottom.

We will call a tableau  $\Theta$  lexically ordered, if either  $\mathfrak{C}_\Theta$  or  $\mathfrak{R}_\Theta$  or both are in lexical order. In particular, we say that  $\Theta$  is column-ordered (resp. row-ordered), if  $\mathfrak{C}_\Theta$  (resp.  $\mathfrak{R}_\Theta$ ) is in lexical order.

For example, the tableau

$$\Phi := \begin{array}{|c|c|c|c|} \hline 1 & 5 & 7 & 9 \\ \hline 2 & 6 & 8 & \\ \hline 3 & & & \\ \hline 4 & & & \\ \hline \end{array} \quad (3.114)$$

---

<sup>20</sup>It should be noted that Definition 3.2 of the row-word is *different* to the definition given in the standard literature such as [95, 96]: there, the row word is read from bottom to top rather than from top to bottom. However, for the purposes of this paper, Definition 3.2 is more useful than the standard definition.

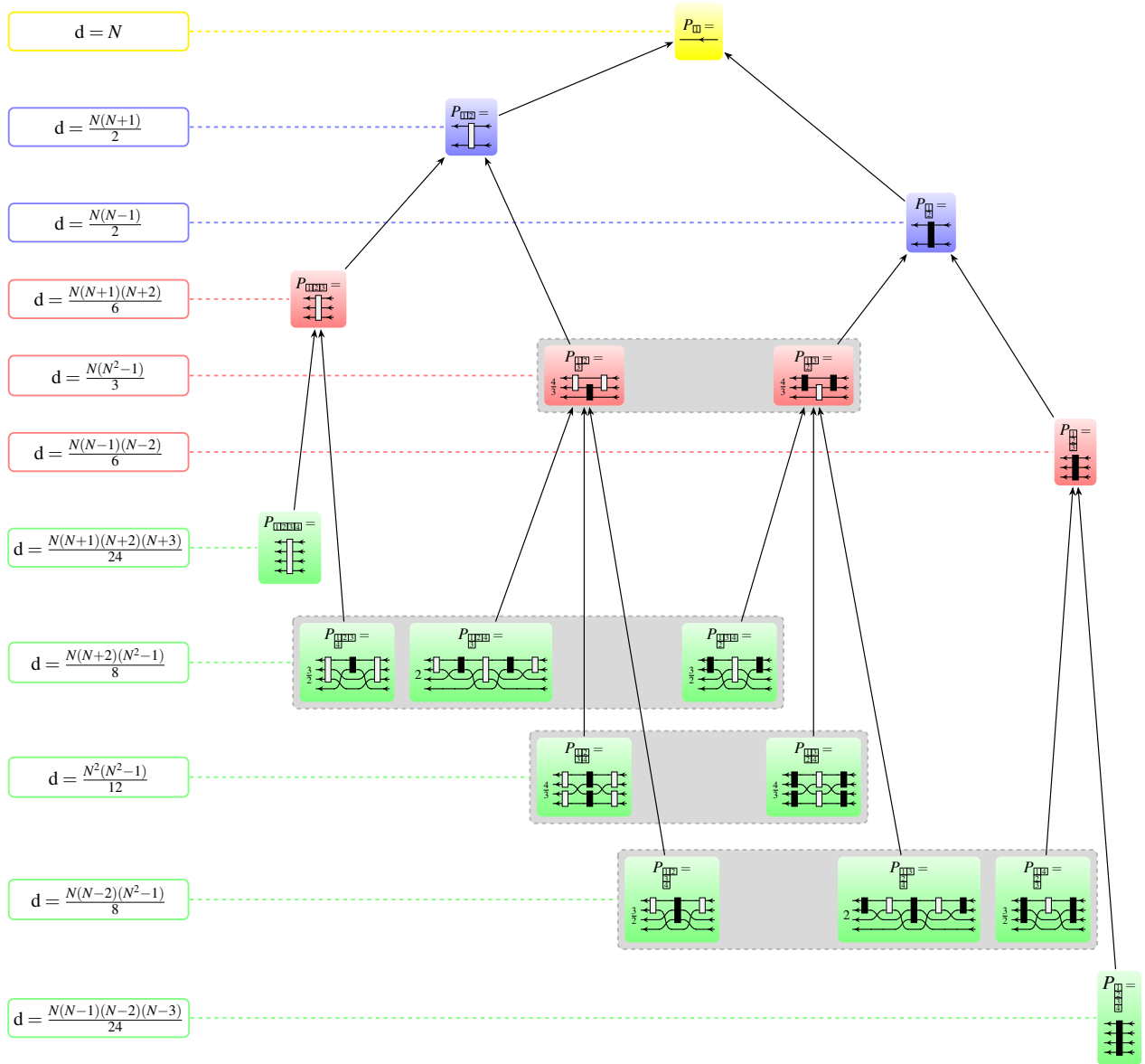


Figure 3.1: Hierarchy of Young tableaux and the associated nested Hermitian Young projector decompositions (in the sense of embeddings into  $\text{API}(\text{SU}(N), V^{\otimes 4})$ ): Projection operators that are contained in a grey box correspond to equivalent irreducible representations of  $\text{SU}(N)$ , as their corresponding Young tableaux have the same shape [72, 93]. The dimension of the irreducible representation corresponding to a (set of) operators(s) is given on the left. The arrows indicate which operators sum to which ancestor. (This figure is based on [72, Fig. 9.1])

has a column-word

$$\mathfrak{C}_\Phi = (1, 2, 3, 4, 5, 6, 7, 8, 9)^t, \quad (3.115)$$

and a row-word

$$\mathfrak{R}_\Phi = (1, 5, 7, 9, 2, 6, 8, 3, 4). \quad (3.116)$$

From this, we see that  $\Phi$  in (3.114) is lexically ordered. In particular, it is column-ordered (but not row-ordered).

In Theorem 3.4, we will describe a construction principle for the Hermitian Young projection operators corresponding to lexically ordered tableaux. This will form a starting point for the general construction principle of the Hermitian Young projectors given in section 3.4.2, as is evident from their proofs in appendix 3.C. It is clear that Keppeler and Sjödhahl had noticed that the projectors associated with ordered tableaux are special: In the appendix of [4], they discuss two examples of Hermitian Young projection operators (which happen to correspond to lexically ordered tableaux) constructed according to the KS Theorem, and argue that these operators can be simplified quite drastically. The procedure leads eventually to the same expressions that emerge directly from Theorem 3.4. However, Keppeler and Sjödhahl do not establish the connection to the lexical order of the Young tableau and do not even hint at a general construction principle.

**■ Theorem 3.4 – lexical Hermitian Young projectors:**

Let  $\Theta \in \mathcal{Y}_n$  be row-ordered. Then, the corresponding Hermitian Young projection operator  $P_\Theta$  is given by

$$P_\Theta = \alpha_\Theta \cdot \bar{Y}_\Theta \bar{Y}_\Theta^\dagger. \quad (3.117a)$$

On the other hand, if  $\Theta \in \mathcal{Y}_n$  is a column-ordered tableau, then the corresponding Hermitian Young projection operator  $P_\Theta$  is given by

$$P_\Theta = \alpha_\Theta \cdot \bar{Y}_\Theta^\dagger \bar{Y}_\Theta. \quad (3.117b)$$

The proof of this Theorem is deferred to appendix 3.C.1. It is directly evident from eqns. (3.117) that  $P_\Theta$  is Hermitian in both cases. Since Hermitian conjugation in birdtrack notation amounts to reflection about a vertical axis, the formulae also guarantee that Hermiticity is directly visible as a reflection symmetry of the associated birdtrack diagrams.

As an example, consider the Young tableau

$$\Theta = \begin{array}{|c|c|} \hline 1 & 2 \\ \hline 3 & \\ \hline \end{array} \quad (3.118)$$

which has a lexically ordered row-word  $\mathfrak{R}_\Theta = (1, 2, 3)$ . The associated Hermitian Young projection operator  $P_\Theta$  according to the Lexical Theorem 3.4 is given by

$$P_\Theta = \underbrace{\frac{4}{3}}_{\alpha_\Theta} \cdot \underbrace{\text{birdtrack}}_{\bar{Y}_\Theta} \underbrace{\text{birdtrack}}_{\bar{Y}_\Theta^\dagger} = \frac{4}{3} \cdot \underbrace{\text{birdtrack}}_{=: P_\Theta}. \quad (3.119)$$

The Hermiticity of this operator is prominently visible in its mirror symmetry.

### 3.4.2 Young tableaux with partial lexical order

We will now give a construction principle for compact expressions of Hermitian Young projection operators corresponding to general, not necessarily lexically ordered, tableaux. The goal is to use what *partial* order there is to a diagram to obtain an optimized iterative procedure. As a first step we need to be able to quantify how “un-ordered” a Young tableau is; we define a *Measure Of Lexical Disorder*:

**■ Definition 3.3 – measure of lexical disorder (MOLD):**

Let  $\Theta \in \mathcal{Y}_n$  be a Young tableau. We define its Measure Of Lexical Disorder (MOLD) to be the smallest natural number  $\mathcal{M}(\Theta) \in \mathbb{N}$  such that

$$\Theta_{(\mathcal{M}(\Theta))} = \pi^{\mathcal{M}(\Theta)}(\Theta) \quad (3.120)$$

is a lexically ordered tableau. (Recall from Definition 3.1 that  $\pi^{\mathcal{M}(\Theta)}$  refers to  $\mathcal{M}(\Theta)$  consecutive applications of the parent map  $\pi$  to the tableau  $\Theta$ .)

We note that the MOLD of a Young tableau is a well-defined quantity, since one will always eventually arrive at a lexically ordered tableau, as, for example, all tableaux in  $\mathcal{Y}_3$  are lexically ordered. This then implies that the MOLD of a tableau  $\Theta \in \mathcal{Y}_n$  has an upper bound,

$$\mathcal{M}(\Theta) \leq n - 3, \quad (3.121)$$

making it a well-defined quantity. As an example, consider the tableau

$$\Phi := \begin{array}{|c|c|c|} \hline 1 & 2 & 4 \\ \hline 3 & 5 & \\ \hline \end{array}. \quad (3.122)$$

The MOLD of the above tableau is  $\mathcal{M}(\Phi) = 2$ , since two applications of the parent map generate a lexically ordered tableau, but just one application of  $\pi$  on  $\Phi$  would not be sufficient,

$$\begin{array}{|c|c|c|} \hline 1 & 2 & 4 \\ \hline 3 & 5 & \\ \hline \end{array} \xrightarrow{\pi} \begin{array}{|c|c|c|} \hline 1 & 2 & 4 \\ \hline 3 & & \\ \hline \end{array} \xrightarrow{\pi} \begin{array}{|c|c|} \hline 1 & 2 \\ \hline 3 & \\ \hline \end{array}. \quad (3.123)$$

We will now give the main Theorem of this section, the construction principle of Hermitian Young projection operators corresponding to Young tableaux  $\Theta$ , using the MOLD of the latter. To do so, we distinguish four cases; the reason why they have to be dealt with separately is given in the analysis following the Theorem, section 3.4.2.1.

**■ Theorem 3.5 – MOLD operators:**

Consider a Young tableau  $\Theta \in \mathcal{Y}_n$  with MOLD  $\mathcal{M}(\Theta) = m$ . Furthermore, suppose that  $\Theta_{(m)}$  has a lexically ordered row-word. Then, the Hermitian Young projection operator corresponding to  $\Theta$ ,  $P_\Theta$ , is, for even  $m$ ,

$$P_\Theta = \beta_\Theta \cdot \mathbf{S}_{\Theta_{(m)}} \mathbf{A}_{\Theta_{(m-1)}} \mathbf{S}_{\Theta_{(m-2)}} \cdots \mathbf{S}_{\Theta_{(2)}} \mathbf{A}_{\Theta_{(1)}} \bar{Y}_\Theta \bar{Y}_\Theta^\dagger \mathbf{A}_{\Theta_{(1)}} \mathbf{S}_{\Theta_{(2)}} \cdots \mathbf{S}_{\Theta_{(m-2)}} \mathbf{A}_{\Theta_{(m-1)}} \mathbf{S}_{\Theta_{(m)}}, \quad (3.124a)$$

and, for odd  $m$ ,

$$P_{\Theta} = \beta_{\Theta} \cdot \mathbf{S}_{\Theta(m)} \mathbf{A}_{\Theta(m-1)} \mathbf{S}_{\Theta(m-2)} \cdots \mathbf{A}_{\Theta(2)} \mathbf{S}_{\Theta(1)} \bar{\mathbf{Y}}_{\Theta}^{\dagger} \bar{\mathbf{Y}}_{\Theta} \mathbf{S}_{\Theta(1)} \mathbf{A}_{\Theta(2)} \cdots \mathbf{S}_{\Theta(m-2)} \mathbf{A}_{\Theta(m-1)} \mathbf{S}_{\Theta(m)}. \quad (3.124b)$$

Similarly, if  $\Theta(m)$  has a lexically ordered column-word,  $P_{\Theta}$  is, for even  $m$ ,

$$P_{\Theta} = \beta_{\Theta} \cdot \mathbf{A}_{\Theta(m)} \mathbf{S}_{\Theta(m-1)} \mathbf{A}_{\Theta(m-2)} \cdots \mathbf{A}_{\Theta(2)} \mathbf{S}_{\Theta(1)} \bar{\mathbf{Y}}_{\Theta}^{\dagger} \bar{\mathbf{Y}}_{\Theta} \mathbf{S}_{\Theta(1)} \mathbf{A}_{\Theta(2)} \cdots \mathbf{A}_{\Theta(m-2)} \mathbf{S}_{\Theta(m-1)} \mathbf{A}_{\Theta(m)}, \quad (3.124c)$$

and, for odd  $m$ ,

$$P_{\Theta} = \beta_{\Theta} \cdot \mathbf{A}_{\Theta(m)} \mathbf{S}_{\Theta(m-1)} \mathbf{A}_{\Theta(m-2)} \cdots \mathbf{S}_{\Theta(2)} \mathbf{A}_{\Theta(1)} \bar{\mathbf{Y}}_{\Theta} \bar{\mathbf{Y}}_{\Theta}^{\dagger} \mathbf{A}_{\Theta(1)} \mathbf{S}_{\Theta(2)} \cdots \mathbf{A}_{\Theta(m-2)} \mathbf{S}_{\Theta(m-1)} \mathbf{A}_{\Theta(m)}. \quad (3.124d)$$

In the above, all symmetrizers and antisymmetrizers are understood to be canonically embedded into  $V^{\otimes n}$ ;  $\beta_{\Theta}$  is a nonzero constant chosen such that  $P_{\Theta}$  is idempotent.

The formal proof of this Theorem can be found in appendix 3.C.2. A comparative example of a Hermitian Young projection operator constructed using MOLD and KS is given in section 3.4.3, Figure 3.2.

It should be noted that we have not provided an explicit expression for the constant  $\beta_{\Theta}$  in Theorem 3.5. This normalization-constant, however, can easily be found for specific operators by direct calculation since the MOLD operators are very well suited for automated calculations on a computer, as is described in section 3.4.3. We would like to draw the reader's attention to the fact that the symmetrizers and antisymmetrizers in all four expressions of Theorem 3.5 *strictly alternate*, including those inside the Young projectors.

As an example, consider the Young tableau

$$\Theta := \begin{array}{|c|c|c|} \hline 1 & 2 & 4 \\ \hline 3 & 5 & \\ \hline \end{array}. \quad (3.125)$$

This tableau has MOLD 2 (i.e. even MOLD), and  $\Theta(2)$  has a lexically ordered row-word. Thus, we have to construct the Hermitian Young projection operator  $P_{\Theta}$  corresponding to  $\Theta$  according to equation (3.124a).  $P_{\Theta}$  is therefore given by

$$\begin{aligned} P_{\Theta} &= \beta_{\Theta} \cdot \mathbf{S}_{\Theta(2)} \mathbf{A}_{\Theta(1)} \mathbf{S}_{\Theta} \mathbf{A}_{\Theta} \mathbf{S}_{\Theta} \mathbf{A}_{\Theta(1)} \mathbf{S}_{\Theta(2)} \\ &= \beta_{\Theta} \cdot \begin{array}{c} \text{[Diagram: A sequence of operators } \mathbf{S}_{\Theta(2)}, \mathbf{A}_{\Theta(1)}, \mathbf{S}_{\Theta}, \mathbf{A}_{\Theta}, \mathbf{S}_{\Theta}, \mathbf{A}_{\Theta(1)}, \mathbf{S}_{\Theta(2)} \text{ represented by strands and crossings. The } \mathbf{S}_{\Theta} \mathbf{A}_{\Theta} \mathbf{S}_{\Theta} \text{ part is highlighted in red.]} \\ \mathbf{S}_{\Theta(2)} \mathbf{A}_{\Theta(1)} \mathbf{S}_{\Theta} \mathbf{A}_{\Theta} \mathbf{S}_{\Theta} \mathbf{A}_{\Theta(1)} \mathbf{S}_{\Theta(2)} \end{array} \\ &= \beta_{\Theta} \cdot \begin{array}{c} \text{[Diagram: A more compact representation of the same operator sequence, showing the overall structure of the Young projector.]} \end{array}. \quad (3.126) \end{aligned}$$

A direct calculation in *Mathematica* reveals that  $\beta_{\Theta} \stackrel{!}{=} 4$  for  $P_{\Theta}$  to be idempotent.

### 3.4.2.1 A Short Analysis of the MOLD Theorem 3.5

We now pause for a moment to look at the four cases presented in Theorem 3.5 in more detail and emphasize their differences. We hope to convey an intuitive feel as to why the corresponding operators are constructed the way they are.

First, let us look at the first two operators (3.124a) and (3.124b). Both these operators  $P_\Theta$  have a symmetrizer on the outside, namely  $\mathbf{S}_{\Theta(m)}$ , opposed to the operators (3.124c) and (3.124d) which have an antisymmetrizer on the outside. This stems from the iterative construction of Hermitian Young projection operators given by the KS Theorem 3.3: By the Lexical Theorem 3.4 we know that  $P_{\Theta(m)}$  is given by

$$P_{\Theta(m)} = \alpha_\Theta \cdot \bar{Y}_{\Theta(m)} \bar{Y}_{\Theta(m)}^\dagger = \alpha_\Theta \cdot \mathbf{S}_{\Theta(m)} \mathbf{A}_{\Theta(m)} \mathbf{S}_{\Theta(m)}, \quad (3.127)$$

since  $P_{\Theta(m)}$  is assumed to correspond to a row-ordered Young tableau. When we thus construct  $P_\Theta$  recursively according to KS [4], we find that

$$P_\Theta = P_{\Theta(m)} \dots Y_\Theta \dots P_{\Theta(m)} \propto \mathbf{S}_{\Theta(m)} \mathbf{A}_{\Theta(m)} \mathbf{S}_{\Theta(m)} \dots Y_\Theta \dots \mathbf{S}_{\Theta(m)} \mathbf{A}_{\Theta(m)} \mathbf{S}_{\Theta(m)}. \quad (3.128)$$

Thus, we expect there to be symmetrizers on the outside of the operators  $P_\Theta$  in expressions (3.124a) and (3.124b). Following a similar logic, we expect there to be antisymmetrizers on the outside of operators (3.124c) and (3.124d).

Lastly, we discuss the importance of the distinction between even and odd  $m$  in the MOLD Theorem 3.5. In the construction of *all*  $P_\Theta$  in the Theorem, we find that they consist of products of alternating symmetrizers and antisymmetrizers to more and more recent generations of  $\Theta$  as we move further to the center of  $P_\Theta$ . If the operator  $P_\Theta$  thus starts with  $\mathbf{S}_{(m)}$  on the outside, as it does in equations (3.124a) and (3.124b), and the product has alternating sets of symmetrizers and antisymmetrizers, each going up one generation, then the parity of  $m$  will decide whether the set corresponding to the tableau  $\Theta_{(1)}$  in the product  $P_\Theta$  is a set of symmetrizers or antisymmetrizers. Thus, the central three sets of symmetrizers and antisymmetrizers in the product  $P_\Theta$  will then either be

$$\mathbf{A}_\Theta \mathbf{S}_\Theta \mathbf{A}_\Theta = \bar{Y}_\Theta^\dagger \bar{Y}_\Theta \quad \text{or} \quad \mathbf{S}_\Theta \mathbf{A}_\Theta \mathbf{S}_\Theta = \bar{Y}_\Theta \bar{Y}_\Theta^\dagger, \quad (3.129)$$

depending on the nature of the sets corresponding to  $\Theta_{(1)}$ , but keeping the alternating structure of symmetrizers and antisymmetrizers.

The fact that the central sets of  $P_\Theta$  in all four equations of the above Theorem 3.5 are either product of (3.129), opposed to simply  $Y_\Theta$  or  $Y_\Theta^\dagger$ , can be attributed to the fact the  $P_\Theta$  is Hermitian and we would like its Hermiticity to be visually explicit.

### 3.4.3 The advantage of using MOLD

The practical advantages of our construction opposed to the KS Theorem 3.3 are striking. To illustrate this, we return to the same example used in [1, Fig. 5.2] [*c.f. chapter 2 Figure 2.2*] to demonstrate the effectiveness of the simplification rules derived there. The Young tableau

$$\Phi := \begin{array}{|c|c|c|c|} \hline 1 & 2 & 4 & 7 \\ \hline 3 & 6 & & \\ \hline 5 & 8 & & \\ \hline 9 & & & \\ \hline \end{array} \quad (3.130)$$

leads to an expression of the corresponding KS projector with 127 symmetrizer- and antisymmetrizer-sets, which reduce to an object with only 13 such sets after applying the cancellation and propagation rules of [1]

[chapter 2].

Both construction principles (KS and MOLD) are iterative in the sense that they both require knowledge about the ancestor tableaux of a tableau  $\Theta \in \mathcal{Y}_n$ . For the construction of KS as it was originally described in [4], one needs all ancestor operators of  $\Theta$  up until  $\Theta_{(n-2)}$ , while the MOLD construction merely uses the ancestor tableaux up until  $\Theta_{\mathcal{M}(\Theta)}$ , which is at most  $\Theta_{(n-3)}$  according to (3.121). This one tableau difference does not seem excessive at first glance, but one should keep in mind that the difference is *at least* one tableau, often more. However the bulk of the computing power used to generate  $\bar{P}_\Phi^{KS}$  comes from the fact that, in addition to the ancestor tableaux of  $\Theta$ , one further requires information about the explicit form of the ancestor Hermitian Young projectors  $P_\Theta$  all the way up to  $P_{\Theta_{(2)}}$ , which have to be calculated separately. The MOLD construction merely uses the Young sets of symmetrizers or antisymmetrizers (**S** and **A** respectively) of the ancestor tableaux of  $\Theta$  up to  $\Theta_{\mathcal{M}(\Theta)}$ , which can be immediately read off the tableaux and thus needs minimal computing power.

Using the MOLD Theorem 3.5, one arrives at the shorter version of [1, Fig. 5.2] [c.f. chapter 2 Figure 2.2] *directly*, after a considerably shorter recursive path and without the need for additional simplifications. One bypasses a long repetitive list of steps altogether! The 127/13 length ratio between  $\bar{P}_\Phi^{KS}$  and  $\bar{P}_\Phi^{MOLD}$ <sup>21</sup>

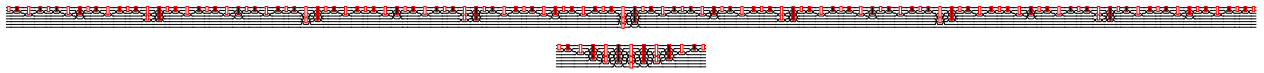


Figure 3.2: For a size comparison, this figure shows  $\bar{P}_\Phi^{KS}$  (top) and  $\bar{P}_\Phi^{MOLD}$  (bottom) for the tableau  $\Phi$  as defined in (3.130) using two different constructions: The top operator was constructed using the KS algorithm, while the bottom operator was constructed using MOLD. Both operators and the associated graphics were generated in *Mathematica*.

is strikingly apparent in Figure 3.2. This makes the MOLD algorithm a lot more practical to work with analytically. The algorithm really comes into its own when used in symbolic algebra programs: the MOLD construction allows us to efficiently create projection operators for considerably larger Young tableaux than the iterative KS equivalent. In particular, for the example in Figure 3.2, the fact that the MOLD algorithm simply avoids a long series of steps makes it over 18600 times faster than its KS counterpart: It generates its result in approximately 0.0038 seconds, while KS takes approximately 71 seconds (not even taking into account the cost of the simplification steps to arrive at the final result) on a modern laptop.

Unlike  $P_\Theta^{KS}$ ,  $P_\Theta^{MOLD}$  is *obviously and visibly* Hermitian by construction.<sup>22</sup> Given that birdtracks are meant to be a tool that makes dealing with these operators *visually* clear, this is an obvious advantage.

We have given a construction principle for compact expressions of Hermitian Young projection operators, the MOLD operators, in section 3.4.2, and we have now seen that the MOLD operators are indeed more useful for practical calculations. We have thus achieved Goal 2 of this paper.

<sup>21</sup>It is important to note that  $\bar{P}_\Phi^{KS}$  and  $\bar{P}_\Phi^{MOLD}$  both differ from  $P_\Phi$  by a constant, but this constant will depend on the construction principle used to find  $\bar{P}_\Phi$ . In that sense,

$$\beta_\Phi^{KS} \cdot \bar{P}_\Phi^{KS} = P_\Phi = \beta_\Phi^{MOLD} \cdot \bar{P}_\Phi^{MOLD} \quad (3.131)$$

but  $\beta_\Phi^{KS} \neq \beta_\Phi^{MOLD}$  in general.

<sup>22</sup> $P_\Theta^{KS}$  do not exhibit their Hermiticity directly since the center-piece of the *KS* operator is the Young projection operator  $\bar{Y}_\Theta$ , which is inherently non-Hermitian. We need to rely on the proof given in [4] to be assured of their Hermiticity.



### 3.5 Chapter conclusion & outlook

The representation theory of  $SU(N)$  is an old theory with many successful applications in physics. Yet, some of the tools remain awkward and only applicable in specific situations, like the general theory of angular momentum or the construction of Young projection operators that lack Hermiticity. Newer tools, like the birdtrack formalism, remain only partially connected with these time honored results. We have a very specific interest in applications to QCD in the context of Jalilian-Marian–Iancu–McLerran–Weigert–Leonidov–Kovner (JIMWLK) [20, 56–59] evolution, in jet physics, in energy loss and generalized parton distributions, so we have aimed at creating a set of tools that we know will aid in these applications and, in the process, have pointed out where the existing tools fall short of our needs.

1. We have found that projection operators built on Young tableaux are uniquely suited to calculations that keep  $N$  as a parameter.

To simply list the irreducible multiplets in  $V^{\otimes m}$ , Young’s procedure forms descendant tableaux of those representing the irreducibles contained in  $V^{\otimes(m-1)}$ , portraying an iterative procedure of “adding a particle” in each step.

To parallel this in terms of projection operators and the associated subspaces (i.e. to implement eq. (3.112), which represents the general case of the summation relations collected in Figure 4.3) — as one needs to do to actually perform calculations in physics applications — we have established that one needs Hermitian versions of these projection operators, as those constructed earlier by Keppeler and Sjö Dahl [4]. This sets the backdrop for the remaining developments.

2. Having motivated the necessity for Hermitian Young projection operators, we are faced with the fact that the KS algorithm quickly becomes unwieldy — the iterative procedures are computationally expensive and produce long expressions (Figure 3.2). We have earlier presented simplification rules [1] [chapter 2] to distill these down to more compact expressions, but that does not alleviate the computational cost.

To address this issue, we have provided a new algorithm based on the Measure Of Lexical Disorder (MOLD) of a tableau in section 3.4.2 that drastically reduces the calculational footprint of the procedure compared to the KS method. It should be noted that the normalized operators constructed using the MOLD algorithm are equal to the KS operators (as is evident from the proof given in appendix 3.C), and thus inherit all properties of the KS operators over  $V^{\otimes m}$ : idempotency, mutual transversality and completeness for all values of  $m$ .

The MOLD algorithm almost completely incorporates the simplifications of [1] [chapter 2] at vastly reduced calculational cost — only isolated cases of MOLD operators still allow for further simplification with the tools presented in [1] [chapter 2]; an example of such an operator is

$$\Theta := \begin{array}{|c|c|} \hline 1 & 3 \\ \hline 2 & \\ \hline 4 & \\ \hline 5 & \\ \hline 6 & \\ \hline \end{array}, \quad P_{\Theta} = \begin{array}{c} \text{Diagram of Young projection operator } P_{\Theta} \text{ with 6 horizontal lines and 3 vertical bars.} \end{array} \xrightarrow[\text{rules}]{\text{simplification}} \begin{array}{c} \text{Simplified diagram of } P_{\Theta} \text{ with 6 horizontal lines and 3 vertical bars.} \end{array}. \quad (3.132)$$

All the algorithms are eminently suited for implementation in symbolic algebra programs: all our explorations and examples have been generated in *Mathematica*.

In particular, the operators shown in Figure 3.2 were generated in *Mathematica*: the operator on the top was constructed using the KS Theorem, while the operator on the bottom resulted from the MOLD construction. The automated calculation was significantly improved with the MOLD algorithm, as the MOLD operator in Figure 3.2 was obtained approximately 18600 times faster than the KS equivalent on a modern laptop — an improvement of 4 orders of magnitude.

Our own list of applications for the tools and insights presented in this paper are QCD centric: Global singlet state projections of Wilson-line operators that appear in a myriad of applications due to factorization of hard and soft contributions help analyzing the physics content in all of them; this will be explored further in [94] [chapter 5]. We hope that our presentation is suitable to unify perspectives provided by the various approaches to representation theory of  $SU(N)$  and that the results prove useful beyond these immediate applications.

# Appendix to chapter 3

## 3.A Littlewood-Young projection operators

For completeness, this appendix summarizes the construction principle of generalized Young projection operators due to Littlewood [85, section 5.3], which corrects for the failure of Young projection operators over  $V^{\otimes n}$  to be transversal or complete beyond  $n = 4$ . We shall call these the Littlewood-Young (LY) projectors and denote them by  $L$ .

Before we give the construction principle of the LY-projectors, let us have a closer look at products of Young projection operators, and criteria, which make these products transversal. Consider two Young tableaux  $\Theta$  and  $\Phi$  in  $\mathcal{Y}_n$ , then the product of their corresponding Young projection operators is given by

$$Y_\Theta Y_\Phi = \alpha_\Theta \alpha_\Phi \cdot \mathbf{S}_\Theta \mathbf{A}_\Theta \mathbf{S}_\Phi \mathbf{A}_\Phi . \quad (3.133)$$

Clearly, if the product  $\mathbf{A}_\Theta \mathbf{S}_\Phi$  vanishes, then so does the product of the Young projectors, but if  $\mathbf{A}_\Theta \mathbf{S}_\Phi \neq 0$ , then  $Y_\Theta Y_\Phi \neq 0$  in general,

$$Y_\Theta Y_\Phi = \alpha_\Theta \alpha_\Phi \cdot \underbrace{\mathbf{S}_\Theta}_{\neq 0} \underbrace{\mathbf{A}_\Theta \mathbf{S}_\Phi}_{\neq 0} \underbrace{\mathbf{A}_\Phi}_{\neq 0} \implies Y_\Theta Y_\Phi \neq 0 \text{ in general} . \quad (3.134)$$

For  $\mathbf{A}_\Theta \mathbf{S}_\Phi$  to vanish indentially, we merely require a particular antisymmetrizer  $\mathbf{A}_i \in \mathbf{A}_\Theta$  to have more than one leg in common with a symmetrizer  $\mathbf{S}_j \in \mathbf{S}_\Phi$ .

If the tableaux  $\Theta$  and  $\Phi$  have different shapes, then this is trivially given, since there must exist at least one pair of boxes  $(\boxed{k}, \boxed{l})$  that appear in the same column in  $\Theta$  and in the same row in  $\Phi$  and vice versa, such that [85, section 5.3, Theorem III]

$$\mathbf{A}_\Theta \mathbf{S}_\Phi = 0 = \mathbf{A}_\Phi \mathbf{S}_\Theta \quad \text{where } \Theta \text{ and } \Phi \text{ have different shapes} . \quad (3.135)$$

If the two tableaux  $\Theta$  and  $\Phi$  have the same shape, one must work harder to see where this criterion applies to force  $\mathbf{A}_\Theta \mathbf{S}_\Phi = 0$ . To see when a pair of boxes  $(\boxed{k}, \boxed{l})$  appears in the same column in  $\Theta$  and in the same row in  $\Phi$  for tableaux of the same shape, we need to introduce an order relation between tableaux of the same shape using their row-words (*c.f.* Definition 3.2):

**■ Definition 3.4 – order relation amongst tableaux of the same shape:**

Let  $\Theta$  and  $\Phi$  be two Young tableaux and let  $\theta_{ij}$  be the entry in the  $i^{\text{th}}$  row and  $j^{\text{th}}$  column of  $\Theta$ , and similarly for  $\phi_{ij}$ . Their corresponding row-words are given by  $\mathfrak{R}_\Theta = (\theta_{11}, \theta_{12}, \dots, \theta_{21}, \dots)$  and  $\mathfrak{R}_\Phi = (\phi_{11}, \phi_{12}, \dots, \phi_{21}, \dots)$

respectively. We say that  $\Theta$  precedes  $\Phi$  and write  $\Theta \prec \Phi$  if  $\theta_{ij} < \phi_{ij}$  for the leftmost  $ij$  where  $\theta_{ij} \in \mathfrak{R}_\Theta$  and  $\phi_{ij} \in \mathfrak{R}_\Phi$  differ.<sup>23</sup>

For example, the Young tableaux of shape  $\begin{array}{|c|c|c|} \hline \square & \square & \square \\ \hline \square & \square & \square \\ \hline \end{array}$  can be ordered as

$$\begin{array}{|c|c|c|} \hline 1 & 2 & 3 \\ \hline 4 & 5 & \\ \hline \end{array} \prec \begin{array}{|c|c|c|} \hline 1 & 2 & 4 \\ \hline 3 & 5 & \\ \hline \end{array} \prec \begin{array}{|c|c|c|} \hline 1 & 2 & 5 \\ \hline 3 & 4 & \\ \hline \end{array} \prec \begin{array}{|c|c|c|} \hline 1 & 3 & 4 \\ \hline 2 & 5 & \\ \hline \end{array} \prec \begin{array}{|c|c|c|} \hline 1 & 3 & 5 \\ \hline 2 & 4 & \\ \hline \end{array} . \quad (3.136)$$

$\mathfrak{R}_\Theta = \underbrace{(1,2,3,4,5)} \quad \mathfrak{R}_\Theta = \underbrace{(1,2,4,3,5)} \quad \mathfrak{R}_\Theta = \underbrace{(1,2,5,3,4)} \quad \mathfrak{R}_\Theta = \underbrace{(1,3,4,2,5)} \quad \mathfrak{R}_\Theta = \underbrace{(1,3,5,2,4)}$

It turns out that this order relation defines exactly when a pair of boxes  $(\square_k, \square_l)$  appearing in the same column of a tableau  $\Theta$  appear in the same row of a tableau  $\Phi$ , forcing the product  $\mathbf{A}_\Theta \mathbf{S}_\Phi$  to vanish [85, section 5.3, Theorem V]. We repeat the proof given by [85]: Let  $\Theta$  and  $\Phi$  be two Young tableaux of the same shape and let  $\Theta \prec \Phi$ . Then, the first entry  $\theta_{ij} \in \mathfrak{R}_\Theta$  distinct from  $\phi_{ij} \in \mathfrak{R}_\Phi$  satisfies  $\theta_{ij} < \phi_{ij}$ . Thus, the entry  $\phi_{kl} \in \mathfrak{R}_\Phi$  such that  $\theta_{ij} = \phi_{kl}$  must appear in a row below row  $i$ , but, by definition of Young tableaux, must be in a column to the left of column  $j$ ,

$$\theta_{ij} = \phi_{kl} \quad \text{with } l < j \text{ and } k > i . \quad (3.137)$$

Since  $l < j$ , the entries  $\theta_{il}$  and  $\phi_{il}$  must be equal (we assumed that the entries  $\theta_{ij}$  and  $\phi_{ij}$  were the *first* distinct entries appearing in the respective row-words),  $\theta_{il} = \phi_{il}$ . Thus, the pair of entries  $(\theta_{ij} = \phi_{kl}, \theta_{il} = \phi_{il})$  appears in the same row in  $\Theta$  (the  $i^{\text{th}}$  row) and in the same column in  $\Phi$  (the  $l^{\text{th}}$  column), yielding  $\mathbf{A}_\Phi \mathbf{S}_\Theta = 0$ . Thus, we can say that

$$\Theta \prec \Phi \implies Y_\Phi Y_\Theta = 0 . \quad (3.138)$$

It should be noted that (3.138) does not necessarily hold for the reverse ordering of the Young projectors, that is

$$\Theta \prec \Phi \not\implies Y_\Theta Y_\Phi = 0 . \quad (3.139)$$

Littlewood uses this one-sided transversality of Young projection operators to create mutually transversal ones:

Let  $\{\Theta_1, \Theta_2, \dots, \Theta_k\}$  be the set of all Young tableaux in  $\mathcal{Y}_n$  with a particular shape  $\mathbf{Y}_\Theta$ , and let them be ordered such that  $\Theta_i \prec \Theta_j$  whenever  $i < j$ . From eq. (3.138), we have that

$$Y_{\Theta_j} Y_{\Theta_i} = 0 \quad \text{whenever } i < j . \quad (3.140)$$

The Littlewood-Young projection operators  $L_{\Theta_i}$  corresponding to the tableaux  $\Theta_i \in \{\Theta_1, \Theta_2, \dots, \Theta_k\} \subset \mathcal{Y}_n$

<sup>23</sup>In words, we order a set of tableaux according to the relative lexical order of their associated row-words. This concept is not to be confused with the lexical order *within* a tableau introduced in Definition 3.2.

are defined as

$$\begin{aligned}
 L_{\Theta_1} &= Y_{\Theta_1} \\
 L_{\Theta_2} &= (1 - L_{\Theta_1})Y_{\Theta_2} \\
 &\vdots \\
 L_{\Theta_k} &= (1 - L_{\Theta_1} - L_{\Theta_2} - \dots - L_{\Theta_{k-1}})Y_{\Theta_k} .
 \end{aligned} \tag{3.141}$$

It should be noticed that the LY-operators corresponding to tableaux in  $\mathcal{Y}_n$  for  $n \leq 4$  reduce to the Young projectors, as, in these instances, the Young projectors are mutually transversal. Even for  $n > 5$ , many LY-projection operators reduce to the regular Young projectors, or at least simplify drastically, since most of the Young projectors remain transversal even for large  $n$ . As an example, at  $n = 5$  the only two Littlewood-Young projection operators that differ from their Young counterpart are given by

$$L_{\begin{array}{|c|c|c|} \hline 1 & 3 & 5 \\ \hline 2 & 4 & \\ \hline \end{array}} = \left(1 - Y_{\begin{array}{|c|c|} \hline 1 & 2 & 3 \\ \hline 4 & 5 & \\ \hline \end{array}}\right) Y_{\begin{array}{|c|c|c|} \hline 1 & 3 & 5 \\ \hline 2 & 4 & \\ \hline \end{array}} \quad \text{and} \quad L_{\begin{array}{|c|c|} \hline 1 & 4 \\ \hline 2 & 5 \\ \hline 3 & \\ \hline \end{array}} = \left(1 - Y_{\begin{array}{|c|c|} \hline 1 & 2 \\ \hline 3 & 4 \\ \hline 5 & \\ \hline \end{array}}\right) Y_{\begin{array}{|c|c|} \hline 1 & 4 \\ \hline 2 & 5 \\ \hline 3 & \\ \hline \end{array}} . \tag{3.142}$$

The LY-operators constructed according to (3.141) are transversal for all values of  $n$ : If two operators  $L_{\Theta}$  and  $L_{\Phi}$  correspond to tableaux of different shapes, then  $L_{\Theta}$  and  $L_{\Phi}$  are transversal since their respective constituent Young projection operators are transversal. If  $L_{\Theta_i}$  and  $L_{\Theta_j}$  correspond to tableaux of the same shape with  $\Theta_i \prec \Theta_j$  ( $i < j$ ), then

$$L_{\Theta_j} L_{\Theta_i} = 0 \quad \text{from eq. (3.140)} \tag{3.143}$$

To show the reverse ( $L_{\Theta_i} L_{\Theta_j} = 0$ ), it is highly advantageous to note that  $L_{\Theta_j}$  as given in (3.141) can be recast as

$$L_{\Theta_j} = (1 - Y_{\Theta_1})(1 - Y_{\Theta_2}) \cdots (1 - Y_{\Theta_{j-1}})Y_{\Theta_j} . \tag{3.144}$$

This can be shown by induction: For  $j = 1, 2$  eq. (3.144) trivially holds, we therefore go through the case  $j = 3$  explicitly:

$$L_{\Theta_3} = \left(1 - \underbrace{Y_{\Theta_1}}_{=L_{\Theta_1}} - \underbrace{(1 - Y_{\Theta_1})Y_{\Theta_2}}_{=L_{\Theta_2}}\right) Y_{\Theta_3} = ((1 - Y_{\Theta_1}) - (1 - Y_{\Theta_1})Y_{\Theta_2})Y_{\Theta_3} = (1 - Y_{\Theta_1})(1 - Y_{\Theta_2})Y_{\Theta_3} . \tag{3.145}$$

Suppose eq. (3.144) holds for all  $L_{\Theta_k}$  up some integer  $k = j - 1$ . Then, by eq. (3.141),  $L_{\Theta_j}$  is given by

$$\begin{aligned}
 L_{\Theta_j} &= \left(\underbrace{1 - Y_{\Theta_1}}_{=(1 - Y_{\Theta_1})} - (1 - Y_{\Theta_1})Y_{\Theta_2} - \dots - (1 - Y_{\Theta_1})(1 - Y_{\Theta_2}) \cdots (1 - Y_{\Theta_{j-2}})Y_{\Theta_{j-1}}\right) Y_{\Theta_j} \\
 &= (1 - Y_{\Theta_1}) \left(\underbrace{1 - Y_{\Theta_2}}_{=(1 - Y_{\Theta_2})} - (1 - Y_{\Theta_2})Y_{\Theta_3} - \dots - (1 - Y_{\Theta_2}) \cdots (1 - Y_{\Theta_{j-2}})Y_{\Theta_{j-1}}\right) Y_{\Theta_j} \\
 &= (1 - Y_{\Theta_1})(1 - Y_{\Theta_2}) \left(\underbrace{1 - Y_{\Theta_3}}_{=(1 - Y_{\Theta_3})} - (1 - Y_{\Theta_3})Y_{\Theta_4} - \dots - (1 - Y_{\Theta_3}) \cdots (1 - Y_{\Theta_{j-2}})Y_{\Theta_{j-1}}\right) Y_{\Theta_j}
 \end{aligned}$$

$$\begin{aligned} & \vdots \\ & = (1 - Y_{\Theta_1})(1 - Y_{\Theta_2}) \cdots (1 - Y_{\Theta_{j-1}})Y_{\Theta_j} , \end{aligned} \quad (3.146)$$

confirming eq. (3.144).

Let

$$M_{\Theta_{i-1}} := (1 - Y_{\Theta_1})(1 - Y_{\Theta_2}) \cdots (1 - Y_{\Theta_{i-1}}) \quad (3.147)$$

such that  $L_{\Theta_i} = M_{\Theta_{i-1}}Y_{\Theta_i}$ . From eq. (3.140) it is clear that

$$Y_{\Theta_k}(1 - Y_{\Theta_l}) = Y_{\Theta_k} - 0 = Y_{\Theta_k} \quad \text{for every } l < k . \quad (3.148)$$

Thus, if  $i < j$  we have that

$$\begin{aligned} L_{\Theta_i} \cdot L_{\Theta_j} &= \underbrace{M_{\Theta_{i-1}}Y_{\Theta_i}}_{=L_{\Theta_i}} \cdot \underbrace{(1 - Y_{\Theta_1}) \cdots (1 - Y_{\Theta_i}) \cdots (1 - Y_{\Theta_{j-1}})Y_{\Theta_j}}_{=L_{\Theta_j}} \\ &\stackrel{\text{eq. (3.148)}}{=} M_{\Theta_{i-1}} \underbrace{Y_{\Theta_i}(1 - Y_{\Theta_i})}_{=Y_{\Theta_i} - Y_{\Theta_i}^2 = 0} \cdots (1 - Y_{\Theta_{j-1}})Y_{\Theta_j} \\ &= 0 , \end{aligned} \quad (3.149)$$

where we used the fact that Young projectors are idempotent ( $Y_{\Theta_i}^2 = Y_{\Theta_i}$ ). Thus,  $L_{\Theta_i}$  and  $L_{\Theta_j}$  are transversal even if  $i < j$ .

We notice that the  $L_{\Theta}$  remain idempotent just like their Young counterparts,

$$L_{\Theta_i} \cdot L_{\Theta_i} = L_{\Theta_i} \underbrace{(1 - L_{\Theta_1} - L_{\Theta_2} - \cdots - L_{\Theta_{i-1}})}_{=L_{\Theta_i}} Y_{\Theta_i} = (L_{\Theta_i} - 0 - 0 - \cdots - 0)Y_{\Theta_i} = L_{\Theta_i}Y_{\Theta_i} = L_{\Theta_i} . \quad (3.150)$$

Putting everything together, we can conclude that

$$L_{\Theta}L_{\Phi} = \delta_{\Theta\Phi}L_{\Phi} \quad \text{for all } \Theta, \Phi \in \mathcal{Y}_n \text{ for all values of } n , \quad (3.151)$$

confirming eqns. (3.6a) and (3.6b).

Since the LY-operators are mutually transversal (eq. (3.151)), they can be simultaneously diagonalised and have images that only intersect at 0. Since they are idempotent, their trace provides the dimension of their image:

$$\text{tr}(L_{\Theta}) = \dim(\Theta) . \quad (3.152)$$

Thus, if we can show that the dimensions of the subspaces corresponding to the  $L_{\Theta}$  sum up to the dimension of the whole space  $\dim(V^{\otimes n}) = N^n$ , it must hold that the transversal operators  $L_{\Theta}$  sum up to the identity on  $V^{\otimes n}$ . To show this, we notice that  $L_{\Theta}$  has the same trace as its counterpart  $Y_{\Theta}$ : Using the cyclic property

of the trace, we have

$$\begin{aligned}
 \operatorname{tr}(L_{\Theta_i}) &= \operatorname{tr}\left(\left(1 - L_{\Theta_1} - L_{\Theta_2} - \dots - L_{\Theta_{i-1}}\right)Y_{\Theta_i}\right) \\
 &= \operatorname{tr}\left(Y_{\Theta_i}\left(1 - L_{\Theta_1} - L_{\Theta_2} - \dots - L_{\Theta_{i-1}}\right)\right) \\
 &= \operatorname{tr}\left(Y_{\Theta_i} - 0 - 0 - \dots - 0\right) \\
 &= \operatorname{tr}\left(Y_{\Theta_i}\right) ,
 \end{aligned} \tag{3.153}$$

which implies that

$$\sum_{\Theta \in \mathcal{Y}_n} \operatorname{tr}(L_{\Theta}) = \sum_{\Theta \in \mathcal{Y}_n} \operatorname{tr}(Y_{\Theta}) = N^n \quad \text{for all } n, \text{ where } N = \dim(V) . \tag{3.154}$$

Therefore, we conclude that the LY-operators sum up to the identity on the space  $V^{\otimes n}$

$$\sum_{\Theta \in \mathcal{Y}_n} L_{\Theta} = \operatorname{id}_n \quad \text{for all } n , \tag{3.155}$$

as was claimed in eq. (3.6c).

### 3.B Young projectors that do not commute with their ancestors

In this appendix, we prove that the standard Young projection operators, which do not project onto subspaces included in the image of their ancestors (unlike their Hermitian counterpart, *c.f.* Lemma 3.2),

$$Y_{\Theta}Y_{\Theta_{(m)}} \neq Y_{\Theta} \quad \text{and/or} \quad Y_{\Theta_{(m)}}Y_{\Theta} \neq Y_{\Theta} \tag{3.156}$$

do not commute with their ancestor operators. While there exist Young projection operators for which one of the two equations (3.156) yields an equality, for example

$$Y_{\begin{smallmatrix} \boxed{12} \\ \boxed{3} \end{smallmatrix}} \cdot Y_{\begin{smallmatrix} \boxed{12} \\ \boxed{3} \end{smallmatrix}} = Y_{\begin{smallmatrix} \boxed{12} \\ \boxed{3} \end{smallmatrix}} , \tag{3.157}$$

for most Young projection operators neither of these conditions hold, e.g.

$$Y_{\begin{smallmatrix} \boxed{12} \\ \boxed{34} \end{smallmatrix}} \cdot Y_{\begin{smallmatrix} \boxed{12} \\ \boxed{3} \end{smallmatrix}} \neq Y_{\begin{smallmatrix} \boxed{12} \\ \boxed{34} \end{smallmatrix}} \quad \text{and} \quad Y_{\begin{smallmatrix} \boxed{12} \\ \boxed{3} \end{smallmatrix}} \cdot Y_{\begin{smallmatrix} \boxed{12} \\ \boxed{34} \end{smallmatrix}} \neq Y_{\begin{smallmatrix} \boxed{12} \\ \boxed{34} \end{smallmatrix}} . \tag{3.158}$$

■ **Lemma 3.2 – Young operators do not generally commute with their ancestor operators:**

Let  $\Theta$  be a Young tableau and  $\Theta_{(m)}$  be its ancestor  $m$  generations back, where  $m$  is a strictly positive integer ( $m > 0$ ). If the images of  $Y_{\Theta}$  and  $Y_{\Theta_{(m)}}$  are not nested, i.e.  $Y_{\Theta}Y_{\Theta_{(m)}} \neq Y_{\Theta}$  and/or  $Y_{\Theta_{(m)}}Y_{\Theta} \neq Y_{\Theta}$ , then  $Y_{\Theta}$  and  $Y_{\Theta_{(m)}}$  do not commute,

$$[Y_{\Theta}, Y_{\Theta_{(m)}}] \neq 0 . \tag{3.159}$$

Conversely, a vanishing commutator  $[Y_{\Theta}, Y_{\Theta_{(m)}}] = 0$  implies image inclusion  $Y_{\Theta}Y_{\Theta_{(m)}} = Y_{\Theta} = Y_{\Theta_{(m)}}Y_{\Theta}$ .

*Proof of Lemma 3.2:* We present a proof by contradiction: Suppose there exists a Young projection operator

$Y_\Theta$  which commutes with its ancestor operator  $Y_{\Theta(m)}$  while  $Y_{\Theta(m)}Y_\Theta \neq Y_\Theta$ ,

$$Y_\Theta Y_{\Theta(m)} = Y_{\Theta(m)} Y_\Theta . \quad (3.160)$$

If we multiply equation (3.160) with the operator  $Y_\Theta$  on the right, and use Theorem 3.1 to simplify the LHS of the resulting equation, we obtain

$$\underbrace{Y_\Theta Y_{\Theta(m)} Y_\Theta}_{=Y_\Theta Y_\Theta = Y_\Theta} = Y_{\Theta(m)} \underbrace{Y_\Theta Y_\Theta}_{=Y_\Theta} \implies Y_\Theta = Y_{\Theta(m)} Y_\Theta , \quad (3.161)$$

a contradiction. The case where  $Y_\Theta Y_{\Theta(m)} \neq Y_\Theta$  follows from left multiplication with  $Y_\Theta$ .  $\square$

We note that Lemma 3.2 is the reason why the proof of the summation property for Hermitian Young projection operators (3.99) breaks down for most Young projectors at the last step (eq. (3.110)), since

$$\left[ \sum_{\Theta \in \mathcal{Y}_{n-1}} \left( \sum_{\Psi \in \{\Theta \otimes \square_n\}} Y_\Psi \right) \right] \cdot Y_{\Theta'} \neq \sum_{\Theta \in \mathcal{Y}_{n-1}} \left( \delta_{\Theta \Theta'} \sum_{\Psi \in \{\Theta \otimes \square_n\}} Y_\Psi \right) . \quad (3.162)$$

## 3.C Proofs of the construction principles for Hermitian Young projection operators

This appendix provides the proofs of the Theorems given in section 3.4.

### 3.C.1 Proof of Theorem 3.4 “lexical Hermitian Young projectors”

The proof of Theorem 3.4 makes use of propagation rules of birdtrack operators [1] [chapter 2]. We thus summarize the applicable rules of [1] [chapter 2] in section 3.C.1.1, before giving the proof of the Lexical Theorem 3.4 in section 3.C.1.2.

#### 3.C.1.1 Propagation rules

We first require the definition of a new quantity, an *amputated* tableau:

**Definition 3.5 – amputated (Young) tableaux:**

Let  $\Theta$  be a (Young) tableau and let  $\mathcal{C}$  denote a particular column in  $\Theta$ . We construct the row-amputated tableau of  $\Theta$  according to  $\mathcal{C}$ ,  $\mathcal{O}_r[\mathcal{C}]$ , by removing all rows of  $\Theta$  which do not overlap with  $\mathcal{C}$ .

Similarly, if  $\mathcal{R}$  is a particular row in  $\Theta$ , we construct the column-amputated tableau of  $\Theta$  according to  $\mathcal{R}$ ,  $\mathcal{O}_c[\mathcal{R}]$ , by removing all columns that do not overlap with  $\mathcal{R}$ .

For example, for the following tableau  $\Theta$ , the row amputated tableau  $\mathcal{O}_r$  according to column  $(3, 4, 7)^t$  is

$$\Theta = \begin{array}{|c|c|c|c|} \hline 1 & 3 & 5 & 9 \\ \hline 2 & 4 & 8 & 10 \\ \hline 6 & 7 & 13 & \\ \hline 11 & & & \\ \hline 12 & & & \\ \hline \end{array} \mapsto \mathcal{O}_r[(3, 4, 7)^t] = \begin{array}{|c|c|c|c|} \hline 1 & 3 & 5 & 9 \\ \hline 2 & 4 & 8 & 10 \\ \hline 6 & 7 & 13 & \\ \hline & & & \\ \hline & & & \\ \hline \end{array} ; \quad (3.163)$$



the rows (11) and (12) were deleted since they did not overlap with the shaded column  $(3, 4, 7)^t$ . An example for column amputation is shown in the step from eq. (3.169) to (3.170). The idea of amputated tableaux is necessary to describe the following simplification rule for birdtrack operators:

■ **Theorem 3.6 – propagation of (anti-)symmetrizers:**

Let  $\Theta$  be a Young tableau and  $O$  be a birdtrack operator of the form

$$O = \mathbf{S}_\Theta \mathbf{A}_\Theta \mathbf{S}_{\Theta \setminus \mathcal{R}} , \quad (3.164)$$

in which the symmetrizer set  $\mathbf{S}_{\Theta \setminus \mathcal{R}}$  arises from  $\mathbf{S}_\Theta$  by removing precisely one symmetrizer  $\mathbf{S}_\mathcal{R}$ . By definition,  $\mathbf{S}_\mathcal{R}$  corresponds to a row  $\mathcal{R}$  in  $\Theta$  such that  $\mathbf{S}_\Theta = \mathbf{S}_{\Theta \setminus \mathcal{R}} \mathbf{S}_\mathcal{R} = \mathbf{S}_\mathcal{R} \mathbf{S}_{\Theta \setminus \mathcal{R}}$ .

If the column-amputated tableau of  $\Theta$  according to the row  $\mathcal{R}$ ,  $\Theta_c[\mathcal{R}]$ , is **rectangular**, then the symmetrizer  $\mathbf{S}_\mathcal{R}$  may be propagated through the set  $\mathbf{A}_\Theta$  from the left to the right, yielding

$$O = \mathbf{S}_\Theta \mathbf{A}_\Theta \mathbf{S}_{\Theta \setminus \mathcal{R}} = \mathbf{S}_{\Theta \setminus \mathcal{R}} \mathbf{A}_\Theta \mathbf{S}_\Theta , \quad (3.165)$$

which implies that  $O$  is Hermitian. We may think of this procedure as moving the missing symmetrizer  $\mathbf{S}_\mathcal{R}$  through the intervening antisymmetrizer set  $\mathbf{A}_\Theta$ .

Noting that  $\mathbf{S}_\Theta = \mathbf{S}_\Theta \mathbf{S}_\mathcal{R} = \mathbf{S}_\mathcal{R} \mathbf{S}_\Theta$ , we immediately augment this statement to

$$\mathbf{S}_\Theta \mathbf{A}_\Theta \mathbf{S}_{\Theta \setminus \mathcal{R}} = \mathbf{S}_{\Theta \setminus \mathcal{R}} \mathbf{A}_\Theta \mathbf{S}_\Theta = \mathbf{S}_\Theta \mathbf{A}_\Theta \mathbf{S}_\Theta . \quad (3.166)$$

If the roles of symmetrizers and antisymmetrizers are exchanged, we need to verify that the row-amputated tableau  $\Theta_r[\mathcal{C}]$  with respect to a column  $\mathcal{C}$  is rectangular to guarantee that

$$\mathbf{A}_\Theta \mathbf{S}_\Theta \mathbf{A}_{\Theta \setminus \mathcal{C}} = \mathbf{A}_{\Theta \setminus \mathcal{C}} \mathbf{S}_\Theta \mathbf{A}_\Theta = \mathbf{A}_\Theta \mathbf{S}_\Theta \mathbf{A}_\Theta . \quad (3.167)$$

This amounts to moving the missing antisymmetrizer  $\mathbf{A}_\mathcal{C}$  through the intervening symmetrizer set  $\mathbf{S}_\Theta$ .

As an example, consider the operator  $Q$  given by

$$Q := \begin{array}{c} \begin{array}{|c|c|c|} \hline \vdots & \vdots & \vdots \\ \hline \vdots & \vdots & \vdots \\ \hline \vdots & \vdots & \vdots \\ \hline \vdots & \vdots & \vdots \\ \hline \end{array} \\ \mathbf{S}_\Theta \end{array} \begin{array}{c} \begin{array}{|c|} \hline \vdots \\ \hline \vdots \\ \hline \vdots \\ \hline \vdots \\ \hline \end{array} \\ \mathbf{A}_\Theta \end{array} \begin{array}{c} \begin{array}{|c|c|c|} \hline \vdots & \vdots & \vdots \\ \hline \vdots & \vdots & \vdots \\ \hline \vdots & \vdots & \vdots \\ \hline \vdots & \vdots & \vdots \\ \hline \end{array} \\ \mathbf{S}_{\Theta \setminus \mathcal{R}} \end{array} , \quad (3.168)$$

To check if the amputated tableau is rectangular, we first need to reconstruct  $\Theta$  with rows corresponding to  $\mathbf{S}_\Theta$  and columns corresponding to  $\mathbf{A}_\Theta$ . Evidently,

$$\Theta = \begin{array}{|c|c|c|} \hline 1 & 2 & 3 \\ \hline 4 & 5 & \\ \hline 6 & 7 & \\ \hline \end{array} . \quad (3.169)$$

In  $\Theta$ , we have marked the row  $(6, 7)$  corresponding to the symmetrizer  $\mathbf{S}_{67}$ , which we would like to propagate through to the right. Thus, in accordance with Theorem 3.6, we form the column-amputated tableau of  $\Theta$

according to the row (6, 7),

$$\mathcal{O}_c[(6, 7)] = \begin{array}{|c|c|} \hline 1 & 2 \\ \hline 4 & 5 \\ \hline 6 & 7 \\ \hline \end{array}, \quad (3.170)$$

and see that it is indeed a rectangular tableau. Thus, we may propagate the symmetrizer  $\mathcal{S}_{67}$  from the left to the right,

$$Q = \begin{array}{c} \text{---} \\ \text{---} \\ \text{---} \\ \text{---} \\ \text{---} \\ \text{---} \end{array} \begin{array}{c} \text{---} \\ \text{---} \\ \text{---} \\ \text{---} \\ \text{---} \\ \text{---} \end{array} = \begin{array}{c} \text{---} \\ \text{---} \\ \text{---} \\ \text{---} \\ \text{---} \\ \text{---} \end{array} \begin{array}{c} \text{---} \\ \text{---} \\ \text{---} \\ \text{---} \\ \text{---} \\ \text{---} \end{array} = \begin{array}{c} \text{---} \\ \text{---} \\ \text{---} \\ \text{---} \\ \text{---} \\ \text{---} \end{array}. \quad (3.171)$$

### 3.C.1.2 Proof of Theorem 3.4:

We will present a proof by induction: First, we prove the *Base Step* for the projection operators of  $\text{SU}(N)$  over  $V^{\otimes 3}$  (i.e with 3 legs), since this is the smallest instant for which the KS algorithm produces a new operator (and also the first instant for which *non-Hermitian* Young projectors occur). Thereafter, we will consider a general projection operator corresponding to a Young tableau  $\Theta \in \mathcal{Y}_{m+1}$  with a lexically ordered column-word (the proof for operators corresponding to row-ordered Young tableaux is very similar and thus left as an exercise to the reader). We will assume that Theorem 3.4 is true for the Hermitian operator corresponding to its parent tableau  $P_{\Theta_{(1)}}$ , where  $\Theta_{(1)} \in \mathcal{Y}_m$ ; this is the *Induction Hypothesis*. Then, we show that the projection operators obtained from the KS Theorem reduce to the expression given in the Lexical Theorem 3.4,

$$P_\Theta = P_{\Theta_{(1)}} Y_\Theta P_{\Theta_{(1)}} = \alpha_\Theta \cdot \bar{Y}_\Theta^\dagger \bar{Y}_\Theta, \quad (3.172)$$

concluding the proof.

**The Base Step:** For the projection operators of  $\text{SU}(N)$  over  $V^{\otimes 1}$  or  $V^{\otimes 2}$  (i.e. with 1 or 2 legs), the proof of (3.172) is trivial since all Young projection operators are automatically Hermitian; thus,  $\bar{Y}_\Theta^\dagger = \bar{Y}_\Theta$ , and (3.172) reduces to

$$\alpha_\Theta \cdot \bar{Y}_\Theta^\dagger \bar{Y}_\Theta = \alpha_\Theta \underbrace{\bar{Y}_\Theta \bar{Y}_\Theta}_{\frac{1}{\alpha_\Theta} \bar{Y}_\Theta} = \bar{Y}_\Theta. \quad (3.173)$$

Since all Young projection operators  $Y_\Theta$  with  $\Theta \in \mathcal{Y}_{1,2}$  have normalization constant 1 (as can easily be checked by looking at all three of them explicitly),  $Y_\Theta = \bar{Y}_\Theta$  holds for these operators. Thus, the Lexical Theorem 3.4 returns the original, already Hermitian operators, as does the KS algorithm. The first nontrivial differences occur for  $n = 3$ . We use this as the base step. Here, we have the following Young projection operators corresponding to their respective Young tableaux,

$$\begin{array}{c} \text{---} \\ \text{---} \\ \text{---} \end{array} \quad \frac{4}{3} \begin{array}{c} \text{---} \\ \text{---} \\ \text{---} \end{array} \quad \frac{4}{3} \begin{array}{c} \text{---} \\ \text{---} \\ \text{---} \end{array} \quad \text{and} \quad \begin{array}{c} \text{---} \\ \text{---} \\ \text{---} \end{array} \quad (3.174a)$$

$$\begin{array}{|c|} \hline 1 \\ \hline 2 \\ \hline 3 \\ \hline \end{array} \quad \begin{array}{|c|c|} \hline 1 & 3 \\ \hline 2 & \\ \hline \end{array} \quad \begin{array}{|c|c|} \hline 1 & 2 \\ \hline 3 & \\ \hline \end{array} \quad \begin{array}{|c|c|c|} \hline 1 & 2 & 3 \\ \hline \end{array}. \quad (3.174b)$$

In (3.174a), the first and last operator are already Hermitian and have normalization constant 1. Therefore, the Lexical Theorem will return these operators unchanged, *c.f.* eq. (3.173).

The second and third tableaux in (3.174b) are lexically column-ordered and row-ordered respectively. Thus, we must construct their Hermitian Young projection operators according to prescriptions (3.117b) and (3.117a) respectively.

Table 3.1 shows that the construction of the Hermitian projection operators corresponding to the tableaux (3.174b) obtained from the Lexical Theorem 3.4 is equivalent that of the KS Theorem 3.3, [4], thus concluding the base step of this proof:

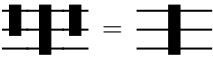
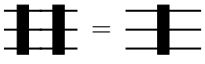
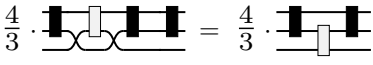
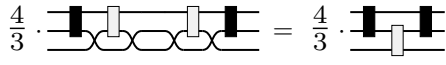
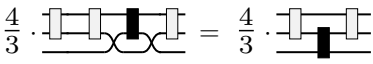
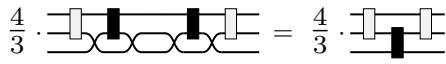
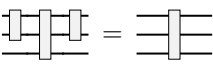
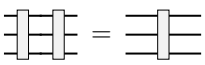
KS Theorem 3.3 [4] (Multiplying Hermitian parent on either side)	Lexical Theorem 3.4 (Multiplying by Hermitian conjugate on appropriate side)
	
	
	
	

Table 3.1: This table contrasts the construction of Hermitian Young projection operators according to the KS Theorem 3.3 (left), with that according to the Lexical Theorem 3.4 (right). Despite visible algorithmic differences, the results are identical.

**The Induction Step:** Let  $\Theta \in \mathcal{Y}_{m+1}$  be a tableau with a lexically ordered column-word, and let  $\Theta_{(1)} \in \mathcal{Y}_m$  be its parent tableau. Clearly, the column-word of  $\Theta_{(1)}$  is also in lexical order. We will assume that the Lexical Theorem 3.4 holds for the Hermitian Young projection operator  $P_{\Theta_{(1)}}$ , i.e. that

$$P_{\Theta_{(1)}} = \alpha_{\Theta} \cdot \bar{Y}_{\Theta_{(1)}}^{\dagger} \bar{Y}_{\Theta_{(1)}}, \quad (3.175)$$

and we will refer to this condition as the *Induction Hypothesis*. Thus, according to this induction hypothesis,  $P_{\Theta_{(1)}}$  can be written in terms of sets of symmetrizers and antisymmetrizers corresponding to the tableau  $\Theta_{(1)}$  as

$$P_{\Theta_{(1)}} = \alpha_{\Theta_{(1)}} \cdot \mathbf{A}_{\Theta_{(1)}} \mathbf{S}_{\Theta_{(1)}} \mathbf{A}_{\Theta_{(1)}}, \quad (3.176)$$

where we used the fact that  $\mathbf{S}_{\Theta_{(1)}} \mathbf{S}_{\Theta_{(1)}} = \mathbf{S}_{\Theta_{(1)}}$ . We now construct  $\bar{P}_{\Theta}$  from  $\bar{P}_{\Theta_{(1)}}$  using the KS Theorem 3.3; we have

$$\bar{P}_{\Theta} = \underbrace{\mathbf{A}_{\Theta_{(1)}} \mathbf{S}_{\Theta_{(1)}} \mathbf{A}_{\Theta_{(1)}}}_{\bar{P}_{\Theta_{(1)}}} \underbrace{\mathbf{S}_{\Theta} \mathbf{A}_{\Theta}}_{\bar{Y}_{\Theta}} \underbrace{\mathbf{A}_{\Theta_{(1)}} \mathbf{S}_{\Theta_{(1)}} \mathbf{A}_{\Theta_{(1)}}}_{\bar{P}_{\Theta_{(1)}}}. \quad (3.177)$$

In the above, we have chosen to ignore the proportionality constant for now, as carrying it with us would draw attention away from the important steps of the proof. Once we have shown that  $\bar{P}_\Theta = \bar{Y}_\Theta^\dagger \bar{Y}_\Theta$ , we will show that the proportionality constant  $\alpha_\Theta$  given in (3.172) (*c.f.* (3.117b)) is indeed the one we require for  $P_\Theta$  to be idempotent.

Since  $\Theta_{(1)}$  is the parent tableau of  $\Theta$ , the images of all symmetrizers and antisymmetrizers in  $Y_\Theta$  (and thus  $P_\Theta$ ) are contained in the images of the symmetrizers and antisymmetrizers in  $Y_{\Theta_{(1)}}$  respectively,<sup>24</sup>

$$\mathbf{S}_\Theta \subset \mathbf{S}_{\Theta_{(1)}} \quad \text{and} \quad \mathbf{A}_\Theta \subset \mathbf{A}_{\Theta_{(1)}}, \quad (3.178)$$

and hence

$$\mathbf{S}_{\Theta_{(1)}} \mathbf{S}_\Theta = \mathbf{S}_\Theta = \mathbf{S}_\Theta \mathbf{S}_{\Theta_{(1)}} \quad \text{and} \quad \mathbf{A}_{\Theta_{(1)}} \mathbf{A}_\Theta = \mathbf{A}_\Theta = \mathbf{A}_\Theta \mathbf{A}_{\Theta_{(1)}}, \quad (3.179)$$

*c.f.* eq. (3.43). Therefore, we are able to factor  $\mathbf{S}_{\Theta_{(1)}}$  out of  $\mathbf{S}_\Theta$  in (3.177) to obtain

$$\bar{P}_\Theta = \underbrace{\mathbf{A}_{\Theta_{(1)}} \mathbf{S}_{\Theta_{(1)}}}_{= \bar{Y}_{\Theta_{(1)}}^\dagger} \underbrace{\mathbf{A}_{\Theta_{(1)}} \mathbf{S}_{\Theta_{(1)}}}_{= \bar{Y}_{\Theta_{(1)}}^\dagger} \overset{\mathbf{S}_\Theta \rightarrow \mathbf{S}_{\Theta_{(1)}} \mathbf{S}_\Theta}{\mathbf{S}_\Theta} \mathbf{A}_\Theta \mathbf{A}_{\Theta_{(1)}} \mathbf{S}_{\Theta_{(1)}} \mathbf{A}_{\Theta_{(1)}}. \quad (3.180)$$

Since  $Y_{\Theta_{(1)}}^\dagger = \alpha_{\Theta_{(1)}} \bar{Y}_{\Theta_{(1)}}^\dagger$  is a projection operator, it follows that  $Y_{\Theta_{(1)}}^\dagger Y_{\Theta_{(1)}}^\dagger = Y_{\Theta_{(1)}}^\dagger$ . Hence, eq. (3.180) reduces to (making use of the bar-notation to retain equality, *c.f.* eq. (3.33))

$$\bar{P}_\Theta = \underbrace{\mathbf{A}_{\Theta_{(1)}} \mathbf{S}_{\Theta_{(1)}}}_{= \bar{Y}_{\Theta_{(1)}}^\dagger} \overset{\mathbf{S}_{\Theta_{(1)}} \mathbf{S}_\Theta \rightarrow \mathbf{S}_\Theta}{\mathbf{S}_\Theta} \mathbf{A}_\Theta \mathbf{A}_{\Theta_{(1)}} \mathbf{S}_{\Theta_{(1)}} \mathbf{A}_{\Theta_{(1)}} = \mathbf{A}_{\Theta_{(1)}} \mathbf{S}_\Theta \mathbf{A}_\Theta \mathbf{S}_{\Theta_{(1)}} \mathbf{A}_{\Theta_{(1)}}, \quad (3.181)$$

$\mathbf{A}_\Theta \mathbf{A}_{\Theta_{(1)}} \rightarrow \mathbf{A}_\Theta$

where we used eq. (3.179) to reabsorb  $\mathbf{S}_{\Theta_{(1)}}$  into  $\mathbf{S}_\Theta$  and  $\mathbf{A}_{\Theta_{(1)}}$  into  $\mathbf{A}_\Theta$ . Thus

$$\bar{P}_\Theta = \mathbf{A}_{\Theta_{(1)}} \mathbf{S}_\Theta \mathbf{A}_\Theta \mathbf{S}_{\Theta_{(1)}} \mathbf{A}_{\Theta_{(1)}}. \quad (3.182)$$

To complete the proof, we have to distinguish two cases: The case where  $\boxed{m+1}$  lies in the first row of  $\Theta$ , and the case where it is positioned in any *but* the first row.

1. Suppose  $\boxed{m+1}$  lies in the first row of  $\Theta$ . Since this is the box containing the highest value in the tableau  $\Theta$ , there is no box positioned below it (otherwise  $\Theta$  would not be a Young tableau). Thus, the leg  $(m+1)$  is not contained in any antisymmetrizer (of length  $> 1$ ), yielding the sets  $\mathbf{A}_{\Theta_{(1)}}$  and  $\mathbf{A}_\Theta$  identical,  $\mathbf{A}_{\Theta_{(1)}} = \mathbf{A}_\Theta$ ,

$$\bar{P}_\Theta = \mathbf{A}_{\Theta_{(1)}} \mathbf{S}_\Theta \mathbf{A}_\Theta \mathbf{S}_{\Theta_{(1)}} \mathbf{A}_{\Theta_{(1)}} = \mathbf{A}_\Theta \boxed{\mathbf{S}_\Theta \mathbf{A}_\Theta \mathbf{S}_{\Theta_{(1)}} \mathbf{A}_\Theta}. \quad (3.183)$$

We now apply the Cancellation Theorem 3.2 to the part of  $P_\Theta$  in the red box to obtain

$$\bar{P}_\Theta = \mathbf{A}_\Theta \mathbf{S}_\Theta \mathbf{A}_\Theta \quad (3.184)$$

<sup>24</sup>We use the notation introduced in section 3.2.2.2.

as required.

2. Suppose now that  $\boxed{m+1}$  is situated in any but the first row of  $\Theta$ . In this case, the leg  $m+1$  does enter an antisymmetrizer (of length  $> 1$ ), thus  $\mathbf{A}_{\Theta_{(1)}} \neq \mathbf{A}_{\Theta}$  — a new strategy is needed. To understand the obstacles, let us once again look at the operator  $P_{\Theta}$  as described by equation (3.182),

$$\bar{P}_{\Theta} = \mathbf{A}_{\Theta_{(1)}} \mathbf{S}_{\Theta} \mathbf{A}_{\Theta} \mathbf{S}_{\Theta_{(1)}} \mathbf{A}_{\Theta_{(1)}}. \quad (3.185)$$

*Describing the strategy:* In (3.185), we have suggestively shaded a part of  $P_{\Theta}$ : if we were allowed to *exchange* the sets  $\mathbf{A}_{\Theta_{(1)}}$  and  $\mathbf{A}_{\Theta}$ , replacing  $\bar{P}_{\Theta}$  by

$$\mathbf{A}_{\Theta} \mathbf{S}_{\Theta} \mathbf{A}_{\Theta_{(1)}} \mathbf{S}_{\Theta_{(1)}} \mathbf{A}_{\Theta_{(1)}}, \quad (3.186)$$

we would be able to factor the symmetrizer  $\mathbf{S}_{\Theta_{(1)}}$  out of  $\mathbf{S}_{\Theta}$  by relation (3.179), and use the fact that  $Y_{\Theta_{(1)}} = \alpha_{\Theta_{(1)}} \bar{Y}_{\Theta_{(1)}}$  is a projection operator to obtain

$$(3.186) = \mathbf{A}_{\Theta} \mathbf{S}_{\Theta} \underbrace{\mathbf{S}_{\Theta_{(1)}} \mathbf{A}_{\Theta_{(1)}}}_{= \bar{Y}_{\Theta_{(1)}}} \underbrace{\mathbf{S}_{\Theta_{(1)}} \mathbf{A}_{\Theta_{(1)}}}_{= \bar{Y}_{\Theta_{(1)}}} = \mathbf{A}_{\Theta} \mathbf{S}_{\Theta} \mathbf{S}_{\Theta_{(1)}} \mathbf{A}_{\Theta_{(1)}}. \quad (3.187)$$

$\mathbf{S}_{\Theta} \rightarrow \mathbf{S}_{\Theta} \mathbf{S}_{\Theta_{(1)}}$

Re-absorbing  $\mathbf{S}_{\Theta_{(1)}}$  into  $\mathbf{S}_{\Theta}$  yields

$$(3.187) = \mathbf{A}_{\Theta} \mathbf{S}_{\Theta} \mathbf{S}_{\Theta_{(1)}} \mathbf{A}_{\Theta_{(1)}} = \mathbf{A}_{\Theta} \mathbf{S}_{\Theta} \mathbf{A}_{\Theta_{(1)}}. \quad (3.188)$$

$\mathbf{S}_{\Theta} \mathbf{S}_{\Theta_{(1)}} \rightarrow \mathbf{S}_{\Theta}$

From there, a similar argument as is needed to justify the missing step from (3.185) to (3.186) can be used to show that

$$\mathbf{A}_{\Theta} \mathbf{S}_{\Theta} \mathbf{A}_{\Theta_{(1)}} = \mathbf{A}_{\Theta} \mathbf{S}_{\Theta} \mathbf{A}_{\Theta}, \quad (3.189)$$

yielding the desired form of  $\bar{P}_{\Theta}$ . The main obstacle in achieving this result thus lies in the justification of the exchange of antisymmetrizers in the step from (3.185) to (3.186).

*The full argument:* We will accomplish this exchange of  $\mathbf{A}_{\Theta_{(1)}}$  and  $\mathbf{A}_{\Theta}$  within the marked region of (3.185) in the following way: Consider the Young tableaux  $\Theta_{(1)}$  and  $\Theta$  as depicted in Figure 3.3:

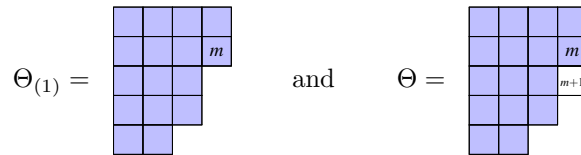


Figure 3.3: This figure gives a schematic depiction of the Young tableaux  $\Theta_{(1)}$  and  $\Theta$ . The boxes that are common in the two tableaux have been shaded in. The box with entry  $(m+1)$  has to lie in the bottom-most position of the last column of  $\Theta$ , as otherwise the column-word of  $\Theta$ ,  $\mathfrak{C}_{\Theta}$ , would not be in lexical order, contradictory to our initial assumption. The requirement that  $\mathfrak{C}_{\Theta}$  is lexically ordered therefore also uniquely determines the position of the box  $m$ , as is indicated in this figure.

Since, by assumption,  $\boxed{m+1}$  does *not* lie in the first row of  $\Theta$ , the leg  $(m+1)$  is contained in an antisymmetrizer (of length  $> 1$ ) in  $\mathbf{A}_\Theta$ , as was already mentioned previously. Let us denote this antisymmetrizer by  $\mathbf{A}_\Theta^{m+1} \in \mathbf{A}_\Theta$ . Furthermore, let  $\mathbf{A}_{\Theta_{(1)}}^m$  be the corresponding antisymmetrizer of the tableau  $\Theta_{(1)}$ : in other words,  $\mathbf{A}_{\Theta_{(1)}}^m$  is the antisymmetrizer  $\mathbf{A}_\Theta^{m+1}$  with the leg  $m+1$  removed. Hence  $\mathbf{A}_{\Theta_{(1)}}^m \supset \mathbf{A}_\Theta^{m+1}$ , using the notation introduced in section 3.2.2.2.

Since  $\Theta_{(1)}$  is the parent tableau of  $\Theta$ , all columns but the last will be identical in the two tableaux, see Figure 3.3. Thus, the antisymmetrizers corresponding to any but the last row will be contained in both sets  $\mathbf{A}_{\Theta_{(1)}}$  and  $\mathbf{A}_\Theta$ , which in particular implies that

$$\mathbf{A}_\Theta = \mathbf{A}_{\Theta_{(1)}} \mathbf{A}_\Theta^{m+1} \quad (3.190)$$

since  $\mathbf{A}_{\Theta_{(1)}}^m \supset \mathbf{A}_\Theta^{m+1}$ . Thus, if we were able to commute the antisymmetrizer  $\mathbf{A}_\Theta^{m+1}$  through the set  $\mathbf{S}_\Theta$  from the right to the left (and then absorb  $\mathbf{A}_{\Theta_{(1)}}^m$  into  $\mathbf{A}_\Theta^{m+1}$ ), we could cast  $P_\Theta$  into the desired form (3.186) (and thus (3.189)). In fact, this is exactly what we will do: According to Theorem 3.6, the antisymmetrizer  $\mathbf{A}_\Theta^{m+1}$  can be propagated through the set  $\mathbf{S}_\Theta$  if the row-amputated Young tableau  $\mathcal{O}_r$  according to the last column of  $\Theta$  is rectangular. Thus, let us form this amputated tableau,

$$\mathcal{O}_r = \begin{array}{|c|c|c|c|} \hline & & & \\ \hline & & & m \\ \hline & & & m+1 \\ \hline \end{array} . \quad (3.191)$$

This tableau is indeed rectangular,<sup>25</sup> allowing us to propagate the antisymmetrizer  $\mathbf{A}_\Theta^{m+1}$  from the right to the left, yielding

$$\bar{P}_\Theta = \mathbf{A}_\Theta \mathbf{S}_\Theta \mathbf{A}_{\Theta_{(1)}} \mathbf{S}_{\Theta_{(1)}} \mathbf{A}_{\Theta_{(1)}} . \quad (3.192)$$

Having demonstrated, that  $\mathbf{A}_{\Theta_{(1)}}$  and  $\mathbf{A}_\Theta$  may be swapped, it is possible to simplify  $\bar{P}_\Theta$  as shown in eqns. (3.187) to (3.188),

$$\bar{P}_\Theta = \mathbf{A}_\Theta \mathbf{S}_\Theta \underbrace{\mathbf{S}_{\Theta_{(1)}} \mathbf{A}_{\Theta_{(1)}}}_{=\bar{Y}_{\Theta_{(1)}}} \underbrace{\mathbf{S}_{\Theta_{(1)}} \mathbf{A}_{\Theta_{(1)}}}_{=\bar{Y}_{\Theta_{(1)}}} = \mathbf{A}_\Theta \mathbf{S}_\Theta \underbrace{\mathbf{S}_{\Theta_{(1)}} \mathbf{A}_{\Theta_{(1)}}}_{=\bar{Y}_{\Theta_{(1)}}} . \quad (3.193)$$

$\mathbf{S}_\Theta \rightarrow \mathbf{S}_\Theta \mathbf{S}_{\Theta_{(1)}} \quad \mathbf{S}_\Theta \mathbf{S}_{\Theta_{(1)}} \rightarrow \mathbf{S}_\Theta$

We once again use Theorem 3.6 to obtain the desired form of  $\bar{P}_\Theta$ ,

$$\bar{P}_\Theta = \mathbf{A}_\Theta \mathbf{S}_\Theta \mathbf{A}_{\Theta_{(1)}} \stackrel{\text{Thm. 3.6}}{=} \mathbf{A}_\Theta \mathbf{S}_\Theta \mathbf{A}_\Theta . \quad (3.194)$$

It remains to show that the normalization constant given in (3.172) is the right one: that is, we will show that  $P_\Theta = \alpha_\Theta \bar{P}_\Theta$ , where  $\bar{P}_\Theta = \bar{Y}_\Theta^\dagger \bar{Y}_\Theta = \mathbf{A}_\Theta \mathbf{S}_\Theta \mathbf{A}_\Theta$  (as was found in (3.184) and (3.194)), is indeed a projection operator. We will establish this by simply squaring  $P_\Theta = \alpha_\Theta \bar{P}_\Theta$  and checking whether it is idempotent:

$$P_\Theta P_\Theta = \alpha_\Theta^2 \cdot (\mathbf{A}_\Theta \mathbf{S}_\Theta \mathbf{A}_\Theta) (\mathbf{A}_\Theta \mathbf{S}_\Theta \mathbf{A}_\Theta) = \alpha_\Theta^2 \cdot \mathbf{A}_\Theta \underbrace{\mathbf{S}_\Theta \mathbf{A}_\Theta}_{=\bar{Y}_\Theta} \underbrace{\mathbf{S}_\Theta \mathbf{A}_\Theta}_{=\bar{Y}_\Theta} , \quad (3.195)$$

<sup>25</sup>It is important to note that this amputated tableau would not necessarily be rectangular if  $\Theta$  were not lexically ordered, as then  $\boxed{m+1}$  could be situated in a column other than the last one. Thus, for non-lexically ordered tableaux, the proof breaks down at this point.

where we have used the fact that  $\mathbf{A}_\Theta \mathbf{A}_\Theta = \mathbf{A}_\Theta$ . By the idempotency of Young projection operators  $Y_\Theta$ , it follows that  $\bar{Y}_\Theta \bar{Y}_\Theta = 1/\alpha_\Theta \bar{Y}_\Theta$ , simplifying (3.195) as

$$P_\Theta P_\Theta = \frac{\alpha_\Theta^2}{\alpha_\Theta} \cdot \mathbf{A}_\Theta \underbrace{\mathbf{S}_\Theta \mathbf{A}_\Theta}_{=Y_\Theta} = \alpha_\Theta \cdot \mathbf{A}_\Theta \mathbf{S}_\Theta \mathbf{A}_\Theta = P_\Theta . \quad (3.196)$$

This concludes the proof of this Theorem 3.4. □

### 3.C.2 Proof of Theorem 3.5 “partially lexical Hermitian Young projectors” (or MOLD Theorem)

We now present a proof of the MOLD Theorem 3.5 by induction, using the Lexical Theorem 3.4 as a base step:

Consider a Young tableau  $\Theta$  with MOLD  $\mathcal{M}(\Theta)$  such that  $\Theta_{(\mathcal{M}(\Theta))}$  has a lexically ordered row-word; the proof for  $\Theta_{(\mathcal{M}(\Theta))}$  having lexically ordered column-word is very similar and thus left as an exercise to the reader. We will provide a *Proof by Induction* on the MOLD of  $\Theta$ ,  $\mathcal{M}(\Theta)$ . Furthermore, we will for now ignore the proportionality constant  $\beta_\Theta$  and concentrate on the birdtrack  $\bar{P}_\Theta$  only. From the steps in the following proof, it will become evident that  $\beta_\Theta \neq 0$  and  $\beta_\Theta < \infty$  (as is explicitly discussed at the appropriate places within the proof), ensuring that  $P_\Theta := \beta_\Theta \bar{P}_\Theta$  is a *non-trivial* (i.e. nonzero) *finite* projection operator.

**The Base Step:** Suppose that  $\mathcal{M}(\Theta) = 0$ . In that case,  $\Theta$  itself has a lexically ordered row-word. Then, by the MOLD Theorem,  $\bar{P}_\Theta$  must be of the following form

$$\bar{P}_\Theta = \underbrace{\mathbf{S}_\Theta \mathbf{A}_\Theta \mathbf{S}_\Theta}_{=Y_\Theta Y_\Theta^\dagger} ; \quad (3.197)$$

this agrees with the result we obtained from the Lexical Theorem 3.4, for which we have already given a full proof in the appendix 3.C.1. Also, the normalization constant  $\beta_\Theta = \alpha_\Theta \neq 0$ , as required by the MOLD Theorem. Thus, the base step of the induction is fulfilled.

**The Induction Step:** Let us now consider a Young tableau  $\Theta$ , such that the MOLD Theorem holds for its parent tableau  $\Theta_{(1)}$ . Further, assume that  $\mathcal{M}(\Theta_{(1)}) = m$ , for some positive integer  $m$ , with  $\Theta_{(m)}$  being row-ordered. Thus, we have that  $\mathcal{M}(\Theta) = m + 1$ . We can now have one of two situations: either  $m$  is even, or  $m$  is odd. First, suppose that  **$m$  is even** (i.e.  **$m + 1$  is odd**). Then, according to the MOLD Theorem, the birdtrack of the projection operator  $P_{\Theta_{(1)}}$  is given by (c.f. eq. (3.124a))

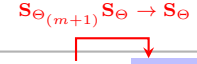
$$\bar{P}_{\Theta_{(1)}} = \mathcal{C} \underbrace{\mathbf{S}_{\Theta_{(1)}} \mathbf{A}_{\Theta_{(1)}} \mathbf{S}_{\Theta_{(1)}}}_{=Y_{\Theta_{(1)}} Y_{\Theta_{(1)}}^\dagger} \mathcal{C}^\dagger , \quad (3.198)$$

where we defined  $\mathcal{C}$  to be

$$\mathcal{C} := \mathbf{S}_{\Theta_{(m+1)}} \mathbf{A}_{\Theta_{(m)}} \mathbf{S}_{\Theta_{(m-1)}} \cdots \mathbf{S}_{\Theta_{(3)}} \mathbf{A}_{\Theta_{(2)}} . \quad (3.199)$$

We will now construct the birdtrack  $\bar{P}_\Theta$  according to the KS Theroerm 3.3 [4]; this yields

$$\begin{aligned} \bar{P}_\Theta &= \bar{P}_{\Theta_{(1)}} \bar{Y}_\Theta \bar{P}_{\Theta_{(1)}} \\ &= \mathcal{C} \left[ \underbrace{\mathbf{S}_{\Theta_{(1)}} \mathbf{A}_{\Theta_{(1)}} \mathbf{S}_{\Theta_{(1)}} \cdots \mathbf{A}_{\Theta_{(m)}} \mathbf{S}_{\Theta_{(m+1)}}}_{\mathcal{C}^\dagger} \mathbf{S}_\Theta \mathbf{A}_\Theta \mathbf{S}_{\Theta_{(m+1)}} \cdots \mathbf{S}_{\Theta_{(1)}} \mathbf{A}_{\Theta_{(1)}} \mathbf{S}_{\Theta_{(1)}} \right] \mathcal{C}^\dagger, \end{aligned} \quad (3.200)$$

$\mathbf{S}_{\Theta_{(m+1)}} \mathbf{S}_\Theta \rightarrow \mathbf{S}_\Theta$   


where we absorbed  $\mathbf{S}_{\Theta_{(m+1)}}$  into  $\mathbf{S}_\Theta$ . We notice that the parts of  $\bar{P}_\Theta$  outside the grey outlined box (denoted by  $\mathcal{C}^\dagger$ ) are already in the form that we want them to be. We thus focus our attention on the part of  $\bar{P}_\Theta$  inside the grey box. If we can show that this part can be written as

$$\bar{P}_\Theta \stackrel{?}{=} \mathcal{C} \left[ \mathbf{S}_{\Theta_{(1)}} \underbrace{\mathbf{A}_\Theta \mathbf{S}_\Theta \mathbf{A}_\Theta \mathbf{S}_{\Theta_{(1)}}}_{\mathbf{Y}_\Theta^\dagger \mathbf{Y}_\Theta} \mathbf{S}_{\Theta_{(1)}} \right] \mathcal{C}^\dagger, \quad (3.201)$$

then we have completed the proof. We will accomplish this goal in two steps:

1. We will use the Cancellation Theorem 3.2 (see section 3.2.3) to cancel the wedged ancestor sets of (anti-)symmetrizers in the grey box and thus reduce  $\bar{P}_\Theta$  to

$$\bar{P}_\Theta = \mathcal{C} \left[ \mathbf{S}_{\Theta_{(1)}} \mathbf{A}_{\Theta_{(1)}} \mathbf{S}_\Theta \mathbf{A}_\Theta \mathbf{S}_{\Theta_{(1)}} \right] \mathcal{C}^\dagger. \quad (3.202)$$

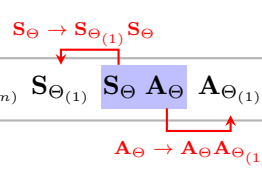
2. We then make use of the Hermiticity of  $P_\Theta$  to show that

$$\bar{P}_\Theta = \mathcal{C} \left[ \mathbf{S}_{\Theta_{(1)}} \mathbf{A}_\Theta \mathbf{S}_\Theta \mathbf{A}_\Theta \mathbf{S}_{\Theta_{(1)}} \right] \mathcal{C}^\dagger. \quad (3.203)$$

Let us start the two-step-process:

1. The first step is easily accomplished: We factor a set  $\mathbf{S}_{\Theta_{(1)}}$  out of  $\mathbf{S}_\Theta$  and a set  $\mathbf{A}_{\Theta_{(1)}}$  out of  $\mathbf{A}_\Theta$ ,

$$\begin{aligned} \bar{P}_\Theta &= \mathcal{C} \left[ \mathbf{S}_{\Theta_{(1)}} \mathbf{A}_{\Theta_{(1)}} \mathbf{S}_{\Theta_{(1)}} \cdots \mathbf{A}_{\Theta_{(m)}} \mathbf{S}_{\Theta_{(1)}} \mathbf{S}_\Theta \mathbf{A}_\Theta \mathbf{A}_{\Theta_{(1)}} \mathbf{S}_{\Theta_{(m+1)}} \cdots \mathbf{S}_{\Theta_{(1)}} \mathbf{A}_{\Theta_{(1)}} \mathbf{S}_{\Theta_{(1)}} \right] \mathcal{C}^\dagger. \\ &\quad \mathbf{S}_\Theta \rightarrow \mathbf{S}_{\Theta_{(1)}} \mathbf{S}_\Theta \quad \mathbf{A}_\Theta \rightarrow \mathbf{A}_\Theta \mathbf{A}_{\Theta_{(1)}} \end{aligned} \quad (3.204)$$



We now encounter sets of symmetrizers and antisymmetrizers corresponding to ancestor tableaux  $\Theta_{(k)}$  with  $1 \leq k \leq m$  wedged between sets belonging to the tableau  $\Theta_{(1)}$ . Thus, we may use Theorem 3.2 to simplify the operator  $\bar{P}_\Theta$  (once again making use of the bar-notation, *c.f.* eq. (3.33), to retain equality in the process)

$$\bar{P}_\Theta = \mathcal{C} \left[ \underbrace{\mathbf{S}_{\Theta_{(1)}} \mathbf{A}_{\Theta_{(1)}} \mathbf{S}_{\Theta_{(1)}} \cdots \mathbf{A}_{\Theta_{(m)}} \mathbf{S}_{\Theta_{(1)}}}_{\propto \mathbf{A}_{\Theta_{(1)}} \mathbf{S}_{\Theta_{(1)}}} \mathbf{S}_\Theta \mathbf{A}_\Theta \mathbf{A}_{\Theta_{(1)}} \mathbf{S}_{\Theta_{(m+1)}} \cdots \mathbf{S}_{\Theta_{(1)}} \mathbf{A}_{\Theta_{(1)}} \mathbf{S}_{\Theta_{(1)}} \right] \mathcal{C}^\dagger$$

$\propto \mathbf{A}_{\Theta_{(1)}} \mathbf{S}_{\Theta_{(1)}} \quad \propto \mathbf{A}_{\Theta_{(1)}} \mathbf{S}_{\Theta_{(1)}}$



$$= \mathcal{C} \left[ \mathbf{S}_{\Theta(1)} \mathbf{A}_{\Theta(1)} \mathbf{S}_{\Theta(1)} \mathbf{S}_{\Theta} \mathbf{A}_{\Theta} \mathbf{A}_{\Theta(1)} \mathbf{S}_{\Theta(1)} \right] \mathcal{C}^{\dagger} . \quad (3.205)$$

Re-absorbing  $\mathbf{S}_{\Theta(1)}$  into  $\mathbf{S}_{\Theta}$  and  $\mathbf{A}_{\Theta(1)}$  into  $\mathbf{A}_{\Theta}$  yields the desired result,

$$\begin{aligned} \bar{P}_{\Theta} &= \mathcal{C} \left[ \mathbf{S}_{\Theta(1)} \mathbf{A}_{\Theta(1)} \mathbf{S}_{\Theta(1)} \mathbf{S}_{\Theta} \mathbf{A}_{\Theta} \mathbf{A}_{\Theta(1)} \mathbf{S}_{\Theta(1)} \right] \mathcal{C}^{\dagger} \\ &= \mathcal{C} \left[ \mathbf{S}_{\Theta(1)} \mathbf{A}_{\Theta(1)} \mathbf{S}_{\Theta} \mathbf{A}_{\Theta} \mathbf{S}_{\Theta(1)} \right] \mathcal{C}^{\dagger} , \end{aligned} \quad (3.206)$$

$\mathbf{S}_{\Theta(1)} \mathbf{S}_{\Theta} \rightarrow \mathbf{S}_{\Theta}$   
 $\mathbf{A}_{\Theta} \mathbf{A}_{\Theta(1)} \rightarrow \mathbf{A}_{\Theta}$

thus concluding this step of the proof.

2. For the second step of the proof, we first notice that the operator obtained in the previous step, operator (3.206), is Hermitian; this is due to the fact that  $\bar{P}_{\Theta}$  (as given in (3.200)) was constructed according to the iterative method described in the KS Theorem 3.3 [4]. In particular, this implies that  $\bar{P}_{\Theta} = \bar{P}_{\Theta}^{\dagger}$ , yielding

$$\bar{P}_{\Theta} = \mathcal{C} \left[ \mathbf{S}_{\Theta(1)} \mathbf{A}_{\Theta(1)} \mathbf{S}_{\Theta} \mathbf{A}_{\Theta} \mathbf{S}_{\Theta(1)} \right] \mathcal{C}^{\dagger} = \mathcal{C} \left[ \mathbf{S}_{\Theta(1)} \mathbf{A}_{\Theta} \mathbf{S}_{\Theta} \mathbf{A}_{\Theta(1)} \mathbf{S}_{\Theta(1)} \right] \mathcal{C}^{\dagger} = \bar{P}_{\Theta}^{\dagger}. \quad (3.207)$$

When we gave the proof of the Lexical Theorem 3.4 in appendix 3.C.1, we were able to prove that  $\mathbf{A}_{\Theta(1)}$  can be extended to become  $\mathbf{A}_{\Theta}$  by using techniques described in Appendix 3.C.1.1. Now however, we are no longer able to use these techniques, as most amputated tableaux  $\mathcal{O}_r$  or  $\mathcal{O}_c$  would *not* be rectangular (as can be easily verified by an example). We therefore need a different strategy to arrive at the desired form for  $\bar{P}_{\Theta}$ .

In addition to  $\bar{P}_{\Theta}$  as given in (3.206), let us define the operator  $\bar{O}$  by

$$\bar{O} := \mathcal{C} \left[ \mathbf{S}_{\Theta(1)} \mathbf{A}_{\Theta} \mathbf{S}_{\Theta} \mathbf{A}_{\Theta} \mathbf{S}_{\Theta(1)} \right] \mathcal{C}^{\dagger}; \quad (3.208)$$

clearly, this operator is Hermitian by construction due to its symmetry. We seek to show that  $\bar{P}_{\Theta} = \bar{O}$  in order to conclude the second step of this proof. This will be accomplished by showing that

$$\bar{O} \subset \bar{P}_{\Theta} \quad \text{and} \quad \bar{P}_{\Theta} \subset \bar{O}, \quad (3.209)$$

where we used the notation introduced in section 3.2.2.2. These inclusions will then lead us to conclude that the subspaces onto which  $\bar{O}$  and  $\bar{P}_{\Theta}$  project are equal, rendering the two operators equal,  $\bar{O} = \bar{P}_{\Theta}$ .

Let us prove the two inclusions (3.209): As discussed in section 3.2.2.2, the first inclusion holds if and only if  $\bar{O} \cdot \bar{P}_{\Theta} = \bar{P}_{\Theta} = \bar{P}_{\Theta} \cdot \bar{O}$  (c.f. equation (3.40)). We thus need to examine the product of  $\bar{O}$  and  $\bar{P}_{\Theta}$ . We consider

$$\bar{O} \cdot \bar{P}_{\Theta} = \mathcal{C} \left[ \mathbf{S}_{\Theta(1)} \mathbf{A}_{\Theta} \mathbf{S}_{\Theta} \mathbf{A}_{\Theta} \mathbf{S}_{\Theta(1)} \right] \mathcal{C}^{\dagger} \cdot \mathcal{C} \left[ \mathbf{S}_{\Theta(1)} \mathbf{A}_{\Theta(1)} \mathbf{S}_{\Theta} \mathbf{A}_{\Theta} \mathbf{S}_{\Theta(1)} \right] \mathcal{C}^{\dagger}. \quad (3.210)$$

Similar to what was done in part 1, we use Theorem 3.2 to simplify the central part of the product

$$\bar{O} \cdot \bar{P}_\Theta$$

$$\bar{O} \cdot \bar{P}_\Theta = \mathcal{C} \mathbf{S}_{\Theta(1)} \mathbf{A}_\Theta \underbrace{\mathbf{S}_\Theta \mathbf{A}_\Theta \mathbf{S}_{\Theta(1)}}_{\propto \mathbf{S}_\Theta \mathbf{A}_\Theta} \mathcal{C}^\dagger \cdot \mathcal{C} \mathbf{S}_{\Theta(1)} \mathbf{A}_{\Theta(1)} \mathbf{S}_\Theta \mathbf{A}_\Theta \mathbf{S}_{\Theta(1)} \mathcal{C}^\dagger, \quad (3.211)$$

yielding (making use of the bar-notation)

$$\bar{O} \cdot \bar{P}_\Theta = \mathcal{C} \mathbf{S}_{\Theta(1)} \mathbf{A}_\Theta \underbrace{\mathbf{S}_\Theta \mathbf{A}_\Theta \mathbf{S}_{\Theta(1)}}_{=\bar{Y}_\Theta} \mathcal{C}^\dagger = \bar{O}. \quad (3.212)$$

Hence, we found that  $\bar{O} \cdot \bar{P}_\Theta = \bar{O}$ . Recalling that both operators  $\bar{O}$  and  $\bar{P}_\Theta$  are Hermitian, it follows that

$$\bar{O} = \bar{O}^\dagger = (\bar{O} \cdot \bar{P}_\Theta)^\dagger = \bar{P}_\Theta^\dagger \cdot \bar{O}^\dagger = \bar{P}_\Theta \cdot \bar{O}. \quad (3.213)$$

Thus, we have shown that both equalities,  $\bar{O} \cdot \bar{P}_\Theta = \bar{O}$  and  $\bar{P}_\Theta \cdot \bar{O} = \bar{O}$ , hold, implying the first inclusion  $\bar{O} \subset \bar{P}_\Theta$ .

To prove the second inclusion in (3.209), we need to consider the product  $\bar{P}_\Theta \cdot \bar{O}$ ,

$$\bar{P}_\Theta \cdot \bar{O} = \mathcal{C} \boxed{\mathbf{S}_{\Theta(1)} \mathbf{A}_{\Theta(1)} \mathbf{S}_\Theta \mathbf{A}_\Theta \mathbf{S}_{\Theta(1)}} \mathcal{C}^\dagger \cdot \mathcal{C} \boxed{\mathbf{S}_{\Theta(1)} \mathbf{A}_\Theta \mathbf{S}_\Theta \mathbf{A}_\Theta \mathbf{S}_{\Theta(1)}} \mathcal{C}^\dagger. \quad (3.214)$$

Once again, we may use Theorem 3.2 to simplify this product as

$$\begin{aligned} \bar{P}_\Theta \cdot \bar{O} &= \mathcal{C} \mathbf{S}_{\Theta(1)} \mathbf{A}_{\Theta(1)} \underbrace{\mathbf{S}_\Theta \mathbf{A}_\Theta \mathbf{S}_{\Theta(1)}}_{\propto \mathbf{S}_\Theta \mathbf{A}_\Theta} \mathcal{C}^\dagger \cdot \mathcal{C} \mathbf{S}_{\Theta(1)} \mathbf{A}_\Theta \mathbf{S}_\Theta \mathbf{A}_\Theta \mathbf{S}_{\Theta(1)} \mathcal{C}^\dagger \\ &= \mathcal{C} \mathbf{S}_{\Theta(1)} \mathbf{A}_{\Theta(1)} \underbrace{\mathbf{S}_\Theta \mathbf{A}_\Theta \mathbf{S}_{\Theta(1)}}_{=\bar{Y}_\Theta} \mathcal{C}^\dagger. \end{aligned} \quad (3.215)$$

We recognize the right hand side of equation (3.215) to be the operator  $\bar{P}_\Theta$ . We thus found that  $\bar{P}_\Theta \cdot \bar{O} = \bar{P}_\Theta$ . Once again, we make use of the Hermiticity of the operators  $\bar{O}$  and  $\bar{P}_\Theta$  to see that

$$\bar{P}_\Theta = \bar{P}_\Theta^\dagger = (\bar{P}_\Theta \cdot \bar{O})^\dagger = \bar{O}^\dagger \cdot \bar{P}_\Theta^\dagger = \bar{O} \cdot \bar{P}_\Theta, \quad (3.216)$$

yielding the desired inclusion  $\bar{P}_\Theta \subset \bar{O}$ . We have thus managed to prove both inclusions in (3.209), forcing us to conclude that the two operators  $\bar{O}$  and  $\bar{P}_\Theta$  are equal,  $\bar{O} = \bar{P}_\Theta$ , yielding

$$\bar{P}_\Theta = \bar{O} = \mathcal{C} \boxed{\mathbf{S}_{\Theta(1)} \mathbf{A}_\Theta \mathbf{S}_\Theta \mathbf{A}_\Theta \mathbf{S}_{\Theta(1)}} \mathcal{C}^\dagger, \quad (3.217)$$

as desired (*c.f.* eq. (3.124b)).

Suppose now that  $m$  is odd (i.e.  $m + 1$  is even). The proof for odd  $m$  will also be conducted in two steps, just as for even  $m$ . We will only give an outline of this proof, as the steps are very similar to those for even  $m$ .

By the induction hypothesis, the projection operator  $P_{\Theta(1)}$  is of the form

$$\bar{P}_{\Theta(1)} = \mathbf{S}_{\Theta(m+1)} \mathbf{A}_{\Theta(m)} \cdots \mathbf{S}_{\Theta(2)} \underbrace{\mathbf{A}_{\Theta(1)} \mathbf{S}_{\Theta(1)} \mathbf{A}_{\Theta(1)}}_{=\bar{Y}_{\Theta(1)}^\dagger \bar{Y}_{\Theta(1)}} \mathbf{S}_{\Theta(2)} \cdots \mathbf{A}_{\Theta(m)} \mathbf{S}_{\Theta(m+1)}. \quad (3.218)$$

Constructing the birdtrack of the Hermitian Young projection operator  $P_\Theta$ ,  $\bar{P}_\Theta$ , according to the KS Theorem 3.3 [4] gives

$$\begin{aligned} \bar{P}_\Theta &= \bar{P}_{\Theta(1)} \bar{Y}_\Theta \bar{P}_{\Theta(1)} \\ &= \mathcal{C}_\Theta \left[ \mathbf{A}_{\Theta(1)} \mathbf{S}_{\Theta(1)} \mathbf{A}_{\Theta(1)} \mathbf{S}_{\Theta(2)} \cdots \mathbf{S}_{\Theta(m+1)} \mathbf{S}_\Theta \mathbf{A}_\Theta \mathbf{S}_{\Theta(m+1)} \cdots \mathbf{S}_{\Theta(2)} \mathbf{A}_{\Theta(1)} \mathbf{S}_{\Theta(1)} \mathbf{A}_{\Theta(1)} \right] \mathcal{C}_\Theta^\dagger, \end{aligned} \quad (3.219)$$

where  $\mathcal{C}_\Theta := \mathbf{S}_{\Theta(m+1)} \cdots \mathbf{S}_{\Theta(2)}$ . We again use Theorem 3.2 to simplify the operator (3.219),

$$\bar{P}_\Theta = \mathbf{S}_{\Theta(m+1)} \cdots \mathbf{S}_{\Theta(2)} \left[ \mathbf{A}_{\Theta(1)} \mathbf{S}_\Theta \mathbf{A}_\Theta \mathbf{S}_{\Theta(1)} \mathbf{A}_{\Theta(1)} \right] \mathbf{S}_{\Theta(2)} \cdots \mathbf{S}_{\Theta(m+1)}. \quad (3.220)$$

We then define an operator  $\bar{O}$  by

$$\bar{O} := \mathbf{S}_{\Theta(m+1)} \cdots \mathbf{S}_{\Theta(2)} \left[ \mathbf{A}_{\Theta(1)} \mathbf{S}_\Theta \mathbf{A}_\Theta \mathbf{S}_\Theta \mathbf{A}_{\Theta(1)} \right] \mathbf{S}_{\Theta(2)} \cdots \mathbf{S}_{\Theta(m+1)}. \quad (3.221)$$

Using Theorem 3.2, as well as the fact that both  $\bar{P}_\Theta$  and  $\bar{O}$  are Hermitian by construction, we may show the inclusions  $\bar{P}_\Theta \subset \bar{O}$  and  $\bar{O} \subset \bar{P}_\Theta$ , to conclude that  $\bar{P}_\Theta = \bar{O}$ , yielding the desired result (*c.f.* eq. (3.124a))

$$\bar{P}_\Theta = \mathbf{S}_{\Theta(m+1)} \cdots \mathbf{S}_{\Theta(2)} \left[ \mathbf{A}_{\Theta(1)} \underbrace{\mathbf{S}_\Theta \mathbf{A}_\Theta \mathbf{S}_\Theta}_{=\bar{Y}_\Theta \bar{Y}_\Theta^\dagger} \mathbf{A}_{\Theta(1)} \right] \mathbf{S}_{\Theta(2)} \cdots \mathbf{S}_{\Theta(m+1)}. \quad (3.222)$$

The proof of equations (3.124c) and (3.124d) in the MOLD Theorem follows the same steps as the proof of equations (3.124a) and (3.124b) given above, and is thus left as an exercise for the reader.

Lastly, we notice that the idempotency of  $P_\Theta$  in each of the cases (3.124) can be verified by using the Cancellation Theorem 3.2: For example if  $P_\Theta$  is constructed according to (3.124a), it follows that

$$\begin{aligned} P_\Theta \cdot P_\Theta &= \beta_\Theta^2 \cdot \mathbf{S}_{\Theta(m)} \cdots \underbrace{\mathbf{S}_\Theta \mathbf{A}_\Theta \mathbf{S}_\Theta \cdots \mathbf{S}_{\Theta(m)} \cdot \mathbf{S}_{\Theta(m)} \cdots \mathbf{S}_\Theta \mathbf{A}_\Theta \mathbf{S}_\Theta}_{=\lambda \cdot \mathbf{S}_\Theta \mathbf{A}_\Theta \mathbf{S}_\Theta} \cdots \mathbf{S}_{\Theta(m)} \\ &= \beta_\Theta^2 \lambda \cdot \mathbf{S}_{\Theta(m)} \cdots \mathbf{S}_\Theta \mathbf{A}_\Theta \mathbf{S}_\Theta \cdots \mathbf{S}_{\Theta(m)}, \end{aligned}$$

where  $\lambda$  is a *nonzero* constant, since all the cancelled sets can be absorbed into  $\mathbf{S}_\Theta$  and  $\mathbf{A}_\Theta$  respectively (*c.f.* Theorem 3.2). Thus, defining

$$\beta_\Theta := \frac{1}{\lambda} < \infty \quad (3.223)$$

ensures that  $P_\Theta$  is indeed a projection operator.  $\square$



## Chapter 4

# Transition Operators

This chapter has been published under the same name in the Journal of Mathematical Physics [3]. In some instances, the present paper (chapter) refers to additional results not given in the paper. Where such work is included in this thesis, a remark in square brackets and italics has been added to refer the reader to the appropriate chapter of this thesis.

**Abstract:** *In this paper, we give a generic algorithm of the transition operators between Hermitian Young projection operators corresponding to equivalent irreducible representations of  $SU(N)$ , using the compact expressions of Hermitian Young projection operators derived in [2] [chapter 3]. We show that the Hermitian Young projection operators together with their transition operators constitute a fully orthogonal basis for the algebra of invariants of  $V^{\otimes m}$  that exhibits a systematically simplified multiplication table. We discuss the full algebra of invariants over  $V^{\otimes 3}$  and  $V^{\otimes 4}$  as explicit examples. In our presentation we make use of various standard concepts, such as Young projection operators, Clebsch-Gordan operators, and invariants (in birdtrack notation). We tie these perspectives together and use them to shed light on each other.*

### 4.1 Introduction

Applications of representation theory generally are concerned with irreducible representations of the group under scrutiny. Physics applications in particular are generally aimed at finding all irreducible representations in an  $m$ -particle Fock space. The textbook example here is of course angular momentum and spin with the group  $SU(2)$  and the construction of the periodic table in quantum mechanics via the irreducible multiplets for  $m$  electrons in an atom with  $m$  protons that classify its orbital configuration, its spectral and chemical properties. In quantum chromodynamics, we meet flavor symmetry (flavor  $SU_f(2)$  or  $SU_f(3)$ ) as an approximate symmetry that guides us through interpreting the mesons and baryons as members of irreducible representations of the flavor group in the *eightfold way* [15, 104]. Gauge invariance and confinement force the same particles into singlets of the color gauge group  $SU_c(3)$ . The latter are of particular interest in the color glass condensate which dominates QCD in high energy applications, i.e. in modern collider experiments. In this set of applications, Wilson line correlators appear, whose color structures are of central importance and the presently existing techniques are limited to explicit calculations at a given order of complexity. In [2] [chapter 3], we have established an efficient algorithm to construct a full set of Hermitian projection operators for the decomposition of a product of  $m$  fundamental representations of  $SU(N)$  as a subset of the

associated algebra of invariants. Here, we aim to find a complete basis for the algebra of invariants that is fully shaped by the irreducible representations that these operators represent, and identify the missing basis elements as transition operators between *equivalent* representations contained in the product. In a future paper [94] [chapter 5], this information will be used to give a full account of all singlets (i.e. all 1-dimensional representations that remain invariant under the group action) constrained in a product of  $m$  fundamental representations with  $m'$  antifundamental representations. In physics parlance, this gives access to the gauge invariant part of the Fock space of  $m$  particles and  $m'$  antiparticles.

There are, of course, several different technologies on the market to address these questions. The most familiar to the practicing physicist are the construction of Clebsch-Gordan coefficients [108] (see [25, 92, 93] for textbook introductions), Elié Cartan's method of roots and weights [103], and Alfred Young's combinatorial method of classifying the idempotents on the algebra of permutations [84]. The *Schur-Weyl duality* [98] relates these idempotents to the irreducible representations of compact, semi-simple Lie groups and thus to  $SU(N)$ . This duality is based on the *theory of invariants* [72, 98], which exploits the invariants (in particular the *primitive invariants*) of a Lie group  $G$  and constructs projection operators corresponding to the irreducible representations of  $G$  from the invariants of that group. It is this method that allows us to carry  $N$  as a parameter throughout, which has important advantages in applications in QCD we are ultimately interested in. The core part of our discussion will deal with a product representations of  $SU(N)$  constructed from the fundamental representation of a Lie group  $G$  on a given vector space  $V$  with  $\dim(V) = N$ , whose action will simply be denoted by  $v \mapsto Uv$  for all  $U \in SU(N)$  and  $v \in V$ . Choosing a basis  $\{e_{(i)} | i = 1, \dots, \dim(V)\}$  such that  $v = v^i e_{(i)}$ , this becomes  $v^i \mapsto U^i_j v^j$ . This immediately induces product representations of  $SU(N)$  on  $V^{\otimes m}$  if one uses this basis of  $V$  to induce a basis on  $V^{\otimes m}$ , so that a general element  $\mathbf{v} \in V^{\otimes m}$  takes the form  $\mathbf{v} = v^{i_1 \dots i_m} e_{(i_1)} \otimes \dots \otimes e_{(i_m)}$ :

$$\mathbf{U} \circ \mathbf{v} = \mathbf{U} \circ v^{i_1 \dots i_m} e_{(i_1)} \otimes \dots \otimes e_{(i_m)} := \underbrace{U^{i_1}_{j_1} \dots U^{i_m}_{j_m}}_{=: \mathbf{U}} v^{j_1 \dots j_m} e_{(i_1)} \otimes \dots \otimes e_{(i_m)}. \quad (4.1)$$

Since all the factors in  $V^{\otimes m}$  are identical, the notion of permuting the factors is a natural one and leads to a linear map on  $V^{\otimes m}$  according to

$$\rho \circ \mathbf{v} = \rho \circ v^{i_1 \dots i_m} e_{(i_1)} \otimes \dots \otimes e_{(i_m)} := v^{i_{\rho(1)} \dots i_{\rho(m)}} e_{(i_1)} \otimes \dots \otimes e_{(i_m)}, \quad (4.2)$$

where  $\rho$  is an element of  $S_m$ , the group of permutations of  $m$  objects.<sup>1</sup> From the definitions (4.1) and (4.2), one immediately infers that the product representation commutes with all permutations on any  $\mathbf{v} \in V^{\otimes m}$ :

$$\mathbf{U} \circ \rho \circ \mathbf{v} = \rho \circ \mathbf{U} \circ \mathbf{v}. \quad (4.3)$$

In other words, any such permutation  $\rho$  is an *invariant* of  $SU(N)$  (or in fact any Lie group  $G$  acting on  $V$ ):

$$\mathbf{U} \circ \rho \circ \mathbf{U}^{-1} = \rho. \quad (4.4)$$

It can further be shown that these permutations span the space of all linear invariants of  $SU(N)$  over  $V^{\otimes m}$  [72]. The permutations are thus referred to as the *primitive invariants* of  $SU(N)$  over  $V^{\otimes m}$ . The full space of

---

<sup>1</sup>Permuting the basis vectors instead involves  $\rho^{-1}$ :  $v^{\rho(i_1) \dots \rho(i_m)} e_{(i_1)} \otimes \dots \otimes e_{(i_m)} = v^{i_1 \dots i_m} e_{(i_{\rho^{-1}(1)})} \otimes \dots \otimes e_{(i_{\rho^{-1}(m)})}$ .

linear invariants is then given by

$$\text{API}(\text{SU}(N), V^{\otimes m}) := \left\{ \sum_{\sigma \in S_m} \alpha_{\sigma} \sigma \mid \alpha_{\sigma} \in \mathbb{R}, \sigma \in S_m \right\} \subset \text{Lin}(V^{\otimes m}) . \quad (4.5)$$

As defined in (4.5),  $\text{API}(\text{SU}(N), V^{\otimes m})$  is a real vector space and becomes a real algebra with the product induced by the product of permutations. It will become obvious from our presentation that this space is large enough to encompass all group-theoretically interesting objects, namely

1. Hermitian projectors onto irreducible representations (see [2, 4]), and
2. any transition operators associated with equivalent representations.

We will show that these operators do not only fit into it, they in fact span the whole space and form an orthogonal basis for  $\text{API}(\text{SU}(N), V^{\otimes m})$ . We will call this the *projector basis* for  $\text{API}(\text{SU}(N), V^{\otimes m})$  in the remainder of this paper (such a basis is referred to as a *multiplet basis* in [102]), and discuss in detail its unique structures and the freedom of choice still left open.

Naively, since the number of permutations in  $S_m$  is  $m!$ , one might expect the dimension of  $\text{API}(\text{SU}(N), V^{\otimes m})$  to be simply  $m!$  and indeed this is the maximal dimension of the algebra. However, this is realized only if  $N = \dim(V) \geq m$ . Failing that, not all permutations remain linearly independent (as elements of the vector space  $\text{Lin}(V^{\otimes m})$ ). This is particularly clearly exhibited in the projector basis. A number of clearly distinguished basis elements will explicitly become null operators, all others will remain nonzero and thus form a basis for the now smaller space of invariants (see appendix 4.A). It is this feature that allows us to use  $N$  as a parameter in calculations.

We begin with a short presentation of some background material, which is needed to fully appreciate the arguments made in this paper, in section 4.2. This section begins by introducing the birdtrack formalism [72], which is particularly suited for dealing with the objects discussed in this paper. We then proceed by summarizing classic textbook material on Young tableaux and their corresponding projection operators (see for example [72, 92, 93, 95, 96]). Lastly, we state some cancellation rules for birdtrack operators [1] [chapter 2].

Section 4.3 provides the first new results. We show that the Young projection operators can be augmented by what we choose to call *transition operators* to give an alternative basis for the algebra of invariants  $\text{API}(\text{SU}(N), V^{\otimes m})$  for  $m \leq 4$ , and proceed to give the full basis for  $\text{API}(\text{SU}(N), V^{\otimes 3})$  (a diagram depicting the full basis up to  $m = 4$  is given in Figure 4.2). Since orthogonality of Young projection operators breaks down beyond  $m = 4$ , the Young basis cannot be generalized to larger  $m$ . This motivates a basis in terms of Hermitian projection operators and their unitary transition operators:

Section 4.4 discusses such a basis through Clebsch-Gordan operators for all  $m$ . As it turns out, Hermiticity and unitarity of these operators automatically guarantee mutual orthogonality of the basis elements with respect to the inner product  $\langle A, B \rangle := \text{tr}(A^\dagger B)$ . Since this method requires the construction of  $N^m$  normalized states to find  $m!$  basis elements for  $\text{API}(\text{SU}(N), V^{\otimes m})$ , we then proceed to present a more efficient algorithm to reach this goal. Our method is based on streamlined methods to construct Hermitian Young projection operators [2] [chapter 3] (themselves based on earlier work by Keppeler and Sjö Dahl [4]). These Hermitian Young projection operators are complemented by unitary transition operators to provide a full basis for  $\text{API}(\text{SU}(N), V^{\otimes m})$  for all  $m$  in section 4.5 (Theorem 4.4). This construction algorithm for transition operators serves as a starting

point for a more efficient method (Theorem 4.5) yielding much shorter expressions of the transition operators. The proof of Theorem 4.5 can be found in appendix 4.D.

We close with some examples. We give the basis of  $\text{API}(\text{SU}(N), V^{\otimes m})$  in terms of Hermitian Young projection operators and unitary transition operators for both  $m = 3$  and  $m = 4$  in section 4.6. Figures 4.2 and 4.3 summarize the most important aspects of Young and Hermitian Young decompositions of  $\text{API}(\text{SU}(N), V^{\otimes m})$  for all  $m \leq 4$ .

## 4.2 Background: birdtracks, Young tableaux, notations and conventions

### 4.2.1 Birdtracks, scalar products, and Hermiticity

In the 1970's, Penrose devised a graphical method of dealing with primitive invariants of Lie groups including Young projection operators [87, 88], which was subsequently applied in a collaboration with MacCallum [89]. This graphical method, now dubbed the *birdtrack formalism*, was modernized and further developed by Cvitanović [72] in recent years. The immense benefit of the birdtrack formalism is that it makes the actions of the operators visually accessible and thus more intuitive. For illustration, we give as an example the permutations of  $S_3$  written both in their cycle notation (see [93] for a textbook introduction) as well as birdtracks:

$$S_3 = \left\{ \underbrace{\begin{array}{c} \longleftrightarrow \\ \longleftrightarrow \\ \longleftrightarrow \end{array}}_{\text{id}}, \underbrace{\begin{array}{c} \longleftrightarrow \\ \text{X} \\ \longleftrightarrow \end{array}}_{(12)}, \underbrace{\begin{array}{c} \longleftrightarrow \\ \text{X} \\ \longleftrightarrow \end{array}}_{(13)}, \underbrace{\begin{array}{c} \longleftrightarrow \\ \text{X} \\ \longleftrightarrow \end{array}}_{(23)}, \underbrace{\begin{array}{c} \longleftrightarrow \\ \text{X} \\ \longleftrightarrow \end{array}}_{(123)}, \underbrace{\begin{array}{c} \longleftrightarrow \\ \text{X} \\ \longleftrightarrow \end{array}}_{(132)} \right\}. \quad (4.6)$$

The action of each of the above permutations on a tensor product  $v_1 \otimes v_2 \otimes v_3$  is clear, for example

$$(123)(v_1 \otimes v_2 \otimes v_3) = v_3 \otimes v_1 \otimes v_2. \quad (4.7)$$

In the birdtrack formalism, this equation is written as

$$\begin{array}{c} \longleftrightarrow \\ \text{X} \\ \longleftrightarrow \end{array} \begin{array}{c} v_1 \\ v_2 \\ v_3 \end{array} = \begin{array}{c} v_3 \\ v_1 \\ v_2 \end{array}, \quad (4.8)$$

where each term in the product  $v_1 \otimes v_2 \otimes v_3$  (written as a tower  $\begin{array}{c} v_1 \\ v_2 \\ v_3 \end{array}$ ) can be thought of as being moved along

the lines of  $\begin{array}{c} \longleftrightarrow \\ \text{X} \\ \longleftrightarrow \end{array}$ . Birdtracks are thus naturally read from right to left as is also indicated by the arrows on the legs.

The graphical structure faithfully represents the multiplication table of  $S_m$  by implementing a “glue and follow the lines prescription” along the lines of

$$\begin{array}{c} \longleftrightarrow \\ \text{X} \\ \longleftrightarrow \end{array} \cdot \begin{array}{c} \longleftrightarrow \\ \text{X} \\ \longleftrightarrow \end{array} := \begin{array}{c} \longleftrightarrow \\ \text{X} \\ \longleftrightarrow \end{array} = \begin{array}{c} \longleftrightarrow \\ \text{X} \\ \longleftrightarrow \end{array}. \quad (4.9)$$

Selecting a set of integers  $\{a_1, \dots, a_n\}$ , we can introduce two prominent types of elements of these algebras:



symmetrizers

$$\mathbf{S}_{a_1, \dots, a_n} := \frac{1}{n!} \sum_{\sigma \in S_n} \sigma_{a_1, \dots, a_n} , \quad (4.10a)$$

where  $\sigma_{a_1, \dots, a_n}$  denotes a permutation in  $S_n$  over the letters  $a_1, \dots, a_n$ , and antisymmetrizers

$$\mathbf{A}_{a_1, \dots, a_n} := \frac{1}{n!} \sum_{\sigma \in S_n} \text{sign}(\sigma) \sigma_{a_1, \dots, a_n} . \quad (4.10b)$$

These may act on subsets of  $n$  factors in  $V^{\otimes m}$ . Both symmetrizers and antisymmetrizers are by definition idempotent,

$$\mathbf{S}_{a_1, \dots, a_n}^2 = \mathbf{S}_{a_1, \dots, a_n} \quad \text{and} \quad \mathbf{A}_{a_1, \dots, a_n}^2 = \mathbf{A}_{a_1, \dots, a_n} , \quad (4.11)$$

they are projection operators.

All of these have birdtrack representations in which symmetrizers (resp. antisymmetrizers) are shown as unfilled (filled) boxes covering the lines to be symmetrized (resp. antisymmetrized). Take for example  $\mathbf{S}_{134} \in \text{API}(V^{\otimes 5})$  and  $\mathbf{A}_{35} \in \text{API}(V^{\otimes 5})$ , which take the form

$$\mathbf{S}_{134} = \begin{array}{c} \leftarrow \leftarrow \leftarrow \\ \leftarrow \leftarrow \leftarrow \\ \leftarrow \leftarrow \leftarrow \\ \leftarrow \leftarrow \leftarrow \\ \leftarrow \leftarrow \leftarrow \end{array} \in \text{API}(\text{SU}(N), V^{\otimes 5}) \quad \text{and} \quad \mathbf{A}_{35} = \begin{array}{c} \leftarrow \leftarrow \leftarrow \\ \leftarrow \leftarrow \leftarrow \\ \leftarrow \leftarrow \leftarrow \\ \leftarrow \leftarrow \leftarrow \\ \leftarrow \leftarrow \leftarrow \end{array} \in \text{API}(\text{SU}(N), V^{\otimes 5}) . \quad (4.12)$$

We note in passing that Hermitian conjugation for birdtracks (in the sense of linear maps on  $V^{\otimes m}$  with the scalar product inherited from  $V$ ) is achieved by reflection around a vertical axis, followed by a reversal of the arrows (see [72] [or section 3.3.1 in chapter 3]). As an example, take

$$\begin{array}{c} \leftarrow \leftarrow \leftarrow \\ \leftarrow \leftarrow \leftarrow \\ \leftarrow \leftarrow \leftarrow \end{array} \xrightarrow{\text{reflect}} \begin{array}{c} \leftarrow \leftarrow \leftarrow \\ \leftarrow \leftarrow \leftarrow \\ \leftarrow \leftarrow \leftarrow \end{array} \xrightarrow{\text{reverse arrows}} \begin{array}{c} \rightarrow \rightarrow \rightarrow \\ \rightarrow \rightarrow \rightarrow \\ \rightarrow \rightarrow \rightarrow \end{array} , \quad \text{i.e.} \quad \left( \begin{array}{c} \leftarrow \leftarrow \leftarrow \\ \leftarrow \leftarrow \leftarrow \\ \leftarrow \leftarrow \leftarrow \end{array} \right)^\dagger = \begin{array}{c} \rightarrow \rightarrow \rightarrow \\ \rightarrow \rightarrow \rightarrow \\ \rightarrow \rightarrow \rightarrow \end{array} . \quad (4.13)$$

This implies that all symmetrizers and antisymmetrizers as defined in eqns. (4.10) and (4.12) are Hermitian,

$$\mathbf{S}_{a_1, \dots, a_n}^\dagger = \mathbf{S}_{a_1, \dots, a_n} \quad \text{and} \quad \mathbf{A}_{a_1, \dots, a_n}^\dagger = \mathbf{A}_{a_1, \dots, a_n} , \quad (4.14)$$

and that all permutations are unitary:

$$\sigma^{-1} = \sigma^\dagger \quad \text{for all } \sigma \in S_m . \quad (4.15)$$

The direction of arrows on the legs also allows us to account for complex conjugation (*c.f.* [72]). In this paper, we will exclusively be working with real operators and thus suppress the direction of the arrows, for example

$$\text{\textcircled{X}} \quad \text{will refer to} \quad \begin{array}{c} \leftarrow \leftarrow \leftarrow \\ \leftarrow \leftarrow \leftarrow \\ \leftarrow \leftarrow \leftarrow \end{array} . \quad (4.16)$$

Lastly, if a *Hermitian* projection operator  $A$  projects onto a subspace completely contained in the image of

a Hermitian projection operator  $B$ , then we denote this as  $A \subset B$ , transferring the familiar notation of sets to the associated projection operators. In particular,  $A \subset B$  if and only if

$$A \cdot B = B \cdot A = A \tag{4.17}$$

for the following reason: If the subspaces obtained by consecutively applying the operators  $A$  and  $B$  in any order is the same as that obtained by merely applying  $A$ , then not only need the subspaces that  $A$  and  $B$  project onto overlap (as otherwise  $A \cdot B = B \cdot A = 0$ ), but the subspace corresponding to  $A$  must be completely contained in the subspace of  $B$  - otherwise the last equality of (4.17) would not hold. Hermiticity is crucial for these statements — they thus do not apply to most Young projection operators [*c.f. section 3.2.1 and later section 4.2.3*] on  $V^{\otimes m}$  if  $m \geq 3$ .<sup>2</sup> A familiar example for this situation is the relation between symmetrizers of different lengths: a symmetrizer  $\mathcal{S}_{\mathcal{N}}$  can be absorbed into a symmetrizer  $\mathcal{S}_{\mathcal{N}'}$ , as long as the index set  $\mathcal{N}$  is a subset of  $\mathcal{N}'$ , and the same statement holds for antisymmetrizers [72]. For example,

$$\begin{array}{c} \text{---} \\ \text{---} \\ \text{---} \end{array} \begin{array}{c} \text{---} \\ \text{---} \\ \text{---} \end{array} = \begin{array}{c} \text{---} \\ \text{---} \\ \text{---} \end{array} \begin{array}{c} \text{---} \\ \text{---} \\ \text{---} \end{array} = \begin{array}{c} \text{---} \\ \text{---} \\ \text{---} \end{array} \begin{array}{c} \text{---} \\ \text{---} \\ \text{---} \end{array} . \tag{4.18}$$

Thus, by the above notation,  $\mathcal{S}_{\mathcal{N}'} \subset \mathcal{S}_{\mathcal{N}}$  if  $\mathcal{N} \subset \mathcal{N}'$ . Or, as in our example,

$$\begin{array}{c} \text{---} \\ \text{---} \\ \text{---} \end{array} \subset \begin{array}{c} \text{---} \\ \text{---} \\ \text{---} \end{array} . \tag{4.19}$$

$\text{API}(\text{SU}(N), V^{\otimes m})$  itself is equipped with a scalar product for linear maps that is consistent with the scalar product on  $V^{\otimes m}$  and simply given by a trace

$$\langle \cdot, \cdot \rangle : \text{API}(\text{SU}(N), V^{\otimes m}) \times \text{API}(\text{SU}(N), V^{\otimes m}) \rightarrow \mathbb{R}, \quad \langle A, B \rangle := \text{tr}(A^\dagger B) . \tag{4.20}$$

In birdtrack notation, the trace  $\text{tr}$  merely connects each line exiting  $A^\dagger B$  on the left with the line entering  $A^\dagger B$  on the right that is on the same level [72],

$$\text{tr}(A^\dagger B) = \begin{array}{c} \text{---} \\ \text{---} \\ \text{---} \end{array} \begin{array}{c} \text{---} \\ \text{---} \\ \text{---} \end{array} . \tag{4.21}$$

For example,

$$\text{tr} \left( \begin{array}{c} \text{---} \\ \text{---} \end{array} \begin{array}{c} \text{---} \\ \text{---} \end{array} \right)^\dagger \begin{array}{c} \text{---} \\ \text{---} \end{array} \begin{array}{c} \text{---} \\ \text{---} \end{array} = \text{tr} \left( \begin{array}{c} \text{---} \\ \text{---} \end{array} \begin{array}{c} \text{---} \\ \text{---} \end{array} \right) = \text{tr} \left( \begin{array}{c} \text{---} \\ \text{---} \end{array} \begin{array}{c} \text{---} \\ \text{---} \end{array} \right) = \begin{array}{c} \text{---} \\ \text{---} \end{array} \begin{array}{c} \text{---} \\ \text{---} \end{array} = N^2, \tag{4.22}$$

where we have drawn the lines originating from the trace in red for visual clarity. Each closed loop in the trace yields a factor of  $N$  (the dimension of the fundamental representation), so that the scalar product (4.20) will always yield a polynomial of  $N$ . In particular, it is clear that this polynomial will not be identically 0 if  $A, B \in S_m$  (and hence  $A^\dagger \in S_m$ ), since  $S_m$  is a group and thus  $A^\dagger B \in S_m$ . The cyclic property of the trace

<sup>2</sup>As can be explicitly verified by an example.

becomes very apparent in birdtrack notation, as the operator  $A_1$  in

$$\text{tr}(A_1 A_2 \dots A_n) \tag{4.23}$$

can just be “pulled” to the right of  $A_n$  along the lines induced by the trace. [Traces of the elements of  $\text{API}(\text{SU}(N), V^{\otimes m})$  and  $\text{API}(\text{SU}(N), V^{\otimes m} \otimes (V^*)^{\otimes m'})$  are discussed in more detail in chapter 8.]

### 4.2.2 The hierarchical nature of Young tableaux

A Young tableau is a conglomerate of numbered boxes with shape and ordering restrictions imposed. The shape and ordering restrictions automatically emerge if we construct these tableaux iteratively, starting from a single box  $\boxed{1}$  in a process governed by branching rules (see for example [95, 96]). The second box  $\boxed{2}$  and all further boxes are attached (in order) to the right of or below an existing box in all possible ways that lead to a set of boxes in which no row is longer than that above it and no column is longer than the one left of it. The process results in a tree whose first few branchings are displayed in Figure 4.1.

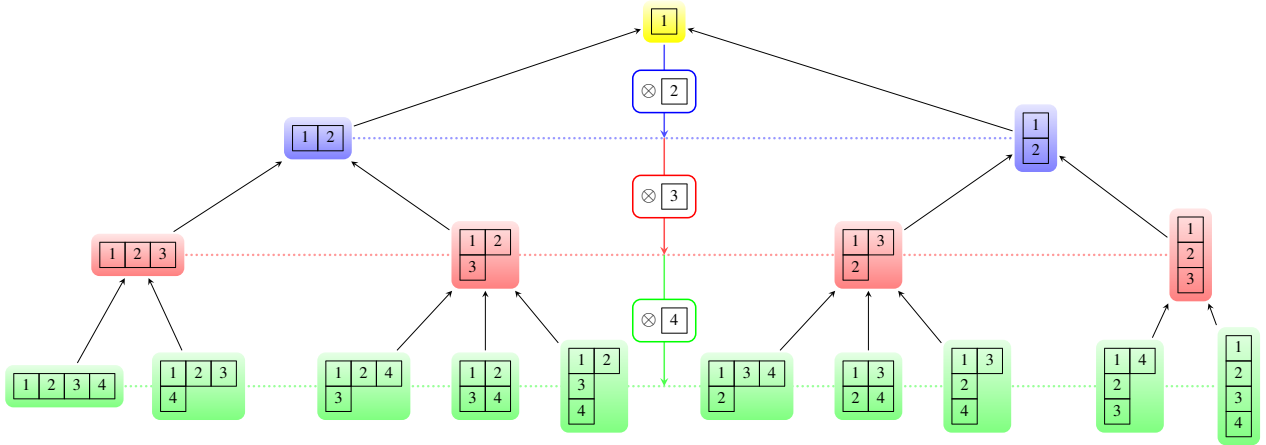


Figure 4.1: Branching tree of Young tableaux from its root to the 4<sup>th</sup> generation.

We denote the set of Young tableaux with  $n$  boxes by  $\mathcal{Y}_n$ , and note that in each branching step every Young tableau  $\Theta \in \mathcal{Y}_{n-1}$  creates a whole set of descendant tableaux in  $\mathcal{Y}_n$ . We will refer to this set by  $\{\Theta \otimes \boxed{n}\}$  and notice that it has no overlap with the descendants of any other element of  $\mathcal{Y}_{n-1}$ . Any  $\mathcal{Y}_n$  is the disjoint union of descendant sets: For example,

$$\mathcal{Y}_3 := \left\{ \begin{array}{|c|c|c|} \hline 1 & 2 & 3 \\ \hline \end{array}, \begin{array}{|c|c|} \hline 1 & 2 \\ \hline 3 \\ \hline \end{array}, \begin{array}{|c|c|} \hline 1 & 3 \\ \hline 2 \\ \hline \end{array}, \begin{array}{|c|} \hline 1 \\ \hline 2 \\ \hline 3 \\ \hline \end{array} \right\} = \left\{ \begin{array}{|c|c|} \hline 1 & 2 \\ \hline \end{array} \otimes \boxed{3} \right\} \cup \left\{ \begin{array}{|c|} \hline 1 \\ \hline 2 \\ \hline \end{array} \otimes \boxed{3} \right\}. \tag{4.24}$$

Traversing the tree of Figure 4.1 downwards is a branching operation, in which each descendant has a well defined ancestry chain: Starting at a Young tableau and taking away the box with the highest entry is a map in the mathematical sense, it yields a unique tableau. We call this map the parent map and denote it by  $\pi$ .  $\pi$  can then repeatedly be applied to the resulting tableau generating the ancestry chain for a given tableau.

An example for part of such a chain is

$$\dots \xrightarrow{\pi} \begin{array}{|c|c|c|} \hline 1 & 3 & 6 \\ \hline 2 & 5 & \\ \hline 4 & & \\ \hline \end{array} \xrightarrow{\pi} \begin{array}{|c|c|} \hline 1 & 3 \\ \hline 2 & 5 \\ \hline 4 & \\ \hline \end{array} \xrightarrow{\pi} \begin{array}{|c|c|} \hline 1 & 3 \\ \hline 2 & \\ \hline 4 & \\ \hline \end{array} \xrightarrow{\pi} \begin{array}{|c|c|} \hline 1 & 3 \\ \hline 2 & \\ \hline \end{array} \xrightarrow{\pi} \dots \quad (4.25)$$

This idea can obviously be formalized in a way that provides some useful notation:

**Definition 4.1 – parent map and ancestor tableaux:**

Let  $\Theta \in \mathcal{Y}_n$  be a Young tableau. We define its parent tableau  $\Theta_{(1)} \in \mathcal{Y}_{n-1}$  to be the tableau obtained from  $\Theta$  by removing the box  $\boxed{n}$  of  $\Theta$ . Furthermore, we will define a parent map  $\pi$  from  $\mathcal{Y}_n$  to  $\mathcal{Y}_{n-1}$ , for a particular  $n$ ,

$$\pi : \mathcal{Y}_n \rightarrow \mathcal{Y}_{n-1} , \quad (4.26)$$

which acts on  $\Theta$  by removing the box  $\boxed{n}$  from  $\Theta$ ,<sup>3</sup>

$$\pi : \Theta \mapsto \Theta_{(1)} . \quad (4.27)$$

In general, we define the successive action of the parent map  $\pi$  by

$$\mathcal{Y}_n \xrightarrow{\pi} \mathcal{Y}_{n-1} \xrightarrow{\pi} \mathcal{Y}_{n-2} \xrightarrow{\pi} \dots \xrightarrow{\pi} \mathcal{Y}_{n-m} , \quad (4.28)$$

and denote it by  $\pi^m$ ,

$$\pi^m : \mathcal{Y}_n \rightarrow \mathcal{Y}_{n-m} , \quad \pi^m := \mathcal{Y}_n \xrightarrow{\pi} \mathcal{Y}_{n-1} \xrightarrow{\pi} \mathcal{Y}_{n-2} \xrightarrow{\pi} \dots \xrightarrow{\pi} \mathcal{Y}_{n-m} . \quad (4.29)$$

We will further denote the tableau obtained from  $\Theta$  by applying the map  $\pi$   $m$  times,  $\pi^m(\Theta)$ , by  $\Theta_{(m)}$ , and refer to it as the ancestor tableau of  $\Theta$   $m$  generations back. Applying the map  $\pi^m$  to a Young tableau  $\Theta$  then yields the unique tableau  $\Theta_{(m)}$ ,

$$\pi^m : \Theta \mapsto \Theta_{(m)} . \quad (4.30)$$

We now reverse direction again and return to thinking about adding boxes. As we keep adding more and more boxes, we encounter more and more tableaux that share their overall shape, they only differ by the ordering of entries. The shape (represented by the boxes with the entries deleted) is commonly referred to as a Young *diagram*. The reordering required to relate two tableaux of the same shape defines a tableau permutation:

**Definition 4.2 – tableau permutation:**

Consider two Young tableaux  $\Theta, \Theta' \in \mathcal{Y}_n$  with the same shape. Then,  $\Theta'$  can be obtained from  $\Theta$  by permuting the numbers of  $\Theta$ ; clearly, the permutation needed to obtain  $\Theta'$  from  $\Theta$  is unique. We denote the permutation that maps  $\Theta'$  into  $\Theta$  by  $\rho_{\Theta\Theta'}$ ,

$$\Theta = \rho_{\Theta\Theta'}(\Theta') \quad \iff \quad \Theta' = \rho_{\Theta\Theta'}^{-1}(\Theta) = \rho_{\Theta'\Theta}(\Theta) . \quad (4.31)$$

<sup>3</sup>We note that the tableau  $\Theta_{(1)}$  is always a Young tableau if  $\Theta$  was a Young tableau, since removing the box with the highest entry cannot possibly destroy the properties of  $\Theta$  (and thus  $\Theta_{(1)}$ ) that make it a Young tableau.

### 4.2.3 From Young tableaux to Young operators

The literature (see for example [93]) provides a standard manner in which each Young tableau is associated with a Young projection operator that is constructed from symmetrizers and antisymmetrizers — symmetrizers for the rows and antisymmetrizers for the columns. (For completeness, we assign the identity permutation for rows or columns of length one. If *all* rows or columns are exactly of length one, we refer to this as the symmetrizers or antisymmetrizers becoming trivial.) As such, the Young projection operators corresponding to tableaux in  $\mathcal{Y}_m$  are elements of the (real) algebra of invariants  $\text{API}(\text{SU}(N), V^{\otimes m})$ .

Take, for example

$$\Theta = \begin{array}{|c|c|c|} \hline 1 & 3 & 4 \\ \hline 2 & 5 & \\ \hline \end{array}. \tag{4.32}$$

The Young projection operator corresponding to this tableau,  $Y_{\Theta}$ , is given by

$$Y_{\begin{array}{|c|c|c|} \hline 1 & 3 & 4 \\ \hline 2 & 5 & \\ \hline \end{array}} = 2 \cdot \mathbf{S}_{134} \mathbf{S}_{25} \mathbf{A}_{12} \mathbf{A}_{35}, \tag{4.33}$$

where the constant 2 ensures idempotency of  $Y_{\begin{array}{|c|c|c|} \hline 1 & 3 & 4 \\ \hline 2 & 5 & \\ \hline \end{array}}$  (*c.f.* eq. (4.37)). (This is a textbook topic. For a reminder on how to construct Young projection operators from Young tableaux, readers are referred to [93, 95, 96].) All the symmetrizers of a tableau commute with each other and so do the antisymmetrizers, since no number appears more than once in any tableau. Thus, when constructing the birdtrack corresponding to  $Y_{\begin{array}{|c|c|c|} \hline 1 & 3 & 4 \\ \hline 2 & 5 & \\ \hline \end{array}}$ , we are able to draw the two symmetrizers appearing in it underneath each other (since they are disjoint), and similarly for the two antisymmetrizers,

$$Y_{\begin{array}{|c|c|c|} \hline 1 & 3 & 4 \\ \hline 2 & 5 & \\ \hline \end{array}} = 2 \cdot \left[ \begin{array}{c} \text{diagram: two horizontal lines with arcs connecting them, representing symmetrizers and antisymmetrizers} \end{array} \right]. \tag{4.34}$$

We denote the set (or product — it does not really matter as they mutually commute) of symmetrizers associated with the tableau  $\Theta$  by  $\mathbf{S}_{\Theta}$ , and the set (or product) of antisymmetrizers by  $\mathbf{A}_{\Theta}$ . However, the symmetrizers of a tableau do not commute with its antisymmetrizers (unless one or both are trivial):

$$[\mathbf{S}_{\Theta}, \mathbf{A}_{\Theta}] \neq 0. \tag{4.35}$$

Therefore their relative order matters in the general definition of a Young projector<sup>4</sup>

$$Y_{\Theta} := \alpha_{\Theta} \mathbf{S}_{\Theta} \mathbf{A}_{\Theta}, \tag{4.36}$$

where  $\alpha_{\Theta} \in \mathbb{R}$  is defined as [72]

$$\alpha_{\Theta} := \frac{\mathcal{H}_{\Theta}}{\prod_{\mathcal{R}} |\text{length}(\mathcal{R})|! \prod_{\mathcal{C}} |\text{length}(\mathcal{C})|!}. \tag{4.37}$$

The products in the denominator run over every row  $\mathcal{R}$  respectively over every column  $\mathcal{C}$  in  $\Theta$  [72], and  $\mathcal{H}_{\Theta}$  is the hook length of the tableau  $\Theta$  [95, 96]: For a particular Young tableau  $\Theta$ , form its underlying Young

<sup>4</sup>Placing the antisymmetrizers to the right of the symmetrizers is a *choice* of convention — the reverse order leads to equivalent structural results, it only matters to stay consistent.

diagram  $\mathbf{Y}_\Theta$  by deleting all entries and then re-fill each box  $c$  in  $\mathbf{Y}_\Theta$  with the integer counting all boxes to the right and below it (including itself), called the *hook* of  $c$   $\mathcal{H}_c$ , for example,

$$\Theta = \begin{array}{|c|c|c|c|} \hline 1 & 3 & 5 & 8 \\ \hline 2 & 6 & 7 & \\ \hline 4 & & & \\ \hline \end{array} \xrightarrow{\text{delete entries}} \begin{array}{|c|c|c|c|} \hline & & & \\ \hline & & & \\ \hline & & & \\ \hline & & & \\ \hline \end{array} \xrightarrow{\text{hooks } \mathcal{H}_c} \begin{array}{|c|c|c|c|} \hline 6 & 4 & 3 & 1 \\ \hline 4 & 2 & 1 & \\ \hline 1 & & & \\ \hline \end{array} . \quad (4.38)$$

The hook length of  $\Theta$ ,  $\mathcal{H}_\Theta$ , (equivalently the hook length of  $\mathbf{Y}_\Theta$ ,  $\mathcal{H}_{\mathbf{Y}_\Theta}$ ) is defined to be the product of all the hooks  $\mathcal{H}_c$ ,

$$\mathcal{H}_\Theta = \mathcal{H}_{\mathbf{Y}_\Theta} := \prod_{c \in \Theta} \mathcal{H}_c ; \quad (4.39)$$

for the tableau in (4.38), the hook length is  $\mathcal{H}_\Theta = 6 \cdot 4^2 \cdot 3 \cdot 2 = 576$ .

The Young projection operators are nonzero precisely if all their columns are at most of length  $N$ , otherwise they vanish identically — we refer to this as being dimensionally zero (see appendix 4.A).

From eqns. (4.35) and (4.36), one infers that  $Y_\Theta$  is not Hermitian (unless at least one of the sets is trivial):

$$Y_\Theta^\dagger = \alpha_\Theta (\mathbf{S}_\Theta \mathbf{A}_\Theta)^\dagger = \alpha_\Theta \mathbf{A}_\Theta \mathbf{S}_\Theta \neq Y_\Theta . \quad (4.40)$$

Hermiticity (or the lack thereof) in birdtrack notation is best judged after expanding in primitive invariants, for example

$$\begin{aligned} Y_{\begin{array}{|c|c|} \hline 1 & 3 \\ \hline 2 & \end{array}} &= \frac{4}{3} \cdot \begin{array}{c} \text{---} \\ \text{---} \\ \text{---} \\ \text{---} \\ \text{---} \\ \text{---} \end{array} \Rightarrow Y_{\begin{array}{|c|c|} \hline 1 & 3 \\ \hline 2 & \end{array}}^\dagger = \frac{4}{3} \cdot \begin{array}{c} \text{---} \\ \text{---} \\ \text{---} \\ \text{---} \\ \text{---} \\ \text{---} \end{array} \\ &= \frac{1}{3} \left( \begin{array}{c} \text{---} \\ \text{---} \\ \text{---} \\ \text{---} \\ \text{---} \\ \text{---} \end{array} - \begin{array}{c} \text{---} \\ \text{---} \\ \text{---} \\ \text{---} \\ \text{---} \\ \text{---} \end{array} + \begin{array}{c} \text{---} \\ \text{---} \\ \text{---} \\ \text{---} \\ \text{---} \\ \text{---} \end{array} - \begin{array}{c} \text{---} \\ \text{---} \\ \text{---} \\ \text{---} \\ \text{---} \\ \text{---} \end{array} \right) \quad (4.41) \\ &= \frac{1}{3} \left( \begin{array}{c} \text{---} \\ \text{---} \\ \text{---} \\ \text{---} \\ \text{---} \\ \text{---} \end{array} - \begin{array}{c} \text{---} \\ \text{---} \\ \text{---} \\ \text{---} \\ \text{---} \\ \text{---} \end{array} + \begin{array}{c} \text{---} \\ \text{---} \\ \text{---} \\ \text{---} \\ \text{---} \\ \text{---} \end{array} - \begin{array}{c} \text{---} \\ \text{---} \\ \text{---} \\ \text{---} \\ \text{---} \\ \text{---} \end{array} \right) . \end{aligned}$$

The definition of  $Y_{\begin{array}{|c|c|c|} \hline 1 & 3 & 4 \\ \hline 2 & 5 & \end{array}}$  in (4.33) speaks of a linear map on  $V^{\otimes 5}$ , i.e. an element of  $\text{Lin}(V^{\otimes 5})$ , or with equal validity of a linear map on a larger space  $V^{\otimes m}$ ,  $m \geq 5$ , in which the factors beyond the first five remain unaffected. We speak of this case as the canonical embedding of  $\text{Lin}(V^{\otimes n}) \hookrightarrow \text{Lin}(V^{\otimes m})$  (with  $m \geq n$ ). For a given tableau  $\Theta \in \mathcal{Y}_n$ , we will, in a slight abuse of notation, employ the same notation,  $Y_\Theta$ , to talk both about the original case or any of the embeddings. The idea of an embedding in birdtrack terms requires to explicitly draw the “unaffected lines”, for example the operator  $\bar{Y}_{\begin{array}{|c|c|} \hline 1 & 2 \\ \hline 3 & \end{array}}$  is canonically embedded into  $\text{Lin}(V^{\otimes 5})$  as

$$\begin{array}{c} \text{---} \\ \text{---} \\ \text{---} \\ \text{---} \\ \text{---} \\ \text{---} \end{array} \hookrightarrow \begin{array}{c} \text{---} \\ \text{---} \\ \text{---} \\ \text{---} \\ \text{---} \\ \text{---} \end{array} . \quad (4.42)$$

Furthermore, for any operator  $O$  consisting of symmetrizers and antisymmetrizers, the symbol  $\bar{O}$  will refer to the equivalence class of operators that are proportional to the product of symmetrizers and antisymmetrizers

of  $O$  without any *additional* scalar factors. For example,

$$Y_{\Theta} := \underbrace{\frac{4}{3}}_{=: \alpha_{\Theta}} \cdot \underbrace{\text{diagram}}_{=: \bar{Y}_{\Theta}} . \tag{4.43}$$

The benefit of this notation is that it allows us to ignore all additional scalar factors; in particular, for a nonzero scalar  $\omega$ ,

$$\omega \cdot \bar{O} = \bar{O} \quad \text{but in general} \quad \omega \cdot O \neq O . \tag{4.44}$$

Tableau permutations (*c.f.* Definition 4.2) can be represented as birdtracks. A graphical procedure is probably the most efficient mean to obtain this representation:

**Definition 4.3 – tableau permutations as birdtracks:**

To construct the birdtrack form of the tableau permutation  $\rho_{\Theta\Phi}$  between tableaux of the same shape (*c.f.* Definition 4.2) explicitly, write the Young tableaux  $\Theta$  and  $\Phi$  next to each other, such that  $\Theta$  is to the left of  $\Phi$ , and then connect the boxes in the corresponding position of the two diagrams, such as



Then, write two columns of numbers from 1 to  $n$  next to each other in descending order; the left column represents the entries of  $\Theta$ , and the right column represents the entries of  $\Phi$ . Lastly, connect the entries in the left and the right column in correspondence to (4.45). The resulting tangle of lines is the birdtrack corresponding to  $\rho_{\Theta\Phi}$  and thus determines the permutation.

As a birdtrack,  $\rho_{\Theta\Phi}$  immediately becomes a linear map in  $\text{API}(\text{SU}(N), V^{\otimes m})$  and as such directly relates the associated Young projectors:

$$Y_{\Theta} = \rho_{\Theta\Phi} Y_{\Phi} \rho_{\Theta\Phi}^{-1} = \rho_{\Theta\Phi} Y_{\Phi} \rho_{\Phi\Theta} . \tag{4.46}$$

This property is in fact part and parcel of the very definition of Young projectors in [93, def. 5.4]. Eq. (4.46) demonstrates that tableaux of the same shape correspond to equivalent representations and  $\rho_{\Theta\Phi}$  is the isomorphism that seals the equivalence. For the Hermitian projection operators (*c.f.* sec. 4.5.1), eq. (4.46) breaks down, as is exemplified in appendix 4.B.

It may help to illustrate this with an example: Take the equivalence pair corresponding to the Young tableaux

$$\Theta := \begin{array}{|c|c|} \hline 1 & 2 \\ \hline 3 & \\ \hline \end{array} \quad \text{and} \quad \Phi := \begin{array}{|c|c|} \hline 1 & 3 \\ \hline 2 & \\ \hline \end{array} \tag{4.47}$$

with

$$Y_{\Theta} = \frac{4}{3} \cdot \text{diagram} \quad \text{and} \quad Y_{\Phi} = \frac{4}{3} \cdot \text{diagram} . \tag{4.48}$$

To find the permutation  $\rho_{\Theta\Phi}$ , we connect boxes between  $\Theta$  and  $\Phi$  as

$$(4.49)$$

and identify  $\rho_{\Theta\Phi}$  as  $\overline{\times}$ . Evidently, eq. (4.46) holds, since

$$(4.50)$$

#### 4.2.4 Cancellation rules

In [1] [chapter 2], we established various rules designed to easily manipulate birdtrack operators comprised of symmetrizers and antisymmetrizers. Since all operators considered in this paper are of this form, the simplification rules of [1] [chapter 2] are immediately applicable here. One of them plays a crucial role throughout this paper, so we recall the result without repeating the proof:

**■ Theorem 4.1 – cancellation of parts of the operator [1]:**

Let  $\Theta \in \mathcal{Y}_n$  be a Young tableau, and  $M \in \text{API}(\text{SU}(N), V^{\otimes n})$  be an algebra element. Then, there exists a (possibly vanishing) constant  $\lambda$  such that

$$O := \mathbf{S}_{\Theta} M \mathbf{A}_{\Theta} = \lambda \cdot Y_{\Theta} . \quad (4.51)$$

Note that if the operator  $O$  is nonzero, then  $\lambda \neq 0$ .

To obtain the maximum benefit of this theorem, we provide some crucial criteria that allow us to identify particularly important cases of nonzero  $O$  in  $\text{API}(\text{SU}(N), V^{\otimes n}) \subset \text{Lin}(V^{\otimes n})$ :

1. Let  $\mathbf{A}_{\Phi_i} \supset \mathbf{A}_{\Theta}$  and  $\mathbf{S}_{\Phi_j} \supset \mathbf{S}_{\Theta}$  be (anti-) symmetrizers that can be absorbed into  $\mathbf{A}_{\Theta}$  and  $\mathbf{S}_{\Theta}$  for every  $i \in \{1, 3, \dots, k-1\}$  and for every  $j \in \{2, 4, \dots, k\}$ . If  $M$  in (4.51) is of the form

$$M = \mathbf{A}_{\Phi_1} \mathbf{S}_{\Phi_2} \mathbf{A}_{\Phi_3} \mathbf{S}_{\Phi_4} \cdots \mathbf{A}_{\Phi_{k-1}} \mathbf{S}_{\Phi_k} , \quad (4.52)$$

then  $O$  is nonzero unless  $Y_{\Theta}$  is dimensionally zero.

2. Let  $\Theta, \Phi \in \mathcal{Y}_n$  be two Young tableaux with the same shape, and construct the permutations  $\rho_{\Theta\Phi}$  and  $\rho_{\Phi\Theta}$  between the two tableaux according to Definition 4.3. Furthermore, let  $\mathcal{D}_{\Phi}$  be a product of symmetrizers and antisymmetrizers which can be absorbed into  $\mathbf{S}_{\Phi}$  and  $\mathbf{A}_{\Phi}$  respectively. If  $M$  in (4.51) is of the form

$$M = \rho_{\Theta\Phi} \mathcal{D}_{\Phi} \rho_{\Phi\Theta} , \quad (4.53)$$

then  $O$  is nonzero unless  $Y_{\Theta}$  is dimensionally zero.

3. If  $M$  is a product of expressions of the forms (4.52) and (4.53), then  $O$  is nonzero unless  $Y_{\Theta}$  is dimensionally zero.



The general proof of these statements can again be found in [1] [chapter 2], but it is apparent that under the conditions listed for the ingredients of (4.52) and (4.53), any dimensional zero of  $O$  manifests itself as a dimensional zero of  $Y_\Theta$ , since  $\mathbf{A}_\Theta$  automatically contains the longest antisymmetrizer in  $O$ .

As an example, consider the operator

$$O := \text{[diagram]} = \{\mathbf{S}_{125}, \mathbf{S}_{34}\} \cdot \{\mathbf{A}_{13}\} \cdot \{\mathbf{S}_{12}, \mathbf{S}_{34}\} \cdot \{\mathbf{A}_{13}, \mathbf{A}_{24}\}. \quad (4.54)$$

This operator meets all conditions of Theorem 4.1: the sets  $\{\mathbf{S}_{125}, \mathbf{S}_{34}\}$  and  $\{\mathbf{A}_{13}, \mathbf{A}_{24}\}$  together constitute the birdtrack of a Young projection operator  $\bar{Y}_\Theta$  corresponding to the tableau

$$\Theta := \begin{array}{|c|c|c|} \hline 1 & 2 & 5 \\ \hline 3 & 4 & \\ \hline \end{array}. \quad (4.55)$$

The set  $\{\mathbf{A}_{13}\}$  corresponds to the ancestor tableau  $\Theta_{(2)}$ , and the set  $\{\mathbf{S}_{12}, \mathbf{S}_{34}\}$  corresponds to the ancestor tableau  $\Theta_{(1)}$  and thus can be absorbed into  $\mathbf{A}_\Theta$  resp.  $\mathbf{S}_\Theta$  (c.f. eq. (4.18)). Hence,  $O$  can be written as

$$O = \mathbf{S}_\Theta \mathbf{A}_{\Theta_{(2)}} \mathbf{S}_{\Theta_{(1)}} \mathbf{A}_\Theta. \quad (4.56)$$

According to the Cancellation Theorem 4.1, we may cancel the wedged ancestor sets  $\mathbf{A}_{\Theta_{(2)}}$  and  $\mathbf{S}_{\Theta_{(1)}}$  at the cost of a nonzero constant  $\lambda$ ,

$$O = \lambda \cdot \text{[diagram]} , \quad (4.57)$$

$\underbrace{\hspace{10em}}_{\bar{O} = \bar{Y}_{\begin{array}{|c|c|c|} \hline 1 & 2 & 5 \\ \hline 3 & 4 & \\ \hline \end{array}}}$

which is proportional to  $Y_{\begin{array}{|c|c|c|} \hline 1 & 2 & 5 \\ \hline 3 & 4 & \\ \hline \end{array}}$ .

### 4.3 Young projection and transition operators over $V^{\otimes m}$ for small $m$ : an inspiration for a multiplet adapted basis for API(SU( $N$ ), $V^{\otimes m}$ )

The group theoretical interest in Young operators is that they project onto irreducible representations. They satisfy the following three properties [85]:

1. Young projection operators are idempotent, that is they satisfy<sup>5</sup>

$$Y_\Theta \cdot Y_\Theta = Y_\Theta . \quad (4.58a)$$

They are mutually transversal as projectors in that their images intersect only at 0: if  $\Theta$  and  $\Phi$  are two distinct Young tableaux in  $\mathcal{Y}_m$ , then

$$Y_\Theta \cdot Y_\Phi = 0 \quad \text{for } m = 1, 2, 3, 4 , \quad (4.58b)$$

<sup>5</sup>This is surprisingly hard to demonstrate unless you have access to the Cancellation Theorem 4.1.

and for all  $m$  if  $\Theta$  and  $\Phi$  have a different shape.

2. The set of Young projection operators for  $\text{SU}(N)$  over  $V^{\otimes m}$  sum up to the identity element of  $V^{\otimes m}$ :

$$\sum_{\Theta \in \mathcal{Y}_m} Y_{\Theta} = \text{id}_{V^{\otimes m}} \quad \text{for } m = 1, 2, 3, 4 . \quad (4.58c)$$

In physics parlance this constitutes a completeness relation.

The Young tableaux underlying the projection operators fully classify the irreducible representations of  $\text{SU}(N)$  over  $V^{\otimes m}$  for any  $m$ . If  $m \leq 4$ , the Young projectors split the space  $V^{\otimes m}$  into mutually transversal subspaces, which can be shown to be irreducible [93]. For  $m \geq 4$ , generalizations of Young projectors take over this role. Such generalizations include subtracted operators [85, 106] and Hermitian Young projection operators [2, 4] [*c.f. chapter 3*]. In this paper, we will focus on the latter.

Besides Young projection operators not being pairwise transversal for  $m \geq 5$  as linear maps, they are not orthogonal with respect to the scalar product on API  $(\text{SU}(N), V^{\otimes m})$  even for smaller  $m$ , for example

$$\text{tr} \left( Y_{\begin{smallmatrix} \square & \square \\ \square \end{smallmatrix}}^{\dagger} Y_{\begin{smallmatrix} \square & \square \\ \square \end{smallmatrix}} \right) \neq 0 , \quad (4.59)$$

as emerges quickly from an explicit calculation:

$$\begin{aligned} \text{tr} \left( Y_{\begin{smallmatrix} \square & \square \\ \square \end{smallmatrix}}^{\dagger} Y_{\begin{smallmatrix} \square & \square \\ \square \end{smallmatrix}} \right) &= \text{Tr} \left( \left( \frac{4}{3} \right)^2 \begin{array}{c} \text{---} \text{---} \text{---} \\ \text{---} \text{---} \end{array} \cdot \begin{array}{c} \text{---} \text{---} \text{---} \\ \text{---} \text{---} \end{array} \right) \\ &= \frac{1}{9} \text{Tr} \left( - \text{---} \text{---} + \text{---} \text{---} - 2 \cdot \text{---} \text{---} + \text{---} \text{---} + 2 \cdot \text{---} \text{---} - \text{---} \text{---} \right) \\ &= -\frac{N_c^3}{9} + \frac{N_c}{9} \neq 0 . \end{aligned}$$

This mishap is only possible since the Young projectors are not Hermitian — otherwise their transversality as projectors would create a zero automatically at least for  $m \leq 4$ .<sup>6</sup>

Nevertheless, the trace of  $Y_{\Theta}$  corresponding to  $\Theta \in \mathcal{Y}_m$ , normalized as a projector, uncovers the dimension of the associated irreducible representation (see [72, appendix B4] for a textbook exposition):

$$\text{tr}(Y_{\Theta}) = \dim(\Theta) \quad \text{for all } m . \quad (4.60)$$

As is evident from Figure 4.1,  $|\mathcal{Y}_m|$ , the number of Young tableaux in  $\mathcal{Y}_m$ , is smaller than the dimension of API  $(\text{SU}(N), V^{\otimes m})$ , which is  $m!$  (up to dimensional zeros).

### 4.3.1 Transition operators for Young projectors over $V^{\otimes m}$ for $m \leq 4$

Generally, the established goal of representation theory is to find a set of operators that satisfy idempotency, transversality and decomposition of unity, nothing more, nothing less, and for  $m \leq 4$ , Young projection operators do just that.

---

<sup>6</sup>This is truly an issue with Hermiticity, not a consequence of choosing an unsuitable scalar product: The sets of left and right eigenvectors differ if  $Y_{\Theta}$  is not Hermitian.

We step beyond this point by noting that there is an additional set of linearly independent operators in  $\text{API}(\text{SU}(N), V^{\otimes m})$  for  $m \leq 4$  that are closely related to the set of Young projectors, and that complete it to a basis of the full algebra in a transparent way. Recall that for any pair of equivalent representations corresponding to tableaux  $\Theta$  and  $\Phi$  in  $\mathcal{Y}_m$ , there exists a unique tableau permutation  $\rho_{\Theta\Phi}$  such that  $Y_\Theta = \rho_{\Theta\Phi} Y_\Phi \rho_{\Phi\Theta}$  (c.f. eq. (4.46)). From this, define *transition operators* as

$$T_{\Theta\Phi} := \rho_{\Theta\Phi} Y_\Phi = Y_\Theta \rho_{\Theta\Phi} = Y_\Theta \rho_{\Theta\Phi} Y_\Phi \quad \text{for } m = 1, 2, 3, 4, \quad (4.61)$$

and observe that they seamlessly extend the multiplication table of the Young projectors:

$$Y_\Theta T_{\Theta\Phi} = T_{\Theta\Phi} = T_{\Theta\Phi} Y_\Phi \quad (4.62a)$$

$$T_{\Theta\Phi} T_{\Phi\Theta} = Y_\Theta \quad (4.62b)$$

$$T_{\Phi\Theta} T_{\Theta\Phi} = Y_\Phi. \quad (4.62c)$$

We see that  $T_{\Theta\Phi}$  maps the image  $Y_\Phi(V^{\otimes m})$  bijectively onto  $Y_\Theta(V^{\otimes m})$  for  $m \leq 4$ . The inverse on the images is  $T_{\Phi\Theta}$ . The operators  $T_{\Theta\Phi}$  are *transition operators* between the irreducible representations. An example of all Young projection and transition operators over  $V^{\otimes 3}$  is given in section 4.3.3.

Note that, in general, the transition operators between Young projectors are not unitary on the subspaces,

$$(T_{\Theta\Phi})^\dagger = Y_\Phi^\dagger \rho_{\Phi\Theta} Y_\Theta^\dagger \neq T_{\Phi\Theta}, \quad (4.63)$$

since the Young projection operators are not Hermitian (for an explicit example, see appendix 4.C).

### 4.3.2 A multiplet adapted basis for $\text{API}(\text{SU}(N), V^{\otimes m})$

In this section, we prove that the set of all mutually orthogonal projection operators corresponding to irreducible representations of  $\text{SU}(N)$  over  $V^{\otimes m}$  and their transition operators — call this set  $\mathfrak{S}_m$  — spans the algebra of invariants  $\text{API}(\text{SU}(N), V^{\otimes m})$ . This proof holds for all  $m$  allowing us to construct  $\mathfrak{S}_m$ : for Young projection operators, this means that  $m \leq 4$ . Later on (section 4.4), we see that  $\mathfrak{S}_m$  can be constructed *for all*  $m$  if *Hermitian* Young projection operators are used.

The projection operators corresponding to irreducible representations of  $\text{SU}(N)$  over  $V^{\otimes m}$  project onto equivalent irreducible representations *if and only if* the corresponding Young tableaux have the same shape [72, 93] and thus correspond to the same underlying Young diagram. Suppose now that a particular Young diagram  $\mathbf{Y}$  gives rise to  $l$  Young tableaux. Then, the set of all projection operators corresponding to these  $l$  tableaux and all transition operators between them — let us denote this set by  $\mathfrak{S}_{\mathbf{Y}}$  — will be of size  $l^2$ ,

$$|\mathfrak{S}_{\mathbf{Y}}| = l^2, \quad (4.64)$$

since one may always arrange the elements of  $\mathfrak{S}_{\mathbf{Y}}$  into an  $l \times l$  matrix which has the projection operators on the diagonal and each off-diagonal element in position  $ij$  is the transition operator between the diagonal elements  $ii$  and  $jj$ . Fortunately, there is a way of counting how many Young tableaux can be obtained from a Young diagram with a particular shape, namely via the hook length  $\mathcal{H}_{\mathbf{Y}}$  [95, 96, 109]<sup>7</sup> (c.f. eq. (4.39)): If

<sup>7</sup>Note that one often finds the statement that “the number of tableaux corresponding to a diagram is given by the hook length.” It would be less misleading to state that it is a function of the hook length.

$\mathbf{Y}$  is a particular Young diagram, then the set  $\mathfrak{S}_{\mathbf{Y}}$  has size  $(m!/\mathcal{H}_{\mathbf{Y}})^2$  [109],

$$|\mathfrak{S}_{\mathbf{Y}}| = \left( \frac{m!}{\mathcal{H}_{\mathbf{Y}}} \right)^2. \quad (4.65)$$

If we sum the  $|\mathfrak{S}_{\mathbf{Y}}|$  over all Young diagrams  $\mathbf{Y}$  consisting of  $m$  boxes, we obtain the aggregate number of all projection and transition operators associated with  $\text{SU}(N)$  over  $V^{\otimes m}$ ,  $|\mathfrak{S}_m|$ ,

$$|\mathfrak{S}_m| = \sum_{\mathbf{Y}} |\mathfrak{S}_{\mathbf{Y}}| = \sum_{\mathbf{Y}} \left( \frac{m!}{\mathcal{H}_{\mathbf{Y}}} \right)^2. \quad (4.66)$$

To proceed further, we need to use some well established facts of the representation theory of the permutation group of  $m$  elements,  $S_m$ , which can be found in many standard textbooks such as [100]. To this end, let us briefly recapitulate: Each irreducible representation of  $S_m$  corresponds to a Young *diagram*  $\mathbf{Y}$  (not a Young tableau!), and the multiplicity of each representation in the regular representation of the symmetric group is given by  $m!/\mathcal{H}_{\mathbf{Y}}$ . From the representation theory of finite groups (such as  $S_m$ ), it is further known that the sum of the square of the multiplicities of all irreducible representations of a finite group  $G$  is equal to the size of the group. In particular, for the finite group  $S_m$ , this means that

$$|S_m| = \sum_{\mathbf{Y}} \left( \frac{m!}{\mathcal{H}_{\mathbf{Y}}} \right)^2, \quad (4.67)$$

where we sum over all Young tableaux  $\mathbf{Y}$  consisting of  $m$  boxes. (For a bijective proof of eq. (4.67) see [96].) However, (4.66) tells us that the sum on the right hand side of equation (4.67) also represents the aggregate number of all Hermitian Young projection and transition operators of  $\text{SU}(N)$  over  $V^{\otimes m}$ , so that

$$|S_m| = |\mathfrak{S}_m|. \quad (4.68)$$

Provided that  $N \geq m$ , so that dimensional zeros are absent, the projection and transition operators in  $\mathfrak{S}_m$  are all linearly independent (see appendix 4.A for the general case). It follows that these operators span the algebra of invariants over  $V^{\otimes m}$ , and thus constitute an alternative basis of this algebra,

$$\text{API}(\text{SU}(N), V^{\otimes m}) = \left\{ \alpha_k \mathfrak{s}_k \mid \alpha_k \in \mathbb{R}, \mathfrak{s}_k \in \mathfrak{S}_m \right\}. \quad (4.69)$$

### 4.3.3 An example: the full algebra over $V^{\otimes 3}$ in a Young projector basis

$\text{API}(\text{SU}(N), V^{\otimes 3})$  is spanned by the primitive invariants

$$\left\{ \overline{\Xi}, \underline{\Xi}, \overline{\mathfrak{X}}, \underline{\mathfrak{X}}, \overline{\mathfrak{Y}}, \underline{\mathfrak{Y}} \right\} \subset \text{Lin}(V^{\otimes 3}). \quad (4.70)$$

If  $N \geq 3$ , its dimension is  $3! = 6$ . There are 3 Young diagrams consisting of 3 boxes, which give rise to a total of 4 Young tableaux,

$$(4.71)$$

Indeed, we find that the sum of the squares of  $3!/\mathcal{H}_{\mathbf{Y}_i}$  corresponding to each diagram  $\mathbf{Y}_i$  is equal to the size of the group  $S_3$ ,

$$3! = |S_3| = \sum_{\mathbf{Y}_i} \left( \frac{3!}{\mathcal{H}_{\mathbf{Y}_i}} \right)^2 = 1^2 + 2^2 + 1^2. \quad (4.72)$$

The first and last Young tableaux have a unique shape and thus project onto unique irreducible representations of  $SU(N)$ . The corresponding Young projection operators are given by

$$Y_1 = \begin{array}{|c|} \hline \text{---} \\ \hline \text{---} \\ \hline \text{---} \\ \hline \end{array} \quad \text{and} \quad Y_4 = \begin{array}{|c|} \hline \text{---} \\ \hline \text{---} \\ \hline \text{---} \\ \hline \end{array}, \quad (4.73)$$

where  $Y_i$  corresponds to the  $i^{\text{th}}$  tableau (read from left to right) in (4.71). The central two tableaux of (4.71) stem from the same Young diagram. Thus, their corresponding projection operators project onto equivalent irreducible representations; there must therefore exist two transition operators between them. The projection operators  $Y_2$  and  $Y_3$  are

$$Y_2 = \frac{4}{3} \begin{array}{|c|} \hline \text{---} \\ \hline \text{---} \\ \hline \text{---} \\ \hline \end{array} \quad \text{and} \quad Y_3 = \frac{4}{3} \begin{array}{|c|} \hline \text{---} \\ \hline \text{---} \\ \hline \text{---} \\ \hline \end{array}, \quad (4.74)$$

and the transition operators  $T_{ij}$  between  $Y_i$  and  $Y_j$  are

$$T_{23} = Y_2 \rho_{23} = \frac{4}{3} \begin{array}{|c|} \hline \text{---} \\ \hline \text{---} \\ \hline \text{---} \\ \hline \end{array} \quad \text{and} \quad T_{32} = Y_3 \rho_{32} = \frac{4}{3} \begin{array}{|c|} \hline \text{---} \\ \hline \text{---} \\ \hline \text{---} \\ \hline \end{array}, \quad (4.75)$$

in accordance with eq. (4.61) (the permutations  $\rho_{23}$  and  $\rho_{32}$  were calculated in eq. (4.49)). Arranging all projection and transition operators in a matrix  $\mathfrak{M}$ , where the diagonal elements  $\mathbf{m}_{ii}$  are projection operators, and each off-diagonal element  $\mathbf{m}_{ij}$  is the transition operator between  $\mathbf{m}_{ii}$  and  $\mathbf{m}_{ij}$ , one obtains the following matrix of operators,

$$\mathfrak{M} = \begin{pmatrix} \begin{array}{|c|} \hline \text{---} \\ \hline \text{---} \\ \hline \text{---} \\ \hline \end{array} & 0 & 0 & 0 \\ 0 & \frac{4}{3} \begin{array}{|c|} \hline \text{---} \\ \hline \text{---} \\ \hline \text{---} \\ \hline \end{array} & \frac{4}{3} \begin{array}{|c|} \hline \text{---} \\ \hline \text{---} \\ \hline \text{---} \\ \hline \end{array} & 0 \\ 0 & \frac{4}{3} \begin{array}{|c|} \hline \text{---} \\ \hline \text{---} \\ \hline \text{---} \\ \hline \end{array} & \frac{4}{3} \begin{array}{|c|} \hline \text{---} \\ \hline \text{---} \\ \hline \text{---} \\ \hline \end{array} & 0 \\ 0 & 0 & 0 & \begin{array}{|c|} \hline \text{---} \\ \hline \text{---} \\ \hline \text{---} \\ \hline \end{array} \end{pmatrix}, \quad (4.76)$$

where all projection operators are highlighted in blue for visual clarity. The sole purpose of arranging the projection and transition operators in the matrix  $\mathfrak{M}$  is to emphasize the structure and multiplication table of the subalgebras corresponding to the equivalence classes (i.e. the blocks in  $\mathfrak{M}$ ).

Notice that the operator in the  $1 \times 1$  block in the bottom right corner contains an antisymmetrizer of length 3. Thus, for  $N \leq 2$ , this operator is a null-operator, and only the remaining two blocks are non-trivial in the above matrix (*c.f.* appendix 4.A). If  $N \leq 1$ , also the central  $2 \times 2$  block vanishes, as it contains antisymmetrizers of length 2.

## 4.4 Orthogonal projector bases

As we have seen in section 4.3, the Young projection and transition operators provide a basis for the algebra of invariants of  $SU(N)$  over  $V^{\otimes m}$ , provided  $m \leq 4$ . Due to a lack of pairwise transversality and completeness of the Young projection operators beyond this point (*c.f.* eqns. (4.58b) and (4.58c) [and appendix 3.A]), the Young basis cannot be generalized to larger  $m$ . This motivates a basis in terms of *Hermitian* Young projection operators, since these are transversal and complete for all values of  $m$  [4].

We restate the most important aspects of Hermitian Young projection operators in section 4.4.1, before discussing transition operators between Hermitian projections in sections 4.4.2 (in terms of Clebsch-Gordan operators) and 4.5 (between Hermitian Young projection operators).

Section 4.4.3 discusses the multiplication table of the basis of the algebra of invariants of  $SU(N)$  over  $V^{\otimes m}$  in terms of Hermitian projectors and their corresponding transition operators.

### 4.4.1 Hermitian projection operators

If we replace the Young projectors  $Y_\Theta$  by their (more complicated) Hermitian counterparts  $P_\Theta$ , either following Keppeler and Sjödalh [4, 82, 102] or our own improved versions thereof [1, 2] [chapters 2 and 3], the group theoretically important features of Young projection operators now apply *for all values of  $m$*  [4]:<sup>8</sup>

1. The Hermitian Young projection operators are *idempotent* and *mutually transversal as projectors*: for any two Young tableaux  $\Theta$  and  $\Phi$  in  $\mathcal{Y}_m$ , they satisfy

$$P_\Theta \cdot P_\Theta = \delta_{\Theta\Phi} P_\Theta \quad \text{for all } m . \quad (4.77a)$$

2. They provide a complete decomposition of unity on  $V^{\otimes m}$

$$\sum_{\Theta \in \mathcal{Y}_m} P_\Theta = \text{id}_{V^{\otimes m}} \quad \text{for all } m \quad (4.77b)$$

into irreducible representations.

3. Unlike their Young counterparts, they *are* Hermitian

$$P_\Theta^\dagger = P_\Theta . \quad (4.77c)$$

---

<sup>8</sup>The constructions used in this paper are summarized in section 4.5.1.

Due to this new property (Hermiticity), several new features appear [2] [chapter 3]:

4. The projectors in the descendant set  $\{\Theta \otimes \boxed{m}\}$  of any  $\Theta \in \mathcal{Y}_{m-1}$  sum to the parent projector, thus augmenting the single identity (4.77b) by a whole nested set of inclusion sums or partial completeness statements [2] [chapter 3]:

$$\sum_{\Phi \in \{\Theta \otimes \boxed{m}\}} P_{\Phi} = P_{\Theta} . \quad (4.77d)$$

This can be generalized further,

$$\sum_{\Phi \in \{\Theta \otimes \boxed{k} \otimes \dots \otimes \boxed{m}\}} P_{\Phi} = P_{\Theta} \quad \text{for } \Theta \in \mathcal{Y}_{k-1}, \Phi \in \mathcal{Y}_m \text{ and } k < m . \quad (4.77e)$$

5. Unlike their conventional Young counterparts  $Y_{\Theta}$  (or the corrected Littlewood-Young operators  $L_{\Theta}$ , see [2, 85] [or appendix 3.A]), the Hermitian Young projectors  $P_{\Theta}$  are automatically orthogonal with respect to the scalar product on  $\text{API}(\text{SU}(N), V^{\otimes m})$ ,

$$\langle P_{\Theta}, P_{\Phi} \rangle = \text{tr} \left( P_{\Theta}^{\dagger} P_{\Phi} \right) \stackrel{(4.77c)}{=} \text{tr} (P_{\Theta} P_{\Phi}) \stackrel{(4.77a)}{=} 0 \quad \text{for } \Theta \neq \Phi . \quad (4.77f)$$

Both of these properties hinge crucially on Hermiticity — standard (Littlewood-) Young projectors do not share them [c.f. chapter 3].

While the existence of projection operators satisfying eqns. (4.77), and transition operators between them, follows directly from Schur's Lemma, we find it beneficial to illustrate the existence of these operators using Clebsch-Gordan operators.<sup>9</sup> This method remains computationally expensive and keeping  $N$  a parameter appears a hopeless task (see section 4.4.2). In section 4.5, we give an effective construction of transition operators between Hermitian Young projection operators.

#### 4.4.2 A full orthogonal basis for $\text{API}(\text{SU}(N), V^{\otimes m})$ via Clebsch-Gordan operators

Consider a general Clebsch-Gordan operator  $C_{\lambda\kappa; j_1 m_1 \dots j_n m_n}$  that implements the projection and basis change from a product of irreducible representations labelled by  $j_1, \dots, j_n$  (with states labelled by  $m_1, \dots, m_n$ ) into an irreducible representation labelled by  $\lambda$  (where  $\lambda$  stands in for a Young tableau, and with states labelled by  $\kappa$ ) [93]:

$$\begin{aligned} C_{\lambda\kappa; j_1 m_1 \dots j_n m_n} &= |\lambda, \kappa\rangle \overbrace{\langle \lambda, \kappa | j_1, m_1 \rangle \langle j_2, m_2 \rangle \dots \langle j_n, m_n \rangle}^{\mathfrak{C}_{\lambda\kappa; j_1 m_1 \dots j_n m_n}} \langle j_1, m_1 | \langle j_2, m_2 | \dots \langle j_n, m_n | \\ &=: |\lambda, \kappa\rangle \mathfrak{K} \left\langle \begin{array}{c} \lambda \\ \leftarrow j_1, m_1 \\ \leftarrow j_2, m_2 \\ \vdots \\ \leftarrow j_{n-1}, m_{n-1} \\ \leftarrow j_n, m_n \end{array} \right\rangle \begin{array}{c} \langle j_1, m_1 | \\ \langle j_2, m_2 | \\ \vdots \\ \langle j_{n-1}, m_{n-1} | \\ \langle j_n, m_n | \end{array} , \end{aligned} \quad (4.78)$$

the part marked as  $\mathfrak{C}_{\lambda\kappa; j_1 m_1 \dots j_n m_n}$  is the usual Clebsch-Gordan coefficient, and the diagram in the second line is the birdtrack representation of  $\mathfrak{C}_{\lambda\kappa; j_1 m_1 \dots j_n m_n}$  (c.f. [72]). Since we are interested only in products

<sup>9</sup>For a more comprehensive discussion on Clebsch-Gordan operators than section 4.4.2, readers are referred to [108, in German] or [93] for a more modern treatment.

of the fundamental representation acting on  $V^{\otimes n}$  (so that the  $j_i$  all refer to this one representation), we can suppress the corresponding label, but we must retain  $\lambda$  to reference a specific irreducible representation contained in this product. The full operator is obtained by summing over all the indices:

$$C_{\lambda,n} := \sum_{\kappa} \sum_{m_i} C_{\lambda\kappa;j_1 m_1 \dots j_n m_n} =: \left\langle \begin{array}{c} \lambda \\ \vdots \end{array} \right\rangle. \quad (4.79)$$

By its very nature, the Clebsch-Gordan operator translates a product representation into its irreducible sub-blocks labelled by  $\lambda$ , i.e.

$$\left\langle \begin{array}{c} \lambda \\ \vdots \end{array} \right\rangle = U_{(\lambda)} \left\langle \begin{array}{c} \lambda \\ \vdots \end{array} \right\rangle \quad \text{and} \quad \left\langle \begin{array}{c} \lambda \\ \vdots \end{array} \right\rangle = U_{(\lambda)}^\dagger \left\langle \begin{array}{c} \lambda \\ \vdots \end{array} \right\rangle \quad (4.80)$$

for all  $U, U^\dagger \in \text{SU}(N)$  and  $U_{(\lambda)}$  in the representation of  $\text{SU}(N)$  labelled by  $\lambda$ . Orthonormality of the new states,

$$\kappa \left\langle \begin{array}{c} \lambda \\ \vdots \end{array} \right\rangle \left\langle \begin{array}{c} \lambda' \\ \vdots \end{array} \right\rangle \kappa' = \delta_{\lambda,\lambda'} \delta_{\kappa,\kappa'}, \quad (4.81)$$

allows us to cast projection operators in the form

$$P_\lambda := \sum_{\kappa} |\lambda, \kappa\rangle \langle \lambda, \kappa| = C_{\lambda,n}^\dagger \cdot C_{\lambda,n} = \left\langle \begin{array}{c} \lambda \\ \vdots \end{array} \right\rangle \left\langle \begin{array}{c} \lambda \\ \vdots \end{array} \right\rangle, \quad (4.82)$$

which are clearly mutually transversal,

$$P_\lambda P_{\lambda'} = \lambda_{\lambda,\lambda'} P_\lambda. \quad (4.83)$$

Equation (4.82) also introduces the birdtrack notation of  $C_{\lambda,n}^\dagger$ , the Hermitian conjugate of  $C_{\lambda,n}$  given in eq. (4.79). The operators  $P_\lambda$  are mutually transversal elements of the algebra of primitive invariants  $\text{API}(\text{SU}(N), V^{\otimes n})$  due to eq. (4.80),

$$\left\langle \begin{array}{c} \lambda \\ \vdots \end{array} \right\rangle \left\langle \begin{array}{c} \lambda \\ \vdots \end{array} \right\rangle = \left\langle \begin{array}{c} \lambda \\ \vdots \end{array} \right\rangle U_{(\lambda)} U_{(\lambda)}^\dagger \left\langle \begin{array}{c} \lambda \\ \vdots \end{array} \right\rangle = \left\langle \begin{array}{c} \lambda \\ \vdots \end{array} \right\rangle \left\langle \begin{array}{c} \lambda \\ \vdots \end{array} \right\rangle, \quad (4.84)$$

and general theory assures us that these yield projectors on all irreducible subspaces contained in  $V^{\otimes n}$  [93].

From the perspective of Clebsch-Gordan operators, there are obvious candidates for transition operators: When two equivalent representations  $\lambda$  and  $\lambda'$  are isomorphic, one can choose the states  $|\lambda, \kappa\rangle$  and  $|\lambda', \kappa\rangle$  such that the representation matrices are identical,  $U_{(\lambda')} = U_{(\lambda)}$ . This allows us to identify the transition operators

$$T_{\lambda'\lambda} := \sum_{\kappa} |\lambda', \kappa\rangle \langle \lambda, \kappa| = C_{\lambda',n}^\dagger \cdot C_{\lambda,n} = \left\langle \begin{array}{c} \lambda' \\ \vdots \end{array} \right\rangle \left\langle \begin{array}{c} \lambda \\ \vdots \end{array} \right\rangle \quad (4.85)$$



as additional algebra elements, since, with this particular basis choice, they also are invariant:

$$(4.86)$$

Unlike the projection operators  $P_\lambda$ , the transition operators  $T_{\lambda'\lambda}$  are clearly not Hermitian. From their definition in terms of states (4.85), it, however, follows that they are unitary (on the subspaces corresponding to  $\lambda$  and  $\lambda'$ ),

$$(T_{\lambda'\lambda})^\dagger = T_{\lambda\lambda'} . \quad (4.87)$$

These operators in fact define the isomorphisms that in the standard perspective allow us to claim equivalence between the two representations in the first place. Our point here is that these isomorphisms are elements of  $\text{API}(\text{SU}(N), V^{\otimes n})$ .

The totality of all projection and transition operators (4.82) and (4.85) obviously exhausts the algebra of invariants due to the completeness of Clebsch-Gordan operators; the transition operators (4.85) provide *all* the missing basis elements, which fixes their total number. This matches with the counting arguments of section 4.3, and seamlessly fits into the multiplication pattern of closed subalgebras discussed in section 4.4.3.

Note that this procedure leads to a particular realization of projectors and associated transition operators, any other equivalent construction may produce results that differ by a similarity transformation as discussed in section 4.4.3.<sup>10</sup> As a means to find a basis in a practical calculation, this procedure is exceedingly inefficient: It relies on finding a total of  $N^n$  normalized states in  $V^{\otimes n}$  as a stepping stone to produce  $n!$  basis states for  $\text{API}(\text{SU}(N), V^{\otimes n})$ , while keeping  $N \geq n$  to avoid dimensional zeros.<sup>11</sup> It clearly is not the most efficient option to achieve this goal, in particular if one aims to keep  $N$  as a parameter. Therefore, we use the Clebsch-Gordan method as a proof of concept, and abstract the main features of the resulting basis as the goalposts for a more efficient construction to be presented in section 4.5.

We observe:

1.  $T_{\Theta\Phi}$ , as a map from  $V^{\otimes n}$  to  $V^{\otimes n}$ , projects onto the image of  $P_\Phi$  and maps that surjectively onto the image of  $P_\Theta$ ,

$$T_{\Theta\Phi}P_\Phi = T_{\Theta\Phi} = P_\Theta T_{\Theta\Phi} . \quad (4.88)$$

It thus can be considered a map from the image of  $P_\Phi$ ,  $P_\Phi(V^{\otimes n})$ , to the image of  $P_\Theta$ ,  $P_\Theta(V^{\otimes n})$ .

2.  $T_{\Theta\Phi}^\dagger$  is the right inverse of  $T_{\Theta\Phi}$  on  $P_\Theta(V^{\otimes n})$ ,

$$T_{\Theta\Phi}T_{\Theta\Phi}^\dagger = P_\Theta . \quad (4.89)$$

3.  $T_{\Theta\Phi}^\dagger$  is the left inverse of  $T_{\Theta\Phi}$  on  $P_\Phi(V^{\otimes n})$ ,

$$T_{\Theta\Phi}^\dagger T_{\Theta\Phi} = P_\Phi . \quad (4.90)$$

<sup>10</sup>We will see that this similarity transform leaves the block structure of the associated matrix  $\mathfrak{M}$  invariant (see section 4.4.3 and refined below in eq. (4.99)).

<sup>11</sup>This forces us into the domain where  $N^n \geq n^n > n!$ . There will always be more states than multiplets.

We see that  $T_{\Theta\Phi}$  maps the image  $P_\Phi(V^{\otimes n})$  bijectively onto  $P_\Theta(V^{\otimes n})$  — the inverse is  $T_{\Phi\Theta} = T_{\Theta\Phi}^\dagger$ . The  $T_{\Theta\Phi}$  are *unitary transition operators* between the irreducible representations.

These properties are sufficient to uniquely characterize the  $T_{\Theta\Phi}$ . The argument for uniqueness follows a similar pattern as the uniqueness proof for inverses in a group.

Alternatively, one may cast the statements 2 and 3 as

$$2'. T_{\Theta\Phi}^\dagger = T_{\Phi\Theta}$$

$$3'. T_{\Theta\Phi}T_{\Phi\Theta} = P_\Theta .$$

This is the form we use in the definition:

**■ Definition 4.4 – unitary transition operators:**

Let  $\Theta, \Phi \in \mathcal{Y}_n$  be two Young tableaux with the same underlying Young diagram, and let  $P_\Theta$  and  $P_\Phi$  be their respective Hermitian Young projection operators. Then, the operator  $T_{\Theta\Phi}$ , satisfying the following three properties

$$T_{\Theta\Phi}P_\Phi = T_{\Theta\Phi} = P_\Theta T_{\Theta\Phi} \tag{4.91a}$$

$$T_{\Theta\Phi}^\dagger = T_{\Phi\Theta} \tag{4.91b}$$

$$T_{\Theta\Phi}T_{\Phi\Theta} = P_\Theta , \tag{4.91c}$$

is called the transition operator between  $P_\Theta$  and  $P_\Phi$ .

### 4.4.3 The multiplication table of the algebra of invariants

If we look at a given Young diagram  $\mathbf{Y}_i$ , then the set of all projection and transition operators corresponding to tableaux with shape  $\mathbf{Y}_i$ ,  $\mathfrak{S}_{\mathbf{Y}_i}$ , forms a closed subalgebra of  $\text{API}(\text{SU}(N), V^{\otimes m})$ . Its multiplication table is given by eqns. (4.83) and (4.91), and evidently decouples from the rest of the algebra. A simple relabelling allows to condense these equations into a single one (see eq. (4.93b) below). To do so, form a matrix pattern in which the projection operators are placed on the diagonals, such that

$$\mathfrak{m}_{ii} = P_{\Theta_i} \quad \text{for all } \Theta_i \in \mathcal{Y}_m \text{ with underlying diagram } \mathbf{Y}_i \tag{4.92a}$$

and populate the off-diagonal sites with the transition operators, such that

$$\mathfrak{m}_{ij} = T_{\Theta_i\Theta_j} \quad \text{for all } \Theta_i, \Theta_j \in \mathcal{Y}_m \text{ with underlying diagram } \mathbf{Y}_i . \tag{4.92b}$$

Calling the matrix of elements for this subalgebra  $\mathfrak{M}_{\mathbf{Y}_i}$  we can then assemble all such blocks into a matrix pattern of independent closed subalgebras by placing the blocks along the diagonal while filling the remainder with zeros (this makes sense since the “transition operators” between projectors belonging to different blocks

have to be zero by Schur's Lemma). Schematically, we obtain

$$\mathfrak{M} = \begin{pmatrix} \mathfrak{M}_{V_1} & & & & \\ & \mathfrak{M}_{V_2} & & & \\ & & \ddots & & \\ & & & \mathfrak{M}_{V_i} & \\ & & & & \ddots \\ & & & & & \mathfrak{M}_{V_k} \end{pmatrix}. \quad (4.93a)$$

This matrix once again illustrates the fact that the sum of all projection operators and transition operators of  $SU(N)$  must be a sum of squares (*c.f.* eq. (4.66)), as  $\mathfrak{M}$  is block diagonal. It is clear that the matrix elements  $\mathfrak{m}_{ij}$  of  $\mathfrak{M}$  in (4.93a) satisfy the property

$$\mathfrak{m}_{ij}\mathfrak{m}_{kl} = \delta_{jk}\mathfrak{m}_{il}. \quad (4.93b)$$

Eq. (4.93b) (together with the statement which of the  $\mathfrak{m}_{ij}$  are zero) is probably the most compact form to encode both eqns. (4.83) and (4.91) simultaneously. In the new notation, we have

$$\text{API}(SU(N), V^{\otimes m}) = \left\{ \alpha_{ij}\mathfrak{m}_{ij} \mid \alpha_{ij} \in \mathbb{R}, \mathfrak{m}_{ij} \in \mathfrak{S}_m \right\}, \quad (4.93c)$$

where the sum is over all  $i, j \in \{1, \dots, m\}$ , and  $\mathfrak{S}_m$  once again denotes the set of all projection and transition operators corresponding to the irreducible representations of  $SU(N)$  over  $V^{\otimes m}$ . This basis has the advantage that dimensional zeros manifest themselves directly as zeros of the basis elements: if a dimensional zero appears at  $N < m$ , it affects whole equivalence blocks. All operators in the block turn into null-operators simultaneously (*c.f.* appendix 4.A, or section 4.6 for an explicit example). No *additional* dimensional zeros can arise from linear combinations of the remaining basis elements.

In particular, the product (4.93b) yields a nonzero result if and only if two elements of the same block are multiplied in the correct order. A special case of this is squaring a projection operator, such that  $i = j = k = l$ . In fact, (4.93b) is the structure of the multiplication table of the multiplet basis for  $\text{API}(SU(N), V^{\otimes m})$ , and even for  $\text{API}(SU(N), V^{\otimes m} \otimes (V^*)^{\otimes m'})$  [*this is discussed in chapter 5*].

The multiplication table (4.93b) is clearly more structured than that of the primitive invariant basis of  $\text{API}(SU(N), V^{\otimes m})$ , which is directly the multiplication table of  $S_m$ :

$$\rho_i\rho_j = A^k_{ij}\rho_k. \quad (4.94)$$

This has consequences: The simpler structure of (4.93b) also gives access to the uniqueness of the operators  $\mathfrak{m}_{ij}$  appearing in it. While the types and equivalence patterns (the block structure) of irreducible representations contained in  $\text{API}(SU(N), V^{\otimes m})$ , or  $\text{API}(SU(N), V^{\otimes m} \otimes (V^*)^{\otimes m'})$ , are uniquely determined by  $N$ ,  $m$  and  $m'$ , the operators themselves are not uniquely determined by the multiplication table and decomposition of unity requirements alone, if the size of the block it falls into is greater than one.

This can be seen as follows: Since the block structure is fixed, two realizations  $\mathfrak{M}$  and  $\tilde{\mathfrak{M}}$  of bases with the

same block structure must satisfy

$$\mathbf{m}_{ij}\mathbf{m}_{kl} = \delta_{jk}\mathbf{m}_{il} \quad \text{and} \quad \tilde{\mathbf{m}}_{ij}\tilde{\mathbf{m}}_{kl} = \delta_{jk}\tilde{\mathbf{m}}_{il} , \quad (4.95)$$

and be related by a general *real* linear transformation as

$$\tilde{\mathbf{m}}_{ij} := a_{i\alpha}\mathbf{m}_{\alpha\beta}b_{\beta j} . \quad (4.96)$$

This implies that (note that the  $\mathbf{m}$  are *operators*, while the  $a_{ij}$  and  $b_{ij}$  are real coefficients that commute with the  $\mathbf{m}$ )

$$\tilde{\mathbf{m}}_{ij}\tilde{\mathbf{m}}_{kl} = a_{i\alpha}\mathbf{m}_{\alpha\beta}b_{\beta j}a_{k\gamma}\mathbf{m}_{\gamma\delta}b_{\delta l} \stackrel{\mathbf{m}_{\alpha\beta}\mathbf{m}_{\gamma\delta}=\mathbf{m}_{\alpha\delta}\delta_{\beta\gamma}}{=} a_{i\alpha}\mathbf{m}_{\alpha\delta}b_{\delta l} \underbrace{(a_{k\beta}b_{\beta j})}_{\stackrel{!}{=} \delta_{kj}} \stackrel{!}{=} \delta_{kj}\tilde{\mathbf{m}}_{il} , \quad \text{i.e. } b = a^{-1} . \quad (4.97)$$

With this constraint,  $a$  must have the same block structure as both  $\mathfrak{M}$  and  $\tilde{\mathfrak{M}}$ .

Everything we said up to this point also holds for a basis of Young projection and transition operators over  $\text{API}(\text{SU}(N), V^{\otimes m})$ , provided  $m \leq 4$ .<sup>12</sup> The main disadvantage (besides being restricted to small  $m$ ) of this basis remains that it is not orthogonal under the standard scalar product on  $\text{API}(\text{SU}(N), V^{\otimes m})$  provided by  $\langle A, B \rangle = \text{tr}(A^\dagger B)$ , as is exemplified in (4.59).

Populating the subalgebra listing  $\mathfrak{M}$  with Hermitian projectors and their unitary transition operators results in an orthogonal basis:

$$\langle \mathbf{m}_{ij}, \mathbf{m}_{kl} \rangle = \text{tr} \left( \mathbf{m}_{ij}^\dagger \mathbf{m}_{kl} \right) \stackrel{(4.91b)}{\stackrel{(4.77c)}}{=} \text{tr}(\mathbf{m}_{ji}\mathbf{m}_{kl}) \stackrel{(4.93b)}{=} \delta_{ik} \text{tr}(\mathbf{m}_{jl}) = \delta_{ik}\delta_{jl} \dim(\Theta_j) , \quad (4.98)$$

where  $\Theta_j$  labels the representation corresponding to the projection operator  $\mathbf{m}_{jj}$ . Note that this is a general statement based purely on the multiplication table, Hermiticity and unitarity, without any reference to a specific realization of the basis elements, and thus automatically also applies to the basis we construct in section 4.5.

Hermiticity and unitarity also restrict the freedom to change the  $\mathbf{m}_{ij}$  beyond what we had seen in eq. (4.97): The Hermiticity properties ( $\mathbf{m}_{ij}^\dagger = \mathbf{m}_{ji}$ ,  $\tilde{\mathbf{m}}_{ij}^\dagger = \tilde{\mathbf{m}}_{ji}$  and  $a_{ij} \in \mathbb{R}$  since the algebra is real) then lead to

$$\tilde{\mathbf{m}}_{ij}^\dagger = a_{i\alpha}\mathbf{m}_{\alpha\beta}^\dagger a_{\beta j}^{-1} = a_{i\alpha}\mathbf{m}_{\beta\alpha} a_{\beta j}^{-1} = (a^{-1})_{j\beta}^t \mathbf{m}_{\beta\alpha} a_{\alpha i}^t \stackrel{!}{=} \tilde{\mathbf{m}}_{ji} \quad \text{i.e.} \quad a^{-1} = a^t , \quad (4.99)$$

the freedom is restricted to (blockwise!) orthogonal transformations of the  $\mathbf{m}_{ij}$ .

## 4.5 Unitary transition operators for Hermitian Young projectors

Like the (non-unitary) transition operators for Young projectors over  $V^{\otimes m}$  ( $m \leq 4$ ) introduced in section 4.3, the unitary transition operators associated with Hermitian Young projectors are based on the projectors themselves. In the present case, the building blocks will be a set  $\{P_\Theta | \Theta \in \mathcal{Y}_m\}$  (with the full list of properties listed in section 4.4.1), where we need not put a restriction on  $m$ . We first recapitulate their ingredients in

<sup>12</sup>We have not provided transition operators for the Littlewood-Young operators, so that at this point we need to switch to Hermitian operators as soon as  $m \geq 5$ .

section 4.5.1 before we use them, and the tableau permutations of Definition 4.3, to construct the transition operators in section 4.5.2.

### 4.5.1 Construction methods of Hermitian Young projection operators

At the present time, there exist three ways of constructing (completely equivalent) Hermitian Young projection operators. The first is an iterative method that goes back to Keppeler and Sjödaahl (KS) and is discussed in [4]. The second method is based on the KS-algorithm, but produces substantially shorter operators [2] [chapter 3]. The third method exploits the structure of Young tableaux and their “lexical ordering” [2] [chapter 3]. Since the second and third method are used in this paper, we summarize these two construction algorithms in the present section.

In the second method, Hermitian Young projection operators are constructed by forming a product of consecutively “older” Young projection operators:

**■ Theorem 4.2 – staircase form of Hermitian Young projectors [2]:**

Let  $\Theta \in \mathcal{Y}_n$  be a Young tableau. Then, the corresponding Hermitian Young projection operator  $P_\Theta$  is given by

$$P_\Theta = Y_{\Theta_{(n-2)}} Y_{\Theta_{(n-3)}} Y_{\Theta_{(n-4)}} \cdots Y_{\Theta_{(2)}} Y_{\Theta_{(1)}} Y_\Theta Y_{\Theta_{(1)}} Y_{\Theta_{(2)}} \cdots Y_{\Theta_{(n-4)}} Y_{\Theta_{(n-3)}} Y_{\Theta_{(n-2)}}. \quad (4.100)$$

In the third method, one takes into account the *lexical ordering* of the Young tableau. In order to accomplish this, we require a few more definitions.

**■ Definition 4.5 – column- & row-words and lexical ordering:**

Let  $\Theta \in \mathcal{Y}_n$  be a Young tableau. We define the column-word of  $\Theta$ ,  $\mathfrak{C}_\Theta$ , to be the column vector whose entries are the entries of  $\Theta$  read column-wise from left to right. Similarly, the row-word of  $\Theta$ ,  $\mathfrak{R}_\Theta$ , is defined to be the row vector whose entries are those of  $\Theta$  read row-wise from top to bottom.

We say that a tableau  $\Theta$  is (lexically) ordered if either its row-word or its column-word (or both) is in lexical order. If we want to be more specific, we might call  $\Theta$  row-ordered resp. column-ordered.

For example, the tableau

$$\Phi := \begin{array}{|c|c|c|c|} \hline 1 & 5 & 7 & 9 \\ \hline 2 & 6 & 8 & \\ \hline 3 & & & \\ \hline 4 & & & \\ \hline \end{array} \quad (4.101)$$

has a column-word

$$\mathfrak{C}_\Phi = (1, 2, 3, 4, 5, 6, 7, 8, 9)^t, \quad (4.102)$$

and a row-word

$$\mathfrak{R}_\Phi = (1, 5, 7, 9, 2, 6, 8, 3, 4). \quad (4.103)$$

Since  $\mathfrak{C}_\Phi$  is lexically ordered, we say that  $\Phi$  is a (column-) ordered tableau.

It should be noted that the above definition of the row-word is *different* to that given in the standard literature such as [95, 96] (there, the row word is read from bottom to top rather than from top to bottom). However, for the purposes of this paper, Definition 4.5 is more useful than the standard definition.

■ **Definition 4.6 – measure of lexical disorder (MOLD):**

Let  $\Theta \in \mathcal{Y}_n$  be a Young tableau. We define its Measure Of Lexical Disorder (*MOLD*) to be the smallest natural number  $\mathcal{M}(\Theta) \in \mathbb{N}$  such that

$$\Theta_{(\mathcal{M}(\Theta))} = \pi^{\mathcal{M}(\Theta)}(\Theta) \quad (4.104)$$

is a lexically ordered tableau. (Recall from Definition 4.1 that  $\pi^{\mathcal{M}(\Theta)}$  refers to  $\mathcal{M}(\Theta)$  consecutive applications of the parent map  $\pi$  to the tableau  $\Theta$ .)

We note that the MOLD of a Young tableau is a well-defined quantity, since one will always eventually arrive at a lexically ordered tableau, as, for example, all tableaux in  $\mathcal{Y}_3$  are lexically ordered. This then implies that the MOLD of a tableau  $\Theta \in \mathcal{Y}_n$  has an upper bound,

$$\mathcal{M}(\Theta) \leq n - 3, \quad (4.105)$$

making it a well-defined quantity. As an example, consider the tableau

$$\Phi := \begin{array}{|c|c|c|} \hline 1 & 2 & 4 \\ \hline 3 & 5 & \\ \hline \end{array}. \quad (4.106)$$

The MOLD of the above tableau is  $\mathcal{M}(\Phi) = 2$ , one needs to apply  $\pi$  twice to arrive at the first lexically ordered ancestor, which in this case is row ordered:

$$\underbrace{\begin{array}{|c|c|c|} \hline 1 & 2 & 4 \\ \hline 3 & 5 & \\ \hline \end{array}}_{\Phi} \xrightarrow{\pi} \underbrace{\begin{array}{|c|c|c|} \hline 1 & 2 & 4 \\ \hline 3 & & \\ \hline \end{array}}_{\Phi_{(1)}} \xrightarrow{\pi} \underbrace{\begin{array}{|c|c|} \hline 1 & 2 \\ \hline 3 & \\ \hline \end{array}}_{\Phi_{(2)}}. \quad (4.107)$$

The following construction algorithm of Hermitian Young projection operators uses the MOLD of the corresponding Young tableau [2] [chapter 3]:

■ **Theorem 4.3 – MOLD operators [2]:**

Consider a Young tableau  $\Theta \in \mathcal{Y}_n$  with MOLD  $\mathcal{M}(\Theta) = m$ . Furthermore, suppose that  $\Theta_{(m)}$  has a lexically ordered row-word. Then, the Hermitian Young projection operator corresponding to  $\Theta$ ,  $P_\Theta$ , is, for even  $m$ ,

$$P_\Theta = \beta_\Theta \cdot \mathbf{S}_{\Theta_{(m)}} \mathbf{A}_{\Theta_{(m-1)}} \mathbf{S}_{\Theta_{(m-2)}} \cdots \mathbf{S}_{\Theta_{(2)}} \mathbf{A}_{\Theta_{(1)}} \bar{Y}_\Theta^\dagger \bar{Y}_\Theta \mathbf{A}_{\Theta_{(1)}} \mathbf{S}_{\Theta_{(2)}} \cdots \mathbf{S}_{\Theta_{(m-2)}} \mathbf{A}_{\Theta_{(m-1)}} \mathbf{S}_{\Theta_{(m)}}, \quad (4.108a)$$

and, for odd  $m$ ,

$$P_\Theta = \beta_\Theta \cdot \mathbf{S}_{\Theta_{(m)}} \mathbf{A}_{\Theta_{(m-1)}} \mathbf{S}_{\Theta_{(m-2)}} \cdots \mathbf{A}_{\Theta_{(2)}} \mathbf{S}_{\Theta_{(1)}} \bar{Y}_\Theta^\dagger \bar{Y}_\Theta \mathbf{S}_{\Theta_{(1)}} \mathbf{A}_{\Theta_{(2)}} \cdots \mathbf{S}_{\Theta_{(m-2)}} \mathbf{A}_{\Theta_{(m-1)}} \mathbf{S}_{\Theta_{(m)}}. \quad (4.108b)$$

Similarly, if  $\Theta_{(m)}$  has a lexically ordered column-word,  $P_\Theta$  is given by, for even  $m$ ,

$$P_\Theta = \beta_\Theta \cdot \mathbf{A}_{\Theta_{(m)}} \mathbf{S}_{\Theta_{(m-1)}} \mathbf{A}_{\Theta_{(m-2)}} \cdots \mathbf{A}_{\Theta_{(2)}} \mathbf{S}_{\Theta_{(1)}} \bar{Y}_\Theta^\dagger \bar{Y}_\Theta \mathbf{S}_{\Theta_{(1)}} \mathbf{A}_{\Theta_{(2)}} \cdots \mathbf{A}_{\Theta_{(m-2)}} \mathbf{S}_{\Theta_{(m-1)}} \mathbf{A}_{\Theta_{(m)}}, \quad (4.108c)$$

and, for odd  $m$ ,

$$P_{\Theta} = \beta_{\Theta} \cdot \mathbf{A}_{\Theta(m)} \mathbf{S}_{\Theta(m-1)} \mathbf{A}_{\Theta(m-2)} \cdots \mathbf{S}_{\Theta(2)} \mathbf{A}_{\Theta(1)} \bar{Y}_{\Theta} \bar{Y}_{\Theta}^{\dagger} \mathbf{A}_{\Theta(1)} \mathbf{S}_{\Theta(2)} \cdots \mathbf{A}_{\Theta(m-2)} \mathbf{S}_{\Theta(m-1)} \mathbf{A}_{\Theta(m)}. \quad (4.108d)$$

In the above, all symmetrizers and antisymmetrizers are understood to be canonically embedded into the algebra over  $V^{\otimes n}$ ;  $\beta_{\Theta}$  is a nonzero constant chosen such that  $P_{\Theta}$  is idempotent.

This construction seems complicated at first glance as four cases need to be considered. In [2] [chapter 3], we discuss why this is necessary and how the structure of Theorem 4.3 can be understood.

## 4.5.2 Unitary transition operators for Hermitian Young projectors

For the standard Young projection operators, the tableau permutation  $\rho_{\Theta\Phi}$ , viewed as an element of  $\text{Lin}(V^{\otimes m})$ , directly relates any associated Young projectors:

$$Y_{\Theta} = \rho_{\Theta\Phi} Y_{\Phi} \rho_{\Theta\Phi}^{-1} \quad (4.109)$$

(c.f. eq. (4.46)). For Hermitian Young projection operators, this is no longer true in general: There exist tableaux  $\Theta$  and  $\Phi$  such that

$$P_{\Theta} \neq \rho_{\Theta\Phi} P_{\Phi} \rho_{\Theta\Phi}^{-1}. \quad (4.110)$$

The simplest example for such a mismatch is probably the equivalence pair corresponding to the Young tableaux from eq. (4.47)

$$\Theta := \begin{array}{|c|c|} \hline 1 & 2 \\ \hline 3 & \\ \hline \end{array} \quad \text{and} \quad \Phi := \begin{array}{|c|c|} \hline 1 & 3 \\ \hline 2 & \\ \hline \end{array} \quad (4.111)$$

with

$$Y_{\Theta} = \frac{4}{3} \cdot \begin{array}{c} \text{---} \text{---} \\ \text{---} \text{---} \\ \text{---} \text{---} \end{array} \quad \text{and} \quad Y_{\Phi} = \frac{4}{3} \cdot \begin{array}{c} \text{---} \text{---} \\ \text{---} \text{---} \\ \text{---} \text{---} \end{array} \quad (4.112)$$

and

$$P_{\Theta} = \frac{4}{3} \cdot \begin{array}{c} \text{---} \text{---} \\ \text{---} \text{---} \\ \text{---} \text{---} \end{array} \quad \text{and} \quad P_{\Phi} = \frac{4}{3} \cdot \begin{array}{c} \text{---} \text{---} \\ \text{---} \text{---} \\ \text{---} \text{---} \end{array} \quad (4.113)$$

respectively. We recall the associated tableau permutation from eq. (4.49):  $\rho_{\Theta\Phi} = \overline{\text{---}}$ . Evidently,

$$\frac{4}{3} \cdot \begin{array}{c} \text{---} \text{---} \\ \text{---} \text{---} \\ \text{---} \text{---} \end{array} = \frac{4}{3} \cdot \begin{array}{c} \text{---} \text{---} \\ \text{---} \text{---} \\ \text{---} \text{---} \end{array}, \quad \text{while} \quad \frac{4}{3} \cdot \begin{array}{c} \text{---} \text{---} \\ \text{---} \text{---} \\ \text{---} \text{---} \end{array} \neq \frac{4}{3} \cdot \begin{array}{c} \text{---} \text{---} \\ \text{---} \text{---} \\ \text{---} \text{---} \end{array}, \quad (4.114)$$

as claimed.

However, what remains true is that

$$P_{\Theta} \cdot \rho_{\Theta\Phi} P_{\Phi} \rho_{\Theta\Phi}^{-1} \neq 0, \quad (4.115)$$

since all symmetrizers and anti-symmetrizers in  $\rho_{\Theta\Phi}P_{\Phi}\rho_{\Theta\Phi}^{-1}$  can be absorbed into  $\mathbf{S}_{\Theta}$  and  $\mathbf{A}_{\Theta}$  respectively, see condition 2 (eq. (4.53)) in section 4.2.4. The fact that  $P_{\Theta} \cdot \rho_{\Theta\Phi}P_{\Phi}\rho_{\Theta\Phi}^{-1} \neq 0$  in eq. (4.115) is the main ingredient that guarantees that the transition operators constructed below fulfill all necessary criteria. A more involved example illustrating the action of  $\rho_{\Theta\Phi}$  on  $P_{\Phi}$  is given in appendix 4.B.

Here is a first version of the construction algorithm for transition operators:

■ **Theorem 4.4 – unitary transition operators:**

Let  $\Theta, \Phi \in \mathcal{Y}_n$  be two Young tableaux with the same underlying Young diagram, and let  $P_{\Theta}$  and  $P_{\Phi}$  be their respective Hermitian Young projection operators, and  $T_{\Theta\Phi}$  the transition operator between them. Then,  $T_{\Theta\Phi}$  is given by

$$T_{\Theta\Phi} = \tau \cdot P_{\Theta}\rho_{\Theta\Phi}P_{\Phi} , \quad (4.116)$$

where  $\tau$  is a nonzero constant, and  $\rho_{\Theta\Phi} \in S_n$  is the permutation constructed according to Definition 4.3. The constant  $\tau$  is constrained by eq. (4.91c) and can be determined through explicit calculation (c.f. eq. (4.128)).

That the operator (4.116) defined in Theorem 4.4 satisfies all conditions (4.91) as is readily seen:

**Property (4.91a),  $T_{\Theta\Phi}P_{\Phi} = T_{\Theta\Phi} = P_{\Theta}T_{\Theta\Phi}$ , is easily shown:** Let

$$T_{\Theta\Phi} := \tau \cdot P_{\Theta}\rho_{\Theta\Phi}P_{\Phi} \quad \text{with } \tau \in \mathbb{R} \setminus \{0\} . \quad (4.117)$$

Then,

$$T_{\Theta\Phi} \cdot P_{\Phi} := \tau \cdot P_{\Theta}\rho_{\Theta\Phi} \underbrace{P_{\Phi} \cdot P_{\Phi}}_{=P_{\Phi}} = \tau \cdot P_{\Theta}\rho_{\Theta\Phi}P_{\Phi} , \quad (4.118)$$

since  $P_{\Phi}$  is a projection operator. Similarly,

$$P_{\Theta} \cdot T_{\Theta\Phi} := \tau \cdot \underbrace{P_{\Theta} \cdot P_{\Theta}}_{=P_{\Theta}} \rho_{\Theta\Phi}P_{\Phi} = \tau \cdot P_{\Theta}\rho_{\Theta\Phi}P_{\Phi} . \quad (4.119)$$

**Property (4.91b),  $T_{\Theta\Phi}^{\dagger} = T_{\Phi\Theta}$ :**

$$T_{\Theta\Phi}^{\dagger} = \left( P_{\Theta}\rho_{\Theta\Phi}P_{\Phi} \right)^{\dagger} = P_{\Phi}\rho_{\Theta\Phi}^{\dagger}P_{\Theta} = T_{\Phi\Theta} , \quad (4.120)$$

where the last equality holds since  $\rho_{\Theta\Phi}^{\dagger} = \rho_{\Phi\Theta}$  is the inverse permutation of  $\rho_{\Theta\Phi}$  (c.f. Definition 4.3).

**Property (4.91c),  $T_{\Theta\Phi}T_{\Phi\Theta} = P_{\Theta}$ :** We unpack

$$T_{\Theta\Phi}T_{\Phi\Theta} = \tau^2 \cdot P_{\Theta}\rho_{\Theta\Phi} \underbrace{P_{\Phi} \cdot P_{\Phi}}_{=P_{\Phi}} \rho_{\Theta\Phi}^{\dagger}P_{\Theta} = \tau^2 \cdot P_{\Theta}\rho_{\Theta\Phi}P_{\Phi}\rho_{\Theta\Phi}^{\dagger}P_{\Theta} , \quad (4.121)$$

writing  $\rho_{\Phi\Theta}$  as  $\rho_{\Theta\Phi}^{\dagger}$  for clarity in the steps to follow. Of the equivalent ways to express the projectors  $P_{\Theta}$  and  $P_{\Phi}$  [2, 4] [c.f. chapter 3], we choose  $P_{\Theta}$  and  $P_{\Phi}$  to be constructed according to the shortened KS Theorem 4.2



(section 4.5.1):

$$\frac{T_{\Theta\Phi}T_{\Phi\Theta}}{\tau^2} = \underbrace{Y_{\Theta(n-2)} \cdots Y_{\Theta} \cdots Y_{\Theta(n-2)}}_{P_{\Theta}} \rho_{\Theta\Phi} \underbrace{Y_{\Phi(n-2)} \cdots Y_{\Phi} \cdots Y_{\Phi(n-2)}}_{P_{\Phi}} \rho_{\Theta\Phi}^{\dagger} \underbrace{Y_{\Theta(n-2)} \cdots Y_{\Theta} \cdots Y_{\Theta(n-2)}}_{P_{\Theta}}. \quad (4.122)$$

Writing each Young projection operator as a product of symmetrizers and antisymmetrizers,  $Y_{\Xi} = \alpha_{\Xi} \mathbf{S}_{\Xi} \mathbf{A}_{\Xi}$ , eq. (4.122) becomes

$$\begin{aligned} \frac{T_{\Theta\Phi}T_{\Phi\Theta}}{\tau^2 \beta_{\Theta}^2 \beta_{\Phi}} = & \quad (4.123) \\ & \underbrace{\mathbf{S}_{\Theta(n-2)} \cdots \mathbf{S}_{\Theta} \mathbf{A}_{\Theta} \mathbf{S}_{\Theta(1)} \cdots \mathbf{A}_{\Theta(n-2)}}_{\tilde{P}_{\Theta}} \underbrace{\rho_{\Theta\Theta'} \mathbf{S}_{\Theta'(n-2)} \cdots \mathbf{S}_{\Theta'} \mathbf{A}_{\Theta'} \cdots \mathbf{A}_{\Theta'(n-2)}}_{\tilde{P}_{\Theta'}} \underbrace{\rho_{\Theta'\Theta} \mathbf{S}_{\Theta(n-2)} \cdots \mathbf{A}_{\Theta(1)} \mathbf{S}_{\Theta} \mathbf{A}_{\Theta}}_{\tilde{P}_{\Theta}} \cdots \mathbf{A}_{\Theta(n-2)}, \end{aligned}$$

$\begin{array}{ccc} \text{=: } M^{(1)} & \text{=: } M^{(2)} & \text{=: } M^{(3)} \\ \hline \mathbf{S}_{\Theta} \mathbf{A}_{\Theta} \mathbf{S}_{\Theta(1)} \cdots \mathbf{A}_{\Theta(n-2)} & \rho_{\Theta\Theta'} \mathbf{S}_{\Theta'(n-2)} \cdots \mathbf{S}_{\Theta'} \mathbf{A}_{\Theta'} \cdots \mathbf{A}_{\Theta'(n-2)} & \rho_{\Theta'\Theta} \mathbf{S}_{\Theta(n-2)} \cdots \mathbf{A}_{\Theta(1)} \mathbf{S}_{\Theta} \mathbf{A}_{\Theta} \end{array}$

where the constants  $\beta_{\Theta}$  and  $\beta_{\Phi}$  lump together all the constants  $\alpha_{\Xi}$  appearing in  $P_{\Theta}$  and  $P_{\Phi}$  respectively. Let us now take a closer look the part of  $T_{\Theta\Phi}T_{\Phi\Theta}$  that is enclosed in a green box in (4.123): We notice that this part is of the form

$$O := \mathbf{S}_{\Theta} M^{(1)} M^{(2)} M^{(3)} \mathbf{A}_{\Theta}, \quad (4.124)$$

where the  $M^{(i)}$  are defined in (4.123). According to the Cancellation Theorem 4.1, there exists a constant  $\lambda$  such that

$$O = \lambda Y_{\Theta}. \quad (4.125)$$

Furthermore, we know that  $\lambda \neq 0$ , if the operator  $O$  itself is nonzero. In section 4.2.4, we gave two conditions under which  $O$  is guaranteed to be nonzero. From the definition of the  $M^{(i)}$  in eq. (4.123), it is clear that  $M^{(1)}$  and  $M^{(3)}$  satisfy the first such condition (condition 1), while  $M^{(2)}$  satisfies the second condition (condition 2). Thus, a combination of the two conditions hold, and  $O$  is nonzero (*c.f.* condition 3). This implies that (4.125) holds for a nonzero constant  $\lambda$ . We may therefore simplify (4.123) as

$$\frac{T_{\Theta\Phi}T_{\Phi\Theta}}{\tau^2 \beta_{\Theta}^2 \beta_{\Phi}} = \lambda \cdot \mathbf{S}_{\Theta(n-2)} \cdots \mathbf{A}_{\Theta(1)} \mathbf{S}_{\Theta} \mathbf{A}_{\Theta} \mathbf{S}_{\Theta(1)} \cdots \mathbf{A}_{\Theta(n-2)}. \quad (4.126)$$

Once again writing the sets of symmetrizers and antisymmetrizers as Young projection operators,  $Y_{\Xi} = \alpha_{\Xi} \mathbf{S}_{\Xi} \mathbf{A}_{\Xi}$  (where we recall that the  $\alpha_{\Xi}$  are encoded in the constants  $\beta$ ), the product  $T_{\Theta\Phi}T_{\Phi\Theta}$  becomes

$$T_{\Theta\Phi}T_{\Phi\Theta} = (\tau^2 \beta_{\Theta} \beta_{\Phi} \lambda) \cdot \underbrace{Y_{\Theta(n-2)} \cdots Y_{\Theta} \cdots Y_{\Theta(n-2)}}_{P_{\Theta}}. \quad (4.127)$$

Thus, for

$$\tau = \frac{1}{\sqrt{\beta_{\Theta} \beta_{\Phi} \lambda}}, \quad (4.128)$$

where obviously  $\tau < \infty$  and  $\tau \neq 0$  since  $\lambda$ ,  $\beta_\Theta$  and  $\beta_\Phi$  are nonzero and finite [c.f. chapters 2 and 3], the transition operator  $T_{\Theta\Phi}$  also satisfies Property 3 of Definition 4.4.

Since  $T_{\Theta\Phi}$  does indeed satisfy all properties laid out in eqs. (4.91), we conclude that it is the transition operator between the Hermitian Young projection operators  $P_\Theta$  and  $P_\Phi$ .  $\square$

Due to the length of the operator expressions, Theorem 4.4 becomes inefficient very easily. We will build on this result to refine our methods in Theorem 4.5, which provides a more efficient way of constructing the transition operators.

Returning to our example of eq. (4.113), we obtain

$$T_{\Theta\Phi} = \tau \cdot \underbrace{\text{[diagram]}}_{P_\Theta} \underbrace{\text{[diagram]}}_{\rho_{\Theta\Phi}} \underbrace{\text{[diagram]}}_{P_\Phi}. \quad (4.129)$$

Using Theorem 4.1, this can be simplified to

$$T_{\Theta\Phi} = \sqrt{\frac{4}{3}} \cdot \text{[diagram]}. \quad (4.130)$$

The constant  $\sqrt{\frac{4}{3}}$  is determined via implementing eq. (4.91c). In fact, one can incorporate this simplification step directly in the construction, arriving at a general efficient algorithm.

Our description of the algorithm is based on a specific graphical convention for the birdtracks used to represent the projection operators: For any birdtrack operator, we will align all sets of symmetrizers and antisymmetrizer at the top. If a particular set of symmetrizers  $\mathbf{S}_\Theta$  contains several symmetrizers such that each  $\mathbf{S}_i \in \mathbf{S}_\Theta$  corresponds to the  $i^{\text{th}}$  row of  $\Theta$ , then we draw  $\mathbf{S}_i$  above  $\mathbf{S}_j$  if  $i < j$ . A similar convention is used for antisymmetrizers corresponding to the columns of  $\Theta$ .

For birdtrack operators containing 3 index lines, we have neglected to follow this convention in two cases for consistency with the literature (for example [72]). This is remedied using the two identities

$$\text{[diagram 1]} = \text{[diagram 2]} \quad \text{and} \quad \text{[diagram 3]} = \text{[diagram 4]}. \quad (4.131)$$

#### ■ Theorem 4.5 – compact transition operators:

Let  $\Theta$  and  $\Phi$  be two Young tableaux of equivalent representations of  $\text{SU}(N)$ . They therefore have the same shape, and the sets of antisymmetrizers  $\mathbf{A}_\Theta$  and  $\mathbf{A}_\Phi$  are in one to one correspondence: For each element of  $\mathbf{A}_\Theta$ , there exists a counterpart in  $\mathbf{A}_\Phi$  with the same length (this is important for the graphical matching described below). Let  $\bar{P}_\Theta$  and  $\bar{P}_\Phi$  be the birdtracks of two Hermitian Young projection operators constructed according to the MOLD Theorem 4.3, drawn using the conventions listed in the previous paragraph. Then  $\bar{P}_\Theta$  and  $\bar{P}_\Phi$  contain  $\mathbf{A}_\Theta$  and  $\mathbf{A}_\Phi$  at least once, but at most twice. This determines how to proceed:

1. If both  $\bar{P}_\Theta$  and  $\bar{P}_\Phi$  each contain exactly one set of  $\mathbf{A}_\Theta$  respectively  $\mathbf{A}_\Phi$ , then pick this set in each operator.
2. If one of  $\bar{P}_\Theta$  and  $\bar{P}_\Phi$  contains one copy of  $\mathbf{A}_\Theta$  respectively  $\mathbf{A}_\Phi$ , the other contains two, then pick the leftmost set  $\mathbf{A}_\Theta$  in  $\bar{P}_\Theta$  and the rightmost set  $\mathbf{A}_\Phi$  in  $\bar{P}_\Phi$ .

3. If both  $\bar{P}_\Theta$  and  $\bar{P}_\Phi$  each contain two sets of  $\mathbf{A}_\Theta$  respectively  $\mathbf{A}_\Phi$ , then pick either the leftmost set or the rightmost set in both operators. (It does not matter which one, but it needs to be the same in both operators.)

Now split  $\bar{P}_\Theta$  and  $\bar{P}_\Phi$  by vertically cutting through the tower of antisymmetrizers chosen according to these rules. The next step discards everything to the right of the cut in  $\bar{P}_\Theta$  and everything to the left of the cut in  $\bar{P}_\Phi$ , and glues the remaining pieces together at the cut. The resulting birdtrack is  $\bar{T}_{\Theta\Phi}$ .<sup>13</sup>

The proof of this Theorem is rather lengthy and thus deferred to appendix 4.D. This proof will also shed light on the three distinctions 1, 2 and 3 we had to make in the Theorem.

To forestall any misunderstanding about the cut, discard and glue procedures (the significance of which is discussed in appendix 4.D.1), we will now clarify them with an example: Consider the two Hermitian Young projection operators

$$P_\Theta = \frac{3}{2} \cdot \text{[diagram]} \quad \text{and} \quad P_\Phi = 2 \cdot \text{[diagram]} \quad (4.132)$$

corresponding to the Young tableaux

$$\Theta = \begin{array}{|c|c|} \hline 1 & 4 \\ \hline 2 & \\ \hline 3 & \\ \hline \end{array} \quad \text{and} \quad \Phi = \begin{array}{|c|c|} \hline 1 & 3 \\ \hline 2 & \\ \hline 4 & \\ \hline \end{array} \quad (4.133)$$

respectively. We construct  $\bar{T}_{\Theta\Phi}$  according to the compact construction Theorem 4.5: we first split the leftmost antisymmetrizer  $\mathbf{A}_{123}$  of  $\bar{P}_\Theta$  and discard everything to the right of the cut,

$$\bar{P}_\Theta = \text{[diagram]} \mapsto \text{[diagram]} = \text{[diagram]} \quad (4.134)$$

Similarly,

$$\bar{P}_\Phi = \text{[diagram]} \mapsto \text{[diagram]} = \text{[diagram]} \quad (4.135)$$

Gluing the remaining pieces together at the cut then yields

$$\bar{T}_{\Theta\Phi} = \text{[diagram]} \quad (4.136)$$

and indeed, the transition operator  $T_{\Theta\Phi} = \sqrt{2} \cdot \bar{T}_{\Theta\Phi}$ , as can be easily checked by direct calculation.

Readers should note that one can replace antisymmetrizer sets ( $\mathbf{A}_\Theta$  respectively  $\mathbf{A}_\Phi$ ) by symmetrizer set ( $\mathbf{S}_\Theta$  respectively  $\mathbf{S}_\Phi$ ) in *all* the steps outlined in Theorem 4.5. This leads to the same birdtrack  $\bar{T}_{\Theta\Phi}$  as

<sup>13</sup>It should be noted that this gluing can always be done, since the two Young tableaux  $\Theta$  and  $\Phi$  have the same shape, thus do their sets of antisymmetrizers  $\mathbf{A}_\Theta$  and  $\mathbf{A}_\Phi$ , and the two sets are top-aligned.

becomes evident in the proof (*c.f.* appendix 4.D). Basing the procedure on antisymmetrizers however makes the discussion on “vanishing representations” in appendix 4.A clearer.

To obtain  $T_{\Theta\Phi} = \tau \cdot \bar{T}_{\Theta\Phi}$ , one still needs to find the normalization constant  $\tau$  from direct calculation by requiring eq. (4.91c) to hold. The relatively compact expression are well suited for an automated treatment (to obtain this constant).

## 4.6 Examples

### 4.6.1 $\text{API}(\text{SU}(N), V^{\otimes 3})$ — the full algebra of 3 quarks

Revisiting the Young tableaux in  $\mathcal{Y}_3$  (eq. (4.71)),

$$(4.137)$$

Denote the Hermitian projection operator corresponding to the  $i^{\text{th}}$  tableau in (4.137) (read from left to right) by  $P_i$ . The Hermitian projectors corresponding to the first and last tableaux in (4.137) are equal to the Young projection operators (4.73)

$$P_1 = \begin{array}{|c|} \hline \text{---} \\ \hline \text{---} \\ \hline \end{array} = Y_1 \quad \text{and} \quad P_4 = \begin{array}{|c|} \hline \text{---} \\ \hline \text{---} \\ \hline \end{array} = Y_4, \quad (4.138)$$

since these Young projectors are Hermitian to begin with. The Hermitian projection operators corresponding to the central two tableaux are different from their Young counterparts (4.74)

$$P_2 = \frac{4}{3} \begin{array}{|c|} \hline \text{---} \\ \hline \text{---} \\ \hline \end{array} \neq Y_2 \quad \text{and} \quad P_3 = \frac{4}{3} \begin{array}{|c|} \hline \text{---} \\ \hline \text{---} \\ \hline \end{array} \neq Y_3, \quad (4.139)$$

and similarly for their transition operators  $T_{ij}$  between  $P_i$  and  $P_j$ ,

$$T_{23} = \sqrt{\frac{4}{3}} \begin{array}{|c|} \hline \text{---} \\ \hline \text{---} \\ \hline \end{array} \quad \text{and} \quad T_{32} = \sqrt{\frac{4}{3}} \begin{array}{|c|} \hline \text{---} \\ \hline \text{---} \\ \hline \end{array}. \quad (4.140)$$

The birdtracks of the  $\bar{T}_{ij}$  were constructed using Theorem 4.5, and the constants were determined to match eq (4.91c). Arranging all projection operators and transition operators in a matrix  $\mathfrak{M}$  as in (4.93a), one

obtains

$$\mathfrak{M}_3 = \begin{pmatrix} \text{[blue box with 3 vertical lines]} & 0 & 0 & 0 \\ 0 & \frac{4}{3} \text{[blue box with 2 vertical lines and a black bar]} & \sqrt{\frac{4}{3}} \text{[diagram with 2 vertical lines and a black bar]} & 0 \\ 0 & \sqrt{\frac{4}{3}} \text{[diagram with 2 vertical lines and a black bar]} & \frac{4}{3} \text{[blue box with 2 vertical lines and a black bar]} & 0 \\ 0 & 0 & 0 & \text{[blue box with 3 vertical lines]} \end{pmatrix}, \tag{4.141}$$

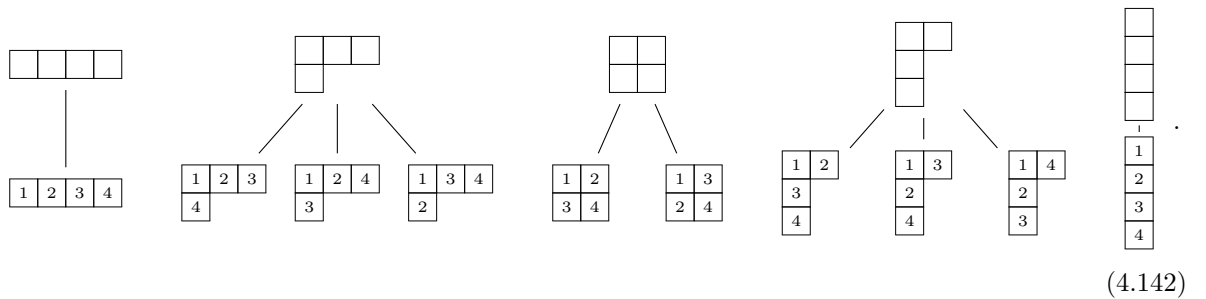
where all projection operators are highlighted in blue. The Hermitian Young projection operators were already known [4, 72]. Ref. [110] also presents the transition operators given in eq. (4.141), and [102] describes a method of obtaining a general transition operators through solving equations. The explicit construction algorithm for transition operators presented here is a new result.

As is the case for the Young projector matrix (4.76), the operator in the bottom right corner in (4.141) becomes a null-operator for  $N \leq 2$ , and so does the  $2 \times 2$  block for  $N \leq 1$ .

### 4.6.2 $\text{API}(\text{SU}(N), V^{\otimes 4})$ — the full algebra of 4 quarks

The general pattern analyzed in section 4.4.3 and once again observed in section 4.6.1 must reappear if  $m$  increases. The case  $m = 4$  provides additional illustration.

All Young tableaux of  $\mathcal{Y}_4$ , and the Young diagrams from which they originate, are



The first and last tableaux each stem from a unique Young diagram, and their corresponding representations thus are not equivalent to any other irreducible representation of  $\text{SU}(N)$ . Tableaux 2, 3 and 4 (as counted from left to right) all have the same shape and therefore correspond to equivalent irreducible representations. The same holds for the tableaux 5 and 6, and the tableaux 7, 8 and 9.

If we arrange the Young projection operators corresponding to the tableaux in (4.142), as well as the transition operators, in a block-diagonal matrix as was done in (4.93a) (with projection operators on the diagonal and

transition operators on the off-diagonal), the resulting block diagonal matrix will be of the form

$$\mathfrak{M}_4 = \begin{pmatrix} \boxed{1} & & & & \\ & \boxed{3} & & & \\ & & \boxed{2} & & \\ & & & \boxed{3} & \\ & & & & \boxed{1} \end{pmatrix}, \quad (4.143)$$

where the number in each block gives the size of the block. Indeed, we again find that

$$4! = |S_4| = \sum_{\mathbf{Y}_i} \left( \frac{4!}{\mathcal{H}_{\mathbf{Y}_i}} \right)^2 = 1^2 + 3^2 + 2^2 + 3^2 + 1^2. \quad (4.144)$$

Since the matrix (4.143) would be rather large, we will now give each block separately. The first block, consisting only of one Hermitian Young projection operator, is

$$\begin{array}{|c|c|c|c|} \hline & & & \\ \hline \end{array} : \quad \left( \begin{array}{|c|} \hline \boxed{1} \\ \hline \end{array} \right), \quad (4.145)$$

and corresponds to an irreducible representation of  $SU(N)$  with dimension  $d = \frac{N(N+1)(N+2)(N+3)}{24}$ . The second block, a  $3 \times 3$  block, is

$$\begin{array}{|c|c|c|} \hline & & \\ \hline \end{array} : \quad \left( \begin{array}{ccc} \boxed{\frac{3}{2}} & \sqrt{2} & \sqrt{\frac{3}{2}} \\ \sqrt{2} & \boxed{2} & \sqrt{3} \\ \sqrt{\frac{3}{2}} & \sqrt{3} & \boxed{\frac{3}{2}} \end{array} \right). \quad (4.146)$$

All Hermitian Young projection operators on the diagonal of this block correspond to equivalent irreducible representations of  $SU(N)$  with dimension  $d = \frac{N(N+2)(N^2-1)}{8}$ . The following  $2 \times 2$  block has projection operators on its diagonal that correspond to equivalent irreducible representations of dimension  $d = \frac{N^2(N^2-1)}{12}$ ,

$$\begin{array}{|c|c|} \hline & \\ \hline \end{array} : \quad \left( \begin{array}{cc} \boxed{\frac{4}{3}} & \sqrt{\frac{4}{3}} \\ \sqrt{\frac{4}{3}} & \boxed{\frac{4}{3}} \end{array} \right). \quad (4.147)$$

The next  $3 \times 3$  block is given by

$$\begin{array}{|c|} \hline \square \\ \hline \square \\ \hline \square \\ \hline \end{array} : \left( \begin{array}{ccc} \begin{array}{|c|} \hline \frac{3}{2} \\ \hline \end{array} & \sqrt{3} & \sqrt{\frac{3}{2}} \\ \hline \sqrt{3} & \begin{array}{|c|} \hline 2 \\ \hline \end{array} & \sqrt{2} \\ \hline \sqrt{\frac{3}{2}} & \sqrt{2} & \begin{array}{|c|} \hline \frac{3}{2} \\ \hline \end{array} \end{array} \right); \tag{4.148}$$

here, the projection operators each correspond to irreducible representations of dimension  $d = \frac{N(N-2)(N^2-1)}{8}$ . What remains is a  $1 \times 1$  block:

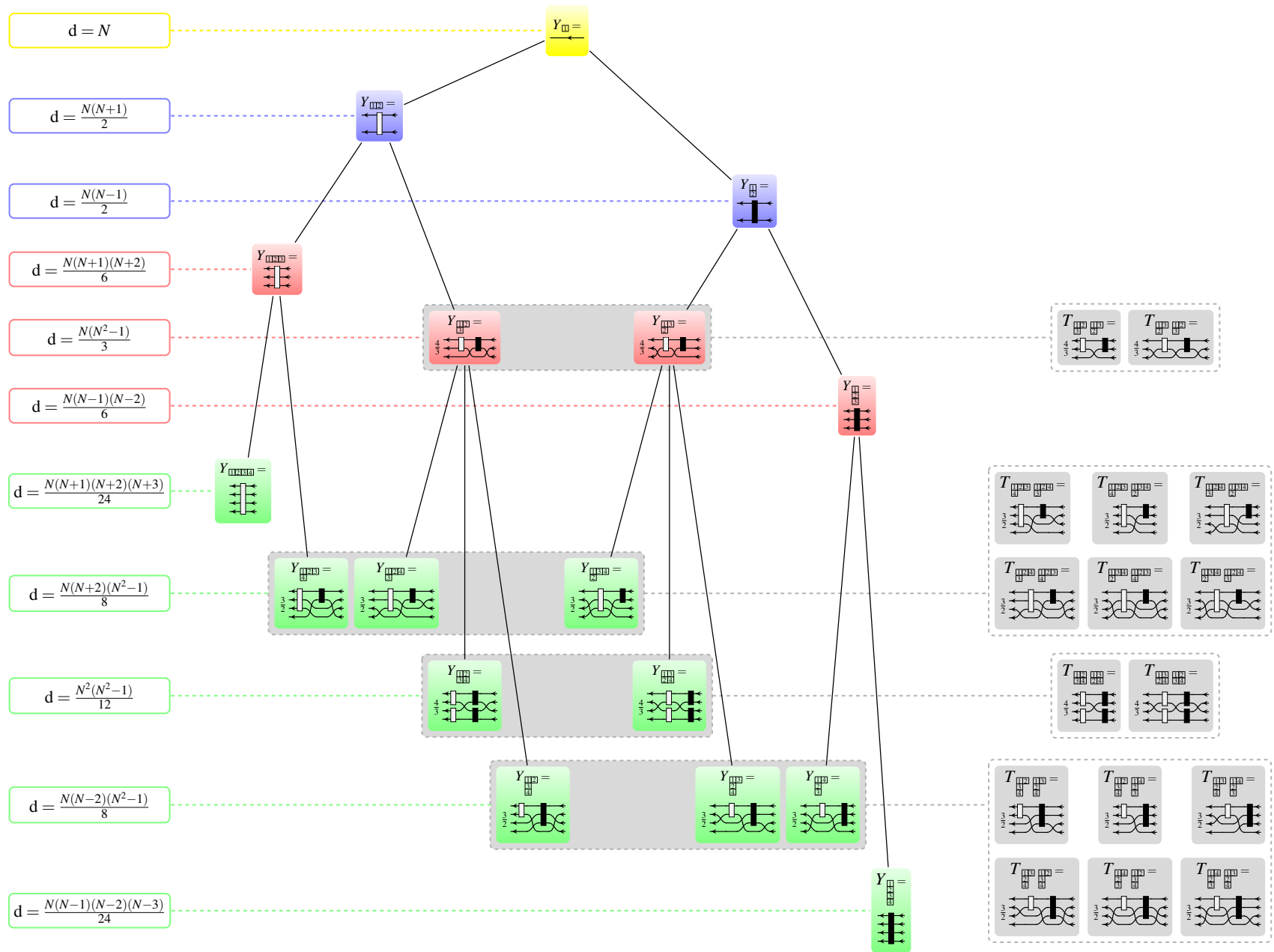
$$\begin{array}{|c|} \hline \square \\ \hline \square \\ \hline \square \\ \hline \end{array} : \left( \begin{array}{|c|} \hline 1 \\ \hline \end{array} \right). \tag{4.149}$$

This operator corresponds to an irreducible representation of dimension  $d = \frac{N(N-1)(N-2)(N-3)}{24}$ .

All the projection operators given above have previously been known [72], the transition operators are a new result.

Similarly to what we observed for the 3-quark algebra, we find that the blocks described above give null-operators from bottom right to top left as we incrementally decrease  $N$  below 4: For  $N = 3$ , only the last  $1 \times 1$  block turns into a null-operator. For  $N = 2$ , the last  $1 \times 1$  block as well as the second-to-last  $3 \times 3$  block consist of null-operators. All but the topmost  $1 \times 1$  block give null-operators for  $N = 1$ . The entire matrix will (trivially) consist of null-operators if we decrease  $N$  to 0. In fact, we can read off which operators will be null-operators from their dimension formula, as  $d = 0$  for a null-operator.

Figures 4.2 and 4.3 expand on the content of Figures 9.1 and 9.2 in Ref. [72] respectively: These figures collect the hierarchy of Young tableaux and the associated nested Hermitian projector decompositions (in the sense of embeddings into  $\text{API}(\text{SU}(N), V^{\otimes 4})$ ) and add the transition operators we have derived in this paper (recall that for  $m \leq 4$ , the construction algorithm for transition operators between Young projectors over  $V^{\otimes m}$  is well-defined). We would like to draw attention to the fact that only the leftmost and rightmost branches in each tree, consisting solely of a single symmetrizer or antisymmetrizer, are fully unique as they are not connected by transition operators listed on the right.



202

Figure 4.2: Hierarchy of Young tableaux and the associated (non-nested) Young projector decompositions over  $V^{\otimes m}$  for  $m = 1, 2, 3, 4$  (in the sense of embeddings into  $\text{API}(\text{SU}(N), V^{\otimes 4})$ ): The solid lines indicate ancestry. The associated transition operators for groups of equivalent representations are listed to the right. Note that this tree cannot be extended beyond  $m = 4$  due to the failure of the corresponding Young projectors to be transversal or complete.



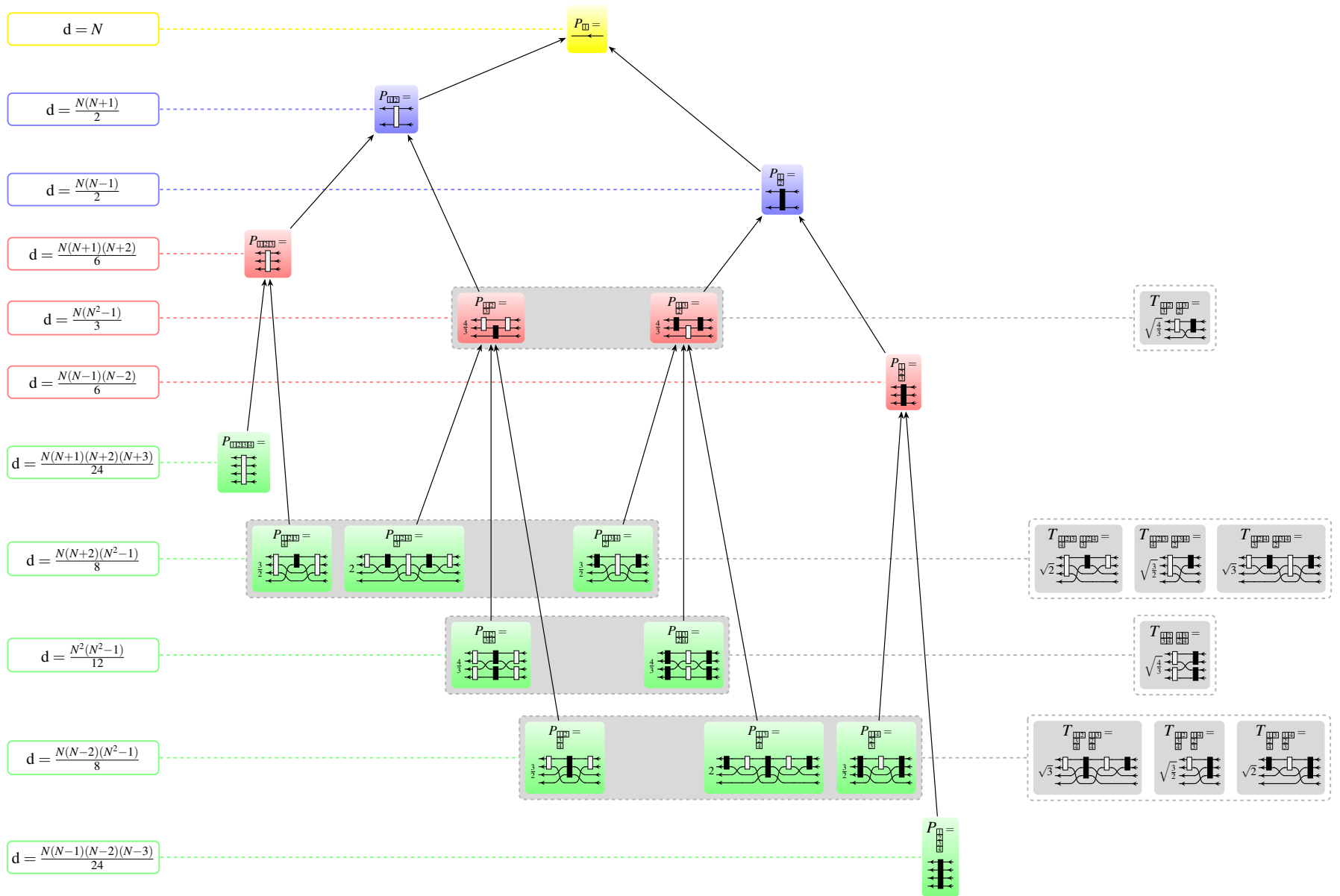


Figure 4.3: Hierarchy of Young tableaux and the associated nested Hermitian Young projector decompositions over  $V^{\otimes m}$  for  $m \leq 4$  (in the sense of embeddings into API  $(\text{SU}(N), V^{\otimes 4})$ ): The arrows indicate which operators sum to which ancestors (see [2] [chapter 3] — this does *not* apply to their standard Young counterparts shown in Figure 4.2). The associated transition operators for groups of equivalent representations are listed to the right (recall that these transition operators are unitary on the image of the projection operators,  $T_{\Phi\Theta} = T_{\Phi\Theta}^\dagger$ ). This tree can be extended to arbitrary  $m$  using the construction algorithm of Hermitian Young projectors [2] [chapter 3] and that of transition operators given in this paper.

## 4.7 Chapter conclusion & outlook

The representation theory of  $SU(N)$  is an old theory with many successful applications in physics. Yet, some of the tools remain awkward and only applicable in specific situations, like the general theory of angular momentum or the construction of Young projection operators that lack Hermiticity. Newer tools, like the birdtrack formalism, remain only partially connected with these time honored results. We have a very specific interest in applications to QCD in the context of Jalilian-Marian–Iancu–McLerran–Weigert–Leonidov–Kovner (JIMWLK) [20, 56–59] evolution, in jet physics, in energy loss and generalized parton distributions, so we have aimed at creating a set of tools that we know will aid in these applications and, in the process have pointed out where the existing tools fall short of our needs.

Building on the previously found Hermitian Young projection operators [2, 4] [*c.f.* chapter 3], the main result of this paper is the inclusion of transition operators that complement the set of multiplet projectors to a basis for the full algebra of invariants  $\text{API}(SU(N), V^{\otimes m})$ ; for Young projectors and their associated transition operators, this is only possible up to  $m = 4$ . Any subset of projectors encoding mutually equivalent representations, together with their transition operators, form closed subalgebras. Relabelling the set of basis operators as  $\mathbf{m}_{ij}$  (with double indices according to (4.92)) so that

$$\text{API}(SU(N), V^{\otimes m}) = \left\{ \alpha_{ij} \mathbf{m}_{ij} \mid \alpha_{ij} \in \mathbb{R}, \mathbf{m}_{ij} \in \mathfrak{S}_m \right\} \quad (4.150)$$

leads to a simplified multiplication table for the new basis elements

$$\mathbf{m}_{ij} \mathbf{m}_{kl} = \delta_{jk} \mathbf{m}_{il}, \quad (4.151)$$

significantly simpler than the standard basis of primitive invariants  $\rho_i \in S_m$ ,  $\rho_i \rho_j = A^k_{ij} \rho_k$ .

The transition operators obtained from Hermitian projectors are automatically unitary, causing the basis elements to be mutually orthogonal and normalized to match the dimension of the irreducible representations,

$$\langle \mathbf{m}_{ij}, \mathbf{m}_{kl} \rangle = \delta_{ik} \delta_{jl} \dim(\Theta_j). \quad (4.152)$$

This is an essential prerequisite for a future publication that aims at constructing an *orthonormal basis* for the space of *all* global color singlet states for a given Fock-space configuration [chapter 5]; it is important to note that (4.152) does *not* hold for the standard Young projectors and their associated transition operators.

We have used the new form of the multiplication table (4.151) to show that the projection operators in  $\text{API}(SU(N), V^{\otimes m})$  are only uniquely determined if the representation occurs precisely once in the decomposition. All Hermitian projectors onto equivalent representations, and their associated transition operators, are only unique up to orthogonal rotations as described in sections 4.4.3 and 4.5. Figures 4.2 and 4.3 collect all the examples worked out in this paper, displaying all their relationships in a compact form for reference.

Our own list of future applications for the tools and insights presented in this paper are QCD centric [*c.f.* chapters 5 and 10]. Global singlet state projections of Wilson-line operators that appear in a myriad of applications due to factorization of hard and soft contributions help analyzing the physics content in all of them. We hope that our presentation is suitable to unify perspectives provided by the various approaches to representation theory of  $SU(N)$ , and that the results prove useful beyond these immediate applications.

# Appendix to chapter 4

## 4.A Dimensional zeros

For small enough values of  $N$  (and we will define what we mean by “small enough” shortly), some of the irreducible representations of  $SU(N)$  over  $V^{\otimes m}$  vanish. The reason for this is simple: An antisymmetrizer over  $p$  legs, viewed as a linear map on  $V^{\otimes p}$ , is a null-operator, if  $\dim(V) < p$ ,

$$\begin{array}{c} \text{---} \\ \text{---} \\ \vdots \\ \text{---} \end{array} \begin{array}{c} 1 \\ 2 \\ \vdots \\ p-1 \\ p \end{array} : V^{\otimes p} \rightarrow 0 \quad \text{if } \dim(V) < p. \quad (4.153)$$

Thus, if an operator in  $\text{Lin}(V^{\otimes m})$  with  $\dim(V) = N$  contains an antisymmetrizer of length  $> N$ , the operator will be a null-operator on the space  $V^{\otimes m}$ . For example, the antisymmetrizer

$$\mathbf{A} = \frac{1}{3!} \left( \text{---} - \text{---} - \text{---} - \text{---} + \text{---} + \text{---} \right) \quad (4.154)$$

acts as a null-operator on the space  $V^{\otimes 3} = V \otimes V \otimes V$  if the dimension of  $V$  is  $\leq 2$ . The reason for this is that the primitive invariants constituting the antisymmetrizer  $\mathbf{A}_{123}$ , as elements of  $\text{Lin}(V^{\otimes 3})$ , are not linearly independent if the vector space  $V$  has dimension  $\leq 2$ . In this situation, the identity permutation (for example) can be expressed as a linear combination of the remaining primitive invariants,

$$\text{---} \stackrel{\dim(V) \leq 2}{=} \text{---} + \text{---} + \text{---} - \text{---} - \text{---}. \quad (4.155)$$

We discussed previously that each irreducible representation of  $SU(N)$  over  $V^{\otimes m}$  corresponds to a particular Young tableau in  $\mathcal{Y}_m$ . From the construction theorems of (Hermitian) Young projection operators (eq. (4.36) for Youngs and section 4.5.1 for Hermitian projectors) and their transition operators (section 4.3 for Youngs up to  $m = 4$  and section 4.5.2 for unitary operators for all  $m$ ), it is evident that the longest antisymmetrizer present in such an operator corresponds to the longest column of the corresponding Young tableau. In particular, if  $N < m$ , there will be at least one Young tableau containing a column which is longer than  $N$ , namely

$$\begin{array}{|c|} \hline 1 \\ \hline 2 \\ \hline \vdots \\ \hline m \\ \hline \end{array}. \quad (4.156)$$

There may be more tableaux with columns longer than  $N$ , depending by how much  $N$  differs from  $m$ . If two (non-) Hermitian Young projection operators  $P_{\Theta}$  and  $P_{\Phi}$  (resp.  $Y_{\Theta}$  and  $Y_{\Phi}$ ) correspond to equivalent irreducible representations of  $SU(N)$ , they both will contain antisymmetrizers of equal length ( $\mathbf{A}_{\Theta}$  or  $\mathbf{A}_{\Phi}$  respectively), and so will their transition operators by construction (see eq. (4.61) for Young operators up to  $m = 4$ , resp. Theorem 4.5 for the unitary operators for all values of  $m$ ). They will therefore all vanish simultaneously if  $N$  is too small. Thus, decreasing  $N$  will render entire block of the matrix  $\mathfrak{M}$  (c.f. eq. (4.93a)) zero

To summarize, we see that *all* multiplets and transition operators are only present in  $\text{API}(SU(N), V^{\otimes m})$  if  $N \geq m$ . If  $N$  is smaller than  $m$ , some of them become null-operators. These can explicitly be identified by their corresponding Young tableau  $\Theta$  or directly by  $\mathbf{A}_{\Theta}$  in the birdtrack notation.

## 4.B Illustrating the action of $\rho_{\Theta\Phi}$ on Hermitian Young projection operators: an example

In this section, we illustrate why eq. (4.115),

$$P_{\Theta} \cdot \rho_{\Theta\Phi} P_{\Phi} \rho_{\Phi\Theta} \neq 0, \quad (4.157)$$

holds by means of an example. In the process, we will show that eq. (4.46) (saying that  $Y_{\Theta} = \rho_{\Theta\Phi} Y_{\Phi} \rho_{\Phi\Theta}$ ) breaks down for Hermitian projection operators,

$$P_{\Theta} \neq \rho_{\Theta\Phi} P_{\Phi} \rho_{\Phi\Theta}. \quad (4.158)$$

Consider two Young tableaux

$$\Theta = \begin{array}{|c|c|c|} \hline 1 & 2 & 5 \\ \hline 3 & 4 & \\ \hline 6 & & \\ \hline \end{array} \quad \text{and} \quad \Phi = \begin{array}{|c|c|c|} \hline 1 & 3 & 5 \\ \hline 2 & 6 & \\ \hline 4 & & \\ \hline \end{array}. \quad (4.159)$$

The permutation  $\rho_{\Theta\Phi}$  according to in Definition 4.3 is given by

$$\rho_{\Theta\Phi} = \overline{\begin{array}{c} \times \\ \times \end{array}}. \quad (4.160)$$

Let us now construct the MOLD operators (c.f. Theorem 4.3) corresponding to  $\Theta$  and  $\Phi$ . To do so, we need to construct their MOLD ancestries (c.f. Definition 4.6 for the MOLD of a tableau),

$$\Theta = \begin{array}{|c|c|c|} \hline 1 & 2 & 5 \\ \hline 3 & 4 & \\ \hline 6 & & \\ \hline \end{array} \rightarrow \begin{array}{|c|c|c|} \hline 1 & 2 & 5 \\ \hline 3 & 4 & \\ \hline \end{array} \rightarrow \begin{array}{|c|c|} \hline 1 & 2 \\ \hline 3 & 4 \\ \hline \end{array} \quad (4.161)$$

and

$$\Phi = \begin{array}{|c|c|c|} \hline 1 & 3 & 5 \\ \hline 2 & 6 & \\ \hline 4 & & \\ \hline \end{array} \rightarrow \begin{array}{|c|c|c|} \hline 1 & 3 & 5 \\ \hline 2 & & \\ \hline 4 & & \\ \hline \end{array} \rightarrow \begin{array}{|c|c|} \hline 1 & 3 \\ \hline 2 & \\ \hline 4 & \\ \hline \end{array} \rightarrow \begin{array}{|c|c|} \hline 1 & 3 \\ \hline 2 & \\ \hline \end{array}. \quad (4.162)$$

The MOLD projectors  $P_\Theta$  and  $P_\Phi$  are thus determined by

$$\bar{P}_\Theta = \begin{array}{c} \text{[Diagram: MOLD projector } \bar{P}_\Theta \text{ with 4 columns and 3 rows of boxes, with vertical bars above and below, and horizontal lines connecting boxes in a specific pattern.]} \end{array} \quad (4.163)$$

$$\bar{P}_\Phi = \begin{array}{c} \text{[Diagram: MOLD projector } \bar{P}_\Phi \text{ with 3 columns and 3 rows of boxes, with vertical bars above and below, and horizontal lines connecting boxes in a specific pattern.]} \end{array}. \quad (4.164)$$

The full projection operators  $P_\Theta$  and  $P_\Phi$  require additional constants  $\beta_\Theta$  and  $\beta_\Phi$ , respectively, to ensure their idempotency. From the differing lengths of  $P_\Theta$  and  $P_\Phi$  (due to the different MOLD of the tableaux  $\Theta$  and  $\Phi$ ), it is abundantly clear that  $P_\Theta \neq \rho_{\Theta\Phi} P_\Phi \rho_{\Theta\Phi}^{-1}$ , confirming eq. (4.158). Let us nonetheless take a closer look at  $\rho_{\Theta\Phi} P_\Phi \rho_{\Theta\Phi}$ ,

$$\rho_{\Theta\Phi} P_\Phi \rho_{\Theta\Phi} = \begin{array}{c} \text{[Diagram: MOLD projector } \rho_{\Theta\Phi} P_\Phi \rho_{\Theta\Phi} \text{ with 4 columns and 3 rows of boxes, with vertical bars above and below, and horizontal lines connecting boxes in a specific pattern.]} \end{array}. \quad (4.165)$$

By transforming  $P_\Phi$  with the permutation  $\rho_{\Theta\Phi}$ , we have transformed each set of (anti-)symmetrizers into a different set of the same shape. In particular, the (anti-)symmetrizers of the ancestor tableaux of  $\Phi$  have been transformed into (anti-)symmetrizers of tableaux obtained from  $\Theta$  by deleting the corresponding boxes,

$$\begin{array}{ccccccc} & \Phi & & \Phi_{(1)} & & \Phi_{(2)} & & \Phi_{(3)} \\ \begin{array}{|c|c|c|} \hline 1 & 3 & 5 \\ \hline 2 & 6 & \\ \hline 4 & & \\ \hline \end{array} & \rightarrow & \begin{array}{|c|c|c|} \hline 1 & 3 & 5 \\ \hline 2 & & \\ \hline 4 & & \\ \hline \end{array} & \rightarrow & \begin{array}{|c|c|} \hline 1 & 3 \\ \hline 2 & \\ \hline 4 & \\ \hline \end{array} & \rightarrow & \begin{array}{|c|c|} \hline 1 & 3 \\ \hline 2 & \\ \hline \end{array} \\ \downarrow & & \downarrow & & \downarrow & & \downarrow \\ \begin{array}{|c|c|c|} \hline 1 & 2 & 5 \\ \hline 3 & 4 & \\ \hline 6 & & \\ \hline \end{array} & \rightarrow & \begin{array}{|c|c|c|} \hline 1 & 2 & 5 \\ \hline 3 & & \\ \hline 6 & & \\ \hline \end{array} & \rightarrow & \begin{array}{|c|c|} \hline 1 & 2 \\ \hline 3 & \\ \hline 6 & \\ \hline \end{array} & \rightarrow & \begin{array}{|c|c|} \hline 1 & 2 \\ \hline 3 & \\ \hline \end{array} \end{array} \quad (4.166a)$$

$$\begin{array}{ccccccc} & \Theta & & \Theta_{(\Phi,1)} & & \Theta_{(\Phi,2)} & & \Theta_{(\Phi,3)} \\ \begin{array}{|c|c|c|} \hline 1 & 2 & 5 \\ \hline 3 & 4 & \\ \hline 6 & & \\ \hline \end{array} & \rightarrow & \begin{array}{|c|c|c|} \hline 1 & 2 & 5 \\ \hline 3 & & \\ \hline 6 & & \\ \hline \end{array} & \rightarrow & \begin{array}{|c|c|} \hline 1 & 2 \\ \hline 3 & \\ \hline 6 & \\ \hline \end{array} & \rightarrow & \begin{array}{|c|c|} \hline 1 & 2 \\ \hline 3 & \\ \hline \end{array} \end{array}. \quad (4.166b)$$

Each tableau  $\Theta_{(\Phi,k)}$  in (4.166b) was obtained from the predecessor  $\Theta_{(\Phi,k-1)}$  by removing the box which is in the same position as the box with the highest number in  $\Phi_{(k-1)}$ . We shall refer to the tableaux in (4.166b) as the  $\Phi$ -MOLD ancestry of  $\Theta$ . Note that most of the tableaux in the  $\Phi$ -MOLD ancestry of  $\Theta$  are *not* the ancestor tableaux of  $\Theta$ ; in fact, most of them are not even Young tableaux. The  $\Theta_{(\Phi,i)}$  emerge by superimposing the  $\Phi_{(i)}$  in cookie cutter fashion over  $\Theta$  and thus intrinsically differ from the ancestry of  $\Theta$

itself — compare

$$\begin{array}{|c|c|c|} \hline 1 & 2 & 5 \\ \hline 3 & 4 & \\ \hline 6 & & \\ \hline \end{array} \rightarrow \begin{array}{|c|c|c|} \hline 1 & 2 & 5 \\ \hline 3 & 4 & \\ \hline & & \\ \hline \end{array} \rightarrow \begin{array}{|c|c|} \hline 1 & 2 \\ \hline 3 & 4 \\ \hline & \\ \hline \end{array} \quad (4.167)$$

$\underbrace{\hspace{10em}}_{\Theta} \qquad \underbrace{\hspace{5em}}_{\Theta_{(1)}} \qquad \underbrace{\hspace{5em}}_{\Theta_{(2)}}$

with eq. (4.166b).

We now see that the symmetrizers and antisymmetrizers in the operator (4.165) are exactly those corresponding to the tableaux in the  $\Phi$ -MOLD ancestry of  $\Theta$  eq. (4.166b). This means that the (anti-)symmetrizers in (4.165) can be obtained from  $\mathbf{S}_\Theta$  and  $\mathbf{A}_\Theta$  by removing index legs. Thus, all symmetrizers (resp. antisymmetrizers) of (4.165) are contained in  $\mathbf{S}_\Theta$  (resp.  $\mathbf{A}_\Theta$ ), yielding the product  $P_\Theta \cdot \rho_{\Theta\Phi} P_\Phi \rho_{\Phi\Theta}$  to be nonzero (*c.f.* eq. (4.52)) as claimed in (4.157).

## 4.C Consequences of non-Hermiticity: an example

In this appendix, we illustrate the non-unitarity of transition operators between Young projection operators as given in eq. (4.63),

$$(T_{\Theta\Phi})^\dagger = Y_\Phi^\dagger \rho_{\Phi\Theta} Y_\Theta^\dagger \neq T_{\Phi\Theta}, \quad (4.168)$$

by means of an example. Consider the two Young tableaux

$$\Theta := \begin{array}{|c|c|} \hline 1 & 2 \\ \hline 3 & \\ \hline \end{array} \quad \text{and} \quad \Phi := \begin{array}{|c|c|} \hline 1 & 3 \\ \hline 2 & \\ \hline \end{array}. \quad (4.169)$$

In eq. (4.49) we found that  $\rho_{\Theta\Phi} = \overline{\times}$ . Using eq. (4.61) we construct  $T_{\Theta\Phi}$

$$\begin{array}{c} \overline{\times} \\ \times \end{array} \underbrace{\begin{array}{|c|c|} \hline \blacksquare & \blacksquare \\ \hline \end{array}}_{Y_\Phi} = \underbrace{\begin{array}{|c|c|} \hline \blacksquare & \blacksquare \\ \hline \end{array}}_{T_{\Theta\Phi}} = \underbrace{\begin{array}{|c|c|} \hline \blacksquare & \blacksquare \\ \hline \end{array}}_{Y_\Theta} \underbrace{\overline{\times}}_{\rho_{\Theta\Phi}} \quad (4.170)$$

and  $T_{\Phi\Theta}$

$$\underbrace{\overline{\times}}_{\rho_{\Phi\Theta}} \underbrace{\begin{array}{|c|c|} \hline \blacksquare & \blacksquare \\ \hline \end{array}}_{Y_\Theta} = \underbrace{\begin{array}{|c|c|} \hline \blacksquare & \blacksquare \\ \hline \end{array}}_{T_{\Phi\Theta}} = \underbrace{\begin{array}{|c|c|} \hline \blacksquare & \blacksquare \\ \hline \end{array}}_{Y_\Phi} \underbrace{\overline{\times}}_{\rho_{\Phi\Theta}}. \quad (4.171)$$

From this example, it is immediately clear that  $(T_{\Theta\Phi})^\dagger \neq T_{\Phi\Theta}$ ,

$$\left( \underbrace{\begin{array}{|c|c|} \hline \blacksquare & \blacksquare \\ \hline \end{array}}_{T_{\Theta\Phi}} \right)^\dagger = \underbrace{\begin{array}{|c|c|} \hline \blacksquare & \blacksquare \\ \hline \end{array}}_{(T_{\Theta\Phi})^\dagger} \neq \underbrace{\begin{array}{|c|c|} \hline \blacksquare & \blacksquare \\ \hline \end{array}}_{T_{\Phi\Theta}}, \quad (4.172)$$

and vice versa

$$\underbrace{\left(\begin{array}{c} \text{---} \\ \text{---} \\ \text{---} \\ \text{---} \end{array}\right)}_{T_{\Phi\Theta}}^\dagger = \underbrace{\left(\begin{array}{c} \text{---} \\ \text{---} \\ \text{---} \\ \text{---} \end{array}\right)}_{(T_{\Phi\Theta})^\dagger} \neq \underbrace{\left(\begin{array}{c} \text{---} \\ \text{---} \\ \text{---} \\ \text{---} \end{array}\right)}_{T_{\Theta\Phi}}, \quad (4.173)$$

confirming eq. (4.168).

## 4.D Proof of Theorem 4.5 “compact transition operators”

### 4.D.1 The significance of the cutting-and-gluing procedure

Before we present the proof of Theorem 4.5, we need to make some observations: Let  $\mathbf{I}$  be any set of symmetrizers or antisymmetrizers, and let  $\rho$  be a permutation. Then, using the fact that  $\rho^\dagger = \rho^{-1}$  for any permutation,<sup>14</sup> we have that

$$\rho \mathbf{I} = \rho \mathbf{I} \underbrace{\rho^\dagger \rho}_{\text{id}} = \rho \underbrace{\mathbf{I} \rho^\dagger}_{=: \mathbf{I}'} \rho = \mathbf{I}' \rho, \quad (4.174)$$

where  $\mathbf{I}'$  is now a set of symmetrizers, respectively antisymmetrizers, over a different set of indices.<sup>15</sup>

In the proof of Theorem 4.5, we will come across a particular such case, namely where  $\rho$  is the permutation  $\rho_{\Theta\Phi}$  as defined in Definition 4.3. The simplest case we encounter are the products  $\rho_{\Theta\Phi} \mathbf{S}_\Phi$  and  $\rho_{\Theta\Phi} \mathbf{A}_\Phi$ . By its very definition  $\rho_{\Theta\Phi}$  explicitly relates  $\Theta$  and  $\Phi$  such that

$$\rho_{\Theta\Phi} \mathbf{S}_\Phi = \mathbf{S}_\Theta \rho_{\Theta\Phi} = \mathbf{S}_\Theta \rho_{\Theta\Phi} \mathbf{S}_\Phi \quad (4.176a)$$

$$\rho_{\Theta\Phi} \mathbf{A}_\Phi = \mathbf{A}_\Theta \rho_{\Theta\Phi} = \mathbf{A}_\Theta \rho_{\Theta\Phi} \mathbf{A}_\Phi, \quad (4.176b)$$

where the last equality follows from the fact that each (anti-) symmetrizer individually is idempotent (4.11). Recognizing the parallel between eq. (4.176) and transition operators eq. (4.116) (between Hermitian projectors, such as symmetrizers  $\mathbf{S}_\Xi$  and antisymmetrizers  $\mathbf{A}_\Xi$ ), the objects (4.176) can be viewed as *transition operators* between individual sets of (anti-) symmetrizers. This observation establishes the connection to the graphical cutting-and-gluing procedure discussed in Theorem 4.5: cutting antisymmetrizers  $\mathbf{A}_\Theta$  and  $\mathbf{A}_\Phi$  vertically and gluing them as suggested by the Theorem is equivalent to forming the product  $\mathbf{A}_\Theta \rho_{\Theta\Phi} \mathbf{A}_\Phi$  (and similarly for symmetrizers). This is illustrated in the following example: For the Young tableaux

$$\Theta = \begin{array}{|c|c|} \hline 1 & 3 \\ \hline 2 & \\ \hline 4 & \\ \hline \end{array} \quad \text{and} \quad \Phi = \begin{array}{|c|c|} \hline 1 & 2 \\ \hline 3 & \\ \hline 4 & \\ \hline \end{array}, \quad (4.177)$$

<sup>14</sup>This becomes evident in the birdtrack formalism, where the inverse of a permutation  $\rho$  is obtained by flipping  $\rho$  about its vertical axis [72], which is incidentally also the process for Hermitian conjugation of a birdtrack [72].

<sup>15</sup>We consider this to be self evident, but an example may help diffuse anxiety:

$$\underbrace{\left(\begin{array}{c} \text{---} \\ \text{---} \\ \text{---} \\ \text{---} \end{array}\right)}_{\rho} \underbrace{\left(\begin{array}{c} \text{---} \\ \text{---} \\ \text{---} \\ \text{---} \end{array}\right)}_{\mathbf{I}} = \underbrace{\left(\begin{array}{c} \text{---} \\ \text{---} \\ \text{---} \\ \text{---} \end{array}\right)}_{\rho} \underbrace{\left(\begin{array}{c} \text{---} \\ \text{---} \\ \text{---} \\ \text{---} \end{array}\right)}_{\mathbf{I}} \underbrace{\left(\begin{array}{c} \text{---} \\ \text{---} \\ \text{---} \\ \text{---} \end{array}\right)}_{\rho^\dagger \rho} = \underbrace{\left(\begin{array}{c} \text{---} \\ \text{---} \\ \text{---} \\ \text{---} \end{array}\right)}_{\mathbf{I}'} \underbrace{\left(\begin{array}{c} \text{---} \\ \text{---} \\ \text{---} \\ \text{---} \end{array}\right)}_{\rho}, \quad (4.175)$$

where we have  $\mathbf{I} = \{\mathbf{S}_{123}, \mathbf{S}_{45}\}$  and  $\mathbf{I}' = \{\mathbf{S}_{124}, \mathbf{S}_{35}\}$ .

we have

$$\underbrace{\begin{array}{c} \text{---} \\ | \\ \text{---} \\ \text{---} \\ | \\ \text{---} \end{array}}_{\mathbf{A}_\Theta} \underbrace{\begin{array}{c} \text{---} \\ \diagdown \diagup \\ \text{---} \\ \diagup \diagdown \\ \text{---} \end{array}}_{\rho_{\Theta\Phi}} \underbrace{\begin{array}{c} \text{---} \\ | \\ \text{---} \\ \text{---} \\ | \\ \text{---} \end{array}}_{\mathbf{A}_\Phi} = \begin{array}{c} \text{---} \\ | \\ \text{---} \\ \text{---} \\ | \\ \text{---} \end{array} = \begin{array}{c} \text{---} \\ | \\ \text{---} \\ \text{---} \\ | \\ \text{---} \end{array}. \quad (4.178)$$

The feature observed in this example is fully general:  $\rho_{\Theta\Phi}$  is *defined* to translate the ordering of the left legs on  $\mathbf{A}_\Phi$  into the ordering of the right legs on  $\mathbf{A}_\Theta$  — this is precisely what the cutting and gluing procedure achieves graphically:

$$\mathbf{A}_\Theta \rightarrow \begin{array}{c} \text{---} \\ | \\ \text{---} \\ \text{---} \\ | \\ \text{---} \end{array} \quad \text{and} \quad \mathbf{A}_\Phi \rightarrow \begin{array}{c} \text{---} \\ \diagdown \diagup \\ \text{---} \\ \diagup \diagdown \\ \text{---} \end{array} \mapsto \begin{array}{c} \text{---} \\ | \\ \text{---} \\ \text{---} \\ | \\ \text{---} \end{array}. \quad (4.179)$$

Both procedures lead to the same result (this is a consequence of relation (4.176)). Thus, we will refer to the algebraic construct (4.176b) as the *cut-antisymmetrizer* and denote it by

$$\mathcal{A}_{\Theta\Phi} := \mathbf{A}_\Theta \rho_{\Theta\Phi} \mathbf{A}_\Phi = \mathbf{A}_\Theta \rho_{\Theta\Phi} = \rho_{\Theta\Phi} \mathbf{A}_\Phi, \quad (4.180)$$

and similarly for the *cut-symmetrizer*  $\mathcal{S}_{\Theta\Phi} := \mathbf{S}_\Theta \rho_{\Theta\Phi} \mathbf{S}_\Phi$ . For the proof of Theorem 4.5, we will only concern ourselves with cut-antisymmetrizers, as we already did in the Theorem. However, all the following arguments hold equally well if we consider cut-symmetrizers instead.

Before we dive into the proof, we need to notice that eqns. (4.176) do not hold for the ancestor sets  $\mathbf{S}_{\Phi_{(k)}}$  and  $\mathbf{A}_{\Phi_{(l)}}$  of  $\mathbf{S}_\Phi$  and  $\mathbf{A}_\Phi$  (*c.f.* eqns. (4.181)). However, such ancestor sets will be transformed (upon commutation with the permutation  $\rho_{\Theta\Phi}$ ) into sets of the same shape that can be obtained from  $\mathbf{S}_\Theta$  resp.  $\mathbf{A}_\Theta$  by dropping lines. Thus, the resulting (anti-)symmetrizers can be absorbed into  $\mathbf{S}_\Theta$  and  $\mathbf{A}_\Theta$  respectively,

$$\rho_{\Theta\Phi} \mathbf{S}_{\Phi_{(k)}} = \mathbf{S}_{\Theta_{(\Phi,k)}} \rho_{\Theta\Phi} \quad \text{for } \mathbf{S}_{\Theta_{(\Phi,k)}} \supset \mathbf{S}_\Theta \quad (4.181a)$$

$$\rho_{\Theta\Phi} \mathbf{A}_{\Phi_{(l)}} = \mathbf{A}_{\Theta_{(\Phi,l)}} \rho_{\Theta\Phi} \quad \text{for } \mathbf{A}_{\Theta_{(\Phi,l)}} \supset \mathbf{A}_\Theta, \quad (4.181b)$$

the (anti-)symmetrizers  $\mathbf{S}_{\Theta_{(\Phi,k)}}$  and  $\mathbf{A}_{\Theta_{(\Phi,l)}}$  correspond to tableaux in the  $\Phi$ -MOLD ancestry of  $\Theta$  (*c.f.* eq. (4.166) in appendix 4.B). For further clarification, we refer the reader to appendix 4.B for an explicit example.

We will now present a proof for the shorthand graphical construction of the birdtracks of transition operators given in Theorem 4.5.

#### 4.D.2 Proof of Theorem 4.5

Let  $\Theta, \Phi \in \mathcal{Y}_n$  be two Young tableaux with the same shape, thus corresponding to equivalent irreducible representations of  $\text{SU}(N)$ , and let the corresponding Hermitian Young projection operators  $P_\Theta$  and  $P_\Phi$  be constructed according to the MOLD Theorem 4.3. Furthermore, let  $\mathbf{I}$  denote either a set of symmetrizers or antisymmetrizers, and  $\mathbf{B}$  denote the other set (that is, if  $\mathbf{I}$  denotes a set of symmetrizers then  $\mathbf{B}$  denotes a set of antisymmetrizers and vice versa): we use these generalized sets rather than the concrete sets  $\mathbf{A}$  and  $\mathbf{S}$



in order to discuss all possible forms of  $P_\Theta$  and  $P_\Phi$  in one go. We then have that  $\bar{P}_\Theta$  is given by

$$\bar{P}_\Theta = \mathcal{C}_\Theta \mathbf{I}_\Theta \mathbf{B}_\Theta \mathbf{I}_\Theta \mathcal{C}_\Theta^\dagger, \quad (4.182)$$

where  $\mathcal{C}_\Theta$  consists of ancestor sets of (anti-)symmetrizers of  $\Theta$ , and the exact structure of  $\mathcal{C}_\Theta$  is determined by the MOLD of  $\Theta$ ,  $\mathcal{M}(\Theta)$ , and the parity of  $\mathcal{M}(\Theta)$ . Similarly,  $\bar{P}_\Phi$  is of the form

$$\bar{P}_\Phi = \mathcal{D}_\Phi \mathbf{I}_\Phi \mathbf{B}_\Phi \mathbf{I}_\Phi \mathcal{D}_\Phi^\dagger \quad \text{or} \quad \bar{P}_\Phi = \mathcal{D}_\Phi \mathbf{B}_\Phi \mathbf{I}_\Phi \mathbf{B}_\Phi \mathcal{D}_\Phi^\dagger, \quad (4.183)$$

where, like  $\mathcal{C}_\Theta$ ,  $\mathcal{D}_\Phi$  consists of ancestor sets of (anti-)symmetrizers of  $\Phi$ . In equation (4.183), we have taken into account that the central part of  $P_\Phi$  can either have the same form as  $P_\Theta$  (which is  $\mathbf{IBI}$ ), or it may have symmetrizers and antisymmetrizers exchanged from  $P_\Theta$ . It should be noted that the set  $\mathcal{D}_\Phi$  will be different whether the central part of  $\bar{P}_\Phi$  is  $\mathbf{I}_\Phi \mathbf{B}_\Phi \mathbf{I}_\Phi$  or  $\mathbf{B}_\Phi \mathbf{I}_\Phi \mathbf{B}_\Phi$ , but in both cases it will consist of ancestor sets of symmetrizers and antisymmetrizers of  $\Theta$ . Understanding this, we have chosen not to introduce different symbols for the set  $\mathcal{D}_\Phi$  in order to introduce the following compact notation for  $\bar{P}_\Phi$ ,

$$\bar{P}_\Phi := \mathcal{D}_\Phi \left\{ \begin{array}{c} \mathbf{I}_\Phi \mathbf{B}_\Phi \mathbf{I}_\Phi \\ \mathbf{B}_\Phi \mathbf{I}_\Phi \mathbf{B}_\Phi \end{array} \right\} \mathcal{D}_\Phi^\dagger, \quad (4.184)$$

which says that the central part of  $\bar{P}_\Phi$  is either given by the top row, or by the bottom row in the curly bracket.<sup>16</sup> According to Theorem 4.4, the birdtrack of the transition operator  $T_{\Theta\Phi}$  is given by

$$\bar{T}_{\Theta\Phi} = \underbrace{\mathcal{C}_\Theta \mathbf{I}_\Theta \mathbf{B}_\Theta \mathbf{I}_\Theta \mathcal{C}_\Theta^\dagger}_{=P_\Theta} \rho_{\Theta\Phi} \underbrace{\mathcal{D}_\Phi \left\{ \begin{array}{c} \mathbf{I}_\Phi \mathbf{B}_\Phi \mathbf{I}_\Phi \\ \mathbf{B}_\Phi \mathbf{I}_\Phi \mathbf{B}_\Phi \end{array} \right\} \mathcal{D}_\Phi^\dagger}_{=\bar{P}_\Phi}. \quad (4.185)$$

As was discussed in section 4.D.1, the permutation  $\rho_{\Theta\Phi}$  can be commuted with  $\mathcal{D}_\Phi$ , in accordance with relations (4.181). Furthermore, equations (4.176) tell us that  $\rho_{\Theta\Phi} \mathbf{I}_\Phi = \mathbf{I}_\Theta \rho_{\Theta\Phi}$  and  $\rho_{\Theta\Phi} \mathbf{B}_\Phi = \mathbf{B}_\Theta \rho_{\Theta\Phi}$ .

In commuting the  $\rho_{\Theta\Phi}$  through the sets  $\mathbf{I}_\Phi$  and  $\mathbf{B}_\Phi$ , it will be convenient to *stop* the commutation in a different place in the top row than the bottom row of  $\bar{T}_{\Theta\Phi}$ ,

$$\bar{T}_{\Theta\Phi} = \mathcal{C}_\Theta \mathbf{I}_\Theta \mathbf{B}_\Theta \mathbf{I}_\Theta \mathcal{C}_\Theta^\dagger \mathcal{D}_\Theta \left\{ \begin{array}{c} \mathbf{I}_\Theta \mathbf{B}_\Phi \rho_{\Theta\Phi} \mathbf{I}_\Phi \\ \mathbf{B}_\Theta \mathbf{I}_\Theta \mathbf{B}_\Theta \rho_{\Theta\Phi} \end{array} \right\} \mathcal{D}_\Phi^\dagger, \quad (4.186)$$

this choice may seem arbitrary at this point, but the position of  $\rho_{\Theta\Phi}$  in (4.186) will turn out to specify the position of the cut in the cutting-and-gluing procedure (*c.f.* section 4.D.1). We emphasize that  $\mathcal{D}_\Theta$  denotes the product of (anti-)symmetrizers in  $\mathcal{D}_\Phi$  when commuting them with  $\rho_{\Theta\Phi}$  (*c.f.* eqns. (4.181)),

$$\mathcal{D}_\Theta \rho_{\Theta\Phi} := \rho_{\Theta\Phi} \mathcal{D}_\Phi. \quad (4.187)$$

We may apply the Cancellation Theorem 4.1 to the operator (4.186) to simplify  $\bar{T}_{\Theta\Phi}$  as

$$\bar{T}_{\Theta\Phi} \stackrel{\text{Thm. 4.1}}{=} \mathcal{C}_\Theta \mathbf{I}_\Theta \mathbf{B}_\Theta \mathbf{I}_\Theta \left\{ \begin{array}{c} \mathbf{I}_\Theta \mathbf{B}_\Theta \rho_{\Theta\Phi} \mathbf{I}_\Phi \\ \mathbf{B}_\Theta \mathbf{I}_\Theta \mathbf{B}_\Theta \rho_{\Theta\Phi} \end{array} \right\} \mathcal{D}_\Phi^\dagger = \mathcal{C}_\Theta \left\{ \begin{array}{c} \mathbf{I}_\Theta \mathbf{B}_\Theta \mathbf{I}_\Theta \mathbf{I}_\Theta \mathbf{B}_\Theta \rho_{\Theta\Phi} \mathbf{I}_\Phi \\ \mathbf{I}_\Theta \mathbf{B}_\Theta \mathbf{I}_\Theta \mathbf{B}_\Theta \mathbf{I}_\Theta \mathbf{B}_\Theta \rho_{\Theta\Phi} \end{array} \right\} \mathcal{D}_\Phi^\dagger. \quad (4.188)$$

<sup>16</sup>This notation is convenient, as it will allow us to discuss both cases simultaneously.

Let us now look at the central part of  $\bar{T}_{\Theta\Phi}$  (the part in the curly brackets) in more detail: Since  $\mathbf{I}_\Theta$  denotes either  $\mathbf{A}_\Theta$  or  $\mathbf{S}_\Theta$ , and  $\mathbf{B}_\Theta$  denotes the other set, then the product  $\mathbf{I}_\Theta\mathbf{B}_\Theta$  is proportional to either a Young projection operator or the Hermitian conjugate thereof,  $\mathbf{I}_\Theta\mathbf{B}_\Theta = \bar{Y}_\Theta^{(\dagger)}$ . Thus, if the central part of  $\bar{T}_{\Theta\Phi}$  is given by the top option (implementing that  $\mathbf{I}_\Theta\mathbf{I}_\Theta = \mathbf{I}_\Theta$ ), we can use the fact that  $\bar{Y}_\Theta^{(\dagger)}$  is quasi-idempotent to obtain

$$\underbrace{\mathbf{I}_\Theta\mathbf{B}_\Theta}_{\bar{Y}_\Theta^{(\dagger)}} \underbrace{\mathbf{I}_\Theta\mathbf{B}_\Theta}_{\bar{Y}_\Theta^{(\dagger)}} \rho_{\Theta\Phi} \mathbf{I}_\Phi \propto \mathbf{I}_\Theta \mathbf{B}_\Theta \rho_{\Theta\Phi} \mathbf{I}_\Phi . \quad (4.189)$$

Similarly, if the central part of  $\bar{T}_{\Theta\Phi}$  is given by the bottom option of (4.188), we may reduce it to

$$\underbrace{\mathbf{I}_\Theta\mathbf{B}_\Theta}_{\bar{Y}_\Theta^{(\dagger)}} \underbrace{\mathbf{I}_\Theta\mathbf{B}_\Theta}_{\bar{Y}_\Theta^{(\dagger)}} \underbrace{\mathbf{I}_\Theta\mathbf{B}_\Theta}_{\bar{Y}_\Theta^{(\dagger)}} \rho_{\Theta\Phi} \propto \mathbf{I}_\Theta \mathbf{B}_\Theta \rho_{\Theta\Phi} . \quad (4.190)$$

This turns (4.188) into (using the bar-notation introduced in eq. (4.44) to retain equality)

$$\bar{T}_{\Theta\Phi} = C_\Theta \left\{ \begin{array}{l} \mathbf{I}_\Theta \mathbf{B}_\Theta \rho_{\Theta\Phi} \mathbf{I}_\Phi \\ \mathbf{I}_\Theta \mathbf{B}_\Theta \rho_{\Theta\Phi} \end{array} \right\} \mathcal{D}_\Phi^\dagger . \quad (4.191)$$

In Theorem 4.5, we discussed three different cutting-and-gluing procedures, depending on the exact structure of the projection operators  $P_\Theta$  and  $P_\Phi$ .

1. Option 1 requires both operators  $\bar{P}_\Theta$  and  $\bar{P}_\Phi$  to contain exactly one set of antisymmetrizers  $\mathbf{A}_\Theta$  and  $\mathbf{A}_\Phi$  respectively. This occurs if we choose the top option of  $\bar{T}_{\Theta\Phi}$  as given in (4.185) (and hence the top line in (4.191)) and if  $\mathbf{B}$  denotes the set of antisymmetrizers and thus  $\mathbf{I}_\Theta$  denotes the set of symmetrizers,

$$(4.191) : \quad \bar{T}_{\Theta\Phi} = C_\Theta \mathbf{I}_\Theta \mathbf{B}_\Theta \rho_{\Theta\Phi} \mathbf{I}_\Phi \mathcal{D}_\Phi^\dagger \xrightarrow{\mathbf{B}=\mathbf{A}, \mathbf{I}=\mathbf{S}} C_\Theta \mathbf{S}_\Theta \underbrace{\mathbf{A}_\Theta \rho_{\Theta\Phi}}_{=\mathcal{A}_{\Theta\Phi}} \mathbf{S}_\Phi \mathcal{D}_\Phi^\dagger , \quad (4.192)$$

where we marked the cut-antisymmetrizer  $\mathcal{A}_{\Theta\Phi}$  (see eq. (4.180)). Clearly, (4.192) coincides with the cutting-and-gluing prescription of Theorem 4.5 if each projector  $P_\Theta$  and  $P_\Phi$  contains exactly one set  $\mathbf{A}_\Theta$  and  $\mathbf{A}_\Phi$  respectively.

2. Option 2 of Theorem 4.5 requires  $\bar{P}_\Theta$  and  $\bar{P}_\Phi$  to have a different number of  $\mathbf{A}_\Theta$  and  $\mathbf{A}_\Phi$ . The bottom option of operator (4.185) (and hence operator (4.191)) corresponds to this case. Dependent on which operator ( $\bar{P}_\Theta$  or  $\bar{P}_\Phi$ ) contains two sets of antisymmetrizers ( $\mathbf{A}_\Theta$  or  $\mathbf{A}_\Phi$ ) is whether  $\mathbf{B}$  denotes the set of antisymmetrizers and  $\mathbf{I}$  the set of symmetrizers, or the other way around: If  $\mathbf{B}$  denotes the set of antisymmetrizers (i.e.  $\bar{P}_\Theta$  contains  $\mathbf{A}_\Theta$  once and  $\bar{P}_\Phi$  contains two copies of  $\mathbf{A}_\Phi$ ), we have

$$(4.191) : \quad \bar{T}_{\Theta\Phi} = C_\Theta \mathbf{I}_\Theta \mathbf{B}_\Theta \rho_{\Theta\Phi} \mathcal{D}_\Phi^\dagger \xrightarrow{\mathbf{B}=\mathbf{A}, \mathbf{I}=\mathbf{S}} C_\Theta \mathbf{S}_\Theta \underbrace{\mathbf{A}_\Theta \rho_{\Theta\Phi}}_{=\mathcal{A}_{\Theta\Phi}} \mathcal{D}_\Phi^\dagger . \quad (4.193a)$$

The operator (4.193a) is the same operator that would have resulted from cutting  $\bar{P}_\Theta$  at its leftmost set  $\mathbf{A}_\Theta$  and  $\bar{P}_\Phi$  at its rightmost set  $\mathbf{A}_\Phi$ , and gluing the pieces in the appropriate manner as described by the Theorem 4.5. On the other hand, if  $\mathbf{I}$  denotes the set of antisymmetrizers (i.e.  $\bar{P}_\Theta$  contains two

copies of  $\mathbf{A}_\Theta$  and  $\bar{P}_\Phi$  contains  $\mathbf{A}_\Phi$  once), then

$$\bar{T}_{\Theta\Phi} \xrightarrow{\mathbf{I}=\mathbf{A}, \mathbf{B}=\mathbf{S}} \mathcal{C}_\Theta \mathbf{A}_\Theta \mathbf{S}_\Theta \rho_{\Theta\Phi} \mathcal{D}_\Phi^\dagger \xrightarrow{\text{eq. (4.176a)}} \mathcal{C}_\Theta \underbrace{\mathbf{A}_\Theta \rho_{\Theta\Phi}}_{=\mathcal{A}_{\Theta\Phi}} \mathbf{S}_\Phi \mathcal{D}_\Phi^\dagger, \quad (4.193b)$$

where we used the commutation relation (4.176a) to commute  $\mathbf{S}_\Theta$  and  $\rho_{\Theta\Phi}$ . This again yields the same result as the cutting-and-gluing procedure of Theorem 4.5.

3. Lastly, suppose that both  $\bar{P}_\Theta$  and  $\bar{P}_\Phi$  each contain two sets of antisymmetrizers  $\mathbf{A}_\Theta$  and  $\mathbf{A}_\Phi$  respectively. Then, we once again need to look at the top option of the operator  $\bar{T}_{\Theta\Phi}$  as given in (4.185) (and hence (4.191)), but this time we require that  $\mathbf{I}$  denotes the set of antisymmetrizers. Then,

$$(4.191): \quad \bar{T}_{\Theta\Phi} = \mathcal{C}_\Theta \mathbf{I}_\Theta \mathbf{B}_\Theta \rho_{\Theta\Phi} \mathbf{I}_\Phi \mathcal{D}_\Phi^\dagger \xrightarrow{\mathbf{I}=\mathbf{A}, \mathbf{B}=\mathbf{S}} \mathcal{C}_\Theta \mathbf{A}_\Theta \mathbf{S}_\Theta \underbrace{\rho_{\Theta\Phi} \mathbf{A}_\Phi}_{=\mathcal{A}_{\Theta\Phi}} \mathcal{D}_\Phi^\dagger. \quad (4.194a)$$

Equivalently,

$$\bar{T}_{\Theta\Phi} = \mathcal{C}_\Theta \mathbf{A}_\Theta \mathbf{S}_\Theta \rho_{\Theta\Phi} \mathbf{A}_\Phi \mathcal{D}_\Phi^\dagger \xrightarrow{\text{eq. (4.176a)}} \mathcal{C}_\Theta \underbrace{\mathbf{A}_\Theta \rho_{\Theta\Phi}}_{=\mathcal{A}_{\Theta\Phi}} \mathbf{S}_\Phi \mathbf{A}_\Phi \mathcal{D}_\Phi^\dagger; \quad (4.194b)$$

eq. (4.194a) corresponds to cutting-and-gluing at the rightmost sets of antisymmetrizers  $\mathbf{A}_\Theta$  and  $\mathbf{A}_\Phi$  (respectively) in both  $\bar{P}_\Theta$  and  $\bar{P}_\Phi$ , while eq. (4.194b) corresponds to cutting-and-gluing the leftmost sets of antisymmetrizers  $\mathbf{A}_\Theta$  and  $\mathbf{A}_\Phi$  in both  $\bar{P}_\Theta$  and  $\bar{P}_\Phi$ .

Thus, we have shown that  $\bar{T}_{\Theta\Phi}$  can indeed be obtained by the graphical cutting-and-gluing prescription given in Theorem 4.5, concluding the proof.  $\square$



## Chapter 5

# Singlets: A Construction Algorithm for the Singlets of $SU(N)$ , and What They Tell Us About Wilson Line Correlators

*We systematically classify all possible singlet states for any given Fock space configuration of quarks and antiquarks. We explain that the currently known method of constructing the projection operators corresponding to irreducible representations of  $SU(N)$  over a mixed tensor product  $V^{\otimes m} \otimes (V^*)^{\otimes n}$  (from Littlewood-Richardson tableaux) is virtually useless in practice due to the enormous computational cost. We give a far more efficient construction algorithm for the projection operators corresponding to 1-dimensional irreducible representations of  $SU(N)$ , the singlet projectors, over an algebra of an equal number of quarks and antiquarks  $V^{\otimes m} \otimes (V^*)^{\otimes m}$ , and provide a counting argument for the number of these singlet projectors. We then show that these singlets may be cast into a different form, giving rise to the remaining singlets of  $SU(N)$  over  $V^{\otimes m} \otimes (V^*)^{\otimes n}$ . We end by looking at the singlet states of the  $3q + 3\bar{q}$ -algebra and use these to construct Wilson line correlators. We examine various coincidence limits of these correlators.*

### 5.1 The necessity of a new construction algorithm for singlet projectors of $SU(N)$

As already discussed in chapters 3 and 4, the irreducible representations of  $SU(N)$  over  $V^{\otimes m}$  can be classified through Young tableaux [84]. In the 1970's, Littlewood and Richardson were able to generalize Young's tableaux to what will be referred to as *Littlewood-Richardson (LR) tableaux*,<sup>1</sup> which correspond to the irreducible representations of  $SU(N)$  over more general product spaces  $W$  (i.e.  $W$  may include spaces derived from  $V$  (such as  $V^*$  or  $V^\dagger$ ) in addition to  $V$  [111]). If one considers a product space consisting of  $V$  and

---

<sup>1</sup>These are not to be confused with Littlewood-Richardson *skew* tableaux [92, 95], which are sometimes simply referred to as Littlewood-Richardson tableaux in the literature.

$V^*$  only, for example  $V^{\otimes m} \otimes (V^*)^{\otimes n}$ , then the projection operators corresponding to the irreducible representations of  $\text{SU}(N)$  over  $V^{\otimes m} \otimes (V^*)^{\otimes n}$  can be extracted from the LR tableaux via Leibniz's formula for determinants [112], as will be exemplified in section 5.1.4.2.

This textbook method is, however, extremely computationally elaborate, and thus virtually useless in practical applications. Luckily, in physics applications one is mainly interested in the *singlet representations* of  $\text{SU}(N)$  over  $V^{\otimes m} \otimes (V^*)^{\otimes n}$  (for  $N = N_c$ , the number of colors), as only these correspond to observable particle configurations — the last statement is imposed on us by *confinement*.

In the following sections, we will elaborate on all the concepts mentioned so far, with the aim of exhibiting their strengths as well as where they fail us in practical applications. This will make the need for an alternative way of constructing singlet projection operators abundantly clear.

We then present a new construction method for the singlet projection operators of  $\text{SU}(N)$  over  $V^{\otimes m} \otimes (V^*)^{\otimes n}$  in section 5.2. Since  $\text{SU}(N)$  has two kinds of invariants, the Kronecker  $\delta$  and the Levi Civita tensor  $\varepsilon^{12\dots N}$ , a general singlet projector of  $\text{SU}(N)$  may be built out of these two invariants. In section 5.2.1, we first discuss the singlets comprised of Kronecker  $\delta$ 's only. The motivation for this will become evident in section 5.2.2, where we show that the singlets that also contain  $\varepsilon$ -tensors do not give new information but are already included in the former kind.

We will see that singlet projectors containing Kronecker  $\delta$ 's only are singlet independently of the value  $N$ , whilst the singlet-ness of projectors containing  $\varepsilon$ -tensors depends on the exact value of  $N$ . This can be intuitively understood when we interpret  $N = N_c$  as the number of colors in QCD, as explained in a short discussion on page 248.

Many of the results presented in this chapter were discovered using the birdtrack formalism [72, 87], as was already the case for the previous chapters of this thesis. However, to conform to the literature, we refrain from proving results in the birdtrack formalism in the main text (unless absolutely necessary) but rather present these proofs in more conventional notation. We do provide the birdtrack version of these proofs in the appendix at the end of this chapter, as we believe that the birdtrack formalism is advantageous in this situation, and to further familiarize readers with this tool of calculation.

### 5.1.1 Theory of invariants & birdtracks

We saw in the previous chapters, 3 (section 3.1.1) and 4 (section 4.1), that the primitive invariants of  $\text{SU}(N)$  over  $V^{\otimes m}$  are given by the permutations over  $m$  objects,

$$S_m = \text{PI}(\text{SU}(N), V^{\otimes m}) . \quad (5.1)$$

The algebra of linear invariants is then given by

$$\text{API}(\text{SU}(N), V^{\otimes m}) := \left\{ \sum_{\sigma \in S_m} \alpha_\sigma \sigma \mid \alpha_\sigma \in \mathbb{R}, \sigma \in S_m \right\} \subset \text{Lin}(V^{\otimes m}) . \quad (5.2)$$

In this chapter, we also want to consider the *antifundamental* representation of  $\text{SU}(N)$  on the dual space  $V^*$ . Again, the irreducible representations of  $\text{SU}(N)$  over a mixed product space  $V^{\otimes m} \otimes (V^*)^{\otimes n}$  can be classified

through the invariants in the algebra [72, 93]

$$\text{API}\left(\text{SU}(N), V^{\otimes m} \otimes (V^*)^{\otimes n}\right) := \left\{ \sum_{\rho \in S_{m,n}} \alpha_{\rho} \rho \mid \alpha_{\rho} \in \mathbb{R} \right\} \subset \text{Lin}\left(V^{\otimes m} \otimes (V^*)^{\otimes n}\right), \quad (5.3)$$

where  $S_{m,n}$  denotes the set of primitive invariants of  $SU(N)$  over  $V^{\otimes m} \otimes (V^*)^{\otimes n}$ ,

$$S_{m,n} = \text{PI}\left(\text{SU}(N), V^{\otimes m} \otimes (V^*)^{\otimes n}\right). \quad (5.4)$$

The primitive invariants  $S_{m,n}$  (over  $V^{\otimes m} \otimes (V^*)^{\otimes n}$ ) are closely related to the primitive invariants  $S_{m+n}$  (over  $V^{\otimes(m+n)}$ ). In fact, the birdtrack formalism allows one to easily construct the primitive invariants  $S_{m,n}$  (eq. (5.4)) from  $S_{m+n}$  (eq. (5.1)) by *swapping fundamental lines out for antifundamental lines* [72]: This is done graphically by swapping the left and right end points on the specific  $V$  in  $V^{\otimes(m+n)}$  to be converted into its dual vector space  $V^*$ . An example will give clarity: The primitive invariants  $S_3 = \text{PI}\left(\text{SU}(N), V^{\otimes 3}\right)$  map onto  $S_{2,1} = \text{PI}\left(\text{SU}(N), V^{\otimes 2} \otimes (V^*)^{\otimes 1}\right)$  as

$$S_3 : \quad \begin{array}{cccccc} \begin{array}{c} \leftarrow \leftarrow \leftarrow \\ \leftarrow \leftarrow \leftarrow \\ \leftarrow \leftarrow \leftarrow \end{array}, & \begin{array}{c} \leftarrow \leftarrow \leftarrow \\ \leftarrow \leftarrow \leftarrow \\ \leftarrow \leftarrow \leftarrow \end{array}, & \begin{array}{c} \leftarrow \leftarrow \leftarrow \\ \leftarrow \leftarrow \leftarrow \\ \leftarrow \leftarrow \leftarrow \end{array}, & \begin{array}{c} \leftarrow \leftarrow \leftarrow \\ \leftarrow \leftarrow \leftarrow \\ \leftarrow \leftarrow \leftarrow \end{array}, & \begin{array}{c} \leftarrow \leftarrow \leftarrow \\ \leftarrow \leftarrow \leftarrow \\ \leftarrow \leftarrow \leftarrow \end{array}, & \begin{array}{c} \leftarrow \leftarrow \leftarrow \\ \leftarrow \leftarrow \leftarrow \\ \leftarrow \leftarrow \leftarrow \end{array} \end{array} \quad (5.5a)$$

$$S_{2,1} : \quad \begin{array}{cccccc} \downarrow & \downarrow & \downarrow & \downarrow & \downarrow & \downarrow \\ \begin{array}{c} \leftarrow \leftarrow \leftarrow \\ \leftarrow \leftarrow \leftarrow \\ \leftarrow \leftarrow \leftarrow \end{array}, & \begin{array}{c} \leftarrow \leftarrow \leftarrow \\ \leftarrow \leftarrow \leftarrow \\ \leftarrow \leftarrow \leftarrow \end{array}, & \begin{array}{c} \leftarrow \leftarrow \leftarrow \\ \leftarrow \leftarrow \leftarrow \\ \leftarrow \leftarrow \leftarrow \end{array}, & \begin{array}{c} \leftarrow \leftarrow \leftarrow \\ \leftarrow \leftarrow \leftarrow \\ \leftarrow \leftarrow \leftarrow \end{array}, & \begin{array}{c} \leftarrow \leftarrow \leftarrow \\ \leftarrow \leftarrow \leftarrow \\ \leftarrow \leftarrow \leftarrow \end{array}, & \begin{array}{c} \leftarrow \leftarrow \leftarrow \\ \leftarrow \leftarrow \leftarrow \\ \leftarrow \leftarrow \leftarrow \end{array} \end{array} \quad (5.5b)$$

in a direct, 1-to-1 correspondence. Since primitive invariants of  $SU(N)$  are Hermitian if and only if their birdtrack expressions are symmetric under a flip about the vertical axis [72] (*c.f.* eq. (3.69)),<sup>2</sup> the graphical procedure of transforming some of its fundamental legs into antifundamental legs does not affect the Hermiticity of a birdtrack. Thus, the subset of Hermitian elements in  $S_{m,n}$  and  $S_{m+n}$  will have the same size.

From the multiplication rule of birdtracks (connect and follow the lines [72]) it immediately follows that  $S_{2,1}$  (unlike  $S_3$ ) is *not* a group, as only the first two elements in (5.5b) have an inverse. In general, the primitive invariants  $S_{m+n}$  form a group, while  $S_{m,n}$  do not — the underlying reason for this is that index contraction does not have an inverse operation, since it is not 1-to-1. Hence, the multiplication tables of the algebras  $\text{API}\left(\text{SU}(N), V^{\otimes(m+n)}\right)$  and  $\text{API}\left(\text{SU}(N), V^{\otimes m} \otimes (V^*)^{\otimes n}\right)$  differ greatly.

### 5.1.2 The irreducible representations of $SU(N)$ over $V^{\otimes m}$ : Young tableaux

The representation theory of  $SU(N)$  over a mixed product space  $V^{\otimes m} \otimes (V^*)^{\otimes n}$  plays an important role in physics applications, as  $V^{\otimes m} \otimes (V^*)^{\otimes n}$  is the Fock space component encapsulating  $m$  quarks and  $n$  antiquarks. In the absence of antiquarks (*i.e.* for  $n = 0$ ), the irreducible representations of  $SU(N)$  can be fully classified using Young's combinatorial method of constructing Young tableaux [84, 95, 96], as was explained in the previous chapters. Even though the construction algorithm for Young tableaux has already been discussed (see, for example, sections 3.1.1 and 4.1), we reiterate it in the present section. The purpose of this is to present a different viewpoint, which aims to emphasize the correspondence between Young's construction and the Littlewood-Richardson tableaux (the latter will be constructed in the following section, 5.1.3).

<sup>2</sup>This is only true for the *primitive* invariants; objects in the algebra of invariants may be Hermitian even if they are not manifestly symmetric under a flip about their vertical axis, *c.f.* the Hermitian operator (3.93) given in chapter 3.

In Young’s construction method for the tableaux, each quark in the fundamental representation is denoted by a box filled with an integer, e.g.  $\boxed{i}$  corresponds to the  $i^{\text{th}}$  quark. A tensor product of  $m$  such boxes corresponds to a product of  $m$  fundamental representations of  $SU(N)$ ,

$$\boxed{1} \otimes \boxed{2} \otimes \dots \otimes \boxed{m} \longrightarrow \begin{array}{c} \longleftrightarrow 1 \\ \longleftrightarrow 2 \\ \longleftrightarrow 3 \\ \vdots \\ \longleftrightarrow m \end{array}, \quad (5.6)$$

which itself is a representation of  $SU(N)$ , albeit not irreducible.

The irreducible representations within the product representation (5.6) is found by stacking the boxes  $\boxed{i}$  in a particular iterative manner: The Young tableaux for 2 quarks are built from  $\boxed{1}$  by positioning  $\boxed{2}$  either to the right of or below  $\boxed{1}$ . One then adds boxes containing consecutively higher numbers (up to  $\boxed{m}$ ) in a way that preserves the *top-alignedness* (the length of each row is always greater than or equal to the row below it) and *left-alignedness* (the length of each column is always greater than or equal to the column to the right of it) of the tableau. This iterative construction was presented up to  $m = 4$  in Figure 4.1.

### 5.1.3 The irreducible representations of $SU(N)$ over $V^{\otimes m} \otimes (V^*)^{\otimes n}$ with standard methods: Littlewood-Richardson tableaux

With Young’s contributions, the representation theory of compact, semi-simple Lie groups over  $V^{\otimes m}$  was considered a fully understood and complete theory from approximately 1950 onward, even though many misconceptions (in particular about the full extent of the theory) remained, especially among casual practitioners.

The situation for the irreducible representations of  $SU(N)$  over a mixed product  $V^{\otimes m} \otimes (V^*)^{\otimes n}$  is not as well developed, despite what a casual glance at the literature might lead us to believe. There exist standard methods to construct the projection operators corresponding to the irreducible representations of  $SU(N)$  over  $V^{\otimes m} \otimes (V^*)^{\otimes n}$ , but these methods are only adequate for classification purposes, not for explicit calculations. In order to drive home our point of its unsuitability for practical calculations, we present a brief account of the standard method. We explain how to construct the tableaux corresponding to the irreducible representations of  $SU(N)$  over  $V^{\otimes m} \otimes (V^*)^{\otimes n}$  and how to obtain the appropriate projection operators from these tableaux. While all pieces of information given in this section are present in the standard literature, we are not aware of a text that describes the entire method from start (constructing the tableaux) to finish (obtaining the projection operators), and thus have chosen to give a full account here.

When constructing the (Hermitian) Young projection operators from Young tableaux, one presupposes each particle (represented by a box in the tableau) to be in the fundamental representation; it is thus identified with a quark. Antiquarks, however, live in the antifundamental representation, thus no longer allowing us to represent them by a single box in a Young tableau. As a result of the Leibniz formula for determinants (*c.f.* section 5.1.4.1, or [112] for a textbook treatment), a single antiquark can be viewed as an antisymmetric combination of  $(N - 1)$  quarks [93]. In the tableau sense, an antiquark is thus represented by a tower of  $(N - 1)$  boxes. Eq. (5.7) shows a few examples of Young tableaux corresponding to a *single particle* in a



particular representation,

$$\begin{array}{ccc}
 \text{fundamental:} & \text{antifundamental:} & \text{adjoint:} \\
 \boxed{1} & \begin{array}{|c|} \hline 1 \\ \hline 2 \\ \hline \vdots \\ \hline N-1 \\ \hline \end{array} & \begin{array}{|c|c|} \hline 1 & N \\ \hline 2 & \\ \hline \vdots & \\ \hline N-1 & \\ \hline \end{array}, & (5.7)
 \end{array}$$

where the numbers here help to keep track of the amount of boxes, but are not necessarily the filling of the box in the tableau sense. Further motivation behind the claim (5.7) is given by the dimension of these tableaux: If we calculated the dimension of the representations corresponding to the tableaux directly from the tableaux (we will explain how to accomplish this shortly), we would find these dimensions to be  $N$ ,  $N$  and  $(N^2 - 1)$  respectively, leading us to conclude that the tableaux (5.7) correspond to the fundamental, the antifundamental and the adjoint representation respectively. We emphasize, however, that the dimension alone is not sufficient to identify a particular tableau with a representation. (This statement is substantiated by realizing that the fundamental and antifundamental representations have the same dimension  $N$ .) Nevertheless, the dimension does provide the first step towards such an identification. The actual reason why the antifundamental representation is classified by the tableau given in (5.7) is the Leibniz identity, as will become clear in section 5.1.4.1.

Let us now explain how to calculate the dimension of a representation directly from the corresponding Young tableau [72, 113].

**Dimension of a representation corresponding to a Young tableau [72, 113]:** Let  $\Theta$  be a Young tableau in  $\mathcal{Y}_m$ , for example

$$\begin{array}{|c|c|c|c|} \hline 1 & 2 & 5 & 7 \\ \hline 3 & 6 & 9 & \\ \hline 4 & & & \\ \hline 8 & & & \\ \hline \end{array} \in \mathcal{Y}_9. \quad (5.8)$$

Each cell  $c$  in the tableau  $\Theta$  can be referred to by the position vector  $(\mathcal{R}, \mathcal{C})$ , where  $\mathcal{R}$  is the row and  $\mathcal{C}$  is the column in which  $c$  appears. For example, the cell  $\boxed{9}$  in (5.8) has the position vector  $(2, 3)$ . To obtain the dimension of the representation corresponding to the Young tableau  $\Theta$ , one deletes all entries in  $\Theta$  to form the underlying *Young diagram*  $\mathbf{Y}_\Theta$ , and re-fills it in two ways:

1. In the first case, each cell  $c$  in  $\mathbf{Y}_\Theta$  is filled with its hook length  $\mathcal{H}_c$  [72, 95, 96] (*c.f.* eq. (4.38)): for every cell  $c$ , one counts the number of boxes appearing below and to the right of  $c$  (including  $c$ ) and writes this number into the cell  $c$ . For the tableau given in (5.8) this procedure yields

$$\text{hook length: } \begin{array}{|c|c|c|c|} \hline 7 & 4 & 3 & 1 \\ \hline 5 & 2 & 1 & \\ \hline 2 & & & \\ \hline 1 & & & \\ \hline \end{array}. \quad (5.9)$$

2. In the second case, we construct a  $k \times k$  matrix  $D$ , where  $k = \max(\text{length}(\mathcal{R}_1), \text{length}(\mathcal{C}_1))$  and  $\mathcal{R}_1$  and  $\mathcal{C}_1$  are the first row resp. column of the diagram  $\mathbf{Y}_\Theta$ . We assign to each entry  $d_{ij}$  of the matrix  $D$  the value  $(j - i)$ , and then cut out the Young diagram  $\mathbf{Y}_\Theta$ , making sure that the top left corners of  $\mathbf{Y}_\Theta$  and  $D$  coincide. As for the tableau given in eq. (5.8), we obtain

$$\text{distance: } D = \begin{pmatrix} 0 & 1 & 2 & 3 \\ -1 & 0 & 1 & 2 \\ -2 & -1 & 0 & 1 \\ -3 & -2 & -1 & 0 \end{pmatrix} \rightarrow \begin{array}{|c|c|c|c|} \hline 0 & 1 & 2 & 3 \\ \hline -1 & 0 & 1 & \\ \hline -2 & & & \\ \hline -3 & & & \\ \hline \end{array}. \quad (5.10)$$

Since the new values in the tableau essentially describe the distance from the diagonal (where positive entries lie above the diagonal and negative entries lie below it), the entry in each cell  $c$  will be referred to as the *distance* and will be denoted by  $d_c$ .

The dimension of the representation corresponding to the tableau  $\Theta$  is then given by [72, 113]

$$\dim(\Theta) = \prod_{c \in \Theta} \frac{N + d_c}{\mathcal{H}_c} = \frac{\prod_{c \in \Theta} (N + d_c)}{\mathcal{H}_\Theta}, \quad (5.11)$$

where the product runs over all cells  $c$  in the Young tableau  $\Theta$ , and

$$\mathcal{H}_\Theta := \prod_{c \in \Theta} \mathcal{H}_c \quad (5.12)$$

defines the hook length of the tableau  $\Theta$ . In the standard literature such as [72, 113], the quantity  $f_c := N + d_c$  is also referred to as the *factor* of the cell  $c$ . Thus, formula (5.11) is also called “factors-over-hooks”.

Using the “factors-over-hooks” formula, the dimension of the representation corresponding to the tableau in eq. (5.8) is

$$\begin{aligned} \dim((5.8)) &= \underbrace{\frac{N+0}{7} \frac{N+1}{4} \frac{N+2}{3} \frac{N+3}{1}}_{\text{row 1}} \cdot \underbrace{\frac{N-1}{5} \frac{N+0}{2} \frac{N+1}{1}}_{\text{row 2}} \cdot \underbrace{\frac{N-2}{2}}_{\text{row 3}} \cdot \underbrace{\frac{N-3}{1}}_{\text{row 4}} \\ &= \frac{N^2(N+1)(N^2-1)(N^2-4)(N^2-9)}{1680}. \end{aligned} \quad (5.13)$$

Formula (5.11) allows one to confirm that the dimensions of the tableaux given in (5.7) are  $N$ ,  $N$ , and  $(N^2 - 1)$  respectively, supporting the claim that they correspond to the fundamental, antifundamental and adjoint representations.

From Young’s algorithm, we know how to add another particle in the fundamental representation to a Young tableau in  $\mathcal{Y}_{k-1}$ . However, to add a particle in a different representation (for example, the antifundamental or adjoint representation), a generalization of the existing algorithm is needed. In the 1970’s, Littlewood and Richardson (LR) did just that [85]: In all its generality, the LR-rule gives a method of multiplying two Young tableaux of arbitrary shape that respects the multiplication properties of their underlying Schur functions.<sup>3</sup>

<sup>3</sup>Each irreducible representation of  $\text{SU}(N)$  corresponds to a unique Schur function. Thus, when we perform the product of two tableaux  $\Theta$  and  $\Phi$ , the product of their underlying Schur functions once again must yield a sum of Schur functions, so that each tableau in the sum  $\Theta \otimes \Phi$  corresponds to an irreducible representation of  $\text{SU}(N)$ . A full treatment of Schur functions is beyond the scope of this thesis — readers are referred to [114], or e.g. [96] for a textbook treatment.

Thus, LR generalize the iterative procedure exemplified in Figure 4.1 beyond the fundamental representation.

In this thesis, we are mainly interested in adding antiquarks, so we quote a simplified version of the LR-rule that applies to adding a particle in the antifundamental representation only. This simplified version is also referred to as *Pieri's formula* [95, 96]. For the fully general algorithm, readers are referred to Littlewood's book [85] or Sagan's book [96], the latter offering a more modern combinatorial view. Furthermore, Howe and Lee [115] provide a wonderfully intuitive proof of the general LR-rule using only classical invariant theory.

■ **Theorem 5.1 – adding antiquarks (LR-rule, Pieri's formula) [85, 95, 96]:**

Let  $\Theta \in \mathcal{Y}_m$  be a Young tableau consisting of  $m$  boxes, and let an antiquark be represented by the Young tableau consisting of one column of length  $(N - 1)$  (c.f. eq. (5.7)),

$$\bar{\Phi} = \begin{array}{|c|} \hline m+1 \\ \hline m+2 \\ \hline m+3 \\ \hline \vdots \\ \hline m+N-1 \\ \hline \end{array} =: \begin{array}{|c|} \hline a_1 \\ \hline a_2 \\ \hline a_3 \\ \hline \vdots \\ \hline a_k \\ \hline \end{array} \quad \text{with } a_{j+1} := a_j + 1, \text{ and end points } a_1 = m + 1 \text{ and } a_k = m + N - 1 . \quad (5.14)$$

Then, the product  $\Theta \otimes \bar{\Phi}$  yields the sum of all tableaux that can be constructed as follows: Take the tableau  $\Theta$  and add each box  $\boxed{a_j} \in \bar{\Phi}$  in the same way as one would using Young's construction (c.f. Figure 4.1). Additionally, we require that each box  $\boxed{a_j}$  appears in a row strictly above  $\boxed{a_{j+1}}$ , and that the resulting tableau has a maximum of  $N$  rows. Evidently, all tableaux in this sum are Young tableaux in  $\mathcal{Y}_{m+N-1}$ .

We may iterate the above described procedure to form the tableaux

$$\Theta \otimes \bar{\Phi}_1 \otimes \cdots \otimes \bar{\Phi}_n , \quad (5.15)$$

where each  $\bar{\Phi}_i$  is a tableau consisting of a single column of length  $(N - 1)$ , as described in eq. (5.14). Let the set of all tableaux appearing in the sum (5.15) be denoted by  $\{\Theta \otimes \bar{\Phi}_1 \otimes \cdots \otimes \bar{\Phi}_n\}$ , and let the union of all such sets over every  $\Theta \in \mathcal{Y}_m$  be denoted by  $\mathcal{Y}_{m,n}$ ,

$$\bigcup_{\Theta \in \mathcal{Y}_m} \{\Theta \otimes \bar{\Phi}_1 \otimes \cdots \otimes \bar{\Phi}_n\} =: \mathcal{Y}_{m,n} . \quad (5.16)$$

All tableaux constructed according to the Littlewood-Richardson rule will be referred to as *Littlewood-Richardson tableaux* in this thesis.<sup>4</sup>

The requirement that the resulting LR-tableau has at most  $N$  rows ensures that the corresponding operator is not **dimensionally zero**:<sup>5</sup> Suppose a particular LR-tableau  $\Theta$  has a column with length  $> N$  (i.e. this tableau has more than  $N$  rows), and let us treat  $\Theta$  as a Young tableau where each box corresponds to an index line in the fundamental representation — that this is a reasonable thing to do will become clear in section 5.1.4.2. Then, the corresponding (Hermitian) Young projection operator contains an antisymmetrizer over more than  $N$  factors in  $V^{\otimes m}$ . Since however  $\dim(V) = N$ , this antisymmetrizer is a null-operator, causing the whole projection operator to become zero. Since this zero is caused by the dimension of  $V$  being “too small”, we say that this operator is *dimensionally zero*.

<sup>4</sup>These are not to be confused with Littlewood-Richardson *skew* tableaux [92, 95], which are sometimes simply referred to as Littlewood-Richardson tableaux in the literature.

<sup>5</sup>C.f. section 4.A for a further discussion on dimensionally null operators.

As an example of the LR-rule described in Theorem 5.1, consider the Young tableau

$$\Theta = \begin{array}{|c|c|} \hline 1 & 3 \\ \hline 2 & \\ \hline \end{array}, \tag{5.17}$$

and let  $N = 4$  such that

$$\bar{\Phi} = \begin{array}{|c|} \hline 4 \\ \hline 5 \\ \hline 6 \\ \hline \end{array}. \tag{5.18}$$

Then, according to Theorem 5.1, the product  $\Theta \otimes \bar{\Phi}$  yields

$$\Theta \otimes \bar{\Phi} = \begin{array}{|c|c|c|} \hline 1 & 2 & 4 \\ \hline 3 & 5 & \\ \hline 6 & & \\ \hline \end{array} \oplus \begin{array}{|c|c|c|} \hline 1 & 2 & 4 \\ \hline 3 & & \\ \hline 5 & & \\ \hline 6 & & \\ \hline \end{array} \oplus \begin{array}{|c|c|} \hline 1 & 2 \\ \hline 3 & 4 \\ \hline 5 & \\ \hline 6 & \\ \hline \end{array}, \tag{5.19}$$

where each tableau in the sum is an element of  $\mathcal{Y}_6 = \mathcal{Y}_{3+N-1}$ . As a further example, we show the branching tree of the tableaux up to  $2q + 2\bar{q}$  in Figure 5.1:

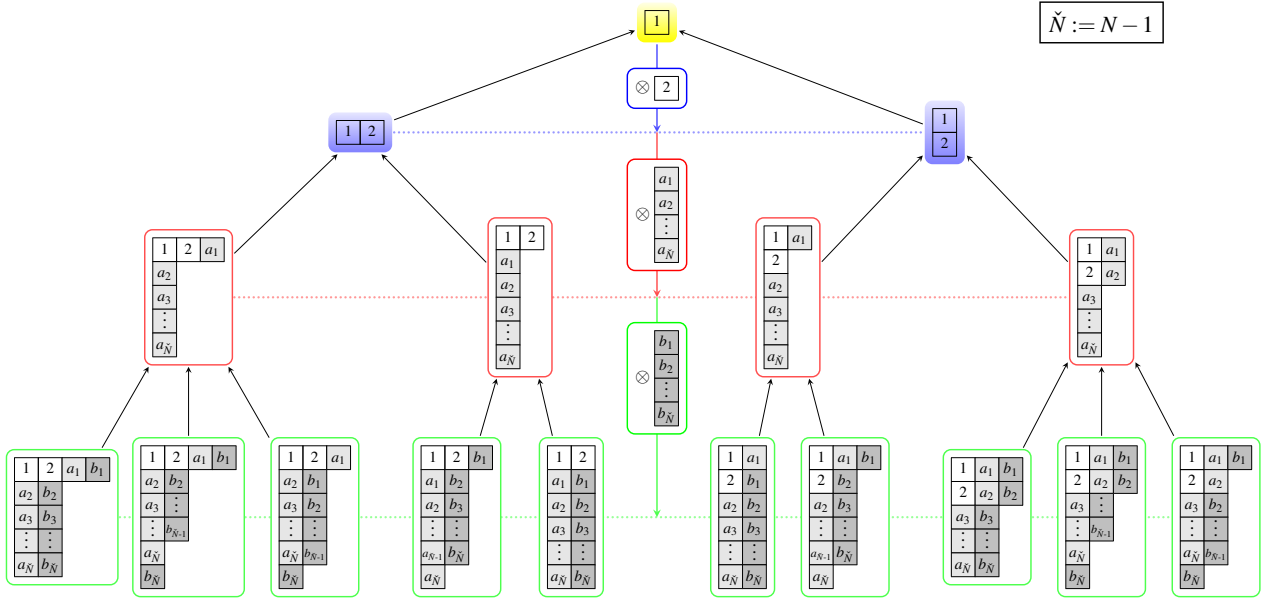


Figure 5.1: This branching tree shows all tableaux up to  $2q + 2\bar{q}$ . In the first two generations, this tree is identical to Figure 4.1, as these generations consist of quarks only. In generations three and four we add one antiquark each, which is given by the light grey and dark grey boxes respectively.

The observant reader might note that the number of tableaux appearing in each generation of Figures 5.1 and 4.1 is the same. This is no mere coincidence, but in fact a general statement, which will be proven in chapter 6, Corollary 6.2.

### 5.1.4 Projection operators from Littlewood-Richardson tableaux using the Leibniz formula for determinants

The LR-rule (Theorem 5.1) allows us to build up the Young tableaux corresponding to the irreducible representations of  $SU(N)$  over  $V^{\otimes m} \otimes (V^*)^{\otimes n}$ . Let us now discuss how to construct the corresponding projection operators. To accomplish this, we first need to recall the Leibniz formula for determinants [112].

#### 5.1.4.1 Leibniz rule for determinants

Let  $U \in SU(N)$  and consider  $U$  to be in the fundamental representation such that it can act on the  $N$ -dimensional vector space  $V$ ; in the physics sense, this means that  $U$  acts on the Fock space constituent corresponding to a quark. Thus,  $U$  itself is given by an  $N \times N$ -matrix, and we denote its components as  $U_{ia_i}$ . The Leibniz formula for determinants [112] allows us to calculate the determinant of any matrix by forming an antisymmetric sum over its columns (or, equivalently, rows) as

$$\det(U) = \varepsilon_{a_1 a_2 \dots a_N} U_{1a_1} U_{2a_2} \dots U_{Na_N} , \quad (5.20)$$

where a sum over repeated indices is implied. Further permuting the rows (resp. columns) of a matrix induces a minus sign in its determinant [107] such that

$$\varepsilon_{b_1 b_2 \dots b_N} \underbrace{\det(U)}_{=1} = \varepsilon_{a_1 a_2 \dots a_N} U_{b_1 a_1} U_{b_2 a_2} \dots U_{b_N a_N} , \quad (5.21)$$

where we have used the fact that, by the definition of the special unitary group, the determinant of  $U$  must equal 1. Lastly, since  $U$  is unitary, it follows that

$$(U_{ia_i})^{-1} = (U_{ia_i})^\dagger = U_{ia_i}^\dagger . \quad (5.22)$$

Eq. (5.21) may, therefore, be cast as

$$\varepsilon_{b_1 b_2 \dots b_N} U_{b_N a_N}^\dagger = \varepsilon_{a_1 a_2 \dots a_N} U_{b_1 a_1} U_{b_2 a_2} \dots U_{b_{(N-1)} a_{(N-1)}} . \quad (5.23)$$

Thus, the Levi-Civita symbol  $\varepsilon_{a_1 a_2 \dots a_N}$  acts as a map that translates a representation on  $V^{\otimes(N-1)}$  into a representation on  $V^*$  — eq. (5.23) allows us to read an antiquark as an antisymmetric product of  $(N-1)$  quarks, in agreement with eq. (5.7). Even more generally, one may write

$$\varepsilon_{b_1 b_2 \dots b_N} \underbrace{U_{b_N a_N}^\dagger \dots U_{b_{(N-j+1)} a_{(N-j+1)}}^\dagger}_{N-j \text{ antiquarks}} = \varepsilon_{a_1 a_2 \dots a_N} \underbrace{U_{b_1 a_1} U_{b_2 a_2} \dots U_{b_{(N-j)} a_{(N-j)}}}_{j \text{ quarks}} . \quad (5.24)$$

Let us now translate the two identities (5.23) and (5.24) into birdtrack notation: Following [72], the Levi-Civita tensor  $\varepsilon_{12\dots N}$  will be denoted by a black box over  $N$  index lines, where all of these lines exit to the left. On the other hand, the index lines of  $\varepsilon_{12\dots N}^\dagger$  will exit the black box to the right. For example,

$$i^\phi \varepsilon_{ijk} = \begin{array}{c} i \leftarrow \\ j \leftarrow \\ k \leftarrow \end{array} \blacksquare \quad \text{and} \quad i^{-\phi} (\varepsilon_{ijk})^\dagger = \blacksquare \begin{array}{c} \rightarrow i \\ \rightarrow j \\ \rightarrow k \end{array} , \quad (5.25)$$

where  $i^{-\phi}$  is a phase factor with  $\phi = n(n-1)/2$ , and  $n$  is the number of legs/indices of the Levi-Civita tensor [72] (for the example (5.25),  $\phi = 3$ ).<sup>6</sup>

As was already done in section 1.4.2.1, we will denote the elements of  $SU(N)$  by pink arrows pointing from right to left,

$$U_{ij} \rightarrow i \text{---} \blacktriangleleft \text{---} j; \quad (5.26a)$$

the placement of the matrix indices shows that  $U$  acts on elements of  $V$  from the left (i.e. the right index  $j$  is contracted with the index of the vector in  $V$ ). As for the primitive invariants, we will eventually drop the index labels on the birdtrack. In our examples,  $U^\dagger$  typically acts on elements of the dual space  $V^*$  from the right, so we define its corresponding birdtrack as

$$U_{ji}^\dagger \rightarrow i \text{---} \blacktriangleright \text{---} j; \quad (5.26b)$$

readers should take note of the placement of the matrix indices on  $U^\dagger$ . If, however, we need to consider the right action of  $U$ , or the left action of  $U^\dagger$ , we need to transpose the matrices of eqns. (5.26). In the birdtrack language (where we do not want to explicitly write the index labels), we will indicate this with a bar over the arrowhead,

$$([U]_{ij})^t = [U]_{ji} \rightarrow i \text{---} \overline{\blacktriangleright} \text{---} j \quad \text{and} \quad (U_{ji}^\dagger)^t = U_{ij}^\dagger \rightarrow i \text{---} \overline{\blacktriangleleft} \text{---} j \quad (5.27)$$

(*c.f.* eqns. (1.145) and (1.146)). As in chapter 1, a tensor product of Wilson lines is represented by a tower of lines with pink arrowheads, for example

$$U_{i_1 j_1} \otimes U_{i_2 j_2} \otimes U_{j_3 i_3}^\dagger = \begin{array}{c} i_1 \blacktriangleleft j_1 \\ i_2 \blacktriangleleft j_2 \\ i_3 \blacktriangleright j_3 \end{array}. \quad (5.28)$$

Writing a bar  $\overline{\phantom{x}}$  over the tower of Wilson lines will indicate that *each* Wilson line in the tower has undergone Hermitian conjugation,

$$(U_{i_1 j_1})^\dagger \otimes (U_{i_2 j_2})^\dagger \otimes (U_{j_3 i_3}^\dagger)^\dagger = U_{i_1 j_1}^\dagger \otimes U_{i_2 j_2}^\dagger \otimes U_{j_3 i_3} = \begin{array}{c} i_1 \overline{\blacktriangleright} j_1 \\ i_2 \overline{\blacktriangleright} j_2 \\ i_3 \overline{\blacktriangleright} j_3 \end{array}. \quad (5.29a)$$

If we only wish to form the Hermitian conjugate of *some* (but not all) of the Wilson lines in the product, then we will graphically gather the arrowheads of the conjugated Wilson lines to one side, such that the bar  $\overline{\phantom{x}}$  only covers the affected arrowheads but not the unaffected ones, for example

$$(U_{i_1 j_1})^\dagger \otimes (U_{i_2 j_2})^\dagger \otimes U_{j_3 i_3}^\dagger = U_{i_1 j_1}^\dagger \otimes U_{i_2 j_2}^\dagger \otimes U_{j_3 i_3}^\dagger = \begin{array}{c} i_1 \overline{\blacktriangleright} j_1 \\ i_2 \overline{\blacktriangleright} j_2 \\ i_3 \blacktriangleright j_3 \end{array} \quad (5.29b)$$

$$\text{or} \quad U_{i_1 j_1} \otimes (U_{i_2 j_2})^\dagger \otimes U_{j_3 i_3}^\dagger = U_{i_1 j_1} \otimes U_{i_2 j_2}^\dagger \otimes U_{j_3 i_3}^\dagger = \begin{array}{c} i_1 \blacktriangleright \overline{j_1} \\ i_2 \overline{\blacktriangleright} j_2 \\ i_3 \blacktriangleright \overline{j_3} \end{array}. \quad (5.29c)$$

<sup>6</sup>The phase factors  $i^{\pm\phi}$  are needed to ensure that the reordering of index lines of  $(\varepsilon_{a_1 a_2 \dots a_N})^\dagger$  brought about by the Hermitian conjugate  $\dagger$  does not destroy the property  $(\varepsilon_{a_1 a_2 \dots a_N})^\dagger \varepsilon_{a_1 a_2 \dots a_N} = \mathbb{1}$ , see [72, section 6.3].

In birdtrack notation, (5.23) amounts to



$$(5.30)$$

and similarly eq. (5.24) becomes



$$(5.31)$$

It further should be noted that, due to the identity [72, eq. (6.28)]



$$(5.32)$$

for Levi-Civita symbols of length  $N$  (where the numbers on the index lines in (5.32) keep track of their amount, but are not necessarily the index label), the product  $(\varepsilon_{a_1 a_2 \dots a_N})^\dagger \varepsilon_{b_1 b_2 \dots b_N}$  is an element of the algebra of invariants  $\text{API}(SU(N), V^{\otimes m})$ .

One now has to ask how the Leibniz formula for determinants introduced in this section can be used to obtain the projection operators from the LR-tableaux. We believe that this is best illustrated by means of an example:

#### 5.1.4.2 The irreducible representations of $SU(N)$ over $V \otimes V^*$ from Littlewood-Richardson tableaux

The Fierz identity is a commonly used tool in many physics calculations. It allows one to decompose the tensor product space of two Kronecker delta's (one in the fundamental, the other in the antifundamental representation)<sup>7</sup> into two irreducible subspaces

$$\delta_{lk} \delta_{ij} = [t^a]_{ik} [t^a]_{jl} + \frac{1}{N} \delta_{ik} \delta_{jl} , \quad (5.33)$$

where  $[t^a]_{ik}$  is the generator of the group. The Fierz identity is easily verifiable — the basic idea is to exploit properties of traces of (products of)  $\gamma$ -matrices [116, sec. 29.3]. We will now show that the projection operators appearing in the Fierz identity, and their summation exhibited in eq. (5.33), can be recovered from the appropriate Littlewood-Richardson tableaux corresponding to 1 fundamental and 1 antifundamental factor: We prove that the LR-tableaux give rise to the two irreducible projection operators

$$\frac{1}{N} \delta_{ik} \delta_{jl} = \frac{1}{N} \curvearrowright \curvearrowleft \quad \text{and} \quad \delta_{lk} \delta_{ij} - \frac{1}{N} \delta_{ik} \delta_{jl} = \overleftarrow{\quad} - \frac{1}{N} \curvearrowright \curvearrowleft \quad (5.34)$$

<sup>7</sup>In practice, we usually consider them to be acted upon by Wilson lines.

of  $SU(N)$  over  $V \otimes V^*$ . We will then utilize the Fierz identity to write the operator  $\delta_{lk}\delta_{ij} - \frac{1}{N}\delta_{ik}\delta_{jl}$  in terms of the generators  $t^a$ . This is sufficient to achieve the main goal of this section, namely to demonstrate that the standard method (starting from LR-tableaux and then using the Leibniz identity to arrive at the desired operators) is not useful for practical calculations.

In birdtrack notation, the Fierz identity can be written as [72]

$$\begin{array}{c} \leftarrow \\ \rightarrow \end{array} = \begin{array}{c} \curvearrowright \\ \curvearrowleft \end{array} + \frac{1}{N} \begin{array}{c} \curvearrowright \\ \curvearrowright \end{array}, \quad (5.35)$$

where the vertex between the dotted and solid lines denotes the generator  $t^a := [t^a]_{ik}$ ,

$$\frac{1}{\sqrt{2}}[t^a]_{ik} := a \cdots \begin{array}{c} \curvearrowright \\ \curvearrowleft \end{array} \begin{array}{c} k \\ i \end{array} \quad \text{and} \quad \frac{1}{\sqrt{2}}[t^b]_{jl} := \begin{array}{c} l \\ j \end{array} \begin{array}{c} \curvearrowright \\ \curvearrowright \end{array} \cdots b. \quad (5.36)$$

As already mentioned, the Fierz identity decomposes the space  $V \otimes V^*$  into irreducible subspaces. Thus, the operators on the right-hand side of eq. (5.35) are projection operators corresponding to the irreducible representations of  $SU(N)$  over  $V \otimes V^*$  (see, for example, [72] or any other standard textbook),

$$\text{adjoint representation:} \quad \begin{array}{c} \curvearrowright \\ \curvearrowleft \end{array} \quad \dim = N^2 - 1 \quad (5.37a)$$

$$\text{singlet representation:} \quad \begin{array}{c} \curvearrowright \\ \curvearrowright \end{array} \quad \dim = 1. \quad (5.37b)$$

Viewing the operators in eq. (5.35) as projectors, the Fierz identity tells us that the projection operators corresponding to the irreducible representations of  $SU(N)$  over  $V \otimes V^*$  sum up to the identity; this is a property that we are already familiar with from Young projection operators over  $V^{\otimes m}$  for  $m \leq 4$ , and their generalization by Littlewood for all  $m$  (c.f. eq. (3.6c)). When deriving the Fierz identity starting from the corresponding LR-tableaux, we will need something stronger than the total summation property of Young projection operators, namely the *partial* summation property of Hermitian Young projection operators eq. (3.112) (c.f. section 3.3.4). This property states that the Hermitian Young projectors sum up to their common Hermitian ancestor operator. This is the reason why the *Hermitian* Young projection operators are of vital importance in the derivation described below.

Consider the branching tree of LR-tableaux for  $1q + 1\bar{q}$  constructed according to Theorem 5.1:



Using the dimension formula for Young tableaux (5.11), we see that the left tableau corresponds to a  $(N^2 - 1)$ -dimensional representation of  $SU(N)$ , while the right tableau corresponds to a 1-dimensional representation of  $SU(N)$ . Thus, we expect these tableaux to give rise to operators (5.37a) and (5.37b) respectively. For the remainder of this section, we will suggestively refer to the projection operators corresponding to the tableaux in (5.38) as the *adjoint* and *singlet*, respectively.

Using the MOLD Theorem 3.5, the Hermitian Young projection operators corresponding to the tableaux (5.38)



are given by<sup>8</sup>

$$P_{\begin{smallmatrix} 1 & 2 \\ 3 & \vdots \\ N & \vdots \end{smallmatrix}} = \frac{2(N-1)}{N} \cdot \begin{array}{c} \begin{array}{c} \leftarrow \square \rightarrow \\ \leftarrow \square \rightarrow \\ \vdots \\ \leftarrow \square \rightarrow \\ \leftarrow \square \rightarrow \end{array} \\ \vdots \\ \begin{array}{c} \leftarrow \square \rightarrow \\ \leftarrow \square \rightarrow \end{array} \end{array} \quad \text{and} \quad P_{\begin{smallmatrix} 1 \\ 2 \\ 3 \\ \vdots \\ N \end{smallmatrix}} = \begin{array}{c} \leftarrow \square \rightarrow \\ \leftarrow \square \rightarrow \\ \leftarrow \square \rightarrow \\ \vdots \\ \leftarrow \square \rightarrow \\ \leftarrow \square \rightarrow \end{array}. \quad (5.39)$$

The Hermitian parent operator of these two projectors corresponds to the tableau  $\begin{array}{|c|} \hline 1 \\ \hline \end{array}$ . The Levi-Civita symbol  $\varepsilon_{a_1 a_2 \dots a_{N-1}}$  embeds  $V^*$  into  $V^{\otimes(N-1)}$  such that we may embed the projection operator  $P_{\begin{array}{|c|} \hline 1 \\ \hline \end{array}}$  into the algebra  $\text{API}(SU(N), V \otimes V^{\otimes(N-1)})$ ,

$$\begin{array}{|c|} \hline 1 \\ \hline \end{array} \hookrightarrow \begin{array}{|c|} \hline 1 \\ \hline \end{array} \otimes \begin{array}{|c|} \hline 2 \\ \hline 3 \\ \hline \vdots \\ \hline N \\ \hline \end{array} \longrightarrow \begin{array}{c} \leftarrow \square \rightarrow \\ \leftarrow \square \rightarrow \\ \vdots \\ \leftarrow \square \rightarrow \\ \leftarrow \square \rightarrow \end{array}; \quad (5.40)$$

notice that in this embedding the antiquark is represented by  $(N-1)$  quark lines in an antisymmetric state, *c.f.* eq. (5.7). The summation property of Hermitian Young projection operators proved in section 3.3.4 predicts that the operators (5.39) sum up to their parent operator (5.40),<sup>9</sup>

$$\begin{array}{c} \leftarrow \square \rightarrow \\ \leftarrow \square \rightarrow \\ \vdots \\ \leftarrow \square \rightarrow \\ \leftarrow \square \rightarrow \end{array} = \begin{array}{c} \leftarrow \square \rightarrow \\ \leftarrow \square \rightarrow \\ \vdots \\ \leftarrow \square \rightarrow \\ \leftarrow \square \rightarrow \end{array} + \frac{2(N-1)}{N} \cdot \begin{array}{c} \begin{array}{c} \leftarrow \square \rightarrow \\ \leftarrow \square \rightarrow \\ \vdots \\ \leftarrow \square \rightarrow \\ \leftarrow \square \rightarrow \end{array} \\ \vdots \\ \begin{array}{c} \leftarrow \square \rightarrow \\ \leftarrow \square \rightarrow \end{array} \end{array}. \quad (5.41)$$

We now wish to translate the fundamental legs  $2 \dots N$  of each operator in (5.41) into an antifundamental leg. This is done by acting an epsilon tensor of length  $N$ ,  $\varepsilon_{2 \dots N(N+1)}$ , on either side of the operators; such a transformation cannot possibly make the operators zero, since the legs  $2 \dots N$  are already in an antisymmetric combination by construction. Having performed this transformation, we may then implement the Leibniz formula (5.30) to regard the last leg exiting  $\varepsilon_{2 \dots N(N+1)}$  as an antifundamental leg. For example, for the singlet operator this procedure yields

$$\begin{array}{c} \leftarrow \square \rightarrow \\ \leftarrow \square \rightarrow \\ \vdots \\ \leftarrow \square \rightarrow \\ \leftarrow \square \rightarrow \end{array} \xrightarrow{\text{act } \varepsilon} N \cdot \begin{array}{c} \leftarrow \square \rightarrow \\ \leftarrow \square \rightarrow \\ \vdots \\ \leftarrow \square \rightarrow \\ \leftarrow \square \rightarrow \end{array} =: N \cdot \begin{array}{c} \leftarrow \square \rightarrow \\ \leftarrow \square \rightarrow \\ \vdots \\ \leftarrow \square \rightarrow \\ \leftarrow \square \rightarrow \end{array} \begin{array}{c} 1 \\ \bar{q} \end{array}, \quad (5.42)$$

where we have decided to suppress the arrows in the last step and, instead, labelled the legs 1 and  $\bar{q}$  for clarity. Notice that the additional factor  $N$  arising from acting  $\varepsilon_{2 \dots N(N+1)}$  on either side of the operator is needed to ensure that the resulting operator is idempotent: when squaring this operator, the two Levi-Civita tensors coming to stand next to each other will combine into an antisymmetrizer of length  $N$ , according to eq. (5.32). However, due to the fact that the bottom leg on each  $\varepsilon$ -tensor is bent, the antisymmetrizer will be traced over its bottom leg, inducing a factor  $1/N$ .

<sup>8</sup>The prefactors of the operators in eq. (5.39) arise from the MOLD algorithm: since both operators correspond to *lexically ordered* tableaux (*c.f.* section 3.4.1), the MOLD algorithm predicts that the Hermitian operators have the same normalization factor as their Young counterparts.

<sup>9</sup>This can easily be double-checked via direct calculation.

Going through the steps demonstrated in (5.42), the operators in eq. (5.41) transform as

$$\begin{array}{c} \leftarrow \\ \leftarrow \\ \vdots \\ \leftarrow \\ \leftarrow \end{array} \rightarrow N \cdot \begin{array}{c} \overline{\quad} \\ \leftarrow \\ \leftarrow \\ \vdots \\ \leftarrow \\ \leftarrow \\ \bar{q} \end{array} \quad (5.43a)$$

$$\begin{array}{c} \leftarrow \\ \leftarrow \\ \vdots \\ \leftarrow \\ \leftarrow \end{array} \rightarrow N \cdot \begin{array}{c} \overline{\quad} \\ \leftarrow \\ \leftarrow \\ \vdots \\ \leftarrow \\ \leftarrow \\ \bar{q} \end{array} \quad (5.43b)$$

$$\frac{2(N-1)}{N} \cdot \begin{array}{c} \leftarrow \\ \leftarrow \\ \vdots \\ \leftarrow \\ \leftarrow \end{array} \rightarrow 2(N-1) \cdot \begin{array}{c} \overline{\quad} \\ \leftarrow \\ \leftarrow \\ \vdots \\ \leftarrow \\ \leftarrow \\ \bar{q} \end{array} \quad (5.43c)$$

These operators do not yet bear any visual resemblance to the objects appearing in the Fierz identity (5.35); it requires approximately four pages of calculation and simplification (see appendix 5.A) to establish the desired outcome:

$$N \cdot \begin{array}{c} \overline{\quad} \\ \leftarrow \\ \leftarrow \\ \vdots \\ \leftarrow \\ \leftarrow \\ \bar{q} \end{array} = \begin{array}{c} \leftarrow \\ \rightarrow \end{array} \quad (5.44a)$$

$$N \cdot \begin{array}{c} \overline{\quad} \\ \leftarrow \\ \leftarrow \\ \vdots \\ \leftarrow \\ \leftarrow \\ \bar{q} \end{array} = \frac{1}{N} \begin{array}{c} \curvearrowright \\ \curvearrowleft \end{array} \quad (5.44b)$$

$$2(N-1) \cdot \begin{array}{c} \overline{\quad} \\ \leftarrow \\ \leftarrow \\ \vdots \\ \leftarrow \\ \leftarrow \\ \bar{q} \end{array} = \begin{array}{c} \curvearrowright \\ \curvearrowleft \end{array}, \quad (5.44c)$$

*c.f.* equations (5.174), (5.185) and (5.194), respectively. Substituting these results back into eq. (5.41) indeed yields the Fierz identity,

$$\begin{array}{c} \leftarrow \\ \rightarrow \end{array} = \frac{1}{N} \begin{array}{c} \curvearrowright \\ \curvearrowleft \end{array} + \begin{array}{c} \curvearrowright \\ \curvearrowleft \end{array}, \quad (5.45)$$

albeit at an excessive computational effort.

At this point, we hope to have convinced the reader that the standard method of obtaining the projection operators from Littlewood-Richardson tableaux is very laborious. In this chapter, we will show that, at least for singlet operators, there exists a more efficient construction method: Note that the singlet projector in the Fierz identity,  $\begin{array}{c} \curvearrowright \\ \curvearrowleft \end{array}$ , could have been obtained by bending and mirroring the projection operator corresponding to the irreducible representation of  $SU(N)$  over  $V$ ,

$$\leftarrow \xrightarrow{\text{bend}} \curvearrowright \xrightarrow{\text{mirror}} \begin{array}{c} \curvearrowright \\ \curvearrowleft \end{array}. \quad (5.46)$$

Eq. (5.46) sets the general strategy for our construction algorithm discussed in section 5.2.

### 5.1.4.3 A comment on the dimension of projection operators obtained from LR-tableaux

As mentioned previously, an operator is **dimensionally nonzero** if  $N$  is large enough to allow for all antisymmetrizers contained in the operator to be nonzero. Thus, we can guarantee a projection operator corresponding to an irreducible representation of  $SU(N)$  over  $V^{\otimes m} \otimes (V^*)^{\otimes n}$  to be dimensionally nonzero if  $N \geq (m+n)$ . In this case, the maximal dimension of the algebra of invariants  $\text{API}\left(SU(N), V^{\otimes m} \otimes (V^*)^{\otimes n}\right)$ , namely  $d = (m+n)!$ , is reached. (The algebra  $\text{API}\left(SU(N), V^{\otimes m} \otimes (V^*)^{\otimes n}\right)$  and its properties will be discussed in more detail in chapters 6 to 8.)

The example of section 5.1.4.2 further shows that the textbook method of talking about irreducible representations of  $SU(N)$  over a mixed space  $V^{\otimes m} \otimes (V^*)^{\otimes n}$  (using LR-tableaux) is rather more indirect than that over a monotone space  $V^{\otimes m}$  (using Young tableaux): The primitive invariants of  $SU(N)$  over  $V^{\otimes m} \otimes (V^*)^{\otimes n}$ , and thus all elements of  $\text{API}\left(SU(N), V^{\otimes m} \otimes (V^*)^{\otimes n}\right)$ , are included in  $\text{API}\left(SU(N), V^{\otimes [m+n(N-1)]}\right)$  in the sense of a subalgebra, as is evident from the corresponding Littlewood-Richardson tableaux  $\mathcal{Y}_{m,n}$  (c.f. eq. (5.16) in Theorem 5.1), which form a subset of  $\mathcal{Y}_{m+n(N-1)}$ . This is due to the presence of  $\varepsilon_{i_1 \dots i_N}$  as a second invariant in addition to  $\delta_{ij}$  (c.f. eq. (5.32)). To be a little more explicit:  $\text{API}\left(SU(N), V^{\otimes [m+n(N-1)]}\right)$  encompasses representations on  $V^{\otimes m} \otimes (V^*)^{\otimes n}$  via the LR-rule, which exploits the determinant condition for  $SU(N)$ , i.e. the invariance of the  $\varepsilon$ -tensor in  $N$  dimensions, and so formally gives access to all these representations as well. The drawback, clearly, is the size of the algebra:  $[m+n(N-1)]! \gg (m+n)!$  generically, and keeping  $N$  as a parameter will not be a trivial task.

In this chapter, we will use what we have learnt about  $\text{API}\left(SU(N), V^{\otimes m}\right)$  in chapters 3 and 4 to construct singlet projectors directly as elements of  $\text{API}\left(SU(N), V^{\otimes m} \otimes (V^*)^{\otimes m}\right)$  (in physics parlance, that is, with  $m$  particles and  $m$  antiparticles), and more generally  $\text{API}\left(SU(N), V^{\otimes m} \otimes (V^*)^{\otimes n}\right)$  without any detour through  $\text{API}\left(SU(N), V^{\otimes [m+m(N-1)]}\right)$  (resp  $\text{API}\left(SU(N), V^{\otimes [m+n(N-1)]}\right)$ ), thus keeping  $N$  as a parameter in the process.

## 5.2 Singlet projection operators

The special unitary group  $SU(N)$  has two kinds of primitive invariants over a mixed product space  $V^{\otimes m} \otimes (V^*)^{\otimes n}$ : a product of Kronecker  $\delta$ 's, and Levi-Civita tensors of size  $N$ ,  $\varepsilon_{12\dots N}$ , where  $N = \dim(V)$  (see [72, 92, 93] or any other standard textbook). Since the projection operators corresponding to (irreducible) representations of  $SU(N)$  must themselves be invariant under the group operation — that is, they are elements of the algebra of invariants  $\text{API}\left(SU(N), V^{\otimes m} \otimes (V^*)^{\otimes n}\right)$  — they have to be comprised of Kronecker  $\delta$ 's and Levi-Civita symbols. In particular, this holds for the singlet projection operators corresponding to the 1-dimensional irreducible representations of  $SU(N)$ . It is clear that a singlet projector containing only Kronecker  $\delta$ 's must act on a product space containing the same amount of fundamental and antifundamental factors  $V^{\otimes m} \otimes (V^*)^{\otimes m}$  [93, 117]; this is best understood in terms of birdtracks, where each Kronecker  $\delta$ , represented by a line,

$$\delta_{ij} = i \longleftarrow j, \tag{5.47}$$

connects each fundamental index to a unique antifundamental index. Only the presence of Levi-Civita tensors allows for singlets over a product space that is not evenly split between  $V$  and  $V^*$ , section 5.2.2.

It can, however, be shown that the singlets including Levi-Civita tensors are completely equivalent to a subset of singlets over  $V^{\otimes k} \otimes (V^*)^{\otimes k}$  for  $N = \dim(V)$ , see section 5.2.2.2. This should come as no surprise since a product of Levi-Civita symbols of length  $N$ ,  $(\varepsilon_{a_1 a_2 \dots a_N})^\dagger \varepsilon_{b_1 b_2 \dots b_N}$ , becomes an antisymmetrizer of length  $N$ , which in turn can again be written as a product of Kronecker  $\delta$ 's [72] (*c.f.* eq. (5.32)),

$$\begin{array}{c} \leftarrow \\ \leftarrow \\ \vdots \\ \leftarrow \end{array} \begin{array}{c} \xrightarrow{1} \\ \xrightarrow{2} \\ \vdots \\ \xrightarrow{N-1} \\ \xrightarrow{N} \end{array} \xrightarrow{\dim(V)=N} \begin{array}{c} \leftarrow \\ \leftarrow \\ \vdots \\ \leftarrow \end{array} \begin{array}{c} \xrightarrow{1} \\ \xrightarrow{2} \\ \vdots \\ \xrightarrow{N-1} \\ \xrightarrow{N} \end{array} . \quad (5.48)$$

Before diving into the general argument, we will motivate this equivalence by taking a closer look at the singlet projector of  $SU(3)$  over  $V^{\otimes 3}$ , which is comprised solely of Levi-Civita tensors,

$$P^S = \begin{array}{c} \leftarrow \\ \leftarrow \\ \leftarrow \end{array} \begin{array}{c} \leftarrow \\ \leftarrow \\ \leftarrow \end{array} \begin{array}{c} \xrightarrow{1} \\ \xrightarrow{2} \\ \xrightarrow{3} \end{array} \begin{array}{c} \xrightarrow{1} \\ \xrightarrow{2} \\ \xrightarrow{3} \end{array} , \quad (5.49)$$

in section 5.2.2.1. This example will be familiar to physicists, as it describes a 3-quark, color neutral representation — a *baryon*.

### 5.2.1 Singlet projectors over $V^{\otimes k} \otimes (V^*)^{\otimes k}$ : Kronecker $\delta$ 's

In this section, we provide an explicit construction algorithm for the singlet projection operators of  $SU(N)$  over a product space consisting of an equal number of quarks and antiquarks,  $V^{\otimes k} \otimes (V^*)^{\otimes k}$ . Our general argument is best understood using Clebsch-Gordan operators over  $V^{\otimes m} \otimes (V^*)^{\otimes n}$  where  $m + n = k$ . We therefore dedicate section 5.2.1.1 to adapting the birdtrack notation for Clebsch-Gordan operators over  $V^{\otimes m}$  (*c.f.* section 4.4.2 in chapter 4) to those over  $V^{\otimes m} \otimes (V^*)^{\otimes n}$ .

In section 4.4.2, we showed (using Clebsch-Gordan operators) that the Hermitian projection and unitary transition operators of  $SU(N)$  over  $V^{\otimes m}$  constitute a basis for the algebra of invariants  $\text{API}(SU(N), V^{\otimes m})$ . This argument will be generalized to mixed spaces  $V^{\otimes m} \otimes (V^*)^{\otimes n}$  in section 5.2.1.2. The fact that the projection and transition operators span  $\text{API}(SU(N), V^{\otimes m} \otimes (V^*)^{\otimes n})$  is a key ingredient in the general construction algorithm for singlet projectors over  $V^{\otimes k} \otimes (V^*)^{\otimes k}$ , which will be given in section 5.2.1.3.

In practical applications, however, Clebsch-Gordan operators are of little use, as obtaining them requires one to first construct all possible states. In section 5.2.1.4 we argue that the Clebsch-Gordan operators used in the construction of the singlet projectors can be substituted for Hermitian Young projection operators (such as MOLD operators, *c.f.* Theorem 3.5) and transition operators (*c.f.* Theorem 4.5). Since the construction algorithms for the MOLD operators and corresponding transition operators are very efficient, these operators are much better suited for practical applications.

Note that the results of sections 5.2.1.2 and 5.2.1.3 could, equally well, be derived from Schur's Lemma, but the *graphical* bending algorithm to generate singlet states (*c.f.* eq. (5.76) in section 5.2.1.3) is best understood in terms of Clebsch-Gordan operators.

#### 5.2.1.1 A short review of Clebsch-Gordan operators

Analogous to the quark-only case (*c.f.* section 4.4.2), we denote a general Clebsch-Gordan operator that implements the projection and basis change from a product of irreducible representations labelled

$q_1, \dots, q_m, \bar{q}_1, \dots, \bar{q}_n$  (with states labelled by  $k_1, \dots, k_m, \bar{k}_1, \dots, \bar{k}_n$ ) into an irreducible representation labelled by  $\lambda$  (where  $\lambda$  stands in for a Littlewood-Richardson tableau and with states labelled by  $\kappa$ ) [93], by  $C_{\lambda\kappa; q_1 \dots q_m k_1 \dots k_m \bar{q}_1 \dots \bar{q}_n \bar{k}_1 \dots \bar{k}_n}$ ,

$$\begin{aligned}
 C_{\lambda\kappa; q_1 \dots q_m k_1 \dots k_m \bar{q}_1 \dots \bar{q}_n \bar{k}_1 \dots \bar{k}_n} &= |\lambda, \kappa\rangle \overbrace{\langle \lambda, \kappa | q_1, k_1 \rangle \dots \langle q_m, k_m | \bar{q}_1, \bar{k}_1 \rangle \dots \langle \bar{q}_n, \bar{k}_n \rangle}^{\mathfrak{C}_{\lambda\kappa; q_1 \dots q_m k_1 \dots k_m \bar{q}_1 \dots \bar{q}_n \bar{k}_1 \dots \bar{k}_n}} \langle q_1, k_1 | \dots \langle q_m, k_m | \langle \bar{q}_1, \bar{k}_1 | \dots \langle \bar{q}_n, \bar{k}_n | \\
 &=: |\lambda, \kappa\rangle \kappa \leftarrow \begin{array}{c} \text{---} q_1, k_1 \quad \langle q_1, k_1 | \\ \vdots \\ \text{---} q_m, k_m \quad \langle q_m, k_m | \\ \vdots \\ \text{---} \bar{q}_1, \bar{k}_1 \quad \langle \bar{q}_1, \bar{k}_1 | \\ \vdots \\ \text{---} \bar{q}_n, \bar{k}_n \quad \langle \bar{q}_n, \bar{k}_n | \end{array} \lambda \end{array} \quad (5.50)
 \end{aligned}$$

The part marked  $\mathfrak{C}_{\lambda\kappa; q_1 \dots q_m k_1 \dots k_m \bar{q}_1 \dots \bar{q}_n \bar{k}_1 \dots \bar{k}_n}$  is the usual Clebsch-Gordan coefficient, and the diagram in the second line is the birdtrack representation of  $\mathfrak{C}_{\lambda\kappa; q_1 \dots q_m k_1 \dots k_m \bar{q}_1 \dots \bar{q}_n \bar{k}_1 \dots \bar{k}_n}$  (c.f. [72] and chapter 4). The full operator is obtained by summing over all the states

$$C_{\lambda, m, n} := \sum_{\kappa} \sum_{k_i, \bar{k}_i} C_{\lambda\kappa; q_1 \dots q_m k_1 \dots k_m \bar{q}_1 \dots \bar{q}_n \bar{k}_1 \dots \bar{k}_n} = \begin{array}{c} \text{---} \\ \vdots \\ \text{---} \end{array} \lambda \begin{array}{c} \text{---} \\ \vdots \\ \text{---} \end{array} \quad (5.51)$$

By their very definition, the Clebsch-Gordan operators (5.51) satisfy analogous properties to their quark-only counterparts,

$$\begin{array}{c} \text{---} \\ \vdots \\ \text{---} \end{array} \lambda \begin{array}{c} \text{---} \\ \vdots \\ \text{---} \end{array} \begin{array}{c} U \\ U^\dagger \\ U^\dagger \end{array} = U_{(\lambda)} \begin{array}{c} \text{---} \\ \vdots \\ \text{---} \end{array} \lambda \begin{array}{c} \text{---} \\ \vdots \\ \text{---} \end{array} \quad \text{and} \quad \begin{array}{c} \text{---} \\ \vdots \\ \text{---} \end{array} \lambda \begin{array}{c} \text{---} \\ \vdots \\ \text{---} \end{array} \begin{array}{c} U^\dagger \\ U \\ U \end{array} = U_{(\lambda)}^\dagger \begin{array}{c} \text{---} \\ \vdots \\ \text{---} \end{array} \lambda \begin{array}{c} \text{---} \\ \vdots \\ \text{---} \end{array} \quad (5.52a)$$

$$\langle \lambda, \kappa | \lambda', \kappa' \rangle = \kappa \leftarrow \begin{array}{c} \text{---} \\ \vdots \\ \text{---} \end{array} \lambda \begin{array}{c} \text{---} \\ \vdots \\ \text{---} \end{array} \lambda' \begin{array}{c} \text{---} \\ \vdots \\ \text{---} \end{array} \kappa' = \delta_{\lambda, \lambda'} \delta_{\kappa, \kappa'}, \quad (5.52b)$$

c.f. eqns. (4.80) and (4.81).

### 5.2.1.2 Projection and transition operators as a basis for the algebra of invariants

In this section, the argument (given in section 4.4.2) that the Hermitian projection and transition operators of  $SU(N)$  over  $V^{\otimes m}$  span  $\text{API}(SU(N), V^{\otimes m})$  will be adapted for the operators over  $V^{\otimes m} \otimes (V^*)^{\otimes n}$ . We begin with a recapitulation of what it means for two representations to be equivalent.

Consider two unitary irreducible representations of  $SU(N)$  labelled  $\lambda$  and  $\lambda'$  respectively. These two representations are said to be *equivalent* if there exists an isomorphism  $S_{\lambda'\lambda}$  between the corresponding vector spaces,

$$\mathcal{S}_{(\lambda'\lambda)} : V_{(\lambda)} \longrightarrow V_{(\lambda')}, \quad (5.53a)$$

such that

$$\mathcal{S}_{(\lambda'\lambda)} U_{(\lambda)} \mathcal{S}_{(\lambda'\lambda)}^{-1} = U_{(\lambda')} \quad \text{for every } U \in SU(N), \quad (5.53b)$$

where  $U_{(\lambda)}$  (resp.  $U_{(\lambda')}$ ) denotes the group element  $U$  in the representation  $\lambda$  (resp.  $\lambda'$ ). The map  $\mathcal{S}_{(\lambda'\lambda)}$  is unitary in the sense that it maps an orthonormal basis of  $V_{(\lambda)}$  to an orthonormal basis of  $V_{(\lambda')}$ . To be explicit, we may now choose an orthonormal basis  $\{|\lambda\kappa\rangle|\kappa = 1, \dots, \dim(V_{(\lambda)})\}$  in the vector space  $V_{(\lambda)}$  so that

$$\langle \lambda\kappa | \lambda\kappa' \rangle = \delta_{\kappa'\kappa} , \quad (5.54)$$

and consider the associated basis in  $V_{(\lambda')}$  given by

$$|\lambda'\kappa\rangle =: \mathcal{S}_{(\lambda'\lambda)}|\lambda\kappa\rangle . \quad (5.55a)$$

The orthonormality of this basis follows from eq. (5.54) and the unitarity of  $\mathcal{S}_{(\lambda'\lambda)}$ ,

$$\langle \lambda'\kappa | \lambda'\kappa' \rangle = \langle \lambda\kappa | \mathcal{S}_{(\lambda'\lambda)}^\dagger \mathcal{S}_{(\lambda'\lambda)} |\lambda\kappa'\rangle = \langle \lambda\kappa | \lambda\kappa' \rangle = \delta_{\kappa'\kappa} . \quad (5.55b)$$

With this choice of basis, the matrix elements of  $\mathcal{S}_{(\lambda'\lambda)}$  become the identity matrix,

$$\langle \lambda'\kappa' | \underbrace{\mathcal{S}_{(\lambda'\lambda)}|\lambda\kappa\rangle}_{=|\lambda'\kappa\rangle} = \langle \lambda'\kappa' | \lambda'\kappa \rangle = \delta_{\kappa'\kappa} . \quad (5.55c)$$

With this synchronized basis choice, the matrices  $U_{(\lambda)}$  and  $U_{(\lambda')}$  are equal for every  $U \in \text{SU}(N)$ :<sup>10</sup>

$$[U_{(\lambda)}]_{\kappa'\kappa} := \langle \lambda\kappa' | U_{(\lambda)} |\lambda\kappa\rangle = \langle \lambda'\kappa' | \mathcal{S}_{(\lambda'\lambda)} U_{(\lambda)} \mathcal{S}_{(\lambda'\lambda)}^{-1} |\lambda'\kappa\rangle \stackrel{\text{eq. (5.53b)}}{=} \langle \lambda'\kappa' | U_{(\lambda')} |\lambda'\kappa\rangle =: [U_{(\lambda')}]_{\kappa'\kappa} . \quad (5.56)$$

It should be noted that for any two representations  $\lambda$  and  $\lambda'$  with the same dimension an isomorphism between the corresponding vector spaces, à la eq. (5.53a), can be found, but the identity (5.53b) holds *if and only if* the two representations are equivalent.

Let us now consider a product of Clebsch-Gordan operators  $C_{\lambda,m,n}^\dagger \mathcal{S}_{\lambda\lambda'} C_{\lambda',m,n}$  (which is a linear map on the space  $V^{\otimes m} \otimes (V^*)^{\otimes n}$ ) in which the representations  $\lambda$  and  $\lambda'$  are equivalent,

$$\begin{aligned} C_{\lambda,m,n}^\dagger \mathcal{S}_{\lambda\lambda'} C_{\lambda',m,n} &= \sum_{\kappa,\kappa'} \sum_{k_i, k'_i, \bar{k}_i, \bar{k}'_i} \left\{ |q_1, k_1\rangle \dots |\bar{q}_n, \bar{k}_n\rangle \mathfrak{C}_{\lambda\kappa; q_1 \dots m k_1 \dots m \bar{q}_1 \dots n \bar{k}_1 \dots n} \times \right. \\ &\quad \left. \times \underbrace{\langle \lambda, \kappa | \mathcal{S}_{\lambda\lambda'} | \lambda', \kappa' \rangle}_{\delta_{\kappa\kappa'}} \mathfrak{C}_{\lambda'\kappa'; q'_1 \dots m k'_1 \dots m \bar{q}'_1 \dots n \bar{k}'_1 \dots n} \langle q'_1, k'_1 | \dots \langle \bar{q}'_n, \bar{k}'_n | \right\} , \end{aligned} \quad (5.57)$$

where we assume the basis choice (5.55) in the last step.

<sup>10</sup>Note that projecting out the matrix elements only makes sense if the basis states are orthonormal, since the underlying procedure is a spectral decomposition of  $U$ .

In birdtrack notation, the product (5.57) is written as <sup>11</sup>

$$C_{\lambda,m,n}^\dagger \mathcal{S}_{\lambda\lambda'} C_{\lambda',m,n} = \begin{array}{c} \text{---} \\ \text{---} \\ \text{---} \\ \text{---} \\ \text{---} \\ \text{---} \\ \text{---} \\ \text{---} \\ \text{---} \\ \text{---} \\ \text{---} \\ \text{---} \end{array} \begin{array}{c} \lambda \\ \lambda' \end{array} \begin{array}{c} \text{---} \\ \text{---} \\ \text{---} \\ \text{---} \\ \text{---} \\ \text{---} \\ \text{---} \\ \text{---} \\ \text{---} \\ \text{---} \\ \text{---} \\ \text{---} \end{array}, \quad (5.58)$$

where  $\delta_{\kappa\kappa'}$  (which is the Kronecker  $\delta$  in the representation  $\lambda$  or, equivalently,  $\lambda'$ ) is explicitly visible,

$$\delta_{\kappa\kappa'} = \kappa \longleftarrow \kappa', \quad (5.59)$$

and thus the map  $\mathcal{S}_{\lambda\lambda'}$  is invisible in the birdtrack formulation. For this reason, displaying  $\mathcal{S}_{\lambda\lambda'}$  on the left-hand side of eq. (5.58) might seem unnecessary, but can be useful as a reminder that we connect different vector spaces  $V_{(\lambda)}$  and  $V_{(\lambda')}$ . Since the Clebsch-Gordan operators  $C_{\lambda,m,n}$  satisfy eqns. (5.52), products of the form  $C_{\lambda,m,n}^\dagger \mathcal{S}_{\lambda\lambda'} C_{\lambda',m,n}$  are explicitly invariant under a global transformation of  $SU(N)$ ,

$$\begin{array}{c} U \\ U \\ U^\dagger \\ U^\dagger \end{array} \begin{array}{c} \lambda \\ \lambda' \end{array} \begin{array}{c} U^\dagger \\ U^\dagger \\ U \\ U \end{array} = \begin{array}{c} \text{---} \\ \text{---} \\ \text{---} \\ \text{---} \\ \text{---} \\ \text{---} \\ \text{---} \\ \text{---} \\ \text{---} \\ \text{---} \\ \text{---} \\ \text{---} \end{array} \begin{array}{c} \lambda \\ \lambda' \end{array} \begin{array}{c} \text{---} \\ \text{---} \\ \text{---} \\ \text{---} \\ \text{---} \\ \text{---} \\ \text{---} \\ \text{---} \\ \text{---} \\ \text{---} \\ \text{---} \\ \text{---} \end{array} \stackrel{\text{eq. (5.56)}}{=} \begin{array}{c} \text{---} \\ \text{---} \\ \text{---} \\ \text{---} \\ \text{---} \\ \text{---} \\ \text{---} \\ \text{---} \\ \text{---} \\ \text{---} \\ \text{---} \\ \text{---} \end{array} \begin{array}{c} \lambda \\ \lambda' \end{array} \begin{array}{c} \text{---} \\ \text{---} \\ \text{---} \\ \text{---} \\ \text{---} \\ \text{---} \\ \text{---} \\ \text{---} \\ \text{---} \\ \text{---} \\ \text{---} \\ \text{---} \end{array}. \quad (5.60)$$

In other words, all products  $C_{\lambda,m,n}^\dagger \mathcal{S}_{\lambda\lambda'} C_{\lambda',m,n}$  are elements of the algebra of invariants  $\text{API}(SU(N), V^{\otimes m} \otimes (V^*)^{\otimes n})$ . This discussion covers both transition and projection operators, the latter arising from the special case that  $V_{(\lambda)} = V_{(\lambda')}$ , so that  $\mathcal{S}_{\lambda\lambda'}$  is the identity map from the outset. For the further discussion, we nevertheless distinguish projection and transition operators notationally,

$$\textbf{Projection ops. } (\lambda = \lambda'): \quad P_\lambda := \sum_{\kappa} |\lambda, \kappa\rangle \langle \lambda, \kappa| = C_{\lambda,m,n}^\dagger \mathcal{S}_{\lambda\lambda} C_{\lambda,m,n} = \begin{array}{c} \text{---} \\ \text{---} \\ \text{---} \\ \text{---} \\ \text{---} \\ \text{---} \\ \text{---} \\ \text{---} \\ \text{---} \\ \text{---} \\ \text{---} \\ \text{---} \end{array} \begin{array}{c} \lambda \\ \lambda \end{array} \begin{array}{c} \text{---} \\ \text{---} \\ \text{---} \\ \text{---} \\ \text{---} \\ \text{---} \\ \text{---} \\ \text{---} \\ \text{---} \\ \text{---} \\ \text{---} \\ \text{---} \end{array} \quad (5.61a)$$

$$\textbf{Transition ops. } (\lambda \neq \lambda'): \quad T_{\lambda\lambda'} := \sum_{\kappa} |\lambda, \kappa\rangle \langle \lambda', \kappa| = C_{\lambda,m,n}^\dagger \mathcal{S}_{\lambda\lambda'} C_{\lambda',m,n} = \begin{array}{c} \text{---} \\ \text{---} \\ \text{---} \\ \text{---} \\ \text{---} \\ \text{---} \\ \text{---} \\ \text{---} \\ \text{---} \\ \text{---} \\ \text{---} \\ \text{---} \end{array} \begin{array}{c} \lambda \\ \lambda' \end{array} \begin{array}{c} \text{---} \\ \text{---} \\ \text{---} \\ \text{---} \\ \text{---} \\ \text{---} \\ \text{---} \\ \text{---} \\ \text{---} \\ \text{---} \\ \text{---} \\ \text{---} \end{array}. \quad (5.61b)$$

This combined set of operators satisfies

$$P_\lambda P_{\lambda'} = \delta_{\lambda\lambda'} P_\lambda \quad (5.62)$$

and

$$T_{\lambda\lambda'} P_{\lambda'} = T_{\lambda\lambda'} = P_\lambda T_{\lambda\lambda'} \quad (5.63a)$$

$$T_{\lambda\lambda'}^\dagger = T_{\lambda'\lambda} \quad (5.63b)$$

$$T_{\lambda\lambda'} T_{\lambda'\lambda} = P_\lambda; \quad (5.63c)$$

these properties are a consequence of the orthogonality of Clebsch-Gordan operators eq. (5.52b). Unlike the

<sup>11</sup>In the birdtrack spirit, the Hermitian conjugate of a Clebsch-Gordan operator is obtained by flipping it about the vertical axis and reversing the arrows [72],  $C_{\lambda,m,n}^\dagger := \begin{array}{c} \text{---} \\ \text{---} \\ \text{---} \\ \text{---} \\ \text{---} \\ \text{---} \\ \text{---} \\ \text{---} \\ \text{---} \\ \text{---} \\ \text{---} \\ \text{---} \end{array} \begin{array}{c} \lambda \end{array} \longleftarrow$ , c.f. section 3.3.1.

projection operators  $P_\lambda$ , the transition operators  $T_{\lambda\lambda'}$  are clearly not Hermitian. However, unitarity follows immediately from their definition in terms of the Clebsch-Gordan states (5.61b),

$$(T_{\lambda'\lambda})^\dagger = T_{\lambda\lambda'} . \quad (5.64)$$

These operators in fact represent the isomorphisms  $\mathcal{S}_{\lambda\lambda'}$  that, in the standard perspective, allow us to claim equivalence between the two representations in the first place. Our point here is that these isomorphisms are elements of the algebra of invariants  $\text{API}\left(\text{SU}(N), V^{\otimes m} \otimes (V^*)^{\otimes n}\right)$ .

By their very definition, the Clebsch-Gordan operators give a *complete set of states* translating the product representation into the representation  $\lambda$  (see, for example, [93, Thm. 3.12]). Furthermore, the totality of all projection and transition operators, eqns. (5.61), gives all nonzero combinations of Clebsch-Gordan operators of the form  $C_{\lambda,m,n}^\dagger \mathcal{S}_{\lambda\lambda'} C_{\lambda',m,n} : V^{\otimes m} \otimes (V^*)^{\otimes n} \rightarrow V^{\otimes m} \otimes (V^*)^{\otimes n}$ . Since these are necessarily invariants of  $\text{SU}(N)$ , **the projection and transition operators exhaust the algebra of invariants and thus constitute a basis for  $\text{API}\left(\text{SU}(N), V^{\otimes m} \otimes (V^*)^{\otimes n}\right)$ .**

### 5.2.1.3 Singlet projectors and transition operators over $V^{\otimes k} \otimes (V^*)^{\otimes k}$ from Clebsch-Gordan operators

We begin this section with an analysis of singlet projectors in the birdtrack language, which will ultimately inspire the general construction algorithm.

In this chapter, “singlet projector” is the name given to an operator that projects onto a 1-dimensional representation of the special unitary group  $\text{SU}(N)$  (*c.f.* [27]). It will be convenient to begin our exposition of the singlet representations of  $\text{SU}(N)$  with the 1-dimensional representations of the unitary group  $\text{U}(N)$  (of which  $\text{SU}(N)$  is a subgroup).

In general, a particular  $n$ -dimensional representation  $\mathcal{R}_{\lambda,n}$  of  $\text{U}(N)$  specifies a group homomorphism  $\pi_{\lambda,n}$  from  $\text{U}(N)$  to the general linear group acting on an  $n$ -dimensional vector space  $V^n$ ,

$$\pi_{\lambda,n} : \text{U}(N) \longrightarrow \text{GL}(V^n) ; \quad (5.65)$$

in this chapter, we will always take  $V = \mathbb{C}$ . Thus, if  $\mathcal{R}_{\lambda,1}$  is a singlet representation,  $\pi_{\lambda,1}$  is a homomorphism into  $\text{GL}(\mathbb{C})$ . Furthermore, since it is a *group* homomorphism,  $\text{U}(N)$  will be mapped to unitary elements in  $\text{GL}(\mathbb{C})$ . These lie along the unit circle,

$$\pi_{\lambda,1} : \text{U}(N) \longrightarrow \text{GL}(\mathbb{C}) \quad (5.66a)$$

$$U \mapsto e^{i\phi(U)} , \quad (5.66b)$$

where the scalars  $\phi(U)$ , giving the phase of the unit circle, depend on the group elements  $U$ .

To restrict the singlet representation (5.66) to the *special* unitary group  $\text{SU}(N) \subset \text{U}(N)$ , the determinant condition  $\det(U) \stackrel{!}{=} 1$  (making  $\text{SU}(N)$  “special”) also has to be satisfied by the elements  $\pi_{\lambda,1}(U)$ , yielding

$$\det(\pi_{\lambda,1}(U)) = \det\left(e^{i\phi(U)}\right) \stackrel{!}{=} 1 \implies \phi(U) = 0 . \quad (5.67)$$



Hence, in a singlet representation, the elements of  $SU(N)$  get mapped to unity,

$$U \xrightarrow{\text{singlet rep.}} 1 . \quad (5.68)$$

What does this mean for a Clebsch-Gordan operator projecting onto a singlet representation in the birdtrack language? In general, we have relation (5.52a)

$$\begin{array}{c} u \\ \vdots \\ u \\ U^\dagger \\ \vdots \\ u^\dagger \end{array} \left\langle \lambda \right\rangle \leftarrow = \left\langle \lambda \right\rangle \leftarrow U_{(\lambda)} . \quad (5.69)$$

If  $\lambda$  corresponds to a singlet representation  $\mathcal{R}_{\lambda,1}$  of  $SU(N)$ , then  $U_{(\lambda)} = 1$ , according to eq. (5.68). In particular, the scalar  $U_{(\lambda)} = 1$  does not carry an index and therefore neither does the “index line”  $\leftarrow$  representing a Kronecker- $\delta$  in the representation  $\mathcal{R}_{\lambda,1}$ ,  $\delta_{ij} \xrightarrow{\mathcal{R}_{\lambda,1}} 1$ . This allows us to omit  $\leftarrow$  altogether,

$$\begin{array}{c} u \\ \vdots \\ u \\ U^\dagger \\ \vdots \\ u^\dagger \end{array} \left\langle \lambda \right\rangle = \begin{array}{c} \vdots \\ \vdots \\ \vdots \end{array} \left\langle \lambda \right\rangle \cdot 1 = \begin{array}{c} \vdots \\ \vdots \\ \vdots \end{array} \left\langle \lambda \right\rangle . \quad (5.70)$$

Eq. (5.70) recovers the defining condition (1.223) of a singlet state,

$$\mathbf{U}|\phi_\lambda^S\rangle = |\phi_\lambda^S\rangle \quad \text{and} \quad \langle \phi_\lambda^S | \mathbf{U}^\dagger = \langle \phi_\lambda^S | , \quad (5.71)$$

where  $\mathbf{U} = U \otimes \dots \otimes U \otimes U^\dagger \otimes \dots \otimes U^\dagger$  and

$$|\phi_\lambda^S\rangle := \begin{array}{c} \vdots \\ \vdots \\ \vdots \end{array} \left\langle \lambda \right\rangle . \quad (5.72)$$

Furthermore, eq. (5.70) teaches us that a projection operator constructed from Clebsch-Gordan operators (*c.f.* eq. (5.61a)) corresponding to singlet representations will take the graphical form

$$\begin{array}{c} \vdots \\ \vdots \\ \vdots \end{array} \left\langle \lambda \right\rangle \left\langle \lambda \right\rangle , \quad (5.73)$$

with the key feature that *no index line passes through the middle*. This characteristic graphical property of a singlet projection operator can also be concluded in a different way:

The *dimension of the irreducible representation of  $SU(N)$  over  $V^{\otimes m} \otimes (V^*)^{\otimes n}$*  corresponding to the projection operator  $P_\lambda$  is given by the trace of  $P_\lambda$  (see, for example, [72] for a textbook exposition): Suppose  $P_\lambda$  corresponds to a  $d$ -dimensional representation of  $SU(N)$ . One may always choose a basis such that  $P_\lambda$  is given by a  $(m+n) \times (m+n)$  matrix with 1 on the diagonal of the  $d \times d$  sub-block onto which  $P_\lambda$  projects, and zeros everywhere else. In this basis, it is easily seen that the trace of  $P_\lambda$  is  $d$ ,  $\text{tr}(P_\lambda) = d$ . Since the trace of an operator is basis-independent, it follows that the trace of  $P_\lambda$  gives the dimension of the irreducible representation of  $SU(N)$  corresponding to  $P_\lambda$  in any basis. Hence

$$d = \text{tr}(P_\lambda) = \sum_{\kappa} \text{tr}(|\lambda, \kappa\rangle \langle \lambda, \kappa|) = \sum_{\kappa} \langle \lambda, \kappa | \lambda, \kappa \rangle = |\{\kappa\}| , \quad (5.74)$$

where the second equality originates from tracing  $P_\lambda$  as given in (5.61a), and  $|\{\kappa\}|$  is the size of the set of states  $\{\kappa\}$  over which  $\kappa$  is summed. If we consider  $\lambda$  to correspond to a singlet representation  $\mathcal{R}_{\lambda,1}$  of  $SU(N)$  (that is,  $d = 1$ ), it follows that  $|\{\kappa\}| = 1$ , which implies that the set  $\{\kappa\}$  contains one element. Hence, no sum over the index  $\kappa$  takes place, and the Kronecker  $\delta$   $\longleftarrow$  in the representation  $\lambda$  inducing the sum may be omitted [72],

$$(5.75)$$

Hence, we have once again arrived at the conclusion that, in the birdtrack sense, a singlet projection operator is visually characterized by an operator with no index lines crossing through the middle (*c.f.* eq. (5.73)).

This observation motivates a graphical construction of singlet states  $|\phi^S\rangle$  of  $SU(N)$  over  $V^{\otimes(m+n)} \otimes (V^*)^{\otimes(m+n)}$  via *reshaping* the projection and transition operators, eqns. (5.61), over  $V^{\otimes m} \otimes (V^*)^{\otimes n}$  (see the following eq. (5.76)), as then the singlet projection operators  $|\phi^S\rangle\langle\phi^S|$  will not have any index lines passing through the middle (*c.f.* eq. (5.84)): Starting from an operator  $T_{\lambda\lambda'}$ <sup>12</sup> and labelling the fundamental lines as  $q, p$  and the antifundamental lines as  $\bar{q}, \bar{p}$  for clarity, we obtain the following state

$$(5.76)$$

Due to the reshaping process the quark lines  $q_1 \dots q_m$  have become antiquark lines, and similarly the antiquark lines  $\bar{q}_1 \dots \bar{q}_n$  have become quark lines in that their transformation behaviour changed: We call a Kronecker  $\delta$  a quark line if we can interpret it as the unit operator in  $\text{Lin}(V)$ , and thus transforms under the associated representation:

$$\text{quark line: } U \longleftarrow U^\dagger = \longleftarrow \in \text{Lin}(V) . \quad (5.77a)$$

Similarly, an antiquark line is a Kronecker  $\delta$  that acts as a the unit operator in  $\text{Lin}(V^*)$  and transforms accordingly as

$$\text{antiquark line: } U^\dagger \longrightarrow U = \longrightarrow \in \text{Lin}(V^*) . \quad (5.77b)$$

The arrow on the index line indicates which transformation behaviour the Kronecker  $\delta$  obeys. Consistently, we interpret  $\curvearrowright$  as an element in  $V \otimes V^*$ , and  $\curvearrowleft$  as an element in  $V^* \otimes V$ , transforming under the associated product representations as invariants,

$$\begin{matrix} U \\ U^\dagger \end{matrix} \curvearrowright = \curvearrowright \in V \otimes V^* \quad (5.78a)$$

$$\begin{matrix} U^\dagger \\ U \end{matrix} \curvearrowleft = \curvearrowleft \in V^* \otimes V . \quad (5.78b)$$

<sup>12</sup>We allow for  $\lambda$  and  $\lambda'$  to be equal,  $T_{\lambda\lambda'} \xrightarrow{\lambda=\lambda'} P_\lambda$ .

This obviously generalizes to the products appearing in the Clebsch-Gordan constructions of eq. (5.76). In this sense, the index lines  $q_1 \dots q_m$  transformed as quark lines in the operators  $T_{\lambda\lambda'}$  but now transform as antiquark lines after the reshaping procedure, and similarly for the index lines labelled  $\bar{q}_1 \dots \bar{q}_n$ .

In summary, the states (5.76) take in the quark lines  $\{p_1, \dots, p_m, \bar{q}_n, \dots, \bar{q}_1\}$  (a total of  $m+n$  quark lines) and the antiquark lines  $\{\bar{p}_1, \dots, \bar{p}_n, q_m, \dots, q_1\}$  (a total of  $n+m$  antiquark lines), and are therefore elements in  $V^{\otimes(m+n)} \otimes (V^*)^{\otimes(m+n)}$ . It immediately follows from eq. (5.60) that the states  $|\phi_{\lambda\lambda'}^S\rangle$  are also *singlet states* in that they satisfy eq. (5.71),

$$\mathbf{U}|\phi_{\lambda\lambda'}^S\rangle = |\phi_{\lambda\lambda'}^S\rangle \quad \text{and} \quad \langle\phi_{\lambda\lambda'}^S|\mathbf{U}^\dagger = \langle\phi_{\lambda\lambda'}^S|, \quad (5.79)$$

where  $\mathbf{U}$  is an appropriate tensor product of  $U, U^\dagger \in SU(N)$ . Lastly, by the completeness of Clebsch-Gordan operators [93], the construction (5.76) exhausts all possible singlet states of  $SU(N)$  over  $V^{\otimes(m+n)} \otimes (V^*)^{\otimes(m+n)}$ , and thus spans the algebra of singlet states.

The singlet states (5.76) can be used to construct the projection operator  $P_{\lambda\lambda'}^S$  (which lies in the algebra of invariants  $\text{API}\left(SU(N), V^{\otimes(m+n)} \otimes (V^*)^{\otimes(m+n)}\right)$ ) as

$$P_{\lambda\lambda'}^S := |\phi_{\lambda\lambda'}^S\rangle\langle\phi_{\lambda\lambda'}^S| = \beta_{\lambda\lambda'} \cdot \begin{array}{c} \text{---} \lambda \text{---} \\ \diagdown \quad \diagup \\ \text{---} \lambda' \text{---} \end{array} \cdot \begin{array}{c} \text{---} \lambda \text{---} \\ \diagup \quad \diagdown \\ \text{---} \lambda' \text{---} \end{array}, \quad \beta_{\lambda\lambda'} \text{ is a constant.} \quad (5.80)$$

The operators (5.80) are *singlet projectors*, as they satisfy

$$\mathbf{U} \cdot P_{\lambda\lambda'}^S = P_{\lambda\lambda'}^S = P_{\lambda\lambda'}^S \cdot \mathbf{U}^\dagger; \quad (5.81)$$

this is an immediate consequence of eq. (5.79). The requirement that  $P_{\lambda\lambda'}^S$  be a projection operator

$$P_{\lambda\lambda'}^S \cdot P_{\lambda\lambda'}^S \stackrel{!}{=} P_{\lambda\lambda'}^S \quad (5.82)$$

fixes the constant  $\beta_{\lambda\lambda'}$ :

$$P_{\lambda\lambda'}^S \cdot P_{\lambda\lambda'}^S = \beta_{\lambda\lambda'}^2 \cdot \begin{array}{c} \text{---} \lambda \text{---} \\ \diagdown \quad \diagup \\ \text{---} \lambda' \text{---} \end{array} \cdot \begin{array}{c} \text{---} \lambda \text{---} \\ \diagup \quad \diagdown \\ \text{---} \lambda' \text{---} \end{array} \cdot \begin{array}{c} \text{---} \lambda \text{---} \\ \diagdown \quad \diagup \\ \text{---} \lambda' \text{---} \end{array} = \beta_{\lambda\lambda'}^2 \cdot \begin{array}{c} \text{---} \lambda \text{---} \\ \diagdown \quad \diagup \\ \text{---} \lambda' \text{---} \end{array} \cdot \begin{array}{c} \text{---} \lambda \text{---} \\ \diagup \quad \diagdown \\ \text{---} \lambda' \text{---} \end{array} \stackrel{!}{=} \beta_{\lambda\lambda'} \cdot \begin{array}{c} \text{---} \lambda \text{---} \\ \diagdown \quad \diagup \\ \text{---} \lambda' \text{---} \end{array} \quad (5.83)$$

such that

$$P_{\lambda\lambda'}^S := \beta_{\lambda\lambda'} \cdot \begin{array}{c} \text{---} \lambda \text{---} \\ \diagdown \quad \diagup \\ \text{---} \lambda' \text{---} \end{array}, \quad \text{where} \quad \beta_{\lambda\lambda'} := \left( \begin{array}{c} \text{---} \lambda \text{---} \\ \diagdown \quad \diagup \\ \text{---} \lambda' \text{---} \end{array} \right)^{-1}. \quad (5.84)$$

Noticing that a trace of birdtrack operators is realized by connecting index lines on the same level [72],

$$\rho = \begin{array}{c} \leftarrow \rightarrow \\ \leftarrow \rightarrow \\ \leftarrow \rightarrow \\ \leftarrow \rightarrow \\ \leftarrow \rightarrow \\ \leftarrow \rightarrow \\ \leftarrow \rightarrow \\ \leftarrow \rightarrow \\ \leftarrow \rightarrow \\ \leftarrow \rightarrow \end{array} \rho \rightarrow \text{tr}(\rho) := \begin{array}{c} \circlearrowleft \\ \circlearrowright \\ \rho \end{array}, \quad (5.85)$$

it follows that

$$\beta_{\lambda\lambda'} = \left( \begin{array}{c} \leftarrow \rightarrow \\ \leftarrow \rightarrow \\ \leftarrow \rightarrow \\ \leftarrow \rightarrow \\ \leftarrow \rightarrow \\ \leftarrow \rightarrow \\ \leftarrow \rightarrow \\ \leftarrow \rightarrow \\ \leftarrow \rightarrow \\ \leftarrow \rightarrow \end{array} \begin{array}{c} \lambda \\ \lambda \\ \lambda \\ \lambda \\ \lambda \\ \lambda \\ \lambda \\ \lambda \\ \lambda \\ \lambda \end{array} \begin{array}{c} \leftarrow \rightarrow \\ \leftarrow \rightarrow \\ \leftarrow \rightarrow \\ \leftarrow \rightarrow \\ \leftarrow \rightarrow \\ \leftarrow \rightarrow \\ \leftarrow \rightarrow \\ \leftarrow \rightarrow \\ \leftarrow \rightarrow \\ \leftarrow \rightarrow \end{array} \begin{array}{c} \lambda \\ \lambda \\ \lambda \\ \lambda \\ \lambda \\ \lambda \\ \lambda \\ \lambda \\ \lambda \\ \lambda \end{array} \right)^{-1} = \left[ \text{tr} \left( \begin{array}{c} \leftarrow \rightarrow \\ \leftarrow \rightarrow \\ \leftarrow \rightarrow \\ \leftarrow \rightarrow \\ \leftarrow \rightarrow \\ \leftarrow \rightarrow \\ \leftarrow \rightarrow \\ \leftarrow \rightarrow \\ \leftarrow \rightarrow \\ \leftarrow \rightarrow \end{array} \begin{array}{c} \lambda \\ \lambda \\ \lambda \\ \lambda \\ \lambda \\ \lambda \\ \lambda \\ \lambda \\ \lambda \\ \lambda \end{array} \begin{array}{c} \leftarrow \rightarrow \\ \leftarrow \rightarrow \\ \leftarrow \rightarrow \\ \leftarrow \rightarrow \\ \leftarrow \rightarrow \\ \leftarrow \rightarrow \\ \leftarrow \rightarrow \\ \leftarrow \rightarrow \\ \leftarrow \rightarrow \\ \leftarrow \rightarrow \end{array} \begin{array}{c} \lambda \\ \lambda \\ \lambda \\ \lambda \\ \lambda \\ \lambda \\ \lambda \\ \lambda \\ \lambda \\ \lambda \end{array} \right) \right]^{-1}. \quad (5.86)$$

With this value of  $\beta_{\lambda\lambda'}$  it becomes clear that the trace of  $P_{\lambda\lambda'}^S$  is 1:

$$\text{tr}(P_{\lambda\lambda'}^S) = \beta_{\lambda\lambda'} \cdot \text{tr} \left( \begin{array}{c} \leftarrow \rightarrow \\ \leftarrow \rightarrow \\ \leftarrow \rightarrow \\ \leftarrow \rightarrow \\ \leftarrow \rightarrow \\ \leftarrow \rightarrow \\ \leftarrow \rightarrow \\ \leftarrow \rightarrow \\ \leftarrow \rightarrow \\ \leftarrow \rightarrow \end{array} \begin{array}{c} \lambda \\ \lambda \\ \lambda \\ \lambda \\ \lambda \\ \lambda \\ \lambda \\ \lambda \\ \lambda \\ \lambda \end{array} \begin{array}{c} \leftarrow \rightarrow \\ \leftarrow \rightarrow \\ \leftarrow \rightarrow \\ \leftarrow \rightarrow \\ \leftarrow \rightarrow \\ \leftarrow \rightarrow \\ \leftarrow \rightarrow \\ \leftarrow \rightarrow \\ \leftarrow \rightarrow \\ \leftarrow \rightarrow \end{array} \begin{array}{c} \lambda \\ \lambda \\ \lambda \\ \lambda \\ \lambda \\ \lambda \\ \lambda \\ \lambda \\ \lambda \\ \lambda \end{array} \right) = 1, \quad (5.87)$$

once again confirming that  $P_{\lambda\lambda'}^S$  corresponds to a singlet representation of  $\text{SU}(N)$ . At this point, we want to emphasize that we have not chosen  $\beta_{\lambda\lambda'}$  such that  $\text{tr}(P_{\lambda\lambda'}^S) = 1$ , but rather so that the idempotency property  $P_{\lambda\lambda'}^S \cdot P_{\lambda\lambda'}^S = P_{\lambda\lambda'}^S$  is satisfied; while it is always possible to force the trace of a projection operator  $O$  to 1 by fixing its normalization constant, this constant may not be the correct one for rendering  $O$  idempotent.

The projection operators constructed in this way are clearly orthonormal from eq. (5.52b). Furthermore, we note that we have not fixed  $\dim(V) = N$  to a particular value in our considerations so far, but have rather kept it as a parameter. Thus, the projector (5.84) is a singlet *independently* of  $N$ .

Lastly, we notice that the singlet projection operators (5.84) all correspond to *equivalent* irreducible representations of  $\text{SU}(N)$  since we can explicitly construct the transition operators between them: Consider two singlet projection operators

$$P_{\lambda\lambda'}^S = \beta_{\lambda\lambda'} \cdot \begin{array}{c} \leftarrow \rightarrow \\ \leftarrow \rightarrow \\ \leftarrow \rightarrow \\ \leftarrow \rightarrow \\ \leftarrow \rightarrow \\ \leftarrow \rightarrow \\ \leftarrow \rightarrow \\ \leftarrow \rightarrow \\ \leftarrow \rightarrow \\ \leftarrow \rightarrow \end{array} \begin{array}{c} \lambda \\ \lambda \\ \lambda \\ \lambda \\ \lambda \\ \lambda \\ \lambda \\ \lambda \\ \lambda \\ \lambda \end{array} \begin{array}{c} \leftarrow \rightarrow \\ \leftarrow \rightarrow \\ \leftarrow \rightarrow \\ \leftarrow \rightarrow \\ \leftarrow \rightarrow \\ \leftarrow \rightarrow \\ \leftarrow \rightarrow \\ \leftarrow \rightarrow \\ \leftarrow \rightarrow \\ \leftarrow \rightarrow \end{array} \begin{array}{c} \lambda \\ \lambda \\ \lambda \\ \lambda \\ \lambda \\ \lambda \\ \lambda \\ \lambda \\ \lambda \\ \lambda \end{array} \quad \text{and} \quad P_{\xi\xi'}^S = \beta_{\xi\xi'} \cdot \begin{array}{c} \leftarrow \rightarrow \\ \leftarrow \rightarrow \\ \leftarrow \rightarrow \\ \leftarrow \rightarrow \\ \leftarrow \rightarrow \\ \leftarrow \rightarrow \\ \leftarrow \rightarrow \\ \leftarrow \rightarrow \\ \leftarrow \rightarrow \\ \leftarrow \rightarrow \end{array} \begin{array}{c} \xi \\ \xi \\ \xi \\ \xi \\ \xi \\ \xi \\ \xi \\ \xi \\ \xi \\ \xi \end{array} \begin{array}{c} \leftarrow \rightarrow \\ \leftarrow \rightarrow \\ \leftarrow \rightarrow \\ \leftarrow \rightarrow \\ \leftarrow \rightarrow \\ \leftarrow \rightarrow \\ \leftarrow \rightarrow \\ \leftarrow \rightarrow \\ \leftarrow \rightarrow \\ \leftarrow \rightarrow \end{array} \begin{array}{c} \xi \\ \xi \\ \xi \\ \xi \\ \xi \\ \xi \\ \xi \\ \xi \\ \xi \\ \xi \end{array}, \quad (5.88)$$

where  $\beta_{\lambda\lambda'}$  and  $\beta_{\xi\xi'}$  are defined according to eq. (5.86). The object  $T_{\lambda\lambda',\xi\xi'}^S$  defined as

$$T_{\lambda\lambda',\xi\xi'}^S := \sqrt{\beta_{\lambda\lambda'}\beta_{\xi\xi'}} \cdot \begin{array}{c} \leftarrow \rightarrow \\ \leftarrow \rightarrow \\ \leftarrow \rightarrow \\ \leftarrow \rightarrow \\ \leftarrow \rightarrow \\ \leftarrow \rightarrow \\ \leftarrow \rightarrow \\ \leftarrow \rightarrow \\ \leftarrow \rightarrow \\ \leftarrow \rightarrow \end{array} \begin{array}{c} \lambda \\ \lambda \\ \lambda \\ \lambda \\ \lambda \\ \lambda \\ \lambda \\ \lambda \\ \lambda \\ \lambda \end{array} \begin{array}{c} \leftarrow \rightarrow \\ \leftarrow \rightarrow \\ \leftarrow \rightarrow \\ \leftarrow \rightarrow \\ \leftarrow \rightarrow \\ \leftarrow \rightarrow \\ \leftarrow \rightarrow \\ \leftarrow \rightarrow \\ \leftarrow \rightarrow \\ \leftarrow \rightarrow \end{array} \begin{array}{c} \xi \\ \xi \\ \xi \\ \xi \\ \xi \\ \xi \\ \xi \\ \xi \\ \xi \\ \xi \end{array} \begin{array}{c} \leftarrow \rightarrow \\ \leftarrow \rightarrow \\ \leftarrow \rightarrow \\ \leftarrow \rightarrow \\ \leftarrow \rightarrow \\ \leftarrow \rightarrow \\ \leftarrow \rightarrow \\ \leftarrow \rightarrow \\ \leftarrow \rightarrow \\ \leftarrow \rightarrow \end{array} \begin{array}{c} \xi \\ \xi \\ \xi \\ \xi \\ \xi \\ \xi \\ \xi \\ \xi \\ \xi \\ \xi \end{array}, \quad (5.89)$$

is the unique transition operator between  $P_{\lambda\lambda'}^S$  and  $P_{\xi\xi'}^S$  as it satisfies the defining properties of transition operators (*c.f.* eqns. (5.63))

$$T_{\lambda\lambda',\xi\xi'}^S \cdot P_{\xi\xi'}^S = T_{\lambda\lambda',\xi\xi'}^S = P_{\lambda\lambda'}^S \cdot T_{\lambda\lambda',\xi\xi'}^S \quad (5.90a)$$

$$(T_{\lambda\lambda',\xi\xi'}^S)^\dagger = T_{\xi\xi',\lambda\lambda'}^S \quad (5.90b)$$

$$T_{\lambda\lambda',\xi\xi'}^S \cdot T_{\xi\xi',\lambda\lambda'}^S = P_{\lambda\lambda'}^S ; \quad (5.90c)$$

this is an immediate consequence of eq. (5.52b). We thus conclude that all singlet projection operators constructed according to (5.84) correspond to equivalent irreducible representations of  $SU(N)$  over  $V^{\otimes(m+n)} \otimes (V^*)^{\otimes(m+n)}$ .

#### 5.2.1.4 Constructing singlet projectors over $V^{\otimes k} \otimes (V^*)^{\otimes k}$ from the projector basis $\mathfrak{S}_k$

In the previous section, we constructed the singlet states of  $SU(N)$  over  $V^{\otimes k} \otimes (V^*)^{\otimes k}$  (where  $k = m + n$ ) by reshaping the Clebsch-Gordan projection (5.61a) and transition (5.61b) operators, *c.f.* eq. (5.76). While the reshaping process itself is very simple and thus ideal for practical applications, these singlet states have one major drawback: one first needs to construct all states over  $V^{\otimes m} \otimes (V^*)^{\otimes n}$  in order to build all Clebsch-Gordan operators to then form the transition and projection operators that will eventually be reshaped into singlet states — a cumbersome and time-consuming task. Thus, in order to make the construction method (5.76) practical, we need to find an alternative to the Clebsch-Gordan operators:

It is important to note that, had we started out with the Clebsch-Gordan operators over a total of  $(m + n)$  particles split into quarks and antiquarks in some other way, we would have obtained equivalent singlet states, which can be made into the states (5.76) by essentially reordering the (anti-) fundamental lines. In particular, this holds for Clebsch-Gordan operators taking in  $k = m + n$  fundamental lines only,

$$C_{\lambda,(m+n)} := \left\langle \begin{array}{c} \lambda \\ \vdots \\ \lambda \end{array} \right\rangle, \quad (5.91)$$

since clearly

$$P_{\lambda\lambda'}^S := \beta_{\lambda\lambda'} \cdot \left( \begin{array}{c} \lambda \\ \vdots \\ \lambda' \end{array} \right) \left( \begin{array}{c} \lambda \\ \vdots \\ \lambda' \end{array} \right) \quad \text{where} \quad \beta_{\lambda\lambda'} := \left( \begin{array}{c} \lambda \\ \vdots \\ \lambda' \end{array} \right)^{-1} \quad (5.92)$$

is a singlet projection operator of  $SU(N)$  over  $V^{\otimes k} \otimes (V^*)^{\otimes k}$ . It should be noted that the algebras of invariants  $\text{API}(SU(N), V^{\otimes m} \otimes (V^*)^{\otimes n})$  and  $\text{API}(SU(N), V^{\otimes(m+n)} = V^{\otimes k})$  have the same size basis, since their bases in terms of primitive invariants are in 1-to-1 correspondence, *c.f.* “swapping fundamental for antifundamental lines” on page 217.

This observation does not seem like a breakthrough yet, as we are still required to construct the Clebsch-Gordan operators in order to arrive at the desired singlet states. However, since the projection and transition operators of  $SU(N)$  over  $V^{\otimes k}$  form a basis for  $\text{API}(SU(N), V^{\otimes k})$ , a different basis will also provide all singlet projection operators over  $V^{\otimes k} \otimes (V^*)^{\otimes k}$  via the reshaping process. Furthermore, we know that the basis of  $\text{API}(SU(N), V^{\otimes k})$  has size  $k!$  and thus gives rise to exactly  $k!$  distinct singlet states.

In section 4.3.2, we showed that the algebra of invariants  $\text{API}(SU(N), V^{\otimes k})$  is spanned by the MOLD operators (*c.f.* Theorem 3.5) and their corresponding transition operators (*c.f.* Theorem 4.5). The algorithm used to construct these operators is very efficient and easily implementable on a computer. Thus, bending

these operators will provide us with a *computationally inexpensive* way of constructing the singlet states and corresponding projection operators of  $SU(N)$  over  $V^{\otimes k} \otimes (V^*)^{\otimes k}$ :

Let  $\mathfrak{S}_k$  denote the set of all MOLD projection and transition operators (*c.f.* section 4.3.2). We arrange the elements of  $\mathfrak{S}_k$  in a matrix  $\mathfrak{M}_k$  where the diagonal elements  $\mathfrak{m}_{ii}$  are the Hermitian projection operators, and the off-diagonal elements  $\mathfrak{m}_{ij}$  are the transition operators between  $\mathfrak{m}_{ii}$  and  $\mathfrak{m}_{jj}$ ; this will yield a block-diagonal matrix where each block corresponds to a set of equivalent representations  $\lambda_i$ ,

$$\begin{pmatrix} \lambda_1 & & & & \\ & \lambda_2 & & & \\ & & \lambda_3 & & \\ & & & \ddots & \\ & & & & \lambda_n \end{pmatrix}. \quad (5.93)$$

For example, the matrix  $\mathfrak{M}_3$  is given by (*c.f.* section 4.6.1)

$$\mathfrak{M}_3 = \begin{pmatrix} \begin{array}{c} \leftarrow \leftarrow \leftarrow \\ \leftarrow \leftarrow \leftarrow \\ \leftarrow \leftarrow \leftarrow \\ \leftarrow \leftarrow \leftarrow \end{array} & 0 & 0 & 0 \\ 0 & \frac{4}{3} \cdot \begin{array}{c} \leftarrow \leftarrow \leftarrow \\ \leftarrow \leftarrow \leftarrow \\ \leftarrow \leftarrow \leftarrow \\ \leftarrow \leftarrow \leftarrow \end{array} & \sqrt{\frac{4}{3}} \cdot \begin{array}{c} \leftarrow \leftarrow \leftarrow \\ \leftarrow \leftarrow \leftarrow \\ \leftarrow \leftarrow \leftarrow \\ \leftarrow \leftarrow \leftarrow \end{array} & 0 \\ 0 & \sqrt{\frac{4}{3}} \cdot \begin{array}{c} \leftarrow \leftarrow \leftarrow \\ \leftarrow \leftarrow \leftarrow \\ \leftarrow \leftarrow \leftarrow \\ \leftarrow \leftarrow \leftarrow \end{array} & \frac{4}{3} \cdot \begin{array}{c} \leftarrow \leftarrow \leftarrow \\ \leftarrow \leftarrow \leftarrow \\ \leftarrow \leftarrow \leftarrow \\ \leftarrow \leftarrow \leftarrow \end{array} & 0 \\ 0 & 0 & 0 & \begin{array}{c} \leftarrow \leftarrow \leftarrow \\ \leftarrow \leftarrow \leftarrow \\ \leftarrow \leftarrow \leftarrow \\ \leftarrow \leftarrow \leftarrow \end{array} \end{pmatrix}, \quad (5.94)$$

where we have highlighted the projection operators  $\mathfrak{m}_{ii}$  for visual clarity. The orthonormal singlet states of  $SU(N)$  over  $V^{\otimes k} \otimes (V^*)^{\otimes k}$  are obtained by bending the operators  $\mathfrak{m}_{ij}$  in  $\mathfrak{M}_k$ ,

$$\frac{|\mathfrak{m}_{ij}\rangle}{\sqrt{\langle \mathfrak{m}_{ij} | \mathfrak{m}_{ij} \rangle}} := \begin{array}{c} \leftarrow \leftarrow \leftarrow \\ \leftarrow \leftarrow \leftarrow \\ \leftarrow \leftarrow \leftarrow \\ \leftarrow \leftarrow \leftarrow \end{array} \mathfrak{m}_{ij} \begin{array}{c} \leftarrow \leftarrow \leftarrow \\ \leftarrow \leftarrow \leftarrow \\ \leftarrow \leftarrow \leftarrow \\ \leftarrow \leftarrow \leftarrow \end{array}. \quad (5.95)$$

These singlet states are clearly orthonormal: The scalar product  $\langle A|B \rangle$  of two operators  $A$  and  $B$  is formed by contracting indices on  $A^\dagger$  and  $B$ . However, this is equivalent to taking their trace,

$$\langle A|B \rangle = \text{tr}(|A\rangle\langle B|) = \text{tr}(A^\dagger B). \quad (5.96)$$

Orthogonality of the operators in  $\mathfrak{S}_k$  under the scalar product (5.96) (*c.f.* chapter 4) in turn renders the singlet states (5.95) orthogonal, since

$$\langle \mathfrak{m}_{ji} | \mathfrak{m}_{kl} \rangle = \text{tr}(\mathfrak{m}_{ji} \mathfrak{m}_{kl}) = \delta_{ik} \delta_{jl} \text{tr}(\mathfrak{m}_{ji} \mathfrak{m}_{ij}) = \delta_{ik} \delta_{jl} \langle \mathfrak{m}_{ji} | \mathfrak{m}_{ij} \rangle, \quad (5.97)$$

where we used the fact that  $\mathfrak{m}_{ij}^\dagger = \mathfrak{m}_{ji}$ .<sup>13</sup> For a proof of the orthogonality of the states (5.95) in the birdtrack

<sup>13</sup> If  $\mathfrak{m}_{ji} = \mathfrak{m}_{ii}$  is a projection operator,  $\mathfrak{m}_{ii}^\dagger = \mathfrak{m}_{ii}$  follows immediately from the Hermiticity property of the MOLD operators. If  $\mathfrak{m}_{ji}$  is a transition operator, then  $\mathfrak{m}_{ij}^\dagger = \mathfrak{m}_{ji}$  is merely the defining property (5.63b) of transition operators.

formalism see appendix 5.B.1.

We may now construct projection operators using the singlet states (5.95),

$$P_{ij}^S := \frac{|\mathbf{m}_{ij}\rangle\langle\mathbf{m}_{ij}|}{\langle\mathbf{m}_{ij}|\mathbf{m}_{ij}\rangle}, \quad (5.98)$$

which, in birdtrack notation, can be written as

$$P_{ij}^S = \frac{1}{\text{tr}(\mathbf{m}_{ij}^\dagger \mathbf{m}_{ij})} \begin{array}{c} \text{---} \circlearrowleft \\ \text{---} \circlearrowright \\ \text{---} \circlearrowleft \\ \text{---} \circlearrowright \end{array} \begin{array}{c} \text{---} \circlearrowleft \\ \text{---} \circlearrowright \\ \text{---} \circlearrowleft \\ \text{---} \circlearrowright \end{array} = \frac{1}{\text{tr}(\mathbf{m}_{ji} \mathbf{m}_{ij})} \begin{array}{c} \text{---} \circlearrowleft \\ \text{---} \circlearrowright \\ \text{---} \circlearrowleft \\ \text{---} \circlearrowright \end{array} \begin{array}{c} \text{---} \circlearrowleft \\ \text{---} \circlearrowright \\ \text{---} \circlearrowleft \\ \text{---} \circlearrowright \end{array}. \quad (5.99)$$

Idempotency and mutual orthogonality of these operators follows from eq. (5.97). From the same token, it can be shown that these operators indeed correspond to 1-dimensional representations of  $SU(N)$  and thus deserve to be called singlet projectors,

$$\dim(P_{ij}^S) = \text{tr}(P_{ij}^S) = \text{tr}\left(\frac{|\mathbf{m}_{ij}\rangle\langle\mathbf{m}_{ij}|}{\langle\mathbf{m}_{ij}|\mathbf{m}_{ij}\rangle}\right) = \frac{\text{tr}(|\mathbf{m}_{ij}\rangle\langle\mathbf{m}_{ij}|)}{\langle\mathbf{m}_{ij}|\mathbf{m}_{ij}\rangle} = \frac{\langle\mathbf{m}_{ij}|\mathbf{m}_{ij}\rangle}{\langle\mathbf{m}_{ij}|\mathbf{m}_{ij}\rangle} = 1. \quad (5.100)$$

Proofs of the mutual orthogonality of these projection operators and their dimension *in birdtrack notation* are given in appendices 5.B.2 and 5.B.3 respectively.

Let us summarize our discussion on singlet projection operators in the following Theorem:

**■ Theorem 5.2 – orthogonal  $N$ -independent singlets & singlet count:**

Consider the irreducible representations of  $SU(N)$  on a product space  $V^{\otimes k} \otimes (V^*)^{\otimes k}$ . There exist exactly  $k!$  singlet states  $|\phi^S\rangle$  satisfying

$$\mathbf{U}|\phi^S\rangle = |\phi^S\rangle \quad \text{and} \quad \langle\phi^S|\mathbf{U}^\dagger = \langle\phi^S|, \quad (5.101)$$

where  $\mathbf{U}$  is a tensor product defined as  $\mathbf{U} := U^{\otimes k} \otimes (U^\dagger)^{\otimes k}$ , and  $U \in SU(N)$  is arbitrary. These singlet states are obtained from reshaping the basis elements of  $\text{API}(SU(N), V^{\otimes k})$ . In particular, if one chooses a basis of Hermitian Young projection operators and transition operators  $\mathfrak{S}_k = \{\mathbf{m}_{ij}\}$ , the resulting normalized singlet states

$$\frac{|\mathbf{m}_{ij}\rangle}{\sqrt{\langle\mathbf{m}_{ij}|\mathbf{m}_{ij}\rangle}} := \begin{array}{c} \text{---} \circlearrowleft \\ \text{---} \circlearrowright \\ \text{---} \circlearrowleft \\ \text{---} \circlearrowright \end{array} \begin{array}{c} \text{---} \circlearrowleft \\ \text{---} \circlearrowright \\ \text{---} \circlearrowleft \\ \text{---} \circlearrowright \end{array} \quad (5.102)$$

are orthonormal

$$\frac{\langle\mathbf{m}_{kl}|\mathbf{m}_{ij}\rangle}{\sqrt{\langle\mathbf{m}_{ij}|\mathbf{m}_{ij}\rangle}\sqrt{\langle\mathbf{m}_{kl}|\mathbf{m}_{kl}\rangle}} = \delta_{ik}\delta_{jl}. \quad (5.103)$$

From these singlet states one can form exactly  $k!$  singlet projection operators corresponding to the  $k!$  1-

dimensional irreducible representations (singlet representations) of  $SU(N)$  over  $V^{\otimes k} \otimes (V^*)^{\otimes k}$ ,

$$P_{ij}^S := \frac{|\mathbf{m}_{ij}\rangle\langle\mathbf{m}_{ij}|}{\langle\mathbf{m}_{ij}|\mathbf{m}_{ij}\rangle} = \frac{1}{\text{tr}(\mathbf{m}_{ij}^\dagger \mathbf{m}_{ij})} \text{Diagram} \quad (5.104)$$

### 5.2.1.5 Transition operators and an example of the complete singlet algebra over $V^{\otimes k} \otimes (V^*)^{\otimes k}$

In section 5.2.1.3 we discussed that all singlet projection operators constructed from bending the basis elements of the algebra of invariants of  $SU(N)$  are equivalent. While a basis for  $\text{API}(SU(N), V^{\otimes m} \otimes (V^*)^{\otimes n})$  (with  $m+n=k$ ) in terms of Clebsch-Gordan operators was used in section 5.2.1.3, the same statement must hold if one chooses a different basis for any  $\text{API}(SU(N), V^{\otimes m} \otimes (V^*)^{\otimes n})$  such that  $m+n=k$ . In particular, one may choose the basis  $\mathfrak{S}_k$  of  $\text{API}(SU(N), V^{\otimes k})$  used in Theorem 5.2 to construct the singlet projectors of  $SU(N)$  over  $V^{\otimes k} \otimes (V^*)^{\otimes k}$ . Theorem 5.3 constructs the transition operators using the basis  $\mathfrak{S}_k$  by analogy to eq. (5.89):

#### ■ Theorem 5.3 – transition operators between singlet projectors:

All 1-dimensional irreducible representations of  $SU(N)$  over the product space  $V^{\otimes k} \otimes (V^*)^{\otimes k}$  are equivalent. Let  $P_{ij}^S$  and  $P_{kl}^S$  be two singlet projection operators corresponding to such 1-dimensional representations, and let them be constructed according to Theorem 5.2, eq. (5.104). Then the transition operator  $T_{ij,kl}^S$  between  $P_{ij}^S$  and  $P_{kl}^S$  is given by

$$T_{ij,kl}^S := \frac{1}{\sqrt{\text{tr}(\mathbf{m}_{ij}^\dagger \mathbf{m}_{ij}) \text{tr}(\mathbf{m}_{kl}^\dagger \mathbf{m}_{kl})}} \text{Diagram} \quad (5.105)$$

In appendix 5.B.4, we explicitly demonstrate *in the birdtrack formalism* that the operators (5.105) satisfy all defining properties of transition operators given in eqns. (5.90).

Having obtained a practical construction algorithm for the singlet states, and thus also for the singlet projection and transition operators of  $SU(N)$  over  $V^{\otimes k} \otimes (V^*)^{\otimes k}$  (Theorems 5.2 and 5.3), we now look at an example: Let us construct all singlet projection and transition operators of  $SU(N)$  over  $V^{\otimes 3} \otimes (V^*)^{\otimes 3}$ . To accomplish this, we bend the elements of  $\mathfrak{S}_3$ <sup>14</sup>

$$\mathfrak{S}_3 = \left\{ \begin{array}{l} \text{Diagram 1}, \quad \frac{4}{3} \cdot \text{Diagram 2}, \quad \sqrt{\frac{4}{3}} \cdot \text{Diagram 3}, \quad \sqrt{\frac{4}{3}} \cdot \text{Diagram 4}, \quad \frac{4}{3} \cdot \text{Diagram 5}, \quad \text{Diagram 6} \end{array} \right\} \quad (5.106)$$

into singlet states

$$\chi_1 \cdot \text{Diagram 1}, \quad \theta_{N>1} \chi_2 \cdot \text{Diagram 2}, \quad \theta_{N>1} \chi_2 \cdot \text{Diagram 3}, \quad \theta_{N>1} \chi_2 \cdot \text{Diagram 4}, \quad \theta_{N>1} \chi_2 \cdot \text{Diagram 5}, \quad \text{and} \quad \theta_{N>2} \chi_3 \cdot \text{Diagram 6}, \quad (5.107)$$

<sup>14</sup>This set can be read off from eq. (5.94). The order of the elements in  $\mathfrak{S}_3$  arises from listing the matrix elements in  $\mathfrak{M}_3$  row-wise from left to right, starting at the top row. This particular order is helpful as it produces explicitly block-diagonal matrices in the coincidence limits discussed in section 5.3.2.1.



where the function  $\theta_{N>p}$  defined as

$$\theta_{N>p} := \begin{cases} 1 & \text{if } N > p \\ 0 & \text{if } N \leq p \end{cases}, \quad p \in \mathbb{N}, \quad (5.108)$$

reminds us that the affected operators in (5.107) are dimensionally zero (*c.f.* appendix 4.A or page 221 for a discussion on dimensional zeros) for values of  $N$  that are smaller than the threshold  $p$ . The normalization constants  $\chi_i$  are given by

$$\chi_1 = \frac{6}{(N+2)(N+1)N}, \quad \chi_2 = \frac{3}{N(N^2-1)} \quad \text{and} \quad \chi_3 = \frac{6}{(N-2)(N-1)N}. \quad (5.109)$$

Using the singlet states (5.107), we can construct the singlet projection and transition operators of  $SU(N)$  over  $V^{\otimes 3} \otimes (V^*)^{\otimes 3}$ . Arranging them into a matrix  $\mathfrak{M}_{3,3}^S$ , which has the projection operators on the diagonal and the transition operators on the off-diagonal (in analogy to eq. (5.93)), we obtain

$$\mathfrak{M}_{3,3}^S = \begin{pmatrix} \chi_{11} \cdot \text{diag} & \chi_{12} \cdot \text{diag} & \chi_{12} \cdot \text{diag} & \chi_{12} \cdot \text{diag} & \chi_{12} \cdot \text{diag} & \chi_{13} \cdot \text{diag} \\ \chi_{21} \cdot \text{diag} & \chi_{22} \cdot \text{diag} & \chi_{22} \cdot \text{diag} & \chi_{22} \cdot \text{diag} & \chi_{22} \cdot \text{diag} & \chi_{23} \cdot \text{diag} \\ \chi_{21} \cdot \text{diag} & \chi_{22} \cdot \text{diag} & \chi_{22} \cdot \text{diag} & \chi_{22} \cdot \text{diag} & \chi_{22} \cdot \text{diag} & \chi_{23} \cdot \text{diag} \\ \chi_{21} \cdot \text{diag} & \chi_{22} \cdot \text{diag} & \chi_{22} \cdot \text{diag} & \chi_{22} \cdot \text{diag} & \chi_{22} \cdot \text{diag} & \chi_{23} \cdot \text{diag} \\ \chi_{21} \cdot \text{diag} & \chi_{22} \cdot \text{diag} & \chi_{22} \cdot \text{diag} & \chi_{22} \cdot \text{diag} & \chi_{22} \cdot \text{diag} & \chi_{23} \cdot \text{diag} \\ \chi_{31} \cdot \text{diag} & \chi_{32} \cdot \text{diag} & \chi_{32} \cdot \text{diag} & \chi_{32} \cdot \text{diag} & \chi_{32} \cdot \text{diag} & \chi_{33} \cdot \text{diag} \end{pmatrix} \quad (5.110)$$

(where we have suppressed the functions  $\theta_{N>p}$  in order not to clutter  $\mathfrak{M}_{3,3}^S$ ). The constants  $\chi_{ij}$  are defined as

$$\chi_{ij} := \sqrt{\chi_i \cdot \chi_j} \quad \text{with } \chi_j \text{ given in eq. (5.109)}, \quad (5.111)$$

and have been marked in color for visual clarity, highlighting that there are only six different constants in the matrix  $\mathfrak{M}_{3,3}^S$

$$\chi_{11}, \chi_{12}, \chi_{13}, \chi_{22}, \chi_{23} \text{ and } \chi_{33}.$$

### 5.2.1.6 Singlet projectors of $SU(N)$ over $V^{\otimes k}$ in a different basis

As already mentioned, the singlet states constructed from bending the operators in  $\mathfrak{S}_k$  give rise to just one basis of the singlet algebra of  $SU(N)$  over  $V^{\otimes k} \otimes (V^*)^{\otimes k}$ ; we will call this basis the *singlet projector basis*. The benefit of this basis is that it yields mutually orthogonal singlet states with minimal computing power.

However, bending the elements of a particular choice of basis for  $\text{API}\left(\text{SU}(N), V^{\otimes m} \otimes (V^*)^{\otimes n}\right)$  with  $m+n = k$  merely provides one way of constructing the singlet projectors of  $\text{SU}(N)$  over  $V^{\otimes k} \otimes (V^*)^{\otimes k}$ . If one constructs these operators by some other means, it is easy to verify whether the resulting set spans the singlet algebra of  $\text{SU}(N)$  over  $V^{\otimes k} \otimes (V^*)^{\otimes k}$  by checking that it has size  $k!$  as required by Theorem 5.2 (provided that the new set of singlet operators that has been constructed is linearly independent).

For example, one may make an Ansatz for singlet states that make the gluons (i.e. adjoint lines) explicit: Recall the notation (5.36) for the group generators  $[t^a]_{ki}$ , and the fact that gluons can couple to each other via the structure constants  $f^{abc}$  and  $d^{abc}$ . Following [72], these constants will be graphically represented, respectively, by a filled (black) and an empty (white) circle at the vertex of the three gluon lines,

$$f^{abc} := \begin{array}{c} a \\ \cdot \\ \cdot \\ \cdot \\ b \end{array} \cdot c \quad \text{and} \quad d^{abc} := \begin{array}{c} a \\ \circ \\ \circ \\ \circ \\ b \end{array} \cdot c . \quad (5.112)$$

With these additional birdtrack notations at hand, we are able to make the following Ansatz for the singlet states over  $V^{\otimes 3} \otimes (V^*)^{\otimes 3}$ ,

$$\xi_1 \cdot \begin{array}{c} \curvearrowright \\ \curvearrowright \\ \curvearrowright \end{array}, \quad \xi_2 \cdot \begin{array}{c} \curvearrowright \\ \curvearrowright \\ \curvearrowright \\ \curvearrowright \end{array}, \quad \xi_2 \cdot \begin{array}{c} \curvearrowright \\ \curvearrowright \\ \curvearrowright \\ \curvearrowright \\ \curvearrowright \end{array}, \quad \xi_2 \cdot \begin{array}{c} \curvearrowright \\ \curvearrowright \\ \curvearrowright \\ \curvearrowright \\ \curvearrowright \\ \curvearrowright \end{array}, \quad \xi_3 \cdot \begin{array}{c} \curvearrowright \\ \curvearrowright \\ \curvearrowright \\ \curvearrowright \\ \curvearrowright \\ \curvearrowright \\ \curvearrowright \end{array} \quad \text{and} \quad \xi_4 \cdot \begin{array}{c} \curvearrowright \\ \curvearrowright \\ \curvearrowright \\ \curvearrowright \\ \curvearrowright \\ \curvearrowright \\ \curvearrowright \\ \curvearrowright \end{array} \quad (5.113)$$

with normalization constants

$$\xi_1 = \frac{1}{\sqrt{N^3}}, \quad \xi_2 = \frac{1}{\sqrt{N(N^2-1)}}, \quad \xi_3 = \frac{1}{\sqrt{2N(N^2-1)}} \quad \text{and} \quad \xi_4 = \sqrt{\frac{N}{2(N^2-4)(N^2-1)}}. \quad (5.114)$$

This basis is orthogonal due to the fact that the generators  $[t^a]_{ki}$  are traceless,

$$0 = \frac{1}{\sqrt{2}} \text{tr}([t^a]_{ki}) = \frac{1}{\sqrt{2}} [t^a]_{ki} \delta_{ik} = a \cdots \begin{array}{c} k \\ \curvearrowright \\ i \end{array} = a \cdots \begin{array}{c} \curvearrowright \end{array}. \quad (5.115)$$

In this basis, the matrix of singlet projection and transition operators becomes

$$\tilde{\mathcal{M}}_{3,3}^S = \begin{pmatrix} \begin{array}{c} \xi_{11} \\ \curvearrowright \\ \curvearrowright \\ \curvearrowright \end{array} & \begin{array}{c} \xi_{12} \\ \curvearrowright \\ \curvearrowright \\ \curvearrowright \end{array} & \begin{array}{c} \xi_{12} \\ \curvearrowright \\ \curvearrowright \\ \curvearrowright \end{array} & \begin{array}{c} \xi_{12} \\ \curvearrowright \\ \curvearrowright \\ \curvearrowright \end{array} & \begin{array}{c} \xi_{13} \\ \curvearrowright \\ \curvearrowright \\ \curvearrowright \end{array} & \begin{array}{c} \xi_{14} \\ \curvearrowright \\ \curvearrowright \\ \curvearrowright \end{array} \\ \begin{array}{c} \xi_{12} \\ \curvearrowright \\ \curvearrowright \\ \curvearrowright \end{array} & \begin{array}{c} \xi_{22} \\ \curvearrowright \\ \curvearrowright \\ \curvearrowright \end{array} & \begin{array}{c} \xi_{22} \\ \curvearrowright \\ \curvearrowright \\ \curvearrowright \end{array} & \begin{array}{c} \xi_{22} \\ \curvearrowright \\ \curvearrowright \\ \curvearrowright \end{array} & \begin{array}{c} \xi_{23} \\ \curvearrowright \\ \curvearrowright \\ \curvearrowright \end{array} & \begin{array}{c} \xi_{24} \\ \curvearrowright \\ \curvearrowright \\ \curvearrowright \end{array} \\ \xi_{12} \cdot \begin{array}{c} \curvearrowright \\ \curvearrowright \\ \curvearrowright \\ \curvearrowright \\ \curvearrowright \end{array} & \xi_{22} \cdot \begin{array}{c} \curvearrowright \\ \curvearrowright \\ \curvearrowright \\ \curvearrowright \\ \curvearrowright \\ \curvearrowright \end{array} & \xi_{22} \cdot \begin{array}{c} \curvearrowright \\ \curvearrowright \\ \curvearrowright \\ \curvearrowright \\ \curvearrowright \\ \curvearrowright \end{array} & \xi_{22} \cdot \begin{array}{c} \curvearrowright \\ \curvearrowright \\ \curvearrowright \\ \curvearrowright \\ \curvearrowright \\ \curvearrowright \end{array} & \xi_{23} \cdot \begin{array}{c} \curvearrowright \\ \curvearrowright \\ \curvearrowright \\ \curvearrowright \\ \curvearrowright \\ \curvearrowright \end{array} & \xi_{24} \cdot \begin{array}{c} \curvearrowright \\ \curvearrowright \\ \curvearrowright \\ \curvearrowright \\ \curvearrowright \\ \curvearrowright \end{array} \\ \xi_{12} \cdot \begin{array}{c} \curvearrowright \\ \curvearrowright \\ \curvearrowright \\ \curvearrowright \\ \curvearrowright \\ \curvearrowright \end{array} & \xi_{22} \cdot \begin{array}{c} \curvearrowright \\ \curvearrowright \\ \curvearrowright \\ \curvearrowright \\ \curvearrowright \\ \curvearrowright \\ \curvearrowright \end{array} & \xi_{22} \cdot \begin{array}{c} \curvearrowright \\ \curvearrowright \\ \curvearrowright \\ \curvearrowright \\ \curvearrowright \\ \curvearrowright \\ \curvearrowright \end{array} & \xi_{22} \cdot \begin{array}{c} \curvearrowright \\ \curvearrowright \\ \curvearrowright \\ \curvearrowright \\ \curvearrowright \\ \curvearrowright \\ \curvearrowright \end{array} & \xi_{23} \cdot \begin{array}{c} \curvearrowright \\ \curvearrowright \\ \curvearrowright \\ \curvearrowright \\ \curvearrowright \\ \curvearrowright \\ \curvearrowright \end{array} & \xi_{24} \cdot \begin{array}{c} \curvearrowright \\ \curvearrowright \\ \curvearrowright \\ \curvearrowright \\ \curvearrowright \\ \curvearrowright \\ \curvearrowright \end{array} \\ \xi_{13} \cdot \begin{array}{c} \curvearrowright \\ \curvearrowright \\ \curvearrowright \\ \curvearrowright \\ \curvearrowright \\ \curvearrowright \\ \curvearrowright \end{array} & \xi_{23} \cdot \begin{array}{c} \curvearrowright \\ \curvearrowright \\ \curvearrowright \\ \curvearrowright \\ \curvearrowright \\ \curvearrowright \\ \curvearrowright \end{array} & \xi_{23} \cdot \begin{array}{c} \curvearrowright \\ \curvearrowright \\ \curvearrowright \\ \curvearrowright \\ \curvearrowright \\ \curvearrowright \\ \curvearrowright \end{array} & \xi_{23} \cdot \begin{array}{c} \curvearrowright \\ \curvearrowright \\ \curvearrowright \\ \curvearrowright \\ \curvearrowright \\ \curvearrowright \\ \curvearrowright \end{array} & \xi_{33} \cdot \begin{array}{c} \curvearrowright \\ \curvearrowright \\ \curvearrowright \\ \curvearrowright \\ \curvearrowright \\ \curvearrowright \\ \curvearrowright \end{array} & \xi_{34} \cdot \begin{array}{c} \curvearrowright \\ \curvearrowright \\ \curvearrowright \\ \curvearrowright \\ \curvearrowright \\ \curvearrowright \\ \curvearrowright \end{array} \\ \xi_{14} \cdot \begin{array}{c} \curvearrowright \\ \curvearrowright \\ \curvearrowright \\ \curvearrowright \\ \curvearrowright \\ \curvearrowright \\ \curvearrowright \end{array} & \xi_{24} \cdot \begin{array}{c} \curvearrowright \\ \curvearrowright \\ \curvearrowright \\ \curvearrowright \\ \curvearrowright \\ \curvearrowright \\ \curvearrowright \end{array} & \xi_{24} \cdot \begin{array}{c} \curvearrowright \\ \curvearrowright \\ \curvearrowright \\ \curvearrowright \\ \curvearrowright \\ \curvearrowright \\ \curvearrowright \end{array} & \xi_{24} \cdot \begin{array}{c} \curvearrowright \\ \curvearrowright \\ \curvearrowright \\ \curvearrowright \\ \curvearrowright \\ \curvearrowright \\ \curvearrowright \end{array} & \xi_{34} \cdot \begin{array}{c} \curvearrowright \\ \curvearrowright \\ \curvearrowright \\ \curvearrowright \\ \curvearrowright \\ \curvearrowright \\ \curvearrowright \end{array} & \xi_{44} \cdot \begin{array}{c} \curvearrowright \\ \curvearrowright \\ \curvearrowright \\ \curvearrowright \\ \curvearrowright \\ \curvearrowright \\ \curvearrowright \end{array} \end{pmatrix}, \quad (5.116)$$

where  $\xi_{ij} := \sqrt{\xi_i \cdot \xi_j}$ , and the  $\xi_i$  are defined in eq. (5.114).

Since (5.116) and (5.110) both give us all the singlet projection and transition operators of  $SU(N)$  over  $V^{\otimes 3} \otimes (V^*)^{\otimes 3}$ , they must be related by a change of basis  $\mathfrak{C}_{3,3}$  such that

$$\mathfrak{M}_{3,3}^S = \mathfrak{C}_{3,3} \tilde{\mathfrak{M}}_{3,3}^S \mathfrak{C}_{3,3}^\dagger. \quad (5.117)$$

For eq. (5.117) to hold, the matrix elements of  $\mathfrak{C}$  have to be of the form

$$[\mathfrak{C}_{3,3}]_{ij} = \sum_k [\mathfrak{M}_{3,3}^S]_{ik} \rho [\tilde{\mathfrak{M}}_{3,3}^S]_{kj}, \quad (5.118)$$

where

$$\rho := \begin{array}{c} \longleftrightarrow \\ \longleftrightarrow \\ \longleftrightarrow \\ \longleftrightarrow \\ \longleftrightarrow \\ \longleftrightarrow \end{array} \text{ is the permutation that re-sorts the fundamental and antifundamental lines.} \quad (5.119)$$

As an example, one term in the sum that is the matrix element  $[\mathfrak{C}_{3,3}]_{14}$  will be

$$[\mathfrak{M}_{3,3}^S]_{11} \rho [\tilde{\mathfrak{M}}_{3,3}^S]_{14} = \begin{array}{c} \text{Diagram 1} \end{array} \begin{array}{c} \text{Diagram 2} \end{array} \begin{array}{c} \text{Diagram 3} \end{array}. \quad (5.120)$$

### 5.2.1.7 Using the primitive invariants $S_k$ or the standard Young projector basis to construct singlet projectors

By Theorem 5.2, one obtains all singlet projectors of  $SU(N)$  over  $V^{\otimes k} \otimes (V^*)^{\otimes k}$  by bending the elements of any basis of the algebra of invariants  $\text{API}(SU(N), V^{\otimes k})$ . It seems natural to use the primitive invariants  $S_k$ , which by definition span  $\text{API}(SU(N), V^{\otimes k})$ , for this task, for example

$$S_3 \longrightarrow \frac{1}{N_c^3} \cdot \begin{array}{c} \text{Diagram 1} \end{array}, \frac{1}{N_c^3} \cdot \begin{array}{c} \text{Diagram 2} \end{array}, \frac{1}{N_c^3} \cdot \begin{array}{c} \text{Diagram 3} \end{array}, \frac{1}{N_c^3} \cdot \begin{array}{c} \text{Diagram 4} \end{array}, \frac{1}{N_c^3} \cdot \begin{array}{c} \text{Diagram 5} \end{array}, \frac{1}{N_c^3} \cdot \begin{array}{c} \text{Diagram 6} \end{array} \quad (5.121)$$

The drawback when using  $S_k$  is that the resulting singlet states are not orthogonal with respect to the scalar product  $\langle \cdot | \cdot \rangle$  introduced in eq. (5.96). The reason for this is that the trace of two primitive invariants  $\text{tr}(\rho^\dagger \sigma)$ , for  $\rho, \sigma \in S_k$ , is nonzero; this statement will be made precise at the end of section 8.2.3 in chapter 8. As an example,

$$\begin{array}{c} \text{Diagram 1} \end{array} = \text{tr} \left( \left( \begin{array}{c} \text{Diagram 2} \end{array} \right)^\dagger \begin{array}{c} \text{Diagram 3} \end{array} \right) = \text{tr} \left( \begin{array}{c} \text{Diagram 4} \end{array} \right) = \text{tr} \left( \begin{array}{c} \text{Diagram 5} \end{array} \right) = \begin{array}{c} \text{Diagram 6} \end{array} = N^2 \neq 0, \quad (5.122)$$

where we have drawn the lines arising from the trace in red for visual clarity.<sup>15</sup>

<sup>15</sup>Each closed loop corresponds to a trace of a Kronecker  $\delta$  in the fundamental representation, and thus gives a factor  $N$ , c.f. [72] or the later section 8.2.1.

Similarly, the Young projection and transition operators are not orthogonal with respect to  $\langle \cdot | \cdot \rangle$ , for example

$$\begin{aligned}
 \text{tr} \left( Y_{\begin{smallmatrix} \square & \square \\ \square \end{smallmatrix}}^\dagger Y_{\begin{smallmatrix} \square & \square \\ \square \end{smallmatrix}} \right) &= \text{tr} \left( \left( \frac{4}{3} \right)^2 \begin{array}{c} \leftarrow \text{---} \square \text{---} \leftarrow \\ \leftarrow \text{---} \square \text{---} \leftarrow \\ \leftarrow \text{---} \square \text{---} \leftarrow \end{array} \cdot \begin{array}{c} \leftarrow \text{---} \square \text{---} \leftarrow \\ \leftarrow \text{---} \square \text{---} \leftarrow \\ \leftarrow \text{---} \square \text{---} \leftarrow \end{array} \right) \\
 &= \frac{1}{9} \text{tr} \left( - \begin{array}{c} \leftarrow \text{---} \leftarrow \\ \leftarrow \text{---} \leftarrow \\ \leftarrow \text{---} \leftarrow \end{array} + \begin{array}{c} \leftarrow \text{---} \leftarrow \\ \leftarrow \text{---} \leftarrow \\ \leftarrow \text{---} \leftarrow \end{array} + \begin{array}{c} \leftarrow \text{---} \leftarrow \\ \leftarrow \text{---} \leftarrow \\ \leftarrow \text{---} \leftarrow \end{array} - 2 \cdot \begin{array}{c} \leftarrow \text{---} \leftarrow \\ \leftarrow \text{---} \leftarrow \\ \leftarrow \text{---} \leftarrow \end{array} + \begin{array}{c} \leftarrow \text{---} \leftarrow \\ \leftarrow \text{---} \leftarrow \\ \leftarrow \text{---} \leftarrow \end{array} + 2 \cdot \begin{array}{c} \leftarrow \text{---} \leftarrow \\ \leftarrow \text{---} \leftarrow \\ \leftarrow \text{---} \leftarrow \end{array} - \begin{array}{c} \leftarrow \text{---} \leftarrow \\ \leftarrow \text{---} \leftarrow \\ \leftarrow \text{---} \leftarrow \end{array} \right) \\
 &= -\frac{N_c^3}{9} + \frac{N_c}{9} \neq 0 .
 \end{aligned} \tag{5.123}$$

Here, we face the additional challenge that the Young projection operators over  $V^{\otimes m}$  are, themselves, only orthogonal up to  $m = 4$ , see [85] or section 3.A.

Thus, both the primitive invariants, as well as the Young projection and transition operators, are not a good basis to use for building singlet states, as the resulting states will not be mutually orthogonal.

## 5.2.2 Singlet projectors over $V^{\otimes m} \otimes (V^*)^{\otimes n}$ : $\varepsilon$ -tensors

We have, so far, discussed the singlets of  $\text{SU}(N)$  that are composed entirely out of Kronecker  $\delta$ 's. Since the  $\varepsilon$ -tensor is an additional invariant of  $\text{SU}(N)$  over mixed product spaces, one ought to discuss their role in constructing singlets. Firstly, it should be noted that a Levi-Civita tensor is only an invariant of  $\text{SU}(N)$  if its length (i.e. its number of index legs) coincides with  $N = \dim(V)$ ,  $\text{length}(\varepsilon) = N$ .

As it turns out, the Levi-Civita tensors do not produce *new* singlets; that is, every singlet of  $\text{SU}(N)$  containing an  $\varepsilon$ -tensor is completely equivalent to a singlet comprised entirely out of Kronecker  $\delta$ 's (those singlets discussed in section 5.2.1). In particular, in this section we will show that, for  $N \stackrel{\text{!}}{=} \text{length}(\varepsilon)$ , every singlet containing a Levi-Civita symbol can be recast into a singlet consisting only of Kronecker  $\delta$ 's, and vice versa.

Before exploring this equivalence in general, let us look at an example:

### 5.2.2.1 Baryon singlet projector $\mathbf{A}_{123}$

Consider the antisymmetrizer  $\mathbf{A}_{123}$

$$\mathbf{A}_{123} = \begin{array}{c} \leftarrow \text{---} \leftarrow \\ \leftarrow \text{---} \leftarrow \\ \leftarrow \text{---} \leftarrow \end{array} \quad \text{with dimension} \quad \dim(\mathbf{A}_{123}) = \frac{(N-2)(N-1)N}{6} . \tag{5.124}$$

From the dimension formula, it immediately follows that  $\mathbf{A}_{123}$  projects onto a singlet representation if  $N = 3$ . This is further highlighted by the fact that, for  $N = 3$ ,  $\mathbf{A}_{123}$  antisymmetrizes over  $N$  legs and thus splits into the product of two Levi-Civita tensors of length 3 in accordance with eq. (5.32),

$$\mathbf{A}_{123} = \begin{array}{c} \leftarrow \text{---} \leftarrow \\ \leftarrow \text{---} \leftarrow \\ \leftarrow \text{---} \leftarrow \end{array} \stackrel{\text{dim}(V)=N=3}{=} \begin{array}{c} \leftarrow \text{---} \leftarrow \\ \leftarrow \text{---} \leftarrow \\ \leftarrow \text{---} \leftarrow \end{array} . \tag{5.125}$$

Hence, for  $\text{length}(\varepsilon) = 3$ ,  $\mathbf{A}_{123}$  becomes a singlet operator (with no index lines crossing through the center, *c.f.* eq. (5.75)) comprised entirely of Levi-Civita tensors. Using the Leibniz identity (5.23), we will now show

that this singlet is completely equivalent to the totally antisymmetric singlet of  $SU(N)$  over  $V^{\otimes 2} \otimes (V^*)^{\otimes 2}$ :

$$\begin{array}{|c|} \hline \text{---} \\ \hline \text{---} \\ \hline \text{---} \\ \hline \end{array} \quad \text{and} \quad \begin{array}{|c|} \hline \text{---} \\ \hline \text{---} \\ \hline \text{---} \\ \hline \end{array} \quad \text{are equivalent for} \quad \dim(V) = N = 3. \quad (5.126)$$

The Leibniz identity (5.23) translates  $N - 1 = 2$  antifundamental intex lines into a fundamental line through the Levi-Civita symbols

$$\begin{array}{|c|} \hline \text{---} \\ \hline \text{---} \\ \hline \text{---} \\ \hline \end{array} \quad \text{and} \quad \begin{array}{|c|} \hline \text{---} \\ \hline \text{---} \\ \hline \text{---} \\ \hline \end{array} \quad (5.127)$$

of size  $N = 3$ . We act a Levi-Civita tensor of length  $N = 3$  on the bottom two antifundamental legs of the antisymmetric  $2q + 2\bar{q}$  singlet, and then absorb the antisymmetrizers into the Levi-Civita tensors

$$\begin{array}{|c|} \hline \text{---} \\ \hline \text{---} \\ \hline \text{---} \\ \hline \end{array} \quad \xrightarrow{\text{act } \varepsilon} \quad \begin{array}{|c|} \hline \text{---} \\ \hline \text{---} \\ \hline \text{---} \\ \hline \end{array} \quad \xrightarrow[\text{antisym.}]{\text{absorb}} \quad \begin{array}{|c|} \hline \text{---} \\ \hline \text{---} \\ \hline \text{---} \\ \hline \end{array}. \quad (5.128)$$

We now flip each antisymmetrizer about its vertical axis, keeping the end points fixed,

$$\begin{array}{|c|} \hline \text{---} \\ \hline \text{---} \\ \hline \text{---} \\ \hline \end{array} \quad \xrightarrow{\text{flip}} \quad (-1)^2 \quad \begin{array}{|c|} \hline \text{---} \\ \hline \text{---} \\ \hline \text{---} \\ \hline \end{array}, \quad (5.129)$$

where we had to absorb a transposition (12) into each  $\varepsilon$ -tensor in the process, inducing a factor of  $(-1)^2 = 1$ .<sup>16</sup> It should be noted that through this flipping procedure each  $\varepsilon$ -tensor in (5.129) will be accompanied by a factor  $i^{\pm\phi}$  (c.f. eq. (5.25)) with the *wrong* sign in the exponent. However, in the product (5.129), each prefactor can be *reassigned* to the other  $\varepsilon$ -tensor, thus remedying the incorrect sign. If this “prefactor conundrum” caused by the flip in (5.129) seems undesirable to the reader, we present a work-around in appendix (5.C), which leaves the prefactors untouched, but still yields the desired result.

It now remains to recombine the two Levi-Civita tensors in (5.129) into the antisymmetrizer  $\mathbf{A}_{123}$  according to eq. (5.32) in order to obtain the desired result,

$$\begin{array}{|c|} \hline \text{---} \\ \hline \text{---} \\ \hline \text{---} \\ \hline \end{array} \quad = \quad \begin{array}{|c|} \hline \text{---} \\ \hline \text{---} \\ \hline \text{---} \\ \hline \end{array} \quad \xrightarrow{\text{eq. (5.32)}} \quad \begin{array}{|c|} \hline \text{---} \\ \hline \text{---} \\ \hline \text{---} \\ \hline \end{array}. \quad (5.130)$$

As we have seen, the antisymmetrizer  $\mathbf{A}_{123}$  is a singlet projection operator of  $SU(N)$  over  $V^{\otimes 3}$  if  $\dim(V) = N \stackrel{!}{=} 3$ . Interpreting  $N = N_c$  as the number of colors in the QCD sense,  $\mathbf{A}_{123}$  corresponds to a color neutral, 3-particle configuration (the Fock space of 3 particles is  $V^{\otimes 3}$ ) — a *baryon*.

In this example, we chose to transform  $(N - 1)$  antifundamental lines into a fundamental line by means of the Leibniz identity (5.30). Equally effectively, we could have transformed  $(N - j)$  antiquarks into  $j$  quarks

<sup>16</sup>Defining  $\kappa_k$  to be the transposition between  $k$  and  $(N - k)$ , longer and thus more “entangled” Levi-Civita tensors will have a prefactor  $[\text{sign}(\kappa_1 \kappa_2 \kappa_3 \dots)]^2 = 1$ .

according to eq. (5.31), for example, if  $j = 2$ ,

$$(5.131)$$

However, the first way of obtaining the baryon singlet projector will be more useful when looking at Wilson line correlators and coincidence limits, see section 5.3.3.

Let us interpret  $N = N_c$  as the number of colors to develop an intuitive sense for the distinction between singlets consisting entirely of Kronecker  $\delta$ 's, and singlets containing  $\varepsilon$ -tensors as well.

**Baryons and mesons:** In this chapter, we have encountered the two projection operators corresponding to the most common quark–antiquark configurations occurring in nature: the meson<sup>17</sup> and the baryon,

$$(5.132)$$

A meson contains one charge of color and one charge of anti-color. This combination gives a color neutral operator (the meson) irrespective of the total number of colors  $N_c$ . On the other hand, the baryon projector exploits the fact that the combination of *all* colors (with equal weight) results in a color neutral object; if, for example,  $N_c = 4$ , then the baryon would have to consist of 4 partons in order to be a color singlet.

Thus, the “singlet-ness” of an operator containing no Levi-Civita symbol (e.g. the meson) is *independent* of the value of  $N$  ( $N_c$ ), while the “singlet-ness” of an operator containing Levi-Civita symbols (e.g. the baryon) *depends* on the exact value of  $N$ .

### 5.2.2.2 Singlets over $V^{\otimes m} \otimes (V^*)^{\otimes n}$ from singlets over $V^{\otimes k} \otimes (V^*)^{\otimes k}$

The procedure exemplified by the antisymmetrizer  $\mathbf{A}_{123}$  may be generalized to antisymmetrizers of length  $\dim(V) = N$  forming part of a larger singlet projector.

A general singlet may contain *several*  $\varepsilon$ -tensors of length  $N$ . The remaining index legs (not entering  $\varepsilon$ ) must be contained in a subsinglet consisting of Kronecker  $\delta$ 's only, in order for the overall operator to be color neutral. This subsinglet therefore contains an equal number of fundamental and antifundamental index lines. A schematic drawing of such a general singlet projection operator of  $\mathbf{SU}(N)$  over  $V^{\otimes m} \otimes (V^*)^{\otimes n}$  is given in Figure 5.2.

<sup>17</sup>The projection operator constructed in eq. (5.46) is the unique singlet projector for one fundamental and one antifundamental factor and thus describes a meson.

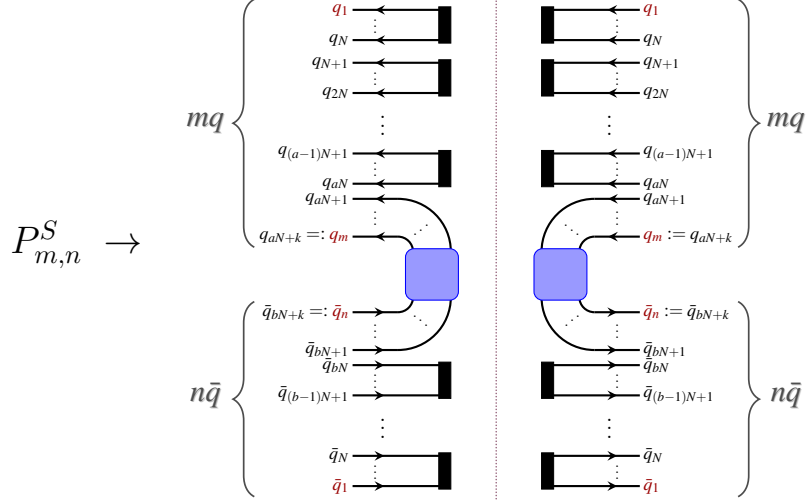


Figure 5.2: This figure depicts a general singlet  $P_{m,n}^S$  over the space  $V^{\otimes m} \otimes (V^*)^{\otimes n}$ , where the top  $m$  index lines  $q_1 \dots q_m$  (counted top to bottom) are in the fundamental representation, and the bottom  $n$  index lines  $\bar{q}_1 \dots \bar{q}_n$  (counted bottom to top) are in the antifundamental representation. This singlet contains  $(a + b)$   $\varepsilon$ -tensors:  $a$  of them over fundamental lines, and  $b$  over antifundamental lines. The remaining  $k = m - aN$  fundamental lines and  $k = n - bN$  antifundamental lines together form a subsinglet containing Kronecker  $\delta$ 's only; this subsinglet is indicated by the blue shaded box. Note that this  $N$ -independent subsinglet contains an equal number of fundamental and antifundamental lines.

Each of the  $\varepsilon$ -tensors appearing in Figure 5.2 can be related to an antisymmetric (sub)singlet over  $N - 1$  fundamental and antifundamental legs, analogously to the example in the previous section 5.2.2.1. Thus, the singlet  $P_{m,n}^S$  of Figure 5.2 can be shown to be equivalent to a singlet over  $V^{\otimes \alpha} \otimes (V^*)^{\otimes \alpha}$  for  $\alpha := (a + b)(N - 1) + k$ , as depicted in Figure 5.3.

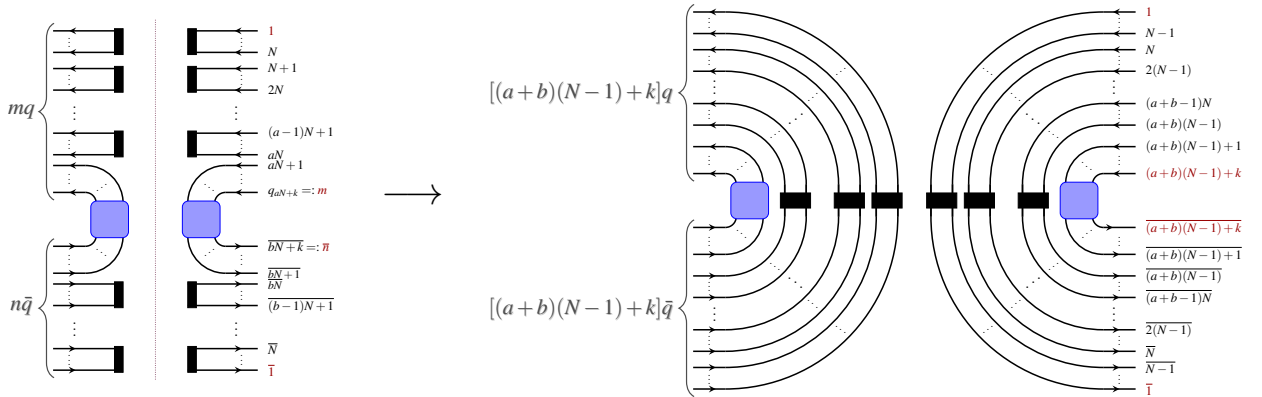


Figure 5.3: The operator of Figure 5.2 is transformed into a singlet projector consisting of Kronecker  $\delta$ 's only (no Levi-Civita symbols): Each  $\varepsilon$ -tensor of length  $N$  in the singlet in Figure 5.2 has been transformed into an antisymmetric subsinglet over  $N - 1$  fundamental and antifundamental legs. The subsinglet of Figure 5.2 containing Kronecker  $\delta$ 's only (blue box) remains unchanged. (In this graphic, we have numbered each fundamental leg and each antifundamental leg (marked by the overbar) to keep track of their number.)

Let us summarize:

■ **Theorem 5.4 – General singlets and equivalences:**

Let  $N$  be a particular integer and let  $P_{m,n}^S$  be a singlet projection operator of  $SU(N)$  over  $V^{\otimes m} \otimes (V^*)^{\otimes n}$ .  $P_{m,n}^S$  has to fulfill the following conditions:

- $P_{m,n}^S$  contains exactly  $(a + b)$  antisymmetrizers of length  $N$  ( $a$  of which are antisymmetrizers over fundamental legs, and  $b$  over antifundamental legs) such that

$$m - aN = n - bN =: k \quad (5.133)$$

for some integer  $k$ . Note that  $N$ ,  $m$  and  $n$  do not uniquely determine  $a$ ,  $b$  and  $k$  through eq. (5.133), allowing for several singlet projectors over  $V^{\otimes m} \otimes (V^*)^{\otimes n}$ .

- The remaining  $k$  fundamental and  $k$  antifundamental legs not contained in a Levi-Civita tensor are joined in an  $N$ -independent subsinglet  $P_{m,n,(k)}^S$ .

Then, there exists an  $N$ -independent singlet projection operator  $P_{\alpha,\alpha}^S$  in  $\text{API}\left(SU(N), V^{\otimes \alpha} \otimes (V^*)^{\otimes \alpha}\right)$  for

$$\alpha := (a + b)(N - 1) + k \quad (5.134)$$

that is equivalent to  $P_{m,n}^S$  for the chosen value of  $N$

$$P_{\alpha,\alpha}^S|_N = P_{m,n}^S. \quad (5.135)$$

In particular,  $P_{\alpha,\alpha}^S$  will have the following subsinglet structure:

- $k$  of its fundamental and antifundamental legs will constitute the subsinglet  $P_{m,n,(k)}^S$ ,
- the remaining legs constitute  $(a + b)$  totally antisymmetric subsinglets, each containing exactly  $N - 1$  fundamental and antifundamental legs.

As mentioned in the theorem, eq. (5.133) does not uniquely determine the integers  $a$ ,  $b$  and  $k$  from  $m$ ,  $n$  and  $N$ . An immediate consequence of this is that two different singlets  $Q_1^S$  and  $Q_2^S$  of  $SU(N)$  over  $V^{\otimes m} \otimes (V^*)^{\otimes n}$  may be equivalent to singlets over  $V^{\otimes \alpha_1} \otimes (V^*)^{\otimes \alpha_1}$  and  $V^{\otimes \alpha_2} \otimes (V^*)^{\otimes \alpha_2}$  respectively, where  $\alpha_1 \neq \alpha_2$ . As singlets,  $Q_1^S$  and  $Q_2^S$  remain equivalent (one can always construct the transition operator between them).

## 5.3 Wilson line correlators

As was explained in section 1.6.1 of chapter 1, partial coincidence limits of Wilson line correlators impose constraints on the  $n$ -point functions  $G_{Y,\mathbf{x}_1 \dots \mathbf{x}_n}^{(j)}$  and  $K_{Y,\mathbf{x}_1 \dots \mathbf{x}_n}^{(j)}$  in the parametrization of  $H_{\text{JIMWLK}}$ . In section 5.3.1, we examine several coincidence limits of the correlators of  $3q + 3\bar{q}$ . To this end, we construct the Wilson line correlators using *two* bases of the  $3q + 3\bar{q}$  singlet states (sections 5.3.2.1 and 5.3.2.2), each suited for a particular kind of coincidence limit.

However, in order to discuss coincidence limits, we need to reintroduce the coordinate dependence of the Wilson lines (*c.f.* section 1.6.2): Up until now, this thesis has given a road map for constructing the *global* singlet states of  $SU(N)$ , which is to say that all Wilson lines in question are considered to be in a *total*



coincidence limit (*c.f.* eq. (1.227)). In the present section, the singlet states will be acted upon by an arbitrary product of Wilson lines, and we will study the behaviour of these Wilson line correlators in a *partial* coincidence limit.

In section 5.3.1, we first discuss the physical picture behind a partial coincidence limit. Thereafter, we pinpoint the reason why the two bases previously discussed in section 1.6.2 yielded a simplification of the matrix of correlators  $\langle \mathcal{A} \rangle (Y)$  for certain partial coincidence limits but not for others. Section 5.3.2 applies this new-found wisdom to the Wilson line correlators over  $V^{\otimes 3} \otimes (V^*)^{\otimes 3}$  in two bases, analogously to the discussion in section 1.6.2 for the  $2q + 2\bar{q}$ -correlators.

We end with a brief comment on the equivalence between singlets containing a Levi-Civita tensor and singlets not containing a Levi-Civita tensor in the light of coordinate dependent Wilson lines in section 5.3.3.

### 5.3.1 Coincidence limits: a tale of two bases

Recall from chapter 1 that an  $n$ -point Wilson line correlator describes a projectile (consisting of  $n$  particles) interacting eikonally with a dense gluonic target. Due to the high Lorentz contraction, the target has a  $\delta$ -function-like support in the  $x^-$ -direction, and is thus fully described by a distribution function depending only on the transverse coordinate  $\mathbf{x}$ . The interaction of a particular parton with the target will depend on the transverse coordinate at which the parton's worldline pierces through the  $x^- = 0$  plane. A priori, there is no reason to believe that the target is uniform in the transverse plane. Hence, each parton will in general be acted upon by a *distinct* Wilson line  $U_{\mathbf{x}_i} \in SU(N)$ . For example, a projectile comprised of 3 quarks probing the target at coordinates  $\mathbf{x}$ ,  $\mathbf{y}$  and  $\mathbf{z}$  respectively will pick up the Wilson lines

$$\mathbf{U} := U_{\mathbf{x}} \otimes U_{\mathbf{y}} \otimes U_{\mathbf{z}} \in SU(N) \times SU(N) \times SU(N), \quad (5.136)$$

which realizes a particular representation of the product group  $SU(N) \times SU(N) \times SU(N)$  on  $V^{\otimes 3}$ . In certain situations, we may, however, have reason to assume that two (or more) particular Wilson lines in the correlator coincide. This may, for example, happen when the distance  $r$  between two partons probing the target is very small (compared to the size of the target), allowing us to approximate  $r \approx 0$ . In this case, the two partons are assumed to probe the target at essentially the same transverse coordinate,  $\mathbf{x} \rightarrow \mathbf{y}$ , and thus pick up the same Wilson line in the interaction,  $U_{\mathbf{x}} \otimes U_{\mathbf{y}} \rightarrow U_{\mathbf{x}} \otimes U_{\mathbf{x}}$ . For example,

$$U_{\mathbf{x}} \otimes U_{\mathbf{y}} \otimes U_{\mathbf{z}} \xrightarrow{\mathbf{x} \rightarrow \mathbf{y}} U_{\mathbf{x}} \otimes U_{\mathbf{x}} \otimes U_{\mathbf{z}}. \quad (5.137)$$

A Wilson line correlator is projected onto global singlet states  $|i\rangle, |j\rangle$  of  $SU(N)$  in order to describe a physical observable (*c.f.* chapter 1). Since we may choose these states to be orthonormal, Wilson line correlators in the coincidence of *all* its coordinates must obey

$$\begin{aligned} \langle j | U_{\mathbf{x}_1} \otimes \cdots \otimes U_{\mathbf{x}_m} \otimes U_{\mathbf{y}_1}^\dagger \otimes \cdots \otimes U_{\mathbf{y}_n}^\dagger | i \rangle \\ \xrightarrow{\text{total coincidence limit}} \langle j | U_{\mathbf{x}_1} \otimes \cdots \otimes U_{\mathbf{x}_1} \otimes U_{\mathbf{x}_1}^\dagger \otimes \cdots \otimes U_{\mathbf{x}_1}^\dagger | i \rangle \\ \xrightarrow{\text{eq. (1.223)}} \langle j | i \rangle = \delta_{ij}. \end{aligned} \quad (5.138)$$

We therefore naively expect more and more Wilson line correlators to vanish as increasingly more coincidence limits are considered. We may think of partial coincidence limits as “activating” more and more of the

orthogonality between the singlet states. In section 1.6.1, we found this to be partly true: While a certain partial coincidence limit causes several Wilson line correlators to vanish in one basis, the same limit in a different basis may merely establish a complicated relation between correlators, *c.f.* eqns. (1.247) and (1.248). In particular, we looked at two kinds of bases: one consisting of symmetrizers and antisymmetrizers, and one consisting of (anti-) fundamental as well as adjoint index lines. We then proceeded to claim that the fact that certain limits are better suited for one basis than the other can be attributed to the properties of the building blocks of the specific basis. In this section, we will make this statement more precise.

### 5.3.1.1 Symmetrizers and antisymmetrizers

Let us first consider a basis for the singlet states that consists of symmetrizers and antisymmetrizers; an example of this are the operators in  $\mathfrak{S}_k$  and the singlet states constructed from it, *c.f.* Theorem 5.2.

In such a basis, a particular Wilson line correlator may contain two index lines that are in an antisymmetric combination before the interaction and in a symmetric combination after the interaction,

$$\mathbf{S}_{12}(U_{\mathbf{x}} \otimes U_{\mathbf{y}})\mathbf{A}_{12} = \begin{array}{c} \leftarrow U_{\mathbf{x}} \rightarrow \\ \leftarrow U_{\mathbf{y}} \rightarrow \end{array} \begin{array}{c} \leftarrow \\ \leftarrow \end{array}, \quad \text{where } U_{\mathbf{x}} \otimes U_{\mathbf{y}} \in \text{SU}(N) \times \text{SU}(N), \quad (5.139)$$

or vice versa. An example of this are the top two index lines in the Wilson line correlator

$$\left\langle \frac{3}{N(N^2-1)} \begin{array}{c} \text{Wilson line correlator diagram} \end{array} \right\rangle (Y), \quad (5.140)$$

where the blue slab behind the Wilson line arrowheads reminds us that not all Wilson lines are equal (i.e. gauge equivalent to  $\mathbb{1}$ ), *c.f.* Figure 1.6 in chapter 1.

Let us decompose the symmetrizer and antisymmetrizer in (5.139) into their primitive invariants,

$$\begin{array}{c} \leftarrow U_{\mathbf{x}} \rightarrow \\ \leftarrow U_{\mathbf{y}} \rightarrow \end{array} \begin{array}{c} \leftarrow \\ \leftarrow \end{array} = \frac{1}{4} \left\{ \begin{array}{c} \leftarrow U_{\mathbf{x}} \leftarrow \\ \leftarrow U_{\mathbf{y}} \leftarrow \end{array} + \begin{array}{c} \text{Crossing } U_{\mathbf{x}} \\ \text{Crossing } U_{\mathbf{y}} \end{array} - \begin{array}{c} \leftarrow U_{\mathbf{x}} \rightarrow \\ \leftarrow U_{\mathbf{y}} \rightarrow \end{array} \begin{array}{c} \text{Crossing } U_{\mathbf{x}} \\ \text{Crossing } U_{\mathbf{y}} \end{array} \right\}. \quad (5.141)$$

Each index line  $\leftarrow$  represents a Kronecker  $\delta$  and is an invariant of each  $U_i \in \text{SU}(N)$  in the tensor product individually, *c.f.* sections 3.1.1 and 4.1,

$$U_i \leftarrow = \leftarrow U_i. \quad (5.142)$$

Eq. (5.142) allows one to pull each Wilson line  $U_{\mathbf{x}}$  and  $U_{\mathbf{y}}$  across the lines of the birdtrack to the other side, for example

$$\begin{array}{c} \text{Crossing } U_{\mathbf{x}} \\ \text{Crossing } U_{\mathbf{y}} \end{array} = \begin{array}{c} \text{Crossing } U_{\mathbf{y}} \\ \text{Crossing } U_{\mathbf{x}} \end{array}. \quad (5.143)$$

Therefore, the operator (5.141) becomes

$$\begin{array}{c} \leftarrow U_{\mathbf{x}} \rightarrow \\ \leftarrow U_{\mathbf{y}} \rightarrow \end{array} \begin{array}{c} \leftarrow \\ \leftarrow \end{array} = \frac{1}{4} \left\{ \left( \begin{array}{c} \leftarrow U_{\mathbf{x}} \leftarrow \\ \leftarrow U_{\mathbf{y}} \leftarrow \end{array} - \begin{array}{c} \leftarrow U_{\mathbf{y}} \leftarrow \\ \leftarrow U_{\mathbf{x}} \leftarrow \end{array} \right) + \left( \begin{array}{c} \text{Crossing } U_{\mathbf{x}} \\ \text{Crossing } U_{\mathbf{y}} \end{array} - \begin{array}{c} \text{Crossing } U_{\mathbf{y}} \\ \text{Crossing } U_{\mathbf{x}} \end{array} \right) \right\}, \quad (5.144)$$

which is nonzero in general, but vanishes in the limit  $\mathbf{x} \rightarrow \mathbf{y}$ . The underlying reason for this is that the

product  $U_{\mathbf{x}} \otimes U_{\mathbf{y}} \rightarrow U_{\mathbf{x}} \otimes U_{\mathbf{x}}$  commutes with both the symmetrizer and the antisymmetrizer, since the latter are *invariants* of  $SU(N)$  (as explained in sections 3.1.1 and 4.1). Thus, commuting  $U_{\mathbf{x}} \otimes U_{\mathbf{x}}$  to either the left or the right end of the operator (5.144) leaves the symmetrizer and antisymmetrizer to act on each other, yielding a null result.

Let us now adapt our graphical notation for Wilson lines to indicate certain partial coincidence limits: In this thesis, we have denoted a product of Wilson lines that is not in a total coincidence limit by a tower of pink arrowheads on a blue slab, for example,

$$U_{\mathbf{x}} \otimes U_{\mathbf{y}} \otimes U_{\mathbf{z}}^{\dagger} \longrightarrow \begin{array}{c} \text{blue slab} \\ \text{pink arrowheads} \end{array}. \quad (5.145)$$

We will graphically indicate a partial coincidence limit between two (or more) Wilson lines *in the same representation* by coinciding the arrowheads,

$$U_{\mathbf{x}} \otimes U_{\mathbf{y}} \otimes U_{\mathbf{z}}^{\dagger} \xrightarrow{\mathbf{x}=\mathbf{y}} \begin{array}{c} \text{blue slab} \\ \text{coinciding arrowheads} \end{array}. \quad (5.146)$$

This notation is particularly intuitive as it mirrors the physical situation to which it corresponds: Wilson lines picked up in *distinct* transverse locations are drawn in different places on the paper, while Wilson lines with *the same* transverse coordinate are drawn in the same place on the paper.

We emphasize that notation (5.146) can only be used for Wilson lines in the same representation. The graphical notation for a coincidence limit between a fundamental and an antifundamental Wilson line will be discussed in section 5.3.1.2.

In the graphical notation (5.146), the invariance condition

$$\mathbf{U} \circ \rho = \rho \circ \mathbf{U}, \quad \text{where } \mathbf{U} \in SU(N) \times \dots \times SU(N) \text{ and } \rho \text{ is an invariant of } SU(N) \quad (5.147)$$

(*c.f.* eqns. (3.3) and (4.3)) can, for the example of two index legs, be written as

$$\left[ \begin{array}{c} \text{box } \rho \\ \text{two legs} \end{array}, \begin{array}{c} \text{blue slab} \\ \text{coinciding arrowheads} \end{array} \right] = 0. \quad (5.148a)$$

For a general tensor product  $U_{\mathbf{x}} \otimes U_{\mathbf{y}} \in SU(N) \times SU(N)$  with  $\mathbf{x} \neq \mathbf{y}$ , this relation breaks down,

$$\left[ \begin{array}{c} \text{box } \rho \\ \text{two legs} \end{array}, \begin{array}{c} \text{blue slab} \\ \text{separated arrowheads} \end{array} \right] \neq 0, \quad (5.148b)$$

as we have seen in the example (5.144).

Using notation (5.146), the coincidence limit  $\mathbf{x} \rightarrow \mathbf{y}$  of the Wilson line correlator (5.139) is expressed as

$$\mathcal{S}_{12}(U_{\mathbf{x}} \otimes U_{\mathbf{y}}) \mathcal{A}_{12} := \begin{array}{c} \text{diagram with two legs and blue slab} \end{array} \xrightarrow{\mathbf{x} \rightarrow \mathbf{y}} \begin{array}{c} \text{diagram with coinciding arrowheads} \end{array}. \quad (5.149)$$

Since both the symmetrizer and the antisymmetrizer are invariants of  $SU(N)$ , the commutation relation (5.148a)

indeed causes the operator (5.149) to vanish,

$$\begin{array}{c} \left[ \text{diagram: two vertical lines, left one white, right one black, with a red dot between them} \right] \\ \left[ \text{diagram: two vertical lines, left one white, right one black, with a red dot between them, and a blue vertical bar to the right} \right] \end{array} \stackrel{\text{eq. (5.148a)}}{=} \begin{array}{c} \left[ \text{diagram: two vertical lines, left one white, right one black, with a red dot between them} \right] \\ \left[ \text{diagram: two vertical lines, left one white, right one black, with a red dot between them, and a blue vertical bar to the right} \right] \end{array} = \underbrace{\left[ \text{diagram: two vertical lines, left one white, right one black, with a red dot between them} \right]}_{=0} = 0, \quad (5.150)$$

as claimed.

In summary, a basis of singlet states built from symmetrizers and antisymmetrizers (such as the basis constructed from bending the MOLD operators and their transition operators) is particularly well suited for studying coincidence limits of two or more Wilson lines in the same representation. The reason for this is that many Wilson line correlators will vanish due to symmetrizers and antisymmetrizers having more than one common leg when a partial coincidence limit is invoked (as exhibited in eq. (5.150)). We will put this insight to good use in section 5.3.2.1 where we study the  $3q + 3\bar{q}$  Wilson line correlators in such a basis.

### 5.3.1.2 (Anti-) fundamental and adjoint lines

As exemplified in section 1.6.2, a coincidence limit between a fundamental and an antifundamental Wilson line is best studied in what we call a *Fierz basis* (c.f. eqns. (1.232) and (1.233)). The underlying reason for this is that many correlators will become zero by virtue of the generator  $[t^a]_{ki}$  being traceless (c.f. eq. (5.115)). Let us explain: A particular Wilson line correlator in the Fierz basis may contain a fundamental and an antifundamental Wilson line that combine into a singlet before the interaction, and into an adjoint line after the interaction,

$$\frac{1}{\sqrt{2}} t^a \mathbf{U} \delta = a \dots \left( \text{diagram: two curved lines, one labeled } U_{\mathbf{x}} \text{ and the other } U_{\mathbf{x}'}^\dagger \right), \quad \text{for } \mathbf{U} := U_{\mathbf{x}} \otimes U_{\mathbf{x}'}^\dagger \in \text{SU}(N) \times \text{SU}(N) \quad (5.151)$$

(recall the normalization factor  $\frac{1}{\sqrt{2}}$  from eq. (5.36)), or vice versa. An example of this are the top and middle pairs of Wilson lines in the operator

$$\left\langle \frac{1}{N^2 \sqrt{2(N^2-1)}} \left[ \text{diagram: two vertical lines, one blue and one red, with a red dot between them} \right] \right\rangle (Y). \quad (5.152)$$

Let us be more careful when writing eq. (5.151) and add all matrix indices,

$$\frac{1}{\sqrt{2}} [t^a]_{ik} [U_{\mathbf{x}}]_{kl} \delta_{lj} [U_{\mathbf{x}'}^\dagger]_{ji} = \frac{1}{\sqrt{2}} [t^a]_{ik} [U_{\mathbf{x}}]_{kj} [U_{\mathbf{x}'}^\dagger]_{ji}, \quad (5.153)$$

where we have used the property of the Kronecker  $\delta$  to contract indices. In the last expression in (5.153), we encounter a tensor product of two Wilson lines that have been contracted in one index. The coincidence limit  $\mathbf{x} \rightarrow \mathbf{x}'$  together with the unitarity property of the Wilson lines (they are elements of  $\text{SU}(N)$ ) reduces (5.153) to

$$\frac{1}{\sqrt{2}} [t^a]_{ik} [U_{\mathbf{x}}]_{kj} [U_{\mathbf{x}'}^\dagger]_{ji} \xrightarrow{\mathbf{x} \rightarrow \mathbf{x}'} \frac{1}{\sqrt{2}} [t^a]_{ik} \underbrace{[U_{\mathbf{x}}]_{kj} [U_{\mathbf{x}}^\dagger]_{ji}}_{=\delta_{ki}} = \frac{1}{\sqrt{2}} [t^a]_{ik} \delta_{ki} = \frac{1}{\sqrt{2}} \text{tr}(t^a) = 0, \quad (5.154a)$$

yielding the desired simplification. In birdtrack notation, this can equivalently be written as

$$a \cdots \begin{array}{c} \color{blue}{\curvearrowright} \\ \color{red}{\curvearrowleft} \end{array} \xrightarrow{x \rightarrow x'} a \cdots \begin{array}{c} \curvearrowright \\ \curvearrowleft \end{array} \stackrel{\text{eq. (5.36)}}{=} \frac{1}{\sqrt{2}} \text{tr}(t^a) = 0 . \quad (5.154b)$$

Let us now also introduce a graphical notation for the partial coincidence limit between a fundamental and an antifundamental Wilson line. If such a pair of Wilson lines combines into the unique  $q\bar{q}$ -dipole singlet before and after the interaction, a coincidence limit between these two Wilson lines will merely yield a factor  $N$ , such that we can write

$$\begin{array}{c} \color{blue}{\curvearrowright} \\ \color{red}{\curvearrowleft} \end{array} \xrightarrow{x \rightarrow x'} \begin{array}{c} \curvearrowright \\ \curvearrowleft \end{array} = N . \quad (5.155a)$$

On the other hand, if the fundamental and antifundamental Wilson lines combine into a color octet (i.e. a gluon) before and after the interaction, a coincidence limit will yield an adjoint Wilson line, such that

$$a \cdots \begin{array}{c} \color{blue}{\curvearrowright} \\ \color{red}{\curvearrowleft} \end{array} \cdots b \xrightarrow{x \rightarrow x'} a \cdots \color{blue}{\curvearrowright} \cdots b = a \cdots \color{blue}{\curvearrowright} \cdots b , \quad (5.155b)$$

where the second equation follows from the fact that adjoint Wilson lines are real (*c.f.* eq. (1.116)). Eqns. (5.154b) and (5.155) exhaust all possible outcomes of coincidence limits between a fundamental and an antifundamental Wilson line in the Fierz basis.<sup>18</sup>

## 5.3.2 Wilson line correlators of $3q + 3\bar{q}$ and their coincidence limits

In this section, we construct the matrix of Wilson line correlators  $\langle \mathcal{A} \rangle(Y)$  for three  $q\bar{q}$ -pairs. We then investigate  $\langle \mathcal{A} \rangle(Y)$  by considering various coincidence limits between the coordinates of the Wilson lines. As discussed in section 1.6.2, the constraint equations resulting from imposing various coincidence limits bring about simplifications in the matrix  $\langle \mathcal{A} \rangle(Y)$ , provided it is written in a suitable basis. We therefore discuss the Wilson line correlators for  $3q + 3\bar{q}$  in two distinct bases in sections 5.3.2.1 and 5.3.2.2 respectively.

### 5.3.2.1 Hermitian Young projector basis

The elements of the matrix of Wilson line correlators  $\langle \mathcal{A} \rangle(Y)$  take the form

$$\langle \mathbf{m}_{kl} | \mathbf{U} | \mathbf{m}_{ij} \rangle , \quad (5.156)$$

where  $|\mathbf{m}_{ij}\rangle, |\mathbf{m}_{kl}\rangle$  are singlet states of  $SU(N)$  over  $V^{\otimes 3} \otimes (V^*)^{\otimes 3}$ , and  $\mathbf{U}$  is a tensor product of Wilson lines describing the eikonal interaction. Constructing the singlet states by bending the elements of  $\mathfrak{S}_3$  in accordance with Theorem 5.2, the top three index lines of the correlator will be in the fundamental, and the bottom three lines in the antifundamental representation. Thus  $\mathbf{U}$  must be of the form

$$\mathbf{U} := U_x \otimes U_y \otimes U_z \otimes U_{z'}^\dagger \otimes U_{y'}^\dagger \otimes U_{x'}^\dagger . \quad (5.157)$$

<sup>18</sup>That is, provided one wishes to achieve the maximum possible simplification of the matrix of correlators. If one needs to investigate the coincidence limit between a fundamental and an antifundamental Wilson line where neither of the three situations (5.154b) and (5.155) hold, one should consider a change of basis, *c.f.* eq. (1.234) in chapter 1.

In order to avoid clutter when translating the correlators into the birdtrack language, we will suppress the normalization constants and instead indicate that the operators are properly normalized by the symbol  $\blacktriangle$ , for example,

$$\frac{3}{N+1} \sqrt{\frac{2}{(N+1)N(N-1)}} \cdot \text{[Diagram 1]} \stackrel{\blacktriangle}{=} \text{[Diagram 2]}, \quad (5.158)$$

where we have placed  $\blacktriangle$  in the center of the birdtrack to save space. This allows us to focus our discussion on the birdtrack part of the correlators for now. However, we emphasize that one needs to carefully take into account the correct normalization constant in order to obtain meaningful results in physics calculations.

The matrix  $\langle \mathcal{A} \rangle (Y)$  containing all singlet Wilson line correlators for  $3q + 3\bar{q}$  (in a basis of symmetrizers and antisymmetrizers) is given by

$$\langle \mathcal{A} \rangle (Y) = \left( \begin{array}{cccccc} \text{[Diagram 1]} & \text{[Diagram 2]} & \text{[Diagram 3]} & \text{[Diagram 4]} & \text{[Diagram 5]} & \text{[Diagram 6]} \\ \text{[Diagram 7]} & \text{[Diagram 8]} & \text{[Diagram 9]} & \text{[Diagram 10]} & \text{[Diagram 11]} & \text{[Diagram 12]} \\ \text{[Diagram 13]} & \text{[Diagram 14]} & \text{[Diagram 15]} & \text{[Diagram 16]} & \text{[Diagram 17]} & \text{[Diagram 18]} \\ \text{[Diagram 19]} & \text{[Diagram 20]} & \text{[Diagram 21]} & \text{[Diagram 22]} & \text{[Diagram 23]} & \text{[Diagram 24]} \\ \text{[Diagram 25]} & \text{[Diagram 26]} & \text{[Diagram 27]} & \text{[Diagram 28]} & \text{[Diagram 29]} & \text{[Diagram 30]} \\ \text{[Diagram 31]} & \text{[Diagram 32]} & \text{[Diagram 33]} & \text{[Diagram 34]} & \text{[Diagram 35]} & \text{[Diagram 36]} \end{array} \right) (Y). \quad (5.159)$$

Due to the (anti-)symmetrizer structure of the correlators in this matrix, it is particularly suited to the study of coincidence limits between two Wilson lines in the same representation, *c.f.* section 1.6.1. For example, a coincidence limit between the top two Wilson lines ( $\mathbf{x} \rightarrow \mathbf{y}$ ) will cause correlators containing both

a symmetrizer and an antisymmetrizer over the top two indices to vanish (as exemplified in eq. (5.150)),

$$\langle \mathcal{A} \rangle (Y) = \left( \begin{array}{cccccc} \text{diagram} & \text{diagram} & \text{diagram} & \text{diagram} & \text{diagram} & \text{diagram} \\ \text{diagram} & \text{diagram} & \text{diagram} & \text{diagram} & \text{diagram} & \text{diagram} \\ \text{diagram} & \text{diagram} & \text{diagram} & \text{diagram} & \text{diagram} & \text{diagram} \\ \text{diagram} & \text{diagram} & \text{diagram} & \text{diagram} & \text{diagram} & \text{diagram} \\ \text{diagram} & \text{diagram} & \text{diagram} & \text{diagram} & \text{diagram} & \text{diagram} \\ \text{diagram} & \text{diagram} & \text{diagram} & \text{diagram} & \text{diagram} & \text{diagram} \end{array} \right) (Y) \xrightarrow{x \rightarrow y} \left( \begin{array}{cccccc} \text{diagram} & \text{diagram} & \text{diagram} & 0 & 0 & 0 \\ \text{diagram} & \text{diagram} & \text{diagram} & 0 & 0 & 0 \\ \text{diagram} & \text{diagram} & \text{diagram} & 0 & 0 & 0 \\ 0 & 0 & 0 & \text{diagram} & \text{diagram} & \text{diagram} \\ 0 & 0 & 0 & \text{diagram} & \text{diagram} & \text{diagram} \\ 0 & 0 & 0 & \text{diagram} & \text{diagram} & \text{diagram} \end{array} \right) (Y). \quad (5.160)$$

Thus, the limit  $x \rightarrow y$  causes the matrix  $\langle \mathcal{A} \rangle (Y)$  to become block-diagonal. The additional coincidence limit between the bottom two antiquark coordinates ( $x' \rightarrow y'$ ) offers even more simplification,

$$\langle \mathcal{A} \rangle (Y) \xrightarrow{x \rightarrow y} \left( \begin{array}{cccccc} \text{diagram} & \text{diagram} & \text{diagram} & 0 & 0 & 0 \\ \text{diagram} & \text{diagram} & \text{diagram} & 0 & 0 & 0 \\ \text{diagram} & \text{diagram} & \text{diagram} & 0 & 0 & 0 \\ 0 & 0 & 0 & \text{diagram} & \text{diagram} & \text{diagram} \\ 0 & 0 & 0 & \text{diagram} & \text{diagram} & \text{diagram} \\ 0 & 0 & 0 & \text{diagram} & \text{diagram} & \text{diagram} \end{array} \right) (Y) \xrightarrow{x' \rightarrow y'} \left( \begin{array}{cccccc} \text{diagram} & \text{diagram} & 0 & 0 & 0 & 0 \\ \text{diagram} & \text{diagram} & 0 & 0 & 0 & 0 \\ 0 & 0 & \text{diagram} & 0 & 0 & 0 \\ 0 & 0 & 0 & \text{diagram} & 0 & 0 \\ 0 & 0 & 0 & 0 & \text{diagram} & \text{diagram} \\ 0 & 0 & 0 & 0 & \text{diagram} & \text{diagram} \end{array} \right) (Y). \quad (5.161)$$

If both limits ( $x \rightarrow y$  and  $x' \rightarrow y'$ ) are implemented, only two  $2 \times 2$  blocks and two  $1 \times 1$  blocks remain. It is interesting to notice that the  $2 \times 2$  blocks are comprised of the correlators obtained by bending those projection operators in  $\mathfrak{S}_3$  that correspond to Young tableaux with the same parent tableau. On the other hand, the  $1 \times 1$  blocks originate from bending the two transition operators in  $\mathfrak{S}_3$ . This however could have been anticipated since the operators of  $\mathfrak{S}_3$  with the same parent operator have the same symmetry structure in the topmost index pair by construction.<sup>19</sup> We further comment on this phenomenon in section 9.2.

### 5.3.2.2 Fierz basis

Let us now discuss the coincidence limits between a fundamental and an antifundamental representation. As exemplified in section 5.3.1.2, the Fierz basis given in eq. (5.113) yields the most simplification in such a

<sup>19</sup>Depending on the MOLD of the corresponding Young tableaux, two operators in  $\mathfrak{S}_k$  with the same parent operator may have the same symmetry structure in the  $\leq (k-1)$  topmost index lines. This follows immediately from the construction of the MOLD operators, see Theorem 3.5.

limit. In this case, the tensor product of Wilson lines  $\mathbf{U}$  in the correlator must be ordered as

$$\mathbf{U} := U_x \otimes U_{x'}^\dagger \otimes U_y \otimes U_{y'}^\dagger \otimes U_z \otimes U_{z'}^\dagger . \quad (5.162)$$

Once again suppressing the normalization constants to avoid clutter (we indicate that the correlators are properly normalized by the symbol  $\hat{\mathfrak{A}}$ ), the matrix of Wilson line correlators in the basis (5.113) becomes

$$\langle \mathcal{A} \rangle (Y) = \left( \begin{array}{cccccc} \hat{\mathfrak{A}} & \hat{\mathfrak{A}} & \hat{\mathfrak{A}} & \hat{\mathfrak{A}} & \hat{\mathfrak{A}} & \hat{\mathfrak{A}} \\ \hat{\mathfrak{A}} & \hat{\mathfrak{A}} & \hat{\mathfrak{A}} & \hat{\mathfrak{A}} & \hat{\mathfrak{A}} & \hat{\mathfrak{A}} \\ \hat{\mathfrak{A}} & \hat{\mathfrak{A}} & \hat{\mathfrak{A}} & \hat{\mathfrak{A}} & \hat{\mathfrak{A}} & \hat{\mathfrak{A}} \\ \hat{\mathfrak{A}} & \hat{\mathfrak{A}} & \hat{\mathfrak{A}} & \hat{\mathfrak{A}} & \hat{\mathfrak{A}} & \hat{\mathfrak{A}} \\ \hat{\mathfrak{A}} & \hat{\mathfrak{A}} & \hat{\mathfrak{A}} & \hat{\mathfrak{A}} & \hat{\mathfrak{A}} & \hat{\mathfrak{A}} \\ \hat{\mathfrak{A}} & \hat{\mathfrak{A}} & \hat{\mathfrak{A}} & \hat{\mathfrak{A}} & \hat{\mathfrak{A}} & \hat{\mathfrak{A}} \end{array} \right) (Y) . \quad (5.163)$$

Indeed, a coincidence limit between the bottommost two Wilson lines ( $z \rightarrow z'$ ) of the matrix (5.163) causes many of its elements to vanish due to relation (5.154),

$$\langle \mathcal{A} \rangle (Y) = \left( \begin{array}{cccccc} \hat{\mathfrak{A}} & \hat{\mathfrak{A}} & \hat{\mathfrak{A}} & \hat{\mathfrak{A}} & \hat{\mathfrak{A}} & \hat{\mathfrak{A}} \\ \hat{\mathfrak{A}} & \hat{\mathfrak{A}} & \hat{\mathfrak{A}} & \hat{\mathfrak{A}} & \hat{\mathfrak{A}} & \hat{\mathfrak{A}} \\ \hat{\mathfrak{A}} & \hat{\mathfrak{A}} & \hat{\mathfrak{A}} & \hat{\mathfrak{A}} & \hat{\mathfrak{A}} & \hat{\mathfrak{A}} \\ \hat{\mathfrak{A}} & \hat{\mathfrak{A}} & \hat{\mathfrak{A}} & \hat{\mathfrak{A}} & \hat{\mathfrak{A}} & \hat{\mathfrak{A}} \\ \hat{\mathfrak{A}} & \hat{\mathfrak{A}} & \hat{\mathfrak{A}} & \hat{\mathfrak{A}} & \hat{\mathfrak{A}} & \hat{\mathfrak{A}} \\ \hat{\mathfrak{A}} & \hat{\mathfrak{A}} & \hat{\mathfrak{A}} & \hat{\mathfrak{A}} & \hat{\mathfrak{A}} & \hat{\mathfrak{A}} \end{array} \right) (Y) \xrightarrow{z \rightarrow z'} \left( \begin{array}{cccccc} \hat{\mathfrak{A}} & \hat{\mathfrak{A}} & 0 & 0 & 0 & 0 \\ \hat{\mathfrak{A}} & \hat{\mathfrak{A}} & 0 & 0 & 0 & 0 \\ 0 & 0 & \hat{\mathfrak{A}} & \hat{\mathfrak{A}} & \hat{\mathfrak{A}} & \hat{\mathfrak{A}} \\ 0 & 0 & \hat{\mathfrak{A}} & \hat{\mathfrak{A}} & \hat{\mathfrak{A}} & \hat{\mathfrak{A}} \\ 0 & 0 & \hat{\mathfrak{A}} & \hat{\mathfrak{A}} & \hat{\mathfrak{A}} & \hat{\mathfrak{A}} \\ 0 & 0 & \hat{\mathfrak{A}} & \hat{\mathfrak{A}} & \hat{\mathfrak{A}} & \hat{\mathfrak{A}} \end{array} \right) (Y) . \quad (5.164)$$

In the limit  $z \rightarrow z'$ ,  $\langle \mathcal{A} \rangle (Y)$  has become block-diagonal. In fact, the upper left block becomes the matrix of correlators for  $2q + 2\bar{q}$  given in [71] and paraphrased in eq. (1.230). The  $4 \times 4$  block gives the singlet Wilson line correlators for  $2q + 2\bar{q} + g$ .

Performing an additional coincidence limit between the middle pair of Wilson lines ( $y \rightarrow y'$ ) gives rise to



further simplifications,

$$\langle \mathcal{A} \rangle (Y) \xrightarrow{z \rightarrow z'} \left( \begin{array}{cccccc}
 \text{[Diagram 1]} & 0 & 0 & 0 & 0 & 0 \\
 \text{[Diagram 2]} & 0 & 0 & 0 & 0 & 0 \\
 0 & 0 & \text{[Diagram 3]} & \text{[Diagram 4]} & \text{[Diagram 5]} & \text{[Diagram 6]} \\
 0 & 0 & \text{[Diagram 7]} & \text{[Diagram 8]} & \text{[Diagram 9]} & \text{[Diagram 10]} \\
 0 & 0 & \text{[Diagram 11]} & \text{[Diagram 12]} & \text{[Diagram 13]} & \text{[Diagram 14]} \\
 0 & 0 & \text{[Diagram 15]} & \text{[Diagram 16]} & \text{[Diagram 17]} & \text{[Diagram 18]}
 \end{array} \right) (Y) \xrightarrow{y \rightarrow y'} \left( \begin{array}{cccccc}
 \text{[Diagram 19]} & 0 & 0 & 0 & 0 & 0 \\
 0 & \text{[Diagram 20]} & 0 & 0 & 0 & 0 \\
 0 & 0 & \text{[Diagram 21]} & 0 & 0 & 0 \\
 0 & 0 & 0 & \text{[Diagram 22]} & \text{[Diagram 23]} & \text{[Diagram 24]} \\
 0 & 0 & 0 & \text{[Diagram 25]} & \text{[Diagram 26]} & \text{[Diagram 27]} \\
 0 & 0 & 0 & \text{[Diagram 28]} & \text{[Diagram 29]} & \text{[Diagram 30]}
 \end{array} \right) (Y) . \tag{5.165}$$

In this limit, we recover the correlator of the  $q\bar{q}$ -dipole in the top left corner, and the Wilson line correlator for  $q + \bar{q} + g$  twice on the diagonal. The bottom right  $3 \times 3$  block yields the correlators for  $q + \bar{q} + 2g$ .

At leading order, the JIMWLK evolution of the 2-point function (corresponding to a  $q\bar{q}$ -pair) is propelled by the 3-point function containing an additional gluon,  $q\bar{q} + g$ , [71]. In other words, the evolution of the Wilson line correlator in the top left corner of (5.165) is actuated by the second element on the diagonal (equivalently the third element, since they are equal) of (5.165). Their JIMWLK evolution, in turn, is driven by the bottom  $3 \times 3$  block of (5.165), creating an “evolution hierarchy” within the matrix of correlators  $\langle \mathcal{A} \rangle (Y)$ . This hierarchy is currently being investigated by R. Moerman and H. Weigert [83].

### 5.3.3 Singlets containing Levi-Civita tensors

Before concluding this chapter, let us once more comment on the equivalence between singlets containing a Levi-Civita tensor and singlets not containing a Levi-Civita tensor, in the light of coordinate dependent Wilson lines. When we first showed this equivalence in section 5.2.2, we acted *the same* group element  $U^{(\dagger)}$  on each leg of a singlet operator in order to transform fundamental into antifundamental legs (and vice versa) by means of the Leibniz formula (5.30), see section 5.2.2.1. Introducing a coordinate dependence on the group elements  $U^{(\dagger)}$  therefore gives rise to an additional challenge. In this section, we will see how to overcome this.

Consider, once again, the baryon projector

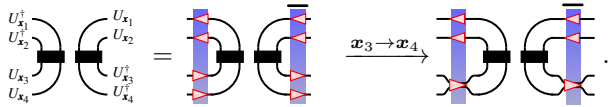
$$\mathbf{A}_{123} = \begin{array}{c} \leftarrow \\ \leftarrow \\ \leftarrow \\ \leftarrow \end{array} \xrightarrow{\dim(V)=N=3} \begin{array}{c} \leftarrow \\ \leftarrow \\ \leftarrow \\ \leftarrow \end{array} . \tag{5.166}$$

As was done in section 5.2.2.1, we will show that  $\mathbf{A}_{123}$  is equivalent to the totally antisymmetric singlet over  $V^{\otimes 2} \otimes (V^*)^{\otimes 2}$ :

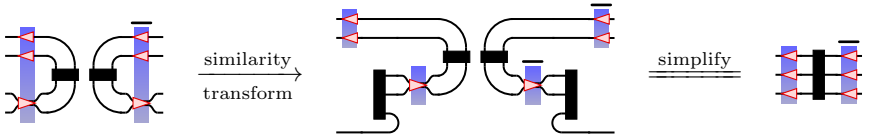
$$\begin{array}{c} \leftarrow \\ \leftarrow \\ \leftarrow \\ \leftarrow \end{array} \quad \text{and} \quad \begin{array}{c} \leftarrow \\ \leftarrow \\ \leftarrow \\ \leftarrow \end{array} \quad \text{are equivalent for } N = 3 . \tag{5.167}$$

Previously, we have acted the same group element of  $SU(N)$  (Wilson line) on each leg of the singlet over  $V^{\otimes 2} \otimes (V^*)^{\otimes 2}$  and then used the Leibniz identity to show the desired equivalence (5.167). In other words, for the Leibniz identity to apply, each Wilson is taken to be at the same transverse coordinate (*c.f.* the sketch of the derivation of the Leibniz identity in section 5.1.4.1).

The following observation will allow us to introduce coordinate dependence on the Wilson lines in the proof of statement (5.167), while still using essentially the same strategy as in section 5.2.2.1: An interaction between the baryon projector and the target gives rise to *at most* three distinct Wilson lines since  $\mathbf{A}_{123}$  contains exactly three legs. Thus, when showing the equivalence (5.167), we need to consider at most three distinct Wilson lines acting on the legs of the  $2q + 2\bar{q}$  operator. In particular, we are allowed to consider a coincidence limit between the two Wilson lines acting on the bottom two legs of this operator,

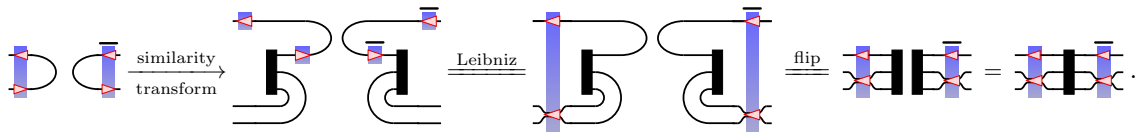

(5.168)

This coincidence limit is sufficient to use the Leibniz identity to transform the two antifundamental index lines into a fundamental line as we did before (in section 5.2.2.1),

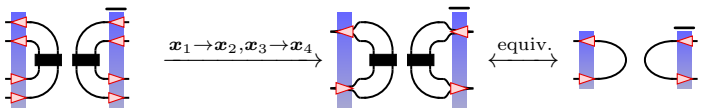

(5.169)

Thus, we conclude that the equivalence (5.167) indeed holds for  $\dim(V) = N = 3$  in the coincidence limit  $\mathbf{x}_3 \rightarrow \mathbf{x}_4$ . The strategy exemplified here can immediately be extended to general singlet projectors such as Figure 5.2.

On the other hand, showing equivalence between the meson and the baryon projectors (as in eq. (5.131)) forces the Wilson lines acting on the bottom two index lines of  $\mathbf{A}_{123}$  into a coincidence limit through the Leibniz identity,


(5.170)

Thus, the meson projector  $\curvearrowright \curvearrowleft$  and the baryon projector  $\curvearrowleft \curvearrowright$  are equivalent for  $\dim(V) = N = 3$  in the coincidence limit  $\mathbf{x}_2 = \mathbf{x}_3$ . This further implies that the projector (5.167) is equivalent to the meson projector in the limit  $\mathbf{x}_1 = \mathbf{x}_1$  and  $\mathbf{x}_3 = \mathbf{x}_4$ ,


(5.171)

## Appendix to chapter 5

### 5.A Simplifying the $1q + 1\bar{q}$ Littlewood-Richardson operators (5.43)

In this appendix, we show how to simplify the three operators in equations (5.43) using the birdtrack formalism.

**The identity operator (5.43a):** First, we absorb the smaller antisymmetrizer of length  $(N - 1)$  into one of the Levi-Civita tensors of length  $N$ . For convenience, we then pull the left Levi-Civita symbol to the right,

$$N \cdot \begin{array}{c} \text{---} 1 \\ | | \\ | | \\ \vdots \\ | | \\ \vdots \\ | | \\ \text{---} \bar{q} \end{array} \xrightarrow{\text{absorb}} N \cdot \begin{array}{c} \text{---} 1 \\ | | \\ \text{---} \\ | | \\ \text{---} \bar{q} \end{array} \xrightarrow{\text{pull } \varepsilon} N \cdot \begin{array}{c} \bigcirc \text{---} 1 \\ \bigcirc \text{---} \\ \bigcirc \text{---} \\ | | \\ \vdots \\ | | \\ \text{---} \bar{q} \end{array} . \tag{5.172}$$

Now, we may use the identity (5.32) (keeping in mind that, by construction, both Levi-Civita tensors have length  $N$ ) to write the product  $(\varepsilon^{a_1 a_2 \dots a_N})^\dagger \varepsilon_{b_1 b_2 \dots b_N}$  as an antisymmetrizer,

$$N \cdot \begin{array}{c} \bigcirc \text{---} 1 \\ \bigcirc \text{---} \\ \bigcirc \text{---} \\ | | \\ \vdots \\ | | \\ \text{---} \bar{q} \end{array} \xrightarrow{\text{eq. (5.32)}} N \cdot \begin{array}{c} \bigcirc \text{---} 1 \\ \bigcirc \text{---} \\ \bigcirc \text{---} \\ | | \\ \vdots \\ | | \\ \text{---} \bar{q} \end{array} . \tag{5.173}$$

This is merely an antisymmetrizer with all but one of its legs traced. Using [72, eq. (6.23)], this trace may be carried out, inducing a factor  $1/N$ . This leaves us with

$$N \cdot \begin{array}{c} \text{---} 1 \\ | | \\ | | \\ \vdots \\ | | \\ \text{---} \bar{q} \end{array} = N \cdot \begin{array}{c} \bigcirc \text{---} 1 \\ \bigcirc \text{---} \\ \bigcirc \text{---} \\ | | \\ \vdots \\ | | \\ \text{---} \bar{q} \end{array} = N \frac{1}{N} \cdot \begin{array}{c} \leftarrow \\ \rightarrow \end{array} = \begin{array}{c} \leftarrow \\ \rightarrow \end{array} . \tag{5.174}$$

**The singlet operator (5.43b):** Once again, we may pull the left Levi-Civita tensor to the right and then use identity (5.32) to simplify this operator as

$$N \cdot \text{Diagram} \xrightarrow{\text{pull } \varepsilon} N \cdot \text{Diagram} \xrightarrow{\text{eq. (5.32)}} N \cdot \text{Diagram} \quad (5.175)$$

For simplicity, we will “disentangle” the  $\bar{q}$ -leg for the remainder of this calculation and treat it as a quark leg,

$$N \cdot \text{Diagram} \rightarrow N \cdot \text{Diagram}, \quad (5.176)$$

but we will reverse this at the end of the calculation (in eq. (5.184)). Furthermore, we wish to explicitly *distinguish* the lengths of the two antisymmetrizers in (5.176) for the sake of clarity in the argument to follow. We thus say that the left antisymmetrizer (originating from the LR-tableau) has length  $p$ , while the right antisymmetrizer (originating from the Levi-Civita tensors) has length  $N$ . At the end of the calculation, we will once again set  $p = N$ .

By identity [72, eq. (6.19)], the right antisymmetrizer of length  $N$  in (5.176) can be decomposed as follows:

$$N \cdot \text{Diagram} = \text{Diagram} - (N-1) \cdot \text{Diagram} \quad (5.177)$$

We may absorb the shorter antisymmetrizer(s) into the longer one in each of the terms — in the last term, we pull the rightmost antisymmetrizer over the top to the left of the longer antisymmetrizer and absorb it from the left. This yields

$$N \cdot \text{Diagram} = \text{Diagram} - (N-1) \cdot \text{Diagram} \quad (5.178)$$

We consider each term separately: The first term is just a free index line and a trace over all but one of the indices of the antisymmetrizer of length  $p$ . Again using [72, eq. (6.23)], we can carry out this trace,

$$\text{Diagram} = \left[ \frac{(N-1)! / [N-(p-1)-1]!}{p!} \right] \text{Diagram} \quad (5.179)$$

Setting  $p = N$ , we find

$$\begin{aligned}
 \left( \text{Diagram: circle with concentric circles and a vertical bar, with arrows pointing left and right} \right) &= \left[ \frac{(N-1)!}{N!} \right] \left( \text{Diagram: two horizontal arrows pointing left and right} \right) = \frac{1}{N} \left( \text{Diagram: two horizontal arrows pointing left and right} \right). \quad (5.180)
 \end{aligned}$$

We now simplify the second term in (5.178). This term is just a trace of all except two indices of the antisymmetrizer of length  $p$ . Again we follow [72, eq. (6.23)] to evaluate this trace,

$$\begin{aligned}
 (N-1) \cdot \left( \text{Diagram: circle with concentric circles and a vertical bar, with arrows pointing left and right} \right) &= (N-1) \left[ \frac{(N-2)! / [N - (p-1) - 1]!}{p! / 2!} \right] \left( \text{Diagram: two horizontal arrows pointing left and right} \right). \quad (5.181)
 \end{aligned}$$

Again setting  $p = N$  we find

$$\begin{aligned}
 (N-1) \cdot \left( \text{Diagram: circle with concentric circles and a vertical bar, with arrows pointing left and right} \right) &= \frac{2}{N} \left( \text{Diagram: two horizontal arrows pointing left and right} \right). \quad (5.182)
 \end{aligned}$$

Substituting (5.180) and (5.182) back into (5.178) yields

$$\begin{aligned}
 N \cdot \left( \text{Diagram: circle with concentric circles and a vertical bar, with arrows pointing left and right} \right) &= \frac{1}{N} \left( \text{Diagram: two horizontal arrows pointing left and right} \right) - \frac{2}{N} \left( \text{Diagram: two horizontal arrows pointing left and right} \right) = \frac{1}{N} \left( \text{Diagram: two horizontal arrows crossing} \right). \quad (5.183)
 \end{aligned}$$

Lastly, we have to transform the bottom index leg back into an antiquark leg,

$$\frac{1}{N} \left( \text{Diagram: two horizontal arrows crossing} \right) \rightarrow \frac{1}{N} \left( \text{Diagram: two horizontal arrows, one pointing right and one pointing left} \right). \quad (5.184)$$

In summary, we found that

$$\left( \text{Diagram: vertical bar with a horizontal line above it and a curved line below it, with arrows pointing left and right} \right) = \frac{1}{N} \left( \text{Diagram: two horizontal arrows, one pointing right and one pointing left} \right). \quad (5.185)$$

**The adjoint operator (5.43c):** Once again, we pull the left Levi-Civita tensor to the right and use eq. (5.32) to combine the two  $\varepsilon$ -tensors into an antisymmetrizer of length  $N$ . Furthermore, as we did in the calculation of the singlet operator, we will treat the antiquark leg  $\bar{q}$  as a quark leg, transforming it back at the end of

our calculation. We have:

$$2(N-1) \cdot \left[ \begin{array}{c} \text{---} \\ | \\ | \\ \vdots \\ | \\ | \\ \text{---} \end{array} \right] \rightarrow 2(N-1) \cdot \left[ \begin{array}{c} \bigcirc \\ \bigcirc \\ \vdots \\ \bigcirc \\ \bigcirc \\ \text{---} \end{array} \right]. \quad (5.186)$$

Using the cancellation rules derived in chapter 2, this operator may be simplified as

$$2(N-1) \cdot \left[ \begin{array}{c} \bigcirc \\ \bigcirc \\ \vdots \\ \bigcirc \\ \bigcirc \\ \text{---} \end{array} \right] = 2(N-1) \cdot \left[ \begin{array}{c} \bigcirc \\ \bigcirc \\ \vdots \\ \bigcirc \\ \bigcirc \\ \text{---} \end{array} \right], \quad (5.187)$$

where no additional constant is induced.<sup>20</sup> We begin the simplification process by decomposing the symmetrizer in (5.187) into its primitive invariants,

$$\begin{aligned} 2(N-1) \cdot \left[ \begin{array}{c} \bigcirc \\ \bigcirc \\ \vdots \\ \bigcirc \\ \bigcirc \\ \text{---} \end{array} \right] &= (N-1) \left[ \begin{array}{c} \bigcirc \\ \bigcirc \\ \vdots \\ \bigcirc \\ \bigcirc \\ \text{---} \end{array} \right] + \left[ \begin{array}{c} \bigcirc \\ \bigcirc \\ \vdots \\ \bigcirc \\ \bigcirc \\ \text{---} \end{array} \right] \\ &= (N-1) \left[ \begin{array}{c} \bigcirc \\ \bigcirc \\ \vdots \\ \bigcirc \\ \bigcirc \\ \text{---} \end{array} \right] + \left[ \begin{array}{c} \bigcirc \\ \bigcirc \\ \vdots \\ \bigcirc \\ \bigcirc \\ \text{---} \end{array} \right], \end{aligned} \quad (5.188)$$

where we merely disentangled the index lines of the second term in the bracket in the last step. The first term in (5.188) is an antisymmetrizer of length  $N$  with all but one of its legs traced. Thus, using [72, eq. (6.23)], this term simplifies to

$$(N-1) \cdot \left[ \begin{array}{c} \bigcirc \\ \bigcirc \\ \vdots \\ \bigcirc \\ \bigcirc \\ \text{---} \end{array} \right] = (N-1) \left[ \frac{(N-1)!/[N-(N-1)-1]!}{N!} \right] \begin{array}{c} \longleftarrow \\ \longleftarrow \\ \longleftarrow \\ \longleftarrow \\ \longleftarrow \end{array} = \frac{(N-1)}{N} \begin{array}{c} \longleftarrow \\ \longleftarrow \\ \longleftarrow \\ \longleftarrow \\ \longleftarrow \end{array}. \quad (5.189)$$

The second term in eq. (5.188) is an antisymmetrizer with all but two indices traced,

$$(N-1) \cdot \left[ \begin{array}{c} \bigcirc \\ \bigcirc \\ \vdots \\ \bigcirc \\ \bigcirc \\ \text{---} \end{array} \right] = (N-1) \left[ \frac{(N-2)!/[N-(N-1)-1]!}{N!/2!} \right] \begin{array}{c} \longleftarrow \text{---} \\ \longleftarrow \text{---} \\ \longleftarrow \text{---} \\ \longleftarrow \text{---} \\ \longleftarrow \text{---} \end{array} = \frac{2}{N} \begin{array}{c} \longleftarrow \text{---} \\ \longleftarrow \text{---} \\ \longleftarrow \text{---} \\ \longleftarrow \text{---} \\ \longleftarrow \text{---} \end{array}. \quad (5.190)$$

<sup>20</sup>This is true since the cancelled part of the operator is a Young projection operator with normalization constant  $2(N-1)$ , as can be verified by direct calculation.

Substituting expressions (5.189) and (5.190) back into (5.188) yields

$$2(N-1) \cdot \left[ \text{Diagram: a circle with a vertical line through its center, and a horizontal line passing through the circle and the vertical line} \right] = \frac{(N-1)}{N} \left[ \text{Diagram: two horizontal lines, one above and one below, with arrows pointing left} \right] + \frac{2}{N} \left[ \text{Diagram: two thick vertical lines, one above and one below, with arrows pointing left} \right]. \quad (5.191)$$

Decomposing the antisymmetrizer into its primitive invariants allows for further simplification,

$$2(N-1) \cdot \left[ \text{Diagram: a circle with a vertical line through its center, and a horizontal line passing through the circle and the vertical line} \right] = \frac{(N-1)}{N} \left[ \text{Diagram: two horizontal lines, one above and one below, with arrows pointing left} \right] + \frac{1}{N} \left( \left[ \text{Diagram: two horizontal lines, one above and one below, with arrows pointing left} \right] - \left[ \text{Diagram: two horizontal lines crossing each other} \right] \right) = \left[ \text{Diagram: two horizontal lines, one above and one below, with arrows pointing left} \right] - \frac{1}{N} \left[ \text{Diagram: two horizontal lines crossing each other} \right]. \quad (5.192)$$

It remains to transform the bottom leg back into the antifundamental representation,

$$\left[ \text{Diagram: two horizontal lines, one above and one below, with arrows pointing left} \right] - \frac{1}{N} \left[ \text{Diagram: two horizontal lines crossing each other} \right] \rightarrow \left[ \text{Diagram: two horizontal lines, one above and one below, with arrows pointing left} \right] - \frac{1}{N} \left[ \text{Diagram: a right-facing and a left-facing arc} \right] = \left[ \text{Diagram: a right-facing and a left-facing arc} \right], \quad (5.193)$$

where we used the Fierz identity (5.35) to obtain the operator  $\left[ \text{Diagram: a right-facing and a left-facing arc} \right]$  in the last step. Thus, we obtain

$$2(N-1) \cdot \left[ \text{Diagram: a vertical line with a horizontal line passing through it, and a thick vertical line below it} \right] = \left[ \text{Diagram: a right-facing and a left-facing arc} \right]. \quad (5.194)$$

## 5.B Calculations in the birdtrack formalism

This appendix aims to show how various calculations of section 5.2 could have been performed in the birdtrack language.

### 5.B.1 Scalar product & orthogonality

Consider two singlet states,

$$|\phi^S\rangle = \left[ \text{Diagram: a box labeled } \phi^S \text{ with four index lines} \right] \quad \text{and} \quad |\psi^S\rangle = \left[ \text{Diagram: a box labeled } \psi^S \text{ with four index lines} \right] \implies \langle \psi^S | = \left[ \text{Diagram: a box labeled } \psi^S \text{ with four index lines} \right]. \quad (5.195)$$

We would like to examine whether these two states are orthogonal: The product  $\langle \psi^S | \phi^S \rangle$  of the according birdtracks is formed by connecting the corresponding index lines (*c.f.* eq. (4.9) or [72]),

$$\langle \psi^S | \phi^S \rangle = \left[ \text{Diagram: two boxes, one labeled } \psi^S \text{ and one labeled } \phi^S, \text{ connected by four index lines} \right]. \quad (5.196)$$

Recalling that the trace of any birdtrack operator  $\rho$  is defined to be the operator  $\rho$  with all index lines on the same level connected [72],

$$\rho = \begin{array}{c} \leftarrow \quad \leftarrow \quad \leftarrow \\ \vdots \\ \leftarrow \quad \leftarrow \quad \leftarrow \\ \rho \\ \leftarrow \quad \leftarrow \quad \leftarrow \\ \vdots \\ \leftarrow \quad \leftarrow \quad \leftarrow \end{array} \rightarrow \text{tr}(\rho) := \begin{array}{c} \circlearrowleft \\ \circlearrowright \\ \rho \\ \circlearrowleft \\ \circlearrowright \end{array}, \quad (5.197)$$

it follows that the inner product (5.196) becomes

$$\langle \psi^S | \phi^S \rangle = \text{tr} \left( (\psi^S)^\dagger \phi^S \right), \quad (5.198)$$

the canonical scalar product on  $V^{\otimes m} \otimes (V^*)^{\otimes m}$ . Thus, the scalar product (5.198) is the natural product to use on the space of singlet states, and we define our notion of orthogonality between singlet states with respect to it.

## 5.B.2 Orthogonal singlet projection operators

We explicitly show in the birdtrack language that two singlet projection operators  $P_{ij}^S$  and  $P_{kl}^S$  constructed according to Theorem 5.2 are orthogonal: In appendix 5.B.1 we found that

$$\langle \mathbf{m}_{ij} | \mathbf{m}_{kl} \rangle = \begin{array}{c} \circlearrowleft \\ \circlearrowright \\ \mathbf{m}_{ji} \quad \mathbf{m}_{kl} \\ \circlearrowleft \\ \circlearrowright \end{array} = \text{tr}(\mathbf{m}_{ji} \mathbf{m}_{kl}), \quad (5.199)$$

where we used the fact that  $\mathbf{m}_{ij}^\dagger = \mathbf{m}_{ji}$  (see footnote 13). For  $\mathbf{m}_{ji}, \mathbf{m}_{kl} \in \mathfrak{S}_m$  (as in Theorem 5.2), the trace  $\text{tr}(\mathbf{m}_{ji} \mathbf{m}_{kl})$  vanishes unless  $i = k$  and  $j = l$  such that

$$\text{tr}(\mathbf{m}_{ji} \mathbf{m}_{kl}) = \delta_{ik} \delta_{jl} \text{tr}(\mathbf{m}_{ji} \mathbf{m}_{kl}). \quad (5.200)$$

Thus, we have

$$P_{ij}^S \cdot P_{kl}^S = \frac{1}{\text{tr}(\mathbf{m}_{ji} \mathbf{m}_{ij})} \frac{1}{\text{tr}(\mathbf{m}_{lk} \mathbf{m}_{kl})} \begin{array}{c} \circlearrowleft \\ \circlearrowright \\ \mathbf{m}_{ij} \quad \mathbf{m}_{ji} \quad \mathbf{m}_{kl} \quad \mathbf{m}_{lk} \\ \circlearrowleft \\ \circlearrowright \end{array} \quad (5.201a)$$

$\text{tr}(\mathbf{m}_{ji} \mathbf{m}_{kl}) \delta_{ik} \delta_{jl}$

$$= \frac{\text{tr}(\mathbf{m}_{ji} \mathbf{m}_{kl}) \delta_{ik} \delta_{jl}}{\text{tr}(\mathbf{m}_{ji} \mathbf{m}_{ij}) \text{tr}(\mathbf{m}_{lk} \mathbf{m}_{kl})} \begin{array}{c} \circlearrowleft \\ \circlearrowright \\ \mathbf{m}_{ij} \quad \mathbf{m}_{lk} \\ \circlearrowleft \\ \circlearrowright \end{array} \quad (5.201b)$$



$$= \frac{\delta_{ik}\delta_{jl}}{\text{tr}(\mathbf{m}_{ji}\mathbf{m}_{ij})} \cdot \text{diagram} \quad (5.201c)$$

In summary, the singlet projection operators obtained from reshaping the basis elements in  $\mathfrak{S}_m$  are indeed orthogonal,

$$P_{ij}^S \cdot P_{kl}^S = \delta_{ik}\delta_{jl}P_{ij}^S. \quad (5.202)$$

### 5.B.3 Dimension of the representations corresponding to singlet projection operators

As explained in section 5.2.1.3 (page 235), the trace of a projection operator gives the dimension of the corresponding representation. In the birdtrack language, the trace of an operator is obtained by connecting the index lines on the same level (*c.f.* eq. (5.197)). Thus, the dimension  $\dim(P_{ij}^S)$  of the irreducible representation corresponding to the singlet projection operator  $P_{ij}^S$  is

$$\dim(P_{ij}^S) = \frac{1}{\text{tr}(\mathbf{m}_{ij}^\dagger \mathbf{m}_{ij})} \cdot \text{diagram} = \frac{1}{\text{tr}(\mathbf{m}_{ij}^\dagger \mathbf{m}_{ij})} \cdot \text{diagram} = \frac{\text{tr}(\mathbf{m}_{ij}^\dagger \mathbf{m}_{ij})}{\text{tr}(\mathbf{m}_{ij}^\dagger \mathbf{m}_{ij})} = 1. \quad (5.203)$$

Therefore, the projection operator  $P_{ij}^S$  does indeed correspond to a 1-dimensional representation of  $SU(N)$  over  $V^{\otimes m} \otimes (V^*)^{\otimes m}$  (irrespective of the value of  $N$ ), making it  $N$ -independently a singlet.

### 5.B.4 Transition operators between singlet projectors

In this section, we verify, in the birdtrack language, that the transition operators constructed according to Theorem 5.3 (eq. (5.105)) satisfy eqns. (5.90),

$$T_{ij,kl}^S \cdot P_{kl}^S = T_{ij,kl}^S = P_{ij}^S \cdot T_{ij,kl}^S \quad (5.204a)$$

$$(T_{ij,kl}^S)^\dagger = T_{kl,ij}^S \quad (5.204b)$$

$$T_{ij,kl}^S \cdot T_{kl,ij}^S = P_{ij}^S. \quad (5.204c)$$

Consider two singlet projection operators  $P_{ij}^S$  and  $P_{kl}^S$  given by

$$P_{ij}^S = \frac{1}{\text{tr}(\mathbf{m}_{ij}^\dagger \mathbf{m}_{ij})} \cdot \text{diagram} \quad \text{and} \quad P_{kl}^S = \frac{1}{\text{tr}(\mathbf{m}_{kl}^\dagger \mathbf{m}_{kl})} \cdot \text{diagram} \quad (5.205)$$

according to Theorem 5.2. It will be convenient to define

$$\beta_{ij}^2 := \frac{1}{\text{tr}(\mathbf{m}_{ij}^\dagger \mathbf{m}_{ij})}, \quad (5.206)$$

such that

$$P_{ij}^S = \beta_{ij}^2 \cdot |\mathbf{m}_{ij}\rangle\langle\mathbf{m}_{ij}| \quad \text{and} \quad P_{kl}^S = \beta_{kl}^2 \cdot |\mathbf{m}_{kl}\rangle\langle\mathbf{m}_{kl}|. \quad (5.207)$$

It should be noted that  $\text{tr}(\mathbf{m}_{ij}^\dagger \mathbf{m}_{ij})$  gives the dimension of the representation corresponding to the operator  $\mathbf{m}_{jj}$  (*c.f.* appendix 5.B.3),

$$\text{tr}(\mathbf{m}_{ij}^\dagger \mathbf{m}_{ij}) = \text{tr}(\mathbf{m}_{jj}) = \dim(\mathbf{m}_{jj}), \quad (5.208)$$

since either  $i = j$ , in which case  $\mathbf{m}_{jj}^\dagger \mathbf{m}_{jj} = \mathbf{m}_{jj} \mathbf{m}_{jj} = \mathbf{m}_{jj}$  as follows from the Hermiticity and idempotency of the MOLD operators, or  $i \neq j$ , such that  $\mathbf{m}_{ij}^\dagger \mathbf{m}_{ij} = \mathbf{m}_{jj}$  is a consequence of the unitarity of the transition operators between MOLD projectors (*c.f.* section 4.5.2). As the dimension  $\dim(\mathbf{m}_{jj})$  must be a strictly positive number, it follows that  $\beta_{ij}$  is finite and real,

$$(\beta_{ij})^* = \beta_{ij} \quad \text{and} \quad \beta_{ij} < \infty. \quad (5.209)$$

Using notation (5.206), the operator  $T_{ij,kl}^S$  defined in (5.105) can be written as

$$T_{ij,kl}^S = \beta_{ij} \beta_{kl} \cdot \begin{array}{c} \text{---} \leftarrow \text{---} \\ \leftarrow \text{---} \leftarrow \text{---} \\ \text{---} \leftarrow \text{---} \\ \leftarrow \text{---} \leftarrow \text{---} \\ \text{---} \leftarrow \text{---} \end{array} \begin{array}{c} \text{---} \leftarrow \text{---} \\ \leftarrow \text{---} \leftarrow \text{---} \\ \text{---} \leftarrow \text{---} \\ \leftarrow \text{---} \leftarrow \text{---} \\ \text{---} \leftarrow \text{---} \end{array} \cdot \quad (5.210)$$

We will now use the birdtrack formalism to show that  $T_{ij,kl}^S$  satisfies all conditions of transition operators given in eqns. (5.204).

**Property (5.204a):** Consider the product  $P_{ij}^S \cdot T_{ij,kl}^S$ ,

$$P_{ij}^S \cdot T_{ij,kl}^S = \beta_{ij}^3 \beta_{kl} \cdot \begin{array}{c} \text{---} \leftarrow \text{---} \\ \leftarrow \text{---} \leftarrow \text{---} \\ \text{---} \leftarrow \text{---} \\ \leftarrow \text{---} \leftarrow \text{---} \\ \text{---} \leftarrow \text{---} \end{array} \underbrace{\begin{array}{c} \text{---} \leftarrow \text{---} \\ \leftarrow \text{---} \leftarrow \text{---} \\ \text{---} \leftarrow \text{---} \\ \leftarrow \text{---} \leftarrow \text{---} \\ \text{---} \leftarrow \text{---} \end{array}}_{=:\beta_{ij}^2} \begin{array}{c} \text{---} \leftarrow \text{---} \\ \leftarrow \text{---} \leftarrow \text{---} \\ \text{---} \leftarrow \text{---} \\ \leftarrow \text{---} \leftarrow \text{---} \\ \text{---} \leftarrow \text{---} \end{array} = \underbrace{\frac{\beta_{ij}^3 \beta_{kl}}{\beta_{ij}^2}}_{=\beta_{ij} \beta_{kl}} \cdot \begin{array}{c} \text{---} \leftarrow \text{---} \\ \leftarrow \text{---} \leftarrow \text{---} \\ \text{---} \leftarrow \text{---} \\ \leftarrow \text{---} \leftarrow \text{---} \\ \text{---} \leftarrow \text{---} \end{array} = T_{ij,kl}^S \cdot \quad (5.211)$$

Similarly, the product  $T_{ij,kl}^S \cdot P_{kl}^S$  becomes

$$T_{ij,kl}^S \cdot P_{kl}^S = \beta_{ij} \beta_{kl}^3 \cdot \text{diagram} = \underbrace{\frac{\beta_{ij} \beta_{kl}^3}{\beta_{kl}^2}}_{=:\beta_{ij} \beta_{kl}} \cdot \text{diagram} = T_{ij,kl}^S. \quad (5.212)$$

Thus, we have that

$$T_{ij,kl}^S \cdot P_{kl}^S = T_{ij,kl}^S = P_{ij}^S \cdot T_{ij,kl}^S \quad (5.213)$$

as required.

**Property (5.204b):** To show this property, we need the Hermitian conjugate of  $T_{ij,kl}^S$ ,  $(T_{ij,kl}^S)^\dagger$ : the Hermitian conjugate of a birdtrack is formed by flipping the birdtrack about its vertical axis and reversing the arrows [72] (*c.f.* section 3.3.1). Thus, we have that  $(T_{ij,kl}^S)^\dagger$  is

$$(T_{ij,kl}^S)^\dagger = \left( \beta_{ij} \beta_{kl} \cdot \text{diagram} \right)^\dagger = (\beta_{ij})^* (\beta_{kl})^* \cdot \text{diagram} = \beta_{ij} \beta_{kl} \cdot \text{diagram}, \quad (5.214)$$

where we used the fact that  $\beta_{ij}$  and  $\beta_{kl}$  are real (see eq (5.209)). The resulting operator in (5.214) can easily be identified as the operator  $T_{kl,ij}^S$ , yielding the desired result

$$(T_{ij,kl}^S)^\dagger = T_{kl,ij}^S. \quad (5.215)$$

**Property (5.204c):** Examine the product  $T_{ij,kl}^S \cdot T_{kl,ij}^S$ ,

$$T_{ij,kl}^S \cdot T_{kl,ij}^S = \beta_{ij}^2 \beta_{kl}^2 \cdot \text{diagram} = \underbrace{\frac{\beta_{ij}^2 \beta_{kl}^2}{\beta_{kl}^2}}_{=:\beta_{ij}^2} \cdot \text{diagram} = P_{ij}^S. \quad (5.216)$$

Thus, we indeed find that

$$T_{ij,kl}^S \cdot T_{kl,ij}^S = P_{ij}^S. \quad (5.217)$$

We showed that the operator  $T_{ij,kl}^S$  as defined in (5.105) (resp eq.(5.210)) does indeed satisfy all the properties of transition operators given in equations (5.204), leading us to conclude that it is the transition operator between  $P_{ij}^S$  and  $P_{kl}^S$ . Thus, the representations corresponding to  $P_{ij}^S$  and  $P_{kl}^S$  are equivalent.

## 5.C Untwisting $\varepsilon$ -tensors without inducing a factor of $i^{\pm\phi}$

In section 5.2.2, we explicitly showed the equivalence between

$$\begin{array}{c} \leftarrow \leftarrow \leftarrow \\ \leftarrow \leftarrow \leftarrow \\ \leftarrow \leftarrow \leftarrow \end{array} \quad \text{and} \quad \begin{array}{c} \leftarrow \leftarrow \leftarrow \\ \leftarrow \leftarrow \leftarrow \\ \leftarrow \leftarrow \leftarrow \end{array} \quad (5.218)$$

for  $\dim(V) = N = 3$ . In the process, we had to flip two Levi-Civita tensors without adjusting the sign of the corresponding prefactor  $i^{\pm\phi}$  (*c.f.* eq. (5.129)), but we saw that in the product each prefactor may be reassigned to the *other*  $\varepsilon$ -tensor, respectively, to counteract the incorrect sign. In this appendix, we present an alternative to the flipping procedure that does not cause havoc with any prefactors.

Let us pick up at eq. (5.128) where we obtained the operator

$$\begin{array}{c} \leftarrow \leftarrow \leftarrow \\ \leftarrow \leftarrow \leftarrow \\ \leftarrow \leftarrow \leftarrow \end{array} \quad \begin{array}{c} \leftarrow \leftarrow \leftarrow \\ \leftarrow \leftarrow \leftarrow \\ \leftarrow \leftarrow \leftarrow \end{array} \quad (5.219)$$

Keeping the end points fixed, we may now move the left  $\varepsilon^\dagger$  to the right of  $\varepsilon$  *without flipping it*; this yields a somewhat entangled operator,

$$\begin{array}{c} \leftarrow \leftarrow \leftarrow \\ \leftarrow \leftarrow \leftarrow \\ \leftarrow \leftarrow \leftarrow \end{array} \quad \begin{array}{c} \leftarrow \leftarrow \leftarrow \\ \leftarrow \leftarrow \leftarrow \\ \leftarrow \leftarrow \leftarrow \end{array} \quad \xrightarrow{\text{move } \varepsilon\text{-tensors}} \quad \begin{array}{c} \leftarrow \leftarrow \leftarrow \\ \leftarrow \leftarrow \leftarrow \\ \leftarrow \leftarrow \leftarrow \end{array} \quad (5.220)$$

The two Levi-Civita tensors of length  $N = 3$  combine into an antisymmetrizer of length  $N = 3$  according to eq. (5.32),

$$\begin{array}{c} \leftarrow \leftarrow \leftarrow \\ \leftarrow \leftarrow \leftarrow \\ \leftarrow \leftarrow \leftarrow \end{array} \quad \xrightarrow{\text{eq. (5.32)}} \quad \begin{array}{c} \leftarrow \leftarrow \leftarrow \\ \leftarrow \leftarrow \leftarrow \\ \leftarrow \leftarrow \leftarrow \end{array} \quad (5.221)$$

The antisymmetrizer in the middle may now be flipped to disentangle the index lines; this does *not* produce any phase factors, as the antisymmetrizer is a real quantity,

$$\begin{array}{c} \leftarrow \leftarrow \leftarrow \\ \leftarrow \leftarrow \leftarrow \\ \leftarrow \leftarrow \leftarrow \end{array} = \begin{array}{c} \leftarrow \leftarrow \leftarrow \\ \leftarrow \leftarrow \leftarrow \\ \leftarrow \leftarrow \leftarrow \end{array} = (-1)^2 \begin{array}{c} \leftarrow \leftarrow \leftarrow \\ \leftarrow \leftarrow \leftarrow \\ \leftarrow \leftarrow \leftarrow \end{array}, \quad (5.222)$$

where, in the disentanglement process, we absorb a transposition (12) on either side of the antisymmetrizer, inducing an additional prefactor  $(-1)^2 = 1$  in the last step (we also encountered this factor when flipping the  $\varepsilon$ -tensors, *c.f.* eq. (5.129) and footnote 16).

Thus, we once again arrive at the desired result (5.130).

## Part II

# *Incidental Results Regarding Multiplets of $SU(N)$*

*or: What to do in a boring Colloquium\**

---

\*The author does not advocate the view that all colloquia are boring, or that one should not pay attention (in fact quite the opposite!). However, some of the results presented in this part have indeed been derived during a colloquium...



## Chapter 6

# On Mixed Multiplets of $SU(N)$ : Counting and General Results

*In this chapter, we provide a counting argument for the irreducible representations of  $SU(N)$  over a mixed product space  $V^{\otimes m} \otimes (V^*)^{\otimes n}$  for general  $m$  and  $n$ , using the Hermiticity properties of the primitive invariants of  $SU(N)$ . For  $n = 0$  (i.e. in the absence of antiquarks) an explicit formula has been known since 1800, but this result seems to be unknown in representation theory circles. Furthermore, we put a modern spin on the recursive count of Young tableaux by Rothe and Chowla et al. by using the birdtrack formalism. For  $n = 1$ , Pieri's formula gives an underlying counting argument. We present a bijection between the Pieri tableaux and Young tableaux.*

### 6.1 Introduction

In chapter 4, it was shown that the set of MOLD-operators (c.f. chapter 3) can be augmented with unitary transition operators to form an *orthogonal* basis of the algebra of invariants of  $SU(N)$  over  $V^{\otimes m}$ , the so-called *projector basis*  $\mathfrak{S}_m$ . That this can be generalized to a mixed product space  $V^{\otimes m} \otimes (V^*)^{\otimes n}$  was demonstrated in chapter 5, section 5.2.1.2:

■ **Theorem 6.1 – projector basis for the algebra of invariants over a mixed product space:**

*The Hermitian projection operators and their unitary transition operators constitute a basis of the algebra of invariants  $\text{API}\left(SU(N), V^{\otimes m} \otimes (V^*)^{\otimes n}\right)$  called the projector basis,  $\mathfrak{S}_{m,n}$ .<sup>1</sup>*

The argument presented in section 5.2.1.2 to prove Theorem 6.1 uses Clebsch-Gordan operators. From this proof, it is apparent that the projector basis is orthogonal with respect to the canonical scalar product  $\langle A|B \rangle = \text{Tr}(A^\dagger B)$  on  $V^{\otimes m} \otimes (V^*)^{\otimes n}$ .

In section 6.2.1, we give a general analysis of transition operators through their relation to intertwining operators, the latter not having been discussed yet in this thesis. This relation allows us to give an alternative proof that the projection and transition operators constitute an orthogonal set with respect to the canonical scalar product.

---

<sup>1</sup>This mirrors the notation we introduced for the set of primitive invariants of  $SU(N)$  over  $V^{\otimes m} \otimes (V^*)^{\otimes n}$ ,  $S_{m,n}$ , c.f. section 5.1.1.

Besides spanning the algebra of invariants, the projector basis  $\mathfrak{S}_{m,n}$  leads to a multitude of new results. The main result presented in this chapter is a counting argument for the number of irreducible representations  $\mathrm{SU}(N)$  over  $V^{\otimes m} \otimes (V^*)^{\otimes n}$ , Theorem 6.2: Denoting the set of all projection operators of  $\mathrm{SU}(N)$  over  $V^{\otimes m} \otimes (V^*)^{\otimes n}$  by  $\mathfrak{P}_{m,n}$  and the set of all transition operators by  $\mathfrak{T}_{m,n}$  such that

$$\mathfrak{P}_{m,n} \cup \mathfrak{T}_{m,n} = \mathfrak{S}_{m,n} , \tag{6.1}$$

we will establish a 1-to-1 correspondence between the elements of  $\mathfrak{P}_{m,n}$  and the Hermitian elements in the set of primitive invariants  $S_{m,n}$  of  $\mathrm{SU}(N)$  over  $V^{\otimes m} \otimes (V^*)^{\otimes n}$ . It will be shown that  $S_{m,n}$  contains the same number of Hermitian elements as  $S_{m+n}$  (the set of primitive invariants of  $\mathrm{SU}(N)$  over  $V^{\otimes(m+n)}$ ), thus allowing us to conclude that the number of irreducible representations of  $\mathrm{SU}(N)$  over  $V^{\otimes m} \otimes (V^*)^{\otimes n}$  only depends on the sum of factors in the product space ( $m+n$ ), but not on the individual values of  $m$  and  $n$ . The fact that the projection operators are Hermitian and the transition operators are unitary (on the corresponding subspaces) is key in proving this counting argument. This result (Theorem 6.2) and some immediate consequences (Corollaries 6.2 to 6.4) are summarized in section 6.3. In fact, the observations made in this section allow us to derive an *explicit* formula for the number of irreducible representations of  $\mathrm{SU}(N)$  over  $V^{\otimes m} \otimes (V^*)^{\otimes n}$  as a function of  $(m+n)$  (Theorem 6.3 in section 6.4).

It turns out that a less general version of Theorem 6.3 had already been developed by Rothe as early as 1800 [118, in German]: In his paper, Rothe presents a recursive formula counting the irreducible representations of  $\mathrm{SU}(N)$  over a *quark-only* Fock space  $V^{\otimes k}$ . From this, one can easily derive the counting formula in Theorem 6.3 (for  $n=0$ ) [97]. However, Rothe's paper seems to be virtually unknown in representation theory circles,<sup>2</sup> presumably in part because it has not been translated into English. This derivation is therefore given in section 6.4. We would, however, like to emphasize that the formula in Theorem 6.3 goes beyond what has been known in the literature in that our argument holds for the irreducible representations of  $\mathrm{SU}(N)$  over  $V^{\otimes m} \otimes (V^*)^{\otimes n}$ , while in Rothe's formula  $n \stackrel{!}{=} 0$  is required.

In section 6.5, we revisit Rothe's recursion formula for the number of Young tableaux. In the 1950's, Chowla, Herstein and Moore [97] supplied a more modern proof of this formula in terms of permutation matrices. We translate [97]'s proof into the language of birdtracks, thus giving it a more modern spin. Furthermore, the birdtrack formalism provides a graphical, more intuitive description of the underpinnings of the formula in question.

Lastly, by this time in the chapter we will have established that the number of irreducible representations of  $\mathrm{SU}(N)$  over  $V^{\otimes m} \otimes (V^*)^{\otimes n}$  is the same as that over  $V^{\otimes(m+n)}$ . In particular, this result holds for  $n=1$ . In this case, we can make the correspondence even more explicit and provide a graphical form of the bijection between the Littlewood-Richardson tableaux (*c.f.* section 5.1.3 in chapter 5) for  $m$  fundamental and 1 antifundamental objects, and the Young tableaux consisting of  $(m+1)$  boxes. This bijection is given in section 6.6.

---

<sup>2</sup>The author only stumbled across it by accident when recreationally reading about a famous problem in graph theory, namely the *telephone number problem*, on Wikipedia [119].



## 6.2 The projector basis of the algebra of invariants

### 6.2.1 Transition operators from intertwining operators

In chapter 4, we went to great lengths to discuss transition operators between equivalent irreducible representations of  $SU(N)$  over a product space  $V^{\otimes m}$ . In particular, an explicit construction principle for these transition operators was given.

As of this point, an explicit construction principle for the transition operators between projection operators corresponding to equivalent irreducible representations of  $SU(N)$  over a mixed product space  $V^{\otimes m} \otimes (V^*)^{\otimes n}$  is not yet known (presumably due to the lack of a practical construction method for the projection operators), but we know that they exist from the argument given section 5.2.1.2 of chapter 5. However, general comments about the structure of transition operators can be made by recognizing that these operators are merely a *generalization of intertwining operators to the whole space*. To see this, let us first give a short summary of intertwining operators. Our main reference for this is [65], but other standard textbooks on representation theory will contain equivalent information.

Suppose  $(V_1, \varphi_1)$  and  $(V_2, \varphi_2)$  are two equivalent irreducible representations of  $SU(N)$  over  $V$ , where  $V_{1,2} \subset V$  are the subspaces and  $\varphi_{1,2} : V \rightarrow V_{1,2}$  are the homomorphisms corresponding to these representations. Then, for every  $U \in SU(N)$ , there exists an intertwining operator  $I_{12} : V_2 \rightarrow V_1$  such that

$$\varphi_1(U) = I_{12} \circ \varphi_2(U) \circ I_{12}^\dagger, \quad (6.2)$$

where  $I_{12}^\dagger =: I_{21}$  translates  $V_1$  into  $V_2$  and  $\circ$  is understood to be the composition of liner maps; from now on we will suppress  $\circ$ . Thus, the intertwining operator  $I_{12}$  translates the group element  $\varphi_2(U)$  from representation  $\varphi_2$  to  $\varphi_1$ . However,  $I_{12}$  merely acts on the subspace  $V_2$  of  $V$ , but not the whole space,

$$\begin{array}{ccc} V_2 & \xrightarrow{I_{12}} & V_1 \\ \varphi_2(U) \downarrow & & \downarrow \varphi_1(U) \\ V_2 & \xrightarrow{I_{12}} & V_1 \end{array} \quad (6.3)$$

We define the *transition operator* to be a generalization of the intertwining operator acting on the whole space  $V$

$$T_{12} : V \rightarrow V \quad \text{such that} \quad T_{12}v = \begin{cases} I_{12}v & \text{if } v \in V_2 \\ 0 & \text{if } v \in V \setminus V_2 \end{cases}, \quad (6.4)$$

that is, the action of  $T_{12}$  restricted onto  $V_2$  becomes the action of  $I_{12}$ ,  $T_{12}|_{V_2} = I_{12}$ . (Note that eq. (6.4) complements the definition of transition operators over  $V^{\otimes m}$  given in Theorem 4.4 in chapter 4.) The operator  $T_{12}$  can be constructed from  $I_{12}$  by first projecting onto the appropriate subspaces. This is done by multiplying the corresponding Hermitian projection operators  $P_{1,2}$  on either side, thus effectively embedding  $I_{12}$  into the whole space,

$$T_{12} := P_1^\dagger I_{12} P_2; \quad (6.5)$$

$P_2 : V \rightarrow V_2$  first projects onto the subspace  $V_2$ , the intertwining operator  $I_{12} : V_2 \rightarrow V_1$  then translates  $V_2$  into  $V_1$ , and finally  $P_1^\dagger$  embeds the result back into the whole space  $V$ :

$$\begin{array}{ccc}
 V & \xrightarrow{T_{12}} & V \\
 P_2 \downarrow & & \uparrow P_1^\dagger \\
 V_2 & \xrightarrow{I_{12}} & V_1
 \end{array} . \tag{6.6}$$

In this chapter, we will be working with Hermitian projection operators such that

$$T_{12} = P_1 I_{12} P_2 . \tag{6.7}$$

Eq. (6.7) can be generalized to product representations of  $SU(N)$  over a product space  $V^{\otimes m} \otimes (V^*)^{\otimes n}$ . In this case, the projection operators  $P$  will be acting on a product of (anti-) fundamental representations of  $SU(N)$

$$U := \underbrace{U \otimes U \otimes \dots \otimes U}_{m \text{ times}} \otimes \underbrace{U^\dagger \otimes U^\dagger \otimes \dots \otimes U^\dagger}_{n \text{ times}} , \tag{6.8}$$

and  $I_{ij}$  will translate each  $V_j \subset V$  and each  $V_j^* \subset V^*$  into  $V_i$  and  $V_i^*$  respectively,

$$I_{ij} : V_j^{\otimes m} \otimes (V_j^*)^{\otimes n} \rightarrow V_i^{\otimes m} \otimes (V_i^*)^{\otimes n} . \tag{6.9}$$

Understanding  $V_i$  and  $V_j$  to be embedded into  $V$  (by acting the identity on elements in  $V \setminus V_{i,j}$ ) makes it clear that  $I_{ij}$  is an element of the algebra of invariants  $\text{API} \left( SU(N), V^{\otimes m} \otimes (V^*)^{\otimes n} \right)$ . The transition operator corresponding to  $I_{ij}$ ,

$$T_{ij} = P_i I_{ij} P_j , \tag{6.10}$$

is then of the form  $P_i \rho P_j$  where  $\rho = I_{ij}$  is an element of  $\text{API} \left( SU(N), V^{\otimes m} \otimes (V^*)^{\otimes n} \right)$ . This resembles the construction of transition operators given in Theorem 4.4.

From eq. (6.10) it immediately follows that  $T_{ij}$  satisfies the following conditions:

$$P_i T_{ij} = T_{ij} = T_{ij} P_j \tag{6.11a}$$

$$T_{ij} = T_{ji}^\dagger \tag{6.11b}$$

$$T_{ij} T_{ji} = P_i , \tag{6.11c}$$

thus allowing us to treat eqns. (6.11) as the defining properties of transition operators. That eqns. (6.11) hold true also immediately follows from their definition in terms of Clebsch-Gordan operators (*c.f.* section 5.2.1.2, as well as our treatment of transition operators in the absence of anti-quarks in section 4.4.2).

If we set  $i = j$ , eq. (6.2) forces the intertwining operator  $I_{ij}$  to become the identity  $\text{id}$  (also on the product space),

$$T_{ij} := P_i I_{ij} P_j \xrightarrow{i=j} T_{ii} = P_i \underbrace{I_{ii}}_{=\text{id}} P_i = P_i P_i = P_i , \tag{6.12}$$

reducing the transition operator  $T_{ij}$  to the projection operator  $P_i$ .

### 6.2.2 The projector basis is orthogonal

An immediate consequence of the projector basis in terms of Clebsch-Gordan operators (*c.f.* section 5.2.1.2 of chapter 5) is that this basis is orthogonal with respect to the canonical scalar product on  $V^{\otimes m} \otimes (V^*)^{\otimes n}$ ,

$$\langle A|B \rangle := \text{Tr} (A^\dagger B) \quad \text{for } A, B \text{ acting on } V^{\otimes m} \otimes (V^*)^{\otimes n} . \quad (6.13)$$

However, with the structural identities of transition operators discussed in the previous section 6.2.1 at hand, we are able to give an alternative proof of the orthogonality of the projector basis  $\mathfrak{S}_{m,n}$  with respect to the scalar product (6.13):

**■ Corollary 6.1 – projector basis is orthogonal:**

The projector basis of  $\text{API} \left( SU(N), V^{\otimes m} \otimes (V^*)^{\otimes n} \right)$  is orthogonal under the canonical scalar product  $\langle A|B \rangle = \text{Tr} (A^\dagger B)$ .

*Proof of Corollary 6.1:* All projection operators in  $\mathfrak{P}_{m,n} \subset \mathfrak{S}_{m,n}$  are Hermitian and mutually orthogonal as linear maps, see section 5.2.1.2. Any two projection operators  $P_i, P_j \in \mathfrak{P}_{m,n}$  therefore satisfy

$$\langle P_i|P_j \rangle = \text{tr} \left( P_i^\dagger P_j \right) \stackrel{P_i^\dagger = P_i}{=} \text{tr} (P_i P_j) \stackrel{P_i P_j = \delta_{ij} P_i}{=} \text{tr} (\delta_{ij} P_i) = \delta_{ij} \dim(P_i) , \quad (6.14)$$

where we use the fact that  $\text{tr} (P_i)$  is the dimension of the representation corresponding to  $P_i$ ,  $\dim(P_i)$ , as explained in [72] and in chapter 5 on page 235. Thus, the inner product  $\langle P_i|P_j \rangle$  of two projection operators  $P_i, P_j \in \mathfrak{P}_{m,n} \subset \mathfrak{S}_{m,n}$  vanishes unless  $i = j$ .

Eq. (6.10) tells us that the transition operator  $T_{ij}$  between two projection operators  $P_i$  and  $P_j$  corresponding to equivalent representations is of the form

$$T_{ij} = P_i I_{ij} P_j, \quad (6.15)$$

where  $I_{ij}$  lies in the algebra of invariants  $\text{API} \left( SU(N), V^{\otimes m} \otimes (V^*)^{\otimes n} \right)$ . Thus, using the cyclic property of the trace, the inner product between a Hermitian projection operator  $P_k$  and the transition operator  $T_{ij}$  is given by

$$\langle P_k|T_{ij} \rangle = \text{Tr} \left( P_k^\dagger P_i I_{ij} P_j \right) \stackrel{P_k^\dagger = P_k}{=} \text{Tr} (P_k P_i I_{ij} P_j) = \text{Tr} (P_j P_k P_i I_{ij}) . \quad (6.16)$$

From the mutual orthogonality of the Hermitian projection operators (*c.f.* section 5.2.1.2 in chapter 5), the product  $P_j P_k P_i$  is nonzero if and only if  $i = j = k$ . However, if  $i = j$ , the transition operator  $T_{ij} = P_i I_{ij} P_j$  reduces to  $P_i$  (*c.f.* eq. (6.12)) which poses a contradiction to our initial assumption that  $T_{ij}$  is a transition operator. Thus, we conclude that

$$\langle P_k|T_{ij} \rangle = 0 \quad \text{for all } P_k \in \mathfrak{P}_{m,n} \text{ and } T_{ij} \in \mathfrak{T}_{m,n} . \quad (6.17)$$

Lastly, we consider the inner product between two transition operators  $T_{kl}$  and  $T_{ij}$  in  $\mathfrak{T}_{m,n} \subset \mathfrak{S}_{m,n}$ ,

$$\langle T_{kl} | T_{ij} \rangle = \text{tr} \left( T_{kl}^\dagger T_{ij} \right) = \text{tr} \left( (P_k I_{kl} P_l)^\dagger P_i I_{ij} P_j \right) = \text{tr} \left( P_l I_{kl}^\dagger P_k P_i I_{ij} P_j \right) . \quad (6.18)$$

Using the cyclic property of the trace and the orthogonality of projection operators as linear maps, eq. (6.18) becomes

$$\text{tr} \left( P_l I_{kl}^\dagger P_k P_i I_{ij} P_j \right) = \text{tr} \left( \underbrace{P_j P_l}_{\delta_{jl} P_l} I_{kl}^\dagger \underbrace{P_k P_i}_{\delta_{ki} P_i} I_{ij} \right) . \quad (6.19)$$

This shows that the inner product between  $T_{kl}$  and  $T_{ij}$  vanishes unless  $i = k$  and  $j = l$ , making the two transition operators equal. Using properties (6.11b) and (6.11c) of transition operators finally yields

$$\langle T_{kl} | T_{ij} \rangle = \delta_{ki} \delta_{jl} \text{tr} \left( T_{il}^\dagger T_{il} \right) = \delta_{ki} \delta_{jl} \text{tr} (P_l) = \delta_{ki} \delta_{jl} \dim(P_l) . \quad (6.20)$$

In summary, eqns. (6.14), (6.17) and (6.20) show that the elements of  $\mathfrak{S}_{m,n}$  are mutually orthogonal.  $\square$

### 6.3 A counting argument of the number of irreducible representations of $SU(N)$

In this section, we give a counting argument for the number of irreducible representations of  $SU(N)$  over a product space  $W = V^{\otimes m} \otimes (V^*)^{\otimes n}$  consisting of a total of  $k$  factors (i.e.  $k = m + n$ ) in Theorem 6.3. As demonstrated in chapter 5, the standard method of constructing the projection operators of  $SU(N)$  over a mixed product space  $V^{\otimes m} \otimes (V^*)^{\otimes n}$  (which involves the Littlewood-Richardson tableaux and the Leibniz formula for determinants), is extremely cumbersome and computationally expensive. The benefit of knowing *a priori* how many irreducible representations exist is that one may determine whether a set of projection operators obtained by some other means (for example by making a suitable Ansatz) is complete and thus classifies the irreducible representations of  $SU(N)$ .

Suppose first that  $n = 0$ , that is,  $W = V^{\otimes k}$  consists of factors  $V$  only. Then, the primitive invariants of  $SU(N)$  over  $W = V^{\otimes k}$  are given by the permutations in the symmetric group  $S_k$ . Since all permutations in  $S_k$  are unitary,

$$\rho^{-1} = \rho^\dagger \quad \text{for all } \rho \in S_k , \quad (6.21)$$

the Hermitian elements of  $S_k$  are those that are their own inverse, also referred to as *involutions* [96]. Furthermore, for  $W = V^{\otimes k}$ , the irreducible representations of  $SU(N)$  are classified by the Young tableaux in  $\mathcal{Y}_k$ . Thus, our general counting argument (which also allows for  $W$  to include factors of  $V^*$  as well as  $V$ ) will have the consequence that the number of Young tableaux in  $\mathcal{Y}_k$  is equal to the number of involutions in  $S_k$ . Knuth [120, section 5.1.4 page 49] once said that

*“This connection between involutions and tableaux is by no means obvious, and there is probably no very simple way to prove it.”*

He then proceeds to present a lengthy proof (approximately 18 pages) involving inserting boxes into Young tableaux to establish this connection. In particular, he re-derives Rothe's recursive formula [118] counting the number of Young tableaux of  $k$  boxes,

$$|\mathcal{Y}_k| = |\mathcal{Y}_{k-1}| + (k-1)|\mathcal{Y}_{k-2}| . \quad (6.22)$$

In this chapter we demonstrate that Knuth should have been more optimistic by presenting a proof (of a more general statement!) that is approximately one page long. It turns out that the necessary ingredients for this proof, that Knuth did not have at his disposal, are the transition operators between Hermitian projection operators. In particular, the key observation in establishing the relation between the Hermitian primitive invariants and the projection operators of  $SU(N)$  over  $V^{\otimes m} \otimes (V^*)^{\otimes n}$  is that they form part of the basis of the algebra of invariants, as will be shown in the present section.

Before stating the counting argument (Theorem 6.2), let us stress once more that this result goes beyond the previously known results in that it gives the number of irreducible representations of  $SU(N)$  over a *mixed* product space  $V^{\otimes m} \otimes (V^*)^{\otimes n}$ , while the currently known results require the absence of  $V^*$ , that is  $n \stackrel{!}{=} 0$ .

■ **Theorem 6.2 – counting argument for the irreducible representations of  $SU(N)$ :**

*Consider the irreducible representations of  $SU(N)$  over the mixed product space  $V^{\otimes m} \otimes (V^*)^{\otimes n}$ . The following three statements hold:*

1. *The set union  $\mathfrak{S}_{m,n} = \mathfrak{P}_{m,n} \cup \mathfrak{T}_{m,n}$  of all Hermitian projection and unitary transition operators and the set  $S_{m,n}$  of all primitive invariants have the same size,*

$$|\mathfrak{S}_{m,n}| = |\mathfrak{P}_{m,n} \cup \mathfrak{T}_{m,n}| = |S_{m,n}| . \quad (6.23a)$$

2. *Let  $n_P(Q)$  denote the number of non-Hermitian elements in a set  $Q$ . The non-Hermitian elements in  $S_{m,n}$  occur in Hermitian conjugate pairs such that  $n_P(S_{m,n})$  is an even number. Furthermore,*

$$|\mathfrak{T}_{m,n}| = n_P(\mathfrak{S}_{m,n}) = n_P(S_{m,n}) , \quad (6.23b)$$

*the number of transition operators in  $\mathfrak{S}_{m,n}$  is the same as the number of non-Hermitian elements in  $S_{m,n}$ .*

3. *Let  $n_H(Q)$  denote the number of Hermitian elements in a set  $Q$ . Then,*

$$|\mathfrak{P}_{m,n}| = n_H(\mathfrak{S}_{m,n}) = n_H(S_{m,n}) , \quad (6.23c)$$

*stating that there are as many projection operators in  $\mathfrak{S}_{m,n}$  as there are Hermitian elements in  $S_{m,n}$ .*

We emphasize that  $\mathfrak{S}_{m,n}$  and  $S_{m,n}$  are the *sets* of projection and transition operators resp. primitive invariants, *not* the algebras spanned by these sets.

*Proof of Theorem 6.2:* 1. Equation (6.23a) is a consequence of the fact that both  $\mathfrak{S}_{m,n}$  and  $S_{m,n}$  constitute a basis of the algebra of primitive invariants  $\text{API}(SU(N), V^{\otimes m} \otimes (V^*)^{\otimes n})$  (c.f. Theorem 6.1) and therefore must contain the same number of elements.

2. Since  $S_{m+n}$  is a group and all its elements are unitary (i.e.  $\rho^{-1} = \rho^\dagger$ ), the elements of  $S_{m+n}$  either are self-inverse  $\rho^{-1} = \rho$ , or occur in Hermitian conjugate pairs  $(\rho, \rho^\dagger)$ . Translating  $n$  of the  $(m+n)$  fundamental

legs of the elements in  $S_{m+n}$  into antifundamental legs does not change their Hermiticity property (as is apparent from the graphical mapping between  $S_{m+n}$  and  $S_{m,n}$ , *c.f.* section 5.1.1). Thus, the elements of  $S_{m,n}$  are either Hermitian or occur in Hermitian conjugate pairs, forcing  $n_P(S_{m,n})$  to be an even number. For each such pair  $(\rho, \rho^\dagger)$  we can form a Hermitian element  $h_\rho$  and an anti-Hermitian element  $a_\rho$  as

$$h_\rho := \rho + \rho^\dagger \quad \text{and} \quad a_\rho := \rho - \rho^\dagger . \quad (6.24)$$

Thus, after such a change of basis,  $S_{m,n}$  splits into two disjoint subsets:

1. the set  $H_{m,n} \subset S_{m,n}$  consisting of all Hermitian elements in  $S_{m,n}$  with size

$$|H_{m,n}| = n_H(S_{m,n}) + \frac{n_P(S_{m,n})}{2} , \quad (6.25a)$$

2. the set  $A_{m,n} \subset S_{m,n}$  containing all anti-Hermitian elements in  $S_{m,n}$  with size

$$|A_{m,n}| = \frac{n_P(S_{m,n})}{2} . \quad (6.25b)$$

Similarly, the projector basis of  $\text{API}(SU(N), V^{\otimes m} \otimes (V^*)^{\otimes n})$ ,  $\mathfrak{S}_{m,n}$ , consists of Hermitian elements (the projection operators) and elements that occur in Hermitian conjugate pairs (the transition operators). Thus,  $\mathfrak{S}_{m,n}$  again splits into disjoint sets  $\mathfrak{H}_{m,n}$  and  $\mathfrak{A}_{m,n}$  consisting of Hermitian and anti-Hermitian elements respectively, analogous to eqns. (6.24) and (6.25).

Since  $H_{m,n}$  and  $A_{m,n}$  (resp.  $\mathfrak{H}_{m,n}$  and  $\mathfrak{A}_{m,n}$ ) are disjoint, it follows that

$$|H_{m,n}| \stackrel{!}{=} |\mathfrak{H}_{m,n}| \quad \text{and} \quad |A_{m,n}| \stackrel{!}{=} |\mathfrak{A}_{m,n}| \quad (6.26)$$

for both unions  $H_{m,n} \cup A_{m,n}$  and  $\mathfrak{H}_{m,n} \cup \mathfrak{A}_{m,n}$  to constitute a basis of the algebra of invariants of  $SU(N)$  over  $V^{\otimes m} \otimes (V^*)^{\otimes n}$ ,  $\text{API}(SU(N), V^{\otimes m} \otimes (V^*)^{\otimes n})$ .

Clearly, a linear combination of Hermitian objects will be Hermitian. Thus, only the elements of  $A_{m,n}$  and  $\mathfrak{A}_{m,n}$  can be used to form the non-Hermitian subsets of  $S_{m,n}$  respectively  $\mathfrak{S}_{m,n}$ . From eq. (6.26) it then follows that

$$n_P(\mathfrak{S}_{m,n}) = |\mathfrak{S}_{m,n}| = 2|\mathfrak{A}_{m,n}| = 2|A_{m,n}| = n_P(S_{m,n}) , \quad (6.27)$$

proving equation (6.23b).

3. We have already shown that the sets  $\mathfrak{S}_{m,n}$  and  $S_{m,n}$  have the same size (eq. (6.23a)) as do their subsets containing only the non-Hermitian elements (eq. (6.23b)). By construction, we further have

$$|\mathfrak{S}_{m,n}| = n_H(\mathfrak{S}_{m,n}) + n_P(\mathfrak{S}_{m,n}) \quad \text{and} \quad |S_{m,n}| = n_H(S_{m,n}) + n_P(S_{m,n}) , \quad (6.28)$$

such that the number of projection operators  $|\mathfrak{P}_{m,n}|$  is given by

$$|\mathfrak{P}_{m,n}| = n_H(\mathfrak{S}_{m,n}) = |\mathfrak{S}_{m,n}| - n_P(\mathfrak{S}_{m,n}) \stackrel{\text{eq. (6.23a)}}{=} |S_{m,n}| - n_P(S_{m,n}) = n_H(S_{m,n}) , \quad (6.29)$$

thus also proving eq. (6.23c) of the Theorem. □

Theorem 6.2 has some immediate consequences which are summarized in Corollaries 6.2 to 6.4:

Eq. (6.23c) of Theorem 6.2 states that the number of irreducible representations of  $SU(N)$  over  $V^{\otimes m} \otimes (V^*)^{\otimes n}$  is given by the number of *Hermitian* primitive invariants in  $S_{m,n}$ . In section 5.1.1 we summarized a graphical method of constructing the elements in  $S_{m,n}$  from those in  $S_{m+n}$  [72], which preserves Hermiticity. Thus,

$$n_H(S_{m,n}) = n_H(S_{m+n}) , \quad (6.30)$$

giving rise to the following Corollary:

■ **Corollary 6.2 – the irreducible representations of  $SU(N)$  and the total particle count:**

*The number of irreducible representations of  $SU(N)$  over a product space  $V^{\otimes m} \otimes (V^*)^{\otimes n}$  does not depend on  $m$  and  $n$  individually, but only on the sum  $(m+n)$ . In physics parlance, the number of irreducible representations of  $SU(N)$  over a particular Fock space only depends on the total number of particles; it is irrelevant how this number is split into particles and anti-particles.*

This is a rather astonishing result: Since the primitive invariants  $S_{m+n}$  of  $SU(N)$  over an only-quark space constitute a group but the primitive invariants  $S_{m,n}$  over a mixed product space do not, the multiplication tables of their respective algebras of invariants are vastly different. It is therefore natural to assume that the algebras  $\text{API}(SU(N), V^{\otimes(m+n)})$  and  $\text{API}(SU(N), V^{\otimes m} \otimes (V^*)^{\otimes n})$  spanned by  $S_{m+n}$  and  $S_{m,n}$  respectively have significant structural differences. Just from this consideration, there is no a priori reason to believe that there should be an equal number of irreducible representations of  $SU(N)$  over  $V^{\otimes(m+n)}$  and  $V^{\otimes m} \otimes (V^*)^{\otimes n}$ ; Corollary 6.2 nonetheless ensures us that this is the case.

In chapter 7, we analyze the irreducible representations of  $SU(N)$  over a 4-particle product space for all particle-antiparticle configurations. This analysis will show that the block structure (signifying which irreducible representations are equivalent) of the multiplication tables  $\mathfrak{M}_{4\text{-particles}}$  may differ, while the number of projection operators remains fixed as predicted by Corollary 6.2.

In chapter 4, we explained that the size of the symmetric group  $S_k$  (and thus the size of the set  $\mathfrak{S}_k$  from Theorem 6.2) is given by a sum of squares, since one can always arrange the elements of  $\mathfrak{S}_k$  into a matrix  $\mathfrak{M}_k$ , which has all projection operators on the diagonal, and each off-diagonal element  $\mathfrak{m}_{ij}$  is the transition operator between  $\mathfrak{m}_{i1}$  and  $\mathfrak{m}_{j1}$ . Analogously, the elements of  $\mathfrak{S}_{m,n}$  can also be arranged into a matrix  $\mathfrak{M}_{m,n}$ , causing this matrix to be block-diagonal. This implies that the size of  $\mathfrak{S}_{m,n}$  (and thus the size of  $S_{m,n}$ ) is also a sum of squares:

■ **Corollary 6.3 – number of primitive invariants as a sum of squares:**

*Consider the irreducible representations of  $SU(N)$  over a mixed product space  $V^{\otimes m} \otimes (V^*)^{\otimes n}$ . The number of primitive invariants of  $SU(N)$  over  $V^{\otimes m} \otimes (V^*)^{\otimes n}$ , as well as the number of all Hermitian projection and transition operators, can be written as a sum of squares,*

$$(m+n)! = |S_{m,n}| = |\mathfrak{S}_{m,n}| = \sum_{i=1}^q k_i^2 , \quad (6.31)$$

where  $q$  is the number of inequivalent irreducible representations of  $SU(N)$ , and  $k_i$  is the number of projection operators projecting onto a particular representation  $R_i$  (or a representation equivalent to it).

It should be noted that the  $k_i$ 's are not in 1-to-1 correspondence with the factors  $(m+n)!/\mathcal{H}_{\mathbf{Y}}$  in eq. (4.67) in general. An example of this is the matrix  $\mathfrak{M}_{2,2}$ , which has a different block-structure to  $\mathfrak{M}_4$  (see chapter 7).

Nonetheless,  $\mathfrak{M}_{2,2}$  and  $\mathfrak{M}_4$  are both  $10 \times 10$  matrices since  $\mathrm{SU}(N)$  has equally many irreducible representations on  $V^{\otimes 2} \otimes (V^*)^{\otimes 2}$  as on  $V^{\otimes 4}$  (by Corollary 6.2) translating into  $\mathfrak{M}_{2,2}$  and  $\mathfrak{M}_4$  having equally many diagonal elements.

Lastly, notice that there is an upper bound on the number of irreducible representations of  $\mathrm{SU}(N)$  over a (possibly mixed) product space:

**Corollary 6.4 – upper bound for the number of projection operators:**

Let  $\mathfrak{T}_{m,n}$  denote the set of all transition operators between equivalent irreducible representations of  $\mathrm{SU}(N)$  over the space  $V^{\otimes m} \otimes (V^*)^{\otimes n}$ . Then, if  $m + n > 2$ ,  $\mathfrak{T}_{m,n}$  is not empty,

$$\mathfrak{T}_{m,n} \neq \emptyset, \tag{6.32a}$$

implying that

$$\mathfrak{P}_{m,n} \leq |\mathfrak{S}_{m,n}| - 2, \tag{6.32b}$$

since transition operators always occur in Hermitian conjugate pairs.

*Proof of Corollary 6.4:* Recall that  $|\mathfrak{T}_{m,n}| = n_P(S_{m,n})$  by Theorem 6.2, where  $S_{m,n}$  is the set of all primitive invariants of  $\mathrm{SU}(N)$  over  $V^{\otimes m} \otimes (V^*)^{\otimes n}$  and  $n_P(S_{m,n})$  denotes the number of non-Hermitian elements in  $S_{m,n}$ .

We first notice that  $n_P(S_{m,n}) = n_P(S_{m+n})$ , since the map transforming the elements of  $S_{m+n}$  into those of  $S_{m,n}$  does not alter their Hermiticity. This allows us to focus on the non-Hermitian elements of  $S_{m+n}$  for the remainder of this proof. The elements of the group  $S_{m+n}$  are Hermitian if and only if they contain no cycles longer than 2 (see the later Lemma 6.1 in section 6.4). Therefore, a permutation that contains cycles of length  $\geq 3$  is not Hermitian. Such a permutation can (and will!) exist in  $S_{m+n}$  if  $m + n \geq 3$  (or equivalently if  $m + n > 2$ ). Since transition operators always occur in Hermitian conjugate pairs, it follows that there exist at least two transition operators between irreducible representations of  $\mathrm{SU}(N)$  over  $V^{\otimes m} \otimes (V^*)^{\otimes n}$  if  $m + n > 2$ , implying both eqns. (6.32).  $\square$

## 6.4 An explicit formula for the number of irreducible representations of $\mathrm{SU}(N)$ over $V^{\otimes m} \otimes (V^*)^{\otimes n}$

The aim of this section is to derive an explicit formula for the number of irreducible representations of  $\mathrm{SU}(N)$  over  $V^{\otimes m} \otimes (V^*)^{\otimes n}$ . Due to Corollary 6.2, we know that this number is the same as the number of irreducible representations of  $\mathrm{SU}(N)$  over  $V^{\otimes(m+n)}$ . It therefore suffices to study the irreducible representations of  $\mathrm{SU}(N)$  on a uniform product space  $V^{\otimes(m+n)}$ .

An explicit formula for the number of irreducible representations of  $\mathrm{SU}(N)$  over  $V^{\otimes(m+n)}$  has already been around for a long time [97, 118] (although this result seems unknown among representation theorists). Note that the proof given in the present section was written before we found out about [97, 118] and therefore does not follow any of these sources in particular. We however are almost certain that a proof similar to the one



given in this section can be found elsewhere in the literature. Lastly, we emphasize that Corollary 6.2 allows us to conclude that the formula presented here not only gives the number of irreducible representations of  $SU(N)$  over  $V^{\otimes(m+n)}$ , but also over all spaces  $V^{\otimes m} \otimes (V^*)^{\otimes n}$ , thus adding new insight and going beyond the standard result.

**An explicit formula:** An immediate consequence of Theorem 6.2 eq. (6.23c) is that the number of irreducible representations of  $SU(N)$  over  $V^{\otimes k}$  is given by the number of Hermitian permutations in  $S_k$

$$|\mathfrak{P}_k| = n_H(S_k) . \quad (6.33)$$

Thus, we need to study the Hermitian permutations in  $S_k$ , which are also referred to as *involutions* [96]. By the unitarity of all elements in  $S_k$ , the Hermitian elements are those that are their own inverse,

$$\rho^{-1} = \rho^\dagger = \rho . \quad (6.34)$$

When written in cycle notation, it becomes clear that a permutation  $\rho$  satisfying eq. (6.34) can only contain disjoint cycles of length  $\leq 2$ : Suppose  $\sigma$  is a cycle of length  $\ell$ ,  $\sigma = (a_1 a_2 \dots a_\ell)$ . Its inverse is given by [100]  $\sigma^{-1} = (a_\ell a_{\ell-1} \dots a_1)$ . Thus, if  $\ell \geq 3$ , it follows that  $\sigma^{-1} \neq \sigma$  [121]:

■ **Lemma 6.1 – permutations that are their own inverse [121]:**

A permutation  $\rho \in S_k$  is its own inverse (and thus Hermitian) if and only if  $\rho$  is comprised of transpositions and 1-cycles solely; that is, it contains no cycles of length  $> 2$ .

Hence, a Hermitian permutation  $\rho \in S_k$  has the disjoint cycle structure<sup>3</sup>  $\lambda_\rho$

$$\lambda_\rho = (\underbrace{2, 2, \dots, 2}_r, \underbrace{1, 1, \dots, 1}_t), \quad (6.35a)$$

such that

$$r \cdot 2 + t \cdot 1 = k . \quad (6.35b)$$

Eq. (6.35a) says that  $\rho$  contains  $r$  2-cycles and  $t$  1-cycles. The number of the irreducible representations of  $SU(N)$  over  $V^{\otimes k}$  is therefore given by the number of permutations in  $S_k$  that have the disjoint cycle structure (6.35a). Counting these permutations amounts to a combinatorial problem:

- If  $r = 0$ , i.e.  $\rho$  contains 1-cycles only, then  $\rho$  is the identity of  $S_k$ . Since the identity element of any group is unique, there exists exactly one element in  $S_k$  for which  $r = 0$ .
- Finding the number of permutations in  $S_k$  for which  $r = 1$  is equivalent to finding the number of transpositions in  $S_k$ . Since a transposition can be written as a cycle containing two letters (or numbers), we need to count how many ways we can choose 2 distinct letters out of  $k$  letters, which is

$$\binom{k}{2} = \frac{k!}{(k-2)!2!} . \quad (6.36)$$

<sup>3</sup>The disjoint cycle structure  $\lambda_\rho$  of a permutation  $\rho$  is the row vector listing the lengths of the disjoint cycles comprising  $\rho$  in decreasing order. For example, the disjoint cycle structure of the permutation  $\rho = (13)(245) \in S_5$  is  $\lambda_\rho = (3, 2)$ , c.f. [121].

- If  $r = 2$ , then  $\rho$  is a disjoint product of two transpositions. The number of such permutations in  $S_k$  corresponds to the number of ways one can choose two disjoint pairs of letters out of  $k$  letters: The first pair is chosen in the same way as for  $r = 1$ , *c.f.* equation (6.36). The second pair has to be chosen out of the  $k - 2$  remaining letters thus yielding a total number of

$$\binom{k}{2} \cdot \binom{k-2}{2} \tag{6.37}$$

ways to choose two disjoint pairs of letters out of  $k$  letters. However, we have been double counting: So far, we have treated the case where a particular pair  $(ab)$  is chosen before a pair  $(cd)$  as distinct from the case where they are chosen in the opposite order. However, the permutations corresponding to these two choices are identical,  $(ab) \cdot (cd) = (cd) \cdot (ab)$ , since the two transpositions  $(ab)$  and  $(cd)$  are disjoint. Correcting for this, the number of permutations with  $r = 2$  is given by

$$\frac{1}{2!} \cdot \binom{k}{2} \cdot \binom{k-2}{2} \tag{6.38}$$

- Following this pattern, the number of permutations with  $r = p$  for some integer  $p$  is given by

$$\frac{1}{p!} \cdot \binom{k}{2} \cdot \binom{k-2}{2} \cdot \binom{k-4}{2} \cdots \binom{k-2(p-1)}{2} = \frac{1}{p!} \cdot \prod_{l=0}^{p-1} \binom{k-2l}{2} \tag{6.39}$$

It will be convenient to define  $j := p - 1$  such that the counting for  $r = j + 1$  becomes

$$\frac{1}{(j+1)!} \cdot \prod_{l=0}^j \binom{k-2l}{2} \tag{6.40}$$

It now remains to add up all the contributions we obtained for each  $r$  from 0 up to some maximum value  $r_{\max}$ ,

$$1 + \sum_{j=0}^{r_{\max}} \frac{1}{(j+1)!} \cdot \prod_{l=0}^j \binom{k-2l}{2} \tag{6.41}$$

The value  $r_{\max}$  is the maximum number of 2-cycles that can make up a Hermitian permutation  $\rho$  in  $S_k$ . Since there are exactly  $k$  letters at our disposal,  $\rho$  can contain at most  $(k-2)/2$  transpositions if  $k$  is even, and at most  $(k-3)/2$  transpositions if  $k$  is odd. Using the floor function<sup>4</sup>  $\lfloor \cdot \rfloor$ , one may define  $r_{\max}$  as

$$r_{\max} := \left\lfloor \frac{(k-2)}{2} \right\rfloor \tag{6.42}$$

since

$$\left\lfloor \frac{(k-2)}{2} \right\rfloor = \begin{cases} \frac{(k-2)}{2} & \text{if } k \text{ is even} \\ \frac{(k-2)}{2} - \frac{1}{2} = \frac{(k-3)}{2} & \text{if } k \text{ is odd} \end{cases} \tag{6.43}$$

<sup>4</sup>The floor function  $\lfloor n \rfloor$  is defined to return the largest integer  $\leq n$ .

Summarizing our findings yields the following formula counting the irreducible representations of  $SU(N)$  over  $V^{\otimes m} \otimes (V^*)^{\otimes n}$ :

■ **Theorem 6.3 – formula for the number of irreducible representations of  $SU(N)$ :**

Let  $\mathfrak{P}_{m,n}$  be the set of all projection operators corresponding to the irreducible representations of  $SU(N)$  over  $V^{\otimes m} \otimes (V^*)^{\otimes n}$ ; by definition  $|\mathfrak{P}_{m,n}|$  gives the number of irreducible representations of  $SU(N)$  over  $V^{\otimes m} \otimes (V^*)^{\otimes n}$ . Then,

$$|\mathfrak{P}_{m,n}| = 1 + \sum_{j=0}^{\lfloor (m+n-2)/2 \rfloor} \frac{1}{(j+1)!} \cdot \prod_{l=0}^j \binom{(m+n)-2l}{2}. \quad (6.44)$$

As mentioned previously, in the absence of antiparticles (i.e. setting  $n = 0$  in the product  $V^{\otimes m} \otimes (V^*)^{\otimes n}$ ), Theorem 6.3 reduces to a result that has been known for a while [97, 118], namely the number of Young tableaux consisting of  $m$  boxes. The reason we nevertheless chose to explicitly re-derive eq. (6.44) here (even though the derivation is almost exclusively done for  $n = 0$  due to Corollary 6.2) is that practitioners in representation theory seem to be unaware of this result:

- Standard textbooks talking about Young tableaux, such as Fulton’s “Young tableaux” [95] and Sagan’s “Symmetric Group” [96], do not mention this counting argument.
- Sagan’s *Combinatorica* package [122] (rewritten in 2003) for *Mathematica* is designed to deal with permutations and Young tableaux. It includes a function called `NumberOfTableaux[m]` calculating the number of tableaux consisting of  $m$  boxes. The *Mathematica* documentation [123] explains that this function first explicitly constructs the Young diagrams consisting of  $m$  boxes, and then uses the hook length of each diagram to obtain the number of Young tableaux corresponding to it (*c.f.* [109] to see why this can be done). This method of counting the Young tableaux of a given size is, however, impractical and computationally expensive, since it requires each Young diagram to be explicitly generated.<sup>5</sup> The use of eq. (6.44) would appear to be more efficient.

## 6.5 Birdtracks and the recursion formula for the number of irreducible representations of $SU(N)$ over $V^{\otimes m} \otimes (V^*)^{\otimes n}$

In 1800, Rothe [118] published a paper containing a recursion formula for the number of involutions in the symmetric group  $S_k$ , where the recursion occurs over the integer  $k$ . According to Theorem 6.2, this number corresponds to the number of Young tableaux (classifying the irreducible representations of  $SU(N)$  over  $V^{\otimes k}$ ). In the language of Young tableaux, Rothe’s formula reads

$$|\mathcal{Y}_k| = |\mathcal{Y}_{k-1}| + (k-1)|\mathcal{Y}_{k-2}|. \quad (6.45)$$

Going beyond the standard literature, Corollary 6.2 predicts that Rothe’s recursion formula also gives the number of irreducible representations of  $SU(N)$  over a mixed product space consisting of  $k$  factors.

<sup>5</sup>Furthermore, there is, a priori, no way of knowing the number of Young diagrams of size  $m$ , since this number is equal to the number of partitions of the integer  $m$ , which is one of the great unsolved problems in number theory.

Chowla *et.al.* [97] provide an intuitive proof of Rothe’s recursion formula (6.45) using the standard representation of permutations in  $SU(N)$  (in this representation, each permutation  $\rho \in S_k$  is written as a  $k \times k$  matrix where each row and each column contains the integer 1 exactly once and all remaining entries are 0 — see [96, 100, 124]). In this section, [97]’s proof will be adapted to birdtracks: We will follow similar steps as given in [97], but instead of using the standard representation of the elements of the symmetric group we will use their birdtrack representation.

*Proof of eq. (6.45):* A consequence of Theorem 6.2 (in section 6.3) is that the number of Hermitian permutations in  $S_k$  is equal to the number irreducible representations of  $SU(N)$  over  $V^{\otimes k}$ , which in turn is given by the number of Young tableaux with  $k$  boxes  $|\mathcal{Y}_k|$ . As we have seen in Lemma 6.1, a permutation is an involution (i.e. its own inverse and thus Hermitian) if and only if it contains 1-cycles and transpositions only. In birdtrack notation, this means that the birdtrack corresponding to an involution  $\rho$  can contain either:

- horizontal legs corresponding to 1-cycles, e.g.  $\text{id}_3 = (1)(2)(3) = \begin{array}{ccc} \longleftrightarrow & & \\ \longleftrightarrow & & \\ \longleftrightarrow & & \end{array}$ ,
- cross-over between pairs of legs representing transpositions, e.g.  $(12)(3) = \begin{array}{ccc} \begin{array}{c} \nearrow \\ \searrow \end{array} & & \\ \longleftrightarrow & & \\ \begin{array}{c} \searrow \\ \nearrow \end{array} & & \end{array}$ .

Thus, we may sort the Hermitian birdtracks in  $S_k$  into two categories: those where the topmost leg is a horizontal line, and those where the top-most leg crosses over some other leg in the permutation.<sup>6</sup>

1. If the top-most leg is horizontal, then the remaining  $(k - 1)$  legs may constitute any Hermitian permutation found in  $S_{k-1}$ . As we know from Theorem 6.2, there are exactly  $|\mathcal{Y}_{k-1}|$  such permutations.
2. If the top-most leg crosses over another leg in the permutation, then there are  $(k - 2)$  legs left to comprise the Hermitian permutations of  $S_{k-2}$ , of which we know there exist  $|\mathcal{Y}_{k-2}|$ . Since there are  $(k - 1)$  possible legs that can cross over the topmost leg, there are a total of  $(k - 1)|\mathcal{Y}_{k-2}|$  permutations in this category.

As an example, we have arranged the birdtracks corresponding to the Hermitian permutations in  $S_5$  into these two categories in Figure 6.1.

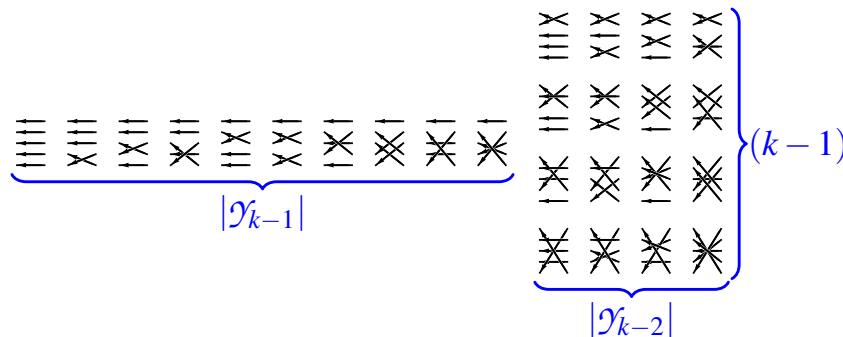


Figure 6.1: The birdtracks corresponding to the Hermitian permutations in  $S_5$ . This figure shows that there are exactly  $|\mathcal{Y}_{k-1}| = |\mathcal{Y}_4|$  permutations with a horizontal topmost leg, and  $(k-1)|\mathcal{Y}_{k-2}| = 4 \cdot |\mathcal{Y}_3|$  permutations where the topmost leg crosses over another leg. (All birdtracks in this figure were generated in *Mathematica*.)

<sup>6</sup>This corresponds to the two categories into which Chowla *et.al.* [97] divide the Hermitian permutations in  $S_k$ : In the standard representation, the integer 1 appearing in the first row may be situated in the first column, or in any *but* the first column.

Thus, the total number of Hermitian permutations in  $S_k$ ,  $|\mathcal{Y}_k|$ , is given by

$$|\mathcal{Y}_k| = |\mathcal{Y}_{k-1}| + (k-1)|\mathcal{Y}_{k-2}| \tag{6.46}$$

as claimed. □

## 6.6 A graphical bijection between the Young tableaux in $\mathcal{Y}_{m+1}$ and the Littlewood-Richardson tableaux in $\mathcal{Y}_{m,1}$

In this section, we present a graphical bijection between the Young tableaux consisting of  $(m+1)$  boxes and the Littlewood-Richardson tableaux  $\mathcal{Y}_{m,1}$ . The latter can be constructed using a simplified version of the LR-rule, often referred to as Pieri's formula [95], which was paraphrased in chapter 5 (*c.f.* Theorem 5.1).

Corollary 6.2 tells us that the number of irreducible representations of  $SU(N)$  over a product space  $V^{\otimes m} \otimes (V^*)^{\otimes n}$  only depends on the sum  $(m+n)$  but not on  $m$  and  $n$  individually. Since this number of irreducible representations over  $V^{\otimes m} \otimes (V^*)^{\otimes n}$  resp.  $V^{\otimes(m+n)}$  is given by the number of Littlewood-Richardson tableaux  $|\mathcal{Y}_{m,n}|$  resp. the number of Young tableaux  $|\mathcal{Y}_{m+n}|$ , an immediate consequence of Corollary 6.2 is that

$$|\mathcal{Y}_{m,n}| = |\mathcal{Y}_{m+n}| \quad \text{for all positive integers } m, n. \tag{6.47}$$

In particular, equation (6.47) must hold true for  $n = 1$  (i.e. tableaux/product spaces consisting of  $m$  fundamental and 1 antifundamental factors). In this specific situation, we are able to formulate a graphical bijection between the tableaux in  $\mathcal{Y}_{m+1}$  and the tableaux in  $\mathcal{Y}_{m,1}$ . The strategy to construct this bijection is as follows: Let  $\Theta$  be an arbitrary tableau in  $\mathcal{Y}_m$ . We will establish a 1-to-1 correspondence from each tableau in the sum

$$\Theta \otimes \boxed{m+1} \tag{6.48a}$$

to each tableau in the sum

$$\Theta \otimes \underbrace{\begin{array}{|c|} \hline m+1 \\ \hline m+2 \\ \hline m+3 \\ \hline \vdots \\ \hline m+N-1 \\ \hline \end{array}}_{=: \bar{\Phi}}, \tag{6.48b}$$

and vice versa. Since  $\Theta$  was chosen arbitrarily, the correspondence between the tableaux in (6.48a) and in (6.48b) immediately establishes a bijection between  $\mathcal{Y}_{(m+1)}$  and  $\mathcal{Y}_{m,1}$ .

According to Pieri's formula (Theorem 5.1), the tableaux in (6.48b) have each box  $\boxed{m+i}$  placed in a row lower than  $\boxed{m+j}$  for every  $N-1 \geq i > j$ . In particular, one tableau in the sum  $\Theta \otimes \bar{\Phi}$  will have each  $\boxed{m+i}$  situated in the  $i^{\text{th}}$  row. Call this tableau  $\Psi_1^\Theta$ .

Notice that the first column of  $\Psi_1^\ominus$  will have length  $(N - 1)$ . Since we may consider tableaux with columns of length at most  $N$ , we are, in principle, allowed to “add” another box to this first column and still obtain a valid tableau: we will signify this by drawing a dot  $\bullet$  in the place where this additional box could be added (i.e. below the first column). This dot will from now on be referred to as the *empty space*. As an example, consider the tableau

$$\Theta = \begin{array}{|c|c|c|c|} \hline 1 & 2 & 4 & 6 \\ \hline 3 & 5 & & \\ \hline 7 & 9 & & \\ \hline 8 & & & \\ \hline \end{array} \in \mathcal{Y}_9 . \tag{6.49}$$

To add one anti-quark, we need to form the tensor product of  $\Theta$  with the tableau consisting of one column and  $N - 1$  rows (let us denote  $\tilde{N} := N - 1$ ),

$$\bar{\varphi} = \begin{array}{|c|} \hline a_1 \\ \hline a_2 \\ \hline \vdots \\ \hline a_{\tilde{N}} \\ \hline \end{array} . \tag{6.50}$$

The corresponding tableau  $\Psi_1^\ominus$  is formed from  $\Theta$  by adding the box  $a_i$  at the end of the  $i^{\text{th}}$  row of  $\Theta$ ,

$$\Psi_1^\ominus = \begin{array}{|c|c|c|c|c|} \hline 1 & 2 & 4 & 6 & a_1 \\ \hline 3 & 5 & a_2 & & \\ \hline 7 & 9 & a_3 & & \\ \hline 8 & a_4 & & & \\ \hline a_5 & & & & \\ \hline \vdots & & & & \\ \hline a_{\tilde{N}} & & & & \\ \hline \bullet & & & & \\ \hline \end{array} , \tag{6.51}$$

where we have marked the empty spot with a dot  $\bullet$ .

The remaining tableaux in the sum (6.48b) can be constructed from  $\Psi_1^\ominus$  by playing a game of exchanging the empty space  $\bullet$  consecutively with the boxes  $a_i$  until another valid Young tableau  $\Psi_2^\ominus$  is obtained. To return to our example (6.51), we begin by exchanging the empty space with the box  $a_{\tilde{N}}$ . This, however, yields a disjoint tableau, not a Young tableau, requiring us to slide the empty space further up. For  $\Psi_1^\ominus$  in eq. (6.51), it becomes evident that all boxes  $a_{\tilde{N}}$  up to  $a_4$  have to be swapped with the empty space before another valid tableau is obtained; this tableau will be called  $\Psi_2^\ominus$

$$\Psi_2^\ominus = \begin{array}{|c|c|c|c|c|} \hline 1 & 2 & 4 & 6 & a_1 \\ \hline 3 & 5 & a_2 & & \\ \hline 7 & 9 & a_3 & & \\ \hline 8 & \bullet & & & \\ \hline a_4 & & & & \\ \hline a_5 & & & & \\ \hline \vdots & & & & \\ \hline a_{\tilde{N}} & & & & \\ \hline \end{array} . \tag{6.52}$$

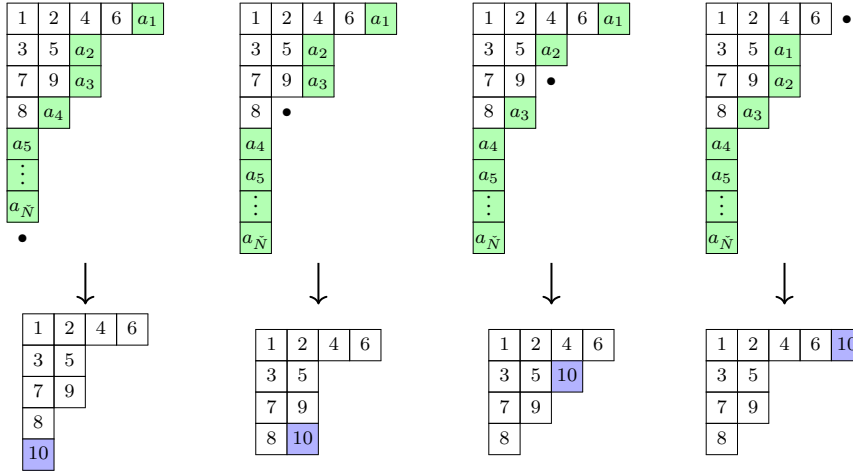
One may continue this swapping game, moving the empty spot  $\bullet$  to consecutively higher rows, to yield further

tableaux  $\Psi_i^\ominus$ . The final tableau is obtained when the empty space  $\bullet$  appears in the first row. For our example, this procedure yields two more tableaux,

$$\Psi_3^\ominus = \begin{array}{cccc} 1 & 2 & 4 & 6 \\ 3 & 5 & a_2 & \\ 7 & 9 & \bullet & \\ 8 & a_3 & & \\ a_4 & & & \\ a_5 & & & \\ \vdots & & & \\ a_{\tilde{N}} & & & \end{array} \quad \text{and} \quad \Psi_4^\ominus = \begin{array}{cccc} 1 & 2 & 4 & 6 \\ 3 & 5 & a_1 & \bullet \\ 7 & 9 & a_2 & \\ 8 & a_3 & & \\ a_4 & & & \\ a_5 & & & \\ \vdots & & & \\ a_{\tilde{N}} & & & \end{array} . \quad (6.53)$$

With the empty space clearly marked as illustrated in the example, it is easy to establish a 1-to-1 correspondence between the tableaux in the sum  $\Theta \otimes \boxed{m+1}$  and those in  $\{\Psi_1^\ominus, \Psi_2^\ominus, \dots, \Psi_l^\ominus\}$ , by identifying the two tableaux in which  $\boxed{m+1}$  and the empty space  $\bullet$  appear in the same column.<sup>7</sup>

In our example, the correspondence between  $\{\Psi_1^\ominus, \Psi_2^\ominus, \Psi_3^\ominus, \Psi_4^\ominus\}$  and the tableaux in  $\Theta \otimes \boxed{10}$  is given by



This clearly yields a unique correspondence, as the empty space  $\bullet$  as well as the box  $\boxed{10}$  can only appear in one spot in a particular column for the resulting tableau to be a Young tableau. Thus, there exists a 1-to-1 mapping between the tableaux in  $\mathcal{Y}_{m+1}$  and the tableaux in  $\mathcal{Y}_{m,1}$ , confirming the equality

$$|\mathcal{Y}_{m,1}| = |\mathcal{Y}_{m+1}| . \quad (6.54)$$

We suspect that an easy bijection between individual tableaux in  $\mathcal{Y}_{m,n}$  and  $\mathcal{Y}_{m+n}$  no longer exists for  $n > 1$ , since in this case the block structures of the associated matrices  $\mathfrak{M}_{m,n}$  and  $\mathfrak{M}_{m+n}$  may be different (as exemplified in chapter 7 for  $m = n = 2$ ). However, there exists, as yet, no conclusive proof for this statement (as far as the author is aware).

<sup>7</sup>It should be noted that both  $\bullet$  and  $\boxed{m+1}$  can only appear in a specific set of columns in the resulting tableaux, since all the  $a_i$  as well as  $\boxed{m+1}$  have to be added to  $\Theta$  according to the branching rules [95, 96].





## Chapter 7

# The Irreducible Representations of $SU(N)$ over the 4-Particle Fock Spaces: An Example

*In the present chapter, the results derived in chapter 6 will be verified in an example. We explicitly study the irreducible representations of  $SU(N)$  over  $V^{\otimes m} \otimes (V^*)^{\otimes n}$  for all positive integers  $m, n$  such that  $m+n = 4$ . We begin by examining the projection and transition operators in each of the cases. In particular, the orthogonality and completeness of the projectors will be verified (where it is not obvious).*

*Thereafter, in section 7.5, we explore what happens to these representations if we fix  $N = 2$ . This is particularly interesting in a physics context since  $SU(2)$  is the symmetry group of the theory of spin. Furthermore, since particles (composed of partons) do carry spin, it no longer suffices to consider the singlet representations of  $SU(2)$  only in this context. We review general results of  $SU(2)$  using standard methods found in many modern textbooks, and then subject the projection operators given previously to the limit  $N = 2$ , verifying the standard results.*

Having established various general results with regards to the irreducible representation of  $SU(N)$  over  $V^{\otimes m} \otimes (V^*)^{\otimes n}$  – most notably a counting argument for the number of irreducible representations – in chapter 6, we will now see these results applied in an example. In the present chapter, we will discuss the irreducible representations of  $SU(N)$  over the 4-particle Fock spaces, that is, all spaces  $V^{\otimes m} \otimes (V^*)^{\otimes n}$  such that  $m+n = 4$ . The focus here will be on a practical calculation to verify the general results. All examples in this chapter are performed in the birdtrack formalism [72, 87].

We will examine the irreducible representations over  $V^{\otimes 4}$  in section 7.2. The irreducible representations over  $(V^*)^{\otimes 4}$  are isomorphic to those over  $V^{\otimes 4}$  (this isomorphism is given in section 7.2.3) and are thus not discussed separately. The irreducible representations over  $V^{\otimes 3} \otimes (V^*)^{\otimes 1}$  are analyzed in section 7.3. Since the irreducible representations over  $V^{\otimes 1} \otimes (V^*)^{\otimes 3}$  are again isomorphic to those over  $V^{\otimes 3} \otimes (V^*)^{\otimes 1}$  (see section 7.3.3) we refrain from discussing them in any further detail. Lastly, we inspect the irreducible representations of  $SU(N)$  over  $V^{\otimes 2} \otimes (V^*)^{\otimes 2}$  in section 7.4.1.





## 7.2 The $4q$ -algebra

We begin our discussion with the irreducible representations of  $SU(N)$  over the product space  $V^{\otimes 4}$ , this being the most familiar of all examples discussed in this chapter. However, since the Hermitian Young projection<sup>2</sup> and transition operators of  $SU(N)$  over this space were discussed in chapters 3 and 4 respectively, this section will be kept brief – we merely state the operators.

### 7.2.1 The projection operators of the $4q$ -algebra

The Hermitian Young projection operators each correspond to a unique Young tableau in  $\mathcal{Y}_4$ :

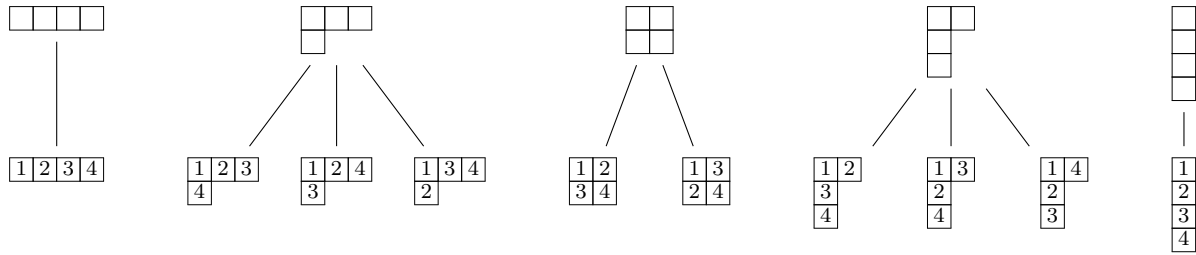


Figure 7.1: This graphic depicts all Young tableaux in  $\mathcal{Y}_4$ , indicating the Young diagrams from which they stem. A full ancestry tree of the tableaux in  $\mathcal{Y}_4$  is given in Fig. 4.1.

The projection operators  $P_i$  (where  $P_i$  corresponds to the  $i^{\text{th}}$  tableau in Fig. 7.1 read from left to right) and the dimension  $d$  of their corresponding representations are given by

$$P_1 = \begin{array}{c} \leftarrow \rightarrow \\ \leftarrow \rightarrow \\ \leftarrow \rightarrow \\ \leftarrow \rightarrow \end{array} \quad d_1 = \frac{N(N+1)(N+2)(N+3)}{24} \quad (7.5a)$$

$$P_2 = \frac{3}{2} \begin{array}{c} \leftarrow \rightarrow \\ \leftarrow \rightarrow \\ \leftarrow \rightarrow \\ \leftarrow \rightarrow \end{array} \quad d_2 = \frac{N(N+2)(N^2-1)}{8} \quad (7.5b)$$

$$P_3 = 2 \begin{array}{c} \leftarrow \rightarrow \\ \leftarrow \rightarrow \\ \leftarrow \rightarrow \\ \leftarrow \rightarrow \end{array} \quad d_3 = \frac{N(N+2)(N^2-1)}{8} \quad (7.5c)$$

$$P_4 = \frac{3}{2} \begin{array}{c} \leftarrow \rightarrow \\ \leftarrow \rightarrow \\ \leftarrow \rightarrow \\ \leftarrow \rightarrow \end{array} \quad d_4 = \frac{N(N+2)(N^2-1)}{8} \quad (7.5d)$$

$$P_5 = \frac{4}{3} \begin{array}{c} \leftarrow \rightarrow \\ \leftarrow \rightarrow \\ \leftarrow \rightarrow \\ \leftarrow \rightarrow \end{array} \quad d_5 = \frac{N^2(N^2-1)}{12} \quad (7.5e)$$

$$P_6 = \frac{4}{3} \begin{array}{c} \leftarrow \rightarrow \\ \leftarrow \rightarrow \\ \leftarrow \rightarrow \\ \leftarrow \rightarrow \end{array} \quad d_6 = \frac{N^2(N^2-1)}{12} \quad (7.5f)$$

<sup>2</sup>The Hermitian Young projection operators without corresponding transition operators were first given in [72].

$$P_7 = \frac{\theta_{N>2} \cdot 3}{2} \begin{array}{c} \text{Diagram: 4 strands, 2 crossings, 2 vertical bars} \\ \text{Diagram: 4 strands, 2 crossings, 2 vertical bars} \end{array} \quad d_7 = \frac{N(N-2)(N^2-1)}{8} \quad (7.5g)$$

$$P_8 = \theta_{N>2} \cdot 2 \begin{array}{c} \text{Diagram: 4 strands, 2 crossings, 3 vertical bars} \\ \text{Diagram: 4 strands, 2 crossings, 3 vertical bars} \end{array} \quad d_8 = \frac{N(N-2)(N^2-1)}{8} \quad (7.5h)$$

$$P_9 = \frac{\theta_{N>2} \cdot 3}{2} \begin{array}{c} \text{Diagram: 4 strands, 2 crossings, 2 vertical bars} \\ \text{Diagram: 4 strands, 2 crossings, 2 vertical bars} \end{array} \quad d_9 = \frac{N(N-2)(N^2-1)}{8} \quad (7.5i)$$

$$P_{10} = \theta_{N>3} \cdot \begin{array}{c} \text{Diagram: 4 strands, 1 crossing, 3 vertical bars} \\ \text{Diagram: 4 strands, 1 crossing, 3 vertical bars} \end{array} \quad d_{10} = \frac{N(N-1)(N-2)(N-3)}{24} \quad (7.5j)$$

In eqns. (7.5), we have added prefactors  $\theta_{N>k}$  (where  $\theta_{N>k} := 1$  if  $N > k$  and  $\theta_{N>k} := 0$  if  $N \leq k$ , *c.f.* later eq. (7.10)) to highlight dimensionally null operators. While the length of the longest antisymmetrizer in each operator in (7.5) immediately determines the value of  $N$  at which it becomes dimensionally zero, this reasoning no longer holds true for the projection and transition operators of  $SU(N)$  over mixed product spaces  $V^{\otimes m} \otimes (V^*)^{\otimes n}$  (as becomes evident in the following sections 7.3 and 7.4), and the prefactor  $\theta_{N>k}$  has to be added to mark the dimensionally null operators over  $V^{\otimes m} \otimes (V^*)^{\otimes n}$ . For the sake of consistency, we have therefore also added the prefactor  $\theta_{N>k}$  to the relevant operators here.

### 7.2.2 The full $4q$ -algebra: transition operators

Young tableaux with the same shape correspond to equivalent irreducible representations of  $SU(N)$  [93]. Thus, the block-structure of the matrix  $\mathfrak{M}_4$  can be read off from Figure 7.1,

$$\mathfrak{M}_4 = \begin{pmatrix} \boxed{1} & & & & \\ & \boxed{3} & & & \\ & & \boxed{2} & & \\ & & & \boxed{3} & \\ & & & & \boxed{1} \end{pmatrix}. \quad (7.6)$$

Explicitly, these blocks are as follows (we have highlighted the projection operators for visual clarity):

$$\begin{array}{|c|c|c|c|} \hline \square & \square & \square & \square \\ \hline \end{array} : \left( \begin{array}{c} \text{Diagram: 4 strands, 1 crossing, 3 vertical bars} \\ \text{Diagram: 4 strands, 1 crossing, 3 vertical bars} \end{array} \right) \quad (7.7a)$$

$$\begin{array}{|c|c|c|} \hline \square & \square & \square \\ \hline \end{array} : \left( \begin{array}{ccc} \begin{array}{c} \text{Diagram: 4 strands, 2 crossings, 2 vertical bars} \\ \text{Diagram: 4 strands, 2 crossings, 2 vertical bars} \end{array} & \begin{array}{c} \text{Diagram: 4 strands, 2 crossings, 2 vertical bars} \\ \text{Diagram: 4 strands, 2 crossings, 2 vertical bars} \end{array} & \begin{array}{c} \text{Diagram: 4 strands, 2 crossings, 2 vertical bars} \\ \text{Diagram: 4 strands, 2 crossings, 2 vertical bars} \end{array} \\ \begin{array}{c} \text{Diagram: 4 strands, 2 crossings, 2 vertical bars} \\ \text{Diagram: 4 strands, 2 crossings, 2 vertical bars} \end{array} & \begin{array}{c} \text{Diagram: 4 strands, 2 crossings, 3 vertical bars} \\ \text{Diagram: 4 strands, 2 crossings, 3 vertical bars} \end{array} & \begin{array}{c} \text{Diagram: 4 strands, 2 crossings, 3 vertical bars} \\ \text{Diagram: 4 strands, 2 crossings, 3 vertical bars} \end{array} \\ \begin{array}{c} \text{Diagram: 4 strands, 2 crossings, 2 vertical bars} \\ \text{Diagram: 4 strands, 2 crossings, 2 vertical bars} \end{array} & \begin{array}{c} \text{Diagram: 4 strands, 2 crossings, 2 vertical bars} \\ \text{Diagram: 4 strands, 2 crossings, 2 vertical bars} \end{array} & \begin{array}{c} \text{Diagram: 4 strands, 2 crossings, 2 vertical bars} \\ \text{Diagram: 4 strands, 2 crossings, 2 vertical bars} \end{array} \end{array} \right) \quad (7.7b)$$

$$\begin{array}{|c|c|} \hline & \\ \hline & \\ \hline \end{array} : \left( \begin{array}{cc} \begin{array}{c} \text{Diagram 1} \\ \frac{4}{3} \end{array} & \begin{array}{c} \text{Diagram 2} \\ \sqrt{\frac{4}{3}} \end{array} \\ \begin{array}{c} \text{Diagram 3} \\ \sqrt{\frac{4}{3}} \end{array} & \begin{array}{c} \text{Diagram 4} \\ \frac{4}{3} \end{array} \end{array} \right) \quad (7.7c)$$

$$\begin{array}{|c|c|} \hline & \\ \hline & \\ \hline \end{array} : \left( \begin{array}{ccc} \begin{array}{c} \text{Diagram 1} \\ \frac{\theta_{N>2} \cdot 3}{2} \end{array} & \begin{array}{c} \text{Diagram 2} \\ \theta_{N>2} \cdot \sqrt{3} \end{array} & \begin{array}{c} \text{Diagram 3} \\ \theta_{N>2} \cdot \sqrt{\frac{3}{2}} \end{array} \\ \begin{array}{c} \text{Diagram 4} \\ \theta_{N>2} \cdot \sqrt{3} \end{array} & \begin{array}{c} \text{Diagram 5} \\ \theta_{N>2} \cdot 2 \end{array} & \begin{array}{c} \text{Diagram 6} \\ \theta_{N>2} \cdot \sqrt{2} \end{array} \\ \begin{array}{c} \text{Diagram 7} \\ \theta_{N>2} \cdot \sqrt{\frac{3}{2}} \end{array} & \begin{array}{c} \text{Diagram 8} \\ \theta_{N>2} \cdot \sqrt{2} \end{array} & \begin{array}{c} \text{Diagram 9} \\ \frac{\theta_{N>2} \cdot 3}{2} \end{array} \end{array} \right) \quad (7.7d)$$

$$\begin{array}{|c|} \hline \\ \hline \\ \hline \\ \hline \end{array} : \left( \begin{array}{c} \text{Diagram 10} \\ \theta_{N>3} \end{array} \right) \quad (7.7e)$$

### 7.2.3 The $4\bar{q}$ -algebra

In birdtrack notation, it is easy to translate the projection operators on  $V^{\otimes 4}$  into those on  $(V^*)^{\otimes 4}$ ; one merely has to reverse the arrows on the index legs, for example,

$$\begin{array}{c} \text{Diagram 11} \\ \text{Diagram 12} \end{array} \xrightarrow{4q \rightarrow 4\bar{q}} \begin{array}{c} \text{Diagram 13} \\ \text{Diagram 14} \end{array} \quad (7.8)$$

Thus, the projection and transition operators of  $SU(N)$  over  $(V^*)^{\otimes 4}$  immediately follow from eqns. (7.7).

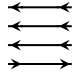
## 7.3 The $3q + 1\bar{q}$ -algebra

### 7.3.1 The projection operators of the $3q + 1\bar{q}$ -algebra

As already mentioned, it is possible to obtain the Hermitian projection operators corresponding to the irreducible representations of  $SU(N)$  over  $V^{\otimes 3} \otimes V^*$  from Littlewood-Richardson tableaux, although the caveat of this method is that it is computationally very expensive.<sup>3</sup> Instead, an Ansatz (based on much trial and error) for the Hermitian projection operators was made. Showing that the operators of our Ansatz satisfy the following four conditions ensures that they indeed correspond to the irreducible representations of  $SU(N)$  over  $V^{\otimes 3} \otimes V^*$ :

1. we must obtain the correct number of operators as predicted by Theorem 6.2, namely 10 operators
2. every operator must be idempotent

<sup>3</sup>C.f. the derivation of the irreducible projectors of  $SU(N)$  over  $V \otimes V^*$  from the appropriate Littlewood-Richardson tableaux in section 5.1.4.2 of chapter 5.

3. the operators must sum up to the identity  of the space  $V^{\otimes 3} \otimes V^*$  (and thus the corresponding dimensions must sum up to  $N^4$ )

4. the operators must be mutually orthogonal.

Our Ansatz is

$$\begin{array}{c} \left[ \begin{array}{c} \leftarrow \leftarrow \leftarrow \\ \leftarrow \leftarrow \leftarrow \\ \leftarrow \leftarrow \leftarrow \\ \leftarrow \leftarrow \leftarrow \end{array} \right] - \frac{3}{N+2} \left[ \begin{array}{c} \leftarrow \leftarrow \leftarrow \\ \leftarrow \leftarrow \leftarrow \\ \leftarrow \leftarrow \leftarrow \\ \leftarrow \leftarrow \leftarrow \end{array} \right] \end{array} \quad d_1 = \frac{N(N^2-1)(N+3)}{6} \quad (7.9a)$$

$$\frac{3}{N+2} \left[ \begin{array}{c} \leftarrow \leftarrow \leftarrow \\ \leftarrow \leftarrow \leftarrow \\ \leftarrow \leftarrow \leftarrow \\ \leftarrow \leftarrow \leftarrow \end{array} \right] \quad d_2 = \frac{N(N+1)}{2} \quad (7.9b)$$

$$\theta_{N>3} \cdot \left\{ \left[ \begin{array}{c} \leftarrow \leftarrow \leftarrow \\ \leftarrow \leftarrow \leftarrow \\ \leftarrow \leftarrow \leftarrow \\ \leftarrow \leftarrow \leftarrow \end{array} \right] - \frac{3}{N-2} \left[ \begin{array}{c} \leftarrow \leftarrow \leftarrow \\ \leftarrow \leftarrow \leftarrow \\ \leftarrow \leftarrow \leftarrow \\ \leftarrow \leftarrow \leftarrow \end{array} \right] \right\} \quad d_3 = \frac{\theta_{N>3} \cdot N(N-3)(N^2-1)}{6} \quad (7.9c)$$

$$\frac{\theta_{N>2} \cdot 3}{N-2} \left[ \begin{array}{c} \leftarrow \leftarrow \leftarrow \\ \leftarrow \leftarrow \leftarrow \\ \leftarrow \leftarrow \leftarrow \\ \leftarrow \leftarrow \leftarrow \end{array} \right] \quad d_4 = \frac{\theta_{N>2} \cdot N(N-1)}{2} \quad (7.9d)$$

$$\theta_{N>2} \cdot \left\{ \frac{4}{3} \left[ \begin{array}{c} \leftarrow \leftarrow \leftarrow \\ \leftarrow \leftarrow \leftarrow \\ \leftarrow \leftarrow \leftarrow \\ \leftarrow \leftarrow \leftarrow \end{array} \right] - \frac{8}{3(N-1)} \left[ \begin{array}{c} \leftarrow \leftarrow \leftarrow \\ \leftarrow \leftarrow \leftarrow \\ \leftarrow \leftarrow \leftarrow \\ \leftarrow \leftarrow \leftarrow \end{array} \right] - \frac{2}{N+1} \left[ \begin{array}{c} \leftarrow \leftarrow \leftarrow \\ \leftarrow \leftarrow \leftarrow \\ \leftarrow \leftarrow \leftarrow \\ \leftarrow \leftarrow \leftarrow \end{array} \right] \right\} \quad d_5 = \frac{\theta_{N>2} \cdot N^2(N^2-4)}{3} \quad (7.9e)$$

$$\frac{8}{3(N-1)} \left[ \begin{array}{c} \leftarrow \leftarrow \leftarrow \\ \leftarrow \leftarrow \leftarrow \\ \leftarrow \leftarrow \leftarrow \\ \leftarrow \leftarrow \leftarrow \end{array} \right] \quad d_6 = \frac{N(N+1)}{2} \quad (7.9f)$$

$$\frac{2}{N+1} \left[ \begin{array}{c} \leftarrow \leftarrow \leftarrow \\ \leftarrow \leftarrow \leftarrow \\ \leftarrow \leftarrow \leftarrow \\ \leftarrow \leftarrow \leftarrow \end{array} \right] \quad d_7 = \frac{N(N-1)}{2} \quad (7.9g)$$

$$\theta_{N>2} \cdot \left\{ \frac{4}{3} \left[ \begin{array}{c} \leftarrow \leftarrow \leftarrow \\ \leftarrow \leftarrow \leftarrow \\ \leftarrow \leftarrow \leftarrow \\ \leftarrow \leftarrow \leftarrow \end{array} \right] - \frac{8}{3(N+1)} \left[ \begin{array}{c} \leftarrow \leftarrow \leftarrow \\ \leftarrow \leftarrow \leftarrow \\ \leftarrow \leftarrow \leftarrow \\ \leftarrow \leftarrow \leftarrow \end{array} \right] - \frac{2}{N-1} \left[ \begin{array}{c} \leftarrow \leftarrow \leftarrow \\ \leftarrow \leftarrow \leftarrow \\ \leftarrow \leftarrow \leftarrow \\ \leftarrow \leftarrow \leftarrow \end{array} \right] \right\} \quad d_8 = \frac{\theta_{N>2} \cdot N^2(N^2-4)}{3} \quad (7.9h)$$

$$\frac{8}{3(N+1)} \left[ \begin{array}{c} \leftarrow \leftarrow \leftarrow \\ \leftarrow \leftarrow \leftarrow \\ \leftarrow \leftarrow \leftarrow \\ \leftarrow \leftarrow \leftarrow \end{array} \right] \quad d_9 = \frac{N(N-1)}{2} \quad (7.9i)$$

$$\frac{2}{N-1} \left[ \begin{array}{c} \leftarrow \leftarrow \leftarrow \\ \leftarrow \leftarrow \leftarrow \\ \leftarrow \leftarrow \leftarrow \\ \leftarrow \leftarrow \leftarrow \end{array} \right] \quad d_{10} = \frac{N(N+1)}{2} \quad (7.9j)$$

We draw attention to the fact that several operators in eqns. (7.9) have a prefactor  $\theta_{N>k}$ , which is defined as

$$\theta_{N>k} := \begin{cases} 1 & \text{if } N > k \\ 0 & \text{if } N \leq k \end{cases}, \quad (7.10)$$

analogous to the Heaviside step function, but with a definite value at  $N = k$ . The reason for adding this prefactor is threefold:

1. For one, the prefactors  $\theta_{N>k}$  conveniently demarcate operators which become dimensionally zero for  $N \leq k$ .<sup>4</sup>
2. Furthermore, the prefactors  $\theta_{N>k}$  prevent certain dimensions from becoming negative: For example, while the birdtrack expression of the operator (7.9c) can be used to show that it vanishes for  $N \leq 3$ , and thus corresponds to a representation of dimension 0, the corresponding dimension formula produces a negative result for  $N = 2$ . This is counteracted by the prefactor  $\theta_{N>3}$ .
3. Lastly, some operators contain constant factors that threaten to become infinite for certain values of  $N$ . (For example, operators (7.9c) and (7.9d) each contain a factor  $\frac{1}{N-2}$ , which would go to infinity as  $N \rightarrow 2$ .) This is again rectified by the prefactor  $\theta_{N>k}$ .

The remainder of this section is devoted to showing that the operators (7.9) satisfy the necessary conditions 1 to 4.

Clearly, the operators (7.9) satisfy condition 1 as there are exactly 10 operators. Furthermore, their idempotency (condition 2) is easily verified (the only ingredients needed to accomplish this are some of the cancellation rules given in chapter 2); we leave this as an exercise for the reader.

With regards to condition 3 (summability), it is important to notice that the operators (7.9) form the following partial sums:

$$(7.9a) + (7.9b) = \begin{array}{c} \leftarrow \leftarrow \leftarrow \\ \leftarrow \leftarrow \leftarrow \\ \leftarrow \leftarrow \leftarrow \\ \leftarrow \leftarrow \leftarrow \\ \leftarrow \leftarrow \leftarrow \\ \leftarrow \leftarrow \leftarrow \\ \leftarrow \leftarrow \leftarrow \\ \leftarrow \leftarrow \leftarrow \\ \leftarrow \leftarrow \leftarrow \\ \leftarrow \leftarrow \leftarrow \end{array} \quad (7.11a)$$

$$(7.9c) + (7.9d) = \begin{array}{c} \leftarrow \leftarrow \leftarrow \\ \leftarrow \leftarrow \leftarrow \\ \leftarrow \leftarrow \leftarrow \\ \leftarrow \leftarrow \leftarrow \\ \leftarrow \leftarrow \leftarrow \\ \leftarrow \leftarrow \leftarrow \\ \leftarrow \leftarrow \leftarrow \\ \leftarrow \leftarrow \leftarrow \\ \leftarrow \leftarrow \leftarrow \\ \leftarrow \leftarrow \leftarrow \end{array} \quad (7.11b)$$

$$(7.9e) + (7.9f) + (7.9g) = \frac{4}{3} \begin{array}{c} \leftarrow \leftarrow \leftarrow \\ \leftarrow \leftarrow \leftarrow \\ \leftarrow \leftarrow \leftarrow \\ \leftarrow \leftarrow \leftarrow \\ \leftarrow \leftarrow \leftarrow \\ \leftarrow \leftarrow \leftarrow \\ \leftarrow \leftarrow \leftarrow \\ \leftarrow \leftarrow \leftarrow \\ \leftarrow \leftarrow \leftarrow \\ \leftarrow \leftarrow \leftarrow \end{array} \quad (7.11c)$$

$$(7.9h) + (7.9i) + (7.9j) = \frac{4}{3} \begin{array}{c} \leftarrow \leftarrow \leftarrow \\ \leftarrow \leftarrow \leftarrow \\ \leftarrow \leftarrow \leftarrow \\ \leftarrow \leftarrow \leftarrow \\ \leftarrow \leftarrow \leftarrow \\ \leftarrow \leftarrow \leftarrow \\ \leftarrow \leftarrow \leftarrow \\ \leftarrow \leftarrow \leftarrow \\ \leftarrow \leftarrow \leftarrow \\ \leftarrow \leftarrow \leftarrow \end{array} \quad (7.11d)$$

The four operators in eqns. (7.11) can be recognized as the Hermitian Young projection operators of  $SU(N)$  over  $V^{\otimes 3}$  canonically embedded into  $V^{\otimes 3} \otimes V^*$ . Thus, the total sum of the operators (7.9) is given by

$$\begin{array}{c} \leftarrow \leftarrow \leftarrow \\ \leftarrow \leftarrow \leftarrow \\ \leftarrow \leftarrow \leftarrow \\ \leftarrow \leftarrow \leftarrow \\ \leftarrow \leftarrow \leftarrow \\ \leftarrow \leftarrow \leftarrow \\ \leftarrow \leftarrow \leftarrow \\ \leftarrow \leftarrow \leftarrow \\ \leftarrow \leftarrow \leftarrow \\ \leftarrow \leftarrow \leftarrow \end{array} + \begin{array}{c} \leftarrow \leftarrow \leftarrow \\ \leftarrow \leftarrow \leftarrow \\ \leftarrow \leftarrow \leftarrow \\ \leftarrow \leftarrow \leftarrow \\ \leftarrow \leftarrow \leftarrow \\ \leftarrow \leftarrow \leftarrow \\ \leftarrow \leftarrow \leftarrow \\ \leftarrow \leftarrow \leftarrow \\ \leftarrow \leftarrow \leftarrow \\ \leftarrow \leftarrow \leftarrow \end{array} + \frac{4}{3} \begin{array}{c} \leftarrow \leftarrow \leftarrow \\ \leftarrow \leftarrow \leftarrow \\ \leftarrow \leftarrow \leftarrow \\ \leftarrow \leftarrow \leftarrow \\ \leftarrow \leftarrow \leftarrow \\ \leftarrow \leftarrow \leftarrow \\ \leftarrow \leftarrow \leftarrow \\ \leftarrow \leftarrow \leftarrow \\ \leftarrow \leftarrow \leftarrow \\ \leftarrow \leftarrow \leftarrow \end{array} + \frac{4}{3} \begin{array}{c} \leftarrow \leftarrow \leftarrow \\ \leftarrow \leftarrow \leftarrow \\ \leftarrow \leftarrow \leftarrow \\ \leftarrow \leftarrow \leftarrow \\ \leftarrow \leftarrow \leftarrow \\ \leftarrow \leftarrow \leftarrow \\ \leftarrow \leftarrow \leftarrow \\ \leftarrow \leftarrow \leftarrow \\ \leftarrow \leftarrow \leftarrow \\ \leftarrow \leftarrow \leftarrow \end{array} = \begin{array}{c} \leftarrow \leftarrow \leftarrow \\ \leftarrow \leftarrow \leftarrow \\ \leftarrow \leftarrow \leftarrow \\ \leftarrow \leftarrow \leftarrow \\ \leftarrow \leftarrow \leftarrow \\ \leftarrow \leftarrow \leftarrow \\ \leftarrow \leftarrow \leftarrow \\ \leftarrow \leftarrow \leftarrow \\ \leftarrow \leftarrow \leftarrow \\ \leftarrow \leftarrow \leftarrow \end{array}, \quad (7.12)$$

as required. Also, the dimensions of the representations corresponding to the operators (7.9) sum up to  $N^4$ , as is easily verified via direct calculation.

Lastly, we investigate the orthogonality of the operators (7.9) (condition 4). Most operators are obviously orthogonal by the orthogonality of the Hermitian Young projection operators (7.11). However, there are

<sup>4</sup>We remind the reader of our discussion on dimensionally null operators in section 4.A.



pairs of operators in (7.9) for which this condition is not sufficient; these pairs are  $\{(7.9f), (7.9g)\}$  and  $\{(7.9i), (7.9j)\}$ .<sup>5</sup> We show the orthogonality of these operators here explicitly.

Let us consider the product of operators (7.9f) and (7.9g)

$$\frac{16}{3(N^2 - 1)} \left[ \text{diagram 1} \right] \cdot \left[ \text{diagram 2} \right] = \frac{16}{3(N^2 - 1)} \left[ \text{diagram 3} \right]. \quad (7.13)$$

In (7.13), we have marked a part of the operator that requires further simplification:

$$\begin{aligned} \left[ \text{diagram 4} \right] &= \frac{1}{2} \left( \left[ \text{diagram 5} \right] - \left[ \text{diagram 6} \right] \right) \\ &= \frac{1}{2} \left( \left[ \text{diagram 7} \right] - \frac{N+1}{2} \left[ \text{diagram 8} \right] \right). \end{aligned} \quad (7.14)$$

Substituting this back into (7.13) yields

$$\begin{aligned} \frac{8}{3(N^2 - 1)} \left( \left[ \text{diagram 9} \right] - \frac{N+1}{2} \left[ \text{diagram 10} \right] \right) \\ = \frac{4(1-N)}{3(N^2 - 1)} \left[ \text{diagram 11} \right]. \end{aligned} \quad (7.15)$$

Eq. (7.15) contains a symmetrizer and an antisymmetrizer (in the shaded box), which have more than one index leg in common. Such a construct vanishes, yielding the operator (7.13) to be zero. Thus, the operators (7.9f) and (7.9g) are indeed orthogonal, as claimed. Similarly, it can be shown that the projectors (7.9i) and (7.9j) are orthogonal.

### 7.3.2 The full $3q + 1\bar{q}$ -algebra: transition operators

The dimensions of the projection operators (7.9) not only suggest the block structure (7.4a) for  $\mathfrak{M}_{3,1}$ <sup>6</sup> but demand it: Since a necessary condition for two operators corresponding to equivalent representations is that the dimensions of the subspaces onto which they project are the same, the block structure (7.4b) immediately disqualifies as there are no four operators in eqns. (7.9) projecting onto subspaces with equal dimensions. Thus,  $\mathfrak{M}_{3,1}$  has the block structure (7.4a),

$$\mathfrak{M}_{3,1} = \begin{pmatrix} \mathbf{1} & & & \\ & \mathbf{3} & & \\ & & \mathbf{2} & \\ & & & \mathbf{3} \\ & & & & \mathbf{1} \end{pmatrix}. \quad (7.16)$$

<sup>5</sup>If these pairs are mutually orthogonal, it immediately follows that the operators (7.9f) and (7.9g) are orthogonal to every other operator in eqns. (7.9), and similarly for the operators (7.9i) and (7.9j).

<sup>6</sup>There are two operators ((7.9a) and (7.9c)) with a unique dimension formula each, two sets of three operators ({(7.9b), (7.9f), (7.9j)} and {(7.9d), (7.9g), (7.9i)}) where each sets corresponds to the same dimension, and a pair of operators ((7.9e) and (7.9h)) corresponding to representations with the same dimension, mirroring the 1-3-2-3-1 pattern of the block structure (7.4a).

This is confirmed by the Littlewood-Richardson (LR) tableaux over  $V^{\otimes 3} \otimes V^*$ , which are given in Figure 7.2.

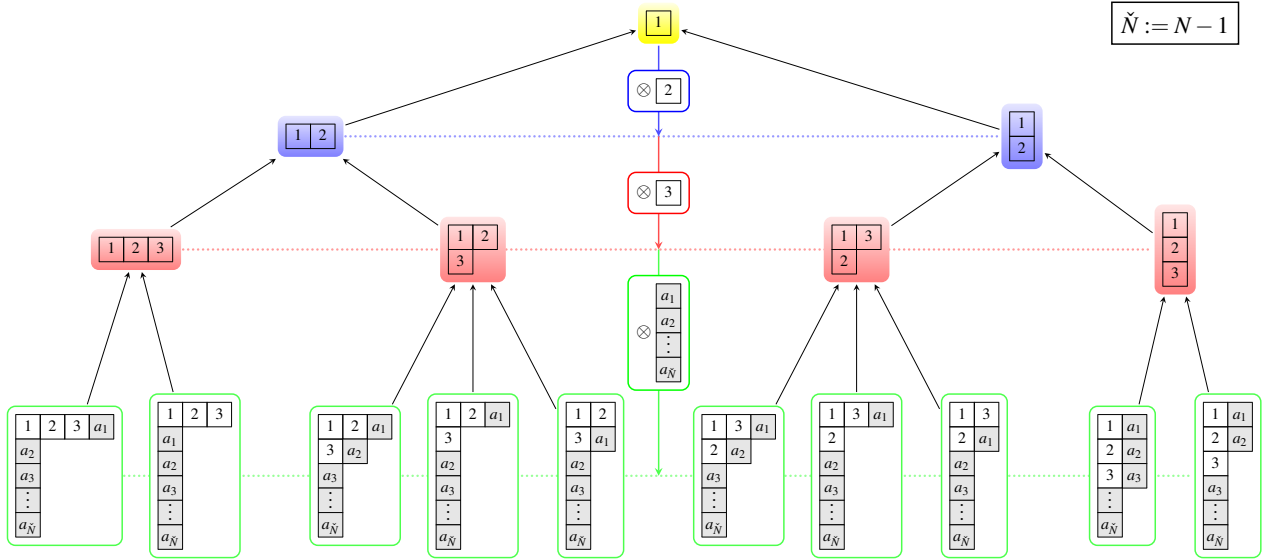


Figure 7.2: This figure gives the ancestry tree of the Littlewood-Richardson tableaux in  $\mathcal{Y}_{3,1}$ , which can be constructed using Pieri’s formula paraphrased in Theorem 5.1. Since tableaux with the same shape correspond to equivalent irreducible representations of  $SU(N)$  (c.f. [93] or the discussion around eq. (7.33)), these tableaux incite the block structure (7.16) for  $\mathfrak{M}_{3,1}$ .

Using the “factors-over-hooks” formula (c.f. [72, 113], or our rendition in section 5.1.3 of chapter 5), one may match each block in the matrix  $\mathfrak{M}_{3,1}$  (corresponding to a representation of dimension d) to a particular LR-diagram.

In particular, the two  $1 \times 1$ -blocks will contain the operators (7.9a) and (7.9c) respectively,

$$\text{length}_{N-1} \left\{ \begin{array}{c} \square \square \square \\ \square \\ \vdots \end{array} \right\} : \left( \begin{array}{c} \leftarrow \leftarrow \leftarrow \\ \leftarrow \leftarrow \leftarrow \\ \leftarrow \leftarrow \leftarrow \\ \leftarrow \leftarrow \leftarrow \\ \leftarrow \leftarrow \leftarrow \end{array} - \frac{3}{N+2} \begin{array}{c} \leftarrow \leftarrow \leftarrow \\ \leftarrow \leftarrow \leftarrow \\ \leftarrow \leftarrow \leftarrow \\ \leftarrow \leftarrow \leftarrow \\ \leftarrow \leftarrow \leftarrow \end{array} \right), \quad \text{length}_{N-1} \left\{ \begin{array}{c} \square \square \\ \square \\ \vdots \end{array} \right\} : \theta_{N>3} \cdot \left( \begin{array}{c} \leftarrow \leftarrow \leftarrow \\ \leftarrow \leftarrow \leftarrow \\ \leftarrow \leftarrow \leftarrow \\ \leftarrow \leftarrow \leftarrow \\ \leftarrow \leftarrow \leftarrow \end{array} - \frac{3}{N-2} \begin{array}{c} \leftarrow \leftarrow \leftarrow \\ \leftarrow \leftarrow \leftarrow \\ \leftarrow \leftarrow \leftarrow \\ \leftarrow \leftarrow \leftarrow \\ \leftarrow \leftarrow \leftarrow \end{array} \right). \quad (7.17)$$

The first  $3 \times 3$ -block corresponds to the equivalent representations of dimension  $\frac{N(N+1)}{2}$ , and thus has the projection operators (7.9b), (7.9f) and (7.9j) on its diagonal. Augmenting the projectors with their transition operators (which were constructed by making an Ansatz that was required to satisfy eqns. (4.91)) yields

$$\text{length}_N \left\{ \begin{array}{c} \square \square \square \\ \square \square \\ \vdots \end{array} \right\} : \left( \begin{array}{ccc} \begin{array}{c} \leftarrow \leftarrow \leftarrow \\ \leftarrow \leftarrow \leftarrow \\ \leftarrow \leftarrow \leftarrow \\ \leftarrow \leftarrow \leftarrow \\ \leftarrow \leftarrow \leftarrow \end{array} & \sqrt{\frac{8}{(N-1)(N+2)}} \begin{array}{c} \leftarrow \leftarrow \leftarrow \\ \leftarrow \leftarrow \leftarrow \\ \leftarrow \leftarrow \leftarrow \\ \leftarrow \leftarrow \leftarrow \\ \leftarrow \leftarrow \leftarrow \end{array} & \sqrt{\frac{6}{(N-1)(N+2)}} \begin{array}{c} \leftarrow \leftarrow \leftarrow \\ \leftarrow \leftarrow \leftarrow \\ \leftarrow \leftarrow \leftarrow \\ \leftarrow \leftarrow \leftarrow \\ \leftarrow \leftarrow \leftarrow \end{array} \\ \sqrt{\frac{8}{(N-1)(N+2)}} \begin{array}{c} \leftarrow \leftarrow \leftarrow \\ \leftarrow \leftarrow \leftarrow \\ \leftarrow \leftarrow \leftarrow \\ \leftarrow \leftarrow \leftarrow \\ \leftarrow \leftarrow \leftarrow \end{array} & \begin{array}{c} \leftarrow \leftarrow \leftarrow \\ \leftarrow \leftarrow \leftarrow \\ \leftarrow \leftarrow \leftarrow \\ \leftarrow \leftarrow \leftarrow \\ \leftarrow \leftarrow \leftarrow \end{array} & \sqrt{\frac{16}{3} \frac{1}{N-1}} \begin{array}{c} \leftarrow \leftarrow \leftarrow \\ \leftarrow \leftarrow \leftarrow \\ \leftarrow \leftarrow \leftarrow \\ \leftarrow \leftarrow \leftarrow \\ \leftarrow \leftarrow \leftarrow \end{array} \\ \sqrt{\frac{6}{(N-1)(N+2)}} \begin{array}{c} \leftarrow \leftarrow \leftarrow \\ \leftarrow \leftarrow \leftarrow \\ \leftarrow \leftarrow \leftarrow \\ \leftarrow \leftarrow \leftarrow \\ \leftarrow \leftarrow \leftarrow \end{array} & \sqrt{\frac{16}{3} \frac{1}{N-1}} \begin{array}{c} \leftarrow \leftarrow \leftarrow \\ \leftarrow \leftarrow \leftarrow \\ \leftarrow \leftarrow \leftarrow \\ \leftarrow \leftarrow \leftarrow \\ \leftarrow \leftarrow \leftarrow \end{array} & \begin{array}{c} \leftarrow \leftarrow \leftarrow \\ \leftarrow \leftarrow \leftarrow \\ \leftarrow \leftarrow \leftarrow \\ \leftarrow \leftarrow \leftarrow \\ \leftarrow \leftarrow \leftarrow \end{array} \end{array} \right). \quad (7.18)$$

The operators (7.9e) and (7.9h) determine the central  $2 \times 2$ -block of  $\mathfrak{M}_{3,1}$ , as they project onto equivalent representations of dimension  $\frac{N(N^2-4)}{3}$ . The two projection operators, which correspond to the LR-diagram

$$\text{length}_{N-1} \left\{ \begin{array}{|c|c|c|} \hline \square & \square & \square \\ \hline \square & \square & \square \\ \hline \vdots & \vdots & \vdots \\ \hline \square & \square & \square \\ \hline \end{array} \right\}, \quad (7.19a)$$

together with their transition operators, are given by

$$\left( \begin{array}{c} \theta_{N>2} \cdot \left\{ \frac{4}{3} \begin{array}{|c|c|c|} \hline \leftarrow \square \rightarrow \\ \hline \leftarrow \square \rightarrow \\ \hline \leftarrow \square \rightarrow \\ \hline \end{array} - \frac{8}{3(N-1)} \begin{array}{|c|c|c|} \hline \leftarrow \square \rightarrow \\ \hline \leftarrow \square \rightarrow \\ \hline \leftarrow \square \rightarrow \\ \hline \end{array} - \frac{2}{N+1} \begin{array}{|c|c|c|} \hline \leftarrow \square \rightarrow \\ \hline \leftarrow \square \rightarrow \\ \hline \leftarrow \square \rightarrow \\ \hline \end{array} \end{array} \right) \theta_{N>2} \cdot \sqrt{\frac{4}{3}} \left( \begin{array}{|c|c|c|} \hline \leftarrow \square \rightarrow \\ \hline \leftarrow \square \rightarrow \\ \hline \leftarrow \square \rightarrow \\ \hline \end{array} - \frac{2}{N-1} \begin{array}{|c|c|c|} \hline \leftarrow \square \rightarrow \\ \hline \leftarrow \square \rightarrow \\ \hline \leftarrow \square \rightarrow \\ \hline \end{array} - \frac{2}{N+1} \begin{array}{|c|c|c|} \hline \leftarrow \square \rightarrow \\ \hline \leftarrow \square \rightarrow \\ \hline \leftarrow \square \rightarrow \\ \hline \end{array} \right) \\ \theta_{N>2} \cdot \sqrt{\frac{4}{3}} \left( \begin{array}{|c|c|c|} \hline \leftarrow \square \rightarrow \\ \hline \leftarrow \square \rightarrow \\ \hline \leftarrow \square \rightarrow \\ \hline \end{array} - \frac{2}{N-1} \begin{array}{|c|c|c|} \hline \leftarrow \square \rightarrow \\ \hline \leftarrow \square \rightarrow \\ \hline \leftarrow \square \rightarrow \\ \hline \end{array} - \frac{2}{N+1} \begin{array}{|c|c|c|} \hline \leftarrow \square \rightarrow \\ \hline \leftarrow \square \rightarrow \\ \hline \leftarrow \square \rightarrow \\ \hline \end{array} \right) \theta_{N>2} \cdot \left\{ \frac{4}{3} \begin{array}{|c|c|c|} \hline \leftarrow \square \rightarrow \\ \hline \leftarrow \square \rightarrow \\ \hline \leftarrow \square \rightarrow \\ \hline \end{array} - \frac{8}{3(N+1)} \begin{array}{|c|c|c|} \hline \leftarrow \square \rightarrow \\ \hline \leftarrow \square \rightarrow \\ \hline \leftarrow \square \rightarrow \\ \hline \end{array} - \frac{2}{N-1} \begin{array}{|c|c|c|} \hline \leftarrow \square \rightarrow \\ \hline \leftarrow \square \rightarrow \\ \hline \leftarrow \square \rightarrow \\ \hline \end{array} \right\} \end{array} \right). \quad (7.19b)$$

Lastly, the operators (7.9d), (7.9g) and (7.9i), corresponding to equivalent irreducible representations of dimension  $\frac{N(N-1)}{2}$ , dictate the structure of the second  $3 \times 3$ -block in  $\mathfrak{M}_{3,1}$ . This block is given by

$$\text{length}_N \left\{ \begin{array}{|c|c|c|} \hline \square & \square & \square \\ \hline \square & \square & \square \\ \hline \vdots & \vdots & \vdots \\ \hline \square & \square & \square \\ \hline \end{array} \right\} : \left( \begin{array}{ccc} \theta_{N>2} \cdot \frac{3}{N+2} \begin{array}{|c|c|c|} \hline \leftarrow \square \rightarrow \\ \hline \leftarrow \square \rightarrow \\ \hline \leftarrow \square \rightarrow \\ \hline \end{array} & \theta_{N>2} \cdot \sqrt{\frac{6}{(N-1)(N+2)}} \begin{array}{|c|c|c|} \hline \leftarrow \square \rightarrow \\ \hline \leftarrow \square \rightarrow \\ \hline \leftarrow \square \rightarrow \\ \hline \end{array} & \theta_{N>2} \cdot \sqrt{\frac{8}{(N-1)(N+2)}} \begin{array}{|c|c|c|} \hline \leftarrow \square \rightarrow \\ \hline \leftarrow \square \rightarrow \\ \hline \leftarrow \square \rightarrow \\ \hline \end{array} \\ \theta_{N>2} \cdot \sqrt{\frac{6}{(N-1)(N+2)}} \begin{array}{|c|c|c|} \hline \leftarrow \square \rightarrow \\ \hline \leftarrow \square \rightarrow \\ \hline \leftarrow \square \rightarrow \\ \hline \end{array} & \frac{2}{N-1} \begin{array}{|c|c|c|} \hline \leftarrow \square \rightarrow \\ \hline \leftarrow \square \rightarrow \\ \hline \leftarrow \square \rightarrow \\ \hline \end{array} & \sqrt{\frac{16}{3}} \frac{1}{N-1} \begin{array}{|c|c|c|} \hline \leftarrow \square \rightarrow \\ \hline \leftarrow \square \rightarrow \\ \hline \leftarrow \square \rightarrow \\ \hline \end{array} \\ \theta_{N>2} \cdot \sqrt{\frac{8}{(N-1)(N+2)}} \begin{array}{|c|c|c|} \hline \leftarrow \square \rightarrow \\ \hline \leftarrow \square \rightarrow \\ \hline \leftarrow \square \rightarrow \\ \hline \end{array} & \sqrt{\frac{16}{3}} \frac{1}{N-1} \begin{array}{|c|c|c|} \hline \leftarrow \square \rightarrow \\ \hline \leftarrow \square \rightarrow \\ \hline \leftarrow \square \rightarrow \\ \hline \end{array} & \frac{8}{3(N-1)} \begin{array}{|c|c|c|} \hline \leftarrow \square \rightarrow \\ \hline \leftarrow \square \rightarrow \\ \hline \leftarrow \square \rightarrow \\ \hline \end{array} \end{array} \right). \quad (7.20)$$

### 7.3.3 The $1q + 3\bar{q}$ -algebra

In section (7.2.3), we presented the isomorphism between the irreducible representations of  $SU(N)$  over  $V^{\otimes 4}$  and those over  $(V^*)^{\otimes 4}$ : the operators are translated into each other by reversing the arrow direction.

If the same method is applied to the operators of  $SU(N)$  over  $V^{\otimes 3} \otimes V^*$  and those over  $V^{\otimes 3} \otimes V^*$ , one obtains the projectors on  $(V^*)^{\otimes 3} \otimes V$  rather than  $V \otimes (V^*)^{\otimes 3}$  (as birdtracks are conventionally read from top to bottom). We need to additionally flip the operators about the horizontal axis, for example

$$\begin{array}{|c|c|c|} \hline \leftarrow \square \rightarrow \\ \hline \leftarrow \square \rightarrow \\ \hline \leftarrow \square \rightarrow \\ \hline \end{array} - \frac{3}{N+2} \begin{array}{|c|c|c|} \hline \leftarrow \square \rightarrow \\ \hline \leftarrow \square \rightarrow \\ \hline \leftarrow \square \rightarrow \\ \hline \end{array} \xrightarrow{3q+1\bar{q} \rightarrow 1q+3\bar{q}} \begin{array}{|c|c|c|} \hline \leftarrow \square \rightarrow \\ \hline \leftarrow \square \rightarrow \\ \hline \leftarrow \square \rightarrow \\ \hline \end{array} - \frac{3}{N+2} \begin{array}{|c|c|c|} \hline \leftarrow \square \rightarrow \\ \hline \leftarrow \square \rightarrow \\ \hline \leftarrow \square \rightarrow \\ \hline \end{array}. \quad (7.21)$$

In physics parlance, the top index line once again represents the quark, and the bottom three index lines represent the antiquarks. This isomorphism implies that the matrices  $\mathfrak{M}_{3,1}$  and  $\mathfrak{M}_{1,3}$  have the same block-structure.

## 7.4 The $2q + 2\bar{q}$ -algebra

In this section, we present all projection and transition operators of  $SU(N)$  over  $V^{\otimes 2} \otimes (V^*)^{\otimes 2}$ . In section 7.4.1, we give the Hermitian projection operators corresponding to the irreducible representations of  $SU(N)$ , and discuss some of their properties. In section 7.4.2, we focus our discussion on the block structure of the matrix  $\mathfrak{M}_{2,2}$ ; we provide the transition operators between projectors onto equivalent irreducible representations, thus completing the basis of the algebra of primitive invariants  $\text{API}(SU(N), V^{\otimes 2} \otimes (V^*)^{\otimes 2})$ .

Cvitanović [72, secs. 8.3 and 9.12] has already provided these operators in a basis of (anti-) fundamental and adjoint lines. We repeat this basis in section 7.4.3 and augment it with the appropriate transition operators.

### 7.4.1 The projection operators of the $2q + 2\bar{q}$ -algebra in an (anti-)symmetrizer basis

Cvitanović [72, sec. 8.3] noted that the projection operators

$$\begin{array}{c} \leftarrow \square \rightarrow \\ \leftarrow \square \rightarrow \\ \leftarrow \square \rightarrow \end{array}, \quad \begin{array}{c} \leftarrow \blacksquare \rightarrow \\ \leftarrow \blacksquare \rightarrow \\ \leftarrow \blacksquare \rightarrow \end{array}, \quad \begin{array}{c} \leftarrow \square \rightarrow \\ \leftarrow \blacksquare \rightarrow \\ \leftarrow \blacksquare \rightarrow \end{array}, \quad \text{and} \quad \begin{array}{c} \leftarrow \blacksquare \rightarrow \\ \leftarrow \blacksquare \rightarrow \\ \leftarrow \blacksquare \rightarrow \end{array} \quad (7.22a)$$

are a decomposition of unity,

$$\begin{array}{c} \leftarrow \square \rightarrow \\ \leftarrow \square \rightarrow \\ \leftarrow \square \rightarrow \end{array} + \begin{array}{c} \leftarrow \blacksquare \rightarrow \\ \leftarrow \blacksquare \rightarrow \\ \leftarrow \blacksquare \rightarrow \end{array} + \begin{array}{c} \leftarrow \square \rightarrow \\ \leftarrow \blacksquare \rightarrow \\ \leftarrow \blacksquare \rightarrow \end{array} + \begin{array}{c} \leftarrow \blacksquare \rightarrow \\ \leftarrow \blacksquare \rightarrow \\ \leftarrow \blacksquare \rightarrow \end{array} = \begin{array}{c} \leftarrow \leftarrow \rightarrow \\ \leftarrow \leftarrow \rightarrow \\ \leftarrow \leftarrow \rightarrow \end{array}, \quad (7.22b)$$

and thus provide a good starting point in finding the projection operators corresponding to the irreducible representations of  $SU(N)$  over  $V^{\otimes 2} \otimes (V^*)^{\otimes 2}$ . [72] then proceeds by giving the  $2q + 2\bar{q}$ -projection operators in an alternative basis, *c.f.* section 7.4.3.

The alternative basis given by Cvitanović teaches us that none of the representations corresponding to the operators (7.22a) are irreducible, but observation (7.22b) motivates the Ansatz that the irreducible operators can be obtained from the operators (7.22a) by subtracting suitable irreducible operators obtained by other means. For example, from chapter 5, we are already familiar with the singlet projection operators

$$\frac{2}{N(N-1)} \begin{array}{c} \leftarrow \blacksquare \rightarrow \\ \leftarrow \blacksquare \rightarrow \\ \leftarrow \blacksquare \rightarrow \end{array} \begin{array}{c} \leftarrow \square \rightarrow \\ \leftarrow \square \rightarrow \\ \leftarrow \square \rightarrow \end{array} \quad \text{and} \quad \frac{2}{N(N+1)} \begin{array}{c} \leftarrow \square \rightarrow \\ \leftarrow \square \rightarrow \\ \leftarrow \square \rightarrow \end{array} \begin{array}{c} \leftarrow \blacksquare \rightarrow \\ \leftarrow \blacksquare \rightarrow \\ \leftarrow \blacksquare \rightarrow \end{array}, \quad (7.23)$$

which correspond to the irreducible singlet representations of  $SU(N)$  over  $V^{\otimes 2} \otimes (V^*)^{\otimes 2}$ . A first Ansatz for two further ‘‘irreducible’’ operators would be

$$\begin{array}{c} \leftarrow \blacksquare \rightarrow \\ \leftarrow \blacksquare \rightarrow \\ \leftarrow \blacksquare \rightarrow \end{array} - \frac{2}{N(N-1)} \begin{array}{c} \leftarrow \blacksquare \rightarrow \\ \leftarrow \blacksquare \rightarrow \\ \leftarrow \blacksquare \rightarrow \end{array} \begin{array}{c} \leftarrow \square \rightarrow \\ \leftarrow \square \rightarrow \\ \leftarrow \square \rightarrow \end{array} \quad \text{and} \quad \begin{array}{c} \leftarrow \square \rightarrow \\ \leftarrow \square \rightarrow \\ \leftarrow \square \rightarrow \end{array} - \frac{2}{N(N+1)} \begin{array}{c} \leftarrow \square \rightarrow \\ \leftarrow \square \rightarrow \\ \leftarrow \square \rightarrow \end{array} \begin{array}{c} \leftarrow \blacksquare \rightarrow \\ \leftarrow \blacksquare \rightarrow \\ \leftarrow \blacksquare \rightarrow \end{array}. \quad (7.24)$$

It turns out that one has to subtract another piece from each operator in (7.24) to obtain an irreducible one, but we hope that the general strategy is now clear.

In this way, we were able to construct 10 projection operators that are:

- mutually orthogonal
- idempotent
- complete (they sum up to the identity).

We can thus be sure that the set of operators we found indeed corresponds to the irreducible representations of  $SU(N)$  over  $V^{\otimes 2} \otimes (V^*)^{\otimes 2}$ . These operators were found to be

$$\begin{array}{c} \begin{array}{c} \leftarrow \leftarrow \leftarrow \\ \leftarrow \leftarrow \leftarrow \\ \rightarrow \rightarrow \rightarrow \\ \rightarrow \rightarrow \rightarrow \end{array} - \frac{4 \cdot \theta_{N>2}}{N-2} \left( \begin{array}{c} \leftarrow \leftarrow \leftarrow \\ \leftarrow \leftarrow \leftarrow \\ \rightarrow \rightarrow \rightarrow \\ \rightarrow \rightarrow \rightarrow \end{array} - \frac{1}{N} \begin{array}{c} \leftarrow \leftarrow \leftarrow \\ \leftarrow \leftarrow \leftarrow \\ \rightarrow \rightarrow \rightarrow \\ \rightarrow \rightarrow \rightarrow \end{array} \right) - \frac{2}{N(N-1)} \begin{array}{c} \leftarrow \leftarrow \leftarrow \\ \leftarrow \leftarrow \leftarrow \\ \rightarrow \rightarrow \rightarrow \\ \rightarrow \rightarrow \rightarrow \end{array} = \end{array} \quad (7.25a)$$

$$= \theta_{N>3} \cdot \left\{ \begin{array}{c} \leftarrow \leftarrow \leftarrow \\ \leftarrow \leftarrow \leftarrow \\ \rightarrow \rightarrow \rightarrow \\ \rightarrow \rightarrow \rightarrow \end{array} - \frac{2}{N-2} \left( 2 \begin{array}{c} \leftarrow \leftarrow \leftarrow \\ \leftarrow \leftarrow \leftarrow \\ \rightarrow \rightarrow \rightarrow \\ \rightarrow \rightarrow \rightarrow \end{array} - \frac{1}{N-1} \begin{array}{c} \leftarrow \leftarrow \leftarrow \\ \leftarrow \leftarrow \leftarrow \\ \rightarrow \rightarrow \rightarrow \\ \rightarrow \rightarrow \rightarrow \end{array} \right) \right\} \quad d_1 = \theta_{N>3} \cdot \frac{N^2(N+1)(N-3)}{4}$$

$$\frac{4 \cdot \theta_{N>2}}{N-2} \left( \begin{array}{c} \leftarrow \leftarrow \leftarrow \\ \leftarrow \leftarrow \leftarrow \\ \rightarrow \rightarrow \rightarrow \\ \rightarrow \rightarrow \rightarrow \end{array} - \frac{1}{N} \begin{array}{c} \leftarrow \leftarrow \leftarrow \\ \leftarrow \leftarrow \leftarrow \\ \rightarrow \rightarrow \rightarrow \\ \rightarrow \rightarrow \rightarrow \end{array} \right) \quad d_2 = \theta_{N>2} (N^2 - 1) \quad (7.25b)$$

$$\frac{2}{N(N-1)} \begin{array}{c} \leftarrow \leftarrow \leftarrow \\ \leftarrow \leftarrow \leftarrow \\ \rightarrow \rightarrow \rightarrow \\ \rightarrow \rightarrow \rightarrow \end{array} \quad d_3 = 1 \quad (7.25c)$$

$$\begin{array}{c} \begin{array}{c} \leftarrow \leftarrow \leftarrow \\ \leftarrow \leftarrow \leftarrow \\ \rightarrow \rightarrow \rightarrow \\ \rightarrow \rightarrow \rightarrow \end{array} - \frac{4}{N+2} \left( \begin{array}{c} \leftarrow \leftarrow \leftarrow \\ \leftarrow \leftarrow \leftarrow \\ \rightarrow \rightarrow \rightarrow \\ \rightarrow \rightarrow \rightarrow \end{array} - \frac{1}{N} \begin{array}{c} \leftarrow \leftarrow \leftarrow \\ \leftarrow \leftarrow \leftarrow \\ \rightarrow \rightarrow \rightarrow \\ \rightarrow \rightarrow \rightarrow \end{array} \right) - \frac{2}{N(N+1)} \begin{array}{c} \leftarrow \leftarrow \leftarrow \\ \leftarrow \leftarrow \leftarrow \\ \rightarrow \rightarrow \rightarrow \\ \rightarrow \rightarrow \rightarrow \end{array} = \end{array} \quad d_4 = \frac{N^2(N-1)(N+3)}{4} \quad (7.25d)$$

$$= \begin{array}{c} \leftarrow \leftarrow \leftarrow \\ \leftarrow \leftarrow \leftarrow \\ \rightarrow \rightarrow \rightarrow \\ \rightarrow \rightarrow \rightarrow \end{array} - \frac{2}{N+2} \left( 2 \begin{array}{c} \leftarrow \leftarrow \leftarrow \\ \leftarrow \leftarrow \leftarrow \\ \rightarrow \rightarrow \rightarrow \\ \rightarrow \rightarrow \rightarrow \end{array} - \frac{1}{N+1} \begin{array}{c} \leftarrow \leftarrow \leftarrow \\ \leftarrow \leftarrow \leftarrow \\ \rightarrow \rightarrow \rightarrow \\ \rightarrow \rightarrow \rightarrow \end{array} \right)$$

$$\frac{4}{N+2} \left( \begin{array}{c} \leftarrow \leftarrow \leftarrow \\ \leftarrow \leftarrow \leftarrow \\ \rightarrow \rightarrow \rightarrow \\ \rightarrow \rightarrow \rightarrow \end{array} - \frac{1}{N} \begin{array}{c} \leftarrow \leftarrow \leftarrow \\ \leftarrow \leftarrow \leftarrow \\ \rightarrow \rightarrow \rightarrow \\ \rightarrow \rightarrow \rightarrow \end{array} \right) \quad d_5 = N^2 - 1 \quad (7.25e)$$

$$\frac{2}{N(N+1)} \begin{array}{c} \leftarrow \leftarrow \leftarrow \\ \leftarrow \leftarrow \leftarrow \\ \rightarrow \rightarrow \rightarrow \\ \rightarrow \rightarrow \rightarrow \end{array} \quad d_6 = 1 \quad (7.25f)$$

$$\theta_{N>2} \cdot \left\{ \begin{array}{c} \leftarrow \leftarrow \leftarrow \\ \leftarrow \leftarrow \leftarrow \\ \rightarrow \rightarrow \rightarrow \\ \rightarrow \rightarrow \rightarrow \end{array} - \frac{4}{N} \begin{array}{c} \leftarrow \leftarrow \leftarrow \\ \leftarrow \leftarrow \leftarrow \\ \rightarrow \rightarrow \rightarrow \\ \rightarrow \rightarrow \rightarrow \end{array} \right\} \quad d_7 = \frac{(N^2-1)(N^2-4)}{4} \quad (7.25g)$$

$$\frac{4}{N} \begin{array}{c} \leftarrow \leftarrow \leftarrow \\ \leftarrow \leftarrow \leftarrow \\ \rightarrow \rightarrow \rightarrow \\ \rightarrow \rightarrow \rightarrow \end{array} \quad d_8 = N^2 - 1 \quad (7.25h)$$

$$\theta_{N>2} \cdot \left\{ \begin{array}{c} \leftarrow \leftarrow \leftarrow \\ \leftarrow \leftarrow \leftarrow \\ \rightarrow \rightarrow \rightarrow \\ \rightarrow \rightarrow \rightarrow \end{array} - \frac{4}{N} \begin{array}{c} \leftarrow \leftarrow \leftarrow \\ \leftarrow \leftarrow \leftarrow \\ \rightarrow \rightarrow \rightarrow \\ \rightarrow \rightarrow \rightarrow \end{array} \right\} \quad d_9 = \frac{(N^2-1)(N^2-4)}{4} \quad (7.25i)$$

$$\frac{4}{N} \begin{array}{c} \leftarrow \leftarrow \leftarrow \\ \leftarrow \leftarrow \leftarrow \\ \rightarrow \rightarrow \rightarrow \\ \rightarrow \rightarrow \rightarrow \end{array} \quad d_{10} = N^2 - 1 \quad (7.25j)$$

By construction, the operators (7.25) sum up to the four operators in (7.22a), which in turn add up to unity, *c.f.* eq. (7.22b). Thus, the projection operators (7.25a) to (7.25j) also sum up to unity, further implying that their dimensions add up to  $N^4$ .

As already mentioned, Cvitanović [72] previously found the projection operators for the  $2q + 2\bar{q}$ -algebra in

a different basis, which is also given in section 7.4.3. For each operator in the alternative basis found by Cvitanović, there exists a corresponding operator in eqns. (7.25) with the same dimension. If the operator projects onto a subspace with no other representation equivalent to it, then the projection operators in the two bases are identical. If there exist equivalent representations, the correspondence between operators in the two bases is no longer (necessarily) 1-to-1 but rather corresponds to a rotation within the associated block in the matrix  $\mathfrak{M}_{2,2}$  (*c.f.* the analogous discussion for quark-only spaces in section 4.4.3).

Some of the operators (7.25) are once again decorated with a prefactor  $\theta_{N>k}$ , which is defined in eq. (7.10). The reason for this is identical to the case of  $3q + 1\bar{q}$  and will thus not be repeated here (*c.f.* the discussion following eq. (7.10)).

That the operators (7.25a) to (7.25j) are orthogonal is easily checked via direct calculation, no computational tricks are necessary. However, as an example we explicitly show that the operators (7.25b) and (7.25c) are orthogonal: Consider their product

$$\begin{aligned} \frac{4 \cdot \theta_{N>2}}{(N-2)} \left[ \text{Diagram 1} - \frac{1}{N} \text{Diagram 2} \right] \cdot \frac{2}{N(N-1)} \text{Diagram 3} = \\ \frac{8 \cdot \theta_{N>2}}{N(N-1)(N-2)} \left[ \text{Diagram 4} - \frac{1}{N} \text{Diagram 5} \right] \end{aligned} \quad (7.26)$$

To simplify each term in the square bracket in (7.26), we recall that antisymmetrizers are projection operators,

$$\text{Diagram 6} \cdot \text{Diagram 7} = \text{Diagram 8}, \quad (7.27)$$

and that the partial and full trace of an antisymmetrizer  $\mathbf{A}_{12}$  is given by [72, eq. (6.23)]

$$\text{Diagram 9} = \frac{N-1}{2} \cdot \text{Diagram 10} \quad \text{and} \quad \text{Diagram 11} = \frac{N(N-1)}{2}. \quad (7.28)$$

Using eqns. (7.27) and (7.28), we simplify the first term in the square bracket in (7.26) as

$$\text{Diagram 12} \stackrel{(7.27)}{=} \text{Diagram 13} \stackrel{(7.28)}{=} \frac{N-1}{2} \text{Diagram 14} \stackrel{(7.27)}{=} \frac{N-1}{2} \text{Diagram 15}. \quad (7.29)$$

The second term in the bracket becomes

$$\frac{1}{N} \text{Diagram 16} \stackrel{(7.27)}{=} \frac{1}{N} \text{Diagram 17} \stackrel{(7.28)}{=} \frac{1}{N} \cdot \frac{N(N-1)}{2} \text{Diagram 18} = \frac{N-1}{2} \text{Diagram 19}. \quad (7.30)$$

Thus, the product (7.26) vanishes,

$$\frac{8 \cdot \theta_{N>2}}{N(N-1)(N-2)} \left[ \text{Diagram 20} - \frac{1}{N} \text{Diagram 21} \right] =$$

$$\frac{8 \cdot \theta_{N>2}}{N(N-1)(N-2)} \left[ \frac{N-1}{2} \left( \text{diagram 1} \right) - \frac{N-1}{2} \left( \text{diagram 2} \right) \right] = 0 \quad (7.31)$$

### 7.4.2 The full $2q + 2\bar{q}$ -algebra: transition operators

The analysis of the  $2q + 2\bar{q}$ -operators given in [72, sec. 9.12] (albeit in a different basis) tells us that the four adjoint operators (with dimension  $(N^2 - 1)$ ) correspond to equivalent irreducible representations, and so do the two singlet projection operators. The two operators (7.25g) and (7.25i) corresponding to subspaces with dimension  $\frac{(N^2-1)(N^2-4)}{4}$  are not equivalent to each other. This is however not surprising when looking at the two LR-tableaux corresponding to the two operators in question: Despite the fact that both tableaux classify representations of dimension  $\frac{(N^2-1)(N^2-4)}{4}$ , they have a *different* shape (i.e. their underlying diagrams are different) and thus cannot produce equivalent representations [93]. These inequivalent tableaux, together with their corresponding projection operators, are given in the later eq. (7.38).

This analysis implies that the block-structure of the matrix  $\mathfrak{M}_{2,2}$  containing all projection and transition operators is given by eq. (7.4b),

$$\mathfrak{M}_{2,2} \mapsto \begin{pmatrix} \begin{array}{cccc} \color{blue}4 & & & \\ & \color{blue}2 & & \\ & & \color{blue}1 & \\ & & & \color{blue}1 \\ & & & & \color{blue}1 \\ & & & & & \color{blue}1 \\ & & & & & & \color{blue}1 \end{array} \\ \vdots \end{pmatrix} . \quad (7.32)$$

This is confirmed by the Littlewood-Richardson tableaux given in Fig. 5.1, where all tableaux with the same shape correspond to equivalent representations [93]. This fact (that Littlewood-Richardson tableaux with the same shape correspond to equivalent representations) can also be extracted from an alternative formulation of the LR-rule in terms of Schur functions (*c.f.* footnote 3): Consider two tableaux with shapes  $\mu$  and  $\nu$ , and let  $s_\mu$  and  $s_\nu$  be their corresponding Schur functions. Then, the Littlewood-Richardson rule can be written as [96]

$$s_\mu \otimes s_\nu = \sum_\lambda c_{\mu\nu}^\lambda s_\lambda , \quad (7.33)$$

where the sum is performed over all tableau shapes  $\lambda$  which can result from multiplying tableaux with shapes  $\mu$  and  $\nu$  according to the LR-rule, and the constants  $c_{\mu\nu}^\lambda$  (also called the *Littlewood-Richardson constants*), giving the number of tableaux of shape  $\lambda$ , result from a multiplication of two tableaux with shapes  $\mu$  and  $\nu$  respectively. Since the Schur function  $s_\lambda$  determining the representation depends only on the shape  $\lambda$  of the LR-tableau but not its filling, two LR-tableaux with the same shape correspond to equivalent irreducible representations of  $SU(N)$  [96].

Again using the ‘‘factors-over-hooks’’ formula (see Refs. [72, 113] or section 5.1.3 in chapter 5), we may identify blocks of  $\mathfrak{M}_{2,2}$  corresponding to a particular representation with a Littlewood-Richardson diagram through its dimension. The birdtrack expressions for the transition operators appearing in the blocks of  $\mathfrak{M}_{2,2}$  can be obtained from the projectors (7.25) without much effort, using the defining properties of transition operators (4.91). We present the result in this section.

As stated earlier, the four operators (7.25b), (7.25e), (7.25h) and (7.25j) correspond to equivalent irreducible

representations of  $SU(N)$  with dimension  $d=N^2-1$ , and thus constitute a  $4 \times 4$ -block in the matrix  $\mathfrak{M}_{2,2}$ . This block, classified by the LR-diagram (*c.f.* Fig. 5.1 for the branching tree of all LR-tableaux over  $V^{\otimes 2} \otimes (V^*)^{\otimes 2}$ )

$$\text{length } \left\{ \begin{array}{c} \square \\ \square \\ \square \\ \vdots \\ \square \end{array} \right\}_N, \quad (7.34a)$$

is given by

$$\left( \begin{array}{cccc} \frac{4 \cdot \theta_{N>2}}{N-2} \left[ \text{diagram} \right] - \frac{1}{N} \left[ \text{diagram} \right] & \frac{4 \cdot \theta_{N>2}}{\sqrt{N^2-4}} \left[ \text{diagram} \right] - \frac{1}{N} \left[ \text{diagram} \right] & \frac{4 \cdot \theta_{N>2}}{\sqrt{N(N-2)}} \left[ \text{diagram} \right] & \frac{4 \cdot \theta_{N>2}}{\sqrt{N(N-2)}} \left[ \text{diagram} \right] \\ \frac{4 \cdot \theta_{N>2}}{\sqrt{N^2-4}} \left[ \text{diagram} \right] - \frac{1}{N} \left[ \text{diagram} \right] & \frac{4}{N+2} \left[ \text{diagram} \right] - \frac{1}{N} \left[ \text{diagram} \right] & \frac{4}{\sqrt{N(N+2)}} \left[ \text{diagram} \right] & \frac{4}{\sqrt{N(N+2)}} \left[ \text{diagram} \right] \\ \frac{4 \cdot \theta_{N>2}}{\sqrt{N(N-2)}} \left[ \text{diagram} \right] & \frac{4}{\sqrt{N(N+2)}} \left[ \text{diagram} \right] & \frac{4}{N} \left[ \text{diagram} \right] & \frac{4}{N} \left[ \text{diagram} \right] \\ \frac{4 \cdot \theta_{N>2}}{\sqrt{N(N-2)}} \left[ \text{diagram} \right] & \frac{4}{\sqrt{N(N+2)}} \left[ \text{diagram} \right] & \frac{4}{N} \left[ \text{diagram} \right] & \frac{4}{N} \left[ \text{diagram} \right] \end{array} \right). \quad (7.34b)$$

From chapter 5 Theorem 5.3 we also know that the two singlet projection operators, (7.25c) and (7.25f), correspond to equivalent representations of  $SU(N)$ . The corresponding  $2 \times 2$ -block in  $\mathfrak{M}_{2,2}$ , together with the associated Littlewood-Richardson diagram, is given by

$$\text{length } \left\{ \begin{array}{c} \square \\ \square \\ \square \\ \vdots \\ \square \end{array} \right\}_N : \left( \begin{array}{cc} \frac{2}{N(N-1)} \left[ \text{diagram} \right] & \frac{2}{N\sqrt{N^2-1}} \left[ \text{diagram} \right] \\ \frac{2}{N\sqrt{N^2-1}} \left[ \text{diagram} \right] & \frac{2}{N(N+1)} \left[ \text{diagram} \right] \end{array} \right). \quad (7.35)$$

The remaining operators (7.25a), (7.25d), (7.25g) and (7.25i) each constitute a  $1 \times 1$ -block in  $\mathfrak{M}_{2,2}$ . Two of these operators ((7.25a) and (7.25d)) can be matched up with a Littlewood-Richardson diagram purely from the dimension of the corresponding representations,

$$\text{length } \left\{ \begin{array}{c} \square \\ \square \\ \square \\ \vdots \\ \square \end{array} \right\}_N : \theta_{N>3} \cdot \left( \left[ \text{diagram} \right] - \frac{2}{N-2} \left( \left[ \text{diagram} \right] - \frac{1}{N-1} \left[ \text{diagram} \right] \right) \right) \quad (7.36)$$

$$\text{length } \left\{ \begin{array}{c} \square \\ \square \\ \square \\ \vdots \\ \square \end{array} \right\}_{N-1} : \left( \left[ \text{diagram} \right] - \frac{2}{N+2} \left( \left[ \text{diagram} \right] - \frac{1}{N+1} \left[ \text{diagram} \right] \right) \right). \quad (7.37)$$

For the remaining two operators, (7.25g) and (7.25i), the dimension alone is not sufficient to uniquely identify them with a LR-diagram, as they correspond to inequivalent irreducible representations that both have dimension  $d = \frac{(N^2-4)(N^2-1)}{4}$ . However, the symmetries between the top two fundamental index lines allow



for a unique identification,

$$\text{length}_N \left\{ \begin{array}{c} \text{[Diagram: Young diagram with 4 boxes in first row, 3 in second, 2 in third, 1 in fourth]} \\ \vdots \\ \text{[Diagram: Young diagram with 4 boxes in first row, 3 in second, 2 in third, 1 in fourth]} \end{array} \right\} : \theta_{N>2} \cdot \left( \begin{array}{c} \text{[Diagram: 4 white boxes with arrows]} \\ \vdots \\ \text{[Diagram: 4 white boxes with arrows]} \end{array} - \frac{4}{N} \begin{array}{c} \text{[Diagram: 4 white boxes with arrows]} \\ \vdots \\ \text{[Diagram: 4 white boxes with arrows]} \end{array} \right) \quad (7.38)$$

$$\text{length}_{N-1} \left\{ \begin{array}{c} \text{[Diagram: Young diagram with 4 boxes in first row, 3 in second, 2 in third, 1 in fourth]} \\ \vdots \\ \text{[Diagram: Young diagram with 4 boxes in first row, 3 in second, 2 in third, 1 in fourth]} \end{array} \right\} : \theta_{N>2} \cdot \left( \begin{array}{c} \text{[Diagram: 4 white boxes with arrows]} \\ \vdots \\ \text{[Diagram: 4 white boxes with arrows]} \end{array} - \frac{4}{N} \begin{array}{c} \text{[Diagram: 4 white boxes with arrows]} \\ \vdots \\ \text{[Diagram: 4 white boxes with arrows]} \end{array} \right), \quad (7.39)$$

where the white boxes correspond to fundamental factors, and the shaded boxes correspond to antifundamental factors (*c.f.* Fig. 5.1).

### 7.4.3 An alternative basis for the $2q + 2\bar{q}$ -algebra

In this section, we present the projection and transition operators of  $SU(N)$  over  $V^{\otimes 2} \otimes (V^*)^{\otimes 2}$  in an alternative basis,  $\tilde{\mathfrak{M}}_{2,2}$ . (If one wanted to be pedantic, one would have to say that we are actually looking at projection and transition operators of  $SU(N)$  over  $(V \otimes V^*)^{\otimes 2}$ , but since there is an isomorphism between the spaces  $(V \otimes V^*)^{\otimes 2}$  and  $V^{\otimes 2} \otimes (V^*)^{\otimes 2}$ , we'll speak of these spaces interchangeably.) As was mentioned previously, [72] gives a set of such projection operators in a basis that makes the gluons explicit. In particular, this basis exploits the fact that a fundamental and an antifundamental line (a  $q\bar{q}$ -pair) can combine to an adjoint line (a gluon) by means of the generators  $[t^a]_{ik}$ , *c.f.* eq. (5.36), and that the adjoint lines couple to each other via the structure constants  $f^{abc}$  and  $d^{abc}$ , *c.f.* eq. (5.112).

The projection operators of [72] are given by<sup>7</sup>

$$\frac{1}{N^2} \begin{array}{c} \text{[Diagram: 4 white boxes with arrows]} \\ \vdots \\ \text{[Diagram: 4 white boxes with arrows]} \end{array} \quad d_1 = 1 \quad (7.40a)$$


$$\frac{1}{N^2 - 1} \begin{array}{c} \text{[Diagram: 4 white boxes with arrows]} \\ \vdots \\ \text{[Diagram: 4 white boxes with arrows]} \end{array} \quad d_2 = 1 \quad (7.40b)$$

$$\frac{1}{N} \begin{array}{c} \text{[Diagram: 4 white boxes with arrows]} \\ \vdots \\ \text{[Diagram: 4 white boxes with arrows]} \end{array} \quad d_3 = N^2 - 1 \quad (7.40c)$$

$$\frac{1}{N} \begin{array}{c} \text{[Diagram: 4 white boxes with arrows]} \\ \vdots \\ \text{[Diagram: 4 white boxes with arrows]} \end{array} \quad d_4 = N^2 - 1 \quad (7.40d)$$

$$\frac{N \cdot \theta_{N>2}}{2(N^2 - 4)} \begin{array}{c} \text{[Diagram: 4 white boxes with arrows]} \\ \vdots \\ \text{[Diagram: 4 white boxes with arrows]} \end{array} \quad d_5 = \theta_{N>2} \cdot (N^2 - 1) \quad (7.40e)$$

$$\frac{1}{2N} \begin{array}{c} \text{[Diagram: 4 white boxes with arrows]} \\ \vdots \\ \text{[Diagram: 4 white boxes with arrows]} \end{array} \quad d_6 = N^2 - 1 \quad (7.40f)$$

<sup>7</sup>Note that there is a printing error in [72, Table 9.4] where the second term in the operator (7.40i) is given as  (note the arrow direction in the fundamental loop). The corrected version was already given in [102].

$$\frac{\theta_{N>3}}{2} \left\{ \begin{array}{l} \text{Diagram 1} - \text{Diagram 2} - \frac{1}{2(N-2)} \text{Diagram 3} - \frac{1}{N(N-1)} \text{Diagram 4} \end{array} \right\} \quad d_7 = \frac{\theta_{N>3} \cdot N^2(N-3)(N+1)}{4} \quad (7.40g)$$

$$\frac{1}{2} \left\{ \begin{array}{l} \text{Diagram 1} + \text{Diagram 2} - \frac{1}{2(N+2)} \text{Diagram 3} - \frac{1}{N(N+1)} \text{Diagram 4} \end{array} \right\} \quad d_8 = \frac{N^2(N+3)(N-1)}{4} \quad (7.40h)$$

$$\frac{\theta_{N>2}}{2} \left\{ \begin{array}{l} \text{Diagram 1} - \text{Diagram 2} - \frac{1}{2N} \text{Diagram 3} \end{array} \right\} \quad d_9 = \frac{(N^2-4)(N^2-1)}{4} \quad (7.40i)$$

$$\frac{\theta_{N>2}}{2} \left\{ \begin{array}{l} \text{Diagram 1} + \text{Diagram 2} - \frac{1}{2N} \text{Diagram 3} \end{array} \right\} \quad d_{10} = \frac{(N^2-4)(N^2-1)}{4} \quad (7.40j)$$

Both [72] and [102] correctly identify the equivalent irreducible representations among the operators (7.40), and thus the block structure of  $\tilde{\mathfrak{M}}_{2,2}$ . Ref. [102] also gives the corresponding transition operators, which can be found by exploiting the defining conditions (4.91) of transition operators; we present these operators again here.

The  $4 \times 4$ -block corresponding to the equivalent irreducible representations of  $SU(N)$  with dimension  $d_{3,4,5,6} = N^2 - 1$  is given by

$$\left( \begin{array}{cccc} \frac{1}{N} \text{Diagram 1} & \frac{1}{\sqrt{N}} \text{Diagram 2} & \frac{\theta_{N>2}}{\sqrt{2(N^2-4)}} \text{Diagram 3} & \frac{1}{\sqrt{2N}} \text{Diagram 4} \\ \frac{1}{\sqrt{N}} \text{Diagram 2} & \frac{1}{N} \text{Diagram 1} & \frac{\theta_{N>2}}{\sqrt{2(N^2-4)}} \text{Diagram 3} & \frac{1}{\sqrt{2N}} \text{Diagram 4} \\ \frac{\theta_{N>2}}{\sqrt{2(N^2-4)}} \text{Diagram 3} & \frac{\theta_{N>2}}{\sqrt{2(N^2-4)}} \text{Diagram 3} & \frac{\theta_{N>2} \cdot N}{2(N^2-4)} \text{Diagram 3} & \frac{\theta_{N>2}}{2\sqrt{N^2-4}} \text{Diagram 4} \\ \frac{1}{\sqrt{2N}} \text{Diagram 4} & \frac{1}{\sqrt{2N}} \text{Diagram 4} & \frac{\theta_{N>2}}{2\sqrt{N^2-4}} \text{Diagram 4} & \frac{1}{2N} \text{Diagram 4} \end{array} \right). \quad (7.41)$$

Similarly, the  $2 \times 2$ -block corresponding to the equivalent singlet representations of  $SU(N)$  is

$$\left( \begin{array}{cc} \frac{1}{N^2} \text{Diagram 1} & \frac{1}{N\sqrt{N^2-1}} \text{Diagram 2} \\ \frac{1}{N\sqrt{N^2-1}} \text{Diagram 2} & \frac{1}{N^2-1} \text{Diagram 1} \end{array} \right). \quad (7.42)$$

This again establishes the block structure (7.32) of  $\tilde{\mathfrak{M}}_{2,2}$  in this basis.

## 7.5 Spin: the special case $N = 2$

### 7.5.1 $SU(2)$ over 4-particle Fock spaces

Having established all Hermitian projection and transition operators of the 4-particle algebra, we now turn to the particular case where we set  $N = 2$ . In other words, we wish to determine the possible spin-states of a 4-particle system, in which each particle has the same spin  $s$ . We will be using standard methods as described in [27, 125] and other standard textbooks.

To find the spin-states of a system of particles, all possible values of the spin quantum number  $s$  for such a composite system need to be known, as  $s$  offers direct access to the dimension  $d$  of the corresponding irreducible representation of  $SU(2)$  via  $d = 2s + 1$ .<sup>8</sup> Furthermore, the multiplicity of the number  $s$  gives access to the block-structure of the matrix  $\mathfrak{M}_{4\text{-particles}}$  at  $N = 2$ , as shown below.

Before turning to explicit examples, let us calculate the possible spins of a 4-particle system (where each of the 4 particles has the same spin  $s$ ) in general, that is, without specifying which of them are particles (living in the Fock space  $V$ ), and which are antiparticles (living in the dual space  $V^*$ ). We will be using a highly condensed notation, only making the quantum number  $s$  specific. For the purpose of this calculation, let  $s = \frac{1}{2}$  (i.e. a fermion), so that the corresponding particle lives in a fundamental (resp. antifundamental) factor  $V^{(*)}$  of the product space. A system of four spin- $1/2$  particles is given by

$$\frac{1}{2} \otimes \frac{1}{2} \otimes \frac{1}{2} \otimes \frac{1}{2}. \quad (7.43)$$

Eq. (7.43) can be refined into the irreducible multiplets of the product: Since the tensor product is associative,

$$\frac{1}{2} \otimes \frac{1}{2} \otimes \frac{1}{2} \otimes \frac{1}{2} = \left[ \left( \frac{1}{2} \otimes \frac{1}{2} \right) \otimes \frac{1}{2} \right] \otimes \frac{1}{2}, \quad (7.44)$$

eq. (7.43) can be calculated in stages. The round bracket in (7.44) becomes

$$\frac{1}{2} \otimes \frac{1}{2} = 0 \oplus 1. \quad (7.45)$$

Remembering that the tensor product  $\otimes$  is distributive over the direct sum  $\oplus$  yields

$$\begin{aligned} \left( \frac{1}{2} \otimes \frac{1}{2} \right) \otimes \frac{1}{2} &= (0 \oplus 1) \otimes \frac{1}{2} \\ &= \left( 0 \otimes \frac{1}{2} \right) \oplus \left( 1 \otimes \frac{1}{2} \right) \\ &= \left( \frac{1}{2} \right) \oplus \left( \frac{1}{2} \oplus \frac{3}{2} \right) \\ &= \frac{1}{2} \oplus \frac{1}{2} \oplus \frac{3}{2}. \end{aligned} \quad (7.46)$$

<sup>8</sup>The reason for this is simple (see [27, 125] or other standard textbooks): First, recall that the quantum number  $s$  gives the positive numerical value of the spin, for example  $s = 0, \frac{1}{2}, 1, \frac{3}{2}, 2, \dots$ . Since the possible values of the spin momentum  $m_s$  of a particle (system) are  $m_s \in \{-s, -s+1, \dots, s-1, s\}$ , there are exactly  $2s+1$  possible values of  $m_s$  for any given  $s$ . Hence, for a particular value of the spin  $s$ , the corresponding particle (system) lives in a spin “ $(2s+1)$ -plet”.

We are now able to perform the final step of the calculation (7.44),

$$\begin{aligned}
 \left[ \frac{1}{2} \otimes \frac{1}{2} \otimes \frac{1}{2} \right] \otimes \frac{1}{2} &= \left[ \frac{1}{2} \oplus \frac{1}{2} \oplus \frac{3}{2} \right] \otimes \frac{1}{2} \\
 &= \left( \frac{1}{2} \otimes \frac{1}{2} \right) \oplus \left( \frac{1}{2} \otimes \frac{1}{2} \right) \oplus \left( \frac{3}{2} \otimes \frac{1}{2} \right) \\
 &= (0 \oplus 1) \oplus (0 \oplus 1) \oplus (1 \oplus 2) \\
 &= 0 \oplus 1 \oplus 0 \oplus 1 \oplus 1 \oplus 2 .
 \end{aligned} \tag{7.47}$$

Eq. (7.47) predicts that there are six irreducible multiplets within the 4-fermion product: two have spin 0, three have spin 1 and the last has spin 2. As explained previously (*c.f.* footnote 8), the dimension  $d$  of the irreducible representations of  $SU(2)$ , corresponding to spin  $s$ , is given by  $d = 2s + 1$ ,

$$\begin{array}{cccccccc}
 s & & 0 & \oplus & 0 & \oplus & 1 & \oplus & 1 & \oplus & 1 & \oplus & 2 \\
 & & \downarrow & & \downarrow & & \downarrow & & \downarrow & & \downarrow & & \downarrow \\
 d = 2s + 1 & & \underbrace{1} & & \underbrace{1} & & \underbrace{3} & & \underbrace{3} & & \underbrace{3} & & \underbrace{5} \\
 & & \text{Singlet} & & \text{Singlet} & & \text{Adjoint} & & \text{Adjoint} & & \text{Adjoint} & & \text{Higher} \\
 & & & & & & & & & & & & \text{dimensional}
 \end{array} . \tag{7.48}$$

Thus, a product state consisting of four spin-1/2 particles gives rise to six irreducible states with spin 0, 0, 1, 1, 1 and 2 corresponding to the irreducible representations of  $SU(2)$  with dimensions 1, 1, 3, 3, 3 and 5 respectively.

Since the spin calculation performed in this section is independent of how many factors in the 4-particle Fock space are  $V$  and how many are  $V^*$ , the obtained result must hold for all 4-fermion algebras at  $N = 2$ . We will show this explicitly in sections 7.5.2 to 7.5.4.

### 7.5.2 $SU(2)$ over $V^{\otimes 4}$ (dimensional zeros)

For the 4-quark representations of  $SU(N)$ , many operators become dimensionally zero as one decreases  $N$  below 4, as discussed in chapter 4. The reason for this is that an antisymmetrizer  $\mathbf{A}$  of length  $\text{length}(\mathbf{A})$  will necessarily vanish if there are fewer than  $\text{length}(\mathbf{A})$  linearly independent objects over which  $\mathbf{A}$  antisymmetrizes. Since the maximum size of a set of linearly independent objects in a vector space  $V$  is given by the dimension  $\dim(V)$  of the vector space, we say that the antisymmetrizer is **dimensionally zero** if  $\text{length}(\mathbf{A}) > \dim(V)$ ; this nomenclature reflects the fact that the dimension of the vector space is not large enough to support an antisymmetrizer of this size. Since furthermore  $N := \dim(V) = \dim(V^*)$ , it follows that any antisymmetrizer of length  $> 2$  will vanish once we fix  $N = 2$ .

For  $N = 2$ , the operators in blocks corresponding to the tableaux of shape

$$\begin{array}{|c|c|} \hline \square & \square \\ \hline \square & \\ \hline \square & \\ \hline \end{array} \quad \text{and} \quad \begin{array}{|c|} \hline \square \\ \hline \square \\ \hline \square \\ \hline \square \\ \hline \end{array} \tag{7.49}$$

become null-operators, since these tableaux contain columns of length  $> 2$  and thus induce antisymmetrizers

in the associated projectors that are longer than 2. The blocks corresponding to the tableaux with shape

$$\begin{array}{|c|c|c|c|} \hline & & & \\ \hline \end{array}, \quad \begin{array}{|c|c|c|} \hline & & \\ \hline & & \\ \hline \end{array} \quad \text{and} \quad \begin{array}{|c|c|} \hline & \\ \hline & \\ \hline \end{array} \quad (7.50)$$

remain and correspond to representations of dimensions 5, 3 and 1 respectively.<sup>9</sup> Thus, the block structure of the matrix  $\mathfrak{M}_4$  restricted to  $N = 2$  becomes

$$\mathfrak{M}_4|_{N=2} = \begin{pmatrix} \color{blue}{1} & & \\ & \color{blue}{3} & \\ & & \color{blue}{2} \end{pmatrix}, \quad (7.51)$$

in agreement with eq. (7.48). For completeness, we repeat the operators on the diagonal of the block matrix (7.51), together with the corresponding dimensions:

$$\begin{array}{|c|c|c|c|} \hline & & & \\ \hline & & & \\ \hline & & & \\ \hline & & & \\ \hline \end{array} \quad d = \frac{2(2+1)(2+2)(2+3)}{24} = 5 \quad (7.52a)$$

$$\begin{array}{|c|c|c|c|} \hline & & & \\ \hline & & & \\ \hline & & & \\ \hline & & & \\ \hline \end{array} \quad d = \frac{2(2+2)(2^2-1)}{8} = 3 \quad (7.52b)$$

$$\begin{array}{|c|c|c|c|} \hline & & & \\ \hline & & & \\ \hline & & & \\ \hline & & & \\ \hline \end{array} \quad d = \frac{2(2+2)(2^2-1)}{8} = 3 \quad (7.52c)$$

$$\begin{array}{|c|c|c|c|} \hline & & & \\ \hline & & & \\ \hline & & & \\ \hline & & & \\ \hline \end{array} \quad d = \frac{2(2+2)(2^2-1)}{8} = 3 \quad (7.52d)$$

$$\begin{array}{|c|c|c|c|} \hline & & & \\ \hline & & & \\ \hline & & & \\ \hline & & & \\ \hline \end{array} \quad d = \frac{2^2(2^2-1)}{12} = 1 \quad (7.52e)$$

$$\begin{array}{|c|c|c|c|} \hline & & & \\ \hline & & & \\ \hline & & & \\ \hline & & & \\ \hline \end{array} \quad d = \frac{2^2(2^2-1)}{12} = 1 \quad (7.52f)$$

### 7.5.2.1 The operators of $SU(2)$ : the standard method vs. simplifying projectors

In standard practice, one obtains the projection operators of  $SU(2)$  over a mixed product space  $V^{\otimes m} \otimes (V^*)^{\otimes n}$  from the operators over  $V^{\otimes(m+n)}$  via the Leibniz formula:

The Leibniz formula for determinants allows us to translate a product of  $(N-1)$  particles into antiparticles [112],

$$\varepsilon_{a_1 a_2 \dots a_N} U_{b_1 a_1} U_{b_2 a_2} \dots U_{b_{(N-1)} a_{(N-1)}} (\varepsilon_{b_1 b_2 \dots b_N})^\dagger = [U^\dagger]_{b_N a_N}; \quad (7.53)$$

this was discussed in detail in chapter 5. If  $N = 2$ , eq. (7.53) simplifies, and in doing so, establishes a 1-to-1 correspondence between particles and antiparticles,

$$\varepsilon_{a_1 a_2} U_{b_1 a_1} (\varepsilon_{b_1 b_2})^\dagger = [U^\dagger]_{b_2 a_2}. \quad (7.54)$$

<sup>9</sup>This can be verified directly from the tableaux using the “factors-over-hooks” method explained in section 5.1.3 of chapter 5.

Thus, replacing a particle with an antiparticle in a projection operator at  $N = 2$  is simply done by conjugating this particle with an epsilon-tensor of length 2. Successive applications of the Levi-Civita tensor to legs of the operators over  $V^{\otimes(m+n)}$  produces the projection operators of  $SU(2)$  over  $V^{\otimes m} \otimes (V^*)^{\otimes n}$ ; this is the standard method described in textbooks, e.g. [93].

On the other hand, if one already knows all projection operators of  $SU(N)$  over the space  $V^{\otimes m} \otimes (V^*)^{\otimes n}$ , one may subject these operators to the limit  $N = 2$ , offering a second method of obtaining the projectors for  $SU(2)$ .

These two methods are, however, not guaranteed to give rise to the same operators: If there exist multiple equivalent representations for a particular  $N$ , then there is no unique basis for constructing the projection operators and their transition operators, as certain linear combinations will yield an equivalent set of operators (this has already been discussed for the operators over  $V^{\otimes k}$  in chapter 4). For the case of the projection operators of  $SU(2)$  over a particular 4-particle Fock space, both methods will yield the same operator for the 5-dimensional representation (when written as a sum of primitive invariants), as it is unique. However, the projectors obtained from the two methods may (and do) differ for the 3- and 1-dimensional representations of  $SU(2)$ , as these representations are characterized by blocks of size  $> 1$  in the multiplication table, *c.f.* eq. (7.51).

In the following sections, we will focus on the second method of obtaining the projection operators of  $SU(2)$  over the 4-particle Fock spaces, since it is the non-standard method and therefore promises new insight.

### 7.5.3 $SU(2)$ over $V^{\otimes 3} \otimes V^*$

For the irreducible representations of  $SU(N)$  over  $V^{\otimes 3} \otimes V^*$ , there are, once more, two operators for which it is immediately obvious that these vanish when we set  $N = 2$ : the operators (7.9c) and (7.9d) contain antisymmetrizers of length 3 in each term and thus become dimensionally zero in the same way as we already observed for certain operators over  $V^{\otimes 4}$ , *c.f.* page 310.

Furthermore, the operators (7.9e) and (7.9h) project onto the zero-dimensional spaces for  $N = 2$ , as is immediately evident from their dimension formula

$$d = \frac{N^2(N+2)(N-2)}{3}. \tag{7.55}$$

We will now show explicitly that these operators vanish:

Let us first consider the operator (7.9e),

$$\frac{4}{3} \left[ \text{diagram 1} \right] - \frac{8}{3(N-1)} \left[ \text{diagram 2} \right] - \frac{2}{N+1} \left[ \text{diagram 3} \right]. \tag{7.56}$$

Our strategy to prove that this operator vanishes if  $N = 2$  is to show that the middle term in (7.56) exactly cancels the remaining two terms. To see this, we first write the antisymmetrizers of length  $2 = N$  in the middle term as a product of Levi-Civita tensors according to [72, sec. 6.3]

$$\left[ \text{diagram 2} \right] \stackrel{N=2}{=} \left[ \text{diagram 3} \right], \tag{7.57}$$

such that

$$\frac{8}{3(N-1)} \begin{array}{c} \leftarrow \square \leftarrow \square \leftarrow \square \\ \leftarrow \blacksquare \leftarrow \blacksquare \\ \rightarrow \blacksquare \rightarrow \blacksquare \\ \rightarrow \square \rightarrow \square \end{array} \xrightarrow{\text{eq. (7.57)}} \frac{8}{3(N-1)} \begin{array}{c} \leftarrow \square \leftarrow \square \leftarrow \square \\ \leftarrow \blacksquare \blacksquare \leftarrow \blacksquare \blacksquare \\ \rightarrow \blacksquare \blacksquare \rightarrow \blacksquare \blacksquare \\ \rightarrow \square \rightarrow \square \end{array}. \quad (7.58)$$

Using eq. (7.57) again, we may recombine the  $\varepsilon$ -tensors into antisymmetrizers in a different way,

$$\frac{8}{3(N-1)} \begin{array}{c} \leftarrow \square \leftarrow \square \leftarrow \square \\ \leftarrow \blacksquare \leftarrow \blacksquare \\ \rightarrow \blacksquare \rightarrow \blacksquare \\ \rightarrow \square \rightarrow \square \end{array} \xrightarrow{\text{eq. (7.57)}} \frac{8}{3(N-1)} \begin{array}{c} \leftarrow \square \leftarrow \square \leftarrow \square \\ \leftarrow \blacksquare \leftarrow \blacksquare \leftarrow \blacksquare \leftarrow \blacksquare \\ \rightarrow \blacksquare \rightarrow \blacksquare \rightarrow \blacksquare \rightarrow \blacksquare \\ \rightarrow \square \rightarrow \square \end{array}. \quad (7.59)$$

We now simplify the shaded part of the operator by decomposing the antisymmetrizer into its primitive invariants,

$$\begin{array}{c} \leftarrow \blacksquare \\ \leftarrow \blacksquare \\ \rightarrow \blacksquare \\ \rightarrow \blacksquare \end{array} = \frac{1}{2} \left( \begin{array}{c} \leftarrow \blacksquare \leftarrow \blacksquare \\ \leftarrow \blacksquare \leftarrow \blacksquare \end{array} - \begin{array}{c} \leftarrow \blacksquare \leftarrow \blacksquare \\ \leftarrow \blacksquare \leftarrow \blacksquare \end{array} \right), \quad (7.60)$$

yielding the following operator,

$$\frac{8}{3(N-1)} \begin{array}{c} \leftarrow \square \leftarrow \square \leftarrow \square \\ \leftarrow \blacksquare \leftarrow \blacksquare \\ \rightarrow \blacksquare \rightarrow \blacksquare \\ \rightarrow \square \rightarrow \square \end{array} = \frac{4}{3(N-1)} \left( \frac{N+1}{2} \begin{array}{c} \leftarrow \square \leftarrow \square \leftarrow \square \\ \leftarrow \blacksquare \leftarrow \blacksquare \\ \rightarrow \blacksquare \rightarrow \blacksquare \\ \rightarrow \square \rightarrow \square \end{array} - \begin{array}{c} \leftarrow \square \leftarrow \square \leftarrow \square \\ \leftarrow \blacksquare \leftarrow \blacksquare \leftarrow \blacksquare \leftarrow \blacksquare \\ \rightarrow \blacksquare \rightarrow \blacksquare \rightarrow \blacksquare \rightarrow \blacksquare \\ \rightarrow \square \rightarrow \square \end{array} \right). \quad (7.61)$$

The first term in this sum simply reduces to

$$\frac{N+1}{2} \begin{array}{c} \leftarrow \square \leftarrow \square \\ \leftarrow \blacksquare \leftarrow \blacksquare \\ \rightarrow \blacksquare \rightarrow \blacksquare \\ \rightarrow \square \rightarrow \square \end{array} \quad (7.62)$$

by eq. (7.57). The second term in the sum (7.61) is found by resolving the shaded symmetrizer as

$$\begin{array}{c} \leftarrow \square \leftarrow \square \\ \leftarrow \blacksquare \leftarrow \blacksquare \\ \rightarrow \blacksquare \rightarrow \blacksquare \\ \rightarrow \square \rightarrow \square \end{array} = \frac{1}{2} \left( \begin{array}{c} \leftarrow \square \leftarrow \square \\ \leftarrow \square \leftarrow \square \end{array} + \begin{array}{c} \leftarrow \square \leftarrow \square \\ \leftarrow \square \leftarrow \square \end{array} \right), \quad (7.63)$$

yielding

$$\begin{array}{c} \leftarrow \square \leftarrow \square \leftarrow \square \\ \leftarrow \blacksquare \leftarrow \blacksquare \\ \rightarrow \blacksquare \rightarrow \blacksquare \\ \rightarrow \square \rightarrow \square \end{array} = \frac{1}{2} \left( \begin{array}{c} \leftarrow \square \leftarrow \square \leftarrow \square \\ \leftarrow \blacksquare \leftarrow \blacksquare \\ \rightarrow \blacksquare \rightarrow \blacksquare \\ \rightarrow \square \rightarrow \square \end{array} + \begin{array}{c} \leftarrow \square \leftarrow \square \leftarrow \square \\ \leftarrow \blacksquare \leftarrow \blacksquare \leftarrow \blacksquare \leftarrow \blacksquare \\ \rightarrow \blacksquare \rightarrow \blacksquare \rightarrow \blacksquare \rightarrow \blacksquare \\ \rightarrow \square \rightarrow \square \end{array} \right). \quad (7.64)$$

A further simplification is possible: We notice that we may move the antisymmetrizer  $A_{23}$ , in the second term in (7.64), up to index lines 1 and 2, and then swap the index lines of the symmetrizers,

$$\begin{array}{c} \leftarrow \square \leftarrow \square \leftarrow \square \\ \leftarrow \blacksquare \leftarrow \blacksquare \\ \rightarrow \blacksquare \rightarrow \blacksquare \\ \rightarrow \square \rightarrow \square \end{array} \xrightarrow{\text{move } A_{23}} \begin{array}{c} \leftarrow \square \leftarrow \square \leftarrow \square \\ \leftarrow \blacksquare \leftarrow \blacksquare \leftarrow \blacksquare \leftarrow \blacksquare \\ \rightarrow \blacksquare \rightarrow \blacksquare \rightarrow \blacksquare \rightarrow \blacksquare \\ \rightarrow \square \rightarrow \square \end{array} \xrightarrow[\text{swap lines in } S_{12}]{\chi \square = \square \chi = \square \chi} \begin{array}{c} \leftarrow \square \leftarrow \square \leftarrow \square \\ \leftarrow \blacksquare \leftarrow \blacksquare \\ \rightarrow \blacksquare \rightarrow \blacksquare \\ \rightarrow \square \rightarrow \square \end{array}. \quad (7.65)$$

Thus, the middle term in the projector (7.56) becomes

$$\begin{aligned} \frac{8}{3(N-1)} \left[ \text{diagram} \right] &= \frac{4}{3(N-1)} \left\{ \frac{N+1}{2} \left[ \text{diagram} \right] - \frac{1}{2} \left( \left[ \text{diagram} \right] + \left[ \text{diagram} \right] \right) \right\} \\ &= \frac{2}{3(N-1)} \left( N \left[ \text{diagram} \right] - \left[ \text{diagram} \right] \right) \end{aligned} \quad (7.66)$$

in the limit  $N = 2$ . We now substitute this result back into the operator (7.56) and evaluate  $N = 2$ ,

$$\begin{aligned} &\left\{ \frac{4}{3} \left[ \text{diagram} \right] - \frac{8}{3(N-1)} \left[ \text{diagram} \right] - \frac{2}{N+1} \left[ \text{diagram} \right] \right\} \\ &\stackrel{N=2}{=} \left\{ \frac{4}{3} \left[ \text{diagram} \right] - \frac{2}{3(N-1)} \left( N \left[ \text{diagram} \right] - \left[ \text{diagram} \right] \right) - \frac{2}{N+1} \left[ \text{diagram} \right] \right\} \Bigg|_{N=2} \\ &= \frac{4}{3} \left[ \text{diagram} \right] - \frac{4}{3} \left[ \text{diagram} \right] + \frac{4}{3} \left[ \text{diagram} \right] - \frac{4}{3} \left[ \text{diagram} \right] \\ &= 0, \end{aligned} \quad (7.67)$$

as desired.

Showing that the operator (7.9h)

$$\frac{4}{3} \left[ \text{diagram} \right] - \frac{8}{3(N+1)} \left[ \text{diagram} \right] - \frac{2}{N-1} \left[ \text{diagram} \right] \quad (7.68)$$

also vanishes for  $N = 2$  is more labour-intensive, since we need to consider each term separately. We will now go through the relevant steps. We begin by simplifying the first term in the sum (7.68): Splitting the two antisymmetrizers into Levi-Civita symbols according to (7.57) and then recombining the central two  $\varepsilon$ -tensors into a new antisymmetrizer yields

$$\frac{4}{3} \left[ \text{diagram} \right] \stackrel{\text{eq. (7.57)}}{=} \frac{4}{3} \left[ \text{diagram} \right] \stackrel{\text{eq. (7.57)}}{=} \frac{4}{3} \left[ \text{diagram} \right]. \quad (7.69)$$

Two index lines in the central part of the operator are now traced over. Evaluating the trace on the antisymmetrizer will give rise to a factor  $\frac{N-1}{2}$  and leave us with a symmetrizer with one leg traced. Evaluating this trace gives a scalar factor  $\frac{N+1}{2}$  such that we finally obtain

$$\frac{4}{3} \left[ \text{diagram} \right] = \frac{4}{3} \cdot \frac{N-1}{2} \left[ \text{diagram} \right] = \frac{4}{3} \cdot \frac{N-1}{2} \cdot \frac{N+1}{2} \left[ \text{diagram} \right] \stackrel{\text{eq. (7.57)}}{=} \frac{N^2-1}{3} \left[ \text{diagram} \right]. \quad (7.70)$$



Thus, in the limit  $N = 2$ , the first term of the operator (7.68) becomes

$$\frac{4}{3} \begin{array}{c} \leftarrow \blacksquare \blacksquare \rightarrow \\ \leftarrow \blacksquare \rightarrow \\ \leftarrow \rightarrow \\ \leftarrow \rightarrow \end{array} \stackrel{N=2}{=} \frac{N^2 - 1}{3} \begin{array}{c} \leftarrow \blacksquare \rightarrow \\ \leftarrow \rightarrow \\ \leftarrow \rightarrow \end{array}. \quad (7.71)$$

To simplify the second term in the operator (7.68), we once again split the antisymmetrizers of length  $2 = N$  into Levi-Civita tensors and recombine them into different antisymmetrizers according to eq. (7.57),

$$\begin{aligned} \frac{8}{3(N+1)} \begin{array}{c} \leftarrow \blacksquare \blacksquare \rightarrow \\ \leftarrow \blacksquare \rightarrow \\ \leftarrow \rightarrow \\ \leftarrow \rightarrow \end{array} &\stackrel{\text{eq. (7.57)}}{=} \frac{8}{3(N+1)} \begin{array}{c} \leftarrow \blacksquare \blacksquare \blacksquare \rightarrow \\ \leftarrow \blacksquare \rightarrow \\ \leftarrow \rightarrow \\ \leftarrow \rightarrow \end{array} \\ &\stackrel{\text{eq. (7.57)}}{=} \frac{8}{3(N+1)} \begin{array}{c} \leftarrow \blacksquare \rightarrow \\ \leftarrow \blacksquare \rightarrow \\ \leftarrow \rightarrow \\ \leftarrow \rightarrow \end{array}. \end{aligned} \quad (7.72)$$

As in eq. (7.70), we can evaluate the traced index lines in (7.72) sequentially at the cost of additional scalar factors, reducing the middle term of the operator (7.68) to

$$\frac{8}{3(N+1)} \begin{array}{c} \leftarrow \blacksquare \blacksquare \rightarrow \\ \leftarrow \blacksquare \rightarrow \\ \leftarrow \rightarrow \\ \leftarrow \rightarrow \end{array} \stackrel{\text{c.f. eq. (7.70)}}{=} \frac{8}{3(N+1)} \left( \frac{N-1}{2} \right)^2 \left( \frac{N+1}{2} \right)^2 \begin{array}{c} \leftarrow \blacksquare \rightarrow \\ \leftarrow \rightarrow \\ \leftarrow \rightarrow \end{array}. \quad (7.73)$$

Our simplification process of the last term of the projection operator (7.68) once again begins with splitting and recombining antisymmetrizers of length  $N = 2$ ,

$$\frac{2}{N-1} \begin{array}{c} \leftarrow \blacksquare \rightarrow \\ \leftarrow \blacksquare \rightarrow \\ \leftarrow \rightarrow \\ \leftarrow \rightarrow \end{array} \stackrel{\text{eq. (7.57)}}{=} \frac{2}{N-1} \begin{array}{c} \leftarrow \blacksquare \blacksquare \rightarrow \\ \leftarrow \blacksquare \rightarrow \\ \leftarrow \rightarrow \\ \leftarrow \rightarrow \end{array} \stackrel{\text{eq. (7.57)}}{=} \frac{2}{N-1} \begin{array}{c} \leftarrow \blacksquare \rightarrow \\ \leftarrow \blacksquare \rightarrow \\ \leftarrow \rightarrow \\ \leftarrow \rightarrow \end{array}. \quad (7.74)$$

The resulting operator contains a traced index leg that is now contained in a symmetrizer and an antisymmetrizer. Thus, we first need to resolve either the symmetrizer or the antisymmetrizer into its primitive invariants before evaluating the trace. We choose to resolve the antisymmetrizer according to eq. (7.60),

$$\frac{2}{N-1} \begin{array}{c} \leftarrow \blacksquare \rightarrow \\ \leftarrow \blacksquare \rightarrow \\ \leftarrow \rightarrow \\ \leftarrow \rightarrow \end{array} = \frac{1}{N-1} \left( \begin{array}{c} \leftarrow \blacksquare \rightarrow \\ \leftarrow \blacksquare \rightarrow \\ \leftarrow \rightarrow \\ \leftarrow \rightarrow \end{array} - \begin{array}{c} \leftarrow \blacksquare \rightarrow \\ \leftarrow \blacksquare \rightarrow \\ \leftarrow \rightarrow \\ \leftarrow \rightarrow \end{array} \right). \quad (7.75)$$

The first term in the resulting sum still has a traced index leg, which, upon evaluation, will give a scalar factor  $\frac{N+1}{2}$ . The second term in (7.75) requires us to resolve the symmetrizer as well,

$$\begin{array}{c} \leftarrow \blacksquare \rightarrow \\ \leftarrow \blacksquare \rightarrow \end{array} = \frac{1}{2} \left( \begin{array}{c} \leftarrow \rightarrow \\ \leftarrow \rightarrow \end{array} + \begin{array}{c} \leftarrow \rightarrow \\ \rightarrow \leftarrow \end{array} \right), \quad (7.76)$$

before allowing further simplification,

$$\frac{2}{N-1} \left[ \text{diagram} \right] = \frac{1}{N-1} \left( \frac{N+1}{2} \left[ \text{diagram} \right] - \frac{1}{2} \left( \left[ \text{diagram} \right] + \left[ \text{diagram} \right] \right) \right). \quad (7.77)$$

What remains are minor algebraic manipulations to obtain the following expression for the last term of operator (7.68) in the limit  $N = 2$ ,

$$\frac{2}{N-1} \left[ \text{diagram} \right] = \frac{1}{2(N-1)} \left( N \left[ \text{diagram} \right] - \left[ \text{diagram} \right] \right). \quad (7.78)$$

Substituting the simplified terms (7.71), (7.73) and (7.78) back into the operator (7.68) (operator (7.9h)) yields

$$\begin{aligned} & \left\{ \frac{4}{3} \left[ \text{diagram} \right] - \frac{8}{3(N+1)} \left[ \text{diagram} \right] - \frac{2}{N-1} \left[ \text{diagram} \right] \right\} \\ & \stackrel{N=2}{=} \left\{ \frac{N^2-1}{3} \left[ \text{diagram} \right] - \frac{(N-1)^2(N+1)}{6} \left[ \text{diagram} \right] - \frac{1}{2(N-1)} \left( N \left[ \text{diagram} \right] - \left[ \text{diagram} \right] \right) \right\} \Big|_{N=2} \\ & = \left[ \text{diagram} \right] - \left[ \text{diagram} \right] - \frac{1}{2} \left[ \text{diagram} \right] + \frac{1}{2} \left[ \text{diagram} \right] \\ & = 0. \end{aligned} \quad (7.79)$$

Thus, the operator (7.68) also vanishes in the limit  $N = 2$ , as expected.

The only operators that remain, together with their associated dimensions are

$$\frac{1}{3} \left[ \text{diagram} \right] - \frac{3}{4} \left[ \text{diagram} \right] \quad d = \frac{2(2-1)(2+1)(2+3)}{6} = 5 \quad (7.80a)$$

$$\frac{3}{4} \left[ \text{diagram} \right] \quad d = \frac{2(2+1)}{2} = 3 \quad (7.80b)$$

$$\frac{4}{3} \left[ \text{diagram} \right] \quad d = \frac{2(2+1)}{2} = 3 \quad (7.80c)$$

$$2 \left[ \text{diagram} \right] \quad d = \frac{2(2+1)}{2} = 3 \quad (7.80d)$$

$$\frac{2}{3} \left[ \text{diagram} \right] \quad d = \frac{2(2-1)}{2} = 1 \quad (7.80e)$$

$$\frac{8}{9} \left[ \text{diagram} \right] \quad d = \frac{2(2-1)}{2} = 1. \quad (7.80f)$$

We previously found transition operators for the projectors (7.80b), (7.80c) and (7.80d) (*c.f.* eq. (7.18)) that remain for  $N = 2$ , thus constituting a  $3 \times 3$ -block in the matrix  $\mathfrak{M}_{3,1}$  for  $N = 2$ . Similarly, the operators (7.80e) and (7.80f) have transition operators (see (7.20)). In fact, the  $3 \times 3$  matrix (7.20) immediately reduces to a  $2 \times 2$  matrix due to many operators becoming dimensionally zero (by virtue of them containing an antisymmetrizer of length  $> 2$ ).

Thus, we once again obtain the block structure

$$\mathfrak{M}_{3,1}|_{N=2} = \begin{pmatrix} \mathbf{1} & & \\ & \mathbf{3} & \\ & & \mathbf{2} \end{pmatrix}. \quad (7.81)$$

#### 7.5.4 $SU(2)$ over $V^{\otimes 2} \otimes (V^*)^{\otimes 2}$

We now analyze the projection operators of the irreducible representations of  $SU(N)$  over  $V^{\otimes 2} \otimes (V^*)^{\otimes 2}$  in the case  $N = 2$ . We will again show that only six irreducible representations remain, and that these representations have dimensions 5, 3, 3, 3, 1 and 1 according to eq. (7.48). In particular, we will explicitly demonstrate how the operators (7.25a), (7.25b), (7.25g) and (7.25i) vanish for  $N = 2$ .

As was already the case for the projectors over  $V^{\otimes 3} \otimes V^*$ , an important step in showing that certain projectors in eqns. (7.25) vanish is that an antisymmetrizer of length  $N$  splits into a product of two Levi-Civita tensors (*c.f.* eq. (7.57))

$$\overleftarrow{\mathbf{1}} \overrightarrow{\mathbf{1}} \stackrel{N=2}{=} \overleftarrow{\mathbf{1}} \overrightarrow{\mathbf{1}}. \quad (7.82)$$

Let us begin with the operator (7.25b),

$$\frac{4 \cdot \theta_{N>2}}{N-2} \left( \overleftarrow{\mathbf{1}} \overrightarrow{\mathbf{1}} \overleftarrow{\mathbf{1}} \overrightarrow{\mathbf{1}} - \frac{1}{N} \overleftarrow{\mathbf{1}} \overrightarrow{\mathbf{1}} \right). \quad (7.83)$$

The antisymmetrizers of the first term in the sum (7.83) can be split and recombined according to eq. (7.82),

$$\overleftarrow{\mathbf{1}} \overrightarrow{\mathbf{1}} \overleftarrow{\mathbf{1}} \overrightarrow{\mathbf{1}} \stackrel{\text{eq. (7.82)}}{=} \overleftarrow{\mathbf{1}} \overrightarrow{\mathbf{1}} \overleftarrow{\mathbf{1}} \overrightarrow{\mathbf{1}} \stackrel{\text{eq. (7.82)}}{=} \overleftarrow{\mathbf{1}} \overrightarrow{\mathbf{1}} \overleftarrow{\mathbf{1}} \overrightarrow{\mathbf{1}} = \overleftarrow{\mathbf{1}} \overrightarrow{\mathbf{1}} \overleftarrow{\mathbf{1}} \overrightarrow{\mathbf{1}}. \quad (7.84)$$

In (7.84) we encounter two antisymmetrizers with several index legs traced over. These traces can be evaluated sequentially: The top traces over each individual antisymmetrizer induce a factor  $\frac{N-1}{2}$  each, and the remaining trace gives a factor  $N$ . Thus, the first term in the operator (7.83) simplifies to

$$\overleftarrow{\mathbf{1}} \overrightarrow{\mathbf{1}} \overleftarrow{\mathbf{1}} \overrightarrow{\mathbf{1}} = \overleftarrow{\mathbf{1}} \overrightarrow{\mathbf{1}} \overleftarrow{\mathbf{1}} \overrightarrow{\mathbf{1}} = \left( \frac{N-1}{2} \right)^2 N \overleftarrow{\mathbf{1}} \overrightarrow{\mathbf{1}}. \quad (7.85)$$

With the simplification (7.85), the part in the bracket of the operator (7.83) vanishes as  $N$  approaches 2,

$$\begin{aligned}
 \left( \text{Diagram 1} - \frac{1}{N} \text{Diagram 2} \right) &\stackrel{N=2}{=} \left\{ \left( \frac{N-1}{2} \right)^2 N \text{Diagram 3} - \frac{1}{N} \text{Diagram 4} \right\} \Big|_{N=2} \\
 &= \frac{1}{2} \text{Diagram 5} - \frac{1}{2} \text{Diagram 6} \\
 &= 0.
 \end{aligned} \tag{7.86}$$

We emphasize that the function  $\theta_{N>2}$  (c.f. eq. (7.10)) was added to the operators to prevent the *prefactor*  $\frac{4}{N-2}$  from becoming infinite as  $N \rightarrow 2$ . Thus, we have shown that the projector (7.25b) indeed vanishes for  $N = 2$ .

We now seek to take the limit  $N \rightarrow 2$  for the operator (7.25a). The first (unsimplified) expression in (7.25a) will be beneficial in this endeavour, as we may recognize the second and third term of (7.25a) as the projection operators (7.25b) and (7.25c),

$$\text{Diagram 7} - \frac{4 \cdot \theta_{N>2}}{N-2} \underbrace{\left( \text{Diagram 8} - \frac{1}{N} \text{Diagram 9} \right)}_{(7.25b)} - \frac{2}{N(N-1)} \underbrace{\text{Diagram 10}}_{(7.25c)}. \tag{7.87}$$

Since we just demonstrated that (7.25b) = 0 in the limit  $N = 2$ , it remains to focus on the first and last terms in the sum (7.87). We begin by splitting and recombining the antisymmetrizers of the first term of (7.87) according to eq. (7.82),

$$\text{Diagram 7} \stackrel{\text{eq. (7.82)}}{=} \text{Diagram 11} \stackrel{\text{eq. (7.82)}}{=} \text{Diagram 12} = \text{Diagram 13}. \tag{7.88}$$

Thus, for  $N = 2$ , operator (7.87) becomes

$$\begin{aligned}
 \text{Diagram 13} - \frac{4}{N-2} \left( \text{Diagram 8} - \frac{1}{N} \text{Diagram 9} \right) - \frac{2}{N(N-1)} \text{Diagram 10} \\
 \stackrel{N=2}{=} \left\{ \text{Diagram 14} - 0 - \frac{2}{N(N-1)} \text{Diagram 10} \right\} \Big|_{N=2} \\
 = \text{Diagram 15} - \text{Diagram 16} \\
 = 0,
 \end{aligned} \tag{7.89}$$

confirming that the operator (7.25a) indeed vanishes for  $N = 2$ .

Lastly, we claimed that the operators (7.25g) and (7.25i) become zero for  $N = 2$ . Since (7.25i) can be viewed as (7.25g) flipped about its vertical axis (with reversed arrows), showing that they vanish will involve the

exact same steps; we thus only present the explicit calculations for the operator (7.25g),

$$\begin{array}{c} \left[ \begin{array}{c} \leftarrow \square \rightarrow \\ \leftarrow \square \rightarrow \\ \leftarrow \blacksquare \rightarrow \\ \leftarrow \blacksquare \rightarrow \end{array} \right] - \frac{4}{N} \left[ \begin{array}{c} \leftarrow \square \rightarrow \\ \leftarrow \square \rightarrow \\ \leftarrow \blacksquare \rightarrow \\ \leftarrow \blacksquare \rightarrow \end{array} \right] \end{array}, \quad (7.90)$$

here. We first split and recombine the antisymmetrizers in the second term in the sum (7.90) according to eq. (7.82),

$$\frac{4}{N} \left[ \begin{array}{c} \leftarrow \square \rightarrow \\ \leftarrow \square \rightarrow \\ \leftarrow \blacksquare \rightarrow \\ \leftarrow \blacksquare \rightarrow \end{array} \right] \xrightarrow{\text{eq. (7.82)}} \frac{4}{N} \left[ \begin{array}{c} \leftarrow \square \rightarrow \\ \leftarrow \square \rightarrow \\ \leftarrow \blacksquare \rightarrow \\ \leftarrow \blacksquare \rightarrow \end{array} \right] \xrightarrow{\text{eq. (7.82)}} \frac{4}{N} \left[ \begin{array}{c} \leftarrow \square \rightarrow \\ \leftarrow \square \rightarrow \\ \leftarrow \blacksquare \rightarrow \\ \leftarrow \blacksquare \rightarrow \end{array} \right] \text{ with a loop on the top two lines.} \quad (7.91)$$

The traced index leg in (7.91) can be evaluated, inducing a constant factor  $\frac{N-1}{2}$ , and the bottom two Levi-Civita tensors may once again be recombined into an antisymmetrizer by virtue of eq. (7.82), such that

$$\frac{4}{N} \left[ \begin{array}{c} \leftarrow \square \rightarrow \\ \leftarrow \square \rightarrow \\ \leftarrow \blacksquare \rightarrow \\ \leftarrow \blacksquare \rightarrow \end{array} \right] \text{ with a loop} = \frac{4}{N} \cdot \frac{N-1}{2} \left[ \begin{array}{c} \leftarrow \square \rightarrow \\ \leftarrow \square \rightarrow \\ \leftarrow \blacksquare \rightarrow \\ \leftarrow \blacksquare \rightarrow \end{array} \right] \xrightarrow{\text{eq. (7.82)}} \frac{2(N-1)}{N} \left[ \begin{array}{c} \leftarrow \square \rightarrow \\ \leftarrow \square \rightarrow \\ \leftarrow \blacksquare \rightarrow \\ \leftarrow \blacksquare \rightarrow \end{array} \right] \text{ with a loop.} \quad (7.92)$$

Thus, in the limit  $N = 2$ , the projection operator (7.25g) becomes

$$\begin{aligned} \left[ \begin{array}{c} \leftarrow \square \rightarrow \\ \leftarrow \square \rightarrow \\ \leftarrow \blacksquare \rightarrow \\ \leftarrow \blacksquare \rightarrow \end{array} \right] - \frac{4}{N} \left[ \begin{array}{c} \leftarrow \square \rightarrow \\ \leftarrow \square \rightarrow \\ \leftarrow \blacksquare \rightarrow \\ \leftarrow \blacksquare \rightarrow \end{array} \right] &\xrightarrow{N=2} \left[ \begin{array}{c} \leftarrow \square \rightarrow \\ \leftarrow \square \rightarrow \\ \leftarrow \blacksquare \rightarrow \\ \leftarrow \blacksquare \rightarrow \end{array} \right] - \frac{2(N-1)}{N} \left[ \begin{array}{c} \leftarrow \square \rightarrow \\ \leftarrow \square \rightarrow \\ \leftarrow \blacksquare \rightarrow \\ \leftarrow \blacksquare \rightarrow \end{array} \right]_{N=2} \\ &= \left[ \begin{array}{c} \leftarrow \square \rightarrow \\ \leftarrow \square \rightarrow \\ \leftarrow \blacksquare \rightarrow \\ \leftarrow \blacksquare \rightarrow \end{array} \right] - \left[ \begin{array}{c} \leftarrow \square \rightarrow \\ \leftarrow \square \rightarrow \\ \leftarrow \blacksquare \rightarrow \\ \leftarrow \blacksquare \rightarrow \end{array} \right] \\ &= 0, \end{aligned} \quad (7.93)$$

as claimed. The same happens for the operator (7.25i),

$$\left[ \begin{array}{c} \leftarrow \blacksquare \rightarrow \\ \leftarrow \blacksquare \rightarrow \\ \leftarrow \square \rightarrow \\ \leftarrow \square \rightarrow \end{array} \right] - \frac{4}{N} \left[ \begin{array}{c} \leftarrow \blacksquare \rightarrow \\ \leftarrow \blacksquare \rightarrow \\ \leftarrow \square \rightarrow \\ \leftarrow \square \rightarrow \end{array} \right] \xrightarrow{N=2} 0. \quad (7.94)$$


In summary, the following multiplets with corresponding dimensions remain for  $N = 2$ :

$$\left[ \begin{array}{c} \leftarrow \square \rightarrow \\ \leftarrow \square \rightarrow \\ \leftarrow \square \rightarrow \\ \leftarrow \square \rightarrow \end{array} \right] - \frac{1}{2} \left( 2 \left[ \begin{array}{c} \leftarrow \square \rightarrow \\ \leftarrow \square \rightarrow \\ \leftarrow \square \rightarrow \\ \leftarrow \square \rightarrow \end{array} \right] - \frac{1}{3} \left[ \begin{array}{c} \leftarrow \square \rightarrow \\ \leftarrow \square \rightarrow \\ \leftarrow \square \rightarrow \\ \leftarrow \square \rightarrow \end{array} \right] \right) \quad d = \frac{2^2(2-1)(2+3)}{4} = 5 \quad (7.95a)$$

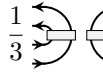
$$\left[ \begin{array}{c} \leftarrow \square \rightarrow \\ \leftarrow \square \rightarrow \\ \leftarrow \square \rightarrow \\ \leftarrow \square \rightarrow \end{array} \right] - \frac{1}{2} \left[ \begin{array}{c} \leftarrow \square \rightarrow \\ \leftarrow \square \rightarrow \\ \leftarrow \square \rightarrow \\ \leftarrow \square \rightarrow \end{array} \right] \quad d = 2^2 - 1 = 3 \quad (7.95b)$$

$$2 \left[ \begin{array}{c} \leftarrow \square \rightarrow \\ \leftarrow \square \rightarrow \\ \leftarrow \blacksquare \rightarrow \\ \leftarrow \blacksquare \rightarrow \end{array} \right] \quad d = 2^2 - 1 = 3 \quad (7.95c)$$

$$2 \left[ \begin{array}{c} \leftarrow \blacksquare \rightarrow \\ \leftarrow \blacksquare \rightarrow \\ \leftarrow \square \rightarrow \\ \leftarrow \square \rightarrow \end{array} \right] \quad d = 2^2 - 1 = 3 \quad (7.95d)$$



$$d = 1 \tag{7.95e}$$



$$\frac{1}{3} d = 1 . \tag{7.95f}$$

Operators (7.95b), (7.95c) and (7.95d) all correspond to equivalent representations, as they are part of the  $4 \times 4$ -block (7.34b) in  $\mathfrak{M}_{2,2}$ . We have shown that one of the operators in the block, namely operator (7.25b), vanishes for  $N = 2$  (*c.f.* eq. (7.86)). Similarly, it can be shown that all transition operators between operator (7.25b) (*resp.* (7.83)) and any other operator in the  $4 \times 4$ -block vanish for  $N = 2$ . This trait is important for establishing a connection to the operators in the alternative basis of  $V^{\otimes 2} \otimes (V^*)^{\otimes 2}$ , which will be the topic of the following section, 7.5.5. In any case, the operators projecting onto representations with dimension 3 constitute a  $3 \times 3$ -block in the matrix  $\mathfrak{M}_{2,2}$  at  $N = 2$ .

Similarly, the singlet operators constitute a  $2 \times 2$ -block (*c.f.* eq. (7.35)). Thus, we again encounter the following block structure

$$\mathfrak{M}_{2,2} \Big|_{N=2} = \begin{pmatrix} \mathbf{1} & & \\ & \mathbf{3} & \\ & & \mathbf{2} \end{pmatrix} . \tag{7.96}$$

### 7.5.5 $SU(2)$ over $V^{\otimes 2} \otimes (V^*)^{\otimes 2}$ — an alternative basis

For completeness, we would like to give a short discussion on the projection operators of  $SU(N)$  over  $V^{\otimes 2} \otimes (V^*)^{\otimes 2}$  for  $N = 2$  in the basis described in section 7.4.3. This discussion will be very brief, as it only serves a comparative purpose to the discussion in the previous section, 7.5.4.

From [72], one may piece together the arguments that show that the operators (7.40e), (7.40g), (7.40i) and (7.40j) vanish for  $N = 2$ . For operators (7.40e) and (7.40g), this is rooted in the fact that  $d^{abc}$ , which is symbolized by the white circle (*c.f.* eq. (5.112))

$$d^{abc} \rightarrow \begin{array}{c} a \\ \circ \\ b \end{array} \cdots c , \tag{7.97}$$

vanishes for  $N \leq 2$ . That the two operators (7.40i) and (7.40j) become zero for  $N = 2$  is apparent from their corresponding dimension formula. Thus, we are once again left with the block structure (7.96) for  $\tilde{\mathfrak{M}}_{2,2} \Big|_{N=2}$  as in the previous section.

We would like to draw attention to the fact that both operators (7.25b) and (7.40e) are part of a  $4 \times 4$  block in their respective algebras. However, the fact that they both vanish for  $N = 2$  means that they translate directly into each other in an explicit change of basis, while the remaining adjoint projectors in the  $4 \times 4$  block are free to form linear combinations in a change of basis. Observations like this show the benefit of an analysis at small  $N$ . We will elaborate on the benefits of a small  $N$  analysis in chapter 9.

# Chapter 8

## On Traces of Primitive Invariants

*This chapter serves to capture various additional results which were obtained in the course of this Ph.D. project. These results largely concern themselves with traces of primitive invariants. A link between the trace of a primitive invariant in  $S_{m+n}$  to the minimum number of transpositions required to express this invariant as a product of transpositions is established. Thereafter, we turn towards the primitive invariants in  $S_{m,n}$  and find that the trace is invariant under the 1-to-1 map  $\overset{N}{\leftarrow\rightarrow}$  (defined in this chapter) between  $S_{m,n}$  and  $S_{m+n}$ . Lastly, we show that the trace commutes with the product operation (viewing primitive invariants as linear maps).*

### 8.1 Introduction and overview

In order to effectively derive the results discussed in the abstract of this chapter, we first remind the reader how to take a trace in the birdtrack formalism. In particular, we recall that a closed loop in the trace of a birdtrack operator contributes a factor of  $N$  to the trace.

We then state our first result: If  $\rho$  is a primitive invariant in the group  $S_k$  acting on a product space  $V^{\otimes m}$  ( $m \geq k$ ), and  $\varkappa(\rho)$  denotes the minimum number of transpositions required to write  $\rho$  as a product of transpositions, then the trace of  $\rho$  is given by

$$\mathrm{tr}(\rho) = N^{m-\varkappa(\rho)} \tag{8.1}$$

(see Theorem 8.2 in section 8.2.3). An immediate consequence of eq. (8.1) is that the trace of a primitive invariant stays the same under Hermitian conjugation or taking the inverse,

$$\mathrm{tr}(\rho) = \mathrm{tr}(\rho^{-1}) = \mathrm{tr}(\rho^\dagger) \tag{8.2}$$

(*c.f.* section 8.2.4). To establish result (8.1), we need to make a detour via the theory of transpositions and their connections to permutations in section 8.2.2. There, we develop a method of representing a permutation  $\rho$  by a graph, where each edge corresponds to a particular transposition in  $\rho$ . This method was inspired by an argument given by Lossers [126] proving that  $\varkappa(\sigma) = p - 1$  for a  $p$ -cycle  $\sigma$ . Our discussion of transpositions gives rise to an interpretation of multiplication with a transposition as a “ladder operation” (*c.f.* Lemma 8.3). This Lemma is of crucial importance when proving the formula (8.1).

Having established an explicit formula for the trace of a primitive invariant in  $S_k$ , we will shift our focus to the primitive invariants  $S_{m,n}$  of  $SU(N)$  over a mixed product space  $V^{\otimes m} \otimes (V^*)^{\otimes n}$ . In section 8.3.1, we remind the reader of the graphical mapping  $\xleftrightarrow{\mathcal{N}}$  that allows us to transform the primitive invariants in  $S_{(m+n)}$  into those in  $S_{m,n}$  (Definition 8.1). We discover that the trace of a primitive invariant remains unchanged under this mapping: If  $\rho \in S_{(m+n)}$ , and  $\overset{\leftrightarrow}{\rho}$  denotes the unique element in  $S_{m,n}$  satisfying  $\xleftrightarrow{\mathcal{N}}: \rho \mapsto \overset{\leftrightarrow}{\rho}$ , then

$$\text{tr}(\rho) = \text{tr}\left(\overset{\leftrightarrow}{\rho}\right) ; \tag{8.3}$$

this is stated in Theorem 8.3.

It should be noted that the map  $\xleftrightarrow{\mathcal{N}}$  does not distribute over a general product  $\rho \cdot \sigma$  for  $\rho, \sigma \in S_{(m+n)}$ ,

$$\xleftrightarrow{\mathcal{N}}_{\rho \cdot \sigma} \neq \xleftrightarrow{\mathcal{N}}_{\rho} \cdot \xleftrightarrow{\mathcal{N}}_{\sigma} \quad \text{in general .} \tag{8.4}$$

Astonishingly however, the distributive quality of  $\xleftrightarrow{\mathcal{N}}$  is restored under the trace,

$$\text{Tr}\left(\xleftrightarrow{\mathcal{N}}_{\rho \cdot \sigma}\right) = \text{Tr}\left(\xleftrightarrow{\mathcal{N}}_{\rho} \cdot \xleftrightarrow{\mathcal{N}}_{\sigma}\right) ; \tag{8.5}$$

this is a consequence of Theorem 8.4, which is summarized in Corollary 8.2.

## 8.2 Traces of primitive invariants in $S_k$

### 8.2.1 Traces of birdtracks

As seen in previous chapters of this thesis, the trace of a birdtrack is formed by connecting the index legs on the same level [72],

$$\text{Tr}(\rho) = \text{Diagram}(\rho) . \tag{8.6a}$$


In birdtrack notation, a closed loop (of a solid line) corresponds to the trace of a Kronecker  $\delta$  in the (anti-)fundamental representation,

$$\text{Diagram}(\text{loop}) = \delta^i_j \delta^j_i = \delta^i_i = N , \tag{8.6b}$$


which induces a factor of  $N$ . Thus, the trace (8.6a) will necessarily yield a polynomial in  $N$  for any birdtrack  $\rho$  consisting of fundamental and antifundamental lines. If  $\rho$  is a *primitive* invariant of  $SU(N)$ , then its trace



will be a single power of  $N$ . For example, we calculate the traces of all primitive invariants in  $S_3$ ,

$$\begin{array}{ll}
 \text{Diagram 1} = N^3 & \text{Diagram 2} = N^2 \\
 \text{Diagram 3} = N^2 & \text{Diagram 4} = N^2 \\
 \text{Diagram 5} = N & \text{Diagram 6} = N
 \end{array} \tag{8.7}$$

In eqns. (8.7), we see that the highest power of  $N$  is achieved by the trace of the identity permutation; all other permutations produce lower powers of  $N$  when traced. This is, in fact, a general feature of the primitive invariants in  $S_k$ . One may go a step further and recognize a pattern in the powers of  $N$  (*c.f.* Theorem 8.2). To do so, we need to make a small detour via the theory of transpositions, which is done in the following section 8.2.2. (Note that even though the results established in section 8.2.2 could be derived for general cycles, we prefer to speak about transpositions as these are the smallest fundamental building blocks of permutations, *c.f.* Theorem 8.1 below.)

### 8.2.2 A graph-theoretic approach to transpositions and permutations

It is commonly known that *any* permutation in  $S_k$  may be expressed as a product of transpositions (see [96, 100, 124] or other standard textbooks). Thus, the study of transpositions promises to provide much insight into  $S_k$  as a whole. It comes as no surprise that transpositions and their connections to the permutations in  $S_k$  are well studied. However, the research in this topic is ongoing, as a recent paper [127] (published in February 2017) giving the number of ways in which a permutation can be written as a product of  $p$  transpositions,  $p \in \mathbb{N}$ , indicates.

A standard result [100] on transpositions and permutations is:

**■ Theorem 8.1 – minimum number of transpositions to express a permutation:**

Let  $\rho \in S_k$  be a permutation. There exists a minimum number of transpositions required to express  $\rho$  as a product of transpositions  $\tau_i$ . This minimum number will be denoted as

$$\varkappa(\rho) \quad \text{such that} \quad \rho = \tau_{\varkappa(\rho)} \tau_{(\varkappa(\rho)-1)} \cdots \tau_2 \tau_1 . \tag{8.8a}$$

In particular, if we write  $\rho$  as a product of disjoint cycles<sup>1</sup>  $\sigma_i$ ,

$$\rho = \sigma_\ell \sigma_{\ell-1} \cdots \sigma_2 \sigma_1 , \tag{8.8b}$$

then

$$\varkappa(\rho) = \sum_{i=1}^{\ell} (|\sigma_i| - 1) , \quad \text{where } |\sigma_i| \text{ is the length of the cycle } \sigma_i . \tag{8.8c}$$

<sup>1</sup>This can always be done – see [96, 100, 124] or other standard textbooks.

The signature of the permutation  $\rho$  is given by

$$\text{sign}(\rho) = (-1)^{\text{sgn}(\rho)} . \tag{8.8d}$$

Theorem 8.1 has been known for a while, and it is this theorem that ultimately allows us to forge a compact formula giving the trace of any permutation in  $S_k$  (see Theorem 8.2). In recent years, Lossers [126] has provided a proof of eq. (8.8c) using a graph-theoretic approach. This proof (which is paraphrased later in the present section on page 325) inspires a representation of permutations in terms of graphs with numbered edges; [126] already represents permutations as graphs with unnumbered edges, however it is the numbering of the edges that prompted us to derive the results given in the present section. We will now develop this graph-theoretic method in detail. Notice that since any permutation can be written as a product of disjoint cycles [96, 100, 124], it suffices to discuss how a particular cycle is represented as a graph.

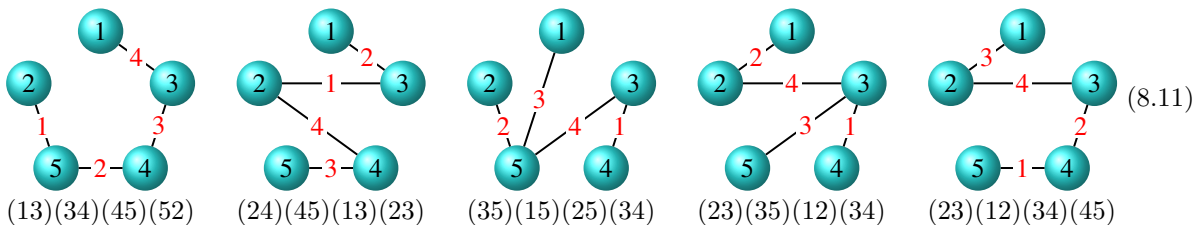
Let  $\sigma := (a_1 a_2 \dots a_p)$  be a  $p$ -cycle (that is a cycle of length  $p$ ) and consider the  $a_i$  to be vertices of a  $p$ -gon ordered clockwise.<sup>2</sup> As an example,



When writing the  $p$ -cycle  $\sigma$  as a product of  $(p - 1)$  transpositions  $\tau_i$  (according to Theorem 8.2 eq. (8.8c)),

$$\sigma = (a_1 a_2 \dots a_p) = \tau_{(p-1)} \tau_{(k-2)} \dots \tau_2 \tau_1 , \tag{8.10}$$

we represent each transposition  $\tau_i = (a_i a_j)$  by an edge marked with the integer  $i$  between the vertices  $a_i$  and  $a_j$ . It should be noted that, since there is no *unique* way of representing  $\sigma$  as a product of  $(p - 1)$  transpositions (in fact, the number of ways can be explicitly calculated [127]), there will be more than one representation of  $\sigma$  as a graph. As an example we provide various ways of writing the cycle (13452) as a product of 4 transpositions and their corresponding graphs,



Since any permutation  $\rho \in S_k$  may be written as a product of disjoint cycles  $\sigma_i$ , the graph  $G$  corresponding to  $\rho$  will consist of subgraphs  $H_i$  (the  $H_i$ 's are disjoint from each other), where each subgraph  $H_i$  corresponds to a cycle  $\sigma_i$ .

Conversely, suppose  $G$  is a graph corresponding to a particular permutation  $\rho$ ; we may recover  $\rho$  directly from its graph  $G$  as follows: It is clear that any node not contained in  $G$  will not enter a cycle of length  $> 1$

<sup>2</sup>This requirement is merely aesthetic as it ensures that the graph corresponding to  $\sigma$  is planar (i.e. has no crossing edges) but may be omitted if the aestheticity is not important to the practitioner.

in  $\rho$  (that is to say that  $\rho$  acts trivially on any element not represented as a node in  $G$ ). For any element  $a$  represented by a node  $a$  in  $G$ , we recover the action of  $\rho$  on  $a$  as follows:

1. Start at node  $a$  and follow the edge with the *lowest* number  $k$  ending on node  $a$ ; if the edge  $k$  runs between nodes  $a$  and  $b$ , this will lead to the vertex  $b$ .
2. From  $b$ , follow the edge with a number strictly greater than  $k$ . If there is more than one edge fulfilling this criterion, select the edge with the lowest such number.
3. Continue in this fashion until you arrive at a vertex  $z$  such that no edges with a number strictly greater than the edge followed to  $z$  leads away from  $z$ .

Once we have arrived at such a vertex  $z$ , we say that the element  $a$  is mapped to  $z$  under the permutation  $\rho$ ,  $\rho : a \mapsto z$ . In this fashion, we can recover the action of  $\rho$  (and thus the permutation  $\rho$  itself) on any element.

As an example, let us reconstruct the permutation  $\rho$  corresponding to the graph



As already stated, the action of  $\rho$  on any element not represented by a node in  $G$  is trivial. Thus, we need only consider the elements 1, 2, 3 and 4. Starting at vertex  $1$ , we move along the edge with the lowest number, edge  $1$ . This brings us to vertex  $2$  where there is no edge with a number  $> 1$  to follow. Thus,  $\rho : 1 \mapsto 2$ . Starting at node  $2$ , we follow edge  $1$  to vertex  $1$ . From there, we may follow edge  $2$  (since  $2 > 1$ ) to node  $3$ . We may follow yet another edge (namely edge  $3$ , since  $3 > 2$ ) to vertex  $4$ , where we no longer have an edge with a number  $> 3$  to follow. Hence,  $\rho : 2 \mapsto 4$ . From vertex  $3$ , we must follow the adjacent edge with the lowest number, edge  $2$ , to node  $1$ . There, we reach our termination condition, since all edges incident on node  $1$  (edges  $1$  and  $2$ ) are not strictly greater than the edge we followed to arrive at  $1$  (edge  $2$ ). This yields  $\rho : 3 \mapsto 1$ . Lastly, starting at node  $4$ , we follow edge  $3$  to node  $3$ , where we again terminate, since  $2, 3 \leq 3$ . Thus,  $\rho : 4 \mapsto 3$ . In summary, we find that the permutation  $\rho$  corresponding to the graph  $G$  in (8.12) is given by

$$\rho = (1243) . \quad (8.13)$$

Armed with this graphical representation of a permutation, we are able to give *Lossers' [126] proof of Theorem 8.2 eq. (8.8c)*: Consider a particular  $p$ -cycle  $\sigma := (a_1 a_2 \dots a_p)$ , and represent each element  $a_1, a_2, \dots, a_p$  by a node on a graph  $G$ . For  $G$  to represent  $\sigma$  as described in this section,  $G$  has to be a connected graph, since each  $a_i$  gets mapped to each  $a_j$  under appropriately many applications of  $\sigma$ . The minimum number of edges needed to connect a graph consisting of  $p$  nodes is  $(p - 1)$ . Since each edge represents a transposition, it follows that  $\varkappa(\sigma) = (p - 1) = |\sigma| - 1$ . If  $\rho$  is a permutation written as a product of  $\ell$  disjoint cycles  $\sigma_i$ ,  $\rho = \sigma_\ell \cdots \sigma_2 \sigma_1$ , then its corresponding graph  $K$  consists of  $\ell$  subgraphs  $H_i$ , where each  $H_i$  corresponds to a

cycle  $\sigma_i$ . Since the  $\sigma_i$  are disjoint, the  $H_i$ 's are disjoint from each other. Thus the minimum number of edges needed for  $K$  to represent  $\rho$  is  $\varkappa(\rho) = \sum_{i=1}^{\ell} (|\sigma_i| - 1) = \sum_{i=1}^{\ell} \varkappa(\sigma_i)$ .  $\square$

So far, we have been considering minimally connected graphs corresponding to permutations. Let us now consider a graph that is a closed loop; in graph theory, such a closed loop is usually referred to as a “cycle” (see [128] or other standard graph theory textbooks), however, to avoid confusion, we reserve the term “cycle” for a particular kind of permutation, and refer to the graph-theoretic cycle as a *multi-node loop* (as a “loop” in graph theory usually only involves one node [128]) in this chapter.

**Lemma 8.1 – multi-node loop graphs correspond to permutations:**

*Consider a multi-node loop graph  $L$  consisting of  $n$  nodes and  $n$  edges, each labeled with a unique number from 1 to  $n$  (not necessarily in order). Such a graph corresponds to a permutation.*

*Proof of Lemma 8.1:* To show that  $L$  corresponds to a permutation, it suffices to show that the mapping  $L : \{a_1, a_2, \dots, a_n\} \rightarrow \{a_1, a_2, \dots, a_n\}$ , according to the rules established in this section, is 1-to-1. If the map is 1-to-1, it automatically has to be onto since the domain and co-domain have the same size.

Consider the pair of nodes  $(a_i, a_j)$  such that  $L : a_i \mapsto a_j$ . Then, there exists a path  $\mathcal{I}$  along the multi-node loop from  $a_i$  to  $a_j$  consisting of edges  $i_1 \dots i_k$  such that  $i_1 < i_2 < \dots < i_k$ ,



Furthermore, edge  $e$ , also incident on  $a_i$ , satisfies  $i_1 < e$  (as we initially followed edge  $i_1$  and not edge  $e$ ), and edge  $f$  ending on  $a_j$  satisfies  $f < i_k$  such that the stopping criterion is reached on node  $a_j$ ,

$$i_1 < e \quad \text{and} \quad f < i_k . \tag{8.15}$$

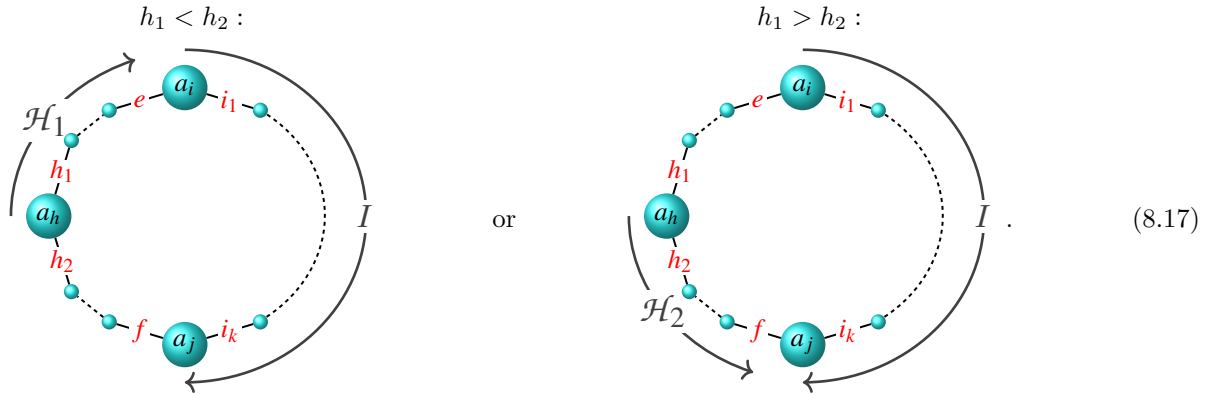
We now wish to show that there cannot be a second element  $a_h \neq a_i$  that also gets mapped to  $a_j$  under the action of  $L$ .

First, assume  $a_h$  lies on the path  $\mathcal{I}$  in  $L$ . Then there exists a pair of edges  $(i_s, i_{s+1})$ ,  $i_s < i_{s+1}$  ending on  $a_h$ ,



To examine the action on  $a_h$  according to  $L$ , we first follow edge  $i_s$  (since  $i_s < i_{s+1}$ ) away from  $a_j$  to the next node. There, we reach the termination criterion since the next edge  $i_{s-1}$  is strictly less than  $i_s$ ,  $i_{s-1} < i_s$ . Thus, an element  $a_h$  lying along the path  $\mathcal{I}$  does not get mapped to  $a_j$  under  $L$ .

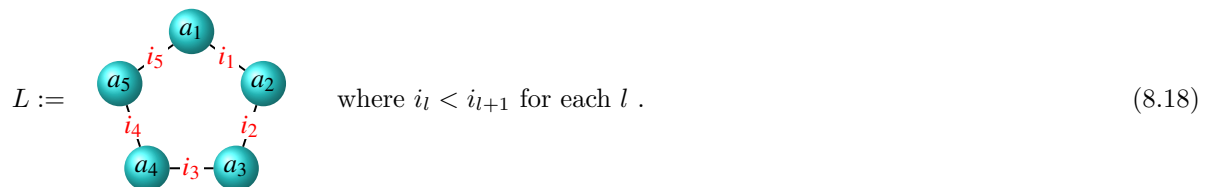
Now consider an element  $a_h$  not lying on the path  $\mathcal{I}$ . Incident on it, there will be two edges; call these edges  $h_1$  and edge  $h_2$ . The path that must be followed away from  $a_h$  is dependent on whether  $h_1 < h_2$  or  $h_1 > h_2$ ,



First suppose that  $h_1 < h_2$  (we follow the path  $\mathcal{H}_1$ ): The termination criterion is, at the latest, reached at node  $a_i$ , since  $i_1 < e$  (c.f. eq. (8.15)). Thus,  $a_h$  does not map to  $a_j$  in this case. Now consider the case  $h_1 > h_2$  (we follow the path  $\mathcal{H}_2$ ): If the termination criterion is reached before we arrive at node  $a_j$ ,  $a_h$  trivially does not map to  $a_j$ . If, however, we may follow edges all the way from  $a_h$  to  $a_j$  along the path  $\mathcal{H}_2$ , then the termination criterion will not be reached on the node  $a_j$  either, since  $f < i_k$  (see eq. (8.15)). Thus,  $a_h$  once again does not map to node  $a_j$  under  $L$ .

We have thus shown that there exists a *unique*  $a_i$  that gets mapped to an element  $a_j$  according to the graph  $L$  (note that we have not excluded the possibility that  $a_i = a_j$ ). Hence, the mapping described by  $L$  is both 1-to-1 and onto, and thus describes a permutation of the elements  $a_1, \dots, a_n$ .  $\square$

As an example, consider the multi-node loop graph  $L$  consisting of vertices  $a_1 \dots a_5$  and edges with numbers increasing clockwise,



Examining the action of  $L$  on each of the  $a_i$ , we notice the following:

- Starting from  $a_1$ , we first follow the edge with the lowest number  $i_1$  to  $a_2$ , then edge  $i_2$  to  $a_3$ , and so on. Once we arrive back at  $a_1$ , we may not follow edge  $i_1$  again, since  $i_i < i_5$ , thus invoking the termination condition. Therefore,  $L : a_1 \mapsto a_1$ .
- From  $a_2$  we follow the edge with the lowest number  $i_1$  to  $a_1$ , and then continue via  $i_5$  to  $a_5$ . There, we once again have to stop, since  $i_4 < i_5$ . Hence,  $L : a_2 \mapsto a_5$ .
- In a similar manner one finds that  $L : a_3 \mapsto a_2$ ,  $L : a_4 \mapsto a_3$  and  $L : a_5 \mapsto a_4$ .

Thus, the permutation  $\rho$  represented by the multi-node loop graph  $L$  can be written in terms of its disjoint cycles as

$$\rho = (a_1)(a_2 a_5 a_4 a_3) . \tag{8.19}$$

Theorem 8.1 teaches us that the number of minimum transpositions  $\varkappa(\rho)$  for  $\rho$  given in eq. (8.19) is 3. Thus,  $\rho$  may equally well be represented by a disjoint graph (each piece corresponding to the disjoint cycles in (8.19)) containing only 3 edges,



where we have essentially deleted edges  $i_1$  and  $i_5$  from (8.18). Thus, the multi-node loop graph in (8.18) and the graph (8.20) act in the same way, and we have to conclude that they are equal as permutations, even though they contain a different number of edges. This observation actually allows a general result:

**■ Lemma 8.2 –  $\varkappa(\rho)$  of a multi-node loop graph:**

Consider a multi-node loop graph  $L$  with  $E$  edges that describes the action of a permutation  $\rho$ . Then

$$\varkappa(\rho) \leq E - 2 . \tag{8.21}$$

*Proof of Lemma 8.2:* Consider a multi-node loop graph  $L$  consisting of  $E$  vertices  $a_1 \dots a_E$  and  $E$  edges  $i_1 \dots i_E$  between them, where  $i_l < i_{l+1}$  for every  $l$  (we note that the edges do not have to be arranged in order within  $L$ ). Suppose edge  $i_1$  runs between nodes  $a_i$  and  $a_{i+1}$ , and edge  $i_E$  lies between  $a_k$  and  $a_{k+1}$ ,



We now aim to show that the permutation  $\rho$  corresponding to the graph (8.22) consists of *at least* two disjoint cycles of length  $p$  and  $(E - p)$  respectively, such that

$$\varkappa(\rho) \stackrel{?}{\leq} (p - 1) + (E - p - 1) = E - 2 . \tag{8.23}$$

In particular, we will show that the nodes  $a_i$  and  $a_k$  are contained in two *separate* disjoint cycles. We present a proof by contradiction: Suppose the graph (8.22) corresponds to a permutation containing the cycle

$$\sigma = (a_i \dots a_k \dots) . \tag{8.24}$$

Then, there exists an integer  $j$  such that  $a_j \mapsto a_k$  under the cycle  $\sigma$ ,  $\sigma = (a_i \dots a_j a_k \dots)$ . Starting from vertex  $a_i$ , we follow edge  $i_1$  (since it is the edge with the smallest number) in a clockwise direction to  $a_{i+1}$ , and then continue clockwise to some node  $a_s$  at which the termination condition is reached. That is, if the

two edges adjacent to  $a_s$  are called  $e$  and  $f$ , and we travelled along edge  $e$  to arrive at  $a_s$ , then  $f < e$  invokes the termination condition,



This establishes that  $\sigma = (a_i a_s \dots a_j a_k \dots)$ . To determine the action of  $\sigma$  on  $a_s$ , we once again have to move along the multi-node loop in a clockwise direction along edge  $f$ , as this is the edge with the lowest number adjacent to  $a_s$ .

In this way we may fill in all elements of the permutation  $\sigma$ . The key observation is that whenever we reach a termination condition on some node  $a_x$  (which is a new element in  $\sigma$ ), we may find the next element in  $\sigma$  by moving away from  $a_x$  in a *clockwise* direction.

Eventually we arrive at node  $a_j$ , which maps onto  $a_k$  under  $\sigma$  by our initial assumption. There are two possible places within the graph  $L$  at which  $a_j$  can be situated; we consider these cases separately.

- Suppose  $a_j$  is situated between nodes  $a_{i+1}$  and  $a_k$ ,<sup>3</sup>



Then, we follow the edges from  $a_j$  to  $a_k$  in a clockwise direction. However, once we arrive at  $a_k$ , we may not stop there since edge  $i_E$  is by definition the edge with the highest number and thus exceeds the number of the previous edge, forcing us to follow it to  $a_{k+1}$  where the termination condition is reached. Thus,  $\sigma : a_j \mapsto a_{k+1} \neq a_k$ .

- Suppose now that  $a_j$  is situated between  $a_{k+1}$  and  $a_i$ ,



where we include the possibility that  $a_j = a_{k+1}$ . We once again need to follow the multi-node loop in a clockwise direction to determine the action of  $\sigma$  on  $a_j$ . However, we reach the termination condition, at the latest, at node  $a_i$ , since  $i_1$  is by definition the node with the smallest number. Thus,  $\sigma : a_j \not\mapsto a_k$ .

In either case, node  $a_j$  does not map to  $a_k$  under the action of the multi-node loop graph  $L$ . We have thus

<sup>3</sup>Note that  $a_j \neq a_{i+1}$ : Since we followed a path in a clockwise direction to  $a_j$ , the edge followed to  $a_{i+1}$  would be edge  $i_1$ , which, by virtue of it being the smallest edge, requires us to follow at least one more edge away from  $a_{i+1}$ .

arrived at a contradiction and are forced to conclude that the permutation  $\rho$  described by the graph (8.22) contains at least two disjoint cycles, one containing  $a_i$  and the other containing  $a_k$ . Thus,

$$\varkappa(\rho) \leq E - 2 \tag{8.28}$$

as required. □

The essence of Lemma 8.2 is that the number of edges  $E$  of a graph  $G$  corresponding to a permutation  $\rho$  is not necessarily equal to the minimum number of transpositions  $\varkappa(\rho)$ , but it has a lower bound,

$$\varkappa(\rho) \leq E . \tag{8.29}$$

This now raises the following question: Suppose we multiply  $\rho$  with a transposition  $(ij)$ , which corresponds to adding an edge between the nodes  $i$  and  $j$  to the graph  $G$ . Does the minimum number of transpositions  $\varkappa((ij) \cdot \rho)$  increase or decrease compared to  $\varkappa(\rho)$ ? This question will turn out to be important when we prove the general formula for the trace of a permutation, Theorem 8.2. It is answered by the following Lemma.

**■ Lemma 8.3 – increasing and decreasing  $\varkappa$  with transpositions:**

Let  $\rho$  be a permutation in  $S_k$  acting on the space  $V^{\otimes m}$ , which, written as a product of disjoint cycles  $\sigma_i$  (including 1-cycles), takes the form

$$\rho = \sigma_\ell \sigma_{\ell-1} \dots \sigma_2 \sigma_1 . \tag{8.30}$$

Furthermore, let  $(ij)$  be a transposition,  $i, j \in \{1, 2, \dots, m\}$ .

1. If  $i$  and  $j$  are contained in the same cycle in (8.30), then

$$\varkappa(\rho \cdot (ij)) = \varkappa((ij) \cdot \rho) \leq \varkappa(\rho) - 1 . \tag{8.31a}$$

2. If  $i$  and  $j$  are contained in the two distinct cycles in (8.30), then

$$\varkappa(\rho \cdot (ij)) = \varkappa((ij) \cdot \rho) = \varkappa(\rho) + 1 . \tag{8.31b}$$

We draw attention to the fact that multiplication of a general permutation  $\rho$  by a transposition in eqns. (8.31) somewhat resembles the action of raising and lowering operators in quantum mechanics, in that a particular choice of transposition will either raise or lower  $\varkappa(\rho)$ .

*Proof of Lemma 8.3:* Consider the permutation  $\rho$  as described in (8.30) and let  $G$  be the corresponding graph consisting of  $\varkappa(\rho)$  edges.  $G$  will consist of  $\ell$  disjoint sub-graphs, each corresponding to a cycle  $\sigma_i$ . Multiplying the permutation  $\rho$  by  $(ij)$  corresponds to adding an edge  $(ij)$  between the vertices  $i$  and  $j$  to the graph  $G$ . For left multiplication, this edge is labelled  $\varkappa(\rho) + 1$ , and for right multiplication, the edge is labelled 1 (while simultaneously increasing the numbers of all previously existing edges in  $G$  by 1).

1. If there exists a  $p$ -cycle  $\sigma_s$  in (8.30) containing both integers  $i$  and  $j$ , then  $i$  and  $j$  are contained in a *connected* sub-graph  $G_s$  of  $G$  consisting of  $p$  vertices and  $(p - 1)$  edges. Adding the edge  $(ij)$  to  $G_s$  necessarily produces a closed multi-node loop in  $G_s$ , thus decreasing the count of  $\varkappa$  by at least 2



according to Lemma 8.2. Hence

$$\varkappa(\rho \cdot (ij)) = \varkappa((ij) \cdot \rho) \leq \left( \underbrace{\varkappa(\rho) + 1}_{\substack{\text{edges in } G \\ + \text{ edge } (ij)}} \right) - 2 = \varkappa(\rho) - 1 . \quad (8.32)$$

2. If the integers  $i$  and  $j$  are contained in two separate cycles  $\sigma_s$  and  $\sigma_t$  respectively, then adding the edge  $(ij)$  corresponds to joining two disjoint sub-graphs into one sub-graph  $G_{st}$ . Notice that  $G_{st}$  is *minimally* connected since it contains  $(\text{length}(\sigma_s) + \text{length}(\sigma_t))$  nodes and

$$(\text{length}(\sigma_s) - 1) + (\text{length}(\sigma_t) - 1) + 1 = \text{length}(\sigma_s) + \text{length}(\sigma_t) - 1 \quad (8.33)$$

edges. Hence,

$$\varkappa(\rho \cdot (ij)) = \varkappa((ij) \cdot \rho) = \varkappa(\rho) + 1 , \quad (8.34)$$

concluding the proof.  $\square$

### 8.2.3 Traces of permutations and minimum number of transpositions

One may now ask the question: Why did we go to great lengths to talk about the minimum number of transpositions  $\varkappa(\rho)$  for a particular permutation  $\rho$ , when actually we aim to find a formula for the trace of  $\rho$ ? It turns out that the power of  $N$  achieved by tracing a primitive invariant  $\rho \in S_k$  is intimately linked with  $\varkappa(\rho)$ . From the example given in eqns. (8.7), one observes an inverse relation between these two quantities. This is made explicit in the following Theorem:

**■ Theorem 8.2 – trace of  $\rho$  from  $\varkappa(\rho)$ :**

Let  $\rho \in S_k$  be a permutation viewed as a linear map over the space  $V^{\otimes m}$ , and let  $\varkappa(\rho)$  be the minimum number of transpositions required to express  $\rho$  as a product of transpositions (c.f. Theorem 8.1). The trace of the permutation  $\rho$  is then given by

$$\text{tr}(\rho) = N^{(m-\varkappa(\rho))} . \quad (8.35)$$

*Proof of Theorem 8.2:* Let  $\rho \in S_k$  be a permutation acting on a product space  $V^{\otimes m}$ . If  $m > k$ , then  $\rho$  is assumed to act on the top  $k$  factors of the product  $V^{\otimes m}$  and the identity acts on the bottom  $(m - k)$  factors of  $V^{\otimes m}$ . We will present a proof by induction on the minimum number of transpositions  $\varkappa(\rho)$  to verify the desired eq. (8.35).

Suppose  $\varkappa(\rho) = 0$ : The unique permutation  $\rho$  satisfying this constraint is the identity  $\rho = \text{id}$ . Translating the corresponding birdtrack back into Kronecker  $\delta$ 's (c.f. eq. (1.107) in section 1.4.2.1) yields

$$\rho = \text{id} = \begin{array}{c} b_1 \longleftarrow a_1 \\ b_2 \longleftarrow a_2 \\ b_3 \longleftarrow a_3 \\ \vdots \\ b_m \longleftarrow a_m \end{array} = \delta_{a_1}^{b_1} \delta_{a_2}^{b_2} \delta_{a_3}^{b_3} \dots \delta_{a_m}^{b_m} . \quad (8.36)$$

As discussed in (8.6b), computing the trace of (8.36) is achieved by connecting the index lines on the same

level, which corresponds to a multiplication of  $\rho$  with

$$\delta_{b_1}^{a_1} \delta_{b_2}^{a_2} \delta_{b_3}^{a_3} \cdots \delta_{b_m}^{a_m} . \quad (8.37)$$

The full trace of the identity element is therefore

$$\text{tr}(\text{id}) = \underbrace{\delta_{a_1}^{b_1} \delta_{a_2}^{b_2} \delta_{a_3}^{b_3} \cdots \delta_{a_m}^{b_m}}_{\text{id}} \underbrace{\delta_{b_1}^{a_1} \delta_{b_2}^{a_2} \delta_{b_3}^{a_3} \cdots \delta_{b_m}^{a_m}}_{\text{trace}} \quad (8.38a)$$

$$= \underbrace{\delta_{a_1}^{b_1} \delta_{b_1}^{a_1}}_{=N} \underbrace{\delta_{a_2}^{b_2} \delta_{b_2}^{a_2}}_{=N} \underbrace{\delta_{a_3}^{b_3} \delta_{b_3}^{a_3}}_{=N} \cdots \underbrace{\delta_{a_m}^{b_m} \delta_{b_m}^{a_m}}_{=N} \quad (8.38b)$$

$$= (N)^m , \quad (8.38c)$$

confirming eq. (8.35) for  $\varkappa(\rho) = 0$ .

Suppose now that eq. (8.35) holds for all permutations with minimum number of transpositions  $n \in \mathbb{N}$ ; this will be referred to as the induction hypothesis. We now aim to show that this implies that eq. (8.35) must hold for all permutations  $\rho'$  such that

$$\varkappa(\rho') = n + 1 , \quad (8.39a)$$

that is, we want to prove that

$$\text{tr}(\rho') \stackrel{?}{=} N^{(m - (\varkappa(\rho) + 1))} . \quad (8.39b)$$

First, let us write  $\rho'$  as a product of transpositions  $\tau_i$

$$\rho' = \underbrace{\tau_{n+1} \tau_n \cdots \tau_2 \tau_1}_{=: \rho} = \rho \cdot \tau_1 . \quad (8.40)$$

The permutation  $\rho$  defined through eq. (8.40) clearly satisfies

$$\varkappa(\rho) = n . \quad (8.41)$$

We thus know that eq. (8.35) holds for this permutation  $\rho$  by the induction hypothesis. Furthermore, when written in terms of its disjoint cycle structure, Lemma 8.3 tells us that the two elements contained in the transposition  $\tau_1$  are not contained in the *same* cycle in  $\rho$ , otherwise eq. (8.39a) would not be satisfied.

The strategy to prove the induction step (8.39b) will be to assume the induction hypothesis for the permutation  $\rho$  and then multiply  $\rho$  with the transposition  $\tau_1$ . This is most easily accomplished in an adapted birdtrack formalism: From now on, instead of merely writing

$$\delta_{a_1}^{b_3} \mapsto \longleftarrow , \quad (8.42)$$

we will make the indices on the Kronecker  $\delta$  explicit,

$$\delta_{a_1}^{b_3} \mapsto \begin{array}{c} \bullet \\ \longleftarrow \\ \bullet \end{array} \begin{array}{c} \bullet \\ \longleftarrow \\ \bullet \end{array} , \quad (8.43)$$

essentially viewing the indices as *nodes* on a graph, and the  $\delta$  as a (directed) edge between them (*c.f.* section 8.2.2). In (8.38), we have indicated the Kronecker  $\delta$ 's stemming from the birdtrack in black, and the  $\delta$ 's originating from the trace in red. We continue in this spirit by color-coding the edges of our graph such that eq. (8.38b) becomes

$$\text{tr}(\text{id}) \mapsto \begin{array}{c} b_1 \\ \curvearrowright \\ a_1 \end{array} \begin{array}{c} b_2 \\ \curvearrowright \\ a_2 \end{array} \cdots \begin{array}{c} b_m \\ \curvearrowright \\ a_m \end{array}, \quad (8.44)$$

where each closed multi-node loop in the graph (8.44) induces a factor of  $N$  (*c.f.* eq. (8.6b)). Since the trace of a birdtrack is always formed via multiplication with the product (8.37) *irregardless of the birdtrack*, the red arrows in a graph representing such a trace remain fixed, while the black arrows change according to the permutation. As an example, the transposition  $\tilde{\tau} := (i(i+1))$  given by

$$\tilde{\tau} = \delta_{a_1}^{b_1} \delta_{a_2}^{b_2} \cdots \delta_{a_i}^{b_{i+1}} \delta_{a_{i+1}}^{b_i} \cdots \delta_{a_m}^{b_m} \quad (8.45)$$

gives rise to the following graph when traced:

$$\text{tr}(\tilde{\tau}) \mapsto \begin{array}{c} b_1 \\ \curvearrowright \\ a_1 \end{array} \begin{array}{c} b_2 \\ \curvearrowright \\ a_2 \end{array} \cdots \begin{array}{c} b_i \\ \curvearrowright \\ a_i \end{array} \begin{array}{c} b_{i+1} \\ \curvearrowright \\ a_{i+1} \end{array} \cdots \begin{array}{c} b_m \\ \curvearrowright \\ a_m \end{array}. \quad (8.46)$$

Let us analyze this example in more detail: If we define  $\rho = \text{id}$  and  $\rho' = \tilde{\tau}$ , then these two permutations satisfy eqns. (8.39a) and (8.40),

$$\varkappa\left(\underbrace{\tilde{\tau}}_{\rho'}\right) = \varkappa\left(\underbrace{\text{id}}_{\rho}\right) + \underbrace{\varkappa(\tilde{\tau})}_1 \quad \text{and} \quad \underbrace{\tilde{\tau}}_{\rho'} = \underbrace{\text{id}}_{\rho} \cdot \underbrace{\tilde{\tau}}_{\tau_1}. \quad (8.47)$$

Thus, if we can show that

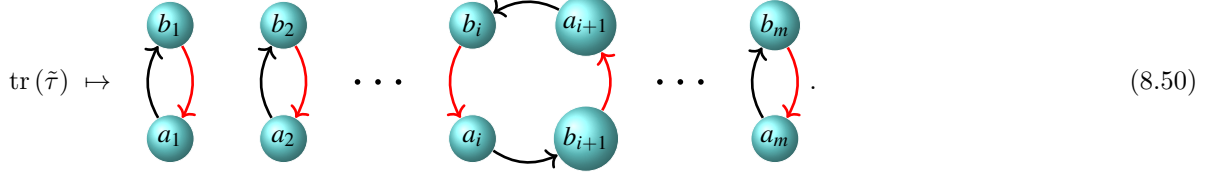
$$\text{tr}(\tilde{\tau}) \stackrel{?}{=} N^{(m - (\varkappa(\text{id}) + 1))} \quad (8.48)$$

we have illustrated that the induction step works in the first instant ( $\varkappa(\rho') = 1$ ), and gain insight into how the proof may be generalized to  $\varkappa(\rho') = n + 1$ . We notice that the graph (8.44) corresponding to  $\text{tr}(\text{id})$  yields the graph (8.46) corresponding to  $\text{tr}(\tilde{\tau})$  when we rearrange two black edges as follows,

$$\underbrace{\begin{array}{c} b_1 \\ \curvearrowright \\ a_1 \end{array} \begin{array}{c} b_2 \\ \curvearrowright \\ a_2 \end{array} \cdots \begin{array}{c} b_i \\ \curvearrowright \\ a_i \end{array} \begin{array}{c} b_{i+1} \\ \curvearrowright \\ a_{i+1} \end{array} \cdots \begin{array}{c} b_m \\ \curvearrowright \\ a_m \end{array}}_{\text{tr}(\text{id})} \rightarrow \underbrace{\begin{array}{c} b_1 \\ \curvearrowright \\ a_1 \end{array} \begin{array}{c} b_2 \\ \curvearrowright \\ a_2 \end{array} \cdots \begin{array}{c} b_i \\ \curvearrowright \\ a_i \end{array} \begin{array}{c} b_{i+1} \\ \curvearrowright \\ a_{i+1} \end{array} \cdots \begin{array}{c} b_m \\ \curvearrowright \\ a_m \end{array}}_{\text{tr}(\tilde{\tau})}; \quad (8.49)$$

this operation joined two separate multi-node loops into one, which becomes immediately clear when rear-

ranging the nodes in the graph corresponding to  $\text{tr}(\tilde{\tau})$  as



Thus, the graph of  $\text{tr}(\tilde{\tau})$  contains one closed multi-node loop fewer than the graph of  $\text{tr}(\text{id})$ , and we have to conclude that

$$\text{tr}(\tilde{\tau}) = \frac{\text{tr}(\text{id})}{N} = N^{(m-\varkappa(\text{id})-1)} = N^{(m-\varkappa(\text{id})+1)} . \quad (8.51)$$

We would like to draw attention to the *key feature* that allowed this step to be proved: Rearranging the black edges in (8.49) combines two multi-node loops into one *because the two edges in question are contained in separate cycles in the permutation id*.

Let us return to the premise in eqns. (8.39). Lemma 8.3 ensures us that the two elements in the transposition  $\tau_1$  are contained in *separate* cycles in  $\rho$ . Thus, altering the black nodes in the graph  $\text{tr}(\rho)$  to become the graph  $\text{tr}(\rho \cdot \tau_1)$  necessarily joins two separate multi-node loops into one, decreasing the total multi-node loop count of  $\text{tr}(\rho')$  compared to that of  $\text{tr}(\rho)$  by 1. Hence, we have that

$$\text{tr}(\rho') = \frac{\text{tr}(\rho)}{N} = N^{(m-\varkappa(\rho)-1)} = N^{(m-\varkappa(\rho)+1)} = N^{(m-\varkappa(\rho'))} , \quad (8.52)$$

concluding the proof.  $\square$

To end this section, we briefly comment on the trace of a product of two primitive invariants in  $S_k$ : Since  $S_k$  is a group, and all its elements are unitary, the product

$$\rho^\dagger \cdot \sigma = \rho^{-1} \cdot \sigma \quad (8.53)$$

lies in the group  $S_k$  for all  $\rho, \sigma \in S_k$ . Theorem 8.2 then implies that the inner product  $\langle \cdot | \cdot \rangle$  (*c.f.* eq. (5.96)) of two permutations in  $S_k$  yields a non-vanishing result,

$$\langle \rho | \sigma \rangle = \text{tr}(\rho^\dagger \cdot \sigma) = N^\alpha \neq 0 \quad (8.54)$$

for some positive integer  $\alpha$ . This is the reason why a basis of singlets states over  $V^{\otimes k} \otimes (V^*)^{\otimes k}$  obtained from bending the primitive invariants in  $S_k$  (as discussed in section 5.2.1.7) can never be orthogonal.

## 8.2.4 Transpositions of inverses and Hermitian conjugates

We would like to note that the minimum number of transpositions  $\varkappa$  must be the same for a permutation  $\rho$  and its inverse  $\rho^{-1}$ . This is most easily seen when writing  $\rho$  in terms of its disjoint cycles,

$$\rho = \sigma_\ell \sigma_{\ell-1} \cdots \sigma_2 \sigma_1 , \quad (8.55)$$

as then its inverse is given by

$$\rho^{-1} = \sigma_1^{-1} \sigma_2^{-1} \cdots \sigma_{\ell-1}^{-1} \sigma_\ell^{-1}, \quad \text{where} \quad (\sigma_i)^{-1} = ((a_1 a_2 \cdots a_{p-1} a_p))^{-1} = (a_p a_{p-1} \cdots a_2 a_1) \quad (8.56)$$

for every  $p$ -cycle  $\sigma_i$  [96, 100, 124]. Thus, we have that  $\varkappa(\rho) = \varkappa(\rho^{-1})$ , immediately implying that

$$\text{tr}(\rho) = N^{m-\varkappa(\rho)} = N^{m-\varkappa(\rho^{-1})} = \text{tr}(\rho^{-1}) . \quad (8.57)$$

Since permutations are unitary,  $\rho^{-1} = \rho^\dagger$ , it immediately follows that

■ **Corollary 8.1 – trace and Hermitian conjugation:**

Let  $\rho \in S_k$ . Then,

$$\text{tr}(\rho) = \text{tr}(\rho^\dagger) , \quad (8.58)$$

where  $\rho^\dagger$  is the Hermitian conjugate of  $\rho$ .

## 8.3 Traces of primitive invariants in $S_{m,n}$ and traces of products

### 8.3.1 Antifundamental factors in the product space

Chapters 2, 3 and 4 concerned themselves almost exclusively with the irreducible representations of  $\text{SU}(N)$  on a product space  $V^{\otimes m}$  consisting only of fundamental factors. In chapters 5, 6 and 7, we include antifundamental representations in the product, discussing various aspects of the representation theory of  $\text{SU}(N)$  over  $V^{\otimes m} \otimes (V^*)^{\otimes n}$ . An important facet of this discussion is the graphical map transforming the birdtracks of the primitive invariants  $S_{(m+n)}$  of  $\text{SU}(N)$  over  $V^{\otimes(m+n)}$  into  $S_{m,n}$ , the primitive invariants of  $\text{SU}(N)$  over a mixed product  $V^{\otimes m} \otimes (V^*)^{\otimes n}$  [72]. We now repeat the definition of this map, also introducing some new notation.

■ **Definition 8.1 – from fundamental to antifundamental lines (the map  $\leftrightarrow$ ):**

Consider the primitive invariants in  $S_{(m+n)}$ . These operators are transformed into the primitive invariants in  $S_{m,n}$  by exchanging the endpoints on the same level of the legs  $(m+1), \dots, (m+n)$ . We denote this map by the symbol

$$\overset{\mathcal{N}}{\leftrightarrow} , \quad \text{where} \quad \mathcal{N} = \{m+1, m+2, \dots, m+n\} \quad (8.59)$$

denotes the set of index lines upon which the map  $\overset{\mathcal{N}}{\leftrightarrow}$  acts. If the set  $\mathcal{N}$  is clear from the context, we may suppress the index set and merely write  $\leftrightarrow$ . Furthermore, for  $\rho \in S_{(m+n)}$ , we will denote the object in  $S_{m,n}$  obtained from  $\rho$  via the map  $\overset{\mathcal{N}}{\leftrightarrow}$  by  $\overset{\mathcal{N}}{\rho}$  (or simply by  $\overset{\leftrightarrow}{\rho}$  if the set  $\mathcal{N}$  is clear),

$$\overset{\mathcal{N}}{\leftrightarrow}: \rho \mapsto \overset{\leftrightarrow}{\rho} . \quad (8.60)$$

The map  $\overset{\mathcal{N}}{\leftrightarrow}$  evidently is a bijection between  $S_{(m+n)}$  and  $S_{m,n}$ .

For example, the primitive invariant

$$\begin{array}{c} \curvearrowright \\ \curvearrowleft \end{array} \quad (8.61)$$

transforms under the map  $\xleftrightarrow{3}$  as

$$\xleftrightarrow{3} : \begin{array}{c} \curvearrowright \\ \curvearrowleft \end{array} \mapsto \begin{array}{c} \curvearrowleft \\ \curvearrowright \end{array} =: \begin{array}{c} \xleftrightarrow{3} \\ \curvearrowright \\ \curvearrowleft \end{array} . \quad (8.62)$$

In fact, all primitive invariants in  $S_{2,1}$  of  $SU(N)$  over  $V^{\otimes 2} \otimes V^*$  are constructed from those in  $S_3$  via the map  $\xleftrightarrow{3}$ ,

$$S_3 : \quad \begin{array}{c} \longleftrightarrow \\ \longleftrightarrow \end{array}, \quad \begin{array}{c} \curvearrowright \\ \curvearrowleft \end{array}, \quad \begin{array}{c} \curvearrowleft \\ \curvearrowright \end{array}, \quad \begin{array}{c} \curvearrowright \\ \curvearrowleft \end{array}, \quad \begin{array}{c} \curvearrowleft \\ \curvearrowright \end{array}, \quad \begin{array}{c} \curvearrowright \\ \curvearrowleft \end{array} \quad (8.63)$$

$$\xleftrightarrow{3} : \quad \begin{array}{c} \downarrow \\ \downarrow \\ \downarrow \\ \downarrow \\ \downarrow \\ \downarrow \end{array} \\ S_{2,1} : \quad \begin{array}{c} \longleftrightarrow \\ \longleftrightarrow \end{array}, \quad \begin{array}{c} \curvearrowright \\ \curvearrowleft \end{array}, \quad \begin{array}{c} \curvearrowleft \\ \curvearrowright \end{array}, \quad \begin{array}{c} \curvearrowright \\ \curvearrowleft \end{array}, \quad \begin{array}{c} \curvearrowleft \\ \curvearrowright \end{array}, \quad \begin{array}{c} \curvearrowright \\ \curvearrowleft \end{array} . \quad (8.64)$$

With regards to birdtracks, we have seen the notion of *swapping lines on the same level* before, namely when taking inverses and for Hermitian conjugation (*c.f.* section 3.3.1). Let us recapitulate:

1. The inverse mapping of a *primitive invariant*  $\rho \in S_k$  is naturally obtained by following the lines of the birdtrack  $\rho$  (indicating the original mapping) in reverse. In other words, the inverse of a primitive invariant in  $S_k$  is formed by mirroring the birdtrack about its vertical axis and reversing the arrows,

$$\begin{array}{c} \curvearrowright \\ \curvearrowleft \end{array} \xrightarrow{\text{mirror}} \begin{array}{c} \curvearrowleft \\ \curvearrowright \end{array} \xrightarrow[\text{arrows}]{\text{reverse}} \begin{array}{c} \curvearrowright \\ \curvearrowleft \end{array} =: \left( \begin{array}{c} \curvearrowright \\ \curvearrowleft \end{array} \right)^{-1} . \quad (8.65)$$

2. The Hermitian conjugate of *any birdtrack operator* is obtained by flipping the birdtrack about its vertical axis and reversing the arrows,

$$\begin{array}{c} \longleftrightarrow \\ \longleftrightarrow \end{array} \xrightarrow{\text{flip}} \begin{array}{c} \longleftrightarrow \\ \longleftrightarrow \end{array} \xrightarrow[\text{arrows}]{\text{reverse}} = \begin{array}{c} \longleftrightarrow \\ \longleftrightarrow \end{array} =: \left( \begin{array}{c} \longleftrightarrow \\ \longleftrightarrow \end{array} \right)^\dagger ; \quad (8.66)$$

this is discussed in detail in [72] and in section 3.3.1 of chapter 3.

For the primitive invariants in  $S_k$ , Hermitian conjugation and forming an inverse involves the same procedure, implying that all elements in  $S_k$  are unitary (*c.f.* section 8.2.4),

$$\rho^{-1} = \rho^\dagger \quad \text{for every } \rho \in S_k . \quad (8.67)$$

It should be noted however that this is not the case for a general element of the algebra of primitive invariants, for example

$$\begin{array}{c} \longleftrightarrow \\ \longleftrightarrow \end{array} = \left( \begin{array}{c} \longleftrightarrow \\ \longleftrightarrow \end{array} \right)^\dagger , \quad \text{but} \quad \begin{array}{c} \longleftrightarrow \\ \longleftrightarrow \end{array} \neq \left( \begin{array}{c} \longleftrightarrow \\ \longleftrightarrow \end{array} \right)^{-1} ; \quad (8.68)$$

in particular, the operators in eq. (8.68) do not have an inverse, as they are quasi-idempotent.<sup>4</sup>

In the group  $S_{(m+n)}$  every element has an inverse. This is not the case for  $S_{m,n}$  (c.f. the last four elements of  $S_{2,1}$  in eq. (8.64)), thus excluding it from being classified as a group. In particular, flipping a birdtrack  $\rho$  in  $S_{m,n}$  about its vertical axis and reversing the arrows, as exemplified in (8.65), only yields  $\rho^{-1}$  if such an inverse exists, which is not true for most elements of  $S_{m,n}$ . What this procedure undoubtedly yields is the Hermitian conjugate  $\rho^\dagger$  of  $\rho$ , as demonstrated in eq. (8.66).

From the definition of the map  $\overleftarrow{\mathcal{N}}$ ,  $\mathcal{N} = \{m+1, \dots, m+n\}$  (c.f. Definition 8.1), it is apparent that the Hermiticity of the elements in  $S_{(m+n)}$  stays unaffected under the map  $\overleftarrow{\mathcal{N}}$ ,

$$\sigma = \rho^\dagger \iff \overleftarrow{\sigma} = \overleftarrow{(\rho^\dagger)} = \left(\overleftarrow{\rho}\right)^\dagger, \tag{8.69}$$

where  $\leftrightarrow$  is understood to be  $\overleftarrow{\mathcal{N}}$ . This is summarized in the following Lemma:

**■ Lemma 8.4 – † and ↔ commute:**

Let  $\rho \in S_{(m+n)}$  and  $\overleftarrow{\rho} \in S_{m,n}$  correspondingly. Then,

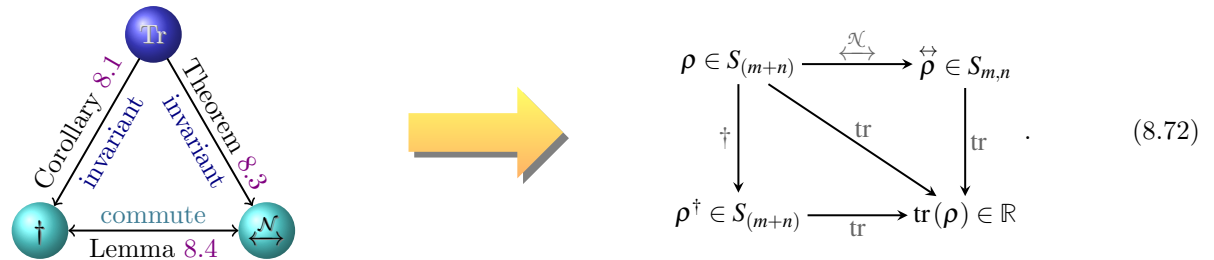
$$\left(\overleftarrow{\rho}\right)^\dagger = \overleftarrow{(\rho^\dagger)}. \tag{8.70}$$

Thus, as already mentioned, the Hermiticity properties of an element  $\rho \in S_{(m+n)}$  stay unchanged under the map  $\overleftarrow{\mathcal{N}}$ . In particular, if  $\rho$  is Hermitian, then  $\overleftarrow{\rho}$  must also be Hermitian,

$$\left(\overleftarrow{\rho}\right)^\dagger \stackrel{\text{Lemma 8.4}}{=} \overleftarrow{(\rho^\dagger)} \stackrel{\rho^\dagger = \rho}{=} \overleftarrow{\rho} = \left(\overleftarrow{\rho}\right). \tag{8.71}$$

### 8.3.2 Traces of primitive invariants in $S_{m,n}$

As we already know, the trace of any birdtrack is calculated by connecting the lines on the same level and assigning a factor  $N$  to each closed loop (c.f. eqs. (8.6)). In section 8.2.2 we showed that the trace of a birdtrack is unaffected under the Hermitian conjugation (Corollary 8.1). We now wish to “close the circle” and show that the trace remains unaffected by the map  $\overleftarrow{\mathcal{N}}$  as well. This notion is encapsulated schematically by the triangle of operations on the left, or more concretely by the commutative diagram on the right



The following Theorem formulates the desired characteristic:

<sup>4</sup>It is easy to show that an idempotent  $P$  (that is  $P^2 = P$ ) can have an inverse  $P^{-1}$  if and only if  $P = \text{id}$ :

$$\text{id} = P \cdot P^{-1} \stackrel{P=P^2}{=} (P^2) \cdot P^{-1} = P \cdot \underbrace{(P \cdot P^{-1})}_{\text{id}} = P \cdot \text{id} = P.$$

**■ Theorem 8.3 – tr is invariant under  $\overset{\mathcal{N}}{\leftrightarrow}$ :**

Let  $\rho \in S_{(m+n)}$  be a permutation and let  $\overset{\mathcal{N}}{\rho}$  be the element in  $S_{m,n}$  that is obtained from  $\rho$  under the map  $\overset{\mathcal{N}}{\leftrightarrow}$ , where  $\mathcal{N}$  is understood to be a subset of  $\{1, \dots, m, m+1, \dots, m+n\}$  of size  $n$ . Then,

$$\text{tr}(\rho) = \text{tr}\left(\overset{\mathcal{N}}{\rho}\right), \tag{8.73}$$

that is, the trace remains invariant under the operation  $\leftrightarrow$ .

*Proof of Theorem 8.3:* Let  $\rho$  and  $\overset{\mathcal{N}}{\rho}$  be as defined in the theorem, and consider the trace of  $\rho$ ,  $\text{tr}(\rho)$ . We will now investigate how this trace changes as we flip consecutive index lines according to the map  $\leftrightarrow$ , thereby building  $\text{tr}\left(\overset{\mathcal{N}}{\rho}\right)$  from  $\text{tr}(\rho)$ . Usually we would start with the bottommost level, but in this case we found that the clarity of the accompanying graphics in this proof is improved if we start with the topmost index line. The index lines ending on the topmost level correspond to the Kronecker  $\delta$ 's  $\delta^{b_i}_{a_1} \delta^{b_1}_{a_j}$  for some integers  $i, j$ . (We include the possibility that  $a_j = b_i$ , inducing a horizontal line  $\delta^{b_1}_{a_1}$  on the top level; flipping  $\delta^{b_1}_{a_1}$ , however, is trivial as it only reverses the arrow on the top index line.) Upon a swap transforming the fundamental lines ending on the top level into antifundamental lines, the product  $\delta^{b_i}_{a_1} \delta^{b_1}_{a_j}$  becomes

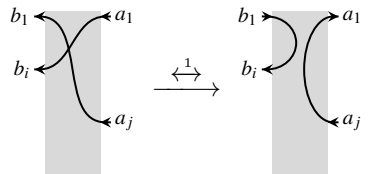
$$\delta^{b_i}_{a_1} \delta^{b_1}_{a_j} \xrightarrow{b_1 \leftrightarrow a_1} \delta^{a_j}_{a_1} \delta^{b_1}_{b_i}. \tag{8.74}$$

Schematically, we represent the birdtrack corresponding to  $\rho$  as



$$\rho \mapsto \text{birdtrack}, \tag{8.75}$$

where we have explicitly drawn the index lines corresponding to the Kronecker  $\delta$ 's  $\delta^{b_i}_{a_1}$  and  $\delta^{b_1}_{a_j}$  and suppressed the remaining index lines constituting  $\rho$  so as not to clutter (and thus mystify) the picture; these remaining index lines are understood to form part of the grey rectangle. Transforming the topmost level into an antifundamental representation is schematically expressed as



$$\text{birdtrack} \xrightarrow{\overset{\mathcal{N}}{\leftrightarrow}} \text{birdtrack}; \tag{8.76}$$

we note that the part of  $\rho$  represented by the grey rectangle is *not* affected by the map  $\overset{\mathcal{N}}{\leftrightarrow}$ . From now on, we will suppress the index labels  $a, b$ .

In order to form the trace of  $\rho$ , we connect each of the index lines on the same level (*c.f.* eqns. (8.6)). Only explicitly drawing  $\delta^{a_1}_{b_1}$ , but understanding all other trace  $\delta$ 's to be present, we schematically represent  $\text{tr}(\rho)$



as

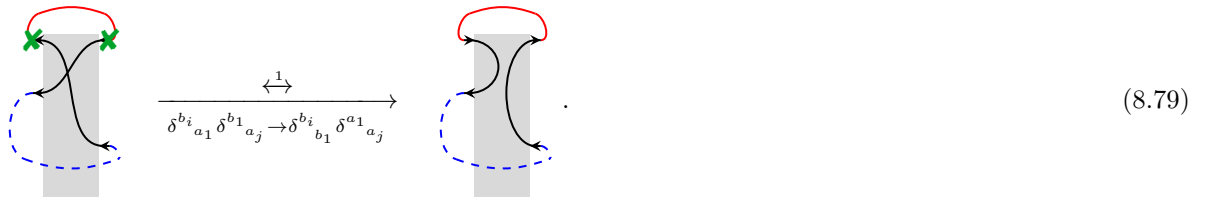


The trace of an operator necessarily yields a scalar, implying that there cannot be any open-ended index legs in  $\text{tr}(\rho)$ . In particular, since the two nodes  $a_1$  and  $b_1$  are connected through the trace  $\delta^{b_1}_{a_1}$ , they form part of a closed loop. This means that the nodes  $a_j$  and  $b_i$  must also be connected through the trace,



we emphasize that the connection between  $a_j$  and  $b_i$  represented by the blue dashed line may contain several other Kronecker deltas  $\delta^{b_u}_{a_v}$  constituting  $\rho$ . The crux of the matter is that the explicitly drawn loop in the above diagram is exactly 1 loop. Thus, if  $\text{tr}(\rho) = (N)^s$  for some  $s \in \mathbb{N}$  (c.f. Theorem 8.2), then the remaining part of  $\text{tr}(\rho)$  not explicitly drawn in (8.78) consists of exactly  $(s - 1)$  closed loops.

We now wish to apply the map  $\overset{1}{\leftarrow}$  to  $\rho$ , exchanging the ends of the index lines on the topmost level. Under the trace, this corresponds to severing the loop in (8.78) at the points  $a_1$  and  $b_1$  (indicated by  $\times$  below), and reconnecting the black index lines as was done in eq. (8.76)



We have not altered the remainder of  $\text{tr}(\rho)$  (the part indicated by the grey box) in any way, so it still consists of exactly  $(s - 1)$  closed loops. Eq. (8.79) illustrates that the map  $\overset{1}{\leftarrow}$  merely “disentangled” the explicitly drawn loop containing all four nodes  $a_1, a_j, b_1, b_i$ , but we remain with exactly 1 closed loop. Therefore, after applying  $\overset{1}{\leftarrow}$  to  $\rho$  inside the trace, the loop count and thus the trace itself is not altered,

$$\text{tr}\left(\overset{1}{\rho}\right) = \text{tr}(\rho). \quad (8.80)$$

We may now repeat the above procedure with any number of indices and will still find that

$$\text{tr}\left(\overset{\leftrightarrow}{\rho}\right) = \text{tr}(\rho), \quad (8.81)$$

concluding the proof of Theorem 8.3.  $\square$

Since any birdtrack operator  $A \in \text{Lin}(V^{\otimes(m+n)})$  is a linear combination of the primitive invariants in  $S_{(m+n)}$ ,

Theorem 8.3 trivially also holds for  $A$ ,

$$\text{tr}(A) = \begin{array}{c} \text{---} \text{---} \text{---} \\ \left. \begin{array}{c} \text{---} \text{---} \text{---} \\ \text{---} \text{---} \text{---} \\ \text{---} \text{---} \text{---} \\ \vdots \\ \text{---} \text{---} \text{---} \\ \vdots \\ \text{---} \text{---} \text{---} \\ \text{---} \text{---} \text{---} \\ \text{---} \text{---} \text{---} \\ \text{---} \text{---} \text{---} \\ \text{---} \text{---} \text{---} \end{array} \right\} A \\ \text{---} \text{---} \text{---} \end{array} = \begin{array}{c} \text{---} \text{---} \text{---} \\ \left. \begin{array}{c} \text{---} \text{---} \text{---} \\ \text{---} \text{---} \text{---} \\ \text{---} \text{---} \text{---} \\ \vdots \\ \text{---} \text{---} \text{---} \\ \vdots \\ \text{---} \text{---} \text{---} \\ \text{---} \text{---} \text{---} \\ \text{---} \text{---} \text{---} \\ \text{---} \text{---} \text{---} \\ \text{---} \text{---} \text{---} \end{array} \right\} A \\ \text{---} \text{---} \text{---} \end{array} = \text{tr} \left( \overset{\leftrightarrow}{A} \right) \quad (8.82)$$

as is illustrated here for the case where  $n = 1$ .

Theorem 8.3 gives an alternative way of computing the trace of a primitive invariant  $\lambda \in S_{m,n}$  (acting on a product space consisting of a total of  $k$  factors): one first transforms  $\lambda$  into a primitive invariant of  $S_{(m+n)}$  (acting on  $V^{\otimes k}$ ) via the map  $\overset{\mathcal{N}}{\leftarrow \rightarrow}$ , and then uses Theorem 8.2 to evaluate the trace,

$$\text{tr} \left( \underbrace{\lambda}_{\in S_{m,n}} \right) \stackrel{\text{Thm. 8.3}}{=} \text{tr} \left( \underbrace{\overset{\mathcal{N}}{\leftarrow \rightarrow} \lambda}_{\in S_{(m+n)}} \right) = N^{k - \varkappa \left( \overset{\mathcal{N}}{\leftarrow \rightarrow} \lambda \right)}. \quad (8.83)$$

### 8.3.3 Traces of products of primitive invariants

Let us now turn our attention to products of primitive invariants. Let  $\rho, \sigma \in S_{(m+n)}$  and let  $\overset{\leftrightarrow}{\rho}$  and  $\overset{\leftrightarrow}{\sigma}$  be their corresponding primitive invariants in  $S_{m,n}$  under the map  $\overset{\mathcal{N}}{\leftarrow \rightarrow}$ ,  $\mathcal{N} = \{m+1, \dots, m+n\}$ . In general, it is true that

$$\overset{\leftarrow \rightarrow}{\rho \cdot \sigma} \neq \overset{\leftrightarrow}{\rho} \cdot \overset{\leftrightarrow}{\sigma}. \quad (8.84)$$

As an example,

$$\left( \overset{1}{\leftarrow \rightarrow} \right) \cdot \left( \overset{1}{\leftarrow \rightarrow} \right) = \begin{array}{c} \text{---} \text{---} \text{---} \\ \left. \begin{array}{c} \text{---} \text{---} \text{---} \\ \text{---} \text{---} \text{---} \\ \text{---} \text{---} \text{---} \\ \text{---} \text{---} \text{---} \\ \text{---} \text{---} \text{---} \end{array} \right\} \cdot \begin{array}{c} \text{---} \text{---} \text{---} \\ \left. \begin{array}{c} \text{---} \text{---} \text{---} \\ \text{---} \text{---} \text{---} \\ \text{---} \text{---} \text{---} \\ \text{---} \text{---} \text{---} \\ \text{---} \text{---} \text{---} \end{array} \right\} \\ \text{---} \text{---} \text{---} \end{array} = \begin{array}{c} \text{---} \text{---} \text{---} \\ \left. \begin{array}{c} \text{---} \text{---} \text{---} \\ \text{---} \text{---} \text{---} \\ \text{---} \text{---} \text{---} \\ \text{---} \text{---} \text{---} \\ \text{---} \text{---} \text{---} \end{array} \right\} \\ \text{---} \text{---} \text{---} \end{array} = \begin{array}{c} \text{---} \text{---} \text{---} \\ \left. \begin{array}{c} \text{---} \text{---} \text{---} \\ \text{---} \text{---} \text{---} \\ \text{---} \text{---} \text{---} \\ \text{---} \text{---} \text{---} \\ \text{---} \text{---} \text{---} \end{array} \right\} \\ \text{---} \text{---} \text{---} \end{array}, \quad (8.85a)$$

but

$$\left( \overset{1}{\leftarrow \rightarrow} \right) \cdot \left( \overset{1}{\leftarrow \rightarrow} \right) = \left( \overset{1}{\leftarrow \rightarrow} \right) = \begin{array}{c} \text{---} \text{---} \text{---} \\ \left. \begin{array}{c} \text{---} \text{---} \text{---} \\ \text{---} \text{---} \text{---} \\ \text{---} \text{---} \text{---} \\ \text{---} \text{---} \text{---} \\ \text{---} \text{---} \text{---} \end{array} \right\} = \begin{array}{c} \text{---} \text{---} \text{---} \\ \left. \begin{array}{c} \text{---} \text{---} \text{---} \\ \text{---} \text{---} \text{---} \\ \text{---} \text{---} \text{---} \\ \text{---} \text{---} \text{---} \\ \text{---} \text{---} \text{---} \end{array} \right\} \neq \begin{array}{c} \text{---} \text{---} \text{---} \\ \left. \begin{array}{c} \text{---} \text{---} \text{---} \\ \text{---} \text{---} \text{---} \\ \text{---} \text{---} \text{---} \\ \text{---} \text{---} \text{---} \\ \text{---} \text{---} \text{---} \end{array} \right\}. \quad (8.85b)$$

Astonishingly, however, the trace of both (8.85a) and (8.85b) is the same,

$$\text{tr} \left( \begin{array}{c} \text{---} \text{---} \text{---} \\ \left. \begin{array}{c} \text{---} \text{---} \text{---} \\ \text{---} \text{---} \text{---} \\ \text{---} \text{---} \text{---} \\ \text{---} \text{---} \text{---} \\ \text{---} \text{---} \text{---} \end{array} \right\} \right) = \text{tr} \left( \begin{array}{c} \text{---} \text{---} \text{---} \\ \left. \begin{array}{c} \text{---} \text{---} \text{---} \\ \text{---} \text{---} \text{---} \\ \text{---} \text{---} \text{---} \\ \text{---} \text{---} \text{---} \\ \text{---} \text{---} \text{---} \end{array} \right\} \right) = N^2. \quad (8.86)$$

This is not a mere coincidence, but a general feature of primitive invariants:

**■ Theorem 8.4 – the trace stays invariant under  $\overset{\mathcal{N}}{\leftarrow \rightarrow}$  for products:**

Let  $\rho, \sigma \in S_{(m+n)}$  and let  $\overset{\leftrightarrow}{\rho}, \overset{\leftrightarrow}{\sigma}$  be the two elements in  $S_{m,n}$  obtained from  $\rho$  and  $\sigma$  via the map  $\overset{\mathcal{N}}{\leftarrow \rightarrow}$ ,  $\mathcal{N}$  is a subset of  $\{1, \dots, m, m+1, \dots, m+n\}$  of size  $n$ .<sup>5</sup> Then,

$$\text{tr}(\rho \cdot \sigma) = \text{tr} \left( \overset{\leftrightarrow}{\rho} \cdot \overset{\leftrightarrow}{\sigma} \right), \quad (8.87)$$

<sup>5</sup>This subset is usually taken to be  $\{m+1, \dots, m+n\}$ .

that is, the trace of the product remains unchanged if the map  $\overleftarrow{\mathcal{N}}$  is applied to the individual primitive invariants.

*Proof of Theorem 8.4:* Let  $\rho, \sigma \in S_{(m+n)}$  and  $\overleftrightarrow{\rho}, \overleftrightarrow{\sigma} \in S_{m,n}$  be as required by the Theorem. To prove the desired eq. (8.87), we will use a similar strategy as in the proof of Theorem 8.3: We will argue that the total number of loops in the trace  $\text{tr}(\rho \cdot \sigma)$  stays the same if each invariant  $\rho, \sigma$  is acted upon by the map  $\overleftarrow{\mathcal{N}}$  individually. We will show this by acting  $\overleftarrow{\mathcal{N}}$  successively on the various index lines of  $\rho$  and  $\sigma$ . Once again, it will be convenient to start with the topmost index line. Let us therefore consider the action of  $\overleftarrow{1}$ :

Written as a product of Kronecker  $\delta$ 's,  $\rho$  and  $\sigma$  will contain terms  $\delta^{b_i}_{a_1} \delta^{b_1}_{a_j}$  and  $\delta^{c_s}_{b_1} \delta^{c_1}_{b_t}$  respectively, which correspond to the index lines ending on the topmost level of the two birdtracks. Schematically, expressing all other index lines except  $\delta^{b_i}_{a_1} \delta^{b_1}_{a_j}$  and  $\delta^{c_s}_{b_1} \delta^{c_1}_{b_t}$  by a grey box, the product  $\rho \cdot \sigma$  is written as

$$\rho \cdot \sigma \mapsto \text{Diagram} \tag{8.88}$$

If we act the map  $\overleftarrow{1}$  on each primitive invariant  $\rho$  or  $\sigma$  individually, the product  $\rho \cdot \sigma$  becomes

$$\text{Diagram} \xrightarrow{\overleftarrow{1}} \text{Diagram} = \text{Diagram} \tag{8.89}$$

For the remainder of this proof, we suppress the index labels  $a, b, c$ .

Taking the trace of the product  $\rho \cdot \sigma$  results in connecting all index lines on the same level (*c.f.* eq. (8.6a)). Only making the topmost such connection explicit, but understanding that *all* are present in the schematic depiction below,  $\text{tr}(\rho \cdot \sigma)$  becomes

$$\text{tr}(\rho \cdot \sigma) \mapsto \text{Diagram} \tag{8.90}$$

A product of any two primitive invariants in  $S_{(m+n)}$  will yield another primitive invariant in  $S_{(m+n)}$  by virtue

of  $S_{(m+n)}$  being a group,

$$\rho \cdot \sigma \in S_{(m+n)} . \tag{8.91}$$

As we know from Theorem 8.2, the trace of a primitive invariant in  $S_{(m+n)}$ , such as  $\rho \cdot \sigma$ , will yield a power of  $N$ ,

$$\text{tr}(\rho \cdot \sigma) = N^q \quad \text{for some } q \in \mathbb{N} . \tag{8.92}$$

Thus, the schematic drawing (8.90) of  $\text{tr}(\rho \cdot \sigma)$  must consist of exactly  $q$  closed loops. We now notice the following: The index lines representing  $\delta^{b_i}_{a_1}$  and  $\delta^{c_1}_{b_i}$  are connected through the trace (red line), therefore forming part of the *same* loop in (8.90); we will indicate this by the blue dashed line in the following eq. (8.93). Similarly, the index lines representing  $\delta^{b_1}_{a_j}$  and  $\delta^{c_s}_{b_1}$  are connected at  $b_1$ , therefore also forming part of the same loop; this loop is indicated by the pink dotted line below,

$$\text{tr}(\rho \cdot \sigma) \mapsto \text{Diagram} . \tag{8.93}$$

It is understood that the dashed and dotted lines may involve other index lines not explicitly represented in this schematic drawing of  $\text{tr}(\rho \cdot \sigma)$ . The key observation to be made is that the Kronecker deltas  $\delta^{b_i}_{a_1}$ ,  $\delta^{b_1}_{a_j}$ ,  $\delta^{c_s}_{b_1}$  and  $\delta^{c_1}_{b_i}$  form part of 2 *distinct closed loops*. Hence, if  $\text{tr}(\rho \cdot \sigma) = N^q$  according to eq. (8.92), the part of  $\text{tr}(\rho \cdot \sigma)$  contained in the grey box in (8.93) consists of exactly  $(q - 2)$  closed loops.

**Remark:** We would like to point out that if the Kronecker  $\delta$ 's ending on the top most level of  $\rho$  and  $\sigma$  (these are  $\delta^{b_i}_{a_1}$ ,  $\delta^{b_1}_{a_j}$ ,  $\delta^{c_s}_{b_1}$  and  $\delta^{c_1}_{b_i}$ ) form part of only one loop, then the proof of Theorem 8.4 reduces to the proof of Theorem 8.3 and we are done.

We now wish to act the map  $\overset{1}{\leftrightarrow}$  on each of the primitive invariants  $\rho$  and  $\sigma$  in  $\text{tr}(\rho \cdot \sigma)$ . Graphically, this results in cutting the loops in (8.93) at points  $a_1, b_1, c_1$  (marked by  $\times$  below) and reconnecting them as demonstrated in eq. (8.89),

$$\text{Diagram} \xrightarrow{\overset{1}{\leftrightarrow}} \text{Diagram} . \tag{8.94}$$

It should be noted that all other closed loops in  $\text{tr}(\rho \cdot \sigma)$  (included in the grey boxes) remain intact under the action of  $\overset{1}{\leftrightarrow}$  on  $\rho$  and  $\sigma$  and thus continue to contribute a factor  $N^{(q-2)}$  to  $\text{tr}\left(\overset{\leftrightarrow}{\rho} \cdot \overset{\leftrightarrow}{\sigma}\right)$  (where  $\leftrightarrow := \overset{1}{\leftrightarrow}$ ).

Furthermore, from eq. (8.94) it is abundantly clear that the two explicitly drawn loops in  $\text{tr}(\rho \cdot \sigma)$  remain two distinct loops in  $\text{tr}(\overset{\leftrightarrow}{\rho} \cdot \overset{\leftrightarrow}{\sigma})$ . Thus, the total loop count in  $\text{tr}(\overset{\leftrightarrow}{\rho} \cdot \overset{\leftrightarrow}{\sigma})$  continues to be  $q$ ,

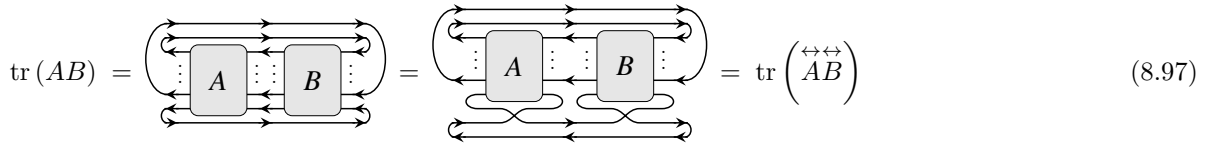
$$\text{tr}(\overset{\leftrightarrow}{\rho} \cdot \overset{\leftrightarrow}{\sigma}) = N^q . \tag{8.95}$$

We conclude, therefore, that

$$\text{tr}(\rho \cdot \sigma) = \text{tr}(\overset{\leftrightarrow}{\rho} \cdot \overset{\leftrightarrow}{\sigma}) , \tag{8.96}$$

where  $\leftrightarrow := \overset{1}{\leftrightarrow}$ , as required. One may now consecutively transform fundamental lines into antifundamental lines under the trace as exhibited above. This will however keep the number of loops in the trace constant, as we have already seen for the case  $\overset{1}{\leftrightarrow}$ . Hence, the trace  $\text{tr}(\rho \cdot \sigma)$  remains invariant under an application of the map  $\overset{\mathcal{N}}{\leftrightarrow}$ .  $\square$

As was already the case for Theorem 8.3, since all birdtrack operators  $A, B \in \text{Lin}(V^{\otimes(m+n)})$  are linear combinations of the primitive invariants in  $S_{(m+n)}$ , Theorem 8.4 trivially also holds for the product  $AB$ ,



$$\text{tr}(AB) = \text{tr}(\overset{\leftrightarrow}{AB}) = \text{tr}(\overset{\leftrightarrow}{A} \cdot \overset{\leftrightarrow}{B}) = \text{tr}(\overset{\leftrightarrow}{A}) \cdot \text{tr}(\overset{\leftrightarrow}{B}) \tag{8.97}$$

as is illustrated here for the case where  $n = 1$ .

Theorem 8.4 indeed explains that the observation made in eqns. (8.85) and (8.86) is completely general: Given that for any  $\rho, \sigma \in S_{(m+n)}$  it is true that  $\lambda := \rho \cdot \sigma$  also lies in  $S_{(m+n)}$  since  $S_{(m+n)}$  is a group, we have that:

**Corollary 8.2** –  $\overset{\mathcal{N}}{\leftrightarrow}$  distributes under Tr:

For any  $\rho, \sigma \in S_{(m+n)}$ , it follows that

$$\text{tr}(\overset{\leftrightarrow}{\rho} \cdot \overset{\leftrightarrow}{\sigma}) \stackrel{\text{Thm. 8.4}}{=} \text{tr}(\rho \cdot \sigma) \stackrel{\text{Thm. 8.3}}{=} \text{tr}(\overset{\mathcal{N}}{\rho} \cdot \overset{\mathcal{N}}{\sigma}) , \tag{8.98}$$

where  $\leftrightarrow$  is understood to mean  $\overset{\mathcal{N}}{\leftrightarrow}$ , for  $\mathcal{N}$  being a subset of  $\{1, \dots, m, m+1, \dots, m+n\}$  of size  $n$  (usually taken to be  $\mathcal{N} = \{m+1, \dots, m+n\}$ ).



**Part *III***

***Conclusion***





## Chapter 9

# Towards a Full Mathematical Theory: Outlook

*While the results given in this thesis are directly applicable to the physics context we are interested in (as discussed in the following chapter 10), there are still some unresolved issues that need to be addressed in order to obtain a full mathematical theory. We list some of these issues in the present chapter.*

### 9.1 A formula for the normalization constants?

For the standard Young projection operators  $Y_\Theta$ , the normalization constant  $\alpha_\Theta$  ensuring their idempotency can be calculated by means of a combinatoric formula involving the Hook length of the tableau  $\Theta$  (*c.f.* eq. (4.37) in chapter 4). The normalization constant  $\beta_\Theta$  corresponding to the MOLD projectors  $P_\Theta$  in Theorem 3.5 was shown to be finite and nonzero, however, no explicit formula to obtain this constant exists up to this point. While calculating the constant  $\beta_\Theta$  via squaring  $P_\Theta$  and requiring that  $P_\Theta \cdot P_\Theta \stackrel{!}{=} P_\Theta$  is easily done (for example in Mathematica), and thus does not cause problems with respect to the practical usability of the MOLD operators in physics examples,<sup>1</sup> an explicit formula for  $\beta_\Theta$  analogous to the Hook rule is desirable to obtain a full mathematical theory.

The underlying reason for the lack of an explicit formula is that the simplification rule used in the construction of the MOLD operators, Corollary 2.2 in chapter 2, is not as well understood as it ought to be. This rule states the conditions under which it is possible to cancel certain sets of symmetrizers and antisymmetrizers in a product at the cost of a nonzero constant  $\lambda$ . This constant must be combinatoric in nature, as it is linked to the number and respective sizes of the sets of (anti-)symmetrizers that are cancelled (this statement is based on observations made when calculating a *large* number of examples), although the precise relation is as yet unclear.

Studying these simplification rules (in particular the cancellation rules of section 2.3) further promises not only better insight into birdtrack operators themselves, but also a deeper understanding of the effect that such cancellation rules have on the operators, hopefully leading us to an explicit formula for the constant

---

<sup>1</sup>Similarly, since the transition operators in chapter 4 are constructed from the MOLD projectors, they also have to be normalized manually. This procedure is also computationally inexpensive, and thus causes no problems in practical applications.

$\lambda$ . This will culminate in an explicit formula for the normalization constant of the MOLD projection and transition operators, thus making their automated implementation on a computer even easier.

## 9.2 Coincidence limits of Wilson lines beyond what is already established

As has been pointed out on numerous occasions, coincidence limits of Wilson line correlators are directly applicable in a physics context. However, from a mathematical point of view, such coincidence limits are interesting in their own right:

In a basis of symmetrizers and antisymmetrizers, we have seen that a particular coincidence limit yields a correlator zero if it essentially causes two legs of a symmetrizer to be connected with two legs of an antisymmetrizer (*c.f.* section 5.3.1.1). For example, a coincidence limit between the top two legs ( $\mathbf{x} \rightarrow \mathbf{y}$ ) of the following operator gives a null result,

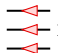
The diagram shows two operators on the left. The first is a symmetrizer with two legs on the left and two on the right, all pointing left. The second is an antisymmetrizer with two legs on the left and two on the right, all pointing right. An arrow labeled  $\mathbf{x} \rightarrow \mathbf{y}$  points to the right-hand side, where the two top legs of the symmetrizer are connected to the two top legs of the antisymmetrizer. The result is  $= 0$ .

(This was already demonstrated in eq. (5.160), we merely “unbent” the singlet states and suppressed the  $U^\dagger$ 's here for clarity.) On the other hand, the same coincidence limit between the following two operators did not vanish,

The diagram shows two operators on the left. The first is a symmetrizer with two legs on the left and two on the right, all pointing left. The second is another symmetrizer with two legs on the left and two on the right, all pointing left. An arrow labeled  $\mathbf{x} \rightarrow \mathbf{y}$  points to the right-hand side, where the two top legs of the first symmetrizer are connected to the two top legs of the second symmetrizer. The result is  $\neq 0$ .

In fact, it would need a coincidence limit of all Wilson lines ( $\mathbf{x} \rightarrow \mathbf{y} \rightarrow \mathbf{z}$ ) to make this operator zero,

The diagram shows two operators on the left. The first is a symmetrizer with two legs on the left and two on the right, all pointing left. The second is an antisymmetrizer with two legs on the left and two on the right, all pointing right. An arrow labeled  $\mathbf{x} \rightarrow \mathbf{y} \rightarrow \mathbf{z}$  points to the right-hand side, where the two top legs of the symmetrizer are connected to the two top legs of the antisymmetrizer, and then these are further connected to a third set of legs. The result is  $= 0$ .

As already mentioned in section 5.3.2.1, the two operators on either side of the Wilson lines  in (9.2) have the same parent operator, while the operators in (9.1) do not. Since the MOLD algorithm (Theorem 3.5) stacks sets of symmetrizers and antisymmetrizers of consecutively older generations of Young tableaux next to each other, it is conceivable that the ancestry of two operators gives information about how many coincidence limits (starting from the top) need to be taken before the resulting operator becomes zero. Since the construction of transition operators has the MOLD operators as its basis (Theorem 3.5), a valid argument for the MOLD operators will immediately transfer to the transition operators.

However, due to the fact that an ancestor tableau of size  $n$  only holds information of the top  $n$  index lines of an operator, it will not be able to give any information about coincidence limits other than the first  $n$ . Thus, information about a coincidence limit of a random subset of index lines cannot be encoded in (ancestor) Young tableaux, and a different approach is required.

Lastly, we emphasize that we have not yet commented on coincidence limits of Wilson lines connecting operators in a different basis. For example, the criterion when a coincidence limit in the basis discussed in

section 5.3.2.2 yields a null operator is very different than in a basis of symmetrizers and antisymmetrizers. Thus, we expect a general argument to involve very different considerations.

### 9.3 Irreducible representations of $SU(N)$ over $V^{\otimes m} \otimes (V^*)^{\otimes n}$

As was demonstrated in chapter 5, section 5.1.4, the standard method of constructing the projection operators of  $SU(N)$  over a mixed product space  $V^{\otimes m} \otimes (V^*)^{\otimes n}$  from the Littlewood-Richardson tableaux is inadequate for practical calculations as it involves an immense computational effort. In section 5.2 of chapter 5, we presented a computationally efficient method of obtaining a subset of these projection operators, namely those corresponding to singlet representations. A practical, easy-to-implement algorithm for the remaining projection operators is (to the author's knowledge) not yet known and thus invites future research on the matter. In particular, such an algorithm will be of interest for physics applications, as it allows one to verify that the  $n$ -point functions  $G_{Y, \mathbf{x}_1 \dots \mathbf{x}_n}^{(j)}$  and  $K_{Y, \mathbf{x}_1 \dots \mathbf{x}_n}^{(j)}$  in the parametrization of JIMWLK behave in the expected way for non-singlets. We will comment further on this topic in section 10.2.4 of chapter 10.

There remains, however, a number of as yet unresolved mathematical oddities standing in the way of attaining the desired construction method. In this section, we focus on those peculiarities that result from making the parameter  $\dim(V) = N$  small enough to produce dimensionally null representations of  $SU(N)$  over  $V^{\otimes m} \otimes (V^*)^{\otimes n}$ . Investigating such phenomena in the future may pave the way to a practical construction algorithm for all projection operators of  $SU(N)$  over  $V^{\otimes m} \otimes (V^*)^{\otimes n}$ . We expect that such an algorithm – once it has been formulated – will enable the study of new properties of the irreducible representations of  $SU(N)$ , which would not have been identified as noteworthy without the explicit expressions of the projection (and transition) operators.

#### 9.3.1 Systematic knowledge of dimensionally null operators of $SU(N)$ over the 4-particle Fock spaces

Let us consider the representations of  $SU(N)$  over a product space  $V^{\otimes m} \otimes (V^*)^{\otimes n}$ , and let  $k := m + n$ . If  $n = 0$ , and hence  $V^{\otimes m} \otimes (V^*)^{\otimes n} = V^{\otimes m} = V^{\otimes k}$ , then the Young tableaux consisting of  $k$  boxes uniquely classify the irreducible representations of  $SU(N)$  over this product space. If, furthermore,  $\dim(V) = N < k$ , then the Young tableaux containing more than  $N$  rows correspond to null representations of  $SU(N)$ , since the associated projection operators include antisymmetrizers of more than  $N$  elements (*c.f.* eq. (3.29) for Young projectors, and Theorem 3.5 for MOLD projectors). In other words, the number of irreducible representations of  $SU(N)$  is reduced if the dimension  $N$  of  $V$  is too small to accommodate all possible representations. For example, the Young tableau

$$\begin{array}{|c|} \hline 1 \\ \hline 2 \\ \hline 3 \\ \hline \vdots \\ \hline k \\ \hline \end{array} \tag{9.4}$$

is the unique tableau that requires  $N \geq k$  in order for the corresponding representation to be nonzero. Notice that the proof of Corollary 6.2, which states that  $SU(N)$  has the same number of representations over all

product spaces  $V^{\otimes m} \otimes (V^*)^{\otimes n}$  with  $m + n = k$  as over  $V^{\otimes(m+n)} = V^{\otimes k}$ , is independent of  $N$ . This implies that Corollary 6.2 holds for all values of  $N$ . There consequently exists a unique projection operator of  $SU(N)$  over every space  $V^{\otimes m} \otimes (V^*)^{\otimes n}$  (with  $m + n = k$ ) whose dimension is nonzero if and only if  $N \geq m + n$ . This was exemplified in chapter 7, where we found that the following operators,<sup>2</sup>

$$V^{\otimes 4} : \quad P^{(4)} = \theta_{N>3} \cdot \begin{array}{c} \leftarrow \rightarrow \\ \leftarrow \rightarrow \\ \leftarrow \rightarrow \\ \leftarrow \rightarrow \end{array} \quad (9.5a)$$

$$V^{\otimes 3} \otimes V^* : \quad P^{(3,1)} = \theta_{N>3} \cdot \left\{ \begin{array}{c} \leftarrow \rightarrow \quad \leftarrow \rightarrow \\ \leftarrow \rightarrow \quad \leftarrow \rightarrow \\ \leftarrow \rightarrow \quad \leftarrow \rightarrow \end{array} - \frac{3}{N-2} \begin{array}{c} \leftarrow \rightarrow \quad \leftarrow \rightarrow \\ \leftarrow \rightarrow \quad \leftarrow \rightarrow \\ \leftarrow \rightarrow \quad \leftarrow \rightarrow \end{array} \right\} \quad (9.5b)$$

$$V^{\otimes 2} \otimes (V^*)^{\otimes 2} : \quad P^{(2,2)} = \theta_{N>3} \cdot \left\{ \begin{array}{c} \leftarrow \rightarrow \quad \leftarrow \rightarrow \\ \leftarrow \rightarrow \quad \leftarrow \rightarrow \\ \leftarrow \rightarrow \quad \leftarrow \rightarrow \end{array} - \frac{2}{N-2} \left( 2 \begin{array}{c} \leftarrow \rightarrow \quad \leftarrow \rightarrow \\ \leftarrow \rightarrow \quad \leftarrow \rightarrow \\ \leftarrow \rightarrow \quad \leftarrow \rightarrow \end{array} - \frac{1}{N-1} \begin{array}{c} \leftarrow \rightarrow \quad \leftarrow \rightarrow \\ \leftarrow \rightarrow \quad \leftarrow \rightarrow \\ \leftarrow \rightarrow \quad \leftarrow \rightarrow \end{array} \right) \right\}, \quad (9.5c)$$

and only these operators for each basis, vanish if  $N$  is decreased below 4. They each constitute a  $1 \times 1$  block in the matrices  $\mathfrak{M}_{4\text{-particle}}$ , and correspond to the respective tableaux

$$P^{(4)} \rightarrow \begin{array}{|c|} \hline 1 \\ \hline 2 \\ \hline 3 \\ \hline 4 \\ \hline \end{array}, \quad P^{(3,1)} \rightarrow \begin{array}{|c|c|} \hline 1 & a_1 \\ \hline 2 & a_2 \\ \hline 3 & a_3 \\ \hline \vdots & \\ \hline a_{\check{N}} & \\ \hline \end{array} \quad \text{and} \quad P^{(2,2)} \rightarrow \begin{array}{|c|c|c|} \hline 1 & a_1 & b_1 \\ \hline 2 & a_2 & b_2 \\ \hline a_3 & \vdots & \\ \hline \vdots & b_{\check{N}-1} & \\ \hline a_{\check{N}} & & \\ \hline b_{\check{N}} & & \\ \hline \end{array}, \quad \check{N} := N - 1, \quad (9.6)$$

as discussed in chapter 7. For completeness, we ought to include the operator

$$\tilde{P}^{(2,2)} = \frac{\theta_{N>3}}{2} \left\{ \begin{array}{c} \leftarrow \rightarrow \quad \leftarrow \rightarrow \\ \leftarrow \rightarrow \quad \leftarrow \rightarrow \end{array} - \begin{array}{c} \leftarrow \rightarrow \quad \leftarrow \rightarrow \\ \leftarrow \rightarrow \quad \leftarrow \rightarrow \end{array} - \frac{1}{2(N-2)} \begin{array}{c} \leftarrow \rightarrow \quad \leftarrow \rightarrow \\ \leftarrow \rightarrow \quad \leftarrow \rightarrow \end{array} - \frac{1}{N(N-1)} \begin{array}{c} \leftarrow \rightarrow \quad \leftarrow \rightarrow \\ \leftarrow \rightarrow \quad \leftarrow \rightarrow \end{array} \right\}, \quad (9.7)$$

as it is also only a nonzero operator if  $N \geq 4$  [72].

Suppose we want to form the singlet states of  $SU(N)$  over  $V^{\otimes 4} \otimes (V^*)^{\otimes 4}$ . According to Theorem 5.2 in chapter 5, we may generate these states via bending the basis elements of  $\text{API}\left(SU(N), V^{\otimes m} \otimes (V^*)^{\otimes n}\right)$  for  $m + n = 4$ . For example, the nonzero matrix elements of  $\mathfrak{M}_4$  (c.f. section 7.3.2) yield all 24 singlet states. As explained in sections 5.2.1.3 and 5.2.1.4, bending the elements of  $\mathfrak{M}_{3,1}$ ,  $\mathfrak{M}_{2,2}$  or  $\tilde{\mathfrak{M}}_{2,2}$  (c.f. sections 7.3.2, 7.4.2 and 7.4.3, respectively) will also lead to sets of 24 singlet states of  $SU(N)$  over  $V^{\otimes 4} \otimes (V^*)^{\otimes 4}$ , all of which are completely equivalent to the first, and thus to each other. Therefore, there exists a change of basis between the various sets of singlets obtained from bending the elements of the different matrices  $\mathfrak{M}_{4\text{-particle}}$ .

In each of these singlet sets, there exists a unique singlet state that is nonzero if and only if  $N \geq 4$ , namely the singlet obtained from bending the operators in eqns. (9.5) and (9.7) respectively. Thus, in a change of basis, these singlets must map directly to each other (as opposed to a linear combination of other singlets).

Spinning this one step further, we notice that there are nine matrix elements in each basis  $\mathfrak{M}_4$ ,  $\mathfrak{M}_{3,1}$ ,  $\mathfrak{M}_{2,2}$  and  $\tilde{\mathfrak{M}}_{2,2}$  that become nonzero for  $N \geq 3$  (this was discussed in great detail in section 7.5). Let us denote

<sup>2</sup>We remind the reader that the function  $\theta_{N>k}$  is defined as (c.f. eq. (7.10))

$$\theta_{N>k} := \begin{cases} 1 & \text{if } N > k \\ 0 & \text{if } N \leq k. \end{cases}$$

this set of operators by  $\mathfrak{S}_{q,\bar{q}}[3]$  (where  $q$  and  $\bar{q}$  denote the number of fundamental resp. antifundamental factors in  $V^{\otimes q} \otimes (V^*)^{\otimes \bar{q}}$ ). Thus, the corresponding subsets of nine singlet states of  $\text{SU}(N)$  over  $V^{\otimes 4} \otimes (V^*)^{\otimes 4}$  must map to each other in a change of basis. However, here we notice something curious: In the matrix  $\mathfrak{M}_4$ , the set  $\mathfrak{S}_4[3]$  is contained in a  $3 \times 3$  block marked below,

$$\mathfrak{S}_4[3] \longrightarrow \begin{pmatrix} \mathbf{1} & & & & & & & & \\ & \color{magenta}{3} & & & & & & & \\ & & \color{cyan}{2} & & & & & & \\ & & & \color{cyan}{3} & & & & & \\ & & & & \color{cyan}{1} & & & & \\ & & & & & \color{magenta}{3} & & & \\ & & & & & & \color{cyan}{1} & & \\ & & & & & & & \color{cyan}{1} & \\ & & & & & & & & \color{cyan}{1} \end{pmatrix}. \quad (9.8a)$$

On the other hand, the nine operators in question are distributed rather oddly in the matrices  $\mathfrak{M}_{3,1}$ ,  $\mathfrak{M}_{2,2}$  and  $\tilde{\mathfrak{M}}_{2,2}$ . In  $\mathfrak{M}_{3,1}$ , the elements of the set  $\mathfrak{S}_{3,1}[3]$  that contain an antisymmetrizer of length 3 (and thus vanish for  $N < 3$ ) populate one row and column in a  $3 \times 3$  block (*c.f.* eq. (7.17)). Additionally, it was shown in section 7.5.3 that the two projection operators of the  $2 \times 2$  block vanish, causing the corresponding transition operators to also become null. Therefore,

$$\mathfrak{S}_{3,1}[3] \longrightarrow \begin{pmatrix} \mathbf{1} & & & & & & & & \\ & \color{cyan}{3} & & & & & & & \\ & & \color{magenta}{2} & & & & & & \\ & & & \color{magenta}{1} & & & & & \\ & & & & \color{magenta}{3} & & & & \\ & & & & & \color{cyan}{1} & & & \\ & & & & & & \color{cyan}{1} & & \\ & & & & & & & \color{cyan}{1} & \\ & & & & & & & & \color{cyan}{1} \end{pmatrix}. \quad (9.8b)$$

For the matrices  $\mathfrak{M}_{2,2}$  and  $\tilde{\mathfrak{M}}_{2,2}$ , one of the projection operators that vanishes for  $N \leq 3$  is contained in a  $4 \times 4$  block (*c.f.* eqns. (7.34b) and (7.41) respectively). Thus, this projection operator, and all six transition operators to it, vanish for  $N \leq 3$ . The remaining two null operators for  $N \leq 3$  are each contained in a  $1 \times 1$  block,

$$\left. \begin{matrix} \mathfrak{S}_{2,2}[3] \\ \tilde{\mathfrak{S}}_{2,2}[3] \end{matrix} \right\} \longrightarrow \begin{pmatrix} \color{magenta}{1} & & & & & & & & \\ & \color{cyan}{4} & & & & & & & \\ & & \color{cyan}{2} & & & & & & \\ & & & \color{cyan}{1} & & & & & \\ & & & & \color{cyan}{1} & & & & \\ & & & & & \color{magenta}{1} & & & \\ & & & & & & \color{magenta}{1} & & \\ & & & & & & & \color{cyan}{1} & \\ & & & & & & & & \color{cyan}{1} \end{pmatrix}. \quad (9.8c)$$

Thus, when forming singlet states out of the matrix elements of the various  $\mathfrak{M}$ 's, the states originating from the marked portions in eqns. (9.8) will be mapped to each other in a change of basis.

We used the case of the 4-factor product space to illustrate certain traits of the bases of singlet states formed from the projection and transition operators over these spaces. As the factors in the product spaces  $V^{\otimes m} \otimes (V^*)^{\otimes n}$  (out of which we build the singlets over  $V^{\otimes(m+n)} \otimes (V^*)^{\otimes(m+n)}$ ) increase, the study of the subsets of operators becoming zero (when incrementally decreasing  $N$ ) becomes more intricate: Let  $N = N_*$  where  $N_* < m + n$ . From the theory of Young tableaux, we know that the operators of  $\mathfrak{S}_{(m+n)}[N_*]$  occupy entire blocks in the matrix  $\mathfrak{M}_{(m+n)}$  – these blocks correspond to Young diagrams with more than  $N_*$  rows. Thus, the size of the set  $\mathfrak{S}_{(m+n)}[N_*]$  must be given by a sum of squares of integers,

$$|\mathfrak{S}_{(m+n)}[N_*]| = \sum_i n_i^2, \quad \text{where } n_i \in \mathbb{N} \text{ for every } i. \quad (9.9)$$

The number of elements of the matrix  $\mathfrak{M}_{m,n}$  that vanish for  $N \leq N_*$  must be the same as that of  $\mathfrak{M}_{(m+n)}$ ,

$$|\mathfrak{S}_{(m+n)}[N_*]| = |\mathfrak{S}_{m,n}[N_*]|, \tag{9.10}$$

even though the elements of  $\mathfrak{S}_{m,n}[N_*]$  need not fill an entire block in the matrix  $\mathfrak{M}_{m,n}$ , as was exhibited in eqns. (9.8b) and (9.8c) for  $\mathfrak{M}_{3,1}$  and  $\mathfrak{M}_{2,2}$  respectively. However, if a certain projection operator in  $\mathfrak{M}_{m,n}$  vanishes for  $N \leq N_*$ , then all transition operators to and from it must vanish as well. Thus, the elements of  $\mathfrak{S}_{m,n}[N_*]$  populate entire rows and columns in  $\mathfrak{M}_{m,n}$ . This puts a restriction on how the elements of  $\mathfrak{S}_{m,n}[N_*]$  can be distributed in  $\mathfrak{M}_{m,n}$ . As an example, we know that there are exactly nine elements in  $\mathfrak{S}_4[3]$ , and hence in  $\mathfrak{S}_{3,1}[3]$  and  $\mathfrak{S}_{2,2}[3]$ . For these nine elements to populate entire rows and columns of the matrices  $\mathfrak{M}_{4\text{-particles}}$ , the only other possible configuration, besides eqns. (9.8), is

$$\left( \begin{array}{cccc} \boxed{1} & & & \\ & \boxed{3} & & \\ & & \boxed{1} & \\ & & & \boxed{2} \\ & & & & \boxed{1} \\ & & & & & \boxed{3} \\ & & & & & & \boxed{1} \end{array} \right), \tag{9.11}$$

which interestingly enough does not occur. Thus, we are presented with an interesting problem in number theory whose solution<sup>3</sup> promises further insight into the representation theory of  $SU(N)$  over  $V^{\otimes m} \otimes (V^*)^{\otimes n}$  and the study of its multiplets.

### 9.3.2 Comparing the projector bases $\mathfrak{S}_3$ and $\mathfrak{S}_{2,1}$

The phenomena discussed in the previous section in fact already occur at the level of three factors in the product space  $V^{\otimes m} \otimes (V^*)^{\otimes n}$ :

We previously presented the projector basis of  $\text{API}(SU(N), V^{\otimes 3})$  in chapter 4, section 4.3.3. To recapitulate, the Hermitian Young projection operators of  $SU(N)$  over  $V^{\otimes 3}$ , together with the dimensions of the corresponding irreducible representations, are

$$\begin{array}{c} \leftarrow \leftarrow \leftarrow \\ \leftarrow \leftarrow \leftarrow \\ \leftarrow \leftarrow \leftarrow \end{array} \quad d = \frac{(N+2)(N+1)N}{6} \tag{9.12a}$$

$$\frac{4}{3} \begin{array}{c} \leftarrow \leftarrow \leftarrow \\ \leftarrow \leftarrow \leftarrow \\ \leftarrow \leftarrow \leftarrow \end{array} \quad d = \frac{N(N^2-1)}{3} \tag{9.12b}$$

$$\frac{4}{3} \begin{array}{c} \leftarrow \leftarrow \leftarrow \\ \leftarrow \leftarrow \leftarrow \\ \leftarrow \leftarrow \leftarrow \end{array} \quad d = \frac{N(N^2-1)}{3} \tag{9.12c}$$

$$\theta_{N>2} \begin{array}{c} \leftarrow \leftarrow \leftarrow \\ \leftarrow \leftarrow \leftarrow \\ \leftarrow \leftarrow \leftarrow \end{array} \quad d = \frac{N(N-1)(N-2)}{6}, \tag{9.12d}$$

<sup>3</sup>The author is not aware of any solution at this point in time.

and the matrix  $\mathfrak{M}_3$ , including the transition operators, is

$$\mathfrak{M}_3 = \begin{pmatrix} \begin{array}{c} \left[ \begin{array}{c} \leftarrow \text{---} \text{---} \text{---} \rightarrow \\ \leftarrow \text{---} \text{---} \text{---} \rightarrow \\ \leftarrow \text{---} \text{---} \text{---} \rightarrow \end{array} \right] & 0 & 0 & 0 \\ 0 & \begin{array}{c} \frac{4}{3} \left[ \begin{array}{c} \leftarrow \text{---} \text{---} \text{---} \rightarrow \\ \leftarrow \text{---} \text{---} \text{---} \rightarrow \\ \leftarrow \text{---} \text{---} \text{---} \rightarrow \end{array} \right] & \sqrt{\frac{4}{3}} \left[ \begin{array}{c} \leftarrow \text{---} \text{---} \text{---} \rightarrow \\ \leftarrow \text{---} \text{---} \text{---} \rightarrow \\ \leftarrow \text{---} \text{---} \text{---} \rightarrow \end{array} \right] & 0 \\ 0 & \sqrt{\frac{4}{3}} \left[ \begin{array}{c} \leftarrow \text{---} \text{---} \text{---} \rightarrow \\ \leftarrow \text{---} \text{---} \text{---} \rightarrow \\ \leftarrow \text{---} \text{---} \text{---} \rightarrow \end{array} \right] & \frac{4}{3} \left[ \begin{array}{c} \leftarrow \text{---} \text{---} \text{---} \rightarrow \\ \leftarrow \text{---} \text{---} \text{---} \rightarrow \\ \leftarrow \text{---} \text{---} \text{---} \rightarrow \end{array} \right] & 0 \\ 0 & 0 & 0 & \theta_{N>2} \cdot \left[ \begin{array}{c} \leftarrow \text{---} \text{---} \text{---} \rightarrow \\ \leftarrow \text{---} \text{---} \text{---} \rightarrow \\ \leftarrow \text{---} \text{---} \text{---} \rightarrow \end{array} \right] \end{array} \end{pmatrix}. \quad (9.13)$$

We have not yet discussed the projection operators of  $\text{SU}(N)$  over  $V^{\otimes 2} \otimes V^*$ . These can be obtained either from the LR-tableaux, or (as in our case) through making an educated guess (Ansatz),

$$\begin{array}{c} \left[ \begin{array}{c} \leftarrow \text{---} \text{---} \text{---} \rightarrow \\ \leftarrow \text{---} \text{---} \text{---} \rightarrow \\ \leftarrow \text{---} \text{---} \text{---} \rightarrow \end{array} \right] - \frac{2}{N+1} \left[ \begin{array}{c} \leftarrow \text{---} \text{---} \text{---} \rightarrow \\ \leftarrow \text{---} \text{---} \text{---} \rightarrow \\ \leftarrow \text{---} \text{---} \text{---} \rightarrow \end{array} \right] \end{array} \quad d = \frac{N(N-1)(N+2)}{2} \quad (9.14a)$$

$$\frac{2}{N+1} \left[ \begin{array}{c} \leftarrow \text{---} \text{---} \text{---} \rightarrow \\ \leftarrow \text{---} \text{---} \text{---} \rightarrow \\ \leftarrow \text{---} \text{---} \text{---} \rightarrow \end{array} \right] \quad d = N \quad (9.14b)$$

$$\frac{2}{N-1} \left[ \begin{array}{c} \leftarrow \text{---} \text{---} \text{---} \rightarrow \\ \leftarrow \text{---} \text{---} \text{---} \rightarrow \\ \leftarrow \text{---} \text{---} \text{---} \rightarrow \end{array} \right] \quad d = N \quad (9.14c)$$

$$\theta_{N>2} \cdot \left\{ \left[ \begin{array}{c} \leftarrow \text{---} \text{---} \text{---} \rightarrow \\ \leftarrow \text{---} \text{---} \text{---} \rightarrow \\ \leftarrow \text{---} \text{---} \text{---} \rightarrow \end{array} \right] - \frac{2}{N-1} \left[ \begin{array}{c} \leftarrow \text{---} \text{---} \text{---} \rightarrow \\ \leftarrow \text{---} \text{---} \text{---} \rightarrow \\ \leftarrow \text{---} \text{---} \text{---} \rightarrow \end{array} \right] \right\} \quad d = \theta_{N>2} \cdot \frac{N(N+1)(N-2)}{2}. \quad (9.14d)$$

Sceptical readers may satisfy themselves that the operators (9.14) indeed correspond to the irreducible representations of  $\text{SU}(N)$  over  $V^{\otimes 2} \otimes V^*$  by checking that

- we have the right number of operators (namely 4 – see Corollary 6.2)
- these operators are mutually orthogonal (left as an exercise)
- their dimension adds up to  $N^3$ ,

$$\frac{N(N-1)(N+2)}{2} + N + N + \frac{N(N+1)(N-2)}{2} = N^3; \quad (9.15)$$

the analogous exercise for the 4-particle operators was presented in chapter 7.

Since there are two transition operators in  $\mathfrak{M}_3$ , Theorem 6.2 predicts that there also need to be two transition operators between the projectors (9.14). This immediately tells us that the operators (9.14b) and (9.14c) correspond to equivalent irreducible representations of  $\text{SU}(N)$ .<sup>4</sup> Using their defining properties (4.91) (see chapter 4, Definition 4.4), one may find the transition operators between these two projectors, yielding the

<sup>4</sup>Recall that their dimension being equal is a *necessary* but not *sufficient* criterion for the equivalence between representations. For example, we saw that there exist two irreducible representations of  $\text{SU}(N)$  over  $V^{\otimes 2} \otimes (V^*)^{\otimes 2}$  with dimension  $\frac{(N^2-1)(N^2-4)}{4}$ , which are not equivalent (*c.f.* section 7.4).

matrix  $\mathfrak{M}_{2,1}$  to be

$$\mathfrak{M}_{2,1} = \begin{pmatrix} \left( \begin{array}{c} \left( \begin{array}{c} \left( \begin{array}{c} \leftarrow \text{---} \text{---} \text{---} \rightarrow \\ \leftarrow \text{---} \text{---} \text{---} \rightarrow \\ \rightarrow \text{---} \text{---} \text{---} \leftarrow \\ \rightarrow \text{---} \text{---} \text{---} \leftarrow \end{array} \right) - \frac{2}{N+1} \left( \begin{array}{c} \leftarrow \text{---} \text{---} \text{---} \rightarrow \\ \leftarrow \text{---} \text{---} \text{---} \rightarrow \\ \rightarrow \text{---} \text{---} \text{---} \leftarrow \\ \rightarrow \text{---} \text{---} \text{---} \leftarrow \end{array} \right) \end{array} \right) & 0 & 0 & 0 \\ 0 & \frac{2}{N+1} \left( \begin{array}{c} \leftarrow \text{---} \text{---} \text{---} \rightarrow \\ \leftarrow \text{---} \text{---} \text{---} \rightarrow \\ \rightarrow \text{---} \text{---} \text{---} \leftarrow \\ \rightarrow \text{---} \text{---} \text{---} \leftarrow \end{array} \right) & \frac{2}{\sqrt{N^2-1}} \left( \begin{array}{c} \leftarrow \text{---} \text{---} \text{---} \rightarrow \\ \leftarrow \text{---} \text{---} \text{---} \rightarrow \\ \rightarrow \text{---} \text{---} \text{---} \leftarrow \\ \rightarrow \text{---} \text{---} \text{---} \leftarrow \end{array} \right) & 0 \\ 0 & \frac{2}{\sqrt{N^2-1}} \left( \begin{array}{c} \leftarrow \text{---} \text{---} \text{---} \rightarrow \\ \leftarrow \text{---} \text{---} \text{---} \rightarrow \\ \rightarrow \text{---} \text{---} \text{---} \leftarrow \\ \rightarrow \text{---} \text{---} \text{---} \leftarrow \end{array} \right) & \frac{2}{N-1} \left( \begin{array}{c} \leftarrow \text{---} \text{---} \text{---} \rightarrow \\ \leftarrow \text{---} \text{---} \text{---} \rightarrow \\ \rightarrow \text{---} \text{---} \text{---} \leftarrow \\ \rightarrow \text{---} \text{---} \text{---} \leftarrow \end{array} \right) & 0 \\ 0 & 0 & 0 & \theta_{N>2} \cdot \left\{ \left( \begin{array}{c} \leftarrow \text{---} \text{---} \text{---} \rightarrow \\ \leftarrow \text{---} \text{---} \text{---} \rightarrow \\ \rightarrow \text{---} \text{---} \text{---} \leftarrow \\ \rightarrow \text{---} \text{---} \text{---} \leftarrow \end{array} \right) - \frac{2}{N-1} \left( \begin{array}{c} \leftarrow \text{---} \text{---} \text{---} \rightarrow \\ \leftarrow \text{---} \text{---} \text{---} \rightarrow \\ \rightarrow \text{---} \text{---} \text{---} \leftarrow \\ \rightarrow \text{---} \text{---} \text{---} \leftarrow \end{array} \right) \right\} \end{array} \right) . \quad (9.16)$$

Cvitanović previously found the projection operators for the algebra of one quark and one gluon  $1q + 1g$  [72, Table 9.3], which forms a subalgebra of  $2q + 1\bar{q}$ . In the  $1q + 1g$ -algebra, there exist three projection operators, of dimensions  $\frac{N(N-1)(N+2)}{2}$ ,  $N$  and  $\frac{N(N+1)(N-2)}{2}$  respectively. The operator of dimension  $N$  as given in [72] may be expressed as a linear combination of the elements in the  $2 \times 2$  block in (9.15) (although the constant prefactors are fairly lengthy).

While Theorem 6.2 ensures that the matrices  $\mathfrak{M}_3$  and  $\mathfrak{M}_{2,1}$  have the same number of nonzero elements, this theorem says nothing about their block structure. However, in the case of the 3-particle Fock space, there is a simple reason why it is to be expected that  $\mathfrak{M}_3$  and  $\mathfrak{M}_{2,1}$  have the same block structure (*c.f.* eqns. (9.13) and (9.16)): It is clear that the total number of projection and transition operators must be a sum of squares, since one may always arrange these operators in a block-diagonal matrix (see section 4.3.2 and Corollary 6.3 for a more detailed argument). Since the totality of projection and transition operators spans the algebra of invariants of  $SU(N)$  over the appropriate product space (see section 5.2.1.2), their number must be the same as the number of primitive invariants,  $|\mathfrak{S}_3| = |S_3|$  and  $|\mathfrak{S}_{2,1}| = |S_{2,1}|$ . This was summarized in Theorem 6.2 and Corollary 6.2. Even further, Theorem 6.2 tells us that all these sets must have the same size

$$3! = 6 = |S_3| = |\mathfrak{S}_3| = |\mathfrak{S}_{2,1}| = |S_{2,1}| . \quad (9.17)$$

Since 6 is a rather small number, there are only two ways to write it as a sum of squares,

$$6 = 1^2 + 1^2 + 1^2 + 1^2 + 1^2 + 1^2 \quad (9.18a)$$

$$= 1^2 + 1^2 + 2^2 . \quad (9.18b)$$

Option (9.18a) requires that there are only inequivalent representations – each block in the associated matrix has size one, so there are no transition operators. However, by Corollary 6.4, we know that this cannot happen if the total number of particles is greater than 2. We are therefore only left with option (9.18b), implying that all matrices  $\mathfrak{M}_{3\text{-particles}}$  have the same block structure,<sup>5</sup>

$$\left. \begin{array}{l} \mathfrak{M}_3 \\ \mathfrak{M}_{2,1} \end{array} \right\} \longrightarrow \left( \begin{array}{ccc} \boxed{1} & & \\ & \boxed{2} & \\ & & \boxed{1} \end{array} \right) . \quad (9.19)$$

<sup>5</sup>As usual, the numbers in the block refer to the size of the block, and the elements outside these blocks are understood to be zero.



For the 4-particle algebra, there are two ways of writing  $4! = 24$  as a sum of squares (which are not all 1, as this is prohibited by Corollary 6.4), *c.f.* section 7.1. These two ways give rise to the two different block structures discussed in the previous section.

**9.3.2.1 Systematic knowledge of dimensionally null operators of  $SU(N)$  over the 3-particle Fock spaces**

Analogously to the 4-particle example, there exists exactly one operator (contained in a  $1 \times 1$  block) that becomes dimensionally zero for  $N < 3$  in each matrix  $\mathfrak{M}_{3\text{-particles}}$ . These operators, and their corresponding Young resp. Littlewood-Richardson tableaux, are

$$P^{(3)} = \theta_{N>2} \cdot \left[ \begin{array}{c} \leftarrow \rightarrow \\ \leftarrow \rightarrow \\ \leftarrow \rightarrow \end{array} \right] \rightarrow \begin{array}{|c|} \hline 1 \\ \hline 2 \\ \hline 3 \\ \hline \end{array}, \quad P^{(2,1)} = \theta_{N>2} \cdot \left\{ \left[ \begin{array}{c} \leftarrow \rightarrow \\ \leftarrow \rightarrow \\ \leftarrow \rightarrow \end{array} \right] - \frac{2}{N-1} \left[ \begin{array}{c} \leftarrow \rightarrow \\ \leftarrow \rightarrow \\ \leftarrow \rightarrow \end{array} \right] \right\} \rightarrow \begin{array}{|c|c|} \hline 1 & a_1 \\ \hline 2 & a_2 \\ \hline a_3 & \\ \hline \vdots & \\ \hline a_{\check{N}} & \\ \hline \end{array}, \quad (9.20)$$

where again  $\check{N} := N - 1$ . For  $N < 2$ , another four operators in each matrix  $\mathfrak{M}_3$  and  $\mathfrak{M}_{2,1}$  vanish. In  $\mathfrak{M}_3$ , these operators constitute the  $2 \times 2$  block. On the other hand (as is easily checked via direct calculation), the vanishing operators in  $\mathfrak{M}_{2,1}$  occupy a  $1 \times 1$  block, and one full row and column in the  $2 \times 2$  block,

$$\mathfrak{S}_3[2] \rightarrow \begin{pmatrix} \boxed{1} & & \\ & \boxed{2} & \\ & & \boxed{1} \end{pmatrix} \quad \text{and} \quad \mathfrak{S}_{2,1}[2] \rightarrow \begin{pmatrix} \boxed{1} & & \\ & \boxed{2} & \\ & & \boxed{1} \\ & & & \boxed{1} \end{pmatrix}, \quad (9.21)$$

using the notation introduced in section 9.3.1.



# Chapter 10

## Summary and Outlook

We summarize the key results that have been derived in the course of this PhD project in section 10.1. Thereafter, in section 10.2, we give an outlook and describe possible future research following on from the results of this thesis.

### 10.1 Thesis summary

The singlet projection operators of  $SU(N)$  are of vital importance in high energy QCD, as they are needed to construct physical Wilson line correlators: Confinement forces color charged partons into color neutral systems, the singlet states of  $SU(N)$ .<sup>1</sup> Hence, a Wilson line correlator describing the eikonal interaction between a system of partons and a dense gluonic target must project onto a singlet state before and after the interaction. As it was argued in chapter 1, such a correlator must be of the the form

$$\langle j | \mathbf{U} | i \rangle, \quad (10.1)$$

where  $\mathbf{U}$  is a tensor products of Wilson lines

$$\mathbf{U} = U_{\mathbf{x}_1} \otimes \dots \otimes U_{\mathbf{x}_m} \otimes U_{\mathbf{y}_1}^\dagger \otimes \dots \otimes U_{\mathbf{y}_n}^\dagger \in \underbrace{SU(N) \times SU(N) \times \dots \times SU(N)}_{(m+n) \text{ times}}, \quad (10.2)$$

and  $|i\rangle, |j\rangle$  are global singlet states of  $SU(N)$ , which is to say that

$$U_{\mathbf{x}_1} \otimes \dots \otimes U_{\mathbf{x}_m} \otimes U_{\mathbf{y}_1}^\dagger \otimes \dots \otimes U_{\mathbf{y}_n}^\dagger |i, j\rangle \xrightarrow[\substack{= \mathbf{y}_1 = \dots = \mathbf{y}_n \\ = \mathbf{x}_1 = \dots = \mathbf{x}_m}]{=} U \otimes \dots \otimes U \otimes U^\dagger \otimes \dots \otimes U^\dagger |i, j\rangle = |i, j\rangle. \quad (10.3)$$

In this thesis, we presented a construction algorithm for the singlet projection operators of  $SU(N)$  over the Fock space  $V^{\otimes m} \otimes (V^*)^{\otimes n}$ .<sup>2</sup> In doing so, we focused on the group theoretic aspects of QCD, particularly in the context of the JIMWLK evolution of Wilson line correlators.

---

<sup>1</sup>We emphasize that we do not claim to have “solved” confinement, but rather that we take this one aspect of confinement (that color charged objects combine into color neutral systems) as an axiom on which we built a large portion of the research conducted in this thesis.

<sup>2</sup>We remind the reader that such a Fock space encapsulates the behaviour of all partons (quarks, antiquarks and gluons), since an adjoint Wilson line can be decomposed into (anti-) fundamental Wilson lines due to the identity  $\tilde{U}_z^{ab} = 2\text{tr} \left( t^a U_z t^b U_z^\dagger \right)$ .

Part **I** (chapters 2 to 5) described the journey of obtaining the singlet states and singlet projection operators of  $SU(N)$ , starting from rudimentary properties of birdtrack operators. In actual fact, our path to the desired singlet projectors was not as streamlined as it is depicted in part **I**, but led us along multiple tangents into other aspects of the study of  $SU(N)$ . The results are given in part **II** (chapters 6 to 8).

Let us now summarize the highlights of parts **I** and **II**:

## Simplification rules for birdtrack operators

In chapter 1, we already identified the birdtrack language as the appropriate formalism to achieve our main goal – constructing the singlet projectors of  $SU(N)$  over a mixed product space  $V^{\otimes m} \otimes (V^*)^{\otimes n}$ . The reason for this is that the birdtrack formalism shed new light on previously studied topics, such as the representation theory of  $SU(N)$  over  $V^{\otimes m}$ , thus allowing us to uncover new properties and structures. However, when we started off in pursuit of this goal, we found that there did not exist any practical rules for the quick manipulation of birdtrack operators in calculations.

Therefore, the first subgoal of this thesis was to find easy-to-use rules allowing us to efficiently manipulate birdtrack operators comprised entirely of symmetrizers and antisymmetrizers. This was achieved in chapter 2, where we presented two classes of rules: *cancellation rules* (Theorem 2.1 and Corollary 2.2), which allow one to shorten the birdtrack expression of a particular operator, and *propagation rules* (Theorems 2.2 and 2.3), which give criteria for when it is possible to commute sets of symmetrizers and antisymmetrizers. We remind the reader of Figure 2.2, where the effectiveness of these rules was illustrated by applying it to a sample operator.

## Hermitian Young projection operators

Slowly building towards the singlet projectors of  $SU(N)$  over a mixed space  $V^{\otimes m} \otimes (V^*)^{\otimes n}$ , we first needed to understand the Hermitian Young projection operators of  $SU(N)$  over the only-quark space  $V^{\otimes m}$ . The only method to construct such operators was by Keppeler and Sjödalh (KS) [4]. This method, beyond the most elementary examples, yields long and unwieldy expressions for the projection operators, and therefore soon becomes impractical (*c.f.* Figure 3.2).

Therefore, the second subgoal of this thesis was to find an alternative construction algorithm for a Hermitian version of the Young projection operators of  $SU(N)$  over  $V^{\otimes m}$ . In chapter 3, we found such an algorithm based on the measure of lexical disorder (MOLD) of the underlying Young tableau. The proof of the MOLD algorithm (Theorem 3.5) uses both the KS operators as well as the simplification rules derived in chapter 2. This algorithm reduced the computing power needed to obtain Hermitian Young projection operators compared to the KS equivalent by a factor of approximately 18000.

In addition, we proved other useful results, for example, the nested summation property of Hermitian Young projectors to their ancestor operator (*c.f.* eq. (3.112)).

## Transition operators

In chapter 4, we used the MOLD operators constructed in chapter 3 to form *unitary transition operators*. As the name suggests, these operators transition between projection operators corresponding to equivalent

irreducible representations of  $SU(N)$  over  $V^{\otimes m}$ .<sup>3</sup> These transition operators are easily obtained from the MOLD operators via a graphical cutting-and-gluing procedure given in Theorem 4.5. This procedure makes the action of the transition operators even more intuitive.

In section 4.3, it was shown that the set of Hermitian Young projection operators and unitary transition operators spans the algebra of invariants of  $SU(N)$  over  $V^{\otimes m}$ , and is thus referred to as the *projector basis*  $\mathfrak{S}_m$ . The reasons why the projector basis is preferable over the primitive invariant basis of  $SU(N)$  (i.e. the symmetric group  $S_m$ ) are twofold: Firstly, unlike the primitive invariants, the elements of  $\mathfrak{S}_m$  are mutually orthogonal with respect to the canonical scalar product  $\langle A|B \rangle = \text{tr}(A^\dagger B)$  (c.f. sections 4.4.2 and 4.4.3). Secondly, the projector basis yields a particularly simple block-diagonal multiplication table (see section 4.4.3). Both of these properties would turn out to be crucial for the construction of the singlet projectors in chapter 5.

## Singlets of $SU(N)$ and Wilson line correlators

Chapter 5 brings together all the work done in the previous chapters to achieve the main goal of this thesis: We use the the projection and transition operators obtained in chapters 3 and 4 to construct the singlet projectors of  $SU(N)$  over  $V^{\otimes m} \otimes (V^*)^{\otimes n}$ :

We began by motivating the need for an alternative construction method of the singlet projection operators of  $SU(N)$  over a mixed product space  $V^{\otimes m} \otimes (V^*)^{\otimes n}$ . In section 5.1.4, we revised the standard method used to construct all projection operators of  $SU(N)$  over  $V^{\otimes m} \otimes (V^*)^{\otimes n}$ ,<sup>4</sup> and exemplified its inadequacy in practical calculations (because of the immense computational effort involved) by deriving the projection operators of  $SU(N)$  over  $V \otimes V^*$ .

While a *practical* construction algorithm for general projection operators of  $SU(N)$  over a mixed space  $V^{\otimes m} \otimes (V^*)^{\otimes n}$  is still outstanding, the singlet operators can be constructed in an easy way. If the mixed product space consists of an equal amount of fundamental and antifundamental factors (i.e.  $m = n$ , c.f. section 5.2.1), then an orthonormal basis of the singlet projectors of  $SU(N)$  over  $V^{\otimes m} \otimes (V^*)^{\otimes m}$  is obtained via bending and mirroring the elements of  $\mathfrak{S}_m$ , as proven in Theorem 5.2. Additionally, we were able to construct the transition operators between all these singlet projection operators, showing that the corresponding singlet representations are indeed all equivalent (Theorem 5.3).

The singlet projectors over  $V^{\otimes m} \otimes (V^*)^{\otimes m}$  in fact give rise to the singlet projection operators over a more general product space  $V^{\otimes m} \otimes (V^*)^{\otimes n}$  (note that  $m \neq n$ ), as shown in section 5.2.2. It turns out that the singlet projectors over  $V^{\otimes m} \otimes (V^*)^{\otimes n}$  are  $N$ -dependent, in that they correspond to a 1-dimensional representation only for a particular value of  $N$ , see section 5.2.2. For this particular  $N$ , the singlets over  $V^{\otimes m} \otimes (V^*)^{\otimes n}$  were shown to be completely equivalent to certain singlet projectors over  $V^{\otimes k} \otimes (V^*)^{\otimes k}$  (where  $k$  is a natural number depending on  $m$  and  $n$ ) in Theorem (5.4).

Chapter 5 ends by constructing Wilson line correlators over a  $3q + 3\bar{q}$  algebra in two bases (section 5.3). We discussed coincidence limits between Wilson lines in these correlators, which can be used in the future to study the parametrization of the JIMWLK equation (c.f. section 10.2).

<sup>3</sup>For two projection operators corresponding to inequivalent (irreducible) representations, one takes the transition operator to be zero, as there exists no change of basis between the corresponding representations.

<sup>4</sup>A reminder: One first constructs tableaux corresponding to the irreducible representations of  $SU(N)$  over  $V^{\otimes m} \otimes (V^*)^{\otimes n}$  according to an algorithm devised by Littlewood and Richardson. Then, one forms the regular MOLD projection operators from these tableaux (treating the boxes corresponding to an antifundamental line as if they corresponded to fundamental lines) and translates this operator into the algebra over  $V^{\otimes m} \otimes (V^*)^{\otimes n}$  by means of the Leibniz formula (c.f. section 5.1.4).

## Multiplets & examples

In chapter 6, we went beyond the singlets of  $SU(N)$  towards studying all irreducible representations over  $V^{\otimes m} \otimes (V^*)^{\otimes n}$ . Whilst a general practical algorithm for the appropriate projection operators is still outstanding, we were nonetheless able to find general properties pertaining to these representations.

For example, we were able to map the Hermitian and non-Hermitian elements of the primitive invariants  $S_{m,n}$  of  $SU(N)$  over  $V^{\otimes m} \otimes (V^*)^{\otimes n}$  to the projection and transition operators in  $\mathfrak{S}_{m,n}$  respectively, *c.f.* Theorem 6.2. (For the special case where  $n = 0$ , this has already been known [120], although the proof given in this thesis (despite being more general) is much shorter and thus more elegant.) An immediate implication of Theorem 6.2 is that  $SU(N)$  has the same number of representations over  $V^{\otimes m} \otimes (V^*)^{\otimes n}$  as over  $V^{\otimes(m+n)}$ , as shown in Corollary 6.2.

As a consequence of the connection between the projection operators in  $\mathfrak{S}_{m,n}$  and the Hermitian elements in  $S_{m,n}$ , we were able to re-derive (fairly unknown) formulae by Rothe [118], which give the number of Young tableaux with  $(m+n)$  boxes either explicitly or recursively (sections 6.4 and 6.5 respectively). Due to Theorem 6.2, we are now able to count the number of representations of  $SU(N)$  over  $V^{\otimes m} \otimes (V^*)^{\otimes n}$ .

In chapter 7, we presented the Hermitian projection and transition operators (in particular bases) of  $SU(N)$  over all product spaces  $V^{\otimes m} \otimes (V^*)^{\otimes n}$  such that  $m+n = 4$ . This confirmed the results given in chapter 6. In addition, we discussed what happens to these operators if  $N = 2$ , thus answering questions such as “Which operators vanish dimensionally?” or “Which operators become equal?”.

## Traces of primitive invariants

Chapter 8 gave further results on traces of primitive invariants of  $SU(N)$  over  $V^{\otimes m} \otimes (V^*)^{\otimes n}$ :

For  $n = 0$ , we were able to relate the trace of a primitive invariant to the minimum number of transpositions required to write this invariant as a product of transpositions (see Theorem 8.2). This theorem allowed us to pinpoint why the singlet states over  $V^{\otimes k} \otimes (V^*)^{\otimes k}$  constructed from the primitive invariants  $S_k$  are not orthogonal (*c.f.* section 8.2.3).

Furthermore, we found that the trace of a primitive invariant stays unchanged under the graphical map  $\leftrightarrow$  (see Definition 8.1) that translates the elements of  $S_{m+n}$  into those of  $S_{m,n}$ , *c.f.* Theorem 8.3. Astonishingly enough, the trace remains invariant even if the map  $\leftrightarrow$  is applied to each primitive invariant in a product individually,

$$\mathrm{tr}(\overleftrightarrow{\rho} \cdot \overleftrightarrow{\sigma}) \stackrel{\text{Thm. 8.4}}{=} \mathrm{tr}(\rho \cdot \sigma) \stackrel{\text{Thm. 8.3}}{=} \mathrm{tr}(\overleftarrow{\rho} \cdot \overrightarrow{\sigma}) . \quad (10.4)$$

## 10.2 Outlook

The research conducted in this PhD project is applicable in a variety of areas. We have already discussed possible future mathematics projects following on from this thesis in chapter 9.

Besides the direct connection to mathematics, there are numerous applications in the physics context. In the present section, we will list several physics applications, and explain how the results of this thesis prompt further research in the areas mentioned here.

### 10.2.1 Wilson line correlators in high energy QCD

Wilson line correlators occur in a multitude of contexts within high energy QCD. We already discussed the JIMWLK equation in chapter 1, but further areas in which Wilson line correlators arise include

- transverse-momentum-dependent parton distributions (TMDs) at small  $x_{Bj}$
- energy loss calculations at high energies
- evolution of non-global observables.

We will briefly discuss each of these topics, and how the results of this thesis may potentially further these fields.

#### 10.2.1.1 Transverse-momentum-dependent parton distributions (TMDs)

In recent years, a lot of progress has been made in marrying the saturation formalism (i.e. the CGC framework) to TMDs, in order to study the latter at small Bjorken- $x$  [129–131]. To illustrate this, we give a brief summary of [130]: One considers the collision of a dilute projectile with a dense target giving rise to the inclusive production of two forward jets,

$$\text{dilute projectile} + \text{dense target} \longrightarrow \text{jet 1} + \text{jet 2} + \text{remainder} . \quad (10.5)$$

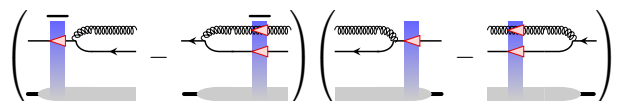
In this system, the projectile (parton) is described by a parton distribution whose evolution is governed by the DGLAP-equation [53–55], while the target is given in terms of TMDs. Since the operator description of the TMDs is process dependent, [130] considers three channels: The two jets in the final state are described by a quark and a gluon ( $qg$ ), a quark and an antiquark ( $q\bar{q}$ ), or two gluons ( $gg$ ). Each of these partons is dressed by a multitude of soft, collinear gluons. It was shown that in the small  $x_{Bj}$  limit (i.e. the Regge-Gribov limit, see section 1.1.2.3), the TMDs of all channels considered in [130] reduce to Fourier transforms of Wilson line correlators depending on the two transverse coordinates  $\mathbf{x}$  and  $\mathbf{y}$  of the jet-partons (where the average is the rapidity dependent average whose evolution with  $Y$  is given by the JIMWLK equation).

On the other hand, starting from the cross sections in the CGC framework yields the same result [130]: One identifies the Feynman diagrams corresponding to the  $qg$ ,  $q\bar{q}$  and  $gg$ -channel, respectively, to calculate the cross section, which yields a sum of Wilson line correlators (*c.f.* the cross sections (1.144) and (1.179)). For example, in the  $q \rightarrow qg$  channel, one encounters the following diagrams for the amplitude [80, 129, 130, 132]



$$\text{Diagram 1} - \text{Diagram 2} , \quad (10.6)$$

where the interaction with the target occurs either before the gluon is radiated (right term) or afterwards (left term). The total cross section therefore becomes



$$\left( \text{Diagram 1} - \text{Diagram 2} \right) + \left( \text{Diagram 2} - \text{Diagram 1} \right) . \quad (10.7)$$

Implicit to this cross section is a trace over the color indices carried by the outgoing quarks, as no net color can occur. Let us suppress the target in diagrams (10.7) (analogous to what was done in section 1.6.2) and multiply out the brackets. Further, making the trace explicit through connecting the quark-lines at the end points yields the following expression,

$$\left\langle \frac{1}{d_f} \text{diagram}_1 - \frac{1}{C_f d_f} \text{diagram}_2 - \frac{1}{C_f d_f} \text{diagram}_3 + \frac{1}{C_f d_f} \text{diagram}_4 \right\rangle (Y), \quad (10.8)$$

where we have chosen to draw the gluon (dotted line) at the bottom of each diagram, as we will establish a correspondence with several diagrams that have already been discussed in this thesis. It can be shown [129] that these Wilson line correlators become

$$\left\langle \frac{1}{d_f} \text{diagram}_1 - \frac{1}{C_f d_f} \text{diagram}_2 - \frac{1}{C_f d_f} \text{diagram}_3 + \frac{1}{C_f d_f} \text{diagram}_4 \right\rangle (Y). \quad (10.9)$$

(The step from eq. (10.8) to (10.9) is non-trivial, as it involves moving Wilson lines across the final state (in the center of each diagram, *c.f.* eq. (1.142)) from the amplitude into the complex conjugate amplitude, and vice versa.) Each diagram in (10.9) corresponds to the following expression in [130, eqns. (49)–(51)],

$$S_{q\bar{q}}^{(2)}[\mathbf{b}, \mathbf{b}'] = \frac{1}{d_f} \left\langle \text{tr} \left( U_{\mathbf{b}'}^\dagger U_{\mathbf{b}} \right) \right\rangle \rightarrow \left\langle \frac{1}{d_f} \text{diagram}_1 \right\rangle (Y) \quad (10.10a)$$

$$S_{q\bar{q}g}^{(3)}[\mathbf{b}, \mathbf{b}', \mathbf{x}] = \frac{1}{d_f C_f} \left\langle \text{tr} \left( U_{\mathbf{b}'}^\dagger t^c U_{\mathbf{b}} t^d \right) [V_{\mathbf{x}}]^{cd} \right\rangle \rightarrow \left\langle \frac{1}{C_f d_f} \text{diagram}_2 \right\rangle (Y) \quad (10.10b)$$

$$S_{q\bar{q}gg}^{(4)}[\mathbf{b}, \mathbf{b}', \mathbf{x}, \mathbf{x}'] = \frac{1}{d_f C_f} \left\langle \text{tr} \left( t^c U_{\mathbf{b}'}^\dagger U_{\mathbf{b}} t^d \right) [V_{\mathbf{x}} V_{\mathbf{x}'}^\dagger]^{cd} \right\rangle \rightarrow \left\langle \frac{1}{C_f d_f} \text{diagram}_3 \right\rangle (Y), \quad (10.10c)$$

where the generators  $t^b$  and the Wilson lines  $U_{\mathbf{b}}$  are in the fundamental representation, and  $V_{\mathbf{x}}^{cb}$  is a Wilson line in the adjoint representation (i.e. a gluon line). We have already encountered the diagrams corresponding to the correlators  $S_{q\bar{q}}^{(2)}[\mathbf{b}, \mathbf{b}']$  and  $S_{q\bar{q}g}^{(3)}[\mathbf{b}, \mathbf{b}', \mathbf{x}]$ ; in particular, these diagrams are contained in the matrix (5.165), which was constructed by imposing two coincidence limits on the matrix of singlet correlators over the  $3q+3\bar{q}$ -algebra. Using the Fierz identity, the operator  $S_{q\bar{q}gg}^{(4)}[\mathbf{b}, \mathbf{b}', \mathbf{x}, \mathbf{x}']$  in (10.10c) may also be related to familiar operators:  $S_{q\bar{q}gg}^{(4)}[\mathbf{b}, \mathbf{b}', \mathbf{x}, \mathbf{x}']$  turns out to be a linear combination of all operators appearing in the 4<sup>th</sup> row of the matrix (5.165),

$$\widehat{\text{diagram}_3} = \alpha_1 \widehat{\text{diagram}_1} + \alpha_2 \widehat{\text{diagram}_2} + \alpha_3 \widehat{\text{diagram}_3}, \quad (10.11)$$

where the  $\alpha_i$  are constants and the hat  $\widehat{\phantom{x}}$  indicates that the correlators are normalized. Thus, all the correlators (10.10) are contained in the matrix (5.165). This shows that the Wilson line correlators constructed



in this thesis are immediately applicable to a typical TMD calculation.

Ref. [130] goes on and rewrites the Wilson line correlators (10.10) in terms of fundamental Wilson lines only. Invoking coincidence limits to ensure that the radiated soft gluons constituting the jet are colinear causes the resulting expression to agree with the cross section obtained in the TMD formalism. This equivalence encourages the use of the CGC formalism to study the structures of TMDs in the small  $x_{Bj}$  regime. However, for this to be done correctly, knowledge about coincidence limits of the appropriate Wilson line correlators is paramount. As demonstrated in the present section, the singlet states found in this thesis (see chapter 5) facilitate the study of these coincidence limits in Wilson line correlators, *c.f.* section 5.3.

In the future, it will be interesting to investigate the  $Y$ -evolution of the Wilson line correlators arising in TMD calculations. This can be done in the CGC formalism via (the parametrization of) the JIMWLK equation. (As already mentioned, the results of this thesis facilitate the study of the color structures and the parameters  $G$  and  $K$  (*c.f.* sections 1.5.3 and 1.5.4) for higher point truncations of the parametrization of JIMWLK.) L. Lippstreu and H. Weigert are currently looking into this [133].

### 10.2.1.2 Energy loss

In  $pp$ -collisions, one observes a particular rate of hadron productions. When naively extrapolating this rate to a  $pA$  collision by modelling it as  $A$  times  $pp$ -collisions,<sup>5</sup> one observes a suppression in hadron production rates [50]. Similar effects are observed for quarkonium production in a  $pA$  collision when extrapolating to  $AA$ -collisions [50]. For quarkonium production, the suppression of hadrons produced in the collision can, to a good approximation, be explained using a model based on coherent energy loss in cold nuclear matter [134, 135].<sup>6</sup>

However, at small Bjorken- $x$  there is a second effect called *shadowing*, which also contributes to the observed suppression rates [50]: Once the medium reaches saturation (as predicted by the color glass condensate effective theory due to the high density), recombination effects balance the rate of gluon production, causing a depletion in the gluon number compared to what would naively be expected [136]. In the literature, this effect is also referred to as *saturation* [21]. It thus seems natural to examine this effect in the saturation formalism.

Munier, Peigné and Petreska [50] describe the gluon radiation in the medium (shadowing) in the saturation formalism. They explicitly discuss processes of the form

$$a + A \longrightarrow a + g + X , \quad (10.12)$$

where  $a = q, g$  is a parton,  $A$  is a nucleus and  $X$  denotes the remainder (besides  $ag$ ) after the interaction. If one takes  $a = q$  to be a quark, one once again obtains the Wilson line correlators (10.10) from such an interaction (*c.f.* [50, eqns. (2.7)–(2.10)]),

$$\left\langle \frac{1}{d_f} \text{[diagram 1]} - \frac{1}{C_f d_f} \text{[diagram 2]} - \frac{1}{C_f d_f} \text{[diagram 3]} + \frac{1}{C_f d_f} \text{[diagram 4]} \right\rangle (Y) . \quad (10.13)$$

<sup>5</sup>Where  $A$  is the nuclear number of the target nucleus.

<sup>6</sup>The cold nuclear matter effects act as a *baseline* to which hot nuclear matter effects (which are present in  $AA$ -collisions) can be added [135].

This once again demonstrates that the results of this thesis may be used to study the energy loss in a medium due to shadowing. Further, one may also tackle energy loss calculations in the saturation formalism for more complicated scatterings involving larger  $n$ -point Wilson line correlators, thus allowing one to study situations that may not be accessible with regular energy loss methods.

As mentioned in [50], the JIMWLK evolution of these correlators has not yet been implemented, but it is desirable to do so. In order to accomplish this, one should parametrize the correlators using the Gaussian truncation and its generalizations (which in turn can be studied using the projectors derived in this thesis). This is currently being done by D. Adamiak and H. Weigert [137].

### 10.2.1.3 Non-global jet observables and the Banfi-Marchesini-Smye equation

Banfi, Marchesini and Smye (BMS) [138] previously derived an equation describing the energy-evolution of non-global jet observables in the large  $N_c$  limit. As the name suggests, these new observables are non-global in that they are restricted to a region of phase space away from the jets.

Ref. [78] draws attention to a striking resemblance between the BMS equation and the Balitsky-Kovchegov (BK) [60–62] equation, the latter being equivalent to a large  $N_c$  limit of JIMWLK. In particular, while outside of the jet region the BMS equation becomes linear, inside the jet region the BMS evolution is identical to BK evolution. This matches our intuition behind the analogy, as the BK equation assumes a nonlinear background field (such as is present in the jets) everywhere [18]. This resemblance seems to suggest a relationship between the transition probabilities  $G_{ab}(E, E_{\text{out}})$  in BMS and the dipole Wilson line correlators  $\text{tr}(U_{\mathbf{x}}U_{\mathbf{y}}^\dagger)$  in BK. If one performs a stereographic projection mapping the transverse coordinates  $\mathbf{x}, \mathbf{y}$  onto the directions  $a, b$  of the two jets, it seems suggestive that [78]

$$G_{ab}(E, E_{\text{out}}) \xrightarrow{?} \left\langle \text{tr}(V_a V_b^\dagger) \right\rangle_E, \quad (10.14)$$

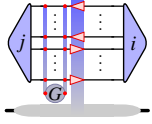
where the right-hand side is some Wilson line correlator, and  $\langle \dots \rangle_E$  denotes an averaging procedure with respect to the energy.

Ref. [78] exploits the analogy between the BMS and BK equations in order to generalize BMS to finite values of  $N_c$ . The result is an energy-evolution equation that strongly resembles the JIMWLK equation. (In particular, the suggested relationship (10.14) is made precise.) Thus, in the context of non-global jet observables, we once again encounter Wilson line correlators, which can be studied using the techniques introduced in this thesis.

## 10.2.2 Parametrization of Wilson line correlators

We have seen that in all areas described in section 10.2.1, one necessarily needs to study Wilson line correlators, as these encode the relevant degrees of freedom. For the more elementary examples, it is still possible to obtain the relevant singlet states to construct these Wilson line correlators by hand. However, more differential observables give rise to larger Wilson line correlators (i.e. involving a multitude of coordinates), calling for a machinery that allows one to easily construct all relevant Wilson line correlators in an automated way. The results of this thesis promise to do just that.

However, studying such larger Wilson line correlators is not a new idea in itself: Any evolution equation of Wilson line correlators can be parametrized analogously to the JIMWLK equation (1.212),



$$\left\langle \left\langle \int_{\mathbf{x}_1 \mathbf{x}_2} G_{\tilde{Y}, \mathbf{x}_1 \mathbf{x}_2}^{(\delta)} \delta^{a_1 a_2} i \bar{\nabla}_{\mathbf{x}_1}^{a_1} i \bar{\nabla}_{\mathbf{x}_2}^{a_2} \right. \right. \quad (10.15a)$$

$$\left. + \int_{\mathbf{x}_1 \mathbf{x}_2 \mathbf{x}_3} \left( G_{\tilde{Y}, \mathbf{x}_1 \mathbf{x}_2 \mathbf{x}_3}^{(d)} d^{a_1 a_2 a_3} + G_{\tilde{Y}, \mathbf{x}_1 \mathbf{x}_2 \mathbf{x}_3}^{(f)} f^{a_1 a_2 a_3} \right) i \bar{\nabla}_{\mathbf{x}_1}^{a_1} i \bar{\nabla}_{\mathbf{x}_2}^{a_2} i \bar{\nabla}_{\mathbf{x}_3}^{a_3} \right. \quad (10.15b)$$

$$\left. + \int_{\mathbf{x}_1 \mathbf{x}_2 \mathbf{x}_3 \mathbf{x}_4} \left( \sum_j G_{\tilde{Y}, \mathbf{x}_1 \mathbf{x}_2 \mathbf{x}_3 \mathbf{x}_4}^{(j)} C_j^{a_1 a_2 a_3 a_4} \right) i \bar{\nabla}_{\mathbf{x}_1}^{a_1} i \bar{\nabla}_{\mathbf{x}_2}^{a_2} i \bar{\nabla}_{\mathbf{x}_3}^{a_3} i \bar{\nabla}_{\mathbf{x}_4}^{a_4} \right. \quad (10.15c)$$

$$\left. + \dots \right\} \mathcal{A} \rangle (Y_0) \Big]_{ji} ,$$

where

$$\int_{\mathbf{x}_1 \mathbf{x}_2 \mathbf{x}_3 \mathbf{x}_4 \dots} := \int \int \int \int d\mathbf{x}_1 d\mathbf{x}_2 d\mathbf{x}_3 d\mathbf{x}_4 \dots , \quad (10.16)$$

for the operators acting on the left, and similarly for the parameters  $K$  acting from the right, *c.f.* section 1.5. However, studying such parametrizations beyond the third order again requires automated machinery, as discussed in section 10.2.2.2. Nonetheless, even up to third order, such a parametrization yields interesting results:

### 10.2.2.1 Beyond the Gaussian truncation: results at third order

Consider only the left parametrization of the JIMWLK equation (10.15), i.e. set all parameters  $K_{\tilde{Y}, \mathbf{x}_1 \dots \mathbf{x}_n}^{(j)}$  acting from the right (*c.f.* eq. (1.211)) to zero. The truncation of this parametrization at the second order (i.e. at (10.15a), the Gaussian truncation) has been used for several years to study the JIMWLK evolution of Wilson line correlators (see for example [18, 30], just to name a few). More recently, [80] set out to study the odderon contribution to the JIMWLK evolution of various Wilson line correlators.

It was found that, for the  $q\bar{q}$ -correlator  $S_{\mathbf{x}\mathbf{y}}$ ,

$$S_{\mathbf{x}\mathbf{y}} = \frac{\langle \text{tr} (U_{\mathbf{x}} U_{\mathbf{y}}^\dagger) \rangle (Y)}{N_c} , \quad \text{where } N_c \text{ is the number of colors ,} \quad (10.17)$$

the odderon contribution enters via an imaginary part in the exponential [80],

$$S_{\mathbf{x}\mathbf{y}} = e^{-C_f (\mathcal{P}_{\mathbf{x}\mathbf{y}} + i \mathcal{O}_{\mathbf{x}\mathbf{y}})(Y)} , \quad (10.18)$$

where  $C_f = \frac{N_c^2 - 1}{2N_c}$  is the Casimir of the fundamental representation. The 2-point functions  $\mathcal{P}_{\mathbf{x}\mathbf{y}}(Y)$  and  $\mathcal{O}_{\mathbf{x}\mathbf{y}}(Y)$  are shown to be symmetric, respectively, antisymmetric under exchange of the transverse coordinates  $\mathbf{x}, \mathbf{y}$ . This symmetry structure links these two functions to the pomeron, respectively, odderon contribution to the dipole-correlator. Since the 2-point function  $G_{\mathbf{x}\mathbf{y}}^{(\delta)}$  is symmetric under the exchange of its indices, the odderon contribution becomes visible for the first time at the third order. In particular,  $\mathcal{O}_{\mathbf{x}\mathbf{y}}(Y)$  emerges

from an antisymmetric combination of the 3-point function  $G_{\mathbf{x}\mathbf{y}\mathbf{z}}^{(d)}$  in a coincidence limit [80],

$$i\mathcal{O}_{\mathbf{x}\mathbf{y}}(\eta) = \frac{C_d}{4} \int_{\eta_0}^{\eta} d\tilde{\eta} \left( G_{\tilde{\eta},\mathbf{y}\mathbf{x}\mathbf{x}}^{(d)} - G_{\tilde{\eta},\mathbf{y}\mathbf{y}\mathbf{x}}^{(d)} \right) + i\mathcal{O}_{\mathbf{x}\mathbf{y}}(\eta_0), \quad (10.19)$$

where  $C_d \delta^{ae} := d^{abc} d^{bce} = \frac{N^2-4}{N} \delta^{ae}$ , and  $\eta := \ln x^-$ , with  $x^-$  being the longitudinal coordinate. Interestingly, not only is the function  $G_{\mathbf{x}\mathbf{y}\mathbf{z}}^{(d)}$  by itself completely symmetric under the exchange of any indices, but the function  $G_{\mathbf{x}\mathbf{y}\mathbf{z}}^{(f)}$ , which has a more complicated symmetry, does not contribute to the  $q\bar{q}$ -correlator at all [80].

The exposition of [80] motivates further study of the parameters  $G$ , in particular their symmetry structure. Recent research by H. Weigert and R. Moerman [83] shows that general statements can be made about whether a particular  $n$ -point function  $G_{\mathbf{x}_1 \dots \mathbf{x}_n}^{(j)}$  (or  $K_{\mathbf{x}_1 \dots \mathbf{x}_n}^{(j)}$ ) with color factor  $C_j^{a_1 \dots a_n}$  gives rise to a real or imaginary contribution in the exponent of the parametrized correlator (*c.f.* eq. (10.18)), thus yielding a symmetric (pomeron) or antisymmetric (odderon) contribution. The symmetry structure of the  $G_{\mathbf{x}_1 \dots \mathbf{x}_n}^{(j)}$ 's (resp.  $K_{\mathbf{x}_1 \dots \mathbf{x}_n}^{(j)}$ 's) and the color factors  $C_j^{a_1 \dots a_n}$  is necessarily dictated by the allowed symmetries of the gauge group  $SU(N)$ , i.e. by the symmetries encapsulated by the irreducible representations of  $SU(N)$  over an appropriate product space. Thus, the results of the present thesis assist in further investigation of the symmetry structures (for example, mixed symmetries) of the parametrization (10.15) at higher orders.

### 10.2.2.2 Generalized structure constants

We have previously alluded to the fact that parametrization (10.15) beyond the third order requires the use of automated machinery. In the present section, we explain why this is the case.

Consider truncating the parametrization (10.15) at the fourth order. One first has to determine the color factors  $C_i^{a_1 a_2 a_3 a_4}$ ; the idea to accomplish this is as follows: We start with a basis of the trace space of the generators  $t^a := t^{a_1}$ ,  $t^b := t^{a_2}$ ,  $t^c := t^{a_3}$  and  $t^d := t^{a_4}$ , for example,

$$\begin{array}{c} \begin{array}{c} a \dots \\ b \dots \\ c \dots \\ d \dots \end{array} \begin{array}{c} \text{---} \\ \text{---} \\ \text{---} \\ \text{---} \end{array} \begin{array}{c} \text{---} \\ \text{---} \\ \text{---} \\ \text{---} \end{array} \end{array}, \quad \begin{array}{c} \begin{array}{c} a \dots \\ b \dots \\ c \dots \\ d \dots \end{array} \begin{array}{c} \text{---} \\ \text{---} \\ \text{---} \\ \text{---} \end{array} \begin{array}{c} \text{---} \\ \text{---} \\ \text{---} \\ \text{---} \end{array} \end{array}, \quad \begin{array}{c} \begin{array}{c} a \dots \\ b \dots \\ c \dots \\ d \dots \end{array} \begin{array}{c} \text{---} \\ \text{---} \\ \text{---} \\ \text{---} \end{array} \begin{array}{c} \text{---} \\ \text{---} \\ \text{---} \\ \text{---} \end{array} \end{array}, \quad (10.20a)$$

$$\text{tr}(t^a t^b) \text{tr}(t^c t^d), \quad \text{tr}(t^a t^c) \text{tr}(t^b t^d), \quad \text{tr}(t^a t^d) \text{tr}(t^c t^b)$$

$$\begin{array}{c} \begin{array}{c} a \dots \\ b \dots \\ c \dots \\ d \dots \end{array} \begin{array}{c} \text{---} \\ \text{---} \\ \text{---} \\ \text{---} \end{array} \end{array}, \quad \begin{array}{c} \begin{array}{c} a \dots \\ b \dots \\ c \dots \\ d \dots \end{array} \begin{array}{c} \text{---} \\ \text{---} \\ \text{---} \\ \text{---} \end{array} \end{array}, \quad \begin{array}{c} \begin{array}{c} a \dots \\ b \dots \\ c \dots \\ d \dots \end{array} \begin{array}{c} \text{---} \\ \text{---} \\ \text{---} \\ \text{---} \end{array} \end{array}, \quad \begin{array}{c} \begin{array}{c} a \dots \\ b \dots \\ c \dots \\ d \dots \end{array} \begin{array}{c} \text{---} \\ \text{---} \\ \text{---} \\ \text{---} \end{array} \end{array}, \quad \begin{array}{c} \begin{array}{c} a \dots \\ b \dots \\ c \dots \\ d \dots \end{array} \begin{array}{c} \text{---} \\ \text{---} \\ \text{---} \\ \text{---} \end{array} \end{array}, \quad \begin{array}{c} \begin{array}{c} a \dots \\ b \dots \\ c \dots \\ d \dots \end{array} \begin{array}{c} \text{---} \\ \text{---} \\ \text{---} \\ \text{---} \end{array} \end{array}. \quad (10.20b)$$

$$\text{tr}(t^a t^b t^c t^d), \quad \text{tr}(t^a t^c t^b t^d), \quad \text{tr}(t^a t^b t^d t^c), \quad \text{tr}(t^a t^d t^c t^b), \quad \text{tr}(t^a t^d t^b t^c), \quad \text{tr}(t^a t^c t^d t^b)$$

The caveat of this basis is that it is not orthogonal,

$$\langle \mu | \nu \rangle \neq 0 \quad \text{for } |\mu\rangle, |\nu\rangle \text{ as defined in (10.20)}. \quad (10.21)$$

As an example,

$$\langle \text{tr}(t^a t^b) \text{tr}(t^c t^d) | \text{tr}(t^a t^c t^d t^b) \rangle = \begin{array}{c} \begin{array}{c} a \dots \\ b \dots \\ c \dots \\ d \dots \end{array} \begin{array}{c} \text{---} \\ \text{---} \\ \text{---} \\ \text{---} \end{array} \end{array} \begin{array}{c} \begin{array}{c} a \dots \\ b \dots \\ c \dots \\ d \dots \end{array} \begin{array}{c} \text{---} \\ \text{---} \\ \text{---} \\ \text{---} \end{array} \end{array} \stackrel{\text{Fierz}}{=} (N^2 - 1)(N - 1) \neq 0, \quad (10.22)$$

where we used the Fierz identity

$$\begin{array}{c} \text{)} \text{)} \\ \text{)} \text{)} \end{array} = \begin{array}{c} \leftarrow \\ \rightarrow \end{array} - \frac{1}{N} \begin{array}{c} \text{)} \text{)} \\ \text{)} \text{)} \end{array} \quad (10.23)$$

repeatedly. However, if each state in (10.20) is projected onto mutually orthogonal subspaces using, for example, the MOLD projection operators  $P_i, P_j$  with four legs (*c.f.* Theorem 3.5), where these four legs are in the adjoint representation, then the resulting states will be orthogonal for  $i \neq j$  since the MOLD projectors are orthogonal: If  $|\mu\rangle, |\nu\rangle$  are states as defined in eqns. (10.20), then the states

$$|\tilde{\mu}_i\rangle := P_i|\mu\rangle \quad \text{and} \quad |\tilde{\nu}_j\rangle := P_j|\nu\rangle \quad (10.24)$$

are orthogonal if  $i \neq j$ ,

$$\langle \tilde{\mu}_i | \tilde{\nu}_j \rangle = \langle \mu | P_i^\dagger P_j | \nu \rangle = \langle \mu | \underbrace{P_i P_j}_{\delta_{ij}} | \nu \rangle = \delta_{ij} \langle \mu | \nu \rangle . \quad (10.25)$$

Eq. (10.25) raises the question: What happens if  $i = j$ ? That is, are the states  $|\tilde{\mu}_i\rangle = P_i|\mu\rangle$  and  $|\tilde{\nu}_i\rangle = P_i|\nu\rangle$  orthogonal? It turns out that many of the states  $P_i|\nu\rangle$  vanish identically [81], such that we are only left with 9 non-vanishing states; this is to be expected, since the trace space is 9-dimensional [102].

While the fact that some of the projections  $P_i|\nu\rangle$  vanish takes care of many instances of the question whether  $|\tilde{\mu}_i\rangle$  and  $|\tilde{\nu}_i\rangle$  are orthogonal, it does not eliminate all such pairs. For these remaining pairs, additional research is necessary. Furthermore, we note that the MOLD projectors, when written with adjoint legs, no longer project onto *irreducible* representations of  $SU(N)$ , albeit still being orthogonal. Therefore, eq. (10.24) produces orthogonal singlets (for  $i \neq j$ ), but not the finest decomposition of the singlet algebra. As an alternative to the MOLD projectors, Keppeler and Sjö Dahl [82, 102] offer a method to construct projection operators over the  $n$ -gluon algebra. However, since we are interested in the singlet states of  $n$  gluons only, constructing all multiplets seems inefficient. Current research is being conducted by H. Weigert, R. Moerman and J. Rayner [81, 83] to streamline the problem at hand.

### 10.2.3 Changing bases for singlet projection operators

In chapter 5, we presented an algorithm giving all singlet states of  $SU(N)$  over  $V^{\otimes m} \otimes (V^*)^{\otimes m}$  (and thus also  $V^{\otimes m} \otimes (V^*)^{\otimes n}$ ) in a particular basis, namely by bending the MOLD projection and transition operators in  $\mathfrak{S}_m$ . However, as demonstrated in section 1.6.2, we often want these singlet states to be written in a different basis, as different bases simplify the constraint equations imposed by different coincidence limits of Wilson line correlators. In particular, we found that a basis containing (anti-) fundamental and adjoint lines (the *Fierz* basis) is particularly well suited for studying coincidence limits between a fundamental and an antifundamental Wilson line (*c.f.* section 5.3.2.2). However, at this point in time, we are still at want for a general, efficient construction algorithm of the singlet states in such a basis.

Alternatively, instead of trying to obtain a construction method for the Fierz basis from scratch, one could investigate the change of basis between the MOLD and the Fierz basis in the currently known examples. Patterns in the change of basis for these examples may allude to the singlet states of the Fierz basis for higher orders, or even to a general construction for the Fierz states in  $m\bar{q} + m\bar{q}$ .

It is, however, important to note that an algorithm to construct such an alternative basis does not yield the results of this thesis null and void. Firstly, coincidence limits between Wilson lines in the same representation are most easily analysed in the basis given in this thesis, as explained in section 5.3.1.1. Furthermore, the basis of singlet states in terms of symmetrizers and antisymmetrizers makes it particularly easy to spot dimensionally null operators – this trait is not shared by, for example, the Fierz basis.

### 10.2.4 Multiplets and physics

Lastly, we emphasize that, even though confinement forces color carrying partons into a singlet representation of  $SU(N)$  (among other things), the study of higher dimensional representations, as discussed in chapter 9, is still of relevance to a physics context:

At leading order, the averaging procedure over the background field governed by the JIMWLK equation suppresses all color non-singlets with a factor  $e^{-\infty}$  [76]. This is rather reassuring in that this aspect of confinement is obeyed by JIMWLK at LO. On the other hand, the parametrization should also vanish for all non-singlet states/projectors of  $SU(N)$ , although, this condition most probably has to be imposed manually on the  $n$ -point parameters  $G_{Y,\mathbf{x}_1\dots\mathbf{x}_n}^{(j)}$  and  $K_{Y,\mathbf{x}_1\dots\mathbf{x}_n}^{(j)}$ . In order to impose this condition, however, one first needs to know the appropriate multiplets of  $SU(N)$ .

If we consider the theory of spin (and thus set  $N = 2$ ), no analogous principle to confinement exists, and the parton system may have any net spin that is allowed by the group  $SU(2)$  (*c.f.* section 7.5), making multiplets of interest here. For  $SU(2)$ , there exists a working method that usually receives fairly in-depth treatment in (physics) textbooks [64, 65, 93, 139, 140]. However, the birdtrack formalism has the potential to make this standard discussion much simpler and therefore more pedagogical.

## 10.3 Concluding remarks

Singlet projection operators are of vital importance in physics, since one aspect of confinement requires color charged particles to combine into color neutral states. However, the textbook method of constructing projection operators corresponding to irreducible representations of  $SU(N)$  over  $V^{\otimes m} \otimes (V^*)^{\otimes n}$  in general, and singlet operators in particular, is computationally costly and thus not useful in practice. Besides giving a simple, computationally efficient construction algorithm for the singlet states and singlet projectors of  $SU(N)$ , this thesis has put forward many results regarding the representation theory of  $SU(N)$  over Fock spaces  $V^{\otimes m} \otimes (V^*)^{\otimes n}$  describing quarks, antiquarks and gluons. While there are still some unresolved issues that need to be addressed in order to obtain a full *mathematical* theory, the focus of this thesis was on *practicality*, such that all results given here directly furnish the study of Wilson line correlators in the context of QCD at high energies. This manifests in the fact that all operators in this thesis require minimal computing time to be constructed, and are thus well suited for practical applications.

# Bibliography

- [1] J. Alcock-Zeilinger and H. Weigert, “Simplification Rules for Birdtrack Operators,” *J. Math. Phys.* **58** no. 5, (2017) 051701, [arXiv:1610.08801 \[math-ph\]](#).
- [2] J. Alcock-Zeilinger and H. Weigert, “Compact Hermitian Young Projection Operators,” *J. Math. Phys.* **58** no. 5, (2017) 051702, [arXiv:1610.10088 \[math-ph\]](#).
- [3] J. Alcock-Zeilinger and H. Weigert, “Transition Operators,” *J. Math. Phys.* **58** no. 5, (2017) 051703, [arXiv:1610.08802 \[math-ph\]](#).
- [4] S. Keppeler and M. Sjö Dahl, “Hermitian Young Operators,” *J. Math. Phys.* **55** (2014) 021702, [arXiv:1307.6147 \[math-ph\]](#).
- [5] C. H. Kahn, *Anaximander and the origins of Greek cosmology*. Hackett Publishing Company, Inc., USA: Indianapolis, 1994. <https://archive.org/details/anaximanderorigi00kahn>.
- [6] E. Chaisson and S. McMillan, *Astronomy Today*. Addison-Wesley, 6th ed., 2008.
- [7] N. Copernicus, *De revolutionibus orbium coelestium (On the Revolution of the Heavenly Spheres)*. Nuremberg, Holy Roman Empire, 1543. [in Latin].
- [8] E. Noether, “Invariante Variationsprobleme,” *Nachrichten von der Gesellschaft der Wissenschaften zu Göttingen, Mathematisch-Physikalische Klasse* (1918) 235–257. <http://eudml.org/doc/59024>. [in German].
- [9] E. Noether, “Invariant Variation Problems,” *Transp. Theory Statist. Phys.* **1** no. 3, (1971) 186–207, [arXiv:physics/0503066 \[physics\]](#). [translated from German by M. A. Travel].
- [10] C. Jordan, “Memoire sur les groupes des mouvements,” *Annali de matematica pura ed applicata, Ser. II*, **II** no. 3, 167–215, (1868) 322–345. [in French].
- [11] M. Gell-Mann, “A Schematic Model of Baryons and Mesons,” *Phys. Lett.* **8** (1964) 214–215.
- [12] G. Zweig, “An SU(3) model for strong interaction symmetry and its breaking. Version 1,”.
- [13] G. Zweig, “An SU(3) model for strong interaction symmetry and its breaking. Version 2,” in *DEVELOPMENTS IN THE QUARK THEORY OF HADRONS. VOL. 1. 1964 – 1978*, D. Lichtenberg and S. P. Rosen, eds., pp. 22–101. CERN-TH-412, 1964. <http://inspirehep.net/record/4674/files/cern-th-412.pdf>.

- [14] R. P. Feynman, *Photon-Hadron Interactions*. W.A. Benjamin (Frontiers in Physics), USA: Massachusetts, 1972.
- [15] M. Gell-Mann and Y. Ne'emam, *The Eightfold way: a review with a collection of reprints*. W.A. Benjamin (Frontiers in Physics), USA: New York, 1964.
- [16] V. E. Barnes *et al.*, “Observation of a Hyperon with Strangeness  $-3$ ,” *Phys. Rev. Lett.* **12** (1964) 204–206.
- [17] V. E. Barnes *et al.*, “Confirmation of the existence of the  $\Omega^-$  hyperon,” *Phys. Lett.* **12** (1964) 134–136.
- [18] H. Weigert, “Evolution at small  $x_{Bj}$ : The Color Glass Condensate,” *Prog. Part. Nucl. Phys.* **55** (2005) 461–565, [arXiv:hep-ph/0501087](#) [[hep-ph](#)].
- [19] H. Fritzsch and M. Gell-Mann, “Current algebra: Quarks and what else?,” *eConf C720906V2* (1972) 135–165, [arXiv:hep-ph/0208010](#) [[hep-ph](#)].
- [20] J. Jalilian-Marian, A. Kovner, L. D. McLerran, and H. Weigert, “The Intrinsic glue distribution at very small  $x$ ,” *Phys. Rev.* **D55** (1997) 5414–5428, [arXiv:hep-ph/9606337](#) [[hep-ph](#)].
- [21] F. Gelis, E. Iancu, J. Jalilian-Marian, and R. Venugopalan, “The Color Glass Condensate,” *Ann. Rev. Nucl. Part. Sci.* **60** (2010) 463–489, [arXiv:1002.0333](#) [[hep-ph](#)].
- [22] L. McLerran and R. Venugopalan, “Computing quark and gluon distribution functions for very large nuclei,” *Phys. Rev.* **D49** (August, 1994) 2233–2241, [arXiv:hep-ph/9309289](#) [[hep-ph](#)].
- [23] L. McLerran and R. Venugopalan, “Gluon distribution functions for very large nuclei at small transverse momentum,” *Phys. Rev.* **D49** (October, 1994) 3352–3355, [arXiv:hep-ph/9311205](#) [[hep-ph](#)].
- [24] **Particle Data Group** Collaboration, C. Patrignani *et al.*, “Review of Particle Physics,” *Chin. Phys.* **C40** no. 10, (2016) 100001.
- [25] M. E. Peskin and D. V. Schroeder, *An Introduction to quantum field theory*. Addison-Wesley, USA: Reading, 1995.
- [26] J.-L. Kneur and A. Neveu, “ $\Lambda_{\overline{\text{MS}}}^{\text{QCD}}$  from Renormalization Group Optimized Perturbation,” *Phys. Rev.* **D85** (2012) 014005, [arXiv:1108.3501](#) [[hep-ph](#)].
- [27] D. Griffiths, *Introduction to elementary particles*. Wiley-VCH, Germany: Weinheim, 2008.
- [28] **ATLAS** Collaboration, M. e. a. Aaboud, “Measurement of the Inelastic Proton-Proton Cross Section at  $\sqrt{s} = 13$  TeV with the ATLAS Detector at the LHC,” *Phys. Rev. Lett.* **117** no. 18, (2016) 182002, [arXiv:1606.02625](#) [[hep-ex](#)].
- [29] H. Weigert, “A compact introduction to evolution at small  $x$  and the color glass condensate,” *Nucl. Phys.* **A783** (2007) 165–172.
- [30] J. Kuokkanen, K. Rummukainen, and H. Weigert, “HERA-Data in the Light of Small  $x$  Evolution with State of the Art NLO Input,” *Nucl. Phys.* **A875** (2012) 29–93, [arXiv:1108.1867](#) [[hep-ph](#)].



- 
- [31] D. Bailin and A. Love, *Introduction to Gauge Field Theory*. Hilger (Graduate Student Series In Physics), UK: Bristol, 1986.
- [32] P. Becher, M. Böhm, and H. Joos, *Gauge Theories of Strong and Electroweak Interactions*. Wiley, UK: Chichester, 1984.
- [33] S. Weinberg, *The Quantum Theory of Fields Vol.II (Modern Applications)*. Cambridge Univ. Pr., UK: Cambridge, 1995.
- [34] T.-P. Cheng and L.-F. Li, *Gauge Theory of Elementary Particle Physics*. Oxford science publications, USA, 1st ed., 1982.
- [35] S. Weinberg, *The Quantum Theory of Fields Vol.I (Foundations)*. Cambridge Univ. Pr., UK: Cambridge, 1995.
- [36] M. Nakahara, *Geometry, topology and physics*. IOP Publishing, USA: Boca Raton, 2003.
- [37] I. O. Cherednikov, T. Mertens, and F. F. Van der Veken, *Wilson lines in quantum field theory*, vol. 24 of *De Gruyter Studies in Mathematical Physics*. de Gruyter, Germany: Berlin, 2014.  
<http://www.degruyter.com/view/product/204486>.
- [38] J. M. Lee, *Introduction to Smooth Manifolds*. Springer, USA: New York, Jan., 2003.
- [39] C.-N. Yang and R. L. Mills, “Conservation of Isotopic Spin and Isotopic Gauge Invariance,” *Phys. Rev.* **96** (1954) 191–195.
- [40] S. M. Carroll, *Spacetime and geometry: An introduction to general relativity*. Addison-Wesley, USA: San Francisco, 2004. <http://www.slac.stanford.edu/spires/find/books/www?cl=QC6:C37:2004>.
- [41] P. Dirac, *The Principles of Quantum Mechanics*. Oxford Univ. Pr., UK: Oxford, 3rd ed., 1947.
- [42] F. Fiorani, G. Marchesini, and L. Reina, “Soft Gluon Factorization and Multi-Gluon Amplitude,” *Nucl. Phys.* **B309** (1988) 439–460.
- [43] J. Collins, *Foundations of perturbative QCD*. Cambridge Univ. Pr., UK: Cambridge, 2013.  
<http://www.cambridge.org/de/knowledge/isbn/item5756723>.
- [44] H. Weigert, “Electromagnetism (Honours).” Lecture Notes, 2017. University of Cape Town.
- [45] J. R. Magnus and H. Neudecker, *Matrix Differential Calculus with Applications in Statistics and Econometrics*. Wiley, UK: Sussex, 3rd ed., 2007.  
<http://www.janmagnus.nl/misc/mdc2007-3rdedition>.
- [46] F. Gelis, “Color Glass Condensate and Glasma,” *Int. J. Mod. Phys.* **A28** (2013) 1330001, [arXiv:1211.3327 \[hep-ph\]](https://arxiv.org/abs/1211.3327).
- [47] L. McLerran, “The Color Glass Condensate and Glasma: Two Lectures,” [arXiv:0804.1736 \[hep-ph\]](https://arxiv.org/abs/0804.1736).
- [48] E. A. Kuraev, L. N. Lipatov, and V. S. Fadin, “The Pomeranchuk Singularity in Nonabelian Gauge Theories,” *Sov. Phys. JETP* **45** (1977) 199–204. [*Zh. Eksp. Teor. Fiz.* 72, 377 (1977)].

- [49] I. I. Balitsky and L. N. Lipatov, “The Pomeranchuk Singularity in Quantum Chromodynamics,” *Sov. J. Nucl. Phys.* **28** (1978) 822–829. [*Yad. Fiz.* 28, 1597 (1978)].
- [50] S. Munier, S. Peigné, and E. Petreska, “Medium-induced gluon radiation in hard forward parton scattering in the saturation formalism,” [arXiv:1603.01028](https://arxiv.org/abs/1603.01028) [[hep-ph](#)].
- [51] H. Weigert. Personal communication, May–July, 2017.
- [52] agsandrew, “Colors In Bloom series. Visually pleasing composition of fractal color textures to serve as background in works on imagination, creativity and design.” Online image. <https://www.shutterstock.com/g/agsandrew>. Stock illustration ID: 170939975.
- [53] Y. L. Dokshitzer, “Calculation of the Structure Functions for Deep Inelastic Scattering and  $e^+e^-$  Annihilation by Perturbation Theory in Quantum Chromodynamics.,” *Sov. Phys. JETP* **46** (1977) 641–653. [*Zh. Eksp. Teor. Fiz.* 73, 1216 (1977)].
- [54] V. N. Gribov and L. N. Lipatov, “Deep inelastic  $ep$  scattering in perturbation theory,” *Sov. J. Nucl. Phys.* **15** (1972) 438–450. [*Yad. Fiz.* 15, 781 (1972)].
- [55] G. Altarelli and G. Parisi, “Asymptotic Freedom in Parton Language,” *Nucl. Phys.* **B126** (1977) 298–318.
- [56] J. Jalilian-Marian, A. Kovner, A. Leonidov, and H. Weigert, “The BFKL equation from the Wilson renormalization group,” *Nucl. Phys.* **B504** (1997) 415–431, [arXiv:hep-ph/9701284](https://arxiv.org/abs/hep-ph/9701284) [[hep-ph](#)].
- [57] J. Jalilian-Marian, A. Kovner, and H. Weigert, “The Wilson renormalization group for low  $x$  physics: Gluon evolution at finite parton density,” *Phys. Rev.* **D59** (1998) 014015, [arXiv:hep-ph/9709432](https://arxiv.org/abs/hep-ph/9709432) [[hep-ph](#)].
- [58] E. Iancu, A. Leonidov, and L. D. McLerran, “Nonlinear gluon evolution in the color glass condensate. 1.,” *Nucl. Phys.* **A692** (2001) 583–645, [arXiv:hep-ph/0011241](https://arxiv.org/abs/hep-ph/0011241) [[hep-ph](#)].
- [59] E. Ferreiro, E. Iancu, A. Leonidov, and L. McLerran, “Nonlinear gluon evolution in the color glass condensate. 2.,” *Nucl. Phys.* **A703** (2002) 489–538, [arXiv:hep-ph/0109115](https://arxiv.org/abs/hep-ph/0109115) [[hep-ph](#)].
- [60] I. Balitsky, “Operator expansion for high-energy scattering,” *Nucl. Phys.* **B463** (1996) 99–160, [arXiv:hep-ph/9509348](https://arxiv.org/abs/hep-ph/9509348) [[hep-ph](#)].
- [61] Y. V. Kovchegov, “Small  $x$   $F(2)$  structure function of a nucleus including multiple pomeron exchanges,” *Phys. Rev.* **D60** (1999) 034008, [arXiv:hep-ph/9901281](https://arxiv.org/abs/hep-ph/9901281) [[hep-ph](#)].
- [62] I. Balitsky and G. A. Chirilli, “Next-to-leading order evolution of color dipoles,” *Phys. Rev.* **D77** (2008) 014019, [arXiv:0710.4330](https://arxiv.org/abs/0710.4330) [[hep-ph](#)].
- [63] A. Haar, “Der Massbegriff in der Theorie der Kontinuierlichen Gruppen,” *Annals of Mathematics* **34** no. 1, (Jan., 1933) 147–169. Second Series, [in German].
- [64] B. Hall, *Lie Groups, Lie Algebras, and Representations - An Elementary Introduction*, 2nd ed. Springer International, Switzerland, 2015.
- [65] Y. Kosmann-Schwarzbach, *Groups and Symmetries - From Finite Groups to Lie Groups*. Springer, USA: New York, 2000.

- 
- [66] H. Weigert, “Unitarity at small Bjorken  $x$ ,” *Nucl. Phys.* **A703** (2002) 823–860, [arXiv:hep-ph/0004044](#) [hep-ph].
- [67] K. Rummukainen and H. Weigert, “Universal features of JIMWLK and BK evolution at small  $x$ ,” *Nucl. Phys.* **A739** (2004) 183–226, [arXiv:hep-ph/0309306](#) [hep-ph].
- [68] A. Kovner, M. Lublinsky, and Y. Mulian, “NLO JIMWLK evolution unabridged,” *JHEP* **08** (2014) 114, [arXiv:1405.0418](#) [hep-ph].
- [69] Y. V. Kovchegov and E. Levin, *Quantum chromodynamics at high energy*, vol. 33. Cambridge Univ. Pr., UK: Cambridge, 2012. <http://www.cambridge.org/de/knowledge/isbn/item6803159>.
- [70] A. H. Mueller, “A Simple derivation of the JIMWLK equation,” *Phys. Lett.* **B523** (2001) 243–248, [arXiv:hep-ph/0110169](#) [hep-ph].
- [71] C. Marquet and H. Weigert, “New observables to test the Color Glass Condensate beyond the large- $N_c$  limit,” *Nucl. Phys.* **A843** (2010) 68–97, [arXiv:1003.0813](#) [hep-ph].
- [72] P. Cvitanović, *Group theory: Birdtracks, Lie’s and exceptional groups*. Princeton Univ. Pr., USA: Princeton, 2008. <http://birdtracks.eu>.
- [73] R. L. Kobes and G. W. Semenoff, “Discontinuities of Green Functions in Field Theory at Finite Temperature and Density,” *Nucl. Phys.* **B260** (1985) 714–746.
- [74] G. ’t Hooft and M. J. G. Veltman, “DIAGRAMMAR,” *NATO Sci. Ser. B* **4** (1974) 177–322.
- [75] Y. V. Kovchegov, J. Kuokkanen, K. Rummukainen, and H. Weigert, “Subleading- $N_c$  corrections in non-linear small- $x$  evolution,” *Nucl. Phys.* **A823** (2009) 47–82, [arXiv:0812.3238](#) [hep-ph].
- [76] H. Weigert, “JIMWLK at NLO,” 2016. (unpublished).
- [77] E. Iancu, A. Leonidov, and L. McLerran, “The Color glass condensate: An Introduction,” in *QCD perspectives on hot and dense matter. Proceedings, NATO Advanced Study Institute, Summer School, Cargese, France, August 6-18, 2001*, pp. 73–145. 2002. [arXiv:hep-ph/0202270](#) [hep-ph]. <http://alice.cern.ch/format/showfull?sysnb=2297268>.
- [78] H. Weigert, “Nonglobal jet evolution at finite  $N_c$ ,” *Nucl. Phys.* **B685** (2004) 321–350, [arXiv:hep-ph/0312050](#) [hep-ph].
- [79] A. Ramnath, H. Weigert, and A. Hamilton, “Exclusive  $J/\Psi$  vector-meson production in high-energy nuclear collisions,” *Nucl. Phys.* **A932** (2014) 274–279.
- [80] T. Lappi, A. Ramnath, K. Rummukainen, and H. Weigert, “JIMWLK evolution of the odderon,” *Phys. Rev.* **D94** (2016) 054014, [arXiv:1606.00551](#) [hep-ph].
- [81] J. Rayner, “Applications of representation theory to a novel approach to JIMWLK,” Master’s thesis, University of Cape Town, South Africa, 2017. [Thesis supervisor: A/Prof. H. Weigert].
- [82] M. Sjödaahl and S. Keppeler, “Tools for calculations in color space,” *PoS (Proceedings of Science), Proceedings, 21st International Workshop on Deep-Inelastic Scattering and Related Subjects DIS2013* (2013) 166, [arXiv:1307.1319](#) [hep-ph].

- [83] R. W. Moerman, “A gauge-invariant, symmetry-preserving truncation of JIMWLK,” Master’s thesis, University of Cape Town, South Africa, 2017. [Thesis supervisor: A/Prof. H. Weigert].
- [84] A. Young, “On Quantitative Substitutional Analysis - III,” *Proc. London Math. Soc.* **s2-28** (1928) 255–292.
- [85] D. E. Littlewood, *The Theory of Group Characters and Matrix Representations of Groups*. Oxford Univ. Pr., UK: Clarendon, 2nd ed., 1950.
- [86] J. D. Dollard and C. N. Friedman, “Product Integration with Application to Differential Equations,” in *Encyclopedia of Mathematics and Its Applications 10*. Cambridge Univ. Pr., UK: Cambridge, 1984.
- [87] R. Penrose, “Applications of negative dimension tensors,” in *Combinatorial mathematics and its applications*, D. Welsh, ed., pp. 221–244. Academic Press, USA: New York, 1971.
- [88] R. Penrose, “Angular momentum: An approach to combinatorial space-time,” in *Quantum Theory and Beyond*, T. Bastin, ed. Cambridge Univ. Pr., UK: Cambridge, 1971.
- [89] R. Penrose and M. A. H. MacCallum, “Twistor theory: An Approach to the quantization of fields and space-time,” *Phys. Rept.* **6** (1972) 241–316.
- [90] G. Falcioni, E. Gardi, M. Harley, L. Magnea, and C. D. White, “Multiple Gluon Exchange Webs,” *JHEP* **10** (2014) 10, [arXiv:1407.3477](https://arxiv.org/abs/1407.3477) [[hep-ph](#)].
- [91] C. J. Bomhof, P. J. Mulders, and F. Pijlman, “The Construction of gauge-links in arbitrary hard processes,” *Eur. Phys. J.* **C47** (2006) 147–162, [arXiv:hep-ph/0601171](https://arxiv.org/abs/hep-ph/0601171) [[hep-ph](#)].
- [92] W. Fulton and J. Harris, *Representation Theory - A First Course*. Springer, USA, 2004.
- [93] W. K. Tung, *Group Theory in Physics*. World Scientific, Singapore, 1985.
- [94] J. Alcock-Zeilinger and H. Weigert, “A Construction Algorithm for the Singlets of  $SU(N)$  and what they tell us about Wilson Line Correlators.”. (in preparation).
- [95] W. Fulton, *Young Tableaux*. Cambridge Univ. Pr., UK: Cambridge, 1997.
- [96] B. Sagan, *The Symmetric Group - Representations, Combinatorial Algorithms, and Symmetric Functions*. Springer, USA: New York, 2nd ed., 2000.
- [97] S. Chowla, I. N. Herstein, and W. K. Moore, “On recursions connected with the symmetric groups I,” *Cannad. J. Math.* **3** (February, 1951) 328–334. <http://cms.math.ca/10.4153/CJM-1951-038-3>.
- [98] H. Weyl, *The Classical Groups: Their Invariants and Representations*. Princeton Univ. Pr., USA: Princeton, 2nd ed., 1946.
- [99] B. van der Waerden, *Moderne Algebra II*. Springer, Germany: Berlin, 1931.
- [100] M. Artin, *Algebra*. Prentice Hall, USA: Boston, 2nd ed., 2011.
- [101] J. C. Collins, D. E. Soper, and G. F. Sterman, “Factorization of Hard Processes in QCD,” *Adv. Ser. Direct. High Energy Phys.* **5** (1989) 1–91, [arXiv:hep-ph/0409313](https://arxiv.org/abs/hep-ph/0409313) [[hep-ph](#)].

- 
- [102] S. Keppeler and M. Sjö Dahl, “Orthogonal multiplet bases in  $SU(N_c)$  color space,” *JHEP* **09** (2012) 124, [arXiv:1207.0609](https://arxiv.org/abs/1207.0609) [hep-ph].
- [103] E. Cartan, *Sur la structure des groupes de transformations finis et continus*. Thèses présentées a la Faculté des Sciences de Paris pour obtenir le grade de docteur ès sciences mathématiques. Nony, 1894. <https://books.google.co.za/books?id=JY8LAAAAYAAJ>. [in French].
- [104] M. Gell-Mann, “The Eightfold Way: A Theory of strong interaction symmetry,” Technical Report CTSL-20, TID-12608, California Inst. of Tech., Pasadena, Synchrotron Lab, March, 1961. <https://digital.library.unt.edu/ark:/67531/metadc867161/m1/>.
- [105] N. Bourbaki, “Lie Groups and Lie Algebras,” in *Elements of Mathematics*, ch. VII–IX. Springer, USA: New York, 2000.
- [106] I. Schensted, *A Course on the Application of Group Theory to Quantum Mechanics*. Neo Press, USA: Peaks Island, ME, 1976.
- [107] S. Lang, *Linear Algebra*. Springer, USA: New York, 3rd ed., 1987.
- [108] A. Clebsch and P. Gordan, *Theorie der abelschen Funktionen*. Teubner, 1866. <https://books.google.co.za/books?id=sNvSngEACAAJ>. [in German].
- [109] K. Glass and C.-K. Ng, “A Simple Proof of the Hook Length Formula,” *Amer. Math. Monthly* **111** no. 8, (Oct., 2004) 700–704.
- [110] P. Cvitanovic, P. G. Lauwers, and P. N. Scharbach, “Gauge Invariance Structure of Quantum Chromodynamics,” *Nucl. Phys.* **B186** (1981) 165–186.
- [111] D. E. Littlewood, “Lie Algebras and Representations of Continuous Groups,” *Int. J. Theor. Phys.* **14** (1976) 97–109.
- [112] N. Jeevanjee, *An Introduction to Tensors and Group Theory for Physicists*. Birkhäuser (Springer), USA: New York, 2nd ed., 2015.
- [113] H. Georgi, “Lie algebras in particle physics,” *Front. Phys.* **54** (1999) 1–320.
- [114] I. Schur, “Über eine Klasse von Matrizen, die sich einer gegebenen Matrix zuordnen lassen.” Inaugural-dissertation, 1901. <https://archive.org/details/bereineklassevo00schugoog>. [in German].
- [115] R. Howe and S. Lee, “Why should the Littlewood-Richardson rule be true?,” *Am. Math. Soc.* **49** no. 2, (April, 2012) 187–236.
- [116] L. B. Okun, *Leptons and Quarks*. North-Holland, Netherlands: Amsterdam, 1982. <http://www.worldscientific.com/worldscibooks/10.1142/9162>.
- [117] R. Howe, “Remarks on Classical Invariant Theory,” *Trans. Amer. Math. Soc.* **313** no. 2, (Jun., 1989) 539–570. <http://www.jstor.org/stable/2001418>.

- [118] H. A. Rothe, “Ueber Permutationen, in Beziehung auf die Stellen ihrer Elemente. Anwendungen der daraus abgeleiteten Sätze auf das Eliminationsproblem.” in *Sammlung Combinatorisch-Analytischer Abhandlungen*, C. F. Hindenburg, ed., pp. 263–305. Gerhard Fleischer dem Jüngeren, Germany: Leipzig, 1800. <http://www.e-rara.ch/zut/content/pageview/1341041>. Zweyte Sammlung, [in German].
- [119] Anon., “Telephone number (mathematics) — Wikipedia, The Free Encyclopedia,” 2016. [https://en.wikipedia.org/wiki/Telephone\\_number\\_\(mathematics\)](https://en.wikipedia.org/wiki/Telephone_number_(mathematics)). [Online; accessed on 20 March 2016].
- [120] D. E. Knuth, *The Art of Computer Programming, Volume 3 - Sorting and Searching*. Addison-Wesley, USA: Boston, 2nd ed., 1998.
- [121] D. Kim and J. S. Kim, “A combinatorial approach to the power of 2 in the number of involutions,” *Journal of Combinatorial Theory, Series A* **117** no. 8, (2010) 1082–1094. <http://www.sciencedirect.com/science/article/pii/S0097316509001204>.
- [122] B. Sagan, “The *Combinatorica* Software Package,” 1990. <http://users.math.msu.edu/users/sagan/papers/old/csp.pdf>.
- [123] “Wolfram Language & System Documentation Center: NumberOfTableaux.” <http://reference.wolfram.com/language/Combinatorica/ref/NumberOfTableaux.html>. [Online; accessed on 15 April 2016].
- [124] N. Jacobson, *Basic Algebra I*. Dover, USA: San Francisco, 1989.
- [125] J. J. Sakurai and J. Napolitano, *Modern Quantum Mechanics*. Addison-Wesley, USA: San Francisco, 2nd ed., 2011.
- [126] O. P. Lossers, “Solution to Problem E3058,” *Am. Math. Monthly* **93** (1986) 820–821.
- [127] M. Anshelevich, M. Gaikema, M. Hansalik, S. He, and N. Mehlhop, “Expansion of permutations as products of transpositions.” <https://arxiv.org/abs/1702.06093>, February, 2017.
- [128] N. Hartsfield and G. Ringel, *Pearls in Graph Theory - A Comprehensive Introduction*. Dover, USA: New York, 1994.
- [129] C. Marquet, “Forward inclusive dijet production and azimuthal correlations in  $pA$  collisions,” *Nucl. Phys.* **A796** (2007) 41–60, [arXiv:0708.0231](https://arxiv.org/abs/0708.0231) [hep-ph].
- [130] C. Marquet, E. Petreska, and C. Roiesnel, “Transverse-momentum-dependent gluon distributions from JIMWLK evolution,” *JHEP* **10** (2016) 065, [arXiv:1608.02577](https://arxiv.org/abs/1608.02577) [hep-ph].
- [131] B.-W. Xiao, F. Yuan, and J. Zhou, “Transverse Momentum Dependent Parton Distributions at Small- $x$ ,” [arXiv:1703.06163](https://arxiv.org/abs/1703.06163) [hep-ph].
- [132] Y. V. Kovchegov and M. D. Sievert, “Sivers function in the quasiclassical approximation,” *Phys. Rev.* **D89** no. 5, (2014) 054035, [arXiv:1310.5028](https://arxiv.org/abs/1310.5028) [hep-ph].
- [133] L. Lippstreu, “Anomalous Cross Dimension Contributions to JIMWLK,” Master’s thesis, University of Cape Town, South Africa, 2017. [Thesis supervisor: A/Prof. H. Weigert].

- 
- [134] F. Arleo and S. Peigné, “Quarkonium suppression from coherent energy loss in fixed-target experiments using LHC beams,” *Adv. High Energy Phys.* **2015** (2015) 961951, [arXiv:1504.07428 \[hep-ph\]](#).
- [135] F. Arleo and S. Peigné, “Quarkonium suppression in heavy-ion collisions from coherent energy loss in cold nuclear matter,” *JHEP* **10** (2014) 73, [arXiv:1407.5054 \[hep-ph\]](#).
- [136] J. Jalilian-Marian and X.-N. Wang, “Shadowing of gluons in perturbative QCD: A Comparison of different models,” *Phys. Rev.* **D63** (2001) 096001, [arXiv:hep-ph/0005071 \[hep-ph\]](#).
- [137] D. Adamiak, “Rapidity Evolution of Observables at High Energies using the Gaussian Truncation,” Master’s thesis, University of Cape Town, South Africa, 2017. [Thesis supervisor: A/Prof. H. Weigert].
- [138] A. Banfi, G. Marchesini, and G. Smye, “Away-from-jet energy flow,” *JHEP* **08** (2002) 006, [arXiv:hep-ph/0206076 \[hep-ph\]](#).
- [139] J. P. Elliott and P. G. Dawber, *Symmetry in Physics Volume 1: Principles and Simple Applications*. Oxford Univ. Pr., UK: Oxford, 1987.
- [140] J. P. Elliott and P. G. Dawber, *Symmetry in Physics Volume 2: Further Applications*. Oxford Univ. Pr., UK: Oxford, 1986.